

Design, Synthesis and Evaluation of Mechanism-Based Inhibitors of IDO1 and PROTAC-Degraders of JAK2

by

Nicholas John Cundy



A thesis submitted to
The University of Birmingham
for the degree of
DOCTOR OF PHILOSOPHY

School of Chemistry
College of Engineering and Physical Sciences
University of Birmingham

December 2019

UNIVERSITY OF
BIRMINGHAM

University of Birmingham Research Archive

e-theses repository

This unpublished thesis/dissertation is copyright of the author and/or third parties. The intellectual property rights of the author or third parties in respect of this work are as defined by The Copyright Designs and Patents Act 1988 or as modified by any successor legislation.

Any use made of information contained in this thesis/dissertation must be in accordance with that legislation and must be properly acknowledged. Further distribution or reproduction in any format is prohibited without the permission of the copyright holder.

Abstract

Over-expression of indolamine-2,3-dioxygenase 1 (IDO1) and programmed death-ligand 1 (PD-L1) are common phenotypes of immunoresistant cancers. The expression of IDO1 and PD-L1 is mediated by the janus kinase-signal transducer and activator of transcription (JAK-STAT) pathway in response to stimulation by interferon- γ (IFN γ), with tumoral signalling specifically transduced *via* JAK2.

IDO1's role in tumour immunoresistance is mediated by both depletion of its substrate, *L*-tryptophan, and by metabolites derived from its product, *N*-formyl-*L*-kynurenine. The mechanism of IDO1-mediated dioxygenation of *L*-tryptophan to *N*-formyl-*L*-kynurenine proceeds by either a radical or electrophilic-based mechanism. Radicals adjacent to cyclopropane rings undergo ring-opening driven by relief of ring strain, with the rate of ring-opening dependent on the stability of the resulting radical. A series of cyclopropane-containing IDO1 substrate mimics were designed to divert the hypothesised radical dioxygenation mechanism, potentially resulting in enzyme inhibition resulting from either a mechanistic 'dead-end' or covalent inactivation of the protein. Based on tryptophan and tryptamine, 1,2-cyclopropanated analogues were synthesised *via* a 1,3-dipolar cycloaddition of an amino acrylate and a indolo-diazo species or the Rh-catalysed cyclopropanation of a terminal olefin. Complimentary spirocyclic cyclopropane analogues of tryptophan and tryptamine were accessed *via* cyclodialkylation of 3-indoleacetonitrile. A library of sulfenylindoles was also synthesised to divert late-stage metabolic intermediates in a non-radical dependent manner. The synthesised inhibitors were exposed to IFN γ -stimulated SCOV-3 cells and demonstrated a broadly poor ability to inhibit IDO1 turnover of tryptophan. Novel cell-free assays were developed to ascertain whether the reduced reactivity was related to compound cell-permeability and to further probe the mechanistic-detail of IDO1. A promising IDO1 inhibitor was identified in the cell-free assays and the further evaluation of the candidate is described.

Study of JAK2's role in tumour immune escape has been complicated by inhibitors direct effects on immune cells, which is thought to be mediated by inhibition of other JAK family members. Proteolysis targeting chimeras (PROTACs) have the ability to degrade proteins within cells by harnessing the ubiquitin-proteasomal system. Based on FDA-approved JAK2 ligand fedratinib, a series of PROTACs were synthesised. The synthesised PROTACs were evaluated in JAK2-expressing HeLa cells. Degradation of JAK2 in HeLa cells was not observed in the preliminary western-blot analysis – future investigations of JAK2 PROTACs is discussed.

Acknowledgements

The production of this thesis was far from a solo endeavor, throughout my PhD I have had the benefit of being surrounded by excellent scientists who have contributed towards this work and my development as a chemist. I have also been fortunate to have had a great support network of friends and family who have made this sometimes grueling three years a great experience. As a result, I owe a few thanks:

A huge thank you is due to Richard and Sam for encouraging my independence and for continually challenging me to keep learning. This experience has been made all the better by your understanding attitudes and eagerness to keep pushing me forward. I'd also like to thank my industrial supervisor, Nick, and the rest of the scientists at Celentyx Ltd for the support of this project. Attending the research meetings and gaining an appreciation of the biology was invaluable for my development as a scientist. This thesis also wouldn't have been what it is without the feedback and discussion from Richard, Sam, Dan and Ian so thank you for your time and helpful comments.

A key ingredient to this PhD has undoubtedly been the people I've shared the lab with over the past three years. So, thank you to the Grainger, Cox and Tucker group members for making work such a fun place to be. A special mention goes out to the members of the breakfast club: Glenn, Mat, Izzy and Russ. I will be sad to give up that tradition. Thanks are also due to the many people who keep/kept this place running and for always being friendly faces around the department: Helen, Lynn, Bernard, Stu, Steve, Cécile, Louise, Chi and Peter. I'd also like to thank John Snaith and Phil for giving me so many opportunities to teach and encouraging me to gain AFHEA status.

Amy, thank you for your support and understanding throughout my PhD, particularly during the write up period. Thank you for also reminding me that there is a world outside of lab and for being a great person to enjoy it with! Chris G, Hannah and Tash, I've missed having you all here in Brum, thank you for being there for me and for the fun over the years. Chris D thanks for all the ale's, the music and being a great friend for so many years. Finally, I owe a lot of thanks to my family – none of this would have been possible without having you with me. Mum and Dad, thank you for giving me every opportunity you possibly could, continually supporting me in all aspects of my life and for setting such a positive example, you have both had more impact on me completing this PhD than you will ever know.

Contents

CHAPTER 1: DESIGN, SYNTHESIS AND EVALUATION OF MECHANISM-BASED INHIBITORS OF IDO1	1
1.1 – IDO1 AND TRYPTOPHAN	2
1.1.1 – <i>The Paradox of IDO1</i>	3
1.1.2 – <i>Early IDO1 Inhibitors</i>	4
1.1.3 – <i>Current IDO Inhibition</i>	5
1.1.4 – <i>Modes of IDO1 Inhibition</i>	6
1.1.5 – <i>Mechanistic Inhibition of IDO1</i>	7
1.1.6 – <i>Development of the Mechanistic Detail of the Heme-Dioxygenases</i>	7
1.2 – RADICALS AND CYCLOPROPANES	20
1.2.1 – <i>Radical Clocks and Rates of Reaction</i>	20
1.2.2 – <i>Captodative Radicals</i>	22
1.2.3 – <i>Radical Ring Opening-Based Therapeutic Agent</i>	23
1.3 – AMINO ACIDS	25
1.3.1 – <i>Proteinogenic Amino Acids</i>	25
1.3.2 – <i>Non-Proteinogenic Amino Acids</i>	25
1.3.3 – <i>Non-α-amino Acids</i>	26
1.3.4 – <i>Cyclopropane-Containing Amino Acids</i>	27
1.3.5 – <i>Synthesis of Cyclopropane-Containing Amino Acids</i>	28
1.4 – AIMS AND OBJECTIVES	36
1.5 – RESULTS AND DISCUSSION: SYNTHESIS OF MECHANISTIC PROBES FOR IDO1	40
1.5.1 – <i>Synthesis of 1,2-Δ-Tryptophan Analogue 61</i>	40
1.5.2 – <i>Synthesis of 1,2-Δ-Tryptamine Analogue 99</i>	51
1.5.3 – <i>Synthesis of Homologated 1,2-Δ-Tryptamine Analogue 182</i>	68

1.5.4 – Synthesis of 1,1'- Δ -Tryptophan and Tryptamine Analogues 100 and 101	71
1.5.5 – Synthesis of Sulfenylindole 102 and a Small Library of Analogues	76
1.6 – RESULTS AND DISCUSSION: WHOLE CELL EVALUATION	81
1.7 – RESULTS AND DISCUSSION: BIOCHEMICAL EVALUATION.....	87
1.7.1 – Steady-State Assay.....	88
1.7.2 – Inhibition Assay	93
1.7.3 – Fluorescence-Based Detection of Kyn.....	98
1.7.4 – Differential Scanning Fluorimetry/Thermal Shift Assay	104
1.8 – CONCLUSIONS AND FUTURE WORK	108
CHAPTER 2: DESIGN, SYNTHESIS AND EVALUATION OF PROTAC-DEGRADERS OF JAK2	110
2.1 – THERAPEUTIC INTERVENTION OF THE JAK/STAT PATHWAY.....	111
2.1.1 – Interferon γ Induction of the JAK/STAT Pathway	111
2.1.2 – Selective Inhibitors of JAK1 and 2	112
2.1.3 – Studying the Role of JAK2 <i>in vivo</i>	115
2.2 – PROTEIN DEGRADATION AS A THERAPEUTIC TOOL	120
2.2.1 – Proteolysis Targeting Chimeras.....	121
2.2.2 – Development of PROTAC Technology	122
2.2.3 – PROTACs Verses Small Molecule Inhibitors <i>in vivo</i>	125
2.2.4 – PROTACs in the Clinic	128
2.3 – AIMS AND OBJECTIVES	131
2.4 – SYNTHESIS OF A SERIES OF JAK2-TARGETING PROTACS	135
2.4.1 – JAK2 Ligand Synthesis.....	135
2.4.2 – Ligase Ligand Synthesis.....	138
2.4.3 – Linker Synthesis.....	142
2.4.4 – Ligase Binder-Linker Synthesis	142
2.4.5 – JAK2 Ligand and Ligase Binder-Linker Complex Coupling.....	145

2.5 – BIOLOGICAL EVALUATION OF THE SYNTHESISED PROTACs	148
2.6 – CONCLUSIONS AND FUTURE WORK	151
CHAPTER 3: APPENDIX	153
CHAPTER 4: EXPERIMENTAL METHODS	169
BIOLOGICAL EVALUATION METHODS	170
<i>General Experimental</i>	170
<i>Whole Cell Evaluation Methods</i>	171
<i>Biochemical Evaluation Methods</i>	172
CHEMICAL SYNTHESIS METHODS.....	175
<i>General Experimental</i>	175
<i>General Synthetic Procedures</i>	177
<i>Chapter 1 Experimental Procedures</i>	178
<i>Chapter 2 Experimental Procedures</i>	246
CHAPTER 5: REFERENCES	300

Abbreviations

)))	Sonication
1-Me-NFK	1-Methyl- <i>N</i> -formyl- <i>L</i> -kynurenine
1-MT	1-Methyl- <i>L</i> -tryptophan
ABCB1	ATP binding cassette subfamily B member 1
Ac	Acetyl
Acac	Acetylacetone
ACC	1-aminocyclopropanecarboxylic acid
ADMET	Absorption, distribution, metabolism, and excretion-toxicology
AIBN	2,2'-azobisisobutyronitrile
Ala	Alanine
ALK	Anaplastic lymphoma kinase
AR	Androgen receptor
ATP	Adenosine triphosphate
AXL	A receptor tyrosine kinase
BET	Bromodomain and extra-terminal domain
Boc	<i>tert</i> -butyloxycarbonyl
Bs	Benzenesulfonyl
BTAC	Benzyltriethylammonium chloride
BTK	Bruton's tyrosine kinase
Cas9	CRISPR associated protein 9
CD20	Cluster of differentiation 20
CD8+	Cluster of differentiation 8+
clAP	Cellular inhibitor of apoptosis
CNS	Central Nervous System
CRABP-I	Cellular retinoic acid binding protein-1
CRBN	Cereblon
CRISPR	Clustered regularly interspaced short palindromic repeats
CTLs	Cytotoxic lymphocytes
Δ	Cyclopropyl
d.r.	Diastereomer ratio
DC ₅₀	Half-maximal degradation concentration
DMEM	Dulbecco's modified eagle medium
DPPA	Diphenylphosphoryl azide
DUBs	De-ubiquitinases
ER	Oestrogen receptor
ET	Essential Thrombocythemia
EDG	Electron withdrawing group
EWG	Electron donating group
FAD	Flavin adenine dinucleotide
FAK	Focal adhesion kinase

FBS	Foetal bovine serum
FDA	Federal drug agency
FGI	Functional group interconversion
FLT3	FMS-like tyrosine kinase 3
<i>g</i>	Gravity (Note: Italics)
GABA	γ -Aminobutyric acid
GST	Glutathione S-transferase
GVHD	Graft-verses-host disease
HATU	<i>N</i> -[(Dimethylamino)-1H-1,2,3-triazolo-[4,5-b]pyridin-1-ylmethylene]- <i>N</i> -methylmethanaminium hexafluorophosphate <i>N</i> -oxide
HeLa	An ovarian cancer cell line
HRMS	High-resolution mass spectrometry
HWE	Horner-Wadsworth-Emmons
IC ₅₀	Half-maximal inhibitory concentration
IDO1	Indoleamine-2,3-dioxygenase 1
IDO2	Indoleamine-2,3-dioxygenase 2
IFN α , β and γ	Interferon α , β and γ
IL	Interleukines
IR	Infrared
JAK	Janus kinase
K_{cat}	Enzyme turnover number
K_d	Dissociation constant
KHMDS	Potassium bis(trimethylsilyl)amide
K_i	Inhibitory constant
K_m	Michaelis constant
Kyn	Kynurenine
LC-MS	Liquid chromatography-mass spectrometry
LRMS	Low-resolution mass spectrometry
LSD1	Lysine-specific histone demethylase 1
Lys	Lysine
mAbs	mono-clonal antibodies
mCRPC	metastatic castration-resistant prostate cancer
MF	Myelofibrosis
MM	Molecular mechanics
MPN	Myeloproliferative neoplasms
M_w	Molecular weight
NADH	Nicotinamide adenine dinucleotide
NADPH	Nicotinamide adenine dinucleotide phosphate
NaHMDS	Sodium bis(trimethylsilyl)amide
NFK	<i>N</i> -Formylkynurenine
NK cells	Natural Killer cells

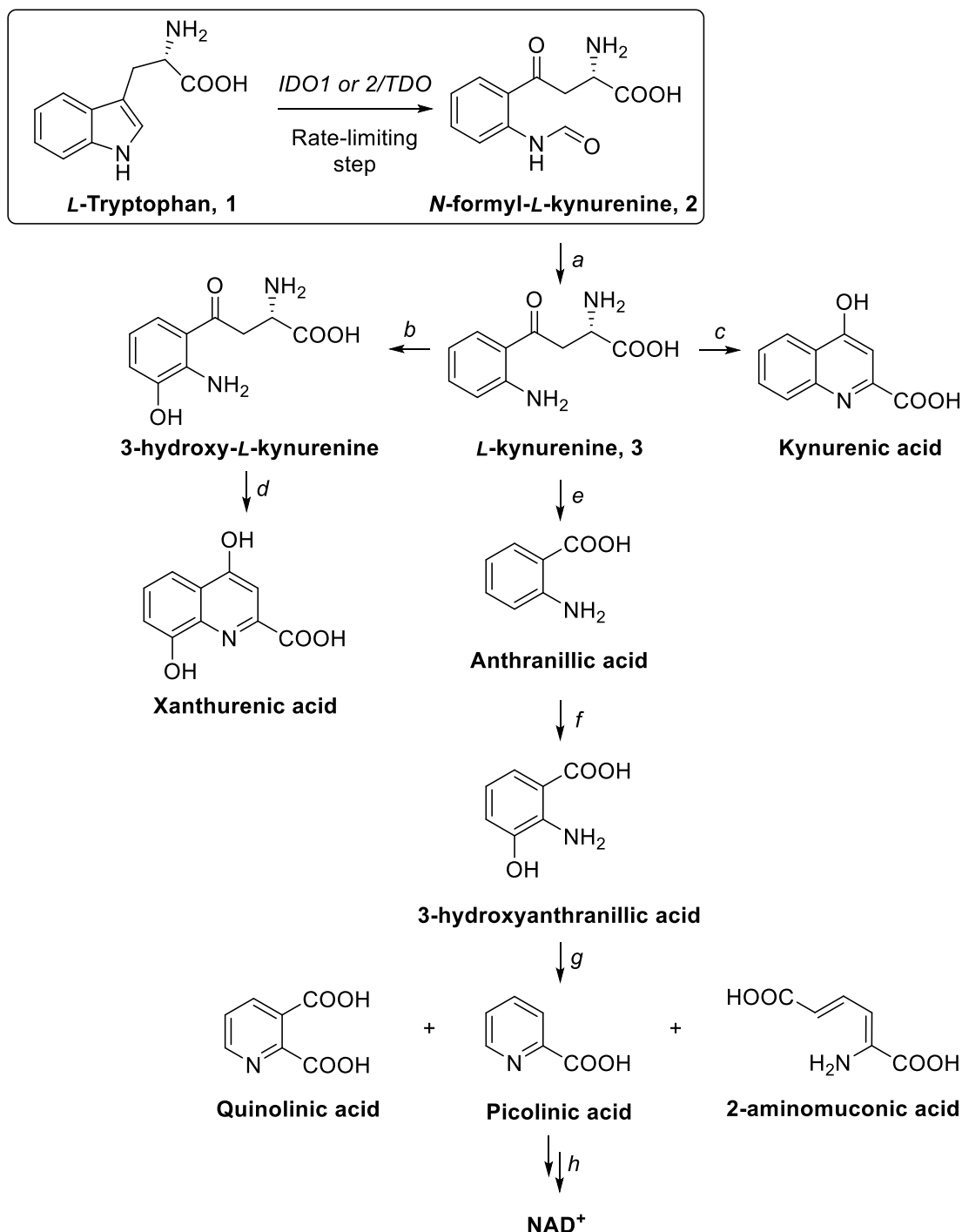
Ns/Nosyl-	4-nitrobenzenesulfonyl
ONIOM	Our own N-layered integrated molecular orbital and molecular mechanics
P/S	Penicillin – streptomycin
<i>p</i> ABA	<i>para</i> -aminobenzoic acid
PBS	Phosphate-buffered saline
PCV	Polycythemia Vera
Pd/C	Palladium on carbon
PD-L1	Programmed death-ligand 1
PNS	Peripheral nervous system
POI	Protein-of-interest
ppm	Parts per million
PROTAC	Proteolysis targeting chimera
PTC	Phase transfer catalyst
QM	Quantum mechanics
RET	Rearrange during transfection
rhIDO1	recombinant human Indoleamine-2,3-Dioxygenase
RNA	Ribonucleic acid
SAR	Structure activity relationship
SCX	Strong cation exchange (resin)
siRNA	small interfering ribonucleic Acid
SKOV	An ovarian cancer cell line
SNIPERs	Specific and non-genetic inhibitor of apoptosis-dependent protein erasers
STAT	Signal transducer and activator of transcription
SVR	Spleen volume reduction
SYPRO Orange	<i>E</i> -3-(4-(4-(dihexylamino)styryl)pyridin-1-ium-1-yl)propane-1-sulfonate
T3P	Propylphosphonic anhydride
TCA	Trichloroacetic acid
TDO	Tryptophan-2,3-dioxygenase
TLC	Thin layer chromatography
T_m	Thermal melting temperature
TNF α	Tumour necrosis factor α
Trp	<i>L</i> -Tryptophan
Ts/Tosyl-	<i>para</i> -Toluenesulfonyl
TSS	Total symptom score
TYK2	Tyrosine kinase 2
UV-vis	Ultra violet-visible
Val	Valine
VHL	von-Hippel Lindau
wtIDO1	wild-type Indoleamine-2,3-Dioxygenase 1
Xantphos	4,5-Bis(diphenylphosphino)-9,9-dimethylxanthene

Chapter 1:

Design, Synthesis and Evaluation of Mechanism-Based inhibitors of IDO1

1.1 – IDO1 and Tryptophan

Indoleamine-2,3-dioxygenase 1 (IDO1) is a key enzyme in the metabolism of tryptophan in the kynurenine pathway (Scheme 1), catalysing the initial dioxidation of *L*-tryptophan **1** to *N*-formyl-*L*-kynurenine **2** (NFK).



Scheme 1 – The kynurenine pathway

a. Formidase; *b.* 3-H Kyn monooxygenase; *c.* Kynurenine aminotransferase (KAT); *d.* KAT; *e.* Kynureninase; *f.* Kynureninase; *g.* 3-Hydroxyanthranillic acid oxygenase (3-HAO), *h.* Quinolinate phosphoribosyl transferase

Until 1967, tryptophan-2,3-dioxygenase (TDO) was the only known dioxygenase enzyme. Studies by Yamamoto confirmed the existence of another tryptophan degrading enzyme that metabolised both *D*- and *L*-tryptophan – the enzyme was tentatively designated *D*-tryptophan pyrrolase and then later Indoleamine-2,3-dioxygenase.¹⁻³ A final tryptophan dioxygenating enzyme was reported independently by three research groups in 2007 and designated Indoleamine-2,3-dioxygenase 2, IDO2 – prompting the re-naming of Indoleamine-2,3-dioxygenase to Indoleamine-2,3-dioxygenase 1, IDO1.⁴⁻⁶

TDO, IDO1 and IDO2 are heme-based enzymes and affect substrate dioxygenation through Lewis acid activation of molecular oxygen.^{7,8} To enable turnover, a ternary complex between the enzyme, molecular oxygen and the substrate must form (Figure 1).⁹ While the substrate scope of TDO and IDO2 is limited to *L*-tryptophan, IDO1 has been demonstrated to metabolise a range of substituted indoles, such as: 5-fluoro, 5-methyl and 5-hydroxytryptophan and 5-hydroxytryptamine.⁹ Crystallographic data shows IDO1's active site as a large, hydrophobic pocket when compared to TDO's and IDO's smaller, more hydrophilic active sites.^{10,11}

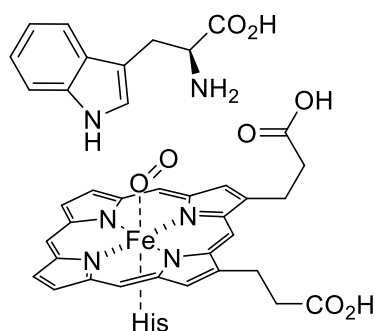


Figure 1 – Required ternary complex within the TDO, IDO1 and IDO2 active sites

The kynurenine pathway is responsible for more than 95% of tryptophan metabolism with its metabolites being the subject of much scrutiny in recent years – largely due to their immunomodulatory effects.^{12,13} IDO1 can be found in many major tissues but its over-expression is a common phenotype in a number of cancers.^{5,14,15} Cellular expression of IDO1 can be induced by various interferons (IFN α , β and γ) and tumour necrosis factor (TNF α).⁵

1.1.1 – The Paradox of IDO1

Under regular cellular function, IDO1 serves as a part of the innate immune response to intracellular viral and bacterial infection.^{16,17} Upregulation of IDO1 leads to depletion of local tryptophan concentrations – an essential amino acid required for the proliferation of the attacking body – and produces anti-pathogenic metabolites preventing the spread of the invading body.¹⁸ The enzyme also plays a significant role in preventing foetal rejection through its ability to modulate T-cell activity.¹⁹ This dual role of IDO1 creates a paradoxical situation where the enzyme can form part of an immune-response whilst simultaneously having the

ability to suppress it – which effect dominates is typically dependent on IDO1 expression levels.²⁰

IDO1 suppresses an immune-response *via* two key mechanisms. The first acts through local tryptophan depletion with many immune cells having tryptophan-sensitive checkpoints within their cell cycle. T-lymphocytes (T-cells) and natural killer cells (NK), key immune response cells, are sensitive to tryptophan starvation leading to a slowing in their proliferation or even cell death.^{21, 22} The second mechanism is a result of the immunosuppressive effects of the downstream metabolites produced in the kynurenine pathway. The metabolites *L*-kynurenine **3**, 3-hydroxykynurenine and 3-hydroxyanthranilic acid have all been implicated in aiding immunoescape of cancers by increasing rates of T-helper and NK cell apoptosis.²³

Over-expression of IDO1 is a common phenotype in numerous cancers, this therefore affords the tumour an ability to avoid immune detection and proliferate.^{15, 24, 25} Attention has therefore been placed on IDO1 to both understand its mode of action and to inhibit its function to deliver new therapeutics.²⁶⁻³¹

1.1.2 – Early IDO1 Inhibitors

By inhibiting IDO1, the therapeutic effect is two-fold: prevention of dropping local tryptophan levels around malignant tumours and halting the production of harmful metabolites. A seminal report from Van den Eynde in 2003 demonstrated that inhibition of IDO1 lead to partial reversal of the immunosuppression afforded by IDO1 and significantly slowed tumour growth in mice.¹⁵

Prior to Van den Eynde's report, only a few examples of IDO inhibitors can be found within the literature. One of the earliest reports of an IDO inhibitor is that of Watanabe's phenylalanine derivative **3**, 2,5-dihydro-*L*-phenylalanine, with an associated K_i of 230 μ M (Figure 2).³² Watanabe later reported a small library of IDO ligands based on β -carboline and indole scaffolds, however none of the compounds screened managed to inhibit IDO with IC_{50} values below micro-molar concentrations.³³

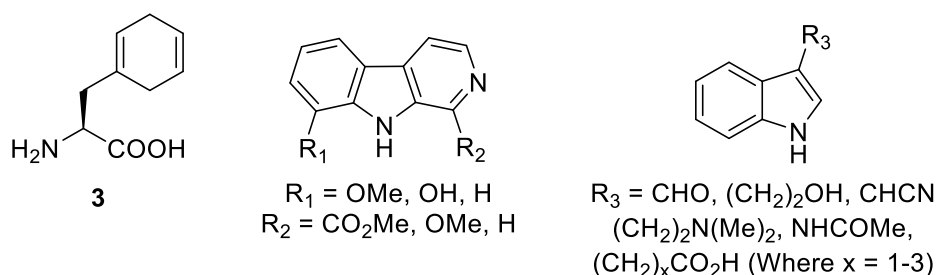


Figure 2 – Watanabe's IDO inhibitors

Another significant discovery in the field of IDO inhibition came from simple tryptophan derivative **4**, *N*-methyl-*L*-tryptophan (1-MT), which achieved K_i values between 19–53 μM (Figure 3).³⁴ Sono had rationally designed **4** based on the then currently available mechanistic understanding of IDO; the inhibitory activity of **4** was rationalised through there being no abstractable proton from the indole nitrogen.

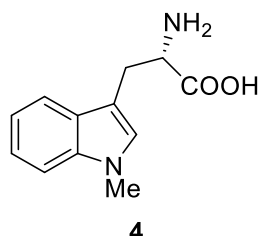


Figure 3 – Sono's IDO inhibitor, 1-MT

Many of the early inhibitors show inhibition at concentrations too high to be readily achieved systematically and, without the understanding of IDO's role in immune escape, no inhibitors entered clinical evaluation. Van der Eynde's 2003 report however ignited a renewed interest and improved inhibitors were soon reported.^{15 35, 36}

1.1.3 – Current IDO Inhibition

Since 2003, many IDO1 inhibitors have been reported from small 4-phenylimidazole derivatives with K_i values $<5 \mu\text{M}$ to large natural products such as halicloic acid possessing a K_i of 10 μM .^{37, 38} A recent, comprehensive review conducted by Röhrig discusses the many IDO1 inhibitors that have been investigated and considers the challenges presented in the field of IDO1 inhibition.³⁹

Considerable effort from the pharmaceutical industry has also been expended and has been the principal driving force in the search for suitable IDO1 inhibitors. During 2014 and 2015 Bristol-Myers Squibb acquired a series of patents that contained inhibitors with sub-nanomolar IC_{50} values.⁴⁰⁻⁴² No subsequent literature has been made available for these compounds. A later patent was then filed in 2016 by BMS which claimed further IDO inhibitors with IC_{50} values below 5 nM and their pipeline states a current phase I IDO1 inhibitor (Figure 4).^{43, 44}

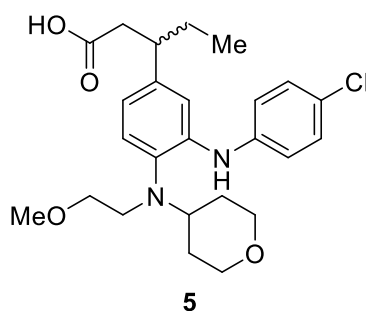


Figure 4 – BMS compound exhibiting $<5 \text{ nM}$ IDO1 inhibition (Example 1257)⁴³

Other commercial advances in IDO inhibition have come from Incyte with the highly effective competitive inhibitor **6**, epacadostat (INCB) (Figure 5).⁴⁵ After an initial setback in early 2016, Incyte have continued the clinical evaluation of epacadostat in combination with Merck's PD-1 checkpoint inhibitor – humanised antibody Keytruda – claiming positive preliminary results in late 2016 (albeit with no data from the comparator arm released).⁴⁶

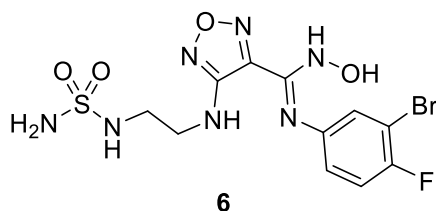


Figure 5 – Epacadostat

In April 2018, Incyte and Merck halted the phase III clinical trials of the epacadostat/Keytruda combination therapy after failing to meet its first endpoint of improving progression-free survival of patients compared with Keytruda alone.⁴⁷ BMS then followed suit in May 2018, halting two of its IDO inhibitor trials leaving fewer active clinical trials for IDO inhibitors.⁴⁸ Currently available data does not indicate if the lack of efficacy is due to poor inhibitor pharmacokinetics or whether the systematic application of IDO1 inhibitors achieves tangible therapeutic benefit for patients.

1.1.4 – Modes of IDO1 Inhibition

Inhibition of enzymes can be achieved through various means, such as: competitive, non-competitive/allosteric and uncompetitive.⁴⁹ Enzymes may also be inhibited by direct chemical reaction with an inhibitor – known as mechanistic or suicide inhibition. An enzyme is particularly susceptible to this type of attack if it contains a redox sensitive region, such as the heme-centre of dioxygenase enzymes.³⁹

The aforementioned inhibitors block IDO1's function through means of competitive inhibition. This however is a mode of inhibition that can be overturned due to it being an equilibrium-driven process. By increasing the concentration of the enzyme's natural substrate, the inhibitor will eventually be out-competed. This ceases to be the case if a branch point for the substrate exists – in this situation, the substrate concentration is reduced *via* an alternative biochemical pathway or substrate transportation mechanism.

IDO1 catalyses the initial step of the kynurenine pathway and is the rate-limiting enzyme for the pathway. As such, there is little opportunity for tryptophan to be metabolised by other means, suggesting that competitive inhibition is not the most suitable mode to inhibit IDO1 for therapeutic benefit.

1.1.5 – Mechanistic Inhibition of IDO1

A study conducted by Malachowski investigated a previously unexplored mode of inhibition in the context of IDO1 – mechanistic inhibition.³⁰ By taking into consideration a proposed alkylperoxy intermediate of tryptophan metabolism, a novel structural class of IDO inhibitors was developed.^{27, 28, 30, 50}

Malachowski's inhibitors were based on Ar-C-X-Y systems where Ar is an aryl substituent, C is a carbon linker and X/Y are heteroatoms. As proof of concept, various commercial systems which closely resemble their design requirements were tested and proven effective – most notably benzylhydrazine giving a K_i of 0.25 μM . The main study focused on the structures of O-alkylhydroxylamines with their lead compound being identified as O-benzylhydroxylamine **7** (oBHA) after achieving an IC_{50} value of 0.81 μM (Figure 6).³⁰

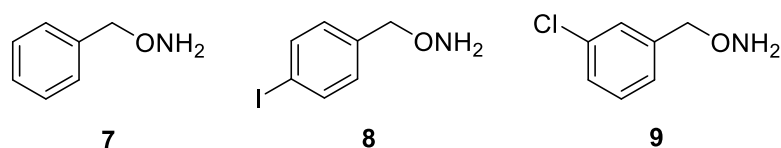


Figure 6 – Malachowski's lead IDO1 inhibitor **7** and two optimised IDO1 inhibitors **8** and **9**

Lead optimisation saw the synthesis and evaluation of 25 derivatives of oBHA, highlighting 4-I-oBHA **8** and 3-Cl-oBHA **9** as promising inhibitors with IC_{50} values of 0.22 and 0.30 μM respectively (Figure 6).³⁰

Malachowski's inhibitors are however likely to exhibit chemical promiscuity and poor pharmacokinetics when tested *in vivo* by virtue of their small size and reactive functionalities. To test this, the inhibitors were tested against other enzyme targets, namely catalase and CYP3A4. Both optimised inhibitors proved less active on these enzymes by a minimum of 20-fold – yet this still provides a narrow therapeutic window.

Despite of the potential limitations of Malachowski's inhibitors, a mechanism-based inhibitor of IDO1 has the potential to yield very positive results and provide therapeutic benefit for patients. No mechanistic inhibitors of IDO have since been reported.

1.1.6 – Development of the Mechanistic Detail of the Heme-Dioxygenases

The mechanism by which the dioxygenase enzymes metabolise *L*-tryptophan to *N*-formyl-*L*-kynurenine is still the subject of much debate.^{28, 30, 50, 51} Isotope effect studies, spectroscopic studies, crystallography and QM/MM calculations have all contributed to the wealth of literature surrounding IDO's mode of action.^{27, 52-56}

Early Work on the Metabolism of Tryptophan

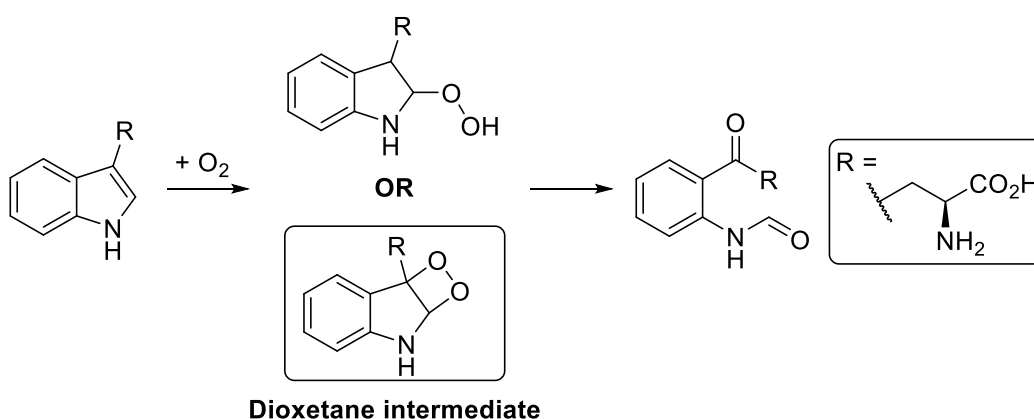
Metabolism of *L*-tryptophan to *L*-kynurenine garnered much attention in the first half of the 20th century due to being one of a few discovered examples of enzymatic aromatic ring oxidation. The earliest description of the enzyme responsible for the dioxygenation of tryptophan was as a tryptophan-pyrrolase.⁵⁷

Early studies of the enzyme concluded the oxidation of tryptophan was carried out by peroxide due to catalases inhibitory effect on the overall reaction.^{58, 59} Experimental evidence later provided by Hayaishi demonstrated that molecular oxygen served as the oxidant in the conversion of tryptophan to *N*-formyl-*L*-kynurenine.^{57, 58, 60}

Hayaishi's experiments indicated that oxidation of tryptophan in an ¹⁸O₂ enriched atmosphere would see incorporation of both ¹⁸O₂ atoms into the downstream products. The same oxidation in a ¹⁶O₂ atmosphere, but in a H₂¹⁸O media, saw almost no incorporation of ¹⁸O atoms into products.⁶⁰

To account for catalases' observed inhibition of the pathway, a two-step reaction was proposed for the overall oxidation: this involved the reduction of molecular oxygen to peroxide and then the use of the peroxide in the oxidation of tryptophan.

Included in this seminal piece of work was the first proposal of two potential intermediates in the oxidation process: a 2-hydroperoxy intermediate and a dioxetane-containing structure (Scheme 2).

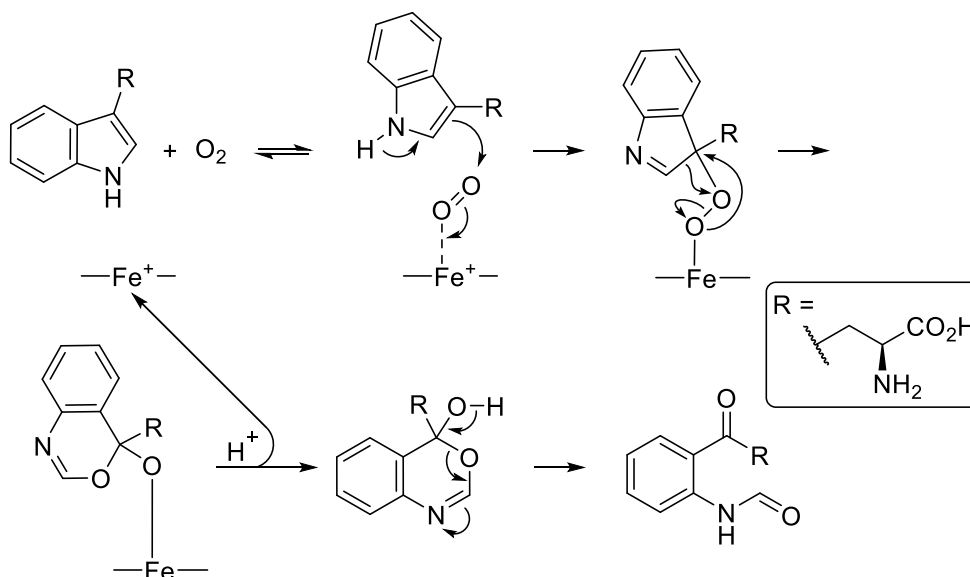


Scheme 2 – Hayaishi's proposed tryptophan oxidation intermediates

In the late 1960s Hamilton proposed an alternative oxidation intermediate.⁶¹ Hamilton argued the dioxetane intermediates loss of aromaticity and formation of a highly strained ring system is energetically unlikely and a more likely mechanism is a Criegee-type rearrangement. Hamilton's proposed mechanism involves abstraction of the indole proton promoting the nucleophilic attack of a ferrous-bound molecular oxygen species forming a ferrous-peroxy

intermediate. Following a Criegee-type rearrangement to a 6-membered species, the intermediate is released from the heme-centre through protonation and undergoes a rapid degradation to afford *N*-formyl-*L*-kynurenine (Scheme 3).⁶¹

Four additional mechanisms for the metabolic oxidation of tryptophan to *N*-formyl-*L*-kynurenine have since been reported. The proposed metabolic oxidations include an electrophilic addition, radical addition and two base-mediated mechanisms.



Scheme 3 – Hamilton's proposed oxidation of tryptophan via a Criegee-type rearrangement

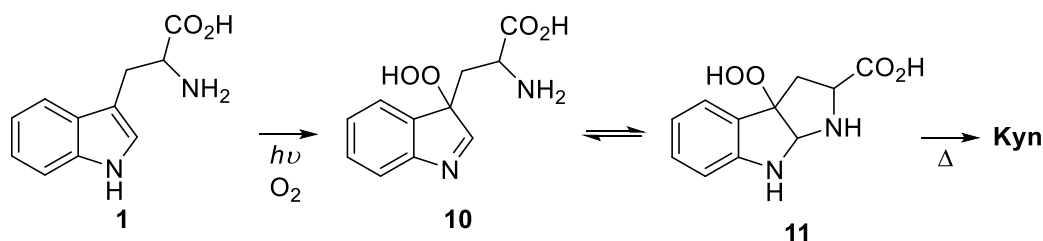
Base-Mediated Metabolism of Tryptophan

As early as the work of Hamilton in 1969, base-mediated mechanisms that abstract the indole NH have been proposed.⁶¹ However, this was based on Hamilton's observation that all of the known dioxygenase-catalysed reactions, at that time, involved substrates which possessed a removable proton.

Support for this hypothesis later came with the discovery of IDO1 inhibitor **4** whose inhibitory properties were attributed to the lack of a removable proton.³⁴ A preceding *in vitro* study on the dioxygenation of indole derivatives by various metalloporphyrins had also highlighted that *N*-methyl skatole was resistant to oxidation.⁶²

Proton abstraction of the indole NH was invoked in Nakagawa's 1977 study of dye-sensitised photooxygenation of tryptophan. Proton abstraction of tryptophan **1** rationalised the observed cyclisation of the α -amine to resultant imine **10** yielding a pyrroloindole intermediate **10** which upon heating degraded to Kyn **3** (Scheme 4).⁶³ Nakagawa later concludes that intermediate **11** was unlikely to be compatible with enzymatic metabolism due to complications arising from

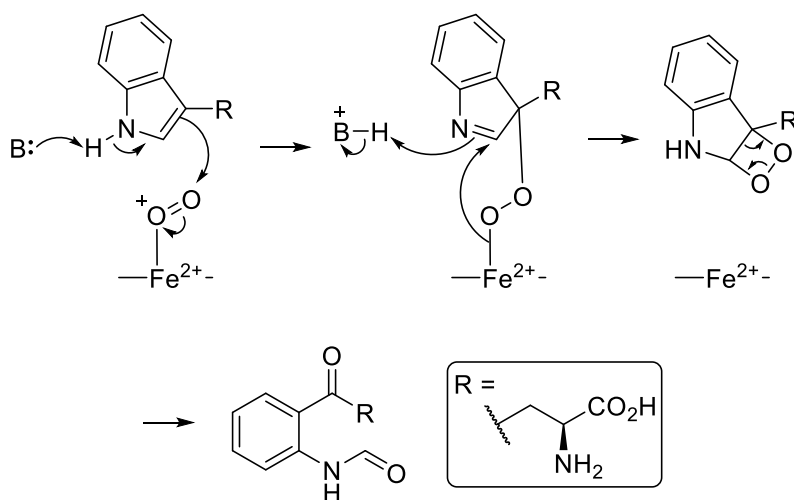
highly strained transition states. However, no comment was made with regards to the feasibility of basic extraction of the indole proton.



Scheme 4 – Nakagawa's dye-sensitized photo-oxygenation of tryptophan

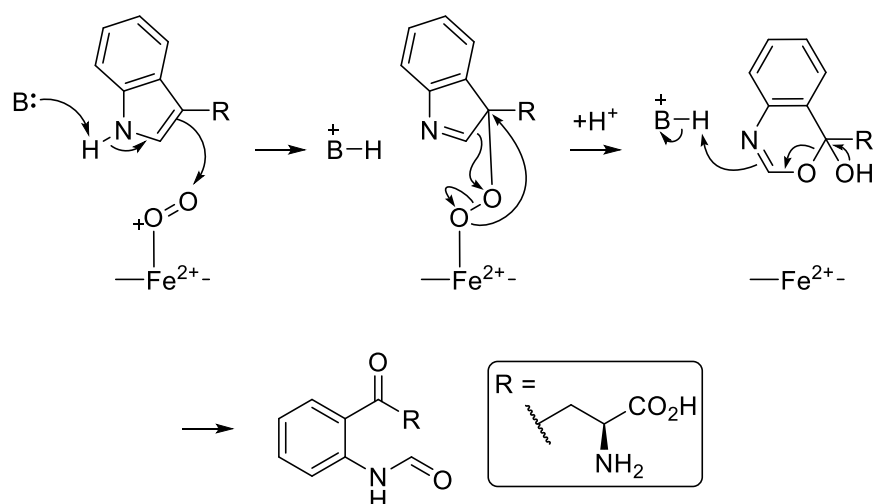
Active Site Base-Mediated Tryptophan Oxidation

Sono was the first to suggest the idea that a basic residue within the active site could be responsible for the deprotonation of the indole amine.⁵¹ The dioxetane-containing mechanism can therefore be represented as shown in Scheme 5. The basic active site residue deprotonates the indole amine and promotes the nucleophilic attack of the activated, heme-bound molecular oxygen. The heme-bound oxygen atom attacks the resultant imine of the indole ring and promotes the re-protonation of the indole nitrogen. The resultant dioxetane intermediate then undergoes a facile retro [2+2] cycloaddition to afford *N*-formyl-*L*-kynurenine



Scheme 5 – Active Site Base Mediated Oxidation of Tryptophan via a Dioxetane Intermediate

By invoking deprotonation *via* an active-site base, the Criegee-type rearrangement can also be represented as shown in Scheme 6.



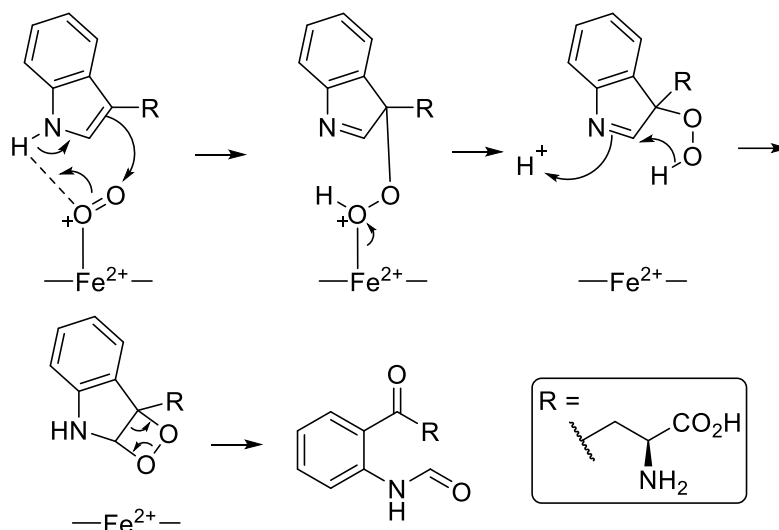
Scheme 6 – Active site base mediated oxidation of tryptophan via a Criegee-type rearrangement

Extraction of a proton by a basic residue within the active site is a reasonable suggestion based on other heme-containing protein structures, such as globins and peroxidases. These heme-proteins contain histidine residues close to the heme centre to aid substrate binding through hydrogen-bond stabilisation – a residue which could also act as a base.⁹

Molecular Oxygen as a Base in Tryptophan Oxidation

An alternative base-mediated mechanism, proposed by Stocker, sees molecular oxygen acting as a base and abstracting the indole NH proton (Scheme 7).⁶⁴ Following Raman spectroscopic studies of the heme environment of IDO1, Stocker suggests an oxidation that proceeds *via* the dioxetane intermediate. The indole NH interacts *via* a hydrogen-bond with the heme-bound molecular oxygen and then undergoes a hetero-ene-like reaction. Here the molecular oxygen acts as a base to give a heme-bound hydroperoxide species that readily dissociates from the heme-centre. Attack of the resulting imine by the C-(3) bound hydroperoxy species, re-protonation of the indole nitrogen and loss of the peroxy proton affords the dioxetane intermediate. A facile retro [2+2] cycloaddition follows to give *N*-formyl-*L*-kynurenine.

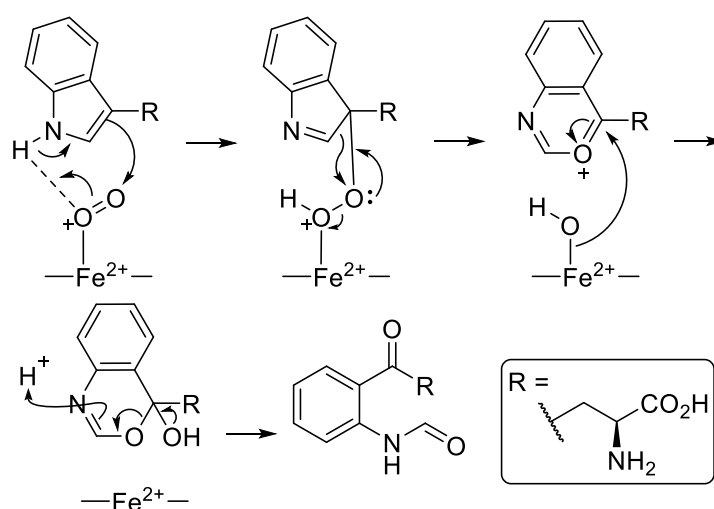
Stocker did not consider the Criegee-type rearrangement due to Witkop's prior assertion that 11-hydroperoxytetrahydrocarbazolenine, an analogous framework, rearranges to 1-aza-8,9-benzcyclonona-2,7-dione *via* a *quasi*-4-membered cyclic species. Here, Witkop argued that imines are more likely to act as electrophiles than electron-donating species.⁶⁵



Scheme 7 – Stocker's proposed O_2 base-mediated oxidation of tryptophan proceeding via a dioxetane intermediate

Experimental evidence for the existence of the highly strained dioxetane intermediates remains unreported and the employment of such a functionality is limited to use in justifying observed mechanistic outcomes.⁶⁶⁻⁶⁸ Additionally no chemiluminescence, a feature strongly associated with the decomposition of dioxetanes, has been observed during tryptophan oxidation experiments.⁶⁹

Chapman later disclosed the first proposition of a molecular oxygen base-mediated Criegee-type mechanism (Scheme 8).²⁷ Chapman's mechanism begins with a hetero-ene-like reaction and is followed by Criegee-type rearrangement. A hydroxyl group remains bound to the heme-centre and serves as an oxidant which attacks the activated carbonyl to give a hemiacetal. Degradation of the hemiacetal then affords *N*-formyl-*L*-kynurenine.



Scheme 8 – Chapman's proposed O_2 base-mediated oxidation of tryptophan proceeding via a Criegee-type rearrangement

Chapman also reports that the formation of a hydrogen-bond between the indole amine and the heme-bound molecular oxygen is key to activating molecular oxygen towards the otherwise spin-forbidden electrophilic attack.²⁷

Investigations into the Base-Mediated Mechanism Proposal

Both the active site and molecular oxygen base mechanisms rely on attack through the 3-position of indole – the expected site of attack when considering the reactivity of indoles.⁷⁰ Electronic perturbation of molecular oxygen by the heme-centre could also potentially allow it to be attacked in the proposed mechanisms.

However, there is no evidence to prove these models are correct. The idea of proton abstraction came from an empirical observation that dioxygenases only act on species with a removable proton.⁶⁰ This was later aligned with the fact that many other heme-based proteins contain a histidine residue within the substrate binding site.

Crystal structures of TDO have shown a basic histidine residue in a position where proton extraction could be feasible.⁷¹ However, site-directed mutagenesis studies have seen this residue replaced with a non-basic group and tryptophan turnover has remained, suggesting the histidine residue is not directly relevant in the mechanism.⁹ Furthermore, crystal structures of IDO1 have shown a non-basic serine residue in the place of the histidine adding to the evidence against an active site base-mediated mechanism.^{9, 10}

An alternative function of the histidine residue in TDO has since been proposed. In the interrogation of the kinetic data for wtTDO, a heightened *L*-Trp K_d for the enzymatically active ferric (Fe^{2+} , 4.1 μM) form over the non-active ferrous (Fe^{3+} , 3.8 mM) was observed.⁷² Mutants which did not possess an active site histidine residue did not demonstrate such a large difference between the ferric and ferrous K_d values. Further electrochemical observations suggest the binding of *L*-Trp to the ferric form is accompanied by the formation of a hydrogen bond which was attributed to the interaction of the substrate indole NH and the histidine residue. The authors therefore hypothesise that histidine's role is a gating residue rather than a base – promoting the binding of substrate to the enzymatically active ferric form over the inactive ferrous form. The authors conclude that the discrimination between the two oxidation states could be achieved through control of water in the active site which, in turn, impacts the overall shape of the active site. To date, no further studies confirming this have been reported.

Deprotonation of the indole amine also appears unlikely due to its weakly acidic nature ($pK_a(\text{H}_2\text{O}) = 16.82$) and the lack of a sufficiently strong base within the active site of IDO1.⁷³ Analysis of the indole deprotonation step was also calculated to be energetically unfeasible.⁵²

The final piece of data supporting the notion of a base-mediated mechanism was Sono's discovery of IDO1 inhibitor 1-MT, **4**.³⁴ Its inhibitory properties were hypothesised to be a result of the lack of a removable proton on the indole nitrogen. This remained the case until two independent studies by Raven and Changyuan proved otherwise.^{54, 74} Both studies showed that, in the absence of tryptophan, **4** acts as a substrate for human IDO1 and IDO1/TDO variants where the active site histidine residue had been removed.^{54, 74} Turnover of **4** was approximately 50-times slower than tryptophan turnover showing **4** to be a poor substrate rather than inhibitor. Turnover of **4** therefore suggested that proton abstraction from the indole NH is not necessary for substrate turnover.

Problems with the Criegee-type and Dioxetane Mechanisms

Of the two mechanisms, the early literature favours the Criegee-type rearrangement over the dioxetane mechanism on thermodynamic grounds.⁶¹ Nakagawa's later *in vitro* studies on the transformation of *L*-tryptophan to *N*-formyl-*L*-kynurenine also viewed the dioxetane intermediate as an extreme of a transition state.⁷⁵

Chung conducted various density functional theory (DFT) calculations on the proposed molecular oxygen base-mediated oxidation of tryptophan.⁵³ Chung investigated both the Criegee-type rearrangement and the dioxetane mechanism and found that the hetero-ene-like step requires a high activation energy due to a highly distorted transition state. Chung also stated that for the Criegee-type mechanism, a large energy barrier exists between the indoline species and the downstream products and would in fact undergo a charge and radical recombination to afford the more stable dioxetane intermediate.

Chung later offers two alternative mechanistic pathways: a direct electrophilic addition or a radical addition to the C(2)- or C(3)-position of indole (*vide infra*).⁵³

A follow-up study employed ONIOM calculations (a combination of QM and MM calculations) and concluded that the Criegee-type and dioxetane mechanisms were not feasible intermediates. The study then suggested the possibility of a radical-based mechanism being more energetically feasible.⁷⁶

Redox Character of the Heme-Centre in the Base-Mediated Pathways

An overlooked feature of the base-mediated Criegee and dioxetane pathways is the lack of redox character invoked at the heme-centre. This is particularly unusual as many heme-based proteins display a rich redox profile in their modes of action. Amongst the most studied examples of this can be found within the activity of the monooxygenase cytochrome P450;

Sono's 1996 review of heme-containing oxygenases describes the varying states of cytochrome P450's oxidation in relation to its function.⁵¹

Cytochromes have long been known to utilise NADH and NADPH to allow for their reductive activation.⁷⁷ Reductive re-activation forms a key step in the cytochrome catalytic cycle as it serves to reduce the inactive ferric Fe^{3+} to the active ferrous Fe^{2+} , allowing the binding of molecular oxygen.⁷⁷ No such associated reductase proteins or co-factors have been identified as part of IDO1's catalytic function, suggesting that either the oxidation state of the iron remains the same throughout its cycle, or that the catalytic cycle begins and ends in the same oxidation state.

Electrophilic Attack and Radical Mechanisms

In recent years, electrophilic attack and radical-based mechanisms have been proposed in response to emerging data on IDO1's structure and binding modes. In these proposals, the heme-centre was also no longer considered to be inert, but instead cycling through a number of oxidation states.⁵³

New Evidence and Initial Proposals

Whilst Chung was the first to propose the direct electrophilic addition route, Raven provided the first mechanistic proposal.⁵⁴ In this study, Raven invoked the proceeding dioxetane and Criegee pathways in the proposal.

Computational studies conducted by Lewis-Bellaster later provided an alternative intermediate in the pathway: an epoxide-containing structure.⁷⁸ Lewis-Bellaster's report also identifies the presence of a ferryl ($\text{Fe}^{4+}=\text{O}$) intermediate *via* Raman spectroscopy. Identification of the ferryl heme oxidation state strongly suggests the iron does vary in oxidation state throughout the catalytic cycle. The ferryl intermediate was later validated in the work of Shiro who independently identified the ferryl intermediate *via* Raman spectroscopy.⁷⁹

Detection of the ferryl intermediate brings the reactivity of the dioxygenases closer to the more familiar monooxygenases which do alter in oxidation state and proceed *via* ferryl intermediates.⁵¹ However, one key difference remains: monooxygenases require reductive activation to remain active while the dioxygenases do not. The data therefore pointed toward the activation of the ferric iron by molecular oxygen.^{80, 81}

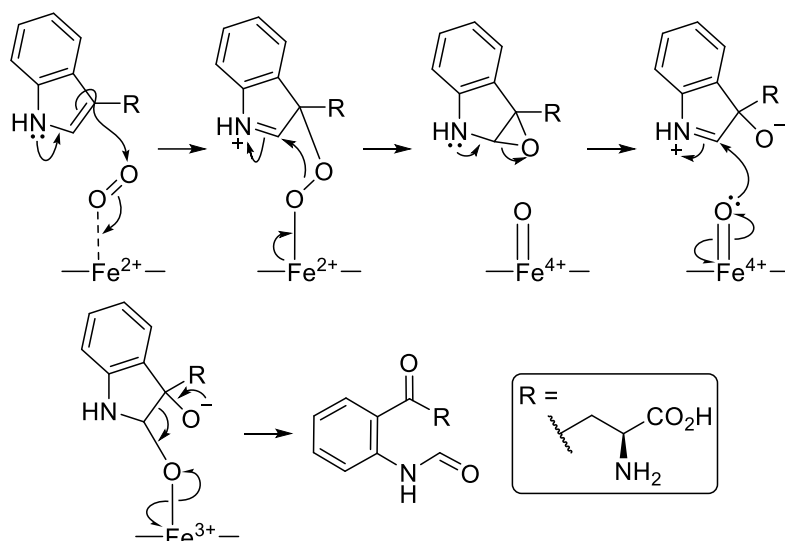
Alongside the spectroscopic identification of a ferryl intermediate, detection of a potential epoxide intermediate *via* mass spectrometry substantiated Lewis-Bellaster's hypothesis.⁵⁰ Coincidentally, epoxide formation is commonplace in cytochromes.^{50, 51, 82}

Direct Electrophilic Attack

Raven was the first to provide an insight to a possible direct electrophilic attack mechanism (Scheme 9).⁵⁴ Lone-pair donation from the indole nitrogen sees the attack of the heme-coordinated oxygen through C(3).⁷⁰ Iron-promoted degradation of the peroxy-intermediate gives rise to both an epoxide intermediate and the ferryl heme centre. Epoxide ring opening is achieved by electron-donation from the indole NH and followed by an attack of the resulting iminium by the ferryl heme-centre. The cleavage of the C(2)–C(3) bond to afford *N*-formyl-*L*-kynurenine is achieved *via* electron-donation from the neighbouring alkoxide.

By providing a mechanism where proton extraction from the indole amine is not necessary for turnover, the observed metabolism of **4** can be rationalised.^{54, 74}

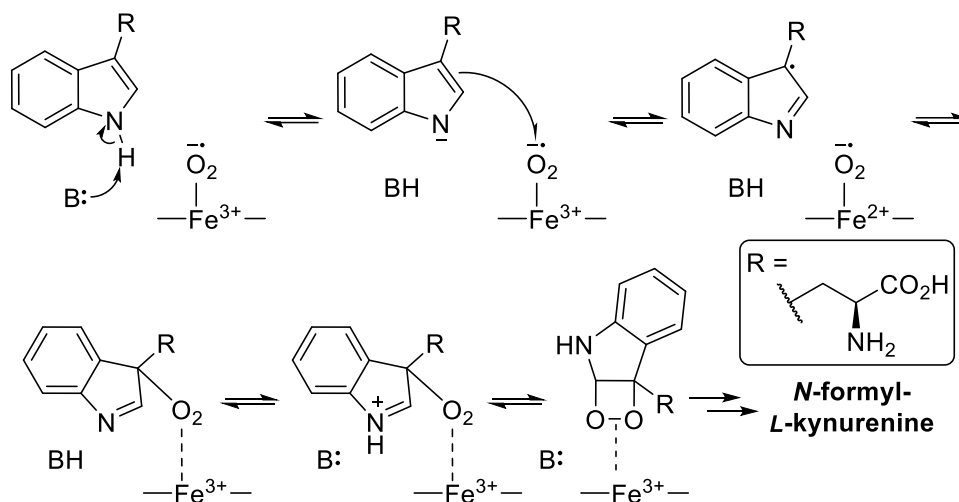
The direct electrophilic attack mechanism provides a reaction pathway that is consistent with the general reactivity of indoles.⁷⁰ Modulation of the iron oxidation state is also in line with the activity of other known heme-containing enzymes.⁵⁰



Scheme 9 – Raven's direct electrophilic attack mechanism⁵⁴

Radical Mechanism

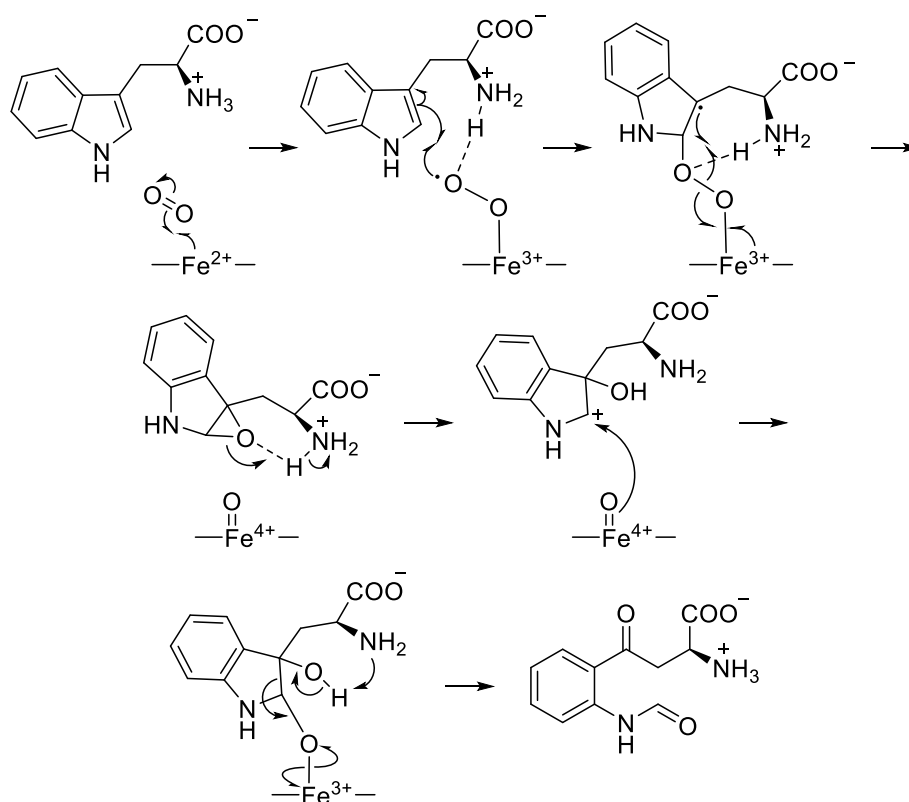
The first report of a radical mechanism was in 1993 when Wiseman calculated the energy of a 1-electron oxidation of tryptophan by a heme-bound oxygen to be significantly lower than the 2-electron mechanism of the dioxetane pathway.⁵² Limited mechanistic detail was given in Wiseman's report and an activating basic species was suggested (Scheme 10).



Scheme 10 – Wiseman's radical mechanism proposal⁵²

Wiseman concluded that the 2-electron pathway proceeded *via* an energetically unfavourable pathway and the 1-electron alternative proved energetically more feasible.⁵² Close inspection of the given mechanism in Wiseman's report provides minimal mechanistic detail and problematic reactivity.

The first complete radical mechanism was included in the same report from Lewis-Ballester which identified a ferryl intermediate by Raman spectroscopy (Scheme 11).⁷⁸

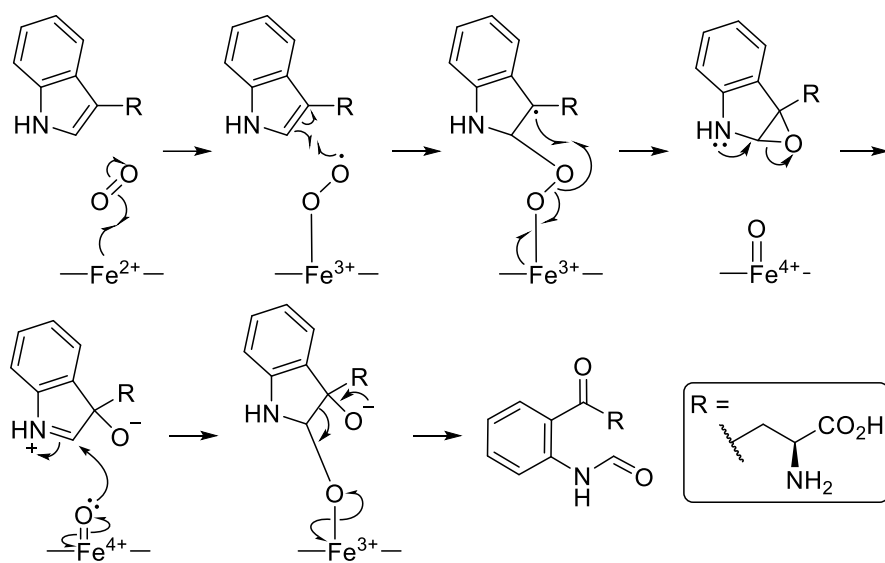


Scheme 11 – Lewis-Ballester's radical mechanism involving proton exchange with the α -amine

The α -amine aids the initial radical addition to the indole C(2) position *via* a hydrogen bonding interaction to form a stabilised benzylic radical. Homolytic cleavage of the peroxy-bond sees the formation of the hypothesised epoxide and the spectroscopically detected ferryl-heme species. Proton exchange from the α -amine activates the epoxide to ring open, leaving a resonance stabilised cation at the C(2) position. Attack of the C(2) position by the ferryl-oxo species is followed by a proton abstraction from the 3-hydroxyl group by the α -amine. The generated alkoxide then collapses cleaving the C(2)–C(3) bond liberating *N*-formyl-*L*-kynurenine.

A follow-up study conducted further QM and MM calculations and supported the notion of a superoxide species and a radical-based mechanism.⁵⁵ Detailed ONIOM calculations by Chung also supported Lewis-Ballester's radical mechanism.⁷⁶

Another mechanism that is commonly reported is the work of Raven. Raven's proposal does not include hydrogen bonding between the α -amine and the superoxy intermediate (Scheme 12).^{8, 50, 81, 83}



Scheme 12 – Raven's proposed radical mechanism

Summary: IDO1 and Tryptophan

Over the past 60 years, considerable effort has gone into understanding the mechanism by which the dioxygenase family of enzymes metabolise a variety of indole-containing substrates. Much of the early work was based on the known reactivity of monooxygenase enzymes and relied on either a dioxetane intermediate or Criegee-type rearrangement and the presence of an active site base. Subsequent crystallographic studies demonstrated that not all of the dioxygenase enzymes have suitable residues within the active site to fulfil this function. Also, the notion of an active site base was frequently disputed due to the relatively high pK_a of the

indole nitrogen. Turnover of **4** by IDO1 provided strong evidence against the active site base proposal; computational studies also disregarded the dioxetane and Criegee-type mechanisms as energetically unfavourable and pointed to either a radical or electrophilic-based mechanism of tryptophan dioxygenation. With the discovery of IDO1's immunomodulatory potential and its role in tumour immune escape, there has been an increased desire to understand how the enzyme functions and how it can be inhibited. To date, the mechanism of tryptophan dioxygenation remains unclear and no IDO1 inhibitors have been approved for clinical use.

1.2 – Radicals and Cyclopropanes

Radical chemistry has often been overlooked due to a perceived lack of predictability in radical reactivity. In recent years, radical chemistry has experienced a renaissance and with this interest has come a greater command by the synthetic chemist over radical reactivity. Numerous accounts of stereo- and regiocontrolled polycyclic ring formations, radical cascades, enantioselective radical reactions, diastereoselective radical reactions and radical carbonylations have been reported, often with excellent yields.⁸⁴⁻⁹⁰ Many reagents have also been developed to initiate radical-based reactivity.⁸⁹

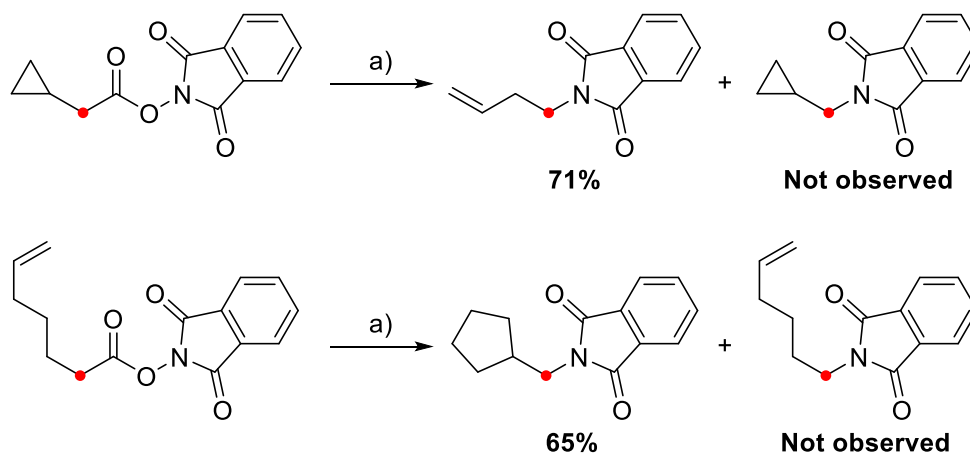
Radical methodology has also been utilised to overcome significant chemical challenges that ionic reactivity struggles to replicate, such as 5-endo-trig cyclisations.⁹¹ Other advantages of radical-based methodologies include fast reaction kinetics, broad functional group tolerance and the ability to initiate radical reactivity under mild conditions.⁹² Such is the utility of radical-based chemistry, notation has been developed to allow radical disconnections to be signified in retrosynthetic analysis.⁹³

Aside from elaborate structural synthesis, one persistent use of radicals in synthetic chemistry has been in the field of mechanistic study.^{94, 95} Few general methodologies exist to measure absolute rate constants for radical processes and those that do exist are too cumbersome for the level of detail often required by the experimentalist.⁹⁴ To ascertain the desired information, competing unimolecular radical reaction precursors, with known rate constants, are incorporated into frameworks to provide an alternative radical pathway. Known as radical clocks, analysis of the product distribution provides a qualitative rate of a radical process since product ratio is directly proportional to the ratio of the rates of the two processes.

1.2.1 – Radical Clocks and Rates of Reaction

Radical clocks provide a standard by which other reactions can be compared against. Numerous radical clocks exist and are designed to probe a variety of radical processes.⁹⁴⁻⁹⁷ In a typical investigation, a number of clocks will be employed with rates which span a region of rates defined by the experimentalist.

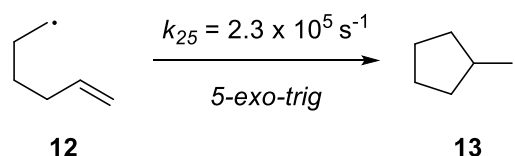
Fu recently utilised two common radical clocks in the investigation of a photoactivated copper-catalysed decarboxylative C-N coupling. The results concluded that the carbon and nitrogen radicals, formed as part of the reaction, recombined at slower rates than the employed clocks suggesting solvent cage-escape occurred prior to the formation of the C-N bond.⁹⁸



Scheme 13 – Fu's use of radical clock experiments

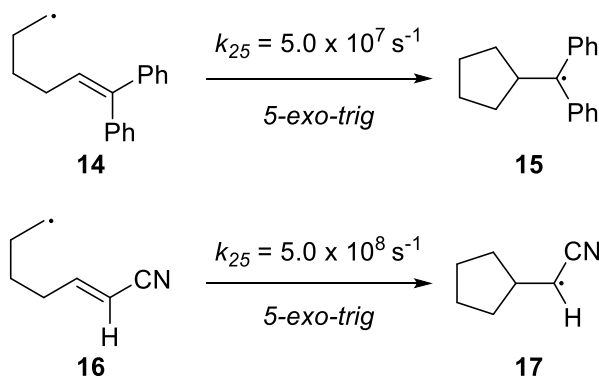
a) $h\nu$ (Blue LED), 10 mol% CuCN, 5 mol% dmp, 15 mol% Xantphos, $\text{ClCH}_2\text{CH}_2\text{Cl}$, 5-10 °C, 24h

Two of the most common clocks employed in rate-determining experiments are radical ring-closing and radical ring-opening reactions. Of the radical ring-closing processes, the best known is the 5-hexenyl radical **12** giving cyclopentylmethyl radical **13** (Scheme 14).^{95, 99, 100} Ring closure of the 5-hexenyl radical relies on the efficient orbital overlap achieved in the chair-like transition state for rapid ring closure. Such efficient overlap is not achieved in the transition state leading to the thermodynamically favoured cyclohexyl radical – hence the observed 98:2 (kinetic:thermodynamic) product ratio.⁹⁹



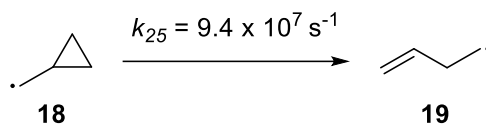
Scheme 14 – 5-exo-trig cyclisation of the cyclopentylmethyl radical

As a radical clock, the 5-hexenyl radical is useful in the low to middle kinetic scale regions. Derivatisation of the terminal alkene can afford the resulting radical increased stability and thus enhance the rate of ring closure (Scheme 15).^{95, 101}



Scheme 15 – Derivatisation of terminal alkene to afford higher ring-closure rates

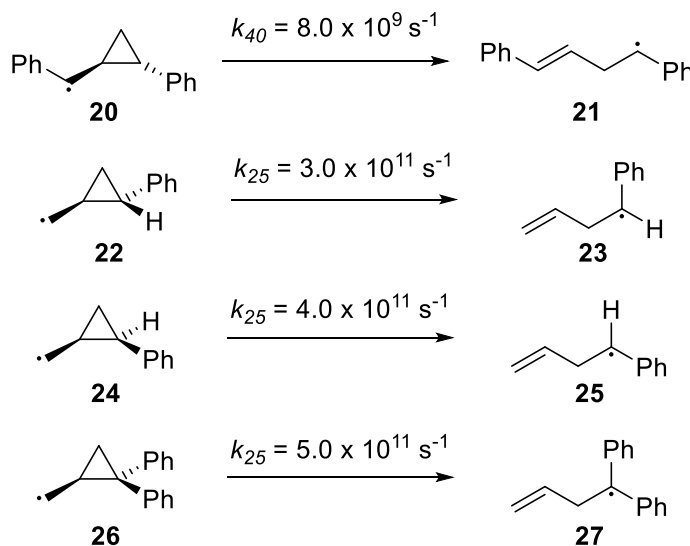
Ring-opening radical clocks however rely on the enthalpic and entropic gain of cleaving small, strained ring systems such as cyclopropanes or cyclobutanes. In this class of radical clock, the ring-opening of cyclopropylcarbinyl radicals are amongst the fastest ring-openings known (Scheme 16).^{94, 102}



Scheme 16 – Ring-opening of a cyclopropylcarbinyl radical

Enhancements in the rates of ring-opening can be achieved by decorating the cyclopropane ring with radical-stabilising moieties (Scheme 17).¹⁰² With ring-opening rates in the picosecond range, phenyl-substituted cyclopropylcarbinyl radicals are the most suitable radical clocks to determine whether a radical intermediate within a reaction is present.¹⁰²

In both cases, the rate of ring-closure or opening is enhanced when the stability of the resulting radical is increased. Addition of phenyl-substituents provides a ‘captor’, or electron-withdrawing, group which stabilises the radical in the transition state structure through delocalisation, lowering the activation energy.^{103, 104} Further enhancements in radical stability, and rate of radical processes, can be achieved by having a ‘dative’, or electron-donating, group adjacent to the radical centre allowing further delocalisation.¹⁰³ Combined, this effect is known as the captodative effect.¹⁰³



Scheme 17 – Substituted cyclopropylcarbinyl radicals and their ring-opening rates

1.2.2 – Captodative Radicals

Captodative radicals are stabilised by the synergistic effect of an electron-withdrawing group (EWG) and an electron-donating group (EDG). Radicals are afforded both kinetic and thermodynamic stability through the captodative effect.¹⁰³ EWGs serve to lower the energy of the singly-occupied orbital through a LUMO-SOMO interaction and thus render the radical

more electrophilic in character. Conversely, EDGs increase the energy of the singly-occupied orbital through a HOMO-SOMO interaction giving the radical more nucleophilic character (Figure 7).

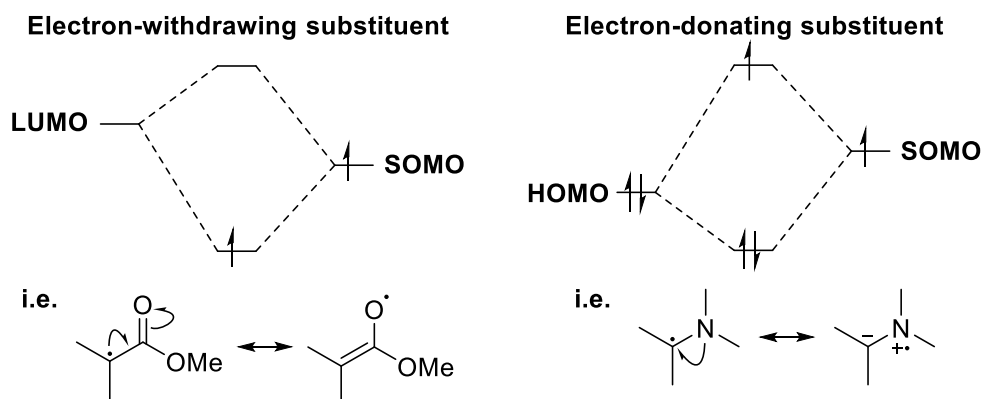
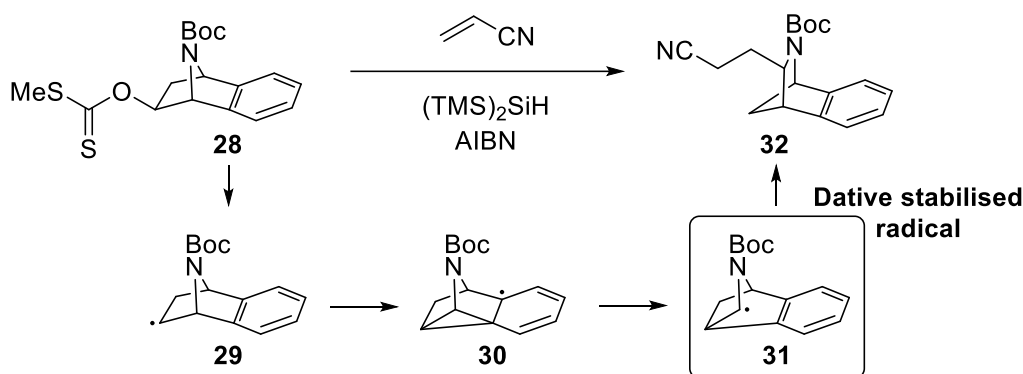


Figure 7 – EWG and EDG effect on radical character

An EWG can therefore offer increased stability to a nucleophilic radical, but a decreased stability toward electrophilic radicals; while EDGs can increase the stability of an electrophilic radical and offer little additional stability to nucleophilic radicals.¹⁰³ Pairing of EWGs and EDGs at a captodative centre offers a reduced stabilisation to the radical when compared to an EDG or EWG pair.¹⁰³

Manifestations of increased nucleophilicity of radicals with an α -EDG have been observed experimentally.^{92, 105} In the synthesis of azatricycle **32**, a radical rearrangement of a homoallylic system affords α -nitrogen radical **31** which is subsequently trapped by an electrophile.⁹² The rearrangement is driven by the release of the cyclopropyl ring strain and re-aromatisation. The gained nucleophilic character of this radical allows for controlled trapping with an electrophile (Scheme 18).



Scheme 18 – Hodgson's radical-deoxygenation rearrangement electrophilic trapping

1.2.3 – Radical Ring Opening-Based Therapeutic Agent

In order to capitalise on radical reactivity, molecular structures are often carefully designed to enable radical reactivity. In medicinal chemistry, compounds are not often designed to react

within a biological system; instead they are designed to bind selectively to target proteins and inhibit their action. However, this is not the case with the FDA approved LSD1 inhibitor tranylcypromine **33** – a mechanism-based inhibitor which acts through radical ring opening of its cyclopropane ring (Figure 8).¹⁰⁶

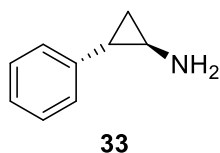
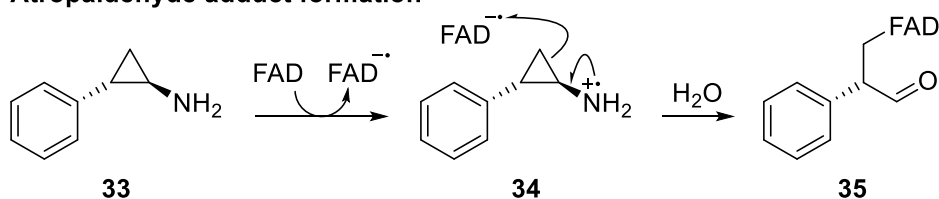


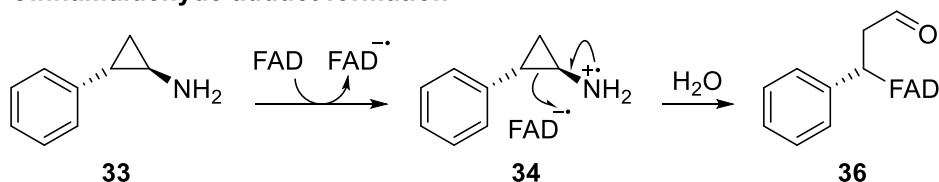
Figure 8 – Tranylcypromine

Tranylcypromine **33** inhibits LSD1 through the inhibition of its co-factor FAD. FAD oxidises amine **33** to the radical cation **34** which leads to ring opening of the α -cyclopropane ring. One of two adducts then forms: atropaldehyde adduct **35** or cinnamaldehyde adduct **36** (Scheme 19).¹⁰⁶ Deactivation of FAD prevents the re-oxidation of the LSD1 enzyme and thus inhibits its function. Tranylcypromine and its analogues have also been investigated as 5-hydroxytryptamine receptor agonists – whether they undergo a radical ring opening is unclear.¹⁰⁷

Atropaldehyde adduct formation



Cinnamaldehyde adduct formation



Scheme 19 – Proposed mechanism for tranylcypromine's inhibition of LSD1 via its interaction with FAD

Summary: Radicals and Cyclopropanes

Radical chemistry has been proven to be an invaluable tool in the synthetic chemist's tool box. Radical character can be modified by electron-withdrawing and donating groups. Radical ring-opening and cyclisation reactions can serve as probes in mechanistic studies. Within medicinal chemistry, radical chemistry remains an under explored area, particular with respect to modes of inhibition. Tranylcypromine serves as a good example of an intentionally designed, radical-based mechanistic inhibitor.

1.3 – Amino acids

Amino acids play a vital role in biological systems, helping to create complex structures such as proteins and enzymes that allow for the regular function of an organism.¹⁰⁸ Over 500 amino acids have been identified and are involved in numerous roles in biological systems from neurotransmitter precursors to plant defence mechanisms.¹⁰⁹⁻¹¹¹

1.3.1 – Proteinogenic Amino Acids

Only 20 amino acids are coded for in the genetic sequence of eukaryotic organisms and are known as canonical, or natural, amino acids.¹⁰⁹ The 20 amino acids found within organisms are more specifically known as α -amino acids due to the presence of an amine group appended to the α -carbon.¹¹² All canonical amino acids, apart from glycine, are chiral molecules and exist in one enantiomeric form in eukaryotes, the *L*-(or *S*)-isomer **37**.¹¹³ Cysteine is an exception to this with the Cahn-Ingold-Prelog rules defining it as the *D*-(or *R*)-isomer **38** (Figure 9).

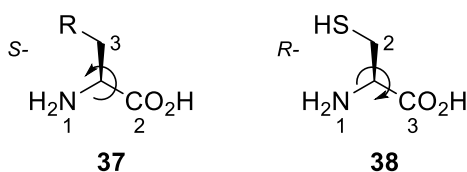


Figure 9 – Generic amino acid structure **37** and cysteine **38**

Amino acids vary in their properties with different R-groups which span from the α -carbon. Different R-groups allow for a variety of intramolecular interactions within proteins and can serve to hold together complex tertiary and quaternary protein structures.¹¹⁴ R-groups can also undergo post-translational modifications to form non-canonical amino acids – those that are not coded for in the genetic sequence – with selenocysteine as the most prevalent in mammalian proteins.¹¹⁵

1.3.2 – Non-Proteinogenic Amino Acids

Amino acids that lack a genetic codon, or a specific RNA carrier, and cannot be incorporated into protein structures are referred to as non-proteinogenic. For example, two non-proteinogenic amino acids play a pivotal role in the urea cycle in mammals.¹¹⁶ Ornithine **39** plays a catalytic role in removing excess amine-containing species from the surrounding media. Citrulline **40** is the product of the subsequent reaction of ornithine and carbamoyl phosphate.¹¹⁶ Neither are found within proteins but both have key biological functions.

Ornithine and citrulline are both α -amino acids, however, non-proteinogenic amino acids are not limited to the α -amino acid core structure. Others such as β -, γ - and δ -amino acids are also found within biological systems.^{112, 117-119}

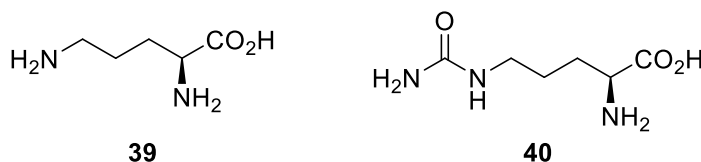


Figure 10 – Ornithine **39** and citrulline **40** structures

1.3.3 – Non- α -amino Acids

γ -Aminobutyric acid (GABA) **41** is an example of a γ -amino acid. GABA serves as an inhibitory neurotransmitter in the mammalian nervous system and is reported to have stimulatory functions in the CNS, PNS and certain non-neuronal tissues (Figure 11).¹¹⁸

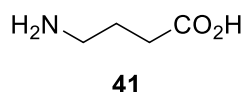


Figure 11 – γ -Aminobutyric acid (GABA) **41** structure

Another example of a biologically important, non- α -amino acid is *p*-aminobenzoic acid (*p*ABA) **42** (Figure 12). *p*ABA is the starting point in the biosynthesis of folic acid in many types of plant and bacteria – a process which is of vital importance to humans as folic acid is one of the essential B vitamins which, when in deficit, can lead to reduced cognitive function.^{120, 121}

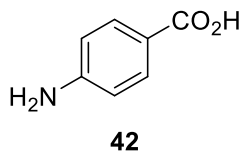


Figure 12 – *p*-Aminobenzoic acid **42** structure

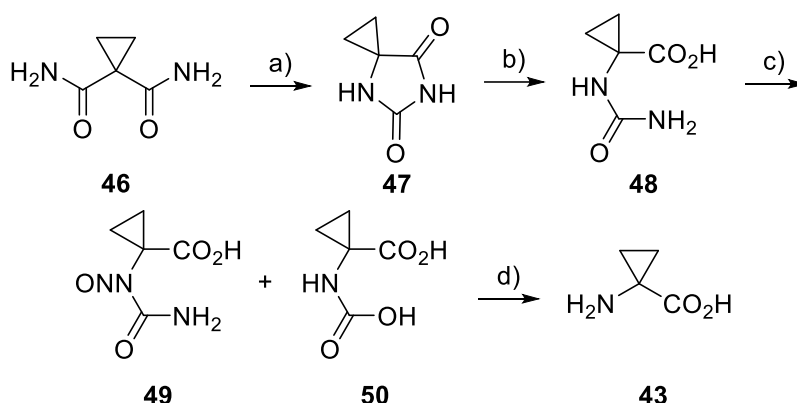
Amino acids play many other roles within biological systems and the structural motifs within them can determine their function. GABA **41** has considerably different properties over its homologue glycine. GABA's conformational freedom and function has been investigated and it was concluded that GABA alters its conformation to allow binding to different receptors in the nervous system.¹²² Other investigations that employed compounds containing conformationally locked GABA-like fragments have however pointed towards GABA having a limited number of active conformations.^{123, 124} It is therefore reasonable to postulate that the additional conformational freedom that is present in the γ -amino acid contributes toward its function over that of its more conformationally restricted α -homologue, glycine.

Conversely certain groups, such as cyclopropanes, can serve to restrict conformational freedom and hold a molecule in a defined conformation – this restriction can bestow the compound with an alternative function.

1.3.5 – Synthesis of Cyclopropane-Containing Amino Acids

In 1922, Ingold was the first to synthesise the cyclopropane-containing amino acid ACC **43** some 30 years before Vähätalo had isolated it from a natural source.¹³⁸

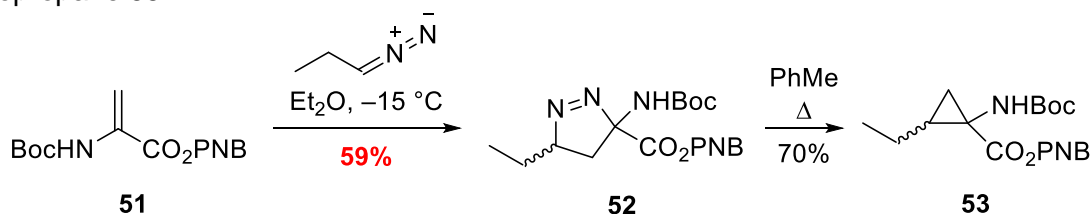
Ingold's synthesis begins with a Hofmann rearrangement of a single amide functionality of dicarboxamide **46**. The resulting isocyanate was trapped by an intramolecular attack giving hydantoin **47** which was hydrolysed to give acid **48**. Treatment of acid **48** with nitrous acid yielded *N*-nitroso **49** and carbamic acid **50**. The later undergoes a spontaneous decarboxylation giving ACC **43** (Scheme 20).¹³⁸



Scheme 20 – Ingold's synthesis of 1-aminocyclopropanecarboxylic acid **43**

a) Br_2 , NaOH ; b) NaOH , H_2O , reflux, 1h, quant.; c) HCl , NaNO_2 , 0 °C, 0.5 h, 29%; d) In situ decomposition of carbamic acid **50** gave HCl salt of **43** which was then neutralised, 60%

An early method that remains a useful tool for accessing cyclopropane derivatives is the use of alkyl diazo-derivatives. This involves the reaction of diazo-compounds with alkenes to affect a 1,3-dipolar cycloaddition across the double bond. An intermediate pyrazoline is formed which, upon heating, extrudes molecular nitrogen and affords a cyclopropane ring.¹³⁹ An example of this protocol can be seen in Suzuki's 1983 synthesis of coronamic acid (Scheme 21).¹⁴⁰ Treatment of amino acrylate **51** with diazopropane affords pyrazoline **52**. At elevated temperatures, in an apolar solvent, pyrazoline **52** extrudes molecular nitrogen to yield cyclopropane **53**.



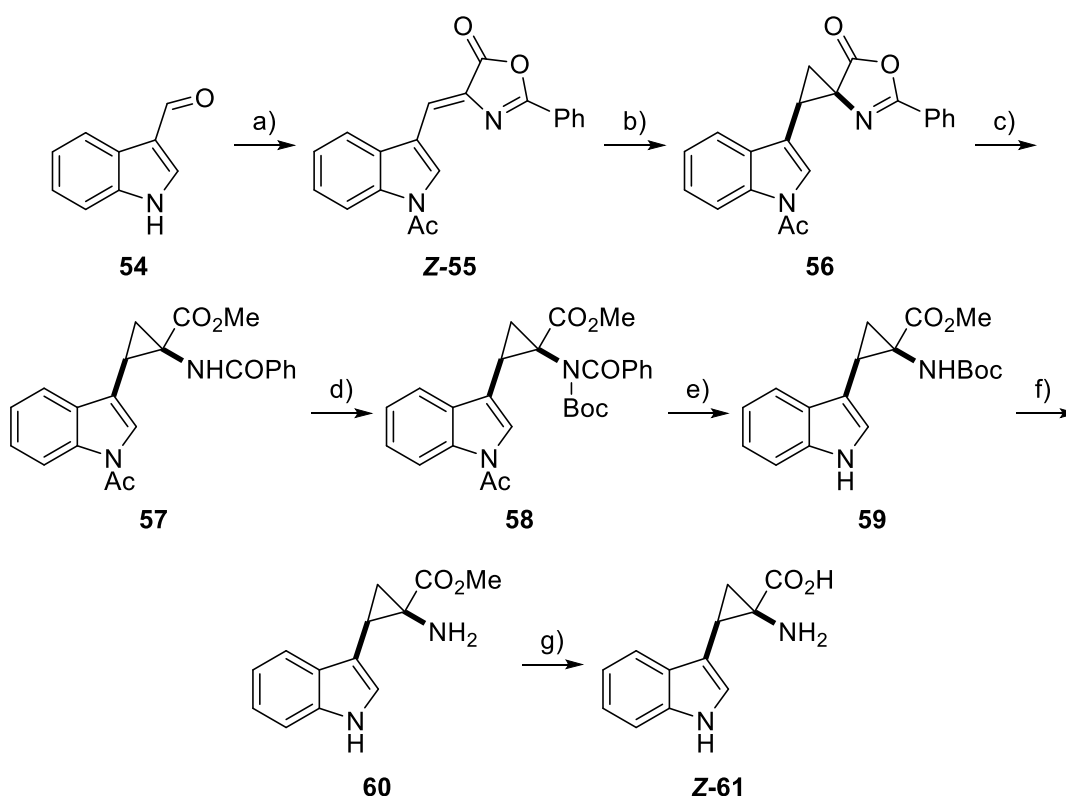
Scheme 21 – Suzuki's synthesis of coronamic acid

Use of diazo compounds in cyclopropane synthesis is a powerful tool with the reactions being reliable and proceeding in good yields, however the use of diazo compounds presents in itself a significant hazard. Diazomethane is highly explosive and a potent carcinogen, longer-chain

alkyl diazo compounds are more stable yet still present significant carcinogenicity as alkylators.^{141, 142}

Other more structurally elaborate amino acids have been accessed *via* the use of alkyl diazo compounds – for example in the diastereoselective synthesis of 2,3-methanotryptophan completed by Donati in 1996.¹⁴³

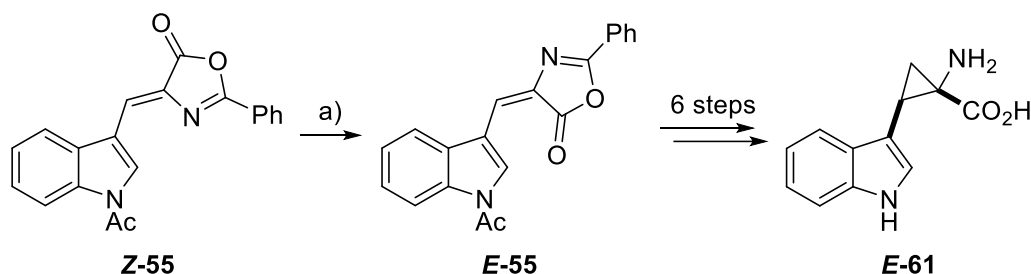
Beginning with an acetic anhydride and sodium acetate mediated condensation of 3-formylindole **54** with hippuric acid, the respective acyl-protected 3-indoymethylene oxazolone **Z-55** was achieved in a 65% yield and 4:1 (*Z*:*E*) isomer ratio. Cyclopropanation of the methylene unit with diazomethane afforded cyclopropane **56** in a poor yield of 46%. Opening of oxazolone **56** *via* a DMAP-catalysed methanolysis proceeded successfully to give the respective methyl ester **57** which was then subjected to Boc-anhydride to access amido carbamate **58**. Hydrazine hydrate cleaved both amide protecting groups leaving the methyl ester and Boc protecting groups present. Subjecting **59** to concentrated HCl in ethyl acetate cleaved the Boc-group, a lithium hydroxide mediated hydrolysis of the resulting ester **60** followed by elution through Dowex resin afforded **Z-61** (Scheme 22).



Scheme 22 – Donati's synthesis of (*Z*)-2,3-methanotryptophan

a) Hippuric acid, NaOAc, (Ac)₂O, 80 °C, 40 min, 46%; b) CH₂N₂, Et₂O, rt, 'overnight', 46%; c) DMAP, MeOH, rt, 35 min, 86%; d) (Boc)₂O, DMAP, Et₃N, CH₂Cl₂, rt, 2 h, 95%; e) NH₂NH₂·H₂O, MeOH, rt, 87%; f) Conc. HCl, EtOAc, rt, 30 min, 98%; g) 1M LiOH_(aq), 1,4-dioxane, rt, 'overnight' then neutralisation with 1M HCl_(aq) then Dowex 50 x 2200, elution with 10% pyridine, 26%

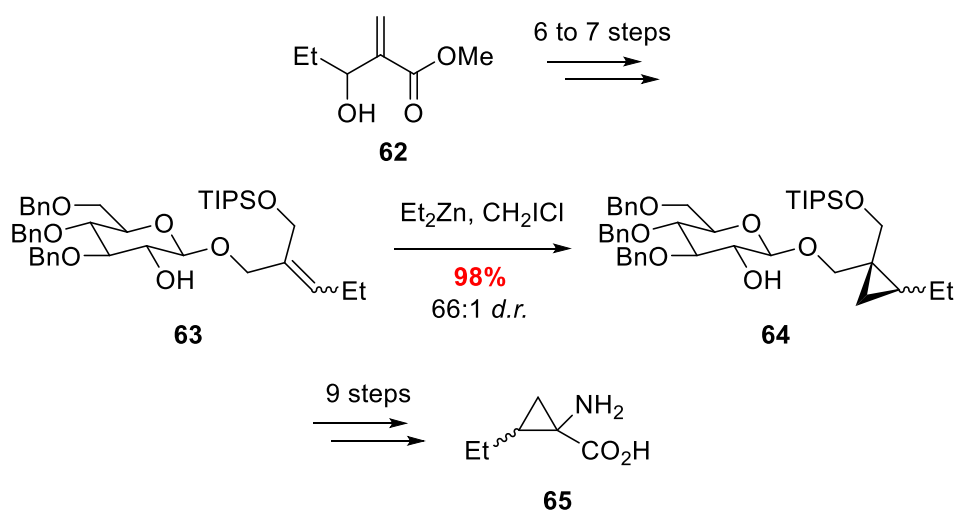
Access to the *E*-diastereomer was achieved by isomerising **Z-55**. Subjecting olefin **Z-55** to an aqueous solution of HBr (48%) under a constant stream of HBr gas granted access to **E-55** in excellent yield (Scheme 23). The desired **E-61** was accessed *via* the same protocol used to synthesise **Z-61**.



Scheme 23 – Donati's synthesis of (*E*)-2,3-methanotryptophan

a) 48% HBr_(aq), HBr_(g), 0 °C, 12 h, 99%

Simmons-Smith methodology has also been used to synthesise cyclopropane-containing amino acid derivatives.¹⁴⁴ Due to the concerted nature of the Simmons-Smith transition state and the directing effect offered by the allylic oxygen, Charette utilised this in the synthesis of a diastereo-enriched mixture of coronamic acid isomers (Scheme 24).

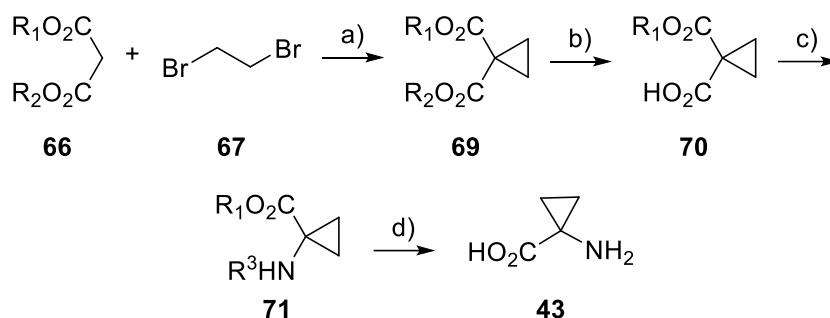


Scheme 24 – Charette's synthesis of coronamic acid

Cyclopropanation of the glucopyranose derivative proceeded with excellent yield and diastereomer ratio. This synthesis however lacks generality and is cumbersome compared to other syntheses of coronamic acid.^{140, 145} Simmons-Smith conditions also requires the use of highly pyrophoric diethyl zinc, limiting the reaction's scalability.

Wheeler utilises an alternative method for cyclopropane synthesis, instead relying on a cyclodialkylation of dialkyl malonate **66** with 1,2-dibromoethane **67**.¹⁴⁶ The resultant diester **69** is then subjected to a basic hydrolysis to give monoacid **70**. A subsequent Curtius

rearrangement and Boc-deprotection affords amino acid **43** in good overall yield (Scheme 25).¹⁴⁶

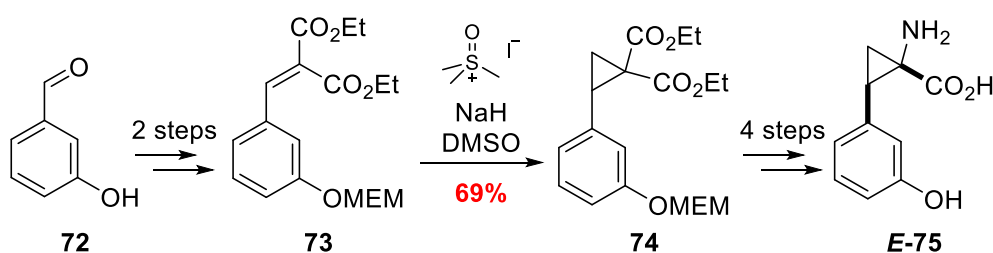


Scheme 25 – Wheeler's synthesis of ACC via a dialkyl malonate

a) NaHCO_3 ; b) $\text{NaOH}_{(\text{aq})}$, EtOH , rt , 72 h, 85%; c) DPPA, $^t\text{BuOH}$, Δ , 8 h, 78%; d) HCl , Δ , 82%
 $R^1 = R^2 = \text{Et}$; $R^3 = \text{Boc}$.

Wheeler's synthesis successfully avoided the use of diazoalkanes yet the scope was not expanded beyond that of ACC. No other 1,2-dibromo derivatives were trialed for potential routes to access other α -cyclopropanated amino acids.

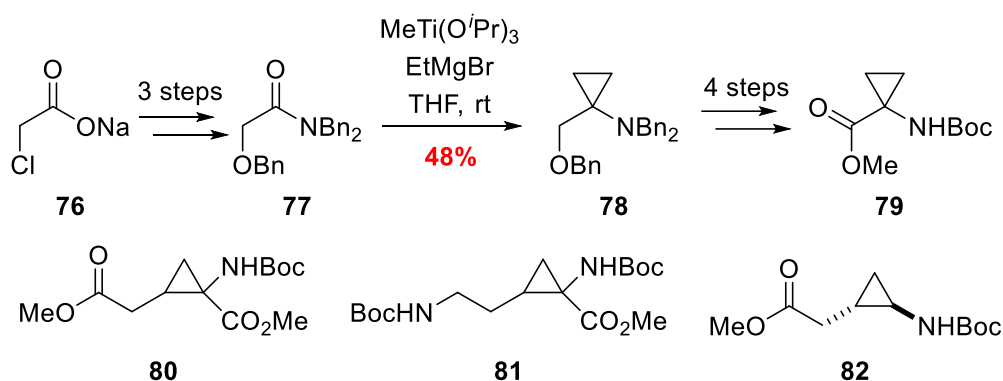
Formation of cyclopropanes can also be accomplished through the use of sulfur ylides.¹⁴⁷ Phillips' employed methods developed by Corey in the synthesis of a medically relevant amino acid analogue **E-75** (Scheme 26).



Scheme 26 – Phillips' synthesis of the **E-75**

Phillips' accessed the **Z-75** through a modified route. Ester **74** was desymmetrised via a KOH-mediated hydrolysis to give the *trans*-potassium carboxylate. Refluxing in ethanolic hydrazine converted the remaining *cis*-ester to a *cis*-acyl hydrazide which was reacted with nitrous acid to give the acyl azide. Upon heating, the acyl azide underwent a Curtius rearrangement to give the protected *Z*-isomer. Quinine and ephedrine were used to enantiomerically resolve the *E*- and *Z*-isomers, respectively.¹⁴⁷

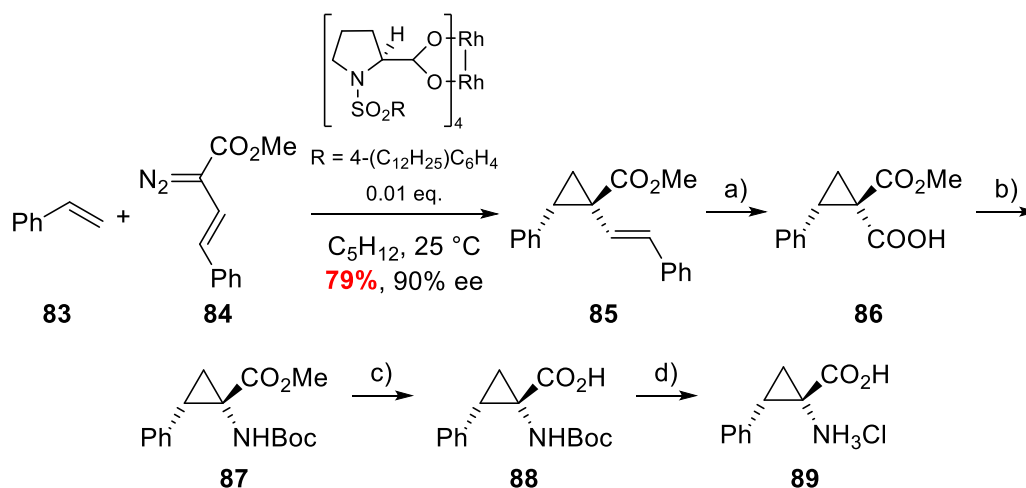
Later reports have accessed cyclopropane-containing amino acids through the use of transition-metals. de Meijere employed a Kulinkovich reaction between amide **77** and alkyl Grignards in the presence of methyltitanium triisopropoxide.¹⁴⁸ This methodology allowed access to protected cyclopropane-containing analogues of coronamic acid, glutamic acid, ornithine and γ -Aminobutyric acid (Scheme 27).



Scheme 27 – de Meijere's Kulinkovich-type synthesis of cyclopropane-containing amino acids **79–82**

Judicious choice of Grignard gave access to protected amino acid analogues **79–82**, showing the potential scope of this approach. The key cyclopropanation steps however proceeded with only moderate yields across the Grignards' used (33–48%) and the titanium-reagent was used in super-stoichiometric amounts.¹⁴⁸

Catalytic transition-metal cyclopropanations have been reported by Davies using chiral dirhodium catalysts and vinyl diazomethanes in the presence of excess styrene **83**.¹⁴⁹ Literature preparations of the dirhodium catalyst and the vinyl diazomethane were followed to gain access to the starting materials.¹⁵⁰ Davies' optimised conditions gave access to α -vinylcyclopropyl **85** in good yield. Oxidative cleavage of alkene **85** afforded acid **86** which was then subjected to a Curtius rearrangement. Saponification of ester **87** and acid-mediated Boc-deprotection gave cyclopropyl amino acid **89** (Scheme 28).¹⁴⁹



Scheme 28 – Davies' asymmetric synthesis of amino acid **89**

a) $\text{RuCl}_3 \cdot \text{H}_2\text{O} / \text{NaIO}_4$, CCl_4 , MeCN , H_2O , rt, 8h, 70%; b) DPPA, Et_3N , $t\text{BuOH}$, C_6H_{14} , reflux, 18 h then $(\text{Boc})_2\text{O}$, reflux, 2 h, 77%; c) KOH , $\text{THF}/\text{H}_2\text{O}$, rt, 18 h, 77%; d) 3 M HCl , EtOAc , rt, 1 h, 83%

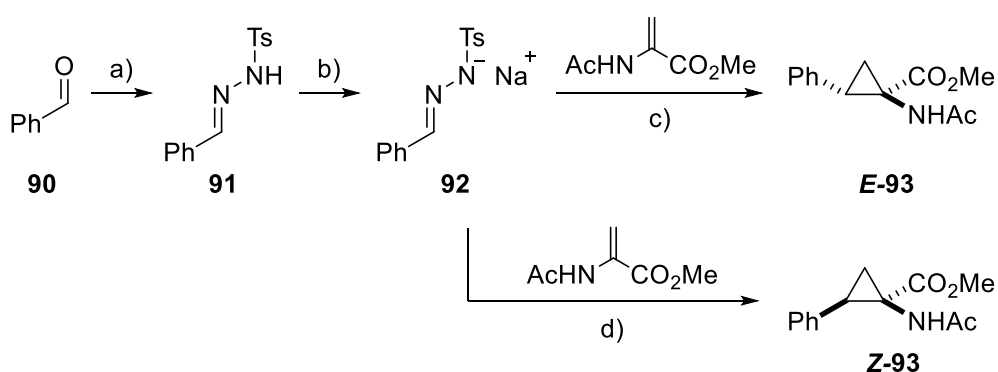
The cyclopropanation protocol developed by Davies proved remarkably successful, achieving high yield and enantiomeric excesses under mild conditions. The methodology was also scalable with the above rhodium-catalysed cyclopropanation to give α -vinylcyclopropyl **85** was achieved on >15 g scale.

Many of the previously discussed routes to cyclopropane-containing amino acids involve functional group transformations post-cyclopropane installation. While cyclopropanes are chemically robust motifs and have been shown to withstand manipulation of surrounding functionalities, additional steps to access the α -amino acid backbone are undesirable.

1,3-Dipolar cycloadditions to dehydroserinate derivatives, as seen in Suzuki's synthesis of coronamic acid (Scheme 21), offer a direct route to the α -amino acid backbone. The drawback of Suzuki's methodology is the use of potentially dangerous alkyldiazomethanes.

Access to both alkyl and aryldiazomethanes through thermolysis of stable tosyl hydrazone salts, in the presence of a phase-transfer catalyst, has since been described by Aggarwal.^{151, 152} Developed as a route to access epoxides, the scope of this chemistry was expanded to incorporate reactivity between tosyl hydrazone salts and aminoacrylate derivatives.¹⁴⁵

Condensation of *p*-toluenesulfonyl hydrazide with benzaldehyde **90** gives access to tosyl hydrazone **91** which is subsequently deprotonated by sodium methoxide to afford tosyl hydrazone sodium salt **92**. It was found in the absence of a transition metal catalyst, cyclopropanation proceeds with diastereoselectivity favouring the *E*-diastereomer **E-93**. In the presence of tetraphenylporphyrin iron(III) chloride this diastereoselectivity was reversed in favour of the *Z*-diastereomer **Z-93** (Scheme 29).



Scheme 29 – Synthesis of (+/-) *E*- & *Z*-2,3-methanophenylalanine

a) *p*-CH₃(C₆H₄)SO₂NHNH₂, MeOH, rt, 0.5 h, 91%; b) Na_(s), MeOH, rt, 0.25 h, 99%; c) BnEt₃NCl, PhMe, 40 °C, 60 h, 48% (*E*:*Z*, 85:15); d) ClFeTPP (1 mol%), BnEt₃NCl, PhMe, 40 °C, 60 h, 84% (*E*:*Z*, 19:81)

Under catalyst-free conditions, a 1,3-dipolar cycloaddition leads to the diastereoselective construction of pyrazoline intermediate **94** with the two bulkiest groups adopting a *trans*-arrangement (Figure 15). The diastereoselectivity is more pronounced when the *N*-Boc protected analogue of the aminoacrylate is employed, achieving a 94:6 (*E*:*Z*) diastereomer ratio.

In the presence of the iron(III) catalyst, iron carbene **95** forms from the phenyldiazomethane and reacts directly with the aminoacrylate. Aggarwal argues that approach by the aminoacrylate must be parallel to the iron carbene. Electron-donation from the amide gives the aminoacrylate-nitrogen positive character and this developing positive charge may well be stabilised by the polarisable π -system of the iron-bound phenyl substituent. This leads to a stabilised reactive conformation where the amide is *cis* to the phenyl group – accounting for the observed diastereoselectivity.^{145, 153} When subjecting alkyl tosyl hydrazones to this chemistry – where there are no π -electrons available to stabilise the transition state – no enhancement in diastereomer ratio is observed (Figure 15).¹⁴⁵

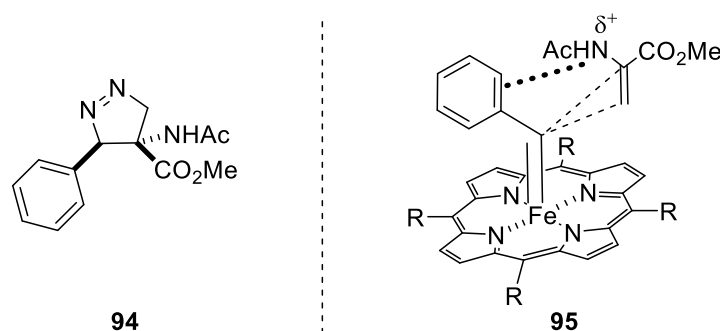
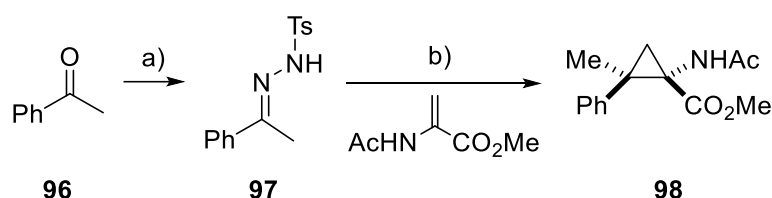


Figure 15 – Pyrazoline intermediate **94** and iron-carbene transition state **95**

Permutations of Aggarwal's methodology have been developed in the laboratories of Jiang and have eliminated the need to form the sodium salt in a discrete reaction. In Jiang's revision, the tosyl hydrazone salt is generated *in situ* by caesium carbonate prior to the addition of the aminoacrylate to the reaction mixture (Scheme 30).¹⁵⁴ The methodology developed by Jiang allows access to the *trans*-cyclopropane, however no attempt to access the *cis*-cyclopropane was reported.

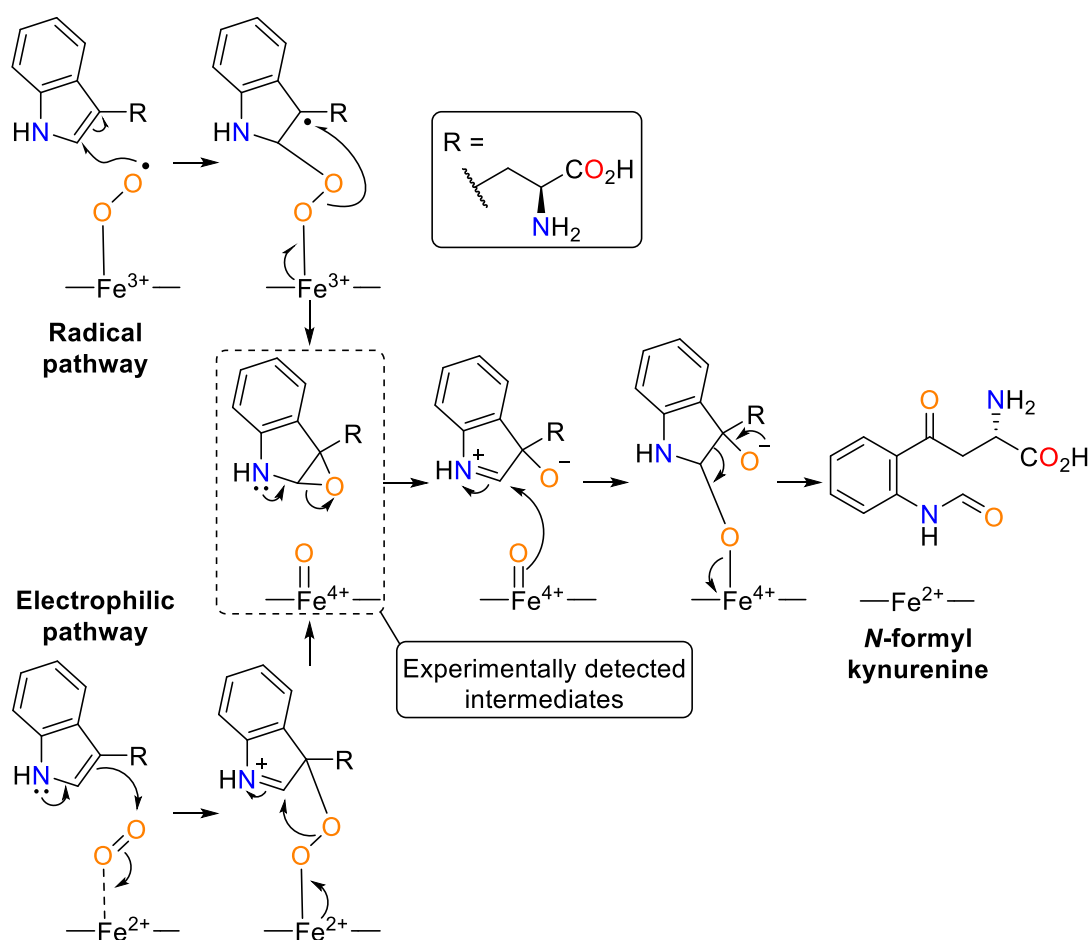


Scheme 30 – Jiang's *in situ* tosyl hydrazone salt generation

a) $p\text{-CH}_3(\text{C}_6\text{H}_4)\text{SO}_2\text{NHNH}_2$, MeOH, rt, 1h, 94%;
 b) i. Cs_2CO_3 , BnEt_3NCl , PhMe, rt, 1h, ii. Methyl 2-acetamidoacrylate, 90 °C, 12 h, 97%
 (combined diastereomer yield: *E*-isomer = 83%, *Z*-isomer = 14%)

1.4 – Aims and objectives

Since the discovery of IDO1 as an attractive immunotherapeutic target, many pharmaceutical companies have developed and clinically evaluated competitive inhibitors of IDO1. Alongside the commercial interest in IDO1, there has also been a renewed academic interest in the enzyme, particularly regarding how the enzyme dioxygenates tryptophan to form *N*-formyl-*L*-kynurenine. Current literature, through experimental observation and theoretical calculation, has proposed either a radical or an electrophilic based metabolic pathway (Scheme 32). By determining IDO1's mode of action, the benefit is potentially two-fold: confirmation of distinct heme-reactivity and the ability to rationally design irreversible inhibitors for therapeutic benefit.



Scheme 32 – Proposed radical- and electrophilic-based metabolic pathways of IDO1

By considering the current mechanistic understanding of IDO1-mediated metabolism of tryptophan to *N*-formyl-*L*-kynurenine, it is possible to design small molecule probes to discriminate between the two mechanistic possibilities. As such substrate mimic ***E/Z*-61·HCl** has been designed, alongside secondary targets **99–102**, to contain a latent chemical motif to divert the reactivity of the enzyme toward a mechanistic 'dead end' (Figure 16).

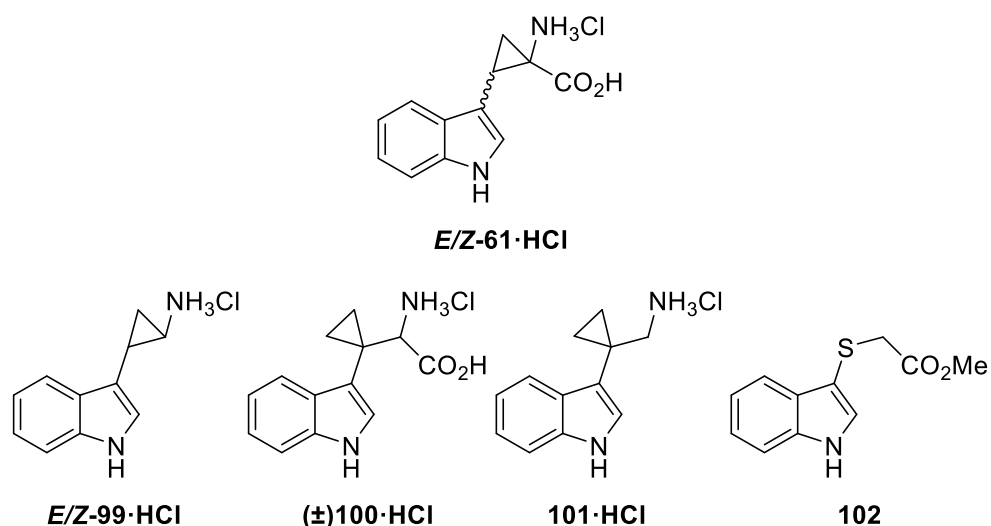


Figure 16 – Rationally designed mechanistic inhibitors of IDO1

Strategic placement of chemically inert functionalities allows for the potential trapping of hypothesised intermediates along the catalytic dioxygenation of the substrate. Due to IDO1's broad substrate scope mimicking the natural substrate by making minor structural changes, indoles **61** & **99–102** are hypothesised to still engage in active site uptake and produce productive enzyme-inhibitor interaction. Analysis of available co-crystal structures of IDO1 and tryptophan indicate sufficient space within the active site to accommodate the proposed structural changes (Figure 17).¹¹

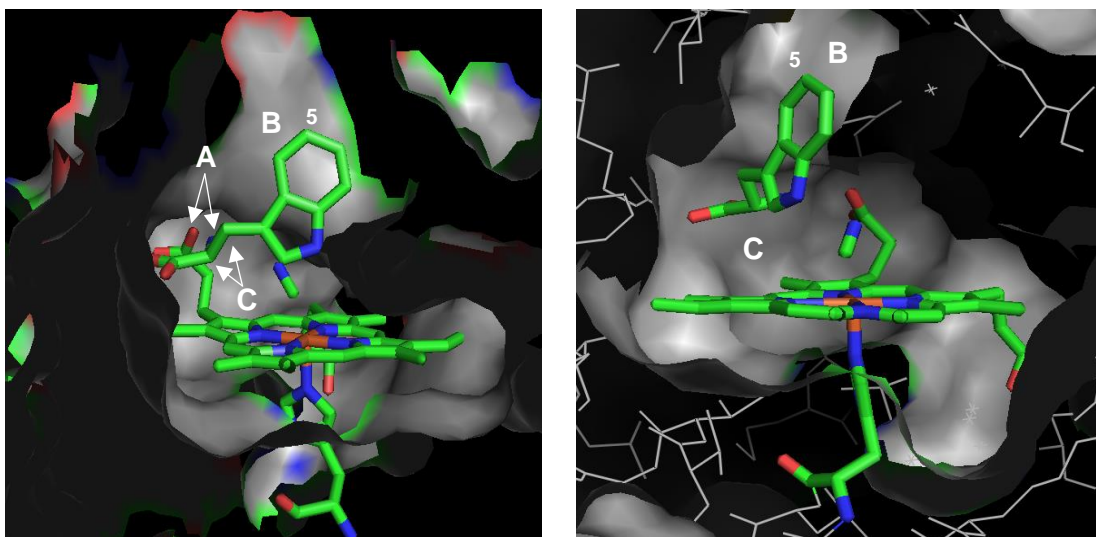
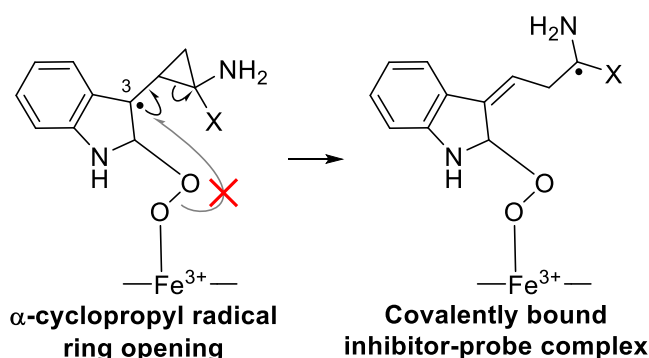


Figure 17 – X-ray co-crystal structure of Trp with rhIDO's active site with a heme-bound cyanide anion

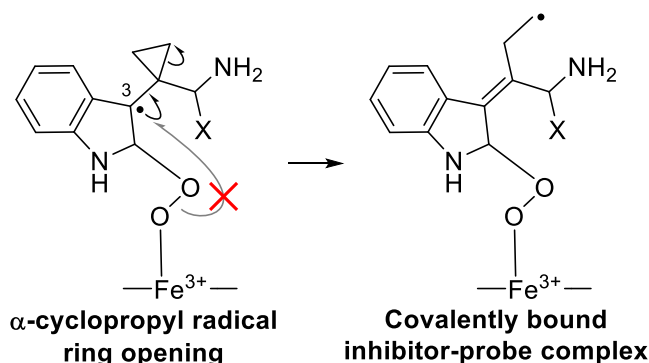
- A** – Stabilising interaction between with α -amine and an acid terminated heme side chain;
- B** – 5-position on the indole ring system points into a hydrophobic pocket;
- C** – Demonstrated the space available within the active site to accommodate a cyclopropane ring

Cyclopropane-containing indoles **61** and **99** are designed to ring open in the presence of a radical at the α -position, with respect to the cyclopropane (Scheme 33). When $X = \text{CO}_2\text{H}$, formation of the α -cyclopropyl radical and subsequent ring opening leads to the formation of a captodative radical. Whereas when $X = \text{H}$, radical ring opening of the cyclopropane leads to the formation of a dative radical. Both resultant radicals are stabilised by the neighbouring electron-donating and/or withdrawing groups, providing a thermodynamic driving force for ring opening. Although the initial radical is a resonance-stabilised benzylic radical, it is hoped that release of ring strain and radical stabilisation will provide a sufficient driving force for the ring opening. The resulting radical from the ring-opening is then available to interact with active site residues *via* proton abstraction or radical addition. Proton abstraction from the active site introduces a radical to the protein structure which could lead to protein degradation.¹⁵⁵ Radical addition to an active site residue would render the active site inaccessible, preventing further substrate turnover.



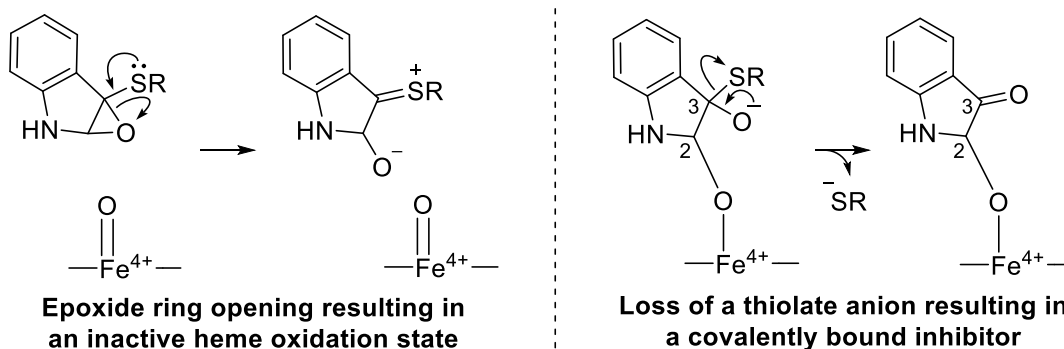
Scheme 33 – Modes of mechanistic diversion for indoles **61** and **99**, where $X = \text{CO}_2\text{H}$ or H

Spirocyclic indoles **100** and **101** are designed to work in a similar manor to indoles **61** and **99** – ring opening in the presence of a radical at the α -position (Scheme 34). In both instances, the radical formed is an unstable primary radical suggesting the thermodynamic driving force for ring opening of the spirocyclic cyclopropanes will be less. However the increased reactivity of the resulting radical could lead to enhanced secondary reactivity with active site residues.



Scheme 34 – Modes of mechanistic diversion for indoles **100** and **101**, where $X = \text{CO}_2\text{H}$ or H

The final mechanistic probe, sulfenylindole **102**, has been designed to target some of the later stage intermediates of IDO1 metabolism that are not reliant on radical reactivity (Scheme 35). There are two intermediates where mechanistic diversion has been envisaged with sulfenylindole **102**. Ring opening of the epoxide intermediate through neighbouring group participation of the sulfide could result in the formation of an inactive oxidation state of the heme-centre. Alternatively, preferential loss of the thiolate anion could lead to a covalently bound enzyme-probe complex.



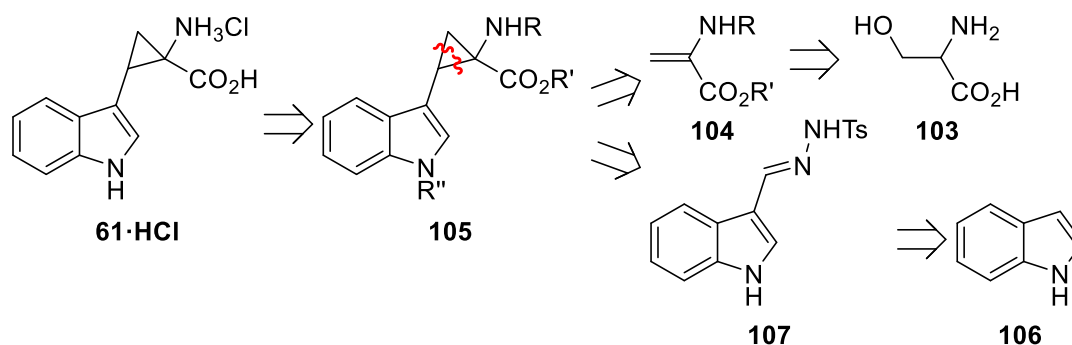
Scheme 35 – Modes of mechanistic diversion for sulfenylindole 102

1.5 – Results and Discussion: Synthesis of mechanistic probes for IDO1

1.5.1 – Synthesis of 1,2- Δ -Tryptophan Analogue **61**

A literature route to tryptophan analogue **61** exists, however the use of diazomethane, a cumbersome deprotection sequence and poor overall yield limited its utility and therefore lead to the genesis of novel routes.¹⁴³ A route to 1,2-methano amino acids that utilised the *in-situ* generation of reactive alkyl diazo-compounds in the presence of amino acrylates was the inspiration for the designed synthesis. Developed by Aggarwal, alkyl and aryl diazo species can be readily generated from sodium hydrazide salts and undergo 1,3-dipolar cycloadditions with amino acrylates to give cyclopropane containing amino acids.¹⁴⁵ Jiang later developed a one-pot strategy which allowed for the *in situ* generation of caesium hydrazide salts, from a tosyl hydrazone, which also undergoes 1,3-dipolar cycloadditions with amino acrylates.¹⁵⁴

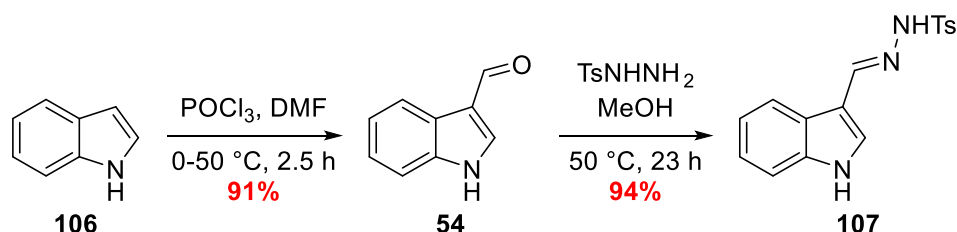
Performing a retrosynthetic analysis utilising Aggarwal's methodology, two key intermediates were identified: tosyl hydrazone **107** and amino acrylate **104** (Scheme 36).



Scheme 36 – Retrosynthetic analysis of 1,2- Δ -tryptophan **61**·HCl

Preliminary 1,3-dipolar cycloadditions

To access tosyl hydrazone **107**, a Vilsmeier-Haack formylation of indole **106** was followed by a condensation with tosyl hydrazide (Scheme 37). Both steps proceeded in excellent yield with no need for purification, isolating **107** as the *E*-isomer with this determined by steric factors.



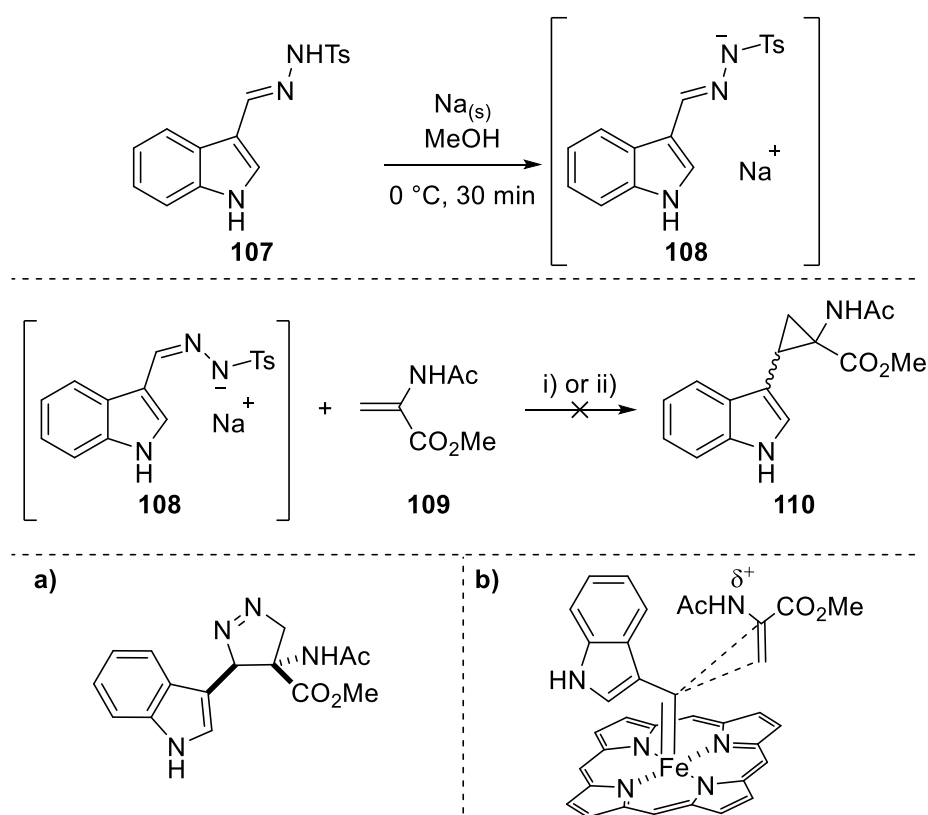
Scheme 37 – Synthesis of tosyl hydrazone **107**

Conversion of tosyl hydrazone **107** to sodium hydrazide **108**, using sodium methoxide, was immediately followed by reaction with amino acrylate **109** in the presence of a phase transfer catalyst benzyltriethylammonium chloride (BTAC) (Scheme 38).

This reaction proceeds *via* a pyrazoline intermediate and the relative stereochemistry of this intermediate is determined *via* steric influence. In this instance, it would be expected that the larger *N*-acetyl group of the amino acrylate adopts a *trans*-conformation with respect to indole. Subsequent extrusion of nitrogen would therefore give rise to the *E*-diastereomer as the major diastereomer (Scheme 38a).

Aggarwal's report also employed a porphyrin catalyst, iron tetraphenylporphyrin chloride (FeTPPCI), to access the *Z*-diastereomer.¹⁴⁵ Formation of an *in-situ* iron-carbenoid species allows the cyclopropanation of alkenes. Stabilisation of the amino acrylate's increasingly positive character on the nitrogen can be achieved by π -electron donation from the electron-rich indole. Consequently, this creates a transition state that places the indole and the amine in a *cis*-conformation. Successful reaction of the two would lead to the formation of the *Z*-diastereomer as the major diastereomer (Scheme 38b).

Both reactions failed to give a productive outcome and a complex mixture of reaction products were isolated; no attempt at isolation and characterisation of these products was made. The failure of these reactions was rationalised through the potential for the electron-rich indole system to destabilise the transient diazo species or iron-carbenoid *via* electron-donation.¹⁵⁶

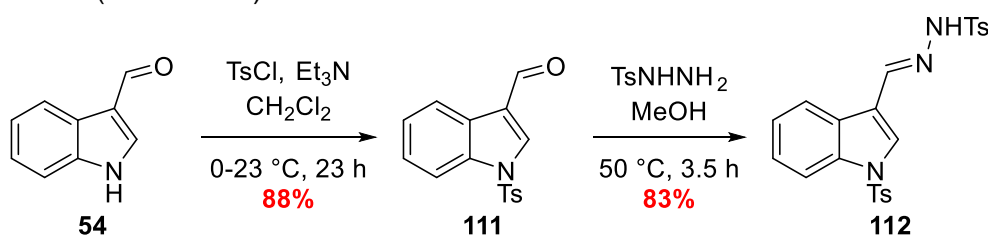


Scheme 38 – Non-catalysed and catalysed cyclopropanations
 i) BTAC, PhMe, 40 °C, 93 h; ii) FeTPPCI, BTAC, PhMe, 40 °C, 94 h

N-Indole Protecting Group Strategy

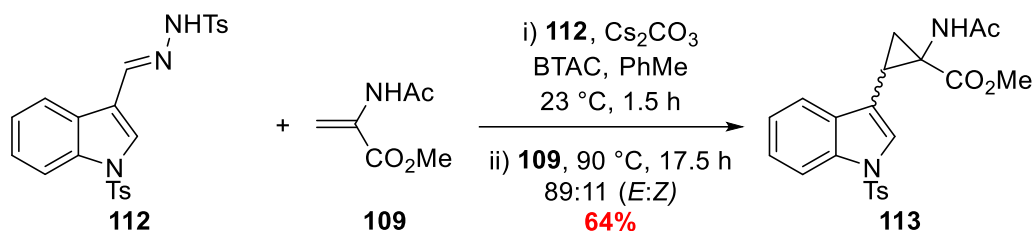
Based on the hypothesis that the electron-donating indole nitrogen prevented a productive outcome, an *N*-protected tosyl hydrazone **111** was synthesised. The *p*-toluenesulfonyl (Ts) group was selected due to its electron-withdrawing nature and the ease of installation.¹⁵⁷

Indole **54** was subjected to *p*-toluenesulfonyl chloride to give corresponding *N*-tosylated indole **111**. The subsequent reaction of **111** with tosyl hydrazide furnished diazo-precursor **112** as a single configurational isomer by ¹H-NMR, presumed to be the *E*-isomer based on steric considerations (Scheme 39).



Scheme 39 – Synthesis of *N*-tosylated tosyl hydrazone **112**

Instead of subjecting tosyl hydrazone **112** to the Aggarwal cyclopropanation conditions, the one-pot strategy developed by Jiang was utilised to access the desired 1,2-methanotryptophan core.¹⁵⁴ The reaction was a success, providing the desired core in a moderate yield and a 89:11 (*E*:*Z*) mixture of diastereomers (Scheme 40).



Scheme 40 – Successful cyclopropanation to form desired 1,2-methano tryptophan core **113**

The diastereomeric ratio of cyclopropane **113** was determined by calculating the ratio between the cyclopropane C-H proton *pseudo*-triplet integrations from analysis of the ¹H-NMR crude reaction mixture (Figure 18).

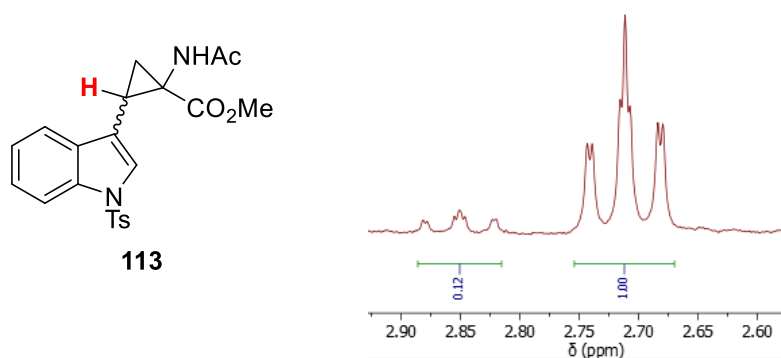


Figure 18 – ¹H-NMR analysis to determine the d.r. for indole **113**

To elucidate the *E/Z* configuration of the diastereomers within the mixture, the methyl ester and *N*-acetyl proton shifts of the major and minor diastereomers were compared. It was hypothesised that when the methyl ester or *N*-acetyl groups were in a *cis*-relationship with respect to the indole ring system, an interaction (or lack thereof) with the induced magnetic field would give rise to differences in the shifts between the two diastereomers. Upon isolation of the two diastereomers, a difference in chemical shift of 0.60 ppm was observed for the methyl ester protons and 0.31 ppm for the *N*-acetyl protons (Figure 19). For the *E*-diastereomer, the methyl ester is placed in a configuration where it can interact with the aromatic system's induced magnetic field (Figure 19a).¹⁵⁸ Interaction with the magnetic field has the effect of shielding the methyl ester protons, shifting the resonance up-field in comparison to the *Z*-diastereomer, where the methyl ester is orientated away from the aromatic system. For the *Z*-diastereomer, the same effect is observed with the *N*-acetyl group which is now orientated toward the aromatic system (Figure 19b).

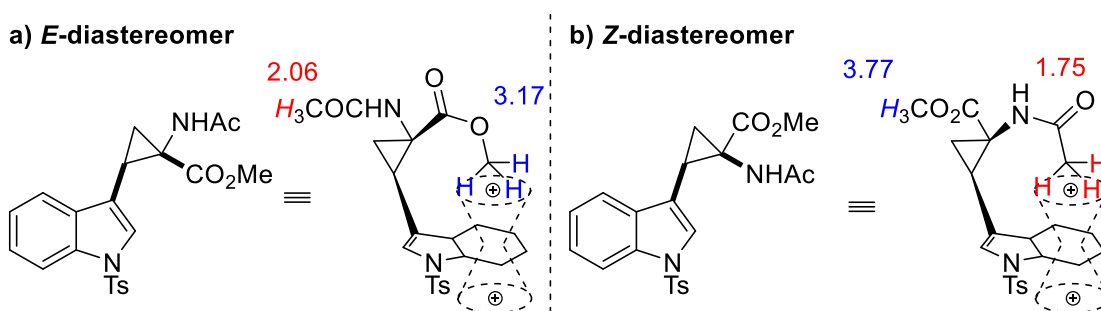


Figure 19 – The effect of magnetic anisotropy on the methyl ester and *N*-acetyl groups

To assess whether this was a viable route to the target compound, a screen of tosyl deprotections was attempted (Scheme 41, Table 1). Many reports cite the use of single-electron reduction type mechanisms for the removal of tosyl groups.¹⁵⁹⁻¹⁶¹ As such, a variety of metal mediated deprotections were trialed (Table 1, Entries 1–5) yet, rather disappointingly, all lead to the recovery of **113**.¹⁵⁹⁻¹⁶¹ Thioglycolic acid in the presence of two equivalents of lithium hydroxide has been reported as a mild nucleophilic method to remove tosyl groups – specifically from *N*-tosyl indole scaffolds.¹⁶² Attempts to replicate this chemistry with indole **113**, both at 23 and 70 °C, lead to the recovery of tosylate **113** (Table 1, Entries 6–7). A final attempt at the tosyl deprotection was made by heating indole **113** in an ethanolic solution of potassium hydroxide. Predictably these conditions hydrolysed the *N*-acetyl group to give amine **115** but did not lead to loss of the tosyl group (Table 1, Entry 8).

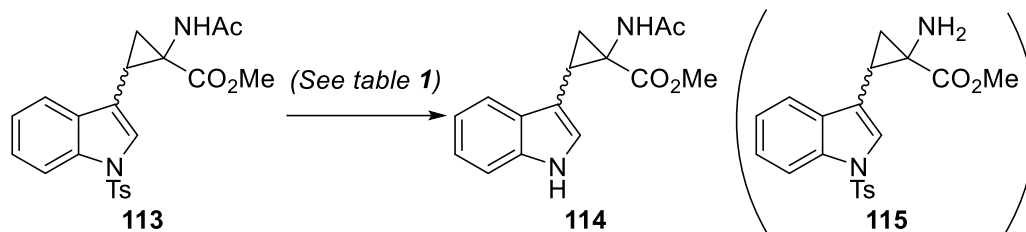
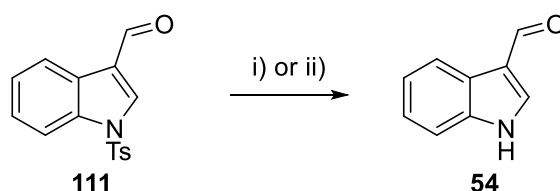


Table 1 – Attempted Tosyl Deprotection conditions

Entry	Conditions	Result
1	Mg(s), MeOH,))) , 23 °C	113
2	Mg(s), THF:MeOH (1:1),))) , 23 °C	113
3	Mg(s), NH ₄ Cl, MeOH,))) 23 °C	113
4	Li(s), naphthalene, THF, -78 °C	113
5	Na(s), MeOH, 23 °C	113
6	Thioglycolic acid, LiOH, DMF, 23 °C	113
7	Thioglycolic acid, LiOH, DMF, 70 °C	113
8	KOH, MeOH, 80 °C	115

To verify whether an observed lack of reactivity was an error of the experimentalist or the chemistry, the conditions used in entry 3 and 6 (Table 1) were replicated on *N*-tosyl aldehyde **111** (Scheme 42). Both reactions proceeded efficiently with calculated ¹H-NMR conversions of 79% and 89% for conditions i and ii, respectively. These results suggest that the failed reactions were likely due to substrate incompatibility.

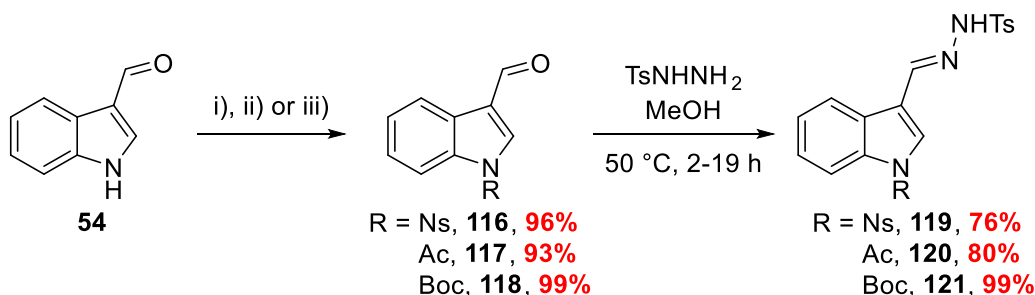


i) Mg(s), NH₄Cl, MeOH,))) 23 °C; ii) Thioglycolic acid, LiOH, DMF, 23 °C

The inability to remove the *N*-tosyl group curtailed further investigation of cyclopropane **113**. However, it did demonstrate the effective use of an electron-withdrawing group to facilitate the cyclopropanation chemistry. As such, the protecting groups *p*-nitrobenzenesulfonyl (Ns),

acetyl (Ac) and *tert*-butyloxycarbonyl (Boc) were investigated due to their electron withdrawing nature and reported ease of removal.

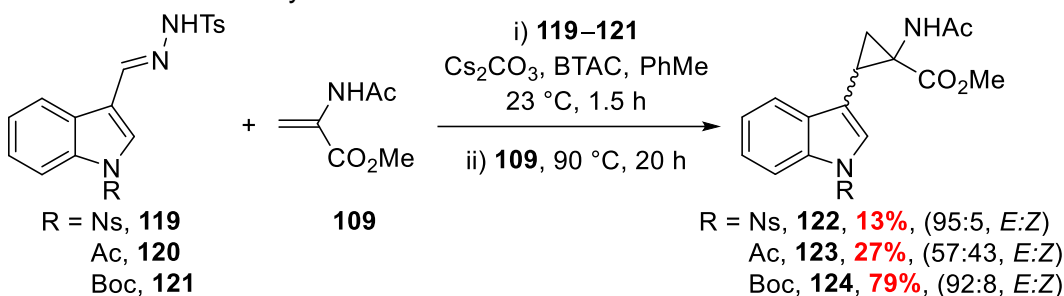
Nosyl-, acetyl- and Boc-protected tosyl hydrazones **119–121** were prepared *via* standard protection procedures of indole **54** followed by subsequent condensation with tosyl hydrazide – all reactions proceeded in good to excellent yield (Scheme 43).¹⁶³⁻¹⁶⁵



Scheme 43 – Protections of indole **54** and subsequent condensation reactions with tosyl hydrazide

i) NsCl , Et_3N , DMAP, CH_2Cl_2 , 23°C , 17 h; ii) Ac_2O , Et_3N , DMAP, CH_2Cl_2 , 23°C , 18 h;
iii) $(\text{Boc})_2\text{O}$, Et_3N , DMAP, CH_2Cl_2 , 23°C , 18 h

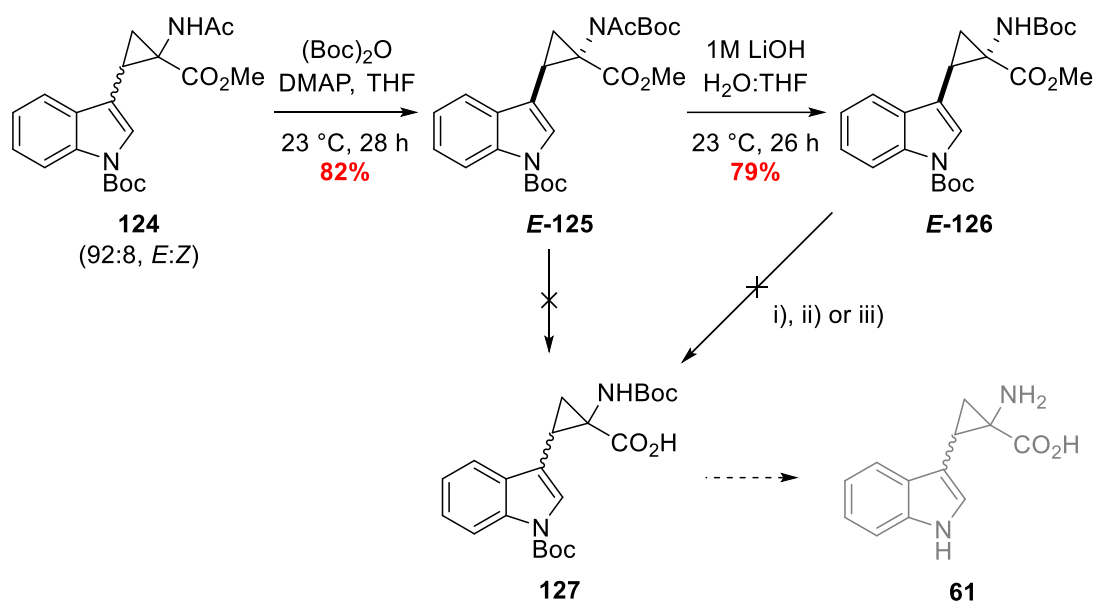
With three *N*-protected tosyl hydrazones in hand, **119–121** were individually subjected to the Jiang one-pot cyclopropanation conditions with amino acrylate **109** (Scheme 44).¹⁵⁴ The *N*-nosyl tosyl hydrazone **119** suffered poor solubility in toluene, even at elevated temperatures, and as a result the reaction gave **122** in very poor yield. *N*-Acetyl hydrazone **120** gave a marginally higher yield of cyclopropane **123**, however the diastereoselectivity was very poor, affording a 57:43 d.r. of diastereomers. *N*-Boc hydrazone **121** was found to be the superior diazo-surrogate, giving an improved yield of the 1,2-methanotryptophan core **124** and excellent diastereoselectivity.



Scheme 44 – Cyclopropanation screen with *N*-protected tosyl hydrazones **119–121**

Precedent set by Donati would provide the deprotection sequence to access target 1,2-methanotryptophan **61**.¹⁴³ First, amide **124** was treated with di-*tert*-butyl dicarbonate to afford the imide-like functionality on cyclopropane **125**. By adding an additional electron-withdrawing group, the base-mediated deprotection of the *N*-acetyl group would occur more readily – a point that became apparent when attempted hydrolysis of *N*-acetyl **124** failed. Interestingly, only the *E*-**125** was isolated from the Boc-protection; the poor reactivity of *Z*-**124** to the Boc-protection could be a result of the steric crowding afforded by the *cis*-*N*-Boc indole

group. Donati's deprotection sequence then utilised hydrazine to remove the amide group. However due to the acute carcinogenicity of hydrazine, imide **125** was subjected to a lithium hydroxide mediated hydrolysis. Under basic hydrolysis conditions it was predicted that the methyl ester would also be hydrolysed. The lithium hydroxide deprotection reaction yielded exclusively the *N*-acetyl deprotected product **E-126**. Subsequent attempts to remove the methyl ester using lithium hydroxide at elevated temperatures, *in-situ* generation of lithium peroxide and a Krapcho-like deprotection failed – starting material was recovered in all cases (Scheme 45).^{166, 167}



Scheme 45 – Attempted deprotection sequence

i) 1M LiOH, H₂O:THF (1:2), reflux, 24 h, decomposed; ii) 1M LiOH, H₂O₂, H₂O:THF (1:2), 23–70 °C, 18 h, decomposed; iii) LiI, EtOAc, reflux, 20 h, **E-126** recovered.

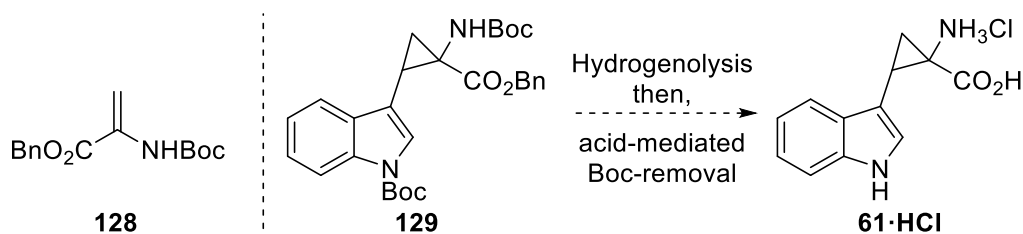
It was discovered that protected tryptophan **125** was not stable in basic solutions of lithium hydroxide at elevated temperature. A number of decomposition products were observed *via* TLC but not isolated and characterised. The unexpected difficulty in the saponification of esters **125** and **126** lead to the re-evaluation of the protecting group strategy.

Alternative Acrylate Protecting Group Strategy

The complications encountered during the deprotection of tryptophan **124** were due to the difficulty of removing the protecting groups from the acrylate **109** synthon. Therefore, an alternative acrylate protecting strategy was designed to enable facile deprotection.

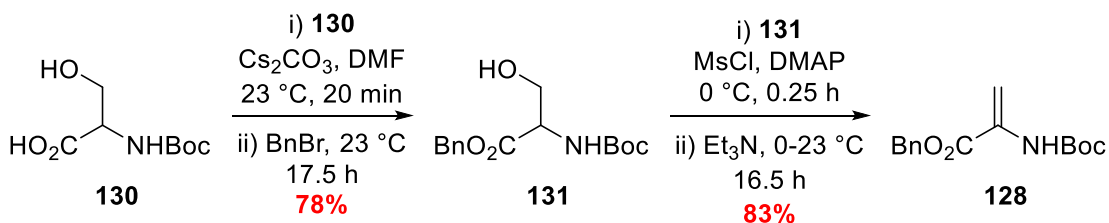
A global deprotection strategy was considered, however, due to the zwitterionic nature of amino acid product **61**, it was recognised that purification would present a significant challenge. Thus, an orthogonal deprotection strategy was seen as an attractive route, as it allows for the

more facile purification of the intermediates. Amino acrylate **128** was therefore designed with a simple two step deprotection sequence in mind (Scheme 46).



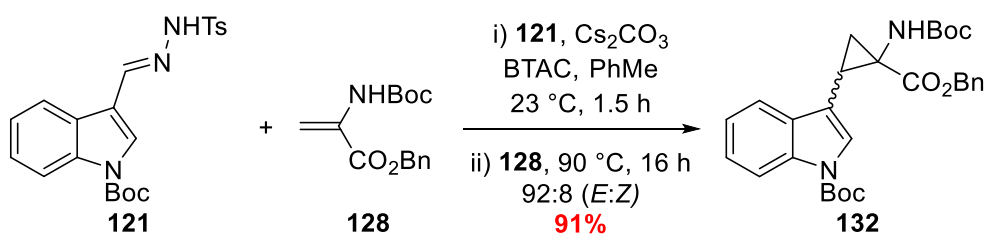
Scheme 46 – Novel amino acrylate **128** design and hypothesised deprotection sequence

The synthesis of amino acrylate **128** began with benzyl protection of *N*-Boc serine **130**, affording benzyl ester **131** in moderate yield. Mesylation of alcohol **131** was followed by a base-mediated elimination to give amino acrylate **128** in good yield (Scheme 47). Alternative routes to affect the elimination included a modified Mitsunobu reaction, however this resulted in poor product recovery and difficulty in removing triphenylphosphine oxide.¹⁶⁸



Scheme 47 – Synthesis of amino acrylate **128**

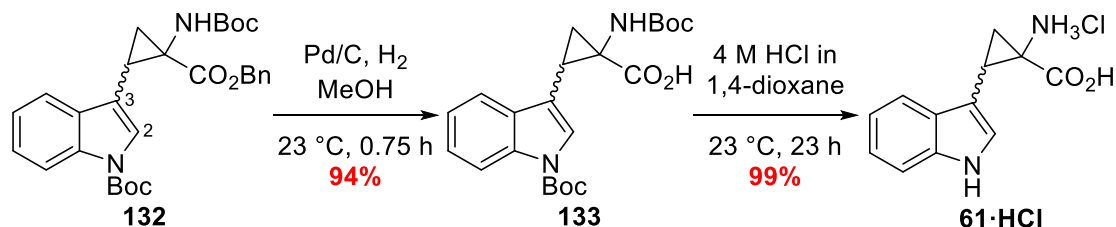
Amino acrylate **128** was then subjected to the Jiang one-pot cyclopropanation conditions, with *N*-Boc protected tosyl hydrazone **121** (Scheme 48).¹⁵⁴ The corresponding 1,2-methanotryptophan core **132** was accessed in an excellent yield and maintained a high diastereoselectivity for the *E*-isomer.



Scheme 48 – Synthesis of 1,2-methanotryptophan **132**

Attempts to remove the benzyl ester by hydrogenolysis lead to complete degradation of tryptophan **132**. Alternative hydrogenolysis catalysts (Pd/C, Pd(OH)₂ and PtO₂) and loading weights had little effect on circumventing the observed degradation. Based on literature precedent, the degradation of the starting material is likely the result of 2,3-double bond reduction in the indole ring.¹⁶⁹ Literature reports concerning the hydrogenolysis of benzyl esters in the presence of an indole ring use short reaction times to overcome the over-reduction of the indole 2,3-double bond.¹⁶⁹ Benzyl ester **132** was therefore subjected to Pd/C-catalysed

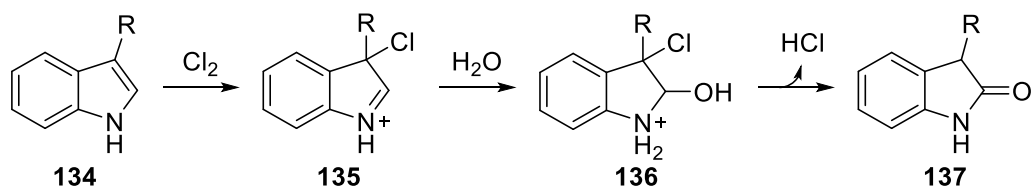
hydrogenolysis for 45 min and clean conversion to acid **133** was observed (Scheme 49). Dicarbamate **132** was treated with 4 M HCl in 1,4-dioxane to give the methanotryptophan **61·HCl** in excellent yield.



Scheme 49 – Deprotection of core **132** to give target compound **61·HCl**

Tryptophan analogue **61·HCl** was isolated as a red solid, which caused unexpected difficulties in its subsequent biological evaluation (Figure 22, *vide infra*). While the compound appeared to be spectroscopically pure, it was proposed that a spectroscopically undetectable quantity of a highly coloured impurity contaminated the sample and as a result was undetectable *via* $^1\text{H-NMR}$ analysis.

Various studies on the degradation of tryptophan in aqueous hydrogen chloride solutions suggest a chlorine-mediated oxidation to form oxindole species **137** (Scheme 50).^{170, 171} Chlorine is a common contaminant in hydrogen chloride solutions and is generated by prolonged exposure to air.¹⁷²

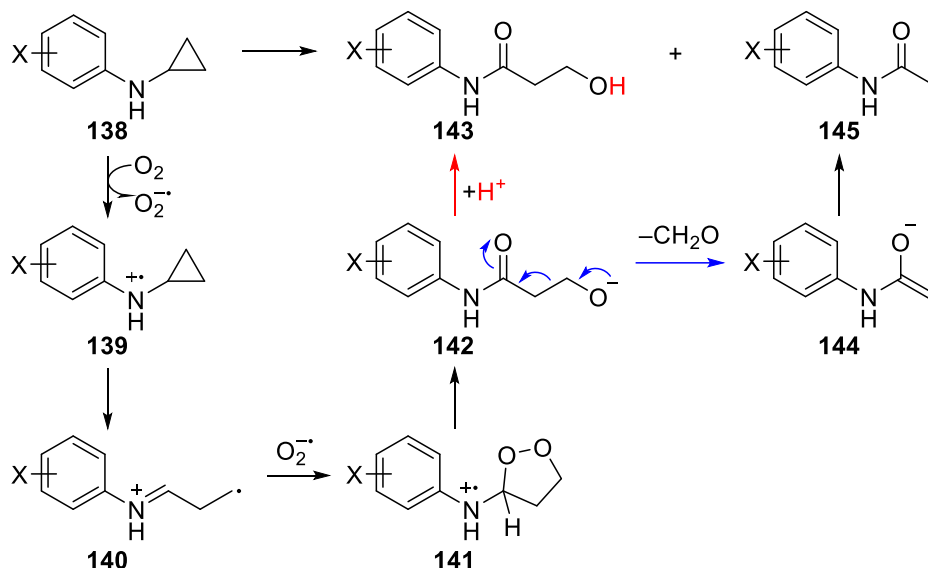


Scheme 50 – Chlorine-mediated oxidation of tryptophan ($R = \text{CH}_2\text{CHNH}_2\text{CO}_2\text{H}$)

The likelihood of tryptophan **61·HCl** degradation *via* a chlorine-mediated mechanism is unclear. The hydrogen chloride was stored under an atmosphere of argon, the reaction was carried out under an argon atmosphere and the reagent was dispersed within a dry, degassed organic solvent. Moreover, no evidence of a possible oxindole-derivative ($M_w = 232.2 \text{ g mol}^{-1}$) was detected by LC-MS analysis.

Other groups have noted the instability of substituted cyclopropylalanines under aerobic conditions – oxidising to form either acetamides or β -hydroxypropionamides (Scheme 51).¹⁷³ A mechanistic proposal for the air-mediated degradation of substituted cyclopropylalanines begins with the oxidation of amine **138** to radical cation **139** by molecular oxygen. A radical is now positioned in the α -position with respect to the cyclopropane and is primed for a radical ring-opening to form primary radical **140**. Reaction of this radical with a further equivalent of molecular oxygen gives radical cation aminodioxolane **141**. Loss of the α -proton, *via* unreacted

S.M./140 or molecular oxygen, sees the degradation of the dioxolane to alkoxide **142**. Alkoxide **142** can be protonated to give β -hydroxypropionamide **143** or undergo a retro-aldol reaction to give acetamide **145**.¹⁷³



Scheme 51 – Mechanistic proposal for the aerobic degradation of aryl cyclopropylamines¹⁷³

A similar mechanism can be envisaged for the degradation of the free amine of tryptophan analogue **61·HCl**. However, this oxidation pathway is unlikely as **61** was present as a hydrochloride salt and no observable degradation was seen by 1H -NMR analysis. It also remains unclear how this degradation could lead to such a marked change in colour.

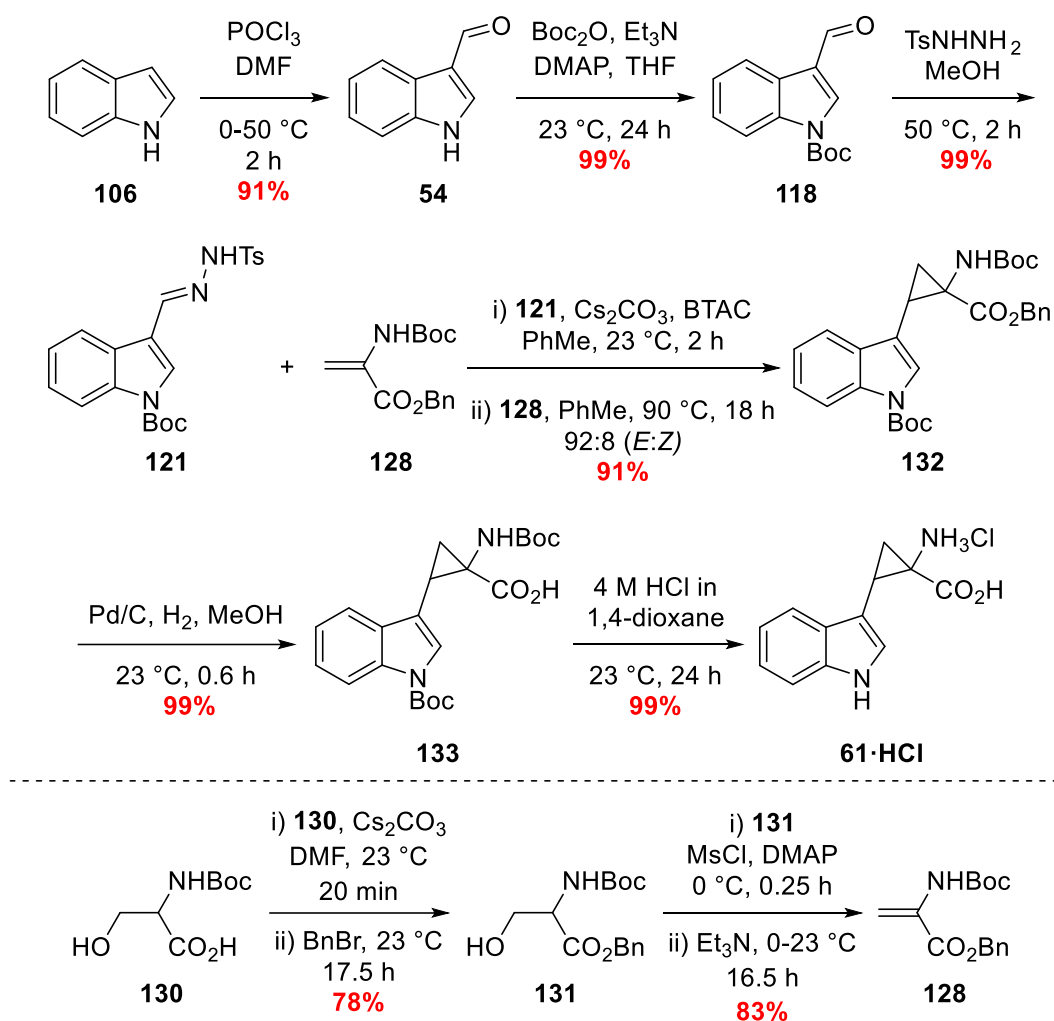
Preparative HPLC was performed to ascertain whether tryptophan **61·HCl** could be separated from the unidentified red impurity. As fractions eluted, aliquots were collected and analysed *via* LC-MS; the fractions containing the desired mass peak ($M_w = 216.5 \text{ g mol}^{-1}$) eluted as colourless solutions. Upon concentration of the compound containing fractions, a red colouration appeared as soon as the concentrated material was exposed to air.

Due to the hitherto unreported instability of **61·HCl** in aerobic conditions, further synthetic optimisations were halted to focus on the synthesis of alternative substrate mimics.

Summary: Synthesis of 1,2- Δ -Tryptophan Analogue **61**

A novel route to 1,2- Δ -tryptophan **61·HCl** was developed which avoided the use of harsh reagents such as diazomethane to install the cyclopropane ring. A novel indolo-diazo species was generated *in situ*, implementing chemistry developed by Aggarwal and Jiang, and reacted *via* a 1,3-dipolar cycloaddition with a novel acrylate **128**.^{145, 154} The discussed synthesis of **61·HCl** far surpassed the literature report in terms of overall yield of tryptophan analogue **61·HCl** (this synthesis, 76%, Donati's synthesis, 4%). The red colouration of tryptophan **61·HCl**

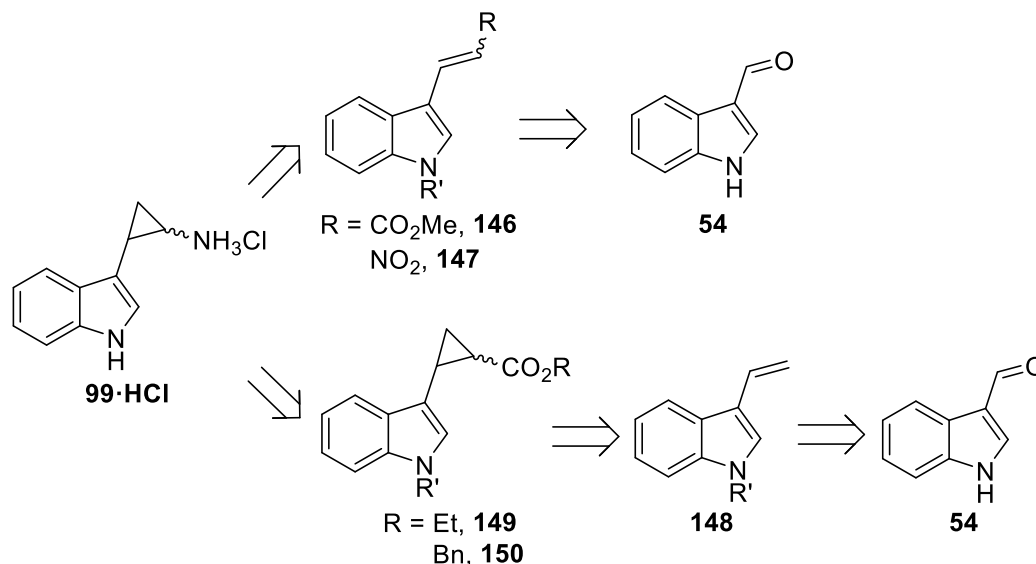
was a result of mild instability to aerobic conditions. Only a small amount of the degradation product was formed and thus was unidentifiable by $^1\text{H-NMR}$ spectroscopy. No mass ions or fragments corresponding to hypothesised degradation products were identified upon MS analysis. The colouration of tryptophan **61·HCl** proved to be troublesome when evaluating its activity (Figure 22, *vide infra*). Despite issues with the instability of **61**, this synthesis remains a marked improvement over the literature route (Scheme 52).



Scheme 52 – Summary of 1,2- Δ -tryptophan analogue **61·HCl** synthesis

1.5.2 – Synthesis of 1,2- Δ -Tryptamine Analogue **99**

IDO1 is known to have a broad substrate scope and is able to metabolise numerous indole-containing substrates.⁹ Therefore, an alternative cyclopropane-containing indole was targeted for synthesis – 1,2- Δ -tryptamine **99·HCl** (Scheme 53).



Scheme 53 – Retrosynthetic analysis of tryptamine analogue **99·HCl**

Access to tryptamine analogue **99·HCl** was envisaged in two ways: cyclopropanation of an α,β -unsaturated system or metal-catalysed cyclopropanation of a terminal olefin. Substrates for the cyclopropanation of an α,β -unsaturated system were identified as α,β -unsaturated esters **146** and nitro **147**, whereas 3-vinyl indole **148** was identified as a suitable terminal olefin for metal-catalysed cyclopropanation.

Ester **146** would be accessed *via* a Horner-Wadsworth-Emmons (HWE) olefination. Judicious choice of reagents when synthesising ester **146** allows for access to either *E*- or *Z*-isomer; trimethyl phosphonoacetate leads to *E*-enriched mixtures while the Still-Gennari modification gives *Z*-selective olefination.¹⁷⁴ The ability to selectively access *E*- and *Z*- α,β -unsaturated esters was seen as a particular advantage of this route as it allows the synthesis of diastereomerically-enriched mixtures of the respective cyclopropane-containing cores.

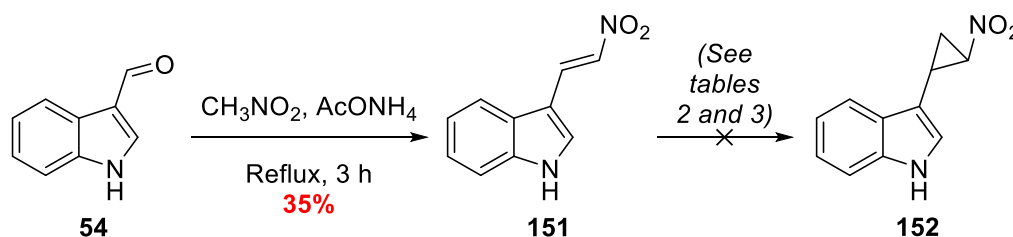
To access α,β -unsaturated nitro compound **147**, a one-pot nitro aldol-dehydration was proposed, which was expected to give a mixture of configurational isomers. Separation of the two isomers by flash column chromatography was envisaged. The α,β -unsaturated ester **146** and nitro **147** would be subjected to cyclopropanation conditions, installing the core cyclopropane ring. For ester **146**, cyclopropanation would be followed by hydrolysis and then

functional group interconversion *via* a Curtius rearrangement to afford the desired amine **99·HCl**. For the nitro **147**, reduction of the nitro group would give access to amine **99·HCl**.

Alternatively, starting from aldehyde **54**, a Wittig olefination would be performed to access vinylogous enamine **148**. Olefin **148** would then be subjected to a copper- or rhodium-catalysed cyclopropanation with ethyl or benzyl diazoacetate to give cyclopropyl ester **149** or **150**.^{175, 176} Final de-esterification followed by a Curtius rearrangement would access tryptamine analogue **99·HCl**.

Nitro Aldol Route

Starting with aldehyde **54**, a nitro aldol was performed using nitromethane and ammonium acetate to access the corresponding α,β -unsaturated nitro **151** (Scheme 54).¹⁷⁷ The reaction proceeded with poor isolated yield and the product was remarkably insoluble in standard organic solvents, increasing the difficulty of isolation and purification. Eventually pure **151** was accessed *via* recrystallisation from hot dichloromethane.



Scheme 54 – Nitro aldol and subsequent cyclopropanation attempts

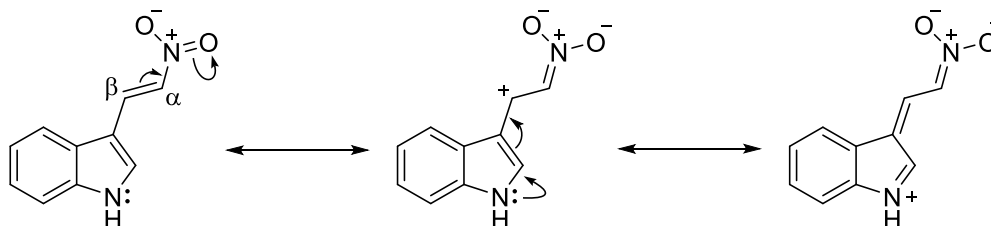
With α,β -unsaturated nitro in hand, a Corey-Chaykovsky cyclopropanation was attempted (Scheme 54).¹⁷⁸ After an initial failure, reaction temperatures were reduced and addition rates of nitroalkene **151** to the ylide mixture were slowed – however after 3 attempts, no productive outcome was observed (Table 2).

Table 2 – Corey-Chaykovsky conditions

Entry	Conditions	Result
1	(Me) ₃ SOI, DMSO, NaH, 23 °C, 19 h	151
2	(Me) ₃ SOI, DMSO, NaH, 0-23 °C, 24 h	151
3	(Me) ₃ SOI, DMSO, NaH, 23 °C, 12 h (addition of 151 over 1 h)	151

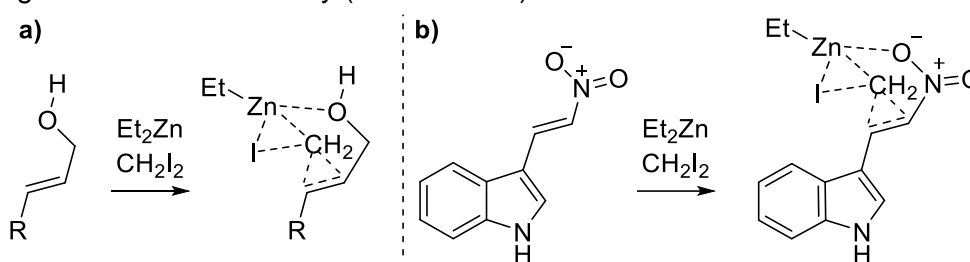
Mechanistically, the Corey-Chaykovsky relies on 1,4-addition to the α,β -unsaturated system – for this to occur, the β -carbon must be sufficiently electrophilic.¹⁷⁸ For α,β -unsaturated nitro **151**, electron donation from the indole amine into the conjugated system would increase the electron density on the β -carbon, thus reducing the ability for nitroalkene **151** to participate in

conjugate addition. This effect can be envisaged by considering the resonance structures that contribute toward the overall π -electronic distribution in indole **151** (Scheme 55).



Scheme 55 – The rationale for reduced electrophilic character of the β -carbon of Indole **151**

Following on from the failed cyclopropanation, an alternative cyclopropanation was attempted that is mechanistically distinct from the Corey-Chaykovsky reaction: the Simmons-Smith reaction. Allylic alcohols can facilitate the Simmons-Smith cyclopropanation *via* chelation to the zinc-carbenoid intermediate, guiding the methylene toward the olefin (Scheme 56b). In nitroalkene **151**, the vinylogous nitro group places an oxygen in a comparable position, suggesting this could aid reactivity (Scheme 56b).



Scheme 56 – Hypothesised directing effect of the nitro group

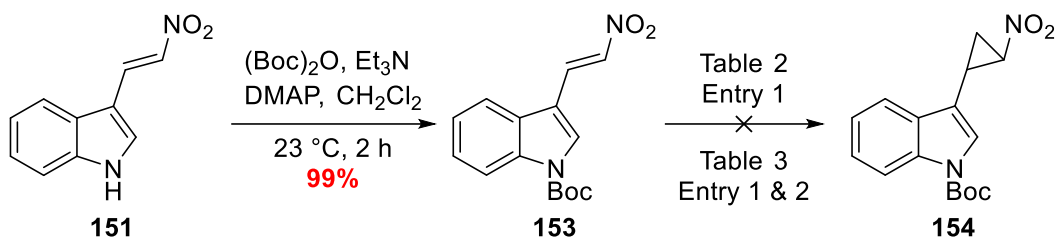
Despite the potential for directing effects, initial attempts to cyclopropanate nitroalkene **151** failed under Simmons-Smith conditions, returning starting material upon work-up (Table 3, Entry 1). Replacing the iodide ligand of the active reagent with a strongly electron-withdrawing group, such as trifluoroacetate, has been reported to give better yields of cyclopropanes in systems with no directing group present.¹⁷⁹ These conditions were replicated on nitro alkene **151** to no avail, suggesting the perturbed electron distribution of the double bond, as a result of the nitro group, was sufficient to prevent reactivity (Table 3, Entry 2).

Table 3 – Attempted Simmons-Smith conditions

Entry	Conditions	Result
1	Et ₂ Zn, CH ₂ I ₂ , CH ₂ Cl ₂ , 0-23 °C, 1.5 h	151
2	Et ₂ Zn, F ₃ CCO ₂ H, CH ₂ I ₂ , CH ₂ Cl ₂ , 0 °C, 5 h	151

In an attempt to overcome the poor solubility and reactivity toward the cyclopropanation conditions, indole **151** was reacted with di-*tert*-butyl dicarbonate to give Boc-protected species **153** (Scheme 57). Boc-protected indole **153** demonstrated improved solubility in a range of standard organic solvents. However, the *N*-protection of the indole amine did not facilitate the

Corey-Chaykovsky or Simmons-Smith cyclopropanation reactions (Conditions attempted: Table 2, Entry 1; Table 3, Entry 1 and 2).



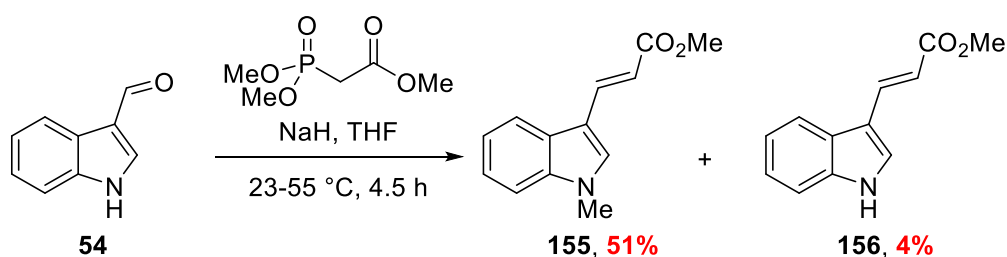
Scheme 57 – *N*-Boc protection and subsequent cyclopropanation attempts

There is little evidence within the literature to suggest that α,β -unsaturated nitro compounds are good substrates for Corey-Chaykovsky cyclopropanations, with most examples proceeding with very poor yields.¹⁸⁰ To date, there is no supporting literature for the cyclopropanation of an α,β -unsaturated nitro compound under Simmons-Smith conditions.

Horner-Wadsworth-Emmons Route (HWE)

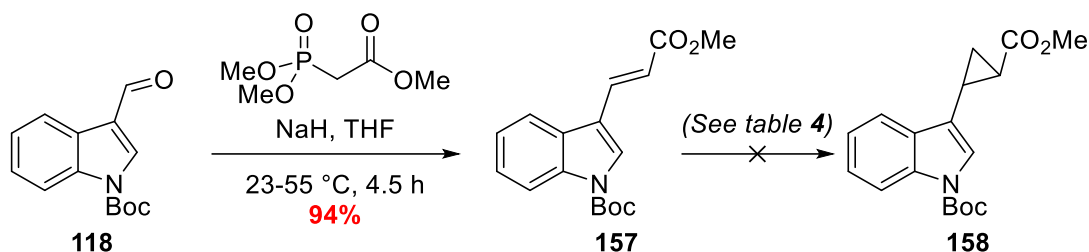
Whilst evaluating the nitro aldol route, a concurrent investigation into the HWE-based preparation of tryptamine **99·HCl** was undertaken.

When subjecting aldehyde **54** to trimethyl phosphonoacetate and base, it became apparent that a protecting group on the indole amine was required. The olefination proceeded with significant methylation of the indole amine, giving *N*-methylated ester **155** as the major product (Scheme 58). The *N*-methylated product is thought to be a result of excess NaH deprotonating the indole amine, followed by subsequent attack of electrophilic methoxy-groups of either the phosphonoacetate or dimethyl phosphate. An analogous methylation can be observed in the action of dimethyl sulfate.¹⁸¹



Scheme 58 – Initial HWE reaction attempt

Subsequent reaction of Boc-protected aldehyde under the HWE conditions proceeded to afford the pure α,β -unsaturated ester **157** in excellent yield, with no need for further purification (Scheme 59).



Scheme 59 – HWE reaction of Boc-protected indole **118**

The resulting α,β -unsaturated ester was then subjected to both the cyclopropanation conditions. The first attempted Corey-Chaykovsky conditions returned only starting material (Table 4, Entry 1). Elevating the temperature had little effect on the reaction and the starting material was recovered after 18 h at 70 °C (Table 4, Entry 2). Standard Simmons-Smith conditions with no additives did not afford the cyclopropyl ester **158** and starting material was recovered quantitatively (Table 4, Entry 3). Use of the additives trifluoroacetic acid and nickel(II) chloride also failed to provide the desired product (Table 4, Entries 4 and 5).^{179, 182}

Table 4 – Attempted cyclopropanation conditions

Entry	Conditions	Result
1	(Me) ₃ SOI, DMSO, NaH, 23 °C, 21 h	157
2	(Me) ₃ SOI, DMSO, NaH, 70 °C, 18 h	157
3	Et ₂ Zn, CH ₂ I ₂ , CH ₂ Cl ₂ , 23 °C, 4 h	157
4	Et ₂ Zn, F ₃ CCO ₂ H, CH ₂ I ₂ , CH ₂ Cl ₂ , 0 °C, 3 h	157
5	Et ₂ Zn, NiCl ₂ (2 mol%), CH ₂ I ₂ , CH ₂ Cl ₂ , 40 °C, 1.5 h	157

A trend of poor isolated yields of Corey-Chaykovsky cyclopropanations can be found within the literature when the α,β -unsaturated ester is appended to an electron rich aromatic system.^{183, 184} Interestingly, cyclopropanation of benzylidenemalonates has been demonstrated to withstand a variety of electron-withdrawing and donating groups on the aromatic ring.¹⁸⁵⁻¹⁸⁷ The increased tolerance to electronic perturbation of the aromatic ring is probably a result of the increased electron-withdrawing capacity of the malonate and the resonance stabilisation of the negative charge after the initial 1,4-addition.

Metal-catalysed Cyclopropanations of Terminal Olefins

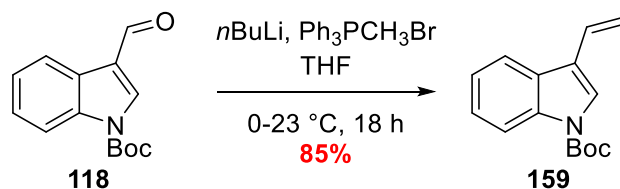
A lack of reactivity of the α,β -unsaturated ester and nitro compounds toward the cyclopropanations prompted the investigation of metal-catalysed cyclopropanations.

Fortuitously, preparations of aryl cyclopropylesters from terminal olefins and diazoacetates have been well documented.^{149, 188, 189}

To access the desired olefin, a Wittig olefination would be performed to methylenate 3-formyl indole. *N*-methylated and non-protected 3-vinyl indoles are liable to significant dimerisation under ambient conditions owing to the electron-donating ability of the indole nitrogen.^{190, 191} Protection of the indole nitrogen with electron-withdrawing groups can be utilised to temper the nucleophilicity of 3-vinyl indoles.¹⁹⁰ As such, an *N*-Boc protecting group would be installed to give aldehyde **118** as the starting substrate for the Wittig methylenation.¹⁹⁰

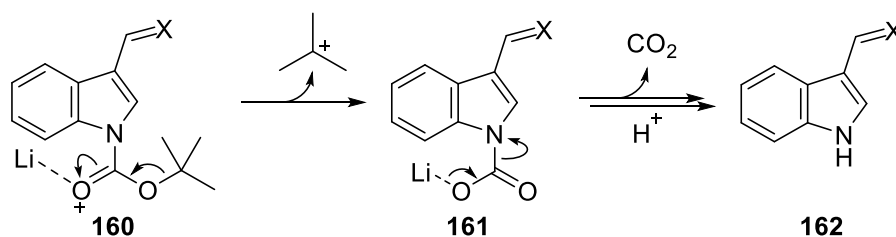
Wittig Olefination Optimisation

Using methyl triphenylphosphonium bromide as the ylide precursor with *n*-butyllithium as the base, the Wittig olefination proceeded to give cyclopropanation precursor **159** in good yield (Scheme 60).



Scheme 60 – Wittig olefination of aldehyde **118**

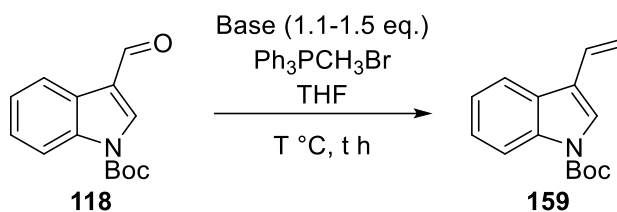
Subsequent olefinations were subject to large variations in isolated yield. Analysis of the crude ¹H-NMR of the methylenation reactions identified the major by-product of the reaction as *N*-Boc deprotected vinyl indole. The *N*-Boc deprotection was rationalised in part through Lewis acid activation by the lithium salts present; chelation of the lithium cation to the carbamate carbonyl could promote the loss of the stabilised *tert*-butyl cation to give lithium carbamate **161**. Spontaneous degradation of carbamic acid **161** affords CO₂ and *N*-deprotected indole **162** (Scheme 61). Other groups have noticed such phenomenon when using *n*BuLi-mediated Wittig olefinations but have not made comment on the rationale.¹⁹²



Scheme 61 – Lithium-mediated *N*-Boc deprotection (*X* = O or CH₂)

By extending the reaction time, higher yields were favoured (Table 5, Entries 1 and 2). Further attempts contradicted these observations when a reaction time of 1.5 h gave a 65% yield (Table 5, Entry 3). In response to literature reports detailing similar preparations, the temperature of the reaction was reduced to 0 °C which in 3 h gave a moderate recovery of **159**

(Table 5, Entry 4).^{193, 194} Reaction temperatures of $-78\text{ }^{\circ}\text{C}$ lead to further increases in the yield until the optimum reaction conditions of $-78\text{ }^{\circ}\text{C}$ for 5.5 h afforded the desired olefin in a 92% yield (Table 5, Entries 5-7).



Scheme 62 – Optimisation of the Wittig olefination

Table 5 – Optimisation of the *n*BuLi-mediated Wittig olefination

Entry	Base eq.	T/ $^{\circ}\text{C}$	t/h	159 yield
1	1.5	0–23 ^a	21	77%
2	1.5	0–23 ^a	16	56%
3	1.5	0–23 ^a	1.5	65%
4	1.2	0	3	53%
5	1.1	-78	3.5	76%
6	1.1	-78	5	78%
7	1.1	-78	5.5	92%

^a Reaction mixtures were left in the ice/water baths until they had warmed to a consistent temperature ($\sim 14\text{--}16\text{ }^{\circ}\text{C}$) and then the reaction mixtures were removed from the bath and allowed to warm to $23\text{ }^{\circ}\text{C}$.

To ascertain whether the hypothesis of the lithium salt-promoted Boc-deprotection of the desired compound was valid, alternative bases for the olefination were investigated. Bases were selected on account of their cation's Lewis acidity; as such, the bases sodium hydride, sodium hexamethyldisilazide and potassium hexamethyldisilazide were identified as suitable reagents (Table 6).

A first attempt using sodium hydride proceeded in relatively poor yield in comparison to *n*BuLi (Table 6, Entry 1). The yield was not suitable for a sustainable synthetic route, however, no *N*-Boc deprotected **159** was observed in the analysis of the $^1\text{H-NMR}$ of the crude reaction mixture. It was suspected that the use of a heterogeneous base could have been a limiting factor in the deprotonation of the phosphonium salt to form the reactive ylide. Use of the homogenous base NaHMDS saw an unexpectedly large reduction in recovered **159** (Table 6, Entry 2). By TLC, aldehyde **118** was not completely consumed and the reduced isolated yield

was later attributed to the incorrect titre of the NaHMDS solution. A solution of KHMDS, of known titre, was used and gave a near quantitative yield of olefin **159** (Table 6, Entry 3). The KHMDS olefination gave repeatable yields of >90% with no *N*-Boc deprotection observed; as such, KHMDS was selected as the optimum base for the olefination.

Table 6 – Wittig optimisations using non-lithium-containing bases

Entry	Base	eq.	T/°C	t/h	159 yield
1	NaH	1.5	0–23 ^a	22	48%
2	NaHMDS	1.5	–78–23	6	9%
3	KHMDS	1.1	–78	6	98%

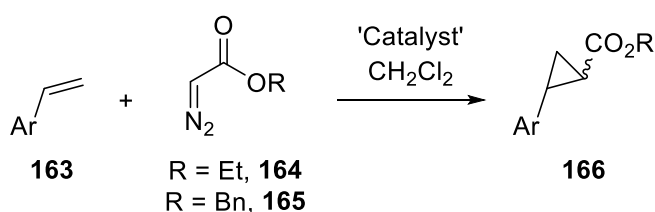
^a Reaction mixtures were left in the ice/water baths until they had warmed to a consistent temperature (~14–16 °C) and then the reaction mixtures were removed and allowed to warm to 23 °C.

The observed trend of no *N*-Boc deprotection when utilising bases with less Lewis acidic cations does not substantiate the hypothesis that lithium bromide was the cause of Boc-deprotection. Precedent within the literature reports the use of lithium bromide in the mono-Boc deprotection of di-Boc-protected amines only.¹⁹⁵

In order to validate whether lithium bromide was capable of Boc-deprotection, *N*-Boc formyl indole **118** was subjected to a solution of LiBr (1.2 eq) in anhydrous THF for 24 h at 23 °C – no subsequent *N*-Boc deprotection was observed. The result of the control experiment suggested the reasons for concomitant *N*-Boc deprotection are more nuanced than the Lewis acidity of the salts present, however investigation into such phenomenon was beyond the scope of the current investigation.

Cyclopropanation of a Terminal Olefin

Installing the key cyclopropane was envisaged to occur *via* a metal-mediated carbene addition across the double bond. Stable diazo sources, such as ethyl and benzyl diazoacetate, have been previously utilised in the synthesis of aryl cyclopropylesters in the presence of copper or rhodium salts (Scheme 63).^{176, 188, 196}



Scheme 63 – General scheme for metal-mediated cyclopropanation of aryl-olefins

Due to the possible cost implication and availability of rare transition metals, an initial procedure utilising copper(II) acetylacetonate (Cu(acac)₂) in the presence of phenylhydrazine

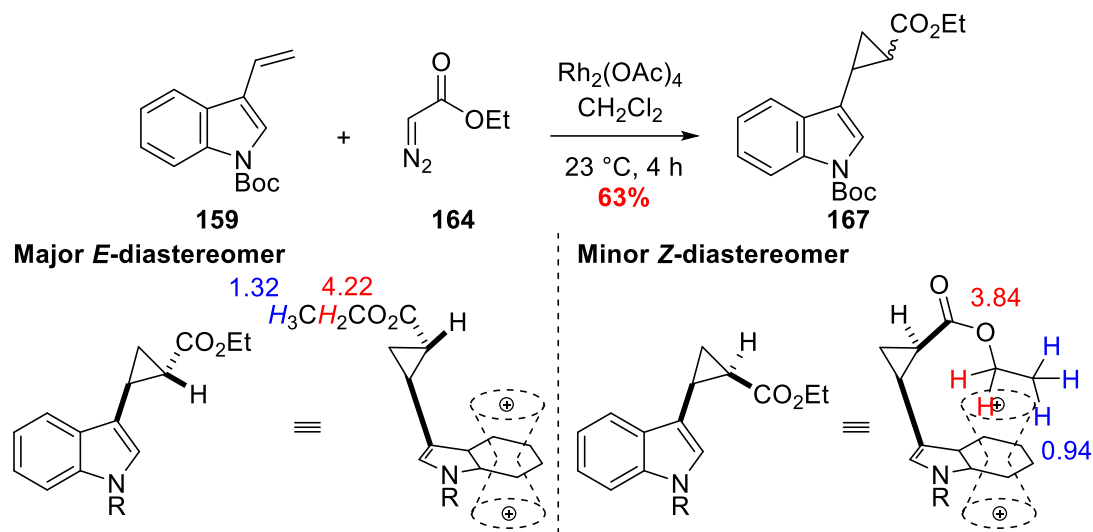
was attempted.¹⁰⁷ The catalyst and phenylhydrazine were refluxed in CH₂Cl₂, prior to addition of olefin **159**; diazoacetate **164** was added over a period of 1 hour. No reaction progress was observed through TLC analysis, and was later confirmed by the recovery of starting olefin **159**.

For a successful cyclopropanation, the copper salt must be reduced to an active oxidation state, Cu(I), and a copper-carbeneoid must form between the Cu(I) and diazoacetate **164**. A literature report of the copper-catalysed cyclopropanation noted the formation of a dark blue solution upon refluxing phenylhydrazine and Cu(acac)₂ in CH₂Cl₂, indicating the *in-situ* reduction by phenylhydrazine to Cu(I).¹⁹⁷ No such observation was made through the time course of this reaction, thus it was proposed that the active Cu(I) species did not form and consequently no copper-carbeneoid species.

In concurrent experiments, a method that employed the more expensive catalyst dirhodium tetraacetate was trialled with diazoacetate **164**. The cyclopropanation proceeded in good yield, affording cyclopropane **167** as a mixture of separable diastereomers in a 56:44 *E:Z* ratio. The isolated quantities of each isomer did not reflect the true d.r. due to isomer co-elution (Scheme 64).

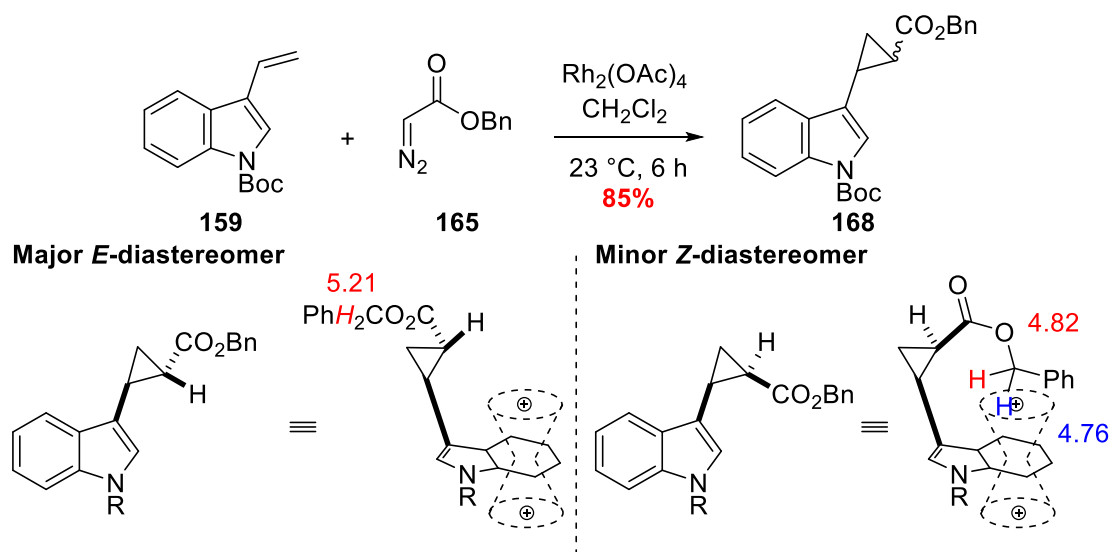
To determine the relative stereochemistry of the diastereomers, differences in chemical shifts between the ethyl-protons of the major and minor diastereomers were analysed. Unfortunately, the relative stereochemistry could not be identified by analysis of the ³*J*-coupling due to stacked resonances that prevented the accurate determination of the coupling constants.

Higher chemical shifts for both CH₂ and CH₃ resonances in the major diastereomer are observed compared to the minor diastereomer – inferring the major isomer is the *E*-isomer (Scheme 64). The minor *Z*-isomer's methylene protons are also non-equivalent, suggesting an interaction with the induced magnetic field from the indole, which renders the two protons magnetically inequivalent.



Scheme 64 – Cyclopropyl-ethyl-ester synthesis and diastereomer rationalisation ($R = \text{Boc}$)

Benzyl diazoacetate **165** was subjected to the rhodium-catalysed cyclopropanation, affording the corresponding cyclopropyl benzyl ester **168** in very good yield (Scheme 65). A 55:45 *E*:*Z* mixture was calculated by $^1\text{H-NMR}$ analysis of the crude product through the relative integrals of the benzyl proton. However, due to the two diastereomers possessing similar polarity, separation of the two diastereomers was not possible by chromatography. The major diastereomer's benzylic CH_2 protons are not shielded by the aromatic system and, as such, display a more downfield resonance in comparison to the minor diastereomer. The further downfield shifted resonance of the benzylic CH_2 protons infers an *E*-configuration. Additionally, the minor diastereomer benzylic CH_2 protons – due to their interaction with the aromatic system's electron density – are diastereotopic, displaying an AB-coupling pattern. Combined with an upfield chemical shift, relative to the major diastereomer, the data is consistent with the minor diastereomer having a *Z*-configuration (Scheme 65).



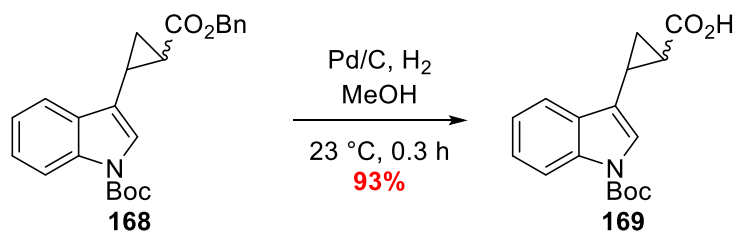
Scheme 65 – Cyclopropyl-benzyl-ester synthesis and diastereomer rationalisation ($R = \text{Boc}$)

The observed d.r. in the above cyclopropanations is a direct result of substrate steric effects, with the catalyst having little to no influence on the diastereomeric outcome of the reaction.¹⁹⁸ Asymmetric catalysts have been reported but their exploration was unimportant to the work at this stage.^{149, 176}

Benzyl- and Ethyl-ester Deprotections

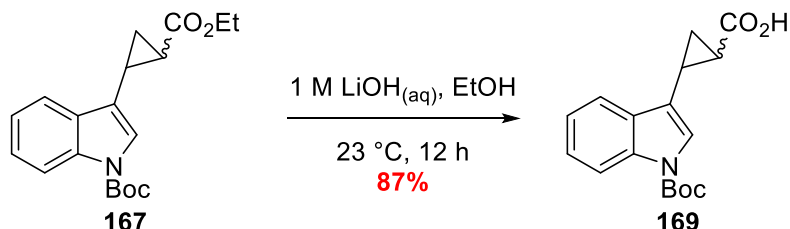
To access tryptamine analogue **99·HCl**, de-esterification of ethyl ester **167** and benzyl ester **168** must take place to provide access to the required acid precursor **169** prior to the Curtius rearrangement.

Hydrogenolysis of benzyl ester **168** initially suffered a analogous over-reduction issue experienced in the deprotection of tryptophan analogue **132**; exposure to hydrogen in the presence of a palladium or platinum source lead to complete decomposition of the starting material. Similar to tryptophan benzyl ester **132**, the over-reduction issue was overcome by shortening the reaction time to 20 minutes, affording the corresponding acid **169** in excellent yield (Scheme 66).



Scheme 66 – Hydrogenolysis of benzyl-ester **168**

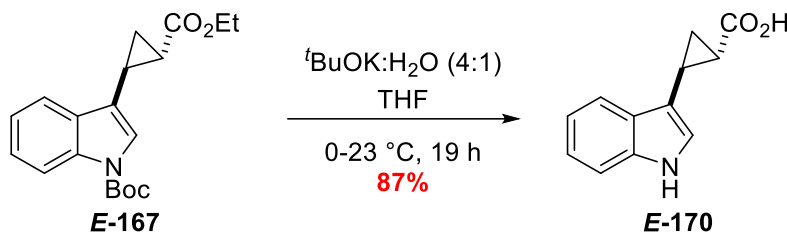
Attempts to saponify ethyl ester **167** in a methanolic solution of sodium hydroxide unexpectedly lead to the degradation of the starting material with no desired product detected *via* ¹H-NMR. An aqueous solution of lithium hydroxide in ethanol was then attempted. Fortunately, no Boc-deprotection was observed and clean cyclopropyl-acid **169** was isolated after an acid/base work-up procedure (Scheme 67).



Scheme 67 – Saponification of ethyl-ester **167**

It was later discovered that a global deprotection of cyclopropyl-ester **E-167** could be achieved by treatment with a 4:1 mixture of potassium *tert*-butoxide and water in anhydrous THF (Scheme 68). Initially this experiment was run as an alternative de-esterification to the lithium

hydroxide-mediated hydrolysis – however upon work-up and subsequent $^1\text{H-NMR}$ analysis of the crude reaction mixture, concomitant removal of the indole *N*-Boc group was evident.



Scheme 68 – Global deprotection of cyclopropyl-ester **E-167**

The authors of this protocol hypothesised that the combination of potassium *tert*-butoxide and water, in an anhydrous ethereal solvent, gives rise to a ‘relatively unsolvated’ hydroxide ion – dubbing it an ‘anhydrous hydroxide’ source.^{199, 200} Through isotopic labelling studies, the hydrolysis was demonstrated to proceed *via* a $\text{B}_{\text{Ac}2}$ mechanism and was capable of hydrolysing sterically encumbered esters and tertiary amides. Boc-deprotection *via* $\text{B}_{\text{Ac}2}$ -type reactivity is seldom seen due to the reduced electrophilicity of the carbamate carbonyl and the steric bulk imposed by the *tert*-butyl group. Aromatic carbamates, such as indole carbamates, can be viewed as more electrophilic due to the delocalisation of the nitrogen lone-pair into the ring system. Based on the currently available literature, the observed deprotection remains a rare anomaly within the chemical literature, with many examples of indole Boc-carbamates surviving aqueous hydrolysis conditions at room temperature.²⁰¹⁻²⁰³ Unsurprisingly, *N*-Boc deprotection is observed when refluxing aromatic *N*-Boc protected compounds in basic solutions.^{204, 205}

The combination of a relatively unsolvated hydroxide ion and an electrophilic carbamate carbonyl could therefore account for the observed Boc-deprotection of carbamate **167**.

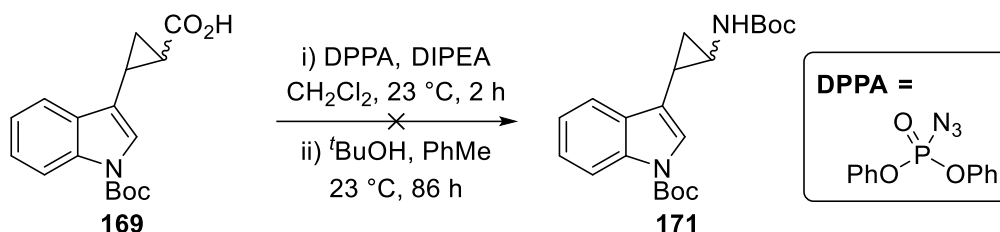
Functional Group Interconversion via the Curtius Rearrangement

With acids **169** and **170** in hand, the next step in the synthesis was to perform a Curtius rearrangement and access the carbamate-protected derivative of tryptamine **171**.

Traditionally the Curtius rearrangement relies on the use of very toxic reagents to prepare the intermediate acyl azide – particularly sodium azide.²⁰⁶ Advances in safer azide sources lead to the development of diphenylphosphoryl azide (DPPA) – a reagent that allows the direct conversion of carboxylic acids to acyl azides.²⁰⁷

Acid **169** was subjected to a solution of DPPA and Hünig’s base in dichloromethane and the reaction was tracked by TLC and IR analysis (Scheme 69). After 2 h no progress was observed by TLC, and determining the formation of the acyl azide by IR was inconclusive as the sample was likely to still contain DPPA. After refluxing the sample in a solution of $^t\text{BuOH}$ in toluene,

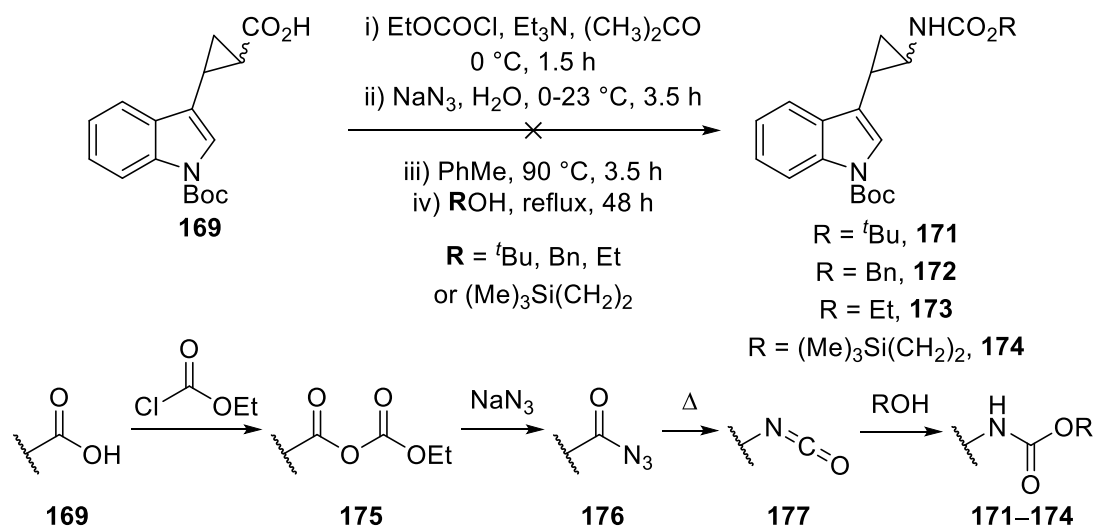
no Boc-protected amine **171** was observed by $^1\text{H-NMR}$ analysis of the crude reaction mixture. A complex mixture of products was observed by TLC which could potentially be attributed to the various possible Boc-thermolysis products. To ascertain whether this was the case, the crude reaction mixture was subjected to Boc-protection conditions and the resulting products were purified by flash column chromatography.¹⁶⁵ No cyclopropyl carbamate **171** was isolated from this mixture, indicating the failure of the DPPA-mediated Curtius rearrangement.



Scheme 69 – Modified Curtius rearrangement attempt

Further attempts at the Curtius rearrangement utilised the protocol developed by Overman.²⁰⁸ While Overman's route consisted of a more involved synthetic sequence, it permitted the simple tracking of each reaction intermediate *via* IR or $^1\text{H-NMR}$ spectroscopy.

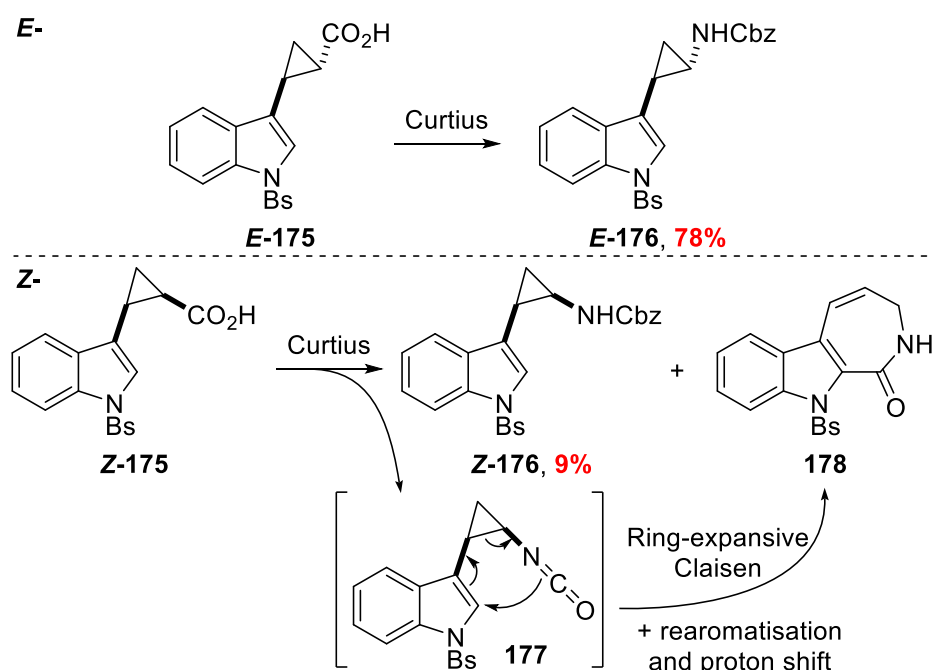
Acid **169** was subjected to a basic solution of ethyl chloroformate to give acyl carbonate **175** – an intermediate that was easily detected by TLC and IR analysis. Treatment of acyl carbonate **175** with sodium azide saw the facile formation of acyl azide **176** which was identified by its characteristic IR-stretching frequency ($2160\text{--}2120\text{ cm}^{-1}$)²⁰⁹ which was followed by a solvent switch to toluene. Heating of the aromatic solution instigated the thermal rearrangement of acyl azide **176** to isocyanate **177**. The isocyanate intermediate **177** was identified from IR by a subtle change in the stretching frequency from the azide ($2280\text{--}2230\text{ cm}^{-1}$).²⁰⁹ However, subsequent trapping of isocyanate **175** with a variety of alcohols appeared to be problematic, and no corresponding carbamate was isolated from any of the reactions (Scheme 70). With the potential thermal instability of the isocyanate in mind, a mild method for isocyanate trapping with an alcohol was attempted.²¹⁰ Isocyanate **177** was isolated and re-solubilised in a solution of Cu(I)Cl and BnOH in DMF, then stirred at $23\text{ }^\circ\text{C}$ for 7 h. TLC analysis of the reaction mixture indicated the formation of multiple reaction products. Only trace quantities of a cyclopropane-containing product was isolated as a mixture from flash column chromatography, suggesting the majority of material degraded under the reaction conditions or had only formed in small quantities. Cyclopropyl-acid **170** was also subjected to Overman's Curtius rearrangement conditions and also failed to give the desired product.



Scheme 70 – Attempted synthesis of **171–174** via Overman's Curtius modification

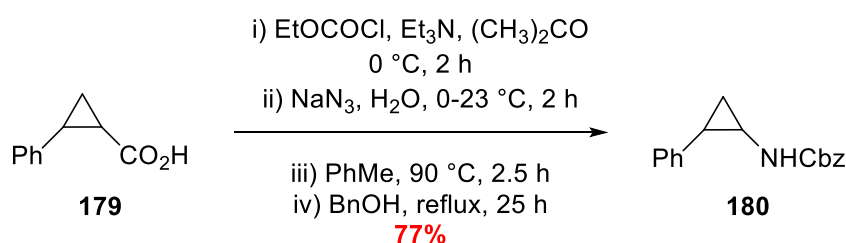
The reported syntheses of tryptamine analogue **99** comment on the intrinsic instability of the electron-rich aryl cyclopropyl amine – noting that the molecule darkened quickly on standing, even under refrigeration, and had to be shielded from light.²¹¹⁻²¹³

Eftink observed differing reactivities of the *E*- and *Z*-diastereomers of the Curtius precursors **E-175** and **Z-175** (Scheme 71). For the *E*-diastereomer, a clean rearrangement was observed giving carbamate **E-176** in good yield. However, subjecting **Z-175** to the Curtius conditions gave a mixture of products; only 9% of **Z-176** was isolated with a major by-product identified as the Claisen rearrangement product **178**. On standing in air, both *E*- and *Z-176* degraded within 24 h.²¹³



Scheme 71 – Eftink's differing Curtius outcomes for the *E*- and *Z*-diastereomers

The instability of the resulting carbamates, and the propensity for the *Z*-diastereomer to undergo the ring-expansive Claisen rearrangement, likely contributed toward the failure of these reactions. Based on literature precedent, it was hypothesised that a cyclopropane with a 1,2-arrangement of an electron-rich aromatic substituent and an electron deficient carbamate is sufficient to polarise the C-C bond, making it susceptible to nucleophilic attack. The polarisation of cyclopropanes by electron-donating and withdrawing groups is a known phenomenon as has been utilised extensively in the synthesis of carbo- and hetrocycles.²¹⁴ To confirm the substrate was not a suitable candidate for the Curtius rearrangement, a test reaction with an *E/Z*-mixture of phenyl-cyclopropyl-acid **179** was conducted (Scheme 72). The test reaction proved a success, giving a mixture of *E/Z*-carbamate **180** in good yield – suggesting indole cyclopropyl-acids are not viable candidates for the Curtius rearrangement.

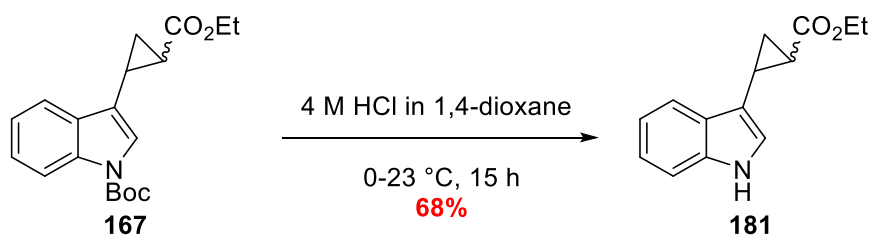


Scheme 72 – Test Curtius rearrangement

Cyclopropyl Ethyl Ester **181**

As a result of the observed instability of the arylcyclopropylamine, and the potential limitations of the compounds ability to serve as a viable mechanistic inhibitor, further attempts to synthesise tryptamine analogue **99-HCl** were abandoned. However, an intermediate along the synthesis route presented itself as a valuable target for isolation; *N*-Boc deprotected indole **181** serves as a close structural analogue to targeted tryptamine **99-HCl**.

The *N*-Boc deprotected indole **181** could be accessed *via* an acid-mediated *N*-Boc deprotection of indole **167** (Scheme 73).



Scheme 73 – *N*-Boc deprotection of cyclopropyl-ester **167**

Summary: 1,2- Δ -tryptamine **99** synthesis

In summary, to install mono-substituted cyclopropanes, and access the desired core framework, a rhodium-catalysed carbene insertion to vinyl indole **159** was required (Scheme 74).

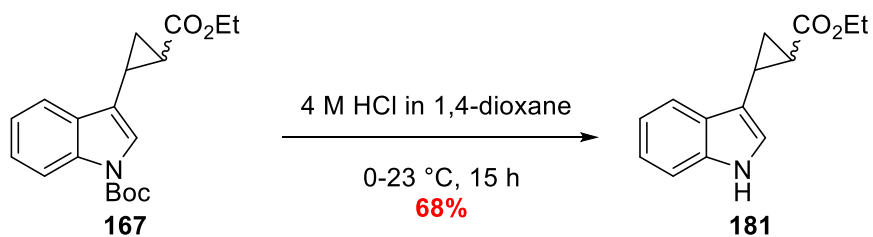
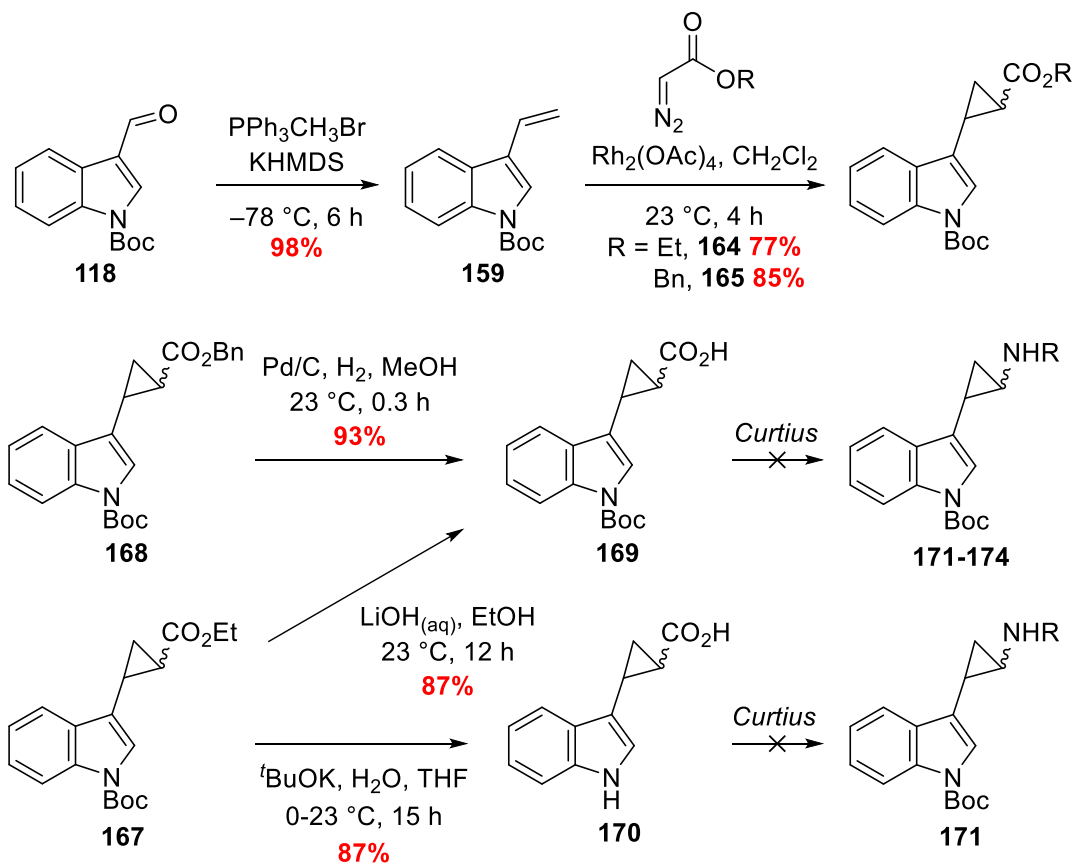
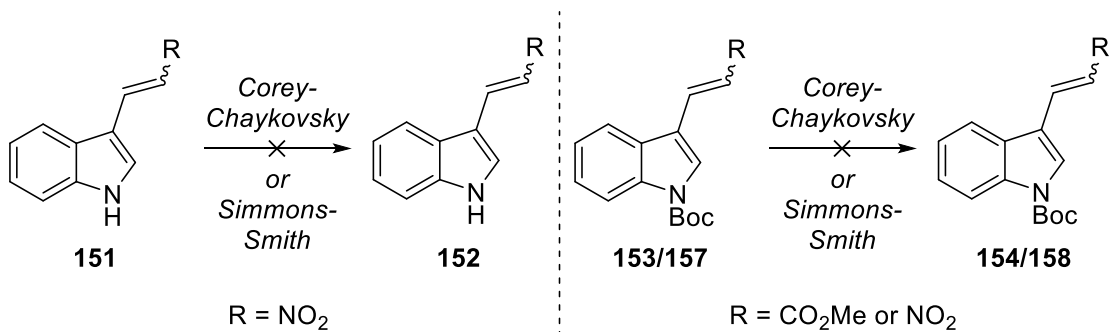
Conjugate addition of trimethylsulfoxonium ylides under Corey-Chaykovsky conditions likely failed due to both the α,β -unsaturated nitros' **151** and **153**, and ester **157** being poor Michael acceptors. A high electron-density aromatic system appended to the β -carbon was seemingly sufficient to see the deactivation of these systems toward 1,4-attack.

The failure of the Simmons-Smith cyclopropanation on the α,β -unsaturated nitro **151** can likely be attributed to the polarity across the double bond and the lack of a sufficient directing group. Use of a Boc-protecting group on the indole nitrogen in nitro **153** and ester **157** also returned the starting material in all attempted reactions suggesting the electronic perturbation of the indole ring offered by the *N*-Boc group was not sufficient. Additional factors such as insufficient resonance stabilisation of the intermediate anionic species in the Corey-Chaykovsky reaction could have also played a part in the reaction's failure.

Due to concomitant *N*-Boc deprotection during the Wittig reaction of aldehyde **118**, optimisation of the olefination conditions was carried out. The use of KHMDS as the base, low reaction temperatures and short reaction times lead to a high yielding olefination.

Both ethyl and benzyl diazoacetate were utilised as carbene precursors, giving access to the corresponding ethyl and benzyl cyclopropyl esters **167** and **168**. Upon accessing ethyl and benzyl ester **167** and **168**, and subsequent deprotection to acid **169** and **170**, a sensitivity to both Overman and DPPA-mediated Curtius conditions was highlighted. A small screen of trapping alcohols and a mild copper-catalysed isocyanate trapping was attempted but all resulted complete loss of the starting material and multiple side-products.

Literature examples of the syntheses of 1,2- Δ -tryptamine analogue **99** note the instability of the *Z*-diastereomer to the Curtius conditions and the sensitivity to temperature of the resulting *E*-carbamate.²¹¹⁻²¹³ The synthesis of 1,2- Δ -tryptamine analogue **99·HCl** was abandoned due to the difficulty in isolating pure product and the challenges posed in biologically-evaluating an unstable compound. In order to test the potential for this structural class of compound to serve as an IDO1 inhibitor, ethyl cyclopropyl ester **181** was synthesised and submitted for biological evaluation.

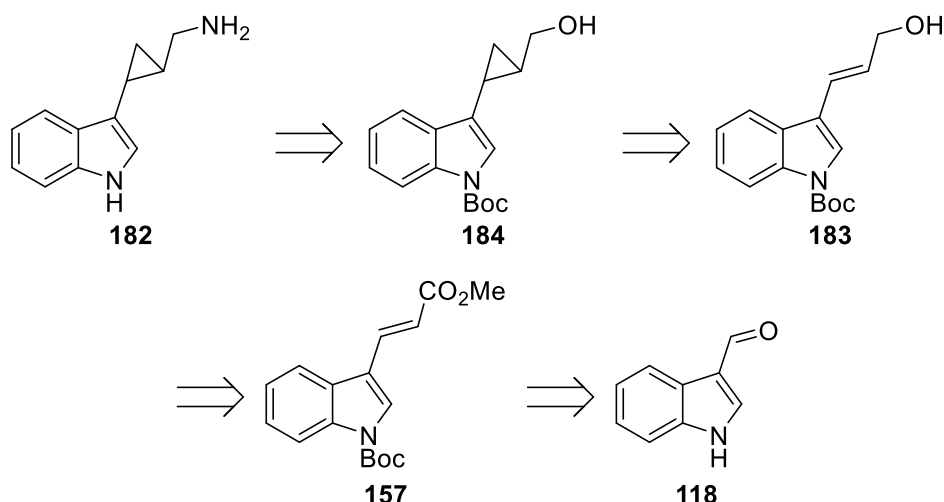


Scheme 74 – 1,2- Δ -tryptamine analogue **99** synthesis summary

1.5.3 – Synthesis of Homologated 1,2- Δ -Tryptamine Analogue **182**

Through an inherent instability, tryptamine analogue **99** was no longer considered a viable target and warranted no further investigation. However the scaffold of a mono-substituted cyclopropyl-indole remained of interest for biological evaluation. The instability of tryptamine **99** was a result the 1,2-arrangement of the electron-rich indole and the electron-deficient carbamate.²¹⁴

To maintain the desired ring-opening mechanistic diversion described previously (Scheme 33, *vide supra*), the cyclopropane must remain appended to the 3-position of the indole ring. However, it was proposed that the amine could be separated from the cyclopropane *via* a methylene group with minimal impact on the desired mechanistic diversion of IDO1 reactivity. As such, a route to homologated 1,2- Δ -tryptamine analogue **182** was designed to reduce the potential polarisation of the cyclopropane ring (Scheme 75).

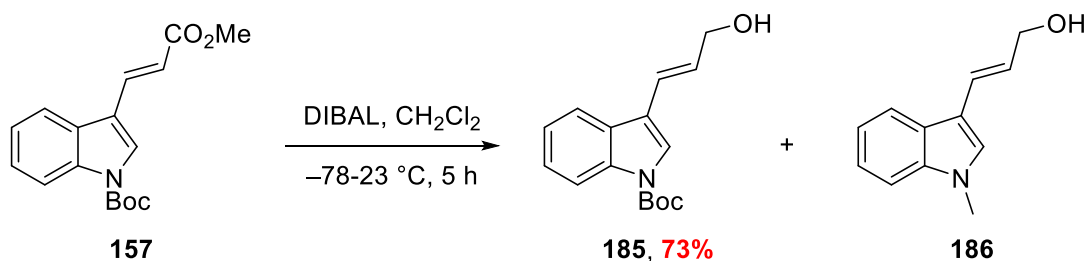


Scheme 75 – Retrosynthetic analysis of homologated tryptamine **182**

Previously described chemistry (Scheme 59) had already set precedent on how α,β -unsaturated ester **157** could be accessed. A chemoselective DIBAL-mediated reduction of ester **157** would be performed to access allylic-alcohol **183**. At this point, the scaffold is predisposed to an allylic alcohol-directed Simmons-Smith cyclopropanation to give cyclopropane **184**. Finally, amine **182** would be accessed *via* a modified Mitsunobu reaction to access an *N*-phthalimide protected amine.²¹⁵⁻²¹⁷ An indole nitrogen protecting group is necessary throughout this synthesis due to the previously encountered methylation in the HWE olefination (Scheme 58).

The previously described *N*-Boc protected ester **157** was subjected to a DIBAL-reduction to afford allylic alcohol **185** (Scheme 76). The reaction proceeded with the formation of *N*-methylated allylic alcohol **186** as an over-reduction by-product (evidenced by LC-MS).

Reduction of *N*-carbamates to *N*-methyl amines with lithium aluminium hydride is not a novel phenomenon, however DIBAL-mediated reduction of *N*-carbamates to *N*-methyl amines is seldom seen. Instances where methyl- and Boc-carbamates remain intact throughout DIBAL-mediated reduction have been reported.^{218, 219} By reducing the equivalents of DIBAL (to 1.2 eq.) and maintaining low reaction temperatures (-78 °C) the over-reduction product was minimised.

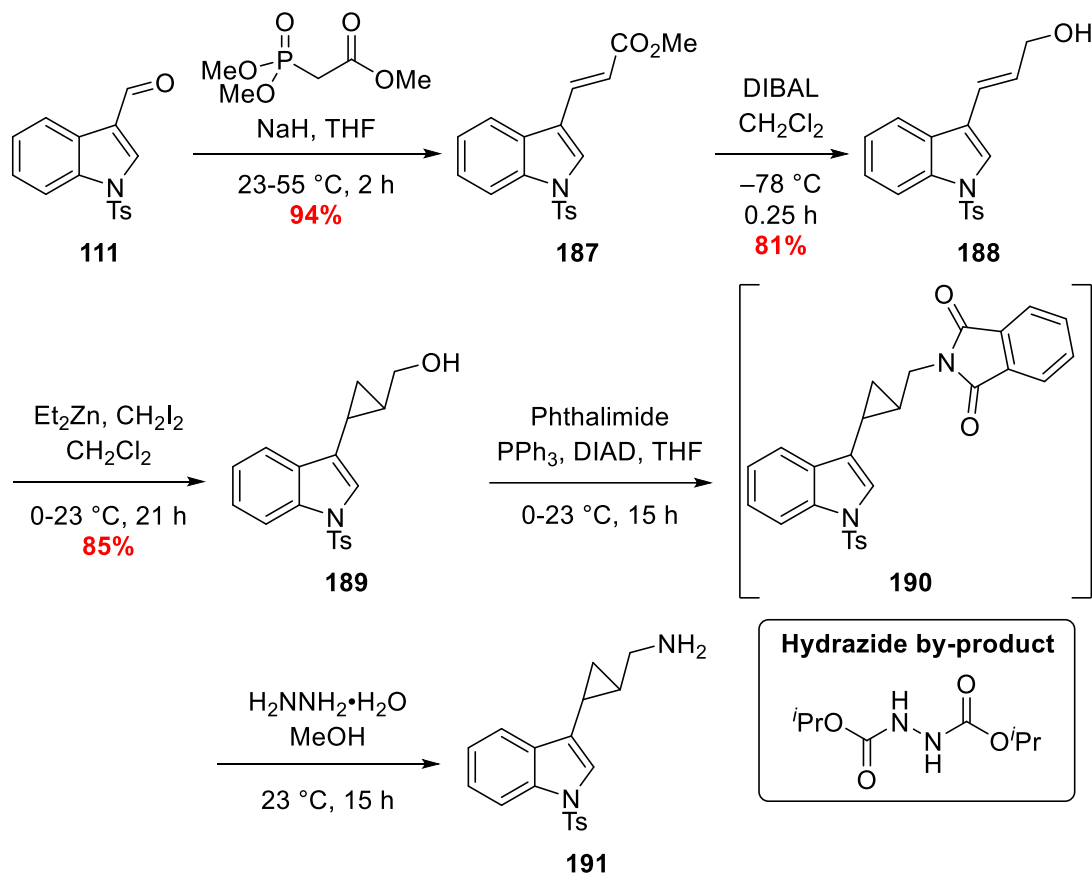


Scheme 76 – DIBAL reduction of N-Boc methyl ester 157

Over-reduction of the Boc-group was a weak point in the overall synthetic strategy; the Boc-group was therefore changed in favour of a more reduction-resistant protecting group – tosyl. *N*-Tosyl protected aldehyde **111** was subjected to the HWE olefination to yield α,β -unsaturated ester **187** which then underwent a DIBAL-reduction to afford allylic alcohol **188**. Allylic alcohol **188** was then subjected to a successful, and scalable, directed Simmons-Smith cyclopropanation to finish the desired core structure **189** in an 85% yield at 1 g scale (Scheme 77).

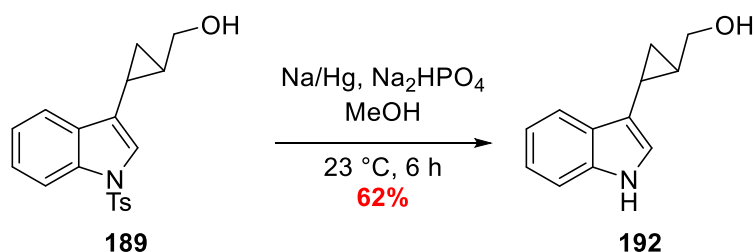
Access to phthalimide **190** would be attempted *via* a modified Mitsunobu reaction for which there exists considerable literature precedent.²¹⁵⁻²¹⁷ Upon flash column chromatography of the crude material, the product co-eluted with the hydrazide by-product of the Mitsunobu reaction (Scheme 77). After numerous failed attempts to remove the hydrazide impurity, the mixture was taken forward to the hydrazine-mediated phthalimide deprotection; the polarity of the resulting amine was hypothesised to be sufficiently different from the hydrazide to allow for successful purification *via* flash column chromatography. Isolation of pure amine **191** soon revealed the instability of the compound to aerobic conditions – degrading completely over a 24 h period at 23 °C. Upon re-synthesis of amine **191**, storage at -20 °C was necessary to avoid oxidative degradation.

After observations of instability, the synthesis of homologated tryptamine **191** warranted no further investigation due to the complications of biologically evaluating a chemically unstable compound.



Scheme 77 – Synthesis of *N*-tosyl cyclopropylmethylalcohol **189**

To provide a compound of this class for biological evaluation, alcohol **189** was subjected to a sodium amalgam-mediated *N*-Tosyl deprotection to give the corresponding *N*-H indole **192** (Scheme 78). Both starting alcohol **189** and the resulting *N*-H indole **192** were stable under aerobic conditions at 23 °C, suggesting the origin of the instability of **191** was the amine functionality.



Scheme 78 – *N*-tosyl deprotection

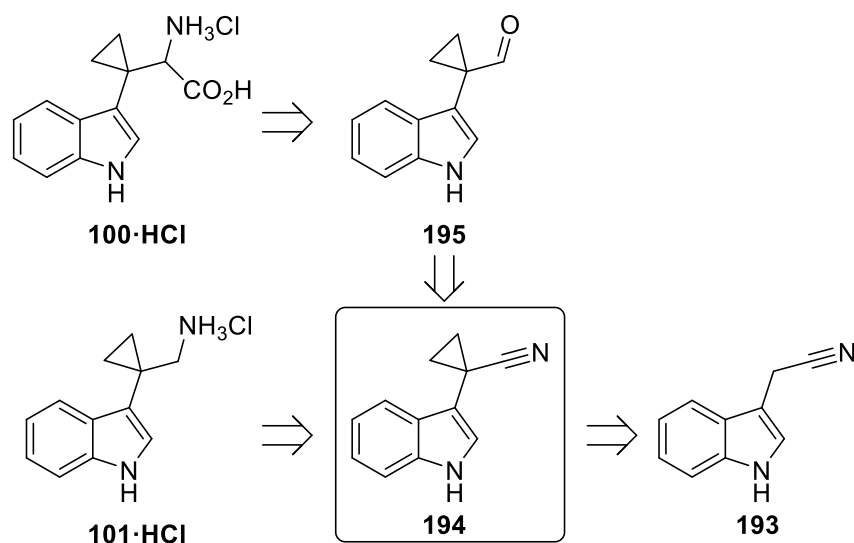
Summary: Synthesis of Homologated 1,2- Δ -tryptamine analogue

After the indole nitrogen protecting group was optimised, an efficient DIBAL-reduction of ester **187** was identified. The resulting allylic alcohol **188** was subjected to a directed Simmons-Smith cyclopropanation which proceeded to give cyclopropane **189** in excellent yield. Co-elution of the hydrazide by-product from the Mitsunobu reaction prevented the isolation of pure **190**, but subjecting the crude to a hydrazine-mediated phthalimide deprotection permitted separation from the contaminating species. Amine **191** subsequently proved unstable to aerobic conditions and completely degraded – further synthetic efforts were abandoned due to the challenges of evaluating chemically unstable compounds. To provide a relevant analogue of this structural class of compounds for biological evaluation, alcohol **189** was subjected to a successful tosyl-deprotection to give alcohol **192**.

1.5.4 – Synthesis of 1,1'- Δ -Tryptophan and Tryptamine Analogues **100** and **101**

During the previously described synthesis of alternative mechanistic inhibitors, the key ring system has remained as a 1,2-cyclopropane. A final attempt to synthesise a mechanistic inhibitor saw the design of spirocyclic cyclopropane-containing analogues of tryptophan and tryptamine – termed 1,1'-cyclopropanes (Scheme 79). A literature report details the divergent synthesis of both tryptophan and tryptamine analogues **100** and **101**, however, minimal experimental detail is provided.²²⁰

From nitrile **193**, a base-mediated cyclodialkylation with a dihaloethane gives access to 1,1'-cyclopropane core **194**, which serves as the point of divergence. Access to 1,1'-cyclopropane-containing tryptophan analogue **100·HCl** would involve a DIBAL-mediated reduction of nitrile **194** to selectively access aldehyde **195**. Tryptophan analogue **100·HCl** would then be accessed by subjecting aldehyde **195** to either a Bucherer-Bergs hydantoin synthesis followed by hydrolysis or a Strecker synthesis. Access to the 1,1'-cyclopropane-containing tryptamine analogue **101·HCl** would be achieved by treatment of nitrile **194** with either a reducing agent or metal-based hydrogenation catalyst. (Scheme 79).



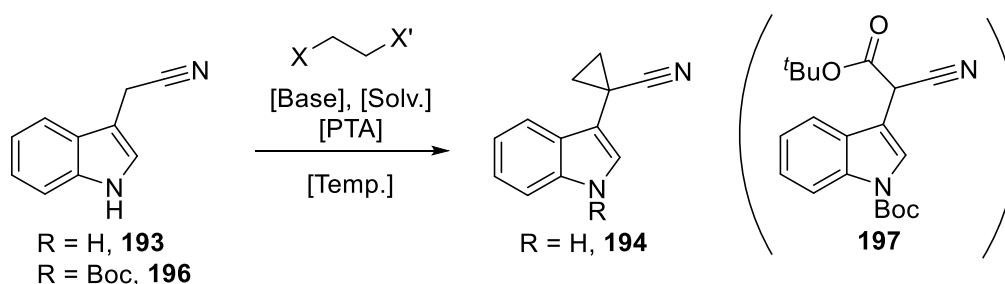
Scheme 79 – Retrosynthetic analysis of 1,1'- Δ -tryptophan and tryptamine analogues 100 and 101

Due to the lack of experimental detail provided in the literature report, multiple variables had to be considered when optimising the cyclodialkylation of nitrile **193** (Scheme 80, Table 7).²²⁰ On account of using a strong base, a protecting group was initially used to prevent unwanted deprotonation of the indole amine. The literature report notes LDA as the optimum base to perform the dialkylation, however, when replicated with nitrile **196** only Claisen-product **197** was isolated (Table 7, Entry 1).

Alternative literature reports of cyclodialkylation utilise the more electrophilic dibromoethane, bi-phasic solutions of sodium hydroxide in organic media with a phase transfer catalyst (PTC).^{221, 222} Subjecting nitrile **196** to these conditions, starting material **196** was recovered (Table 7, Entry 2). Increasing the temperature and using a mixed haloethane also gave disappointing results and lead to the recovery of starting material **196** (Table 7, Entries 3 and 4). The lack of any reactivity with the basic aqueous solution suggested they were not suitable for deprotonation to the nitrile anion.

To ensure deprotonation, LDA was employed again using the mixed haloethane as the alkylating partner (Table 7, Entry 5). Similar to the first attempt with LDA, Claisen product **197** was isolated as the major product – confirming that Boc was not a suitable protecting group for the indole nitrogen.

In order to assess whether an indole nitrogen protecting group was required, nitrile **193** was subjected to the cyclodialkylation conditions. Using an excess of LDA at $-40\text{ }^{\circ}\text{C}$, nitrile **193** was deprotonated to form the nitrile anion. After 30 min the nitrile anion mixture was maintained at $-40\text{ }^{\circ}\text{C}$ and the dihaloethane was added dropwise over 30 min. As a result of careful temperature monitoring and addition rate of the electrophile, spirocyclic cyclopropane **194** was isolated from the reaction mixture in a very good yield (Table 7, Entry 6).



Scheme 80 – Synthesis of 1,1'-spirocyclic cyclopropane **194**

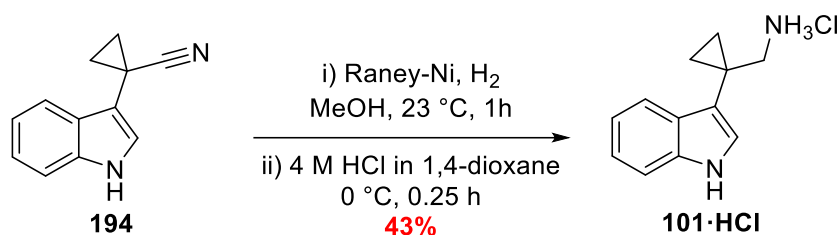
Table 7 – Optimisation conditions for the synthesis of 1,1'-spirocyclic cyclopropane **194**

Entry	R	X	X'	Base	Solv.	PTC	Temp./ $^{\circ}\text{C}$	Result
1	Boc	Cl	Cl	LDA ^a	THF	N/A	$-78-23$	197, 27%
2	Boc	Br	Br	NaOH ^b	PhMe	TBAB	23	196
3	Boc	Br	Cl	NaOH ^b	PhMe	BTAC	70	196
4	Boc	Br	Cl	NaOH ^b	Neat.	BTAC	50	196
5	Boc	Br	Cl	LDA	THF	N/A	$-30-23$	197, 21%
6	H	Br	Cl	LDA	THF	N/A	$-40-23$	194, 83%

^a LDA solutions were prepared from freshly titrated *n*BuLi and distilled (*i*Pr)₂NH.

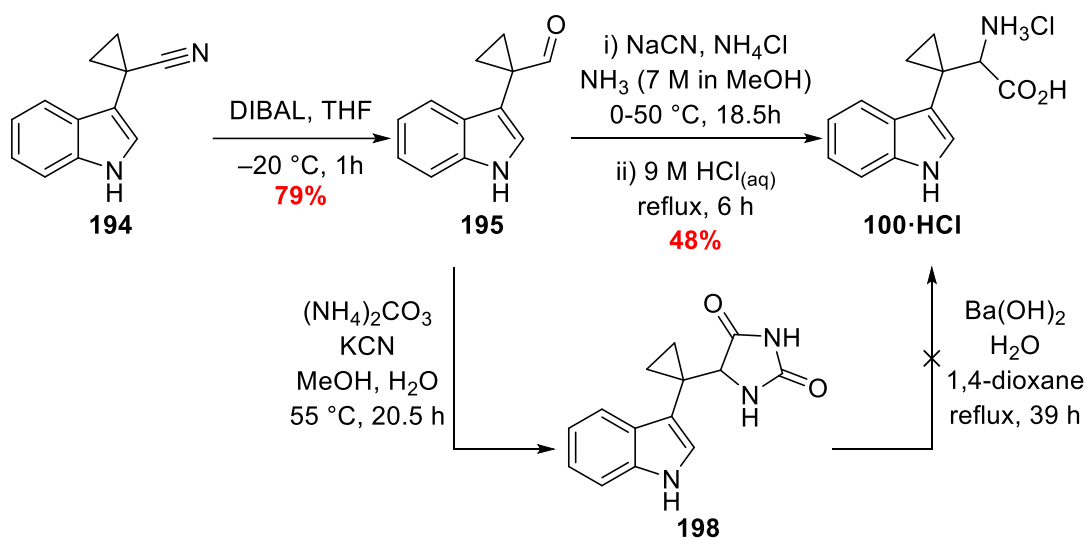
^b 50% aqueous solutions.

With cyclopropyl-nitrile **194** in hand, a change in oxidation state would give access to tryptamine-analogue **101**. A LiAlH₄ reduction was initially attempted but found to produce a complex mixture of products. Raney-nickel affected a clean catalytic hydrogenation, the product amine was then treated with a 4 M solution of HCl in 1,4-dioxane to precipitate the respective hydrochloride salt **101·HCl** (Scheme 81).



Scheme 81 – Synthesis of tryptamine analogue **101·HCl**

Treating nitrile **194** with DIBAL initially displayed no reactivity at $-78\text{ }^\circ\text{C}$. Increasing the reaction temperature to $-20\text{ }^\circ\text{C}$ facilitated a successful reaction to yield aldehyde **195** (Scheme 82). To access tryptophan analogue **100**, two methods were available: a Bucherer-Bergs reaction followed by hydrolysis of the hydantoin intermediate or a one-pot Strecker synthesis. Following precedent, the Bucherer-Bergs was attempted first. Synthesis of hydantoin **198** proved successful, however, isolation of spectroscopically pure material proved a challenge due to the highly polar nature of this intermediate. Subjecting crude hydantoin **198** to a barium hydroxide mediated hydrolysis yielded no amino acid **100**. A Strecker reaction was therefore completed to grant access to 1,1'-spirocyclic tryptophan analogue **100·HCl**, in low isolated yield (Scheme 82).

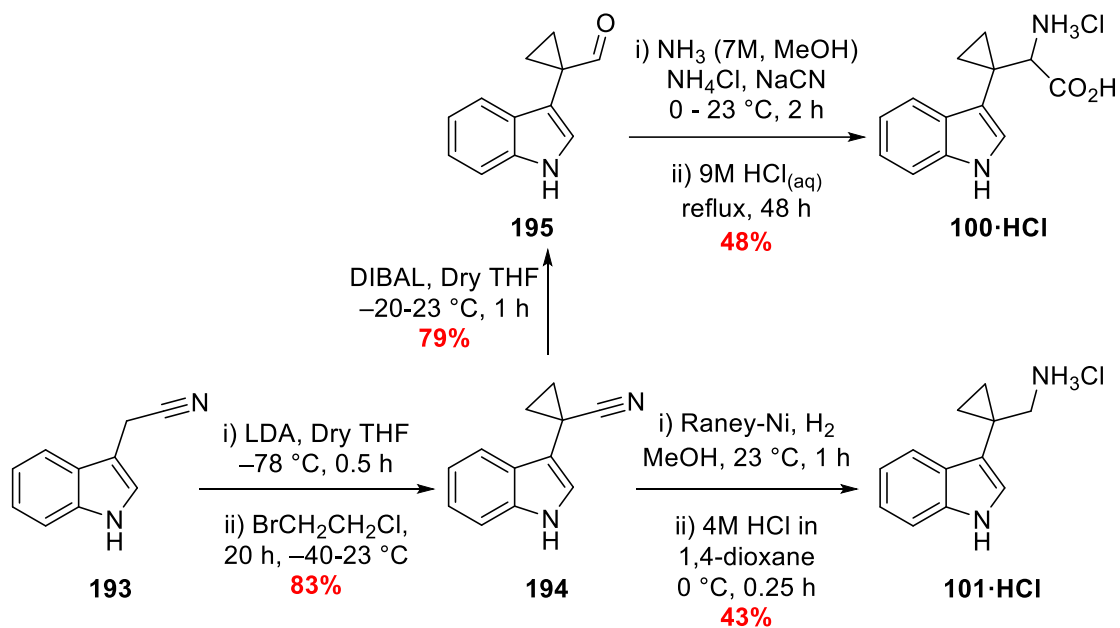


Scheme 82 – Synthesis of 1,1'- Δ -tryptophan analogue **100·HCl**

Summary: 1,1'- Δ -tryptophan and tryptamine synthesis

After optimising the cyclodialkylation of nitrile **194**, the synthesis of tryptophan and tryptamine analogues **100·HCl** and **101·HCl** was achieved successfully (Scheme 83). The successful cyclodialkylation relied on careful control of the reaction temperature and slow addition of the electrophile. Fortunately the product could be isolated *via* recrystallisation and there was no need for removal of a protecting group. Reduction of nitrile **194** to the amine initially proved challenging with lithium aluminium hydride, however this problem was overcome *via* catalytic

hydrogenation with Raney-nickel. To enable facile isolation of pure 1,1'- Δ -tryptamine, the hydrochloride salt **101·HCl** was isolated by precipitation from an ethereal solution of hydrogen chloride. Attempts to replicate the reported Bucherer-Bergs/hydrolysis conditions ultimately failed due to difficulties in isolating spectroscopically pure hydantoin **198** and the failure of the subsequent barium hydroxide-mediated hydrolysis. Therefore, a Strecker reaction was performed on aldehyde **195** which gave amino acid **100·HCl**. Both 1,1'- Δ -analogues were accessed in low overall yield, however enough material was afforded for biological evaluation.

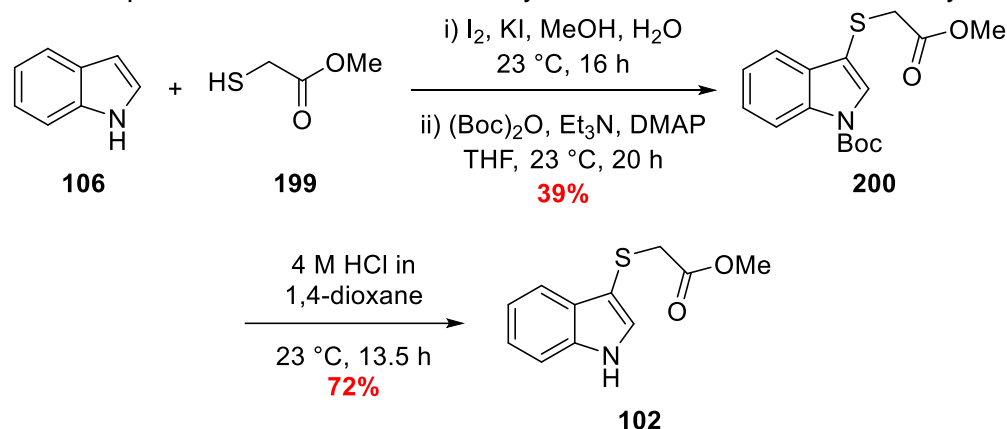


Scheme 83 – Summary of the synthesis of 1,1'- Δ -tryptophan and tryptamine analogues **100** and **101**

1.5.5 – Synthesis of Sulfenylindole **102** and a Small Library of Analogues

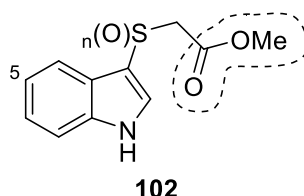
A final structural class of compounds was targeted for synthesis: sulfenylindoles. Unlike the cyclopropane-containing inhibitors, the sulfenylindole structural class of compounds is not intended to divert radical reactivity – instead the sulfenylindoles' are hypothesised to disrupt alternative metabolic intermediates (Scheme 35, *vide supra*).

A literature protocol conveniently describes the synthesis of sulfenylindole **102**.²²³ The initial sulfenylation reaction gave an inseparable mixture of sulfenylindole **102** and a disulfide impurity (identified by ¹H-NMR spectroscopy and MS). Treatment of the mixture with aqueous solutions of sodium hydroxide seemed to have little impact on the amount of disulfide present by ¹H-NMR spectroscopy. To enable clean isolation of the desired material, the crude reaction mixture was subjected to Boc-protection conditions and then purified by flash column chromatography to yield Boc-adduct **200** (Scheme 84). Subjecting Boc-adduct **200** to a HCl-mediated Boc-deprotection then afforded sulfenylindole **102** in moderate overall yield.



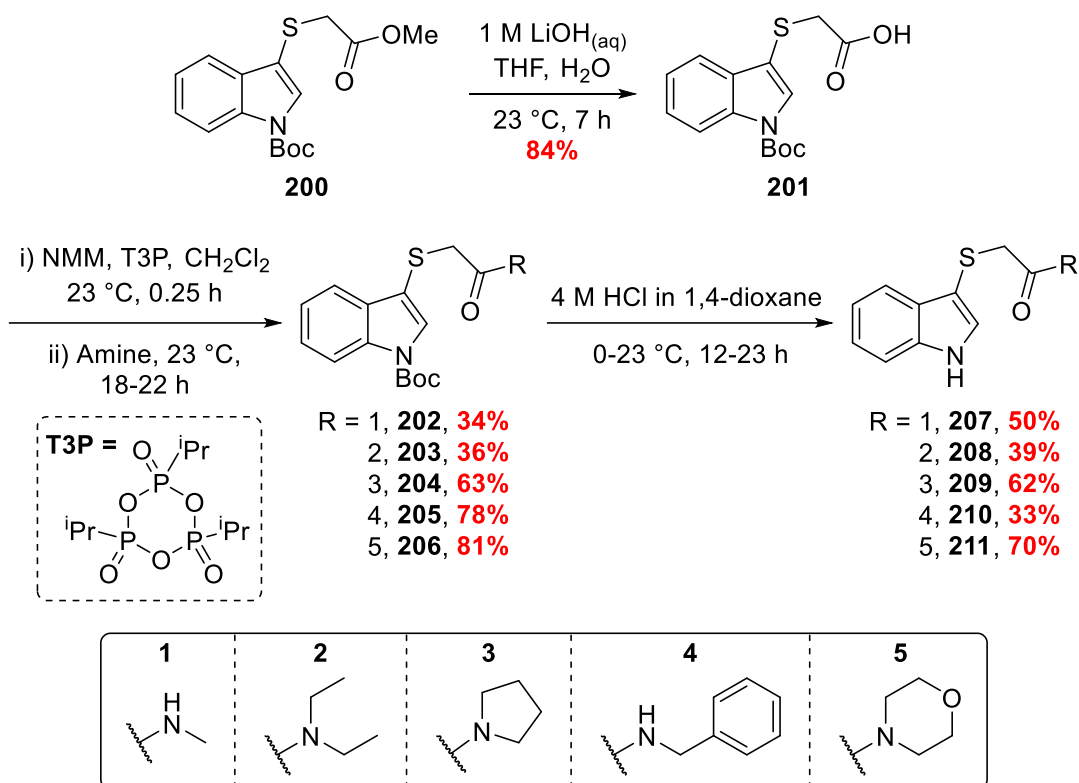
Scheme 84 – Synthesis of sulfenylindole **102**

Initial biological evaluation of sulfenylindole **102** demonstrated promising inhibition of IDO1 in SCOV3 cells (Figure 21, *vide infra*). Combining the knowledge of a good initial hit, IDO1's broad substrate scope and the ease of derivation of sulfenylindole **102**, a small library of indoles would be synthesised. Based on known substrates of IDO1, 3 points of derivatisation were chosen: C₅-substitution, sulfur oxidation state and ester FGIs (Scheme 85).⁹



Scheme 85 – Sulfenylindole **102** points of derivatisation

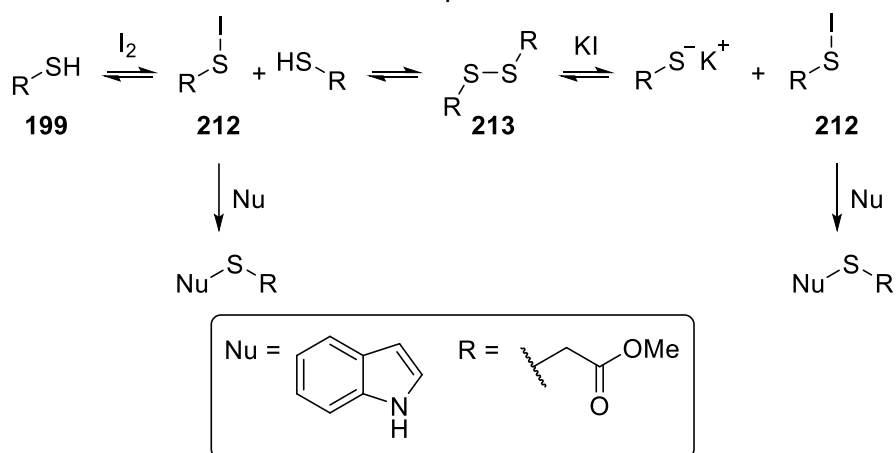
Sulfenylindole **200** was hydrolysed in a biphasic solution of aqueous lithium hydroxide in THF to afford acid **201** in good yield. Acid **201** was then subjected to a series of T3P-mediated amide couplings to give amides **202–206**. Finally, to access the *N*-Boc deprotected compounds, amides **202–206** were treated with a solution of HCl in 1,4-dioxane to afford *N*-Boc deprotected amides **207–211** (Scheme 86).



Scheme 86 – Synthesis of amides **207–211**

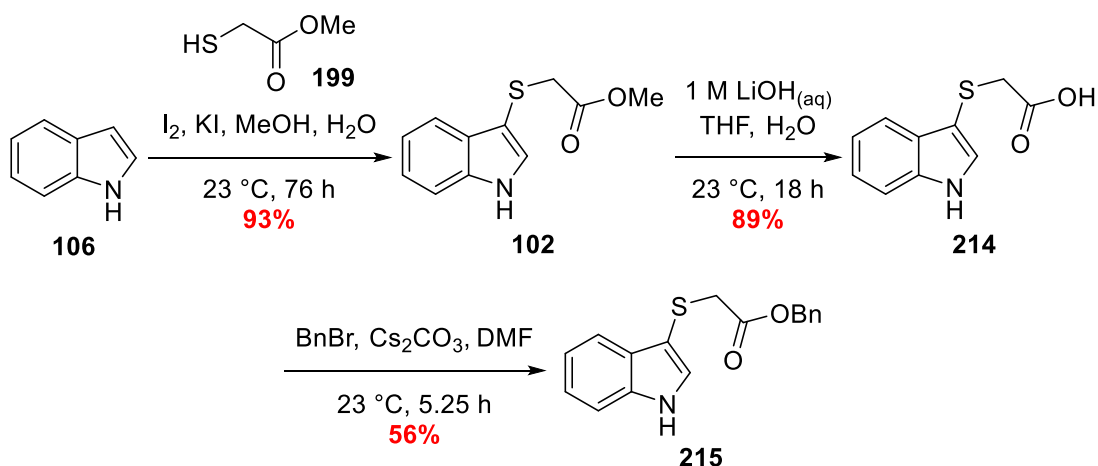
In subsequent sulfenylation reactions, it was found that increasing the reaction time lead to the complete consumption of the *in situ* generated disulfide, rendering the Boc-protection of the crude reaction mixture unnecessary. The suspected reactive intermediate, sulfenyl iodide **212**, in the sulfenylation reaction is thought to be in equilibrium with disulfide **213** and other

spectator species (Scheme 87). With longer reaction times, and an excess of the trapping nucleophile, the reaction can be driven to completion.



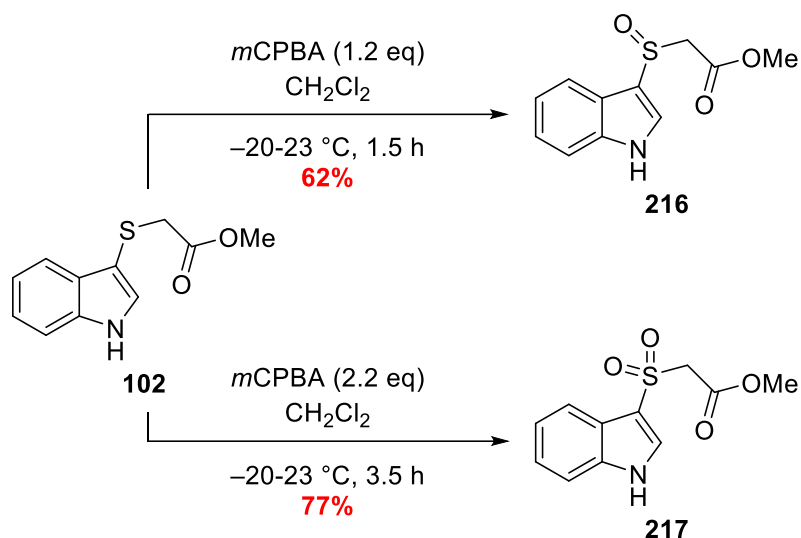
Scheme 87 – Suspected equilibria involved in the sulfenylation reaction

The shortened sequence was then utilised to efficiently access sulfenylindole **102** analogue, acid **214**, in two steps. Acid **214** was then subjected to benzyl bromide in the presence of caesium carbonate to afford benzyl ester **215** in moderate yield (Scheme 88).



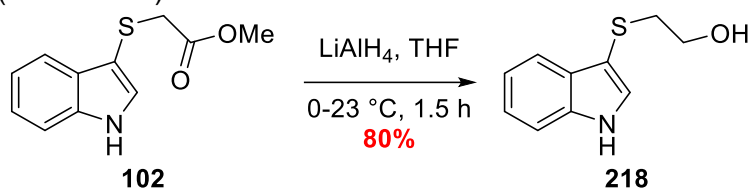
Scheme 88 – Synthesis of acid **214** and benzyl ester **215**

Sulfoxide **216** and sulfone **217** were accessed by careful control of stoichiometry of the oxidant, *meta*-chloroperoxybenzoic acid, in the presence of sulfenylindole **102** (Scheme 89). Initially, oxidation of *N*-Boc protected sulfenylindole **200** was completed but upon HCl-mediate Boc-deprotection the sulfoxide and sulfone degraded. The products of these reactions were not characterised but were presumed to arise from a Pummerer-type reaction pathway.



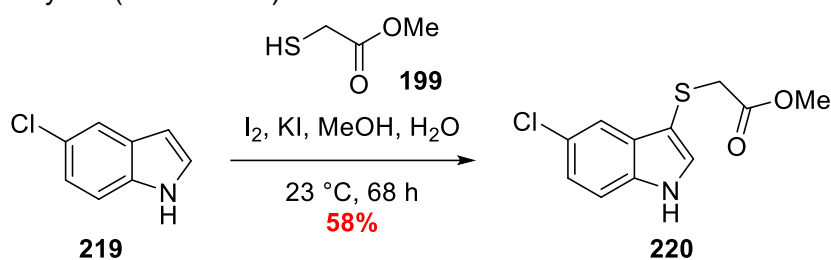
Scheme 89 – Oxidation of sulfenylindole **102** to sulfoxide **217** and sulfone **218**

Conversely, reduction of the sulfenylindole **102** ester functionality would give rise to ethyl-alcohol **218**. Ester **102** was therefore treated with lithium aluminium hydride to give alcohol **218** in high yield (Scheme 90)



Scheme 90 – Reduction of ester **219**

Finally, modifications were made to the C₅-position of the indole ring; to achieve this, a 5-substituted indole replaced indole in the initial sulfenylation reaction. Chloroindole **219** was subjected to the sulfenylation conditions to yield **220**, the 5-chloro analogue of sulfenylindole **102**, in moderate yield (Scheme 91).

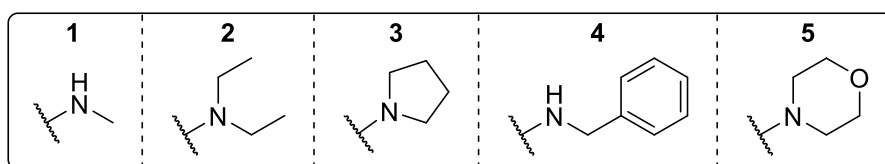
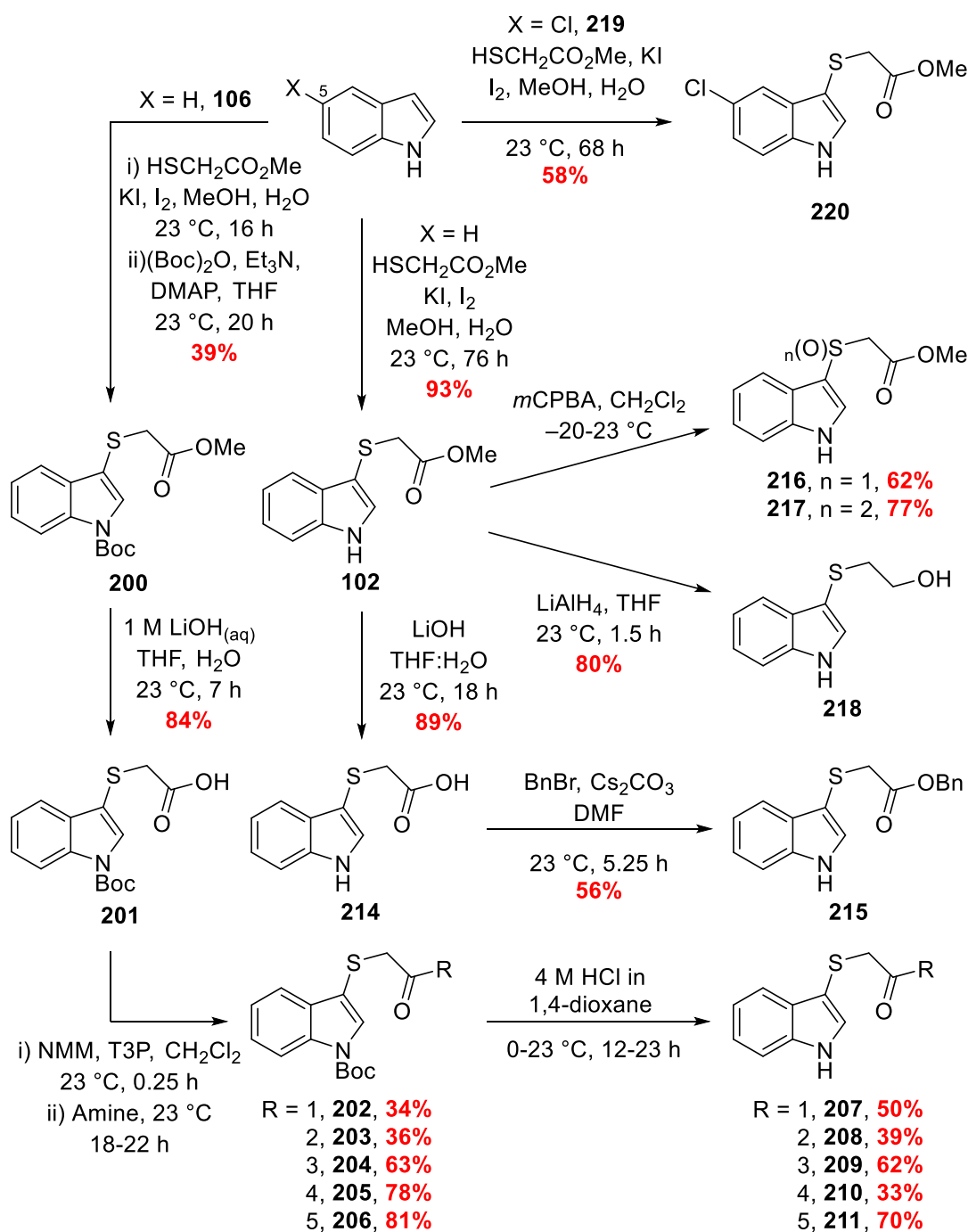


Scheme 91 – Sulfenylation of 5-chloroindole **220**

Summary: synthesis of sulfenylindole **102** and a library of analogues

In summary, a small library of sulfenylindole analogues was synthesised (Scheme 92). Preliminary sulfenylation reactions required subjecting the crude material to a Boc-protection to allow the separation of the desired material from the generated disulfide impurity. This later proved unnecessary and longer reaction times and an excess of the trapping nucleophile would eventually lead to the full conversion to sulfenylindole **102** in one step. Multiple functional

group interconversions were performed to access a range of compounds for biological evaluation – if successful, they represent a novel structural class of IDO inhibitors.



Scheme 92 – Summary of sulfenylindoles synthesised

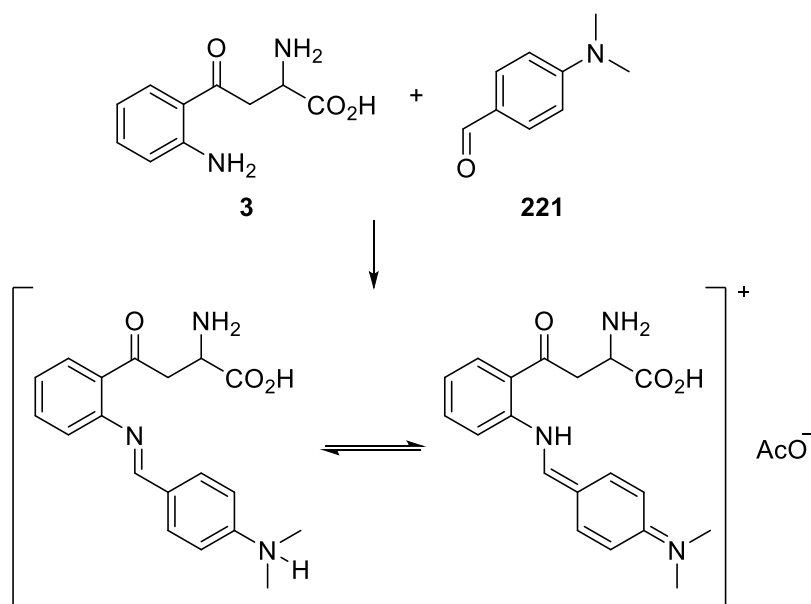
1.6 – Results and Discussion: Whole Cell Evaluation

Whole cell IDO1 inhibition and viability assays were performed by Tina Tang (Celentyx Ltd).

Target compounds **61·HCl**, **100·HCl**, **101·HCl** and **102**, and compounds which shared structural similarities to the target compounds were subjected to whole cell biological evaluation (Figure 20). In many respects whole cell assays are not an ideal screening experiment for novel target-specific compounds, as inhibition data may be compromised by poor membrane permeability or non-specific effects on transporters or cell viability. However, if the molecules are to be useful tool compounds the effects in cells will ultimately need to be demonstrated, therefore the selection of optimal active compounds may be accelerated by directly utilising whole cell assays.

Whole cell assays for IDO1 inhibition were developed and performed Celentyx Ltd utilising immortal ovarian cancer cells (SKOV-3 cell line) which have been treated with IFN γ to stimulate over-expression of IDO1. When treated with Trp the cells synthesise and excrete NFK/Kyn which can be detected in the assay media. Kyn levels were determined by first treating the media with an aqueous TCA solution and heating to convert all NFK to Kyn, then quantified *via* derivatisation with an acidic solution of *p*-dimethylaminobenzaldehyde (Ehrlich's reagent). Measurement of the absorbance of this adduct at 490 nm relative to a standard curve allows calculation of Kyn concentration.

Treatment of the cell lysates with an acidic (glacial AcOH) solution of Ehrlich's reagent **221** initiates a condensation reaction with Kyn **3** to form highly coloured hydrochloride salts (Scheme 93).^{224, 225}



Scheme 93 – Reaction between Kyn **3** and Ehrlich's reagent to give highly coloured imine salts

Two concurrent assays would be run, one in the absence of additional Trp and one with addition of 100 μ M Trp (Figure 21), with cells assessed in parallel for *viability* by staining of cells with Zombie dye and analysing the solutions *via* flow cytometry. Due to the potential time-dependency of the inhibitors, the cells were pre-incubated for two hours with the inhibitors prior to Trp addition.

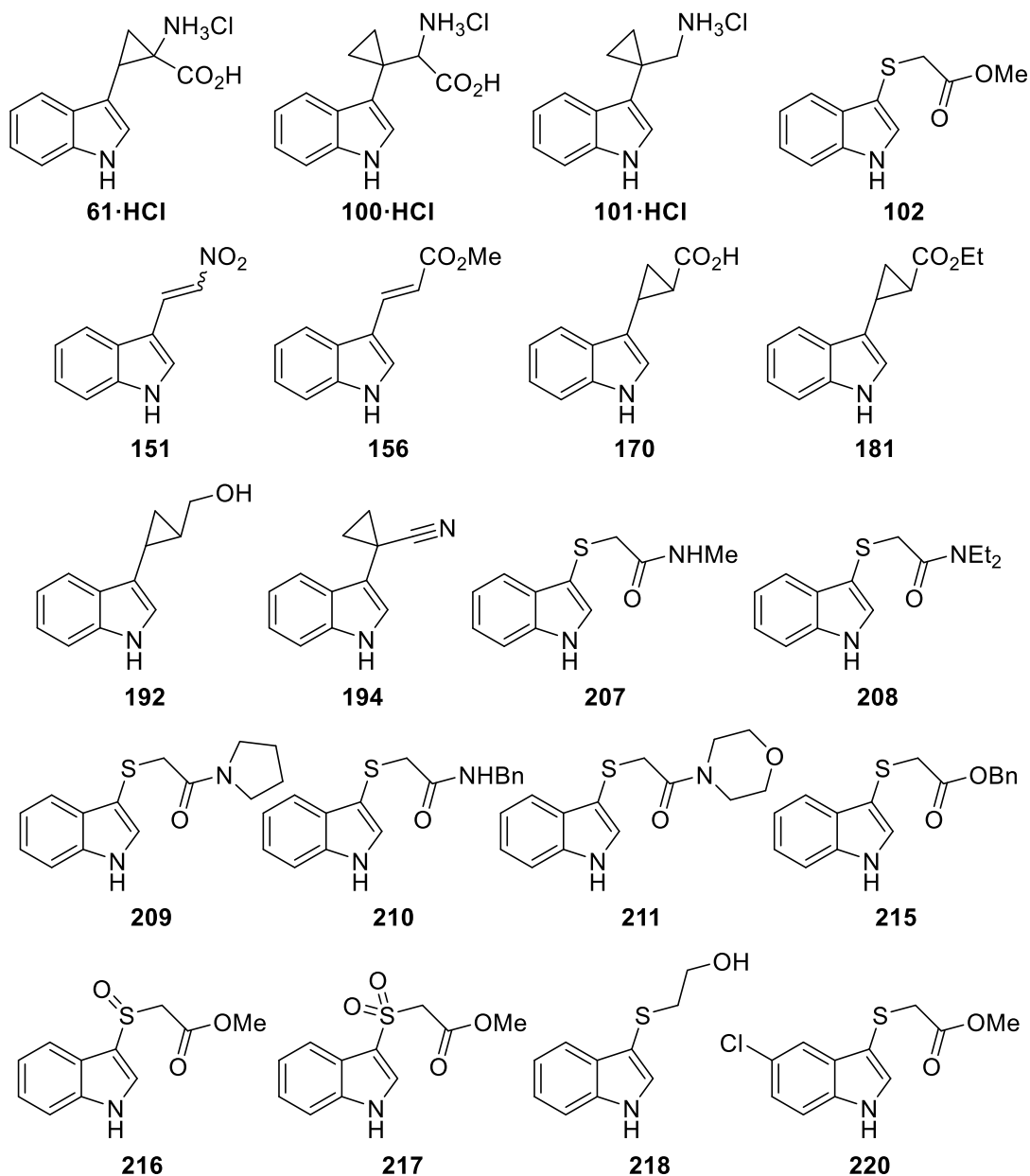


Figure 20 – Compounds Subjected to Whole Cell Evaluation

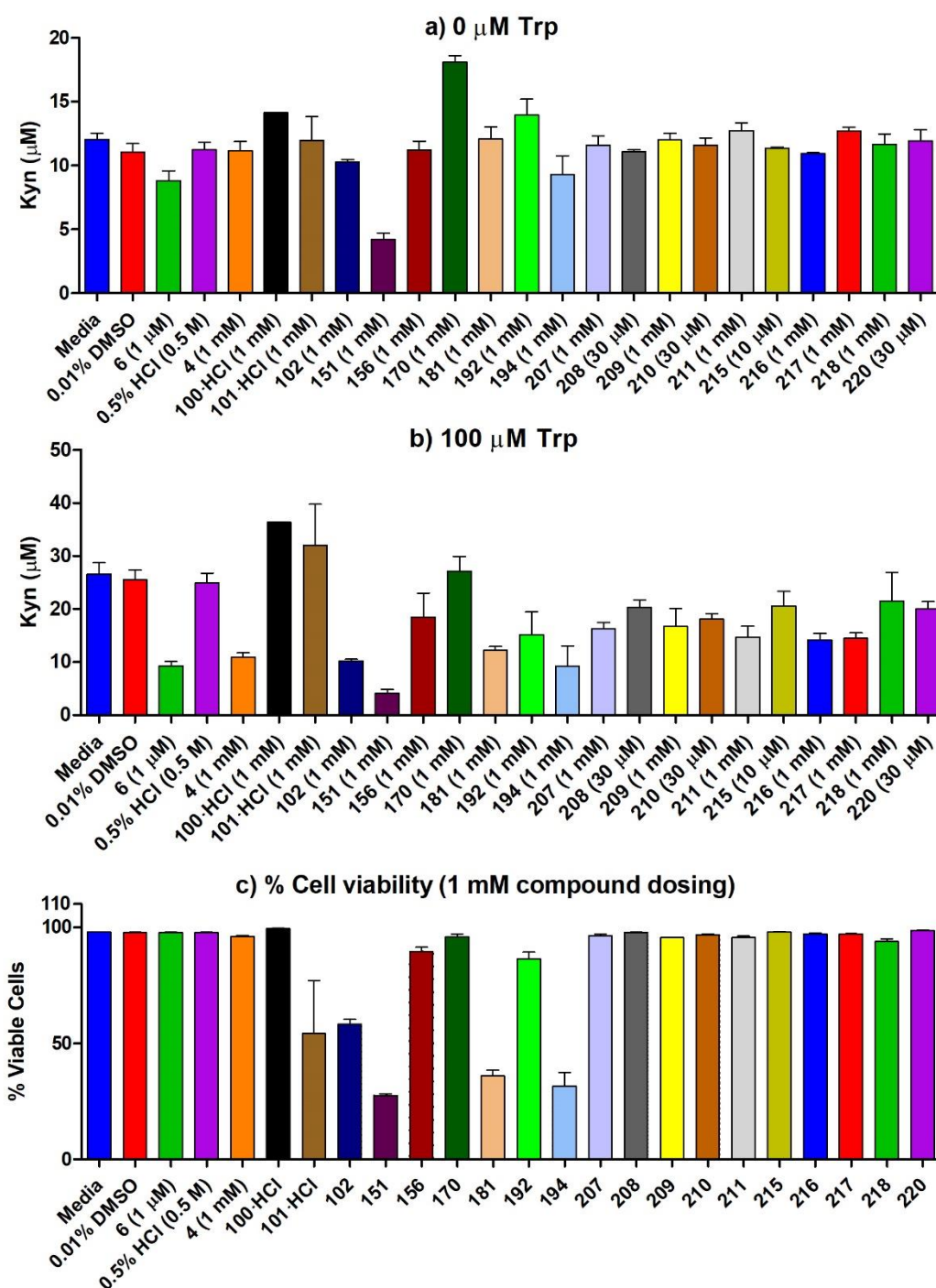


Figure 21 - Whole cell evaluation performed by Celentyx Ltd.

a) & b) – SKOV-3 cells were stimulated with IFN γ for 24 h before being transferred to a 96-well plate (40,000 cell per well). The cells were incubated with vehicle (0.01% DMSO or 0.5% 0.5 M HCl) or inhibitor and then either 0 μM (a) or 100 μM (b) Trp was added and allowed to sit for a further 2 h. Ehrlich's reagent was used to detect Kyn levels in media and visualised at 490 nm. **c)** The above was carried out but instead of staining with Ehrlich's reagent, the cells were stained with Zombie dye and percentage viable cells was measured via flow cytometry.

All novel compounds tested at 1 mM where possible. For examples where solubility was limited, the maximum soluble concentration was used, as assessed by the assay scientists.

While addition of Trp results in an increase in Kyn levels in media, the basal level of Kyn detected in the absence of Trp addition is a result of turnover of the Trp present within the assay solution (Figure 21a). Attempts were made to utilise several Trp-free assay media, but this led to a rapid decline in cell viability.

With the exception of a few examples, the Kyn concentration detected in the absence of additional Trp addition remains consistent with the controls. Notable exceptions include sulfenylindole **102**, nitroalkene **151**, ethyl ester **181** and nitrile **194**; however these compounds demonstrated significant cytotoxicity at the dosed concentrations (Figure 21c). The positive control **6** (INCB) also demonstrates some reduction in Kyn levels, in all cases this can be attributed to loss of IDO1 activity, mediated by either direct inhibition or cell death, resulting in reduced Kyn formation during the pre-incubation period. For acid **170** a gain in signal is seen which is suggestive of interaction between acid **170** and the Ehrlich's reagent used to detect Kyn in media.

When Trp is added, the media control demonstrates an almost two-fold increase in detected Kyn concentration indicating IDO1 turnover of the additional Trp present (Figure 21b). Highly potent positive control, **6**, maintains Kyn concentration at basal levels as a result of complete inhibition of IDO1-mediated turnover of Trp in the second incubation. Additional positive control **4** (1-MT) also demonstrated a similar level of apparent inhibition, albeit at higher test concentration. Disappointingly, tryptophan **100·HCl** and tryptamine **101·HCl** analogues performed poorly in the assays with the data suggesting no inhibition. The high polarity of the compounds and potential poor recognition by cell-surface transport proteins could have prevented cellular entry and thus inhibition. Alternatively, the modifications made to the inhibitor may have completely prevented substrate recognition by the enzyme and entry to the active site – a feature necessary for the proposed mode of inhibition. Sulfenylindole **102**, nitro **151**, ethyl ester **181** and nitrile **194** suffer from the aforementioned cytotoxicity at the dosed concentration. More promising were the results of the sulfenylindole analogues, with the compounds demonstrating drops in Kyn concentration suggestive of inhibition. These results were further supported by the lack of cytotoxicity, which is indicative of the inhibition of IDO1 driving the drop in detected Kyn (Figure 21c).

For 1,2- Δ -tryptophan analogue **61·HCl**, the data was suggestive of a large increase in Kyn levels in the assays where no Trp and 100 μ M Trp was added (Figure 22). It is suspected that the red colouration of the compound contributed to the signal used to detect Kyn levels. Kyn is detected *via* staining with Ehrlich's reagent causing a red colouration, the Kyn concentration

is then inferred from the intensity of the UV absorbance at 590 nm. Additional absorption from the compound therefore results in apparent gain in Kyn concentration.

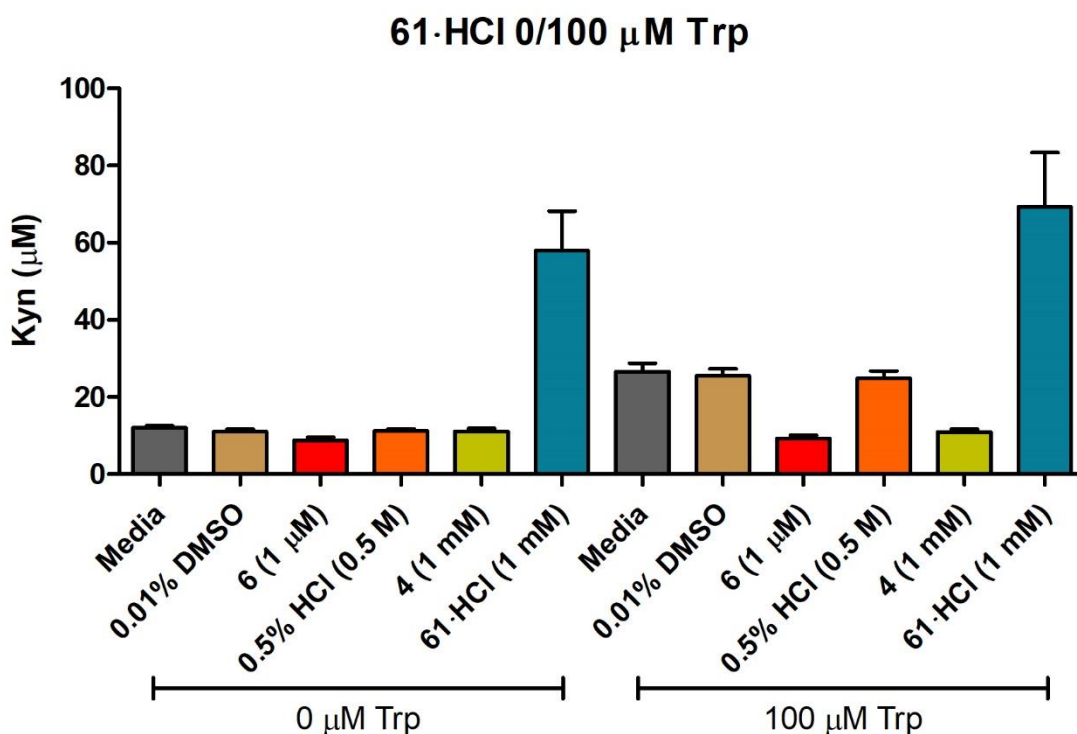


Figure 22 – Whole cell assay data for **61-HCl**

A closer evaluation of sulfenylindole **102** and cyclopropyl ester **181** suggested cytotoxicity was the predominant driver for assay response at high concentrations. Lowering doses revealed sulfenylindole **102** and cyclopropyl ester **181** displayed no cytotoxicity below 300 μ M and 100 μ M respectively (Appendix 1 and 2). A dose response analysis was also performed for sulfenylindole **102** and cyclopropyl ester **181** at two time points to determine whether potency increased over time – a feature of irreversible inhibitors. Time points of 30 and 240 minutes were selected, revealing IC_{50} values of 109 and 83 μ M for sulfenylindole **102** and 96 and 112 μ M for cyclopropyl ester **181** (Appendix 3 and 4). No significant change in IC_{50} was observed across the two time points for sulfenylindole **102** and cyclopropyl ester **181**. In the case of cyclopropyl ester **181** there is a small therapeutic window, the calculated IC_{50} value is close to concentrations where **181** demonstrates cytotoxicity which could complicate further evaluation efforts.

Summary: Whole Cell Evaluation

The whole cell evaluation of the synthesised compounds did not conclusively identify any viable candidates for further evaluation. The best performing inhibitors in the screen were that of the sulfenylindole family of compounds. The red colouration of tryptophan analogue **61·HCl** interfered with accurate determination of its inhibitory properties, however the intrinsic instability of this compound suggests further evaluation is not warranted. Disappointingly the more stable 1,1'- Δ -analogues **100·HCl** and **101·HCl** gave no apparent inhibition when screened. Potential difficulties with either passive or active membrane permeability or loss of substrate recognition by IDO1 could be preventing inhibition. The whole cell assay also failed to provide information on how the enzyme was inhibited or whether the compounds inhibited *via* the mechanisms initially envisaged.

1.7 – Results and Discussion: Biochemical Evaluation

The following biochemical evaluation was performed by Nicholas Cundy at the University of Birmingham, with the exception of the thermal shift assay which was performed by Roseanna Hare at the University of Manchester.

After the disappointing performance of the synthesised compounds in the whole cell assays, another method for evaluating the compounds was necessary. A cell-free biochemical method of evaluation would be the most desirable as membrane permeability is not necessary for the observation of activity. The assay output should also be more closely linked to direct IDO inhibition in this setting, although the potential for non-specific activity in biochemical assays is well established.²²⁶

IDO1's structure and activity profile is well established within the literature and mainly through the extensive work of Emma L. Raven. Raven's research involved the determination of the various kinetic parameters associated with rhIDO1 and several IDO1 mutants.^{7, 227-229} A particularly important piece of this work involved demonstrating that **4** – a long reported and clinically evaluated inhibitor of IDO1 – was in fact a slow substrate rather than an inhibitor.⁵⁴ In establishing this, Raven's lab developed a steady-state kinetics assay that allows tracking of the reaction progress *via* continuous UV-vis absorption readings and the analysis of the metabolic products *via* LC-MS.^{54, 230} Raven utilised this to identify the product of **4** metabolism by IDO1 though identifying the metabolite mass *via* LC-MS.

As such, a collaboration with the Raven lab to assess a selection of the synthesised compounds *via* the steady-state kinetics assay was established. The collaboration sought to determine the metabolic outcome, if any, of the interaction between the synthesised compounds and IDO1.

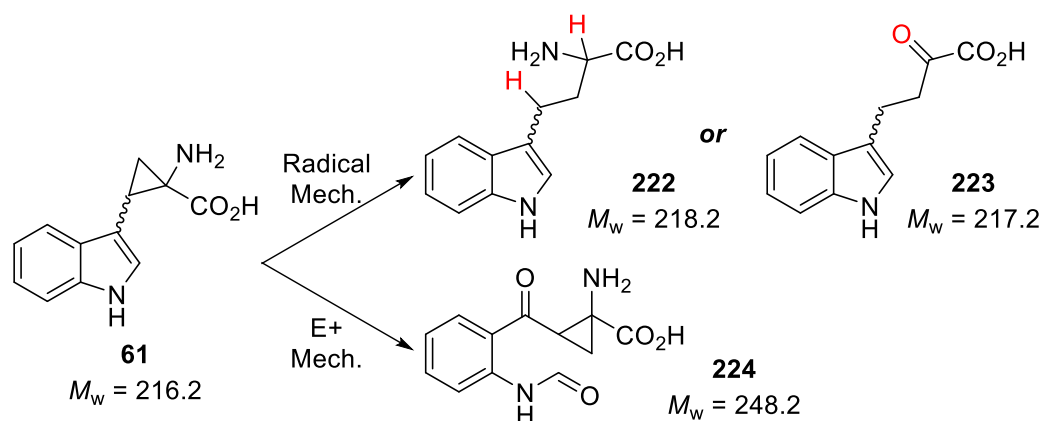
In the cuvette format the assay requires milligram quantities of IDO protein, which are not readily available from commercial suppliers. At the time of conducting these studies the Raven group were not able to prepare fresh protein, but had significant stocks of an IDO1 mutant F164A. The rhIDO1 F164A mutant represents a minor structural change in the distal pocket of the active site where a phenylalanine is replaced with an alanine residue. When compared to wild-type IDO1, the F164A variant demonstrates a K_d and K_m , with respect to *L*-Trp, of 1400 and 210 μ M; this represents a ~5-fold and 30-fold drop in K_d and K_m when compared to wtIDO1.²²⁹ The decrease in K_d and K_m can be rationalised *via* the reduced hydrophobicity of the active site when phenylalanine is replaced by alanine. Raven hypothesised that the π - π stacking interactions offered by the phenylalanine residue assists with the stabilisation of the aromatic indole ring system of tryptophan within the active site. Most importantly however, the

F164A mutant did not suffer a significant drop in the turnover rate (K_{cat}) as a result of the mutation.²²⁹ The data therefore suggests the F164A IDO1 mutant is a suitable protein to conduct mechanistic investigations.

1.7.1 – Steady-State Assay

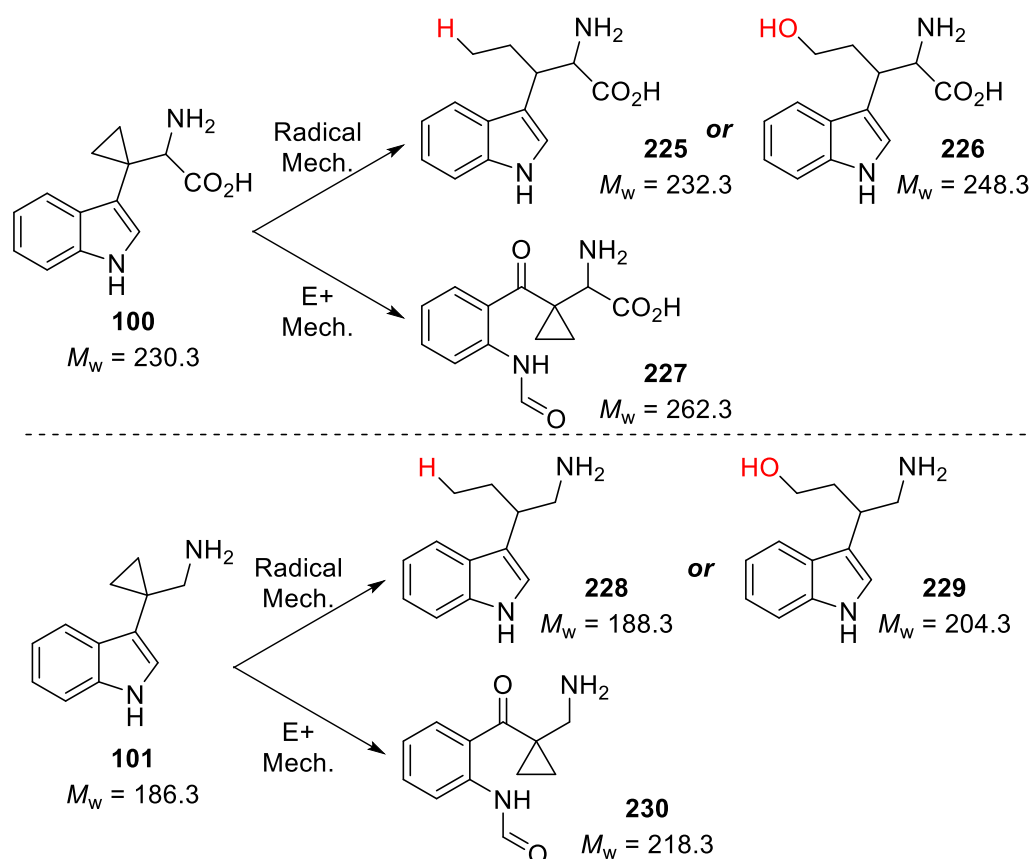
Like in the initial assay run by Raven, it was hypothesised that if the synthesised compounds were to be metabolised by IDO1, a tell-tale mass signature could be detectable *via* LC-MS. The results of these experiments could allow the identification of suitable inhibitors but more importantly it could help infer the detail of the dioxygenation mechanism.

For 1,2- Δ -tryptophan **61**·HCl the observation of different mass outcomes upon metabolism by IDO1 is expected. If the metabolism proceeds *via* the radical mechanism, the cyclopropane ring would open and the predicted homologated tryptophan **222** or α -keto acid **223** would be observed. Homologated tryptophan **222** would be a result of proton abstraction from either IDO1's active site or elsewhere. α -Keto acid **223** would be the product of a radical re-combination with molecular oxygen giving a transient hemi-peroxy aminal, collapse to the iminium species and ultimately the α -keto acid *via* hydrolysis. If the metabolism proceeds *via* the electrophilic mechanism, the cyclopropane would remain and cyclopropane-containing *N*-formyl-*L*-kynurenine **224** would instead be observed. Importantly, all of the possibilities have distinct mass outcomes which point toward a specific mechanistic pathway (Scheme 94).



Scheme 94 – Plausible mechanistic outcomes for the IDO1-mediated metabolism of **61**·HCl

Differences in mass are also expected to be observed between the possible mechanistic products of 1,1'- Δ -tryptophan **100** and tryptamine **101** metabolism (Scheme 95). Radical ring opening of cyclopropanes **100** and **101**, under the radical based metabolism mechanism, is predicted to result in the proton abstraction products **225** and **226** or alkyl hydroxyl compounds **228** and **229**, respectively. Similarly, products of the electrophilic pathway have distinct masses that will enable identification upon LC-MS analysis.

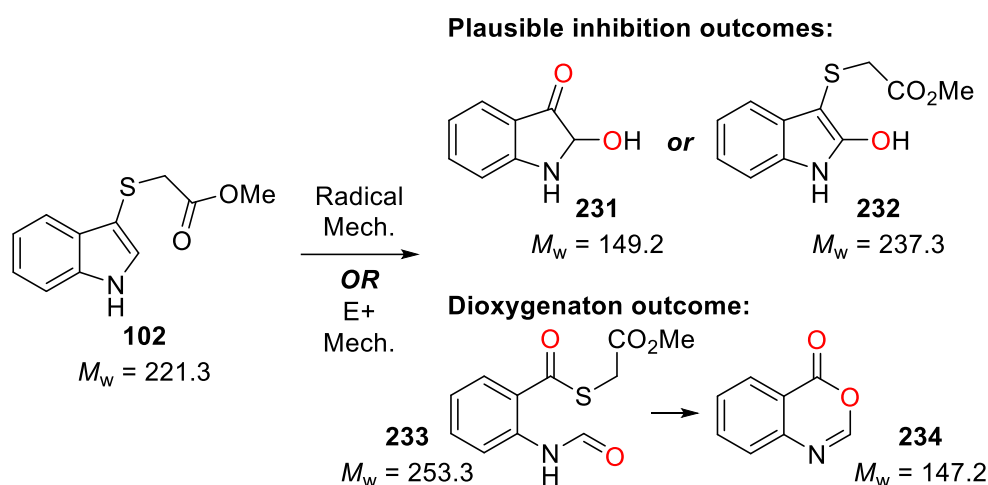


Scheme 95 – Plausible mechanistic outcomes for the IDO1-mediated metabolism of **100** and **101**

For inhibitors **61**, **100** and **101** it is hypothesised that radical ring-opening could lead to either the formation of covalently bound inhibitor-protein adducts or introduce a radical to the protein structure *via* proton abstraction. Radical incorporation into active site residues would lead to irreversible inhibition of IDO1 and the result of this interaction would not be detectable *via* LC-MS alone. Proton abstraction and effective radical transfer to the protein scaffold could lead to protein degradation which could complicate the interpretation of the results.

Sulfenylindole **102** is not predicted to be mechanistically divert the hypothesised radical intermediate, instead it is designed to divert later proposed intermediates in IDO1's substrate metabolism (Scheme 35, *vide supra*). The α -hydroxy ketone **231** is predicted to arise through ring-opening of a proposed epoxide intermediate *via* degradation of a hemithioacetal intermediate followed by hydrolysis of the thionium. 2-Hydroxy sulfenylindole **232** is predicted to arise from the mechanistic diversion of a later intermediate where preferential cleavage of the C-S bond occurs over the cleavage of the indole C(2)-C(3) bond. If no mechanistic diversion takes place, and sulfenylindole **102** is dioxxygenated, thioester **233** is the predicted outcome. A further intramolecular reaction of thioester **233** could also give rise to aryl-1,3-oxazin-4-one **234** (Scheme 96). While these experiments will not provide insight into the

mechanistic detail of IDO1's substrate metabolism, they would provide support for the ability to mechanistically divert the reactivity of IDO1 for potential therapeutic benefit.



Scheme 96 – Plausible Mechanistic Outcomes for the IDO1-mediated Metabolism of **102**

Steady-State Assay Validation

In order to validate the assay, experiments with Trp and **4** were replicated.²³⁰ The dioxygenation reactions were followed by tracking the formation of *N*-formyl-*L*-kynurenine (NFK) *via* its distinct UV-absorption at 321 nm (Figure 23). Addition of Trp to a solution of buffered IDO1 resulted in a linear increase in absorption at 321 nm indicating the steady formation of NFK; at roughly 40 min the absorption plateaus, suggesting either complete consumption of Trp, product-based inhibition of the enzyme or potential IDO1 poisoning as a result of a build-up of superoxy species.²³¹ Addition of **4** results in only a slight increase in absorption as the corresponding 1-methyl-*N*-formyl-*L*-kynurenine (1-Me-NFK) is formed as a significantly slower rate.

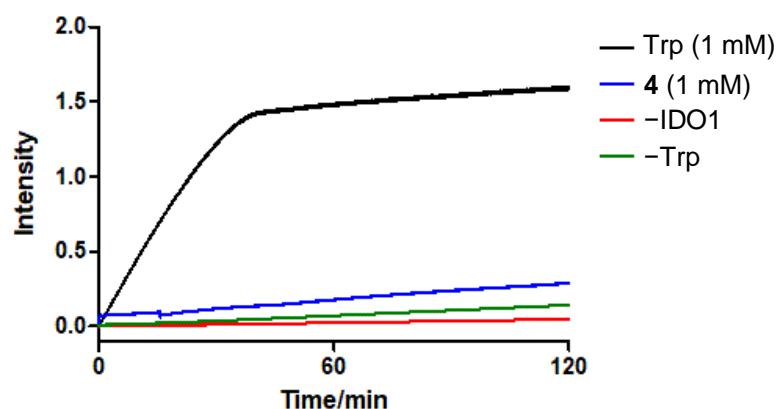


Figure 23 – Steady-state assay validation ($n = 1$)

A stock of Tris buffer (pH 8.0, 50 mM), sodium ascorbate (20 mM) and methylene blue (10 μ M) was oxygenated for 10 min and then transferred to a 1 mL capacity quartz cuvette. A solution of catalase (10 ng mL⁻¹) and then a solution of IDO1 (5 μ M) was added and allowed to equilibrate for 5 min. Trp (1 mM) or **4** (1 mM) was then added and UV-absorption were read for 2 h. The assay mixture was then quenched by addition of TCA_(aq) (30%), centrifuged to remove the enzyme and the submitted for LC-MS analysis.

The quenched assay mixtures were then subjected to LC-MS analysis to identify the mass products of IDO1 metabolism (Figure 24). Analysis of the Trp sample (Figure 24a) identified *N*-formyl-*L*-kynurenine ($M_W = 236.2$) as the $[M + H]^+$ ion. For **4**, a mass ion of 251.2 g mol⁻¹ was identified corresponding to the 1-methyl-*N*-formyl-*L*-kynurenine ($M_W = 250.2$ g mol⁻¹) $[M + H]^+$ ion (Figure 24b). These results corroborate with the observed results for -IDO and -Trp controls and the reported data by Raven and co-workers, confirming the dioxygenation of Trp and **4** to NFK and 1-Me-NFK, respectively, was a direct result of IDO1 activity.²³⁰

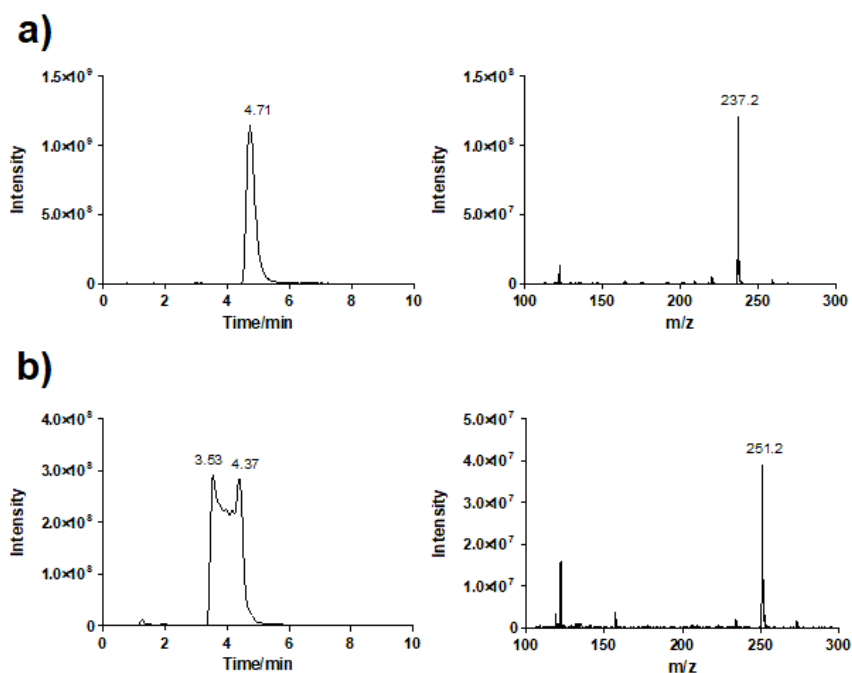


Figure 24 – a) TIC and MS data for metabolism of Trp; b) TIC and MS data for metabolism of **4**

Steady State Assay analysis of Compounds **61·HCl**, **100·HCl**, **101·HCl** and **102**

With the assay validated, the investigation sought to identify the metabolic by-products, if any, of IDO1's metabolism of the synthesised indoles. As such, four compounds were selected for testing based on their ability to probe the radical mechanism or prior performance in the whole cell assay: **61·HCl**, **100·HCl**, **101·HCl** and **102** (Figure 25).

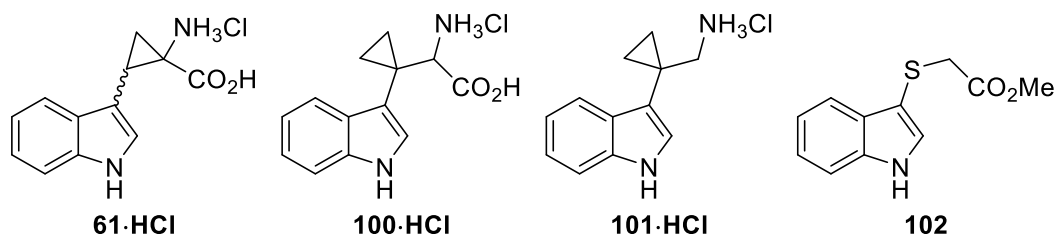


Figure 25 – Compounds selected for the steady-state assay

The assays were performed in an analogous fashion to the Trp and **4** steady state assays with the inhibitors added in the place of Trp/**4**. Throughout the assay the reactions were monitored *via* UV-absorption (Abs = 321 nm) to detect the formation of any NFK-like products. Post-assay the quenched solutions would be subjected to LC-MS and the data analysed to identify any masses that correspond to plausible metabolism products.

Tracking the progress of inhibitor metabolism *via* UV-absorption gave no clear indication that a 321 nm-absorbing chromophore was being generated by the metabolism of **61·HCl**, **100·HCl**, **101·HCl** and **102**. Tryptophan analogue **61·HCl** demonstrated a minor increase in absorbance over time, however this result was difficult to interpret due to **61·HCl** also demonstrating absorbance at 321 nm (Appendix 5).

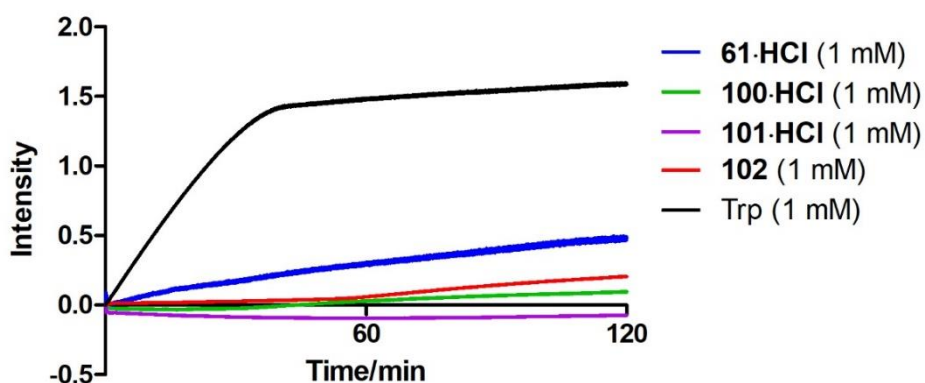


Figure 26 – Steady-state assay UV absorption data for **61·HCl**, **100·HCl**, **101·HCl** and **102** ($n = 1$)

Analysis of the LC-MS data also gave no indication of inhibitor modification though interaction with IDO1. In all cases, none of the plausible metabolic by-product masses were observed and the masses of the inhibitor used were identified within the respective quenched solutions (See Appendix 6.1–7 for LC-MS data of the steady-state assay mixtures, individual compound and assay media LC-MS data).

The lack of observed changes in the steady-state assay could be attributed to multiple factors. The lack of substrate recognition by the enzyme and active site binding; without binding within active site, no turnover of compound will occur. It is also possible that the inhibitors have worked as desired and no further compound turnover is possible due to the deactivation of the enzyme; if this was the case, it would also mean only trace amount of the predicted by-products would be present in the quenched solution. For inhibitors **61·HCl**, **100·HCl** and **101·HCl**, radical ring opening could also see the incorporation of the inhibitor into an active site residue through radical addition. Covalent linkage of the metabolic by-product to the enzyme would prevent the detection *via* LC-MS.

Summary: Steady State Assay

The steady-state assay identified that compounds **61·HCl**, **100·HCl**, **101·HCl** and **102** were not turned over by IDO1. However, very limited conclusions could be drawn from this data. For example, it could not be identified if the compounds were potentially inhibiting the enzyme activity as expected and remaining within the active site, or not interacting with the protein at all. A novel method is therefore required to determine any inhibitory characteristics of **61·HCl**, **100·HCl**, **101·HCl** and **102**.

1.7.2 – Inhibition Assay

We sought to develop an inhibition assay from the methodology published by Raven. Compounds **61·HCl**, **100·HCl** and **101·HCl** are designed to be irreversible inhibitors, as such we expect the inhibition of IDO1 to be time-dependent. The assay must therefore allow an incubation period where the inhibitor is exposed to the enzyme prior to the addition of IDO1's substrate, Trp. To determine a suitable incubation period, the assay mixture was allowed to rest for 15 and 30 minutes prior to the addition of Trp (Figure 27). A pre-incubation period of 30 minutes lead to a significant drop in the detected *N*-formyl-*L*-kynurenine *via* UV-absorbance and LC-MS analysis (Appendix 7.1). The fall in detected *N*-formyl-*L*-kynurenine was interpreted as the degradation of the enzyme over the course of the pre-incubation period. Pre-incubating for 15 minutes lead to only a minor drop in the UV-absorbance signal while maintaining a clear steady-state formation of Kyn suggesting this was a suitable rest period to prevent a significant drop in enzyme activity (Appendix 7.2). This data also further demonstrates that the plateau in the data is driven by enzyme stability rather than Trp consumption or product inhibition.

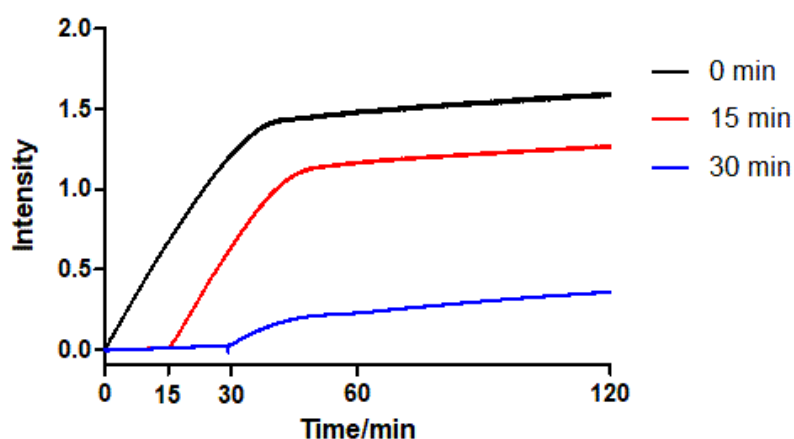


Figure 27 – The effect of pre-incubation of 15 and 30 minutes on NFK production ($n = 1$)

Prior to testing the selected compounds, the assay was validated with respect to its ability detect inhibition of IDO1 activity. For this, known IDO1 inhibitor epacadostat (INCB) **6** and competitive substrate **4** were utilised.

Dosing at $10 \mu\text{M}$ of inhibitor **6** gave complete suppression of UV-absorbance at 321 nm, which was interpreted as complete inhibition of IDO1 (Figure 28). The lack of an NFK mass ion peak in the LC-MS analysis of the assay mixture further supported the complete inhibition of IDO1 activity by inhibitor **6** (Appendix 8). Highly competitive inhibitor **6** was dosed super-stoichiometrically with respect to IDO1 to ensure complete inhibition of enzyme activity. When pre-incubated with **4**, an increase in absorbance can be observed even prior to the addition of Trp at 15 minutes. Upon addition of Trp, the absorbance begins to increase as NFK is produced but not to the same extent as the negative control. Production of NFK from metabolised Trp, and 1-methyl-*N*-formyl-*L*-kynurenine from **4**, was later confirmed by LC-MS (Appendix 9). These data indicate that IDO1 inhibitor **6** is a suitable positive control for these experiments whereas **4** is not a suitable due its conversion to the dioxygenated adduct by IDO1. This data also supports **4** acting as a competitive substrate.⁵⁴

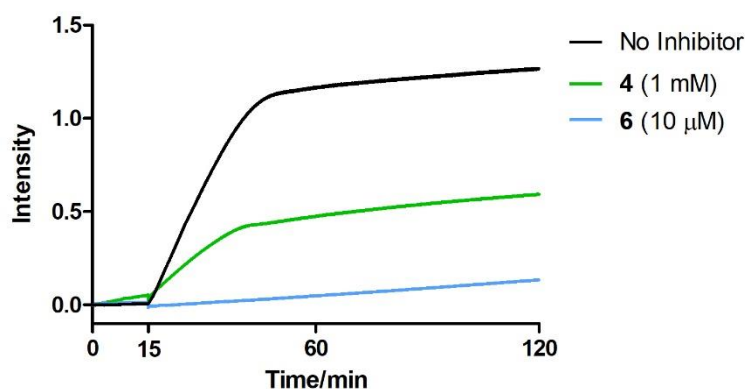


Figure 28 – Inhibition assay validation ($n = 1$)

IDO1 was pre-incubated in the presence of 1 mM of compounds **61·HCl**, **100·HCl**, **101·HCl** or **102** and were assayed against **6** to evaluate their inhibitory activity (Figure 29). Tryptamine analogue **101·HCl** displayed poor inhibition of IDO1 with only a small drop in Kyn production with respect to the no inhibitor control. Sulfenylindole **102** and tryptophan analogues **61·HCl** and **100·HCl** however displayed a significant reduction in absorbance, demonstrating significant inhibition of IDO1 activity.

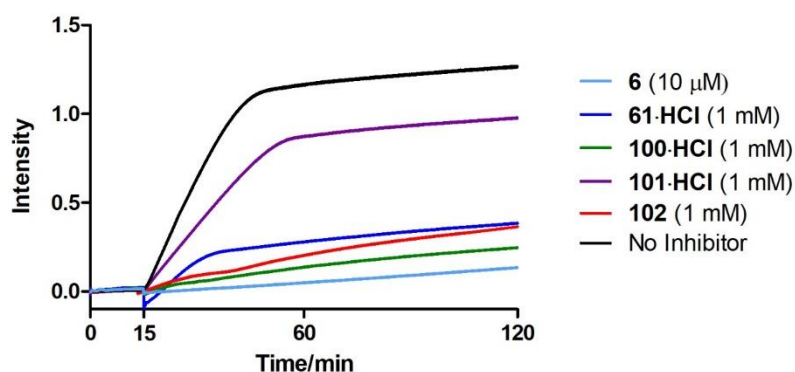


Figure 29 – Inhibition assay data for **61·HCl**, **100·HCl**, **101·HCl** and **102** ($n = 1$)

With these results, further experiments were carried out with **61·HCl**, **100·HCl** and **102**. Reducing the dose concentration 10-fold for 1,2- Δ -tryptophan analogue **61·HCl** saw complete loss of inhibitory activity (Figure 30). For sulfenylindole **102** a 10-fold drop in concentration lead to a small drop in inhibitory activity but the compound retained its ability to suppress IDO1 activity (Figure 31). Further investigation of sulfenylindole **102** was however ceased in favour of other more promising hits due to the narrow therapeutic window observed in the whole cell assays.

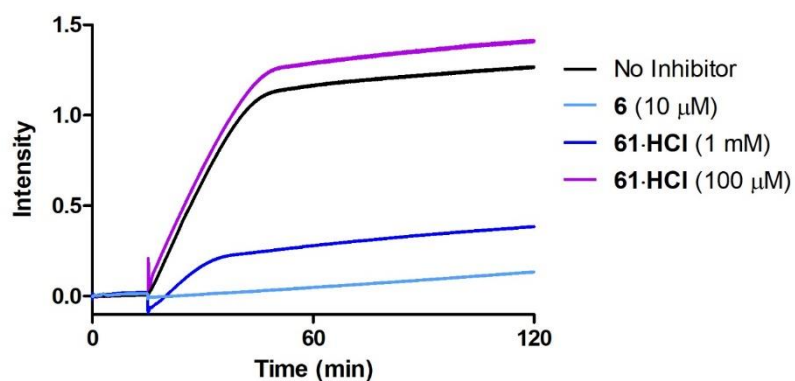


Figure 30 – Reduced dosing of **61·HCl** and the effect on IDO1 activity ($n = 1$)

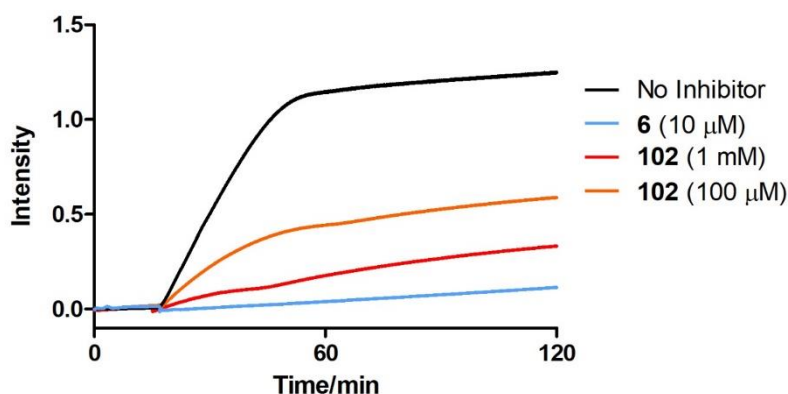


Figure 31 – Reduced dosing of **102** and the effect on IDO1 activity ($n = 1$)

In these preliminary assays, 1,1'- Δ -tryptophan analogue **100·HCl** demonstrated itself to be the most efficacious inhibitor of IDO1 activity (Figure 32). Significant inhibition of IDO1 was achieved at concentrations as low as 10 μ M.

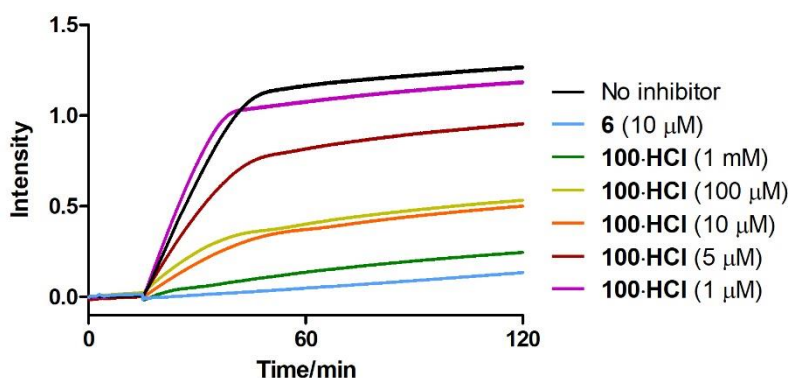


Figure 32 – Reduced concentration dosing of **100·HCl** effect on IDO1 activity ($n = 1$)

The result was treated with much intrigue due to the structure of inhibitor **100·HCl**: a compound that contained a cyclopropane ring that could allow for mechanistic diversion.

Firstly, experiments were designed to determine whether the inhibition of IDO1 by cyclopropane **100·HCl** was time-dependent. In order to assess this, cyclopropane **100·HCl** and Trp were co-administered in equi-molar quantities and the subsequent production of Kyn was monitored *via* UV-absorption (Figure 33). The co-administered mixture initially experiences turnover of Kyn albeit at a significantly slower rate compared to the control – after 20 minutes the production of Kyn beings to plateau. This is contrary to what is observed when **6** and Trp are co-administered: no initial increase in absorbance is seen. The data is therefore suggestive of a time-dependency in the inhibitory activity of cyclopropane **100·HCl**.

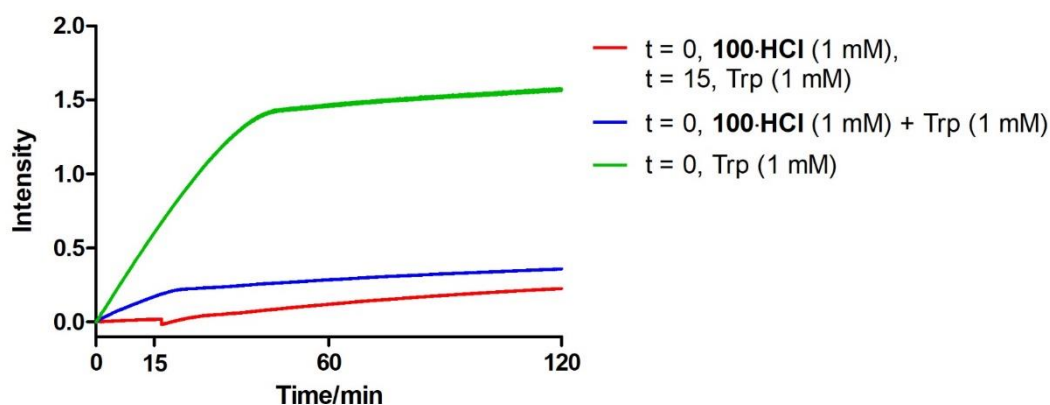


Figure 33 – Time-dependent inhibition of IDO1 by cyclopropane **100·HCl** ($n = 1$)

Encouraged by the apparent time-dependent behaviour of cyclopropane **100·HCl**, the ability of inhibitor **100·HCl** to be out-competed by an excess of IDO1's natural substrate was evaluated. IDO1 was pre-incubated with cyclopropane **100·HCl** and after 15 minutes Trp (10 mM) was added (Figure 34). A 10-fold increase in Trp concentration led to no increase in Kyn production suggesting the inhibitor was not out-competed by excess substrate. This infers one of three possibilities: cyclopropane **100·HCl** is an irreversible inhibitor, the K_i of the inhibitor is significantly lower than the K_d of Trp with respect to IDO1 or the high concentration of Trp resulted in substrate mediated inhibition of IDO1. It therefore became necessary to determine the K_i value for inhibitor **100·HCl**. However the determination of K_i via the current assay would be challenging due to high protein requirements and the time implications when running a single experiment at a time.

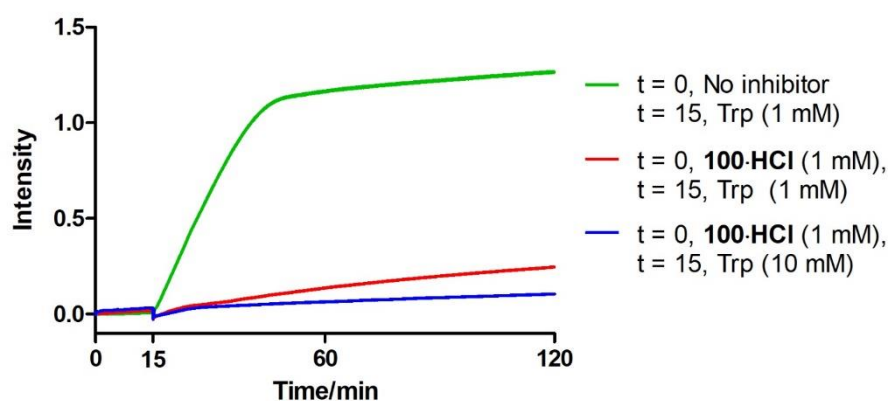


Figure 34 – Inhibitor/substrate competition experiment ($n = 1$)

Summary: Inhibition Assay

A preliminary inhibition assay was developed and helped identify viable candidates for further evaluation. Tryptamine analogue **101·HCl** performed poorly in this assay, demonstrated no significant inhibition of IDO1 activity. Tryptophan **61·HCl** initially demonstrated good inhibition

of protein activity but this was lost when dosed at 100 μ M. However the reliability of the 1 mM concentration data is questionable due to the high background absorbance of compound **61-HCl**. Sulfenylindole **102** demonstrated good inhibition of enzyme activity at the two evaluated concentrations (1 mM and 100 μ M). Further evaluation of this compound was ceased due to the previously discovered narrow therapeutic window. Inhibitor **100-HCl** demonstrated the most favourable inhibition profile: good inhibition in the cell free assays and no observed toxicity at 1 mM. Further experiments also identified a time-dependency in its inhibition of the inability to out-compete the inhibitor – key characteristics of an irreversible inhibitor. The throughput of this assay was however limited by being performed as discrete experiments – this could also limit the reliability and repeatability of the data.

1.7.3 – Fluorescence-Based Detection of NFK

Kyn has been reported to have a fluorescence emission maximum at 434 nm upon excitation at 325 nm suggesting that the assay progress could be tracked *via* following the fluorescence gain during the production of Kyn.²³² Due to the reduced background relative to UV absorption fluorescence spectroscopy is a more sensitive technique and scaling of the 1 mL UV cuvette-based assay to a 384-well plate should therefore be feasible. Use of a fluorescence-based technique could also allow for a higher level of selectivity in tracking the reaction progress – a problem encountered when measuring compound **61-HCl** inhibition of IDO1.

The previously developed inhibition assay was therefore performed on the same volume but analysing in a fluorimeter (ex 324/em 434), with fluorescence reading being taken every 2 minutes. In order to determine whether the assay could be translated to a plate-based format, 50 μ L aliquots were taken at specific time points (10, 20, 25, 30, 40 and 50 min). The aliquots were quenched by dilution into an equivalent volume of DMSO in a 96-well plate and the resulting plate was analysed *via* a plate reader.

The fluorimeter based assay replicated the line shape observed within the UV-absorbance based assay (Figure 35). The quenched aliquots followed the line shape of the fluorimeter readings which demonstrated that both a plate-based assay and a stop-flow assay were feasible options for developing higher throughput assays. Prior UV-absorbance based control experiments had also demonstrated that it is not necessary for the assay mixture to be sealed under an atmosphere of oxygen to observe Trp turnover – a suspected issue of a plate-based assay (Appendix 10).

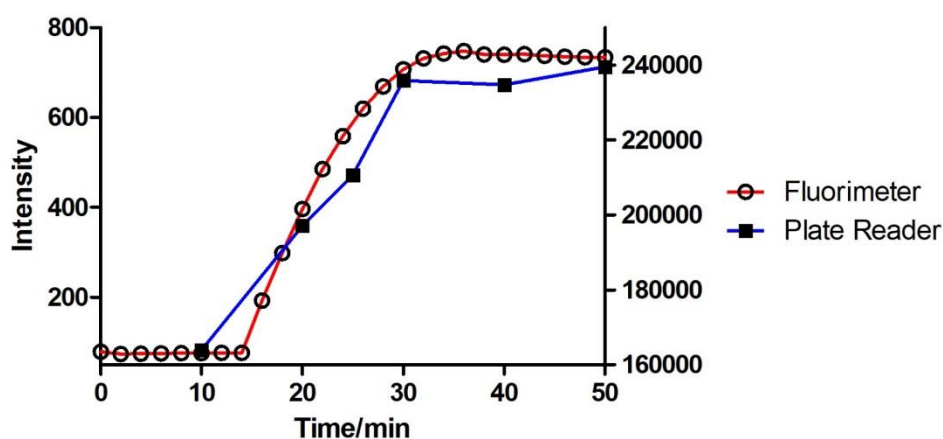


Figure 35 – Validation of fluorescence-based detection of NFK ($n = 1$)

The inhibition assay control (no inhibitor, 1 mM Trp addition at 15 min) was then replicated in a 384-well plate. The resulting readings demonstrating an increase in fluorescence with time – no fluorescence readings were taken during the 15 minute pre-incubation phase (Figure 36).

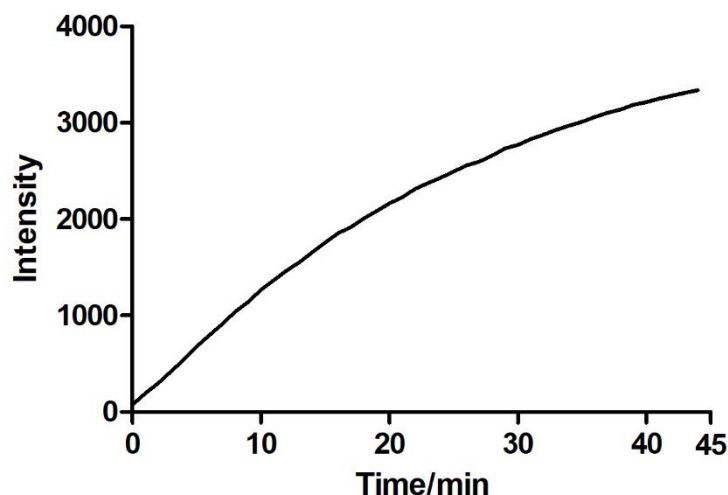


Figure 36 – 384-well plate-based inhibition assay

$n = 3$, data reported as the mean value and is blank corrected

Importantly the assay demonstrated a linear increase in intensity over the first 5–10 min which would allow the development of an assay to estimate inhibitor K_i values *via* a Dixon plot analysis.²³³ To calculate the K_i value using a Dixon plot, 3 or more concentrations of the enzymes natural substrate must be selected. Typically the values lie at a higher and lower concentration than the Michaelis constant (K_m) of the substrate and then a value is selected that is close to the K_m value.²³⁴

Determination of Trp K_m

In order to determine the K_i for tryptophan analogue **100-HCI**, the K_m value of tryptophan for the IDO1 F164A enzyme was verified in the steady-state assay to allow the selection of appropriate concentrations of Trp for use in the Dixon analysis.

The K_m value of tryptophan with respect to the IDO1 F164A mutant was therefore determined by calculating the initial rate of reaction (V_o) of a range of tryptophan concentrations and then plotting V_o versus the tryptophan concentration, with the data fitted to the Michaelis-Menten equation to determine the K_m value.

The IDO F164A mutant has a reported K_m of 210 μM .²²⁹ Based on the reported K_m value, 12 concentrations of tryptophan were selected ranging from 3000–0.02 μM (Figure 37). The data demonstrated a maximum V_o at Trp concentrations of 300–1000 μM ; above 1000 μM , a significant drop in the rate was observed which is suggestive of substrate inhibition afforded by the excess tryptophan present. The observed substrate inhibition has a negative impact on the line fitting and thus the confidence in the estimation of the K_m value. With the 3000 μM included in the Michaelis-Menten fit ($R^2 = 0.865$), a K_m value was calculated as $37.6 \pm 15.3 \mu\text{M}$ (Figure 37a). Excluding the 3000 μM data point from the Michaelis-Menten fit ($R^2 = 0.977$) gave an estimated K_m value of $68.6 \pm 11.01 \mu\text{M}$ (Figure 37b).

The observation of substrate inhibition at concentrations above 1 mM Trp suggests that the prior experiment to out-compete the inhibitor with a higher concentration of substrate (Figure 34) may have not been an appropriate method to evaluate that hypothesis. Other groups have also observed substrate inhibition at higher Trp concentrations.²³⁵

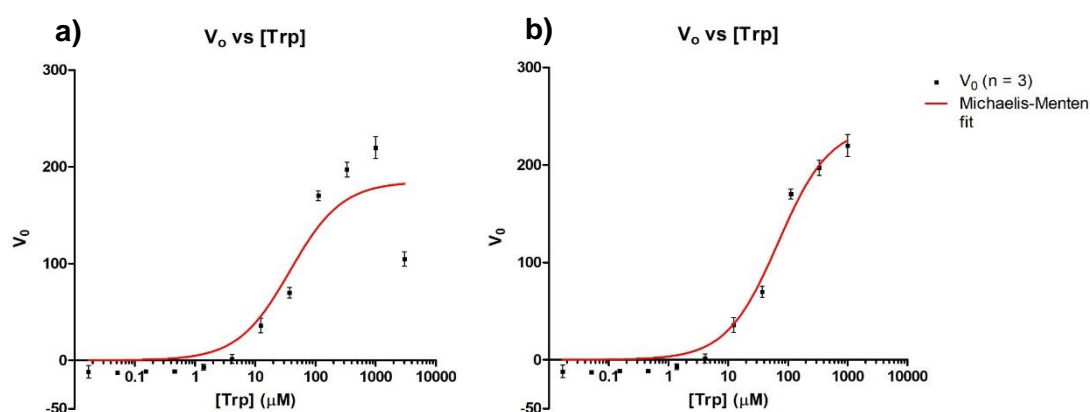


Figure 37 – K_m determination of tryptophan
a) Including the 3 mM data point, b) excluding the 3 mM data point

From these data, the tryptophan concentrations 3, 30 and 300 μM were selected as suitable concentrations to perform the Dixon analysis and determine the K_i of tryptophan analogue **100-HCl**.

Determination of the K_i of INCB 6 and Tryptophan Analogue 100-HCl

Competitive inhibitor **6** was first subjected to the Dixon analysis to confirm the assay could provide a reasonable estimate for the K_i of a known inhibitor. A range of concentrations of inhibitor **6** (10 μM –0.17 nM) were incubated with IDO1 and then treated with 3, 30 or 300 μM Trp. Calculating the V_0 and plotting the reciprocal of V_0 against the concentration gave the Dixon plot (Figure 38).

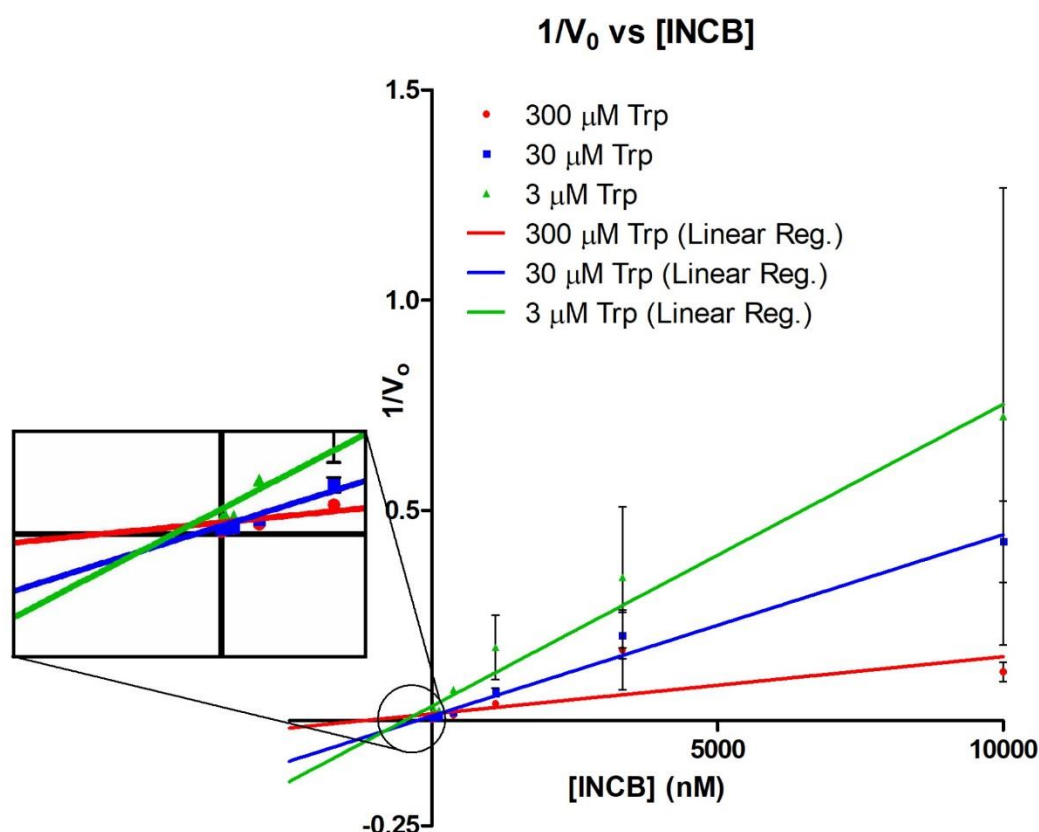


Figure 38 – Dixon plot K_i determination of INCB 6 ($n = 3$)

The Dixon analysis of **6** did not give a reliable intersection of the linear regression lines of the data points to allow the reliable estimation of the K_i value, however this is not especially surprising as the reported K_i of the compound is ~ 10 nM while the concentration of IDO is 1 μM . This means that the degree of inhibition is predominantly driven by the stoichiometry of **6**:IDO1 around the protein concentration and the substrate concentration therefore has a limited impact on the observed K_i .

The analysed data for tryptophan analogue **100·HCl** provided three parallel lines for the three concentrations of Trp utilised which was an unanticipated result and difficult to interpret (Figure 39). Further evaluation of the raw data demonstrated an apparent lack of IDO1 inhibition even at higher compound concentrations, which is inconsistent with the prior observations of IDO1 inhibition in the UV-based inhibition assay (Figure 32).

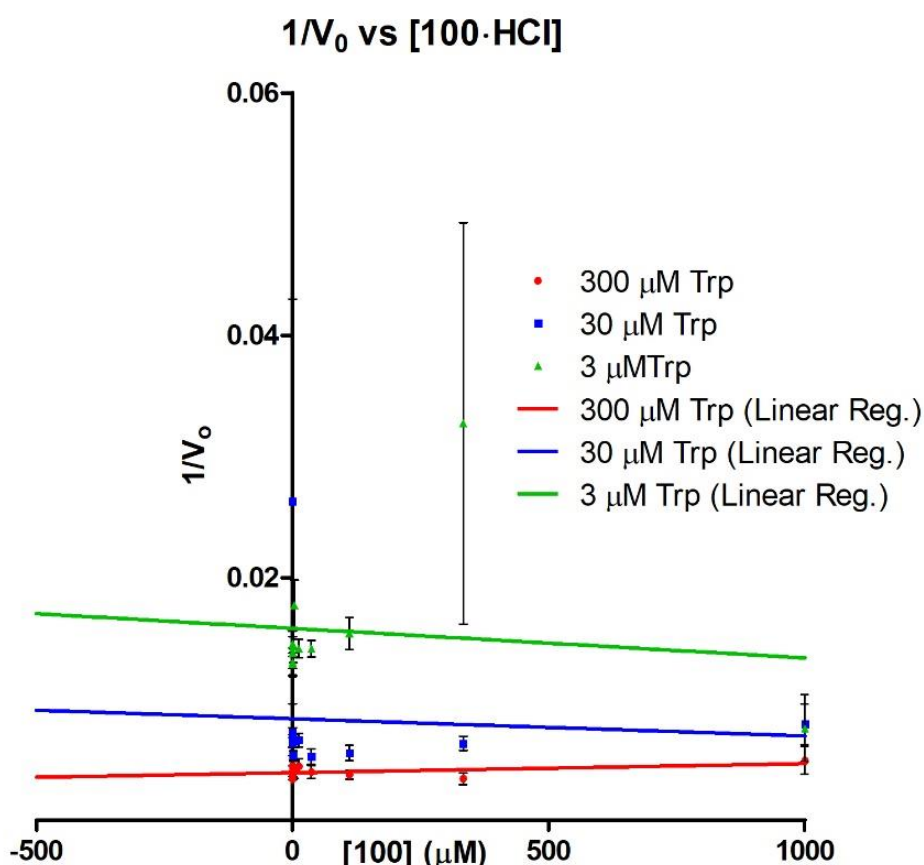


Figure 39 – Dixon plot K_i determination of **100·HCl** ($n = 3$)

Throughout the investigation it was noticed that at high dosing concentrations of **100·HCl**, the assay mixtures demonstrated a high background fluorescence. This was not expected as the molecule itself is structurally related to tryptophan, however one hypothesis was that low level turnover of **100·HCl** by IDO1 could result in formation of a highly fluorescent adduct that interferes with the assay readout.

It was therefore appropriate to determine whether the background changed with time to an extent that could affect the assay result (Figure 40). Three **100·HCl** concentrations were selected and measured over a period of 60 min to determine any changes in fluorescence. Predictably 1 mM **100·HCl** demonstrated high background fluorescence but the level of fluorescence did not change significantly over time. At concentrations of 100 and 10 μM **100·HCl** the level of background fluorescence dropped significantly. Based on these results,

the background fluorescence of **100-HCl** should not have a significant impact on the ability to detect gain in fluorescence as a result of NFK production.

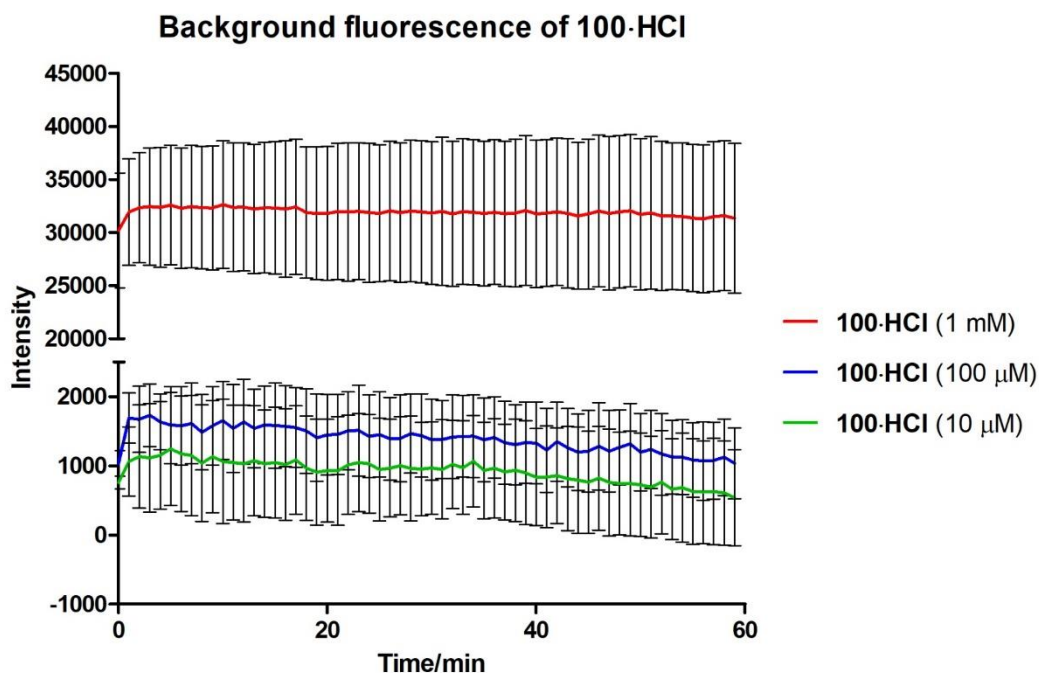


Figure 40 – Change in fluorescence over time at three concentrations of **100-HCl** ($n = 3$)

Summary: Fluorescence-Based Detection of NFK

It was demonstrated that the formation of *N*-formyl-*L*-kynurenine, by IDO1 metabolism of Trp, could be detected *via* fluorescence spectroscopy in a 1 mL cuvette and a 384-well plate with no loss in detection sensitivity.

In order to determine the K_i value for tryptophan **100-HCl**, the K_m of Trp had to first be determined to allow the selection of appropriate substrate concentrations for use in a Dixon plot analysis. A novel assay was developed and the data was fit to the Michaelis-Menten equation to estimate the K_m value. This experiment identified that at high concentration a degree of substrate inhibition is observed. As a result of this finding, the substrate concentrations of 3, 30 and 300 μM were selected as appropriate concentrations for the Dixon plot analysis.

Performing the Dixon plot analysis for known inhibitor **6** gave data with a high degree of error and data that lacked an identifiable intersection of the three linear regression analyses, most likely as a result of the high protein concentration in the assay. Performing the same Dixon analysis with tryptophan analogue **100-HCl** returned three parallel lines which in the context of a Dixon analysis were inexplicable, but probably relate to the low effect levels seen in these

assays. To date we have no explanation as to why the inhibitory effects seen with **100·HCl** in the UV-absorption assay were not reproduced in the plate-based experiment.

1.7.4 – Differential Scanning Fluorimetry/Thermal Shift Assay

To establish whether a binding event was occurring between tryptophan analogue **100·HCl** and IDO1, a thermal shift assay was performed. INCB **6**, 1-MT **4** and **100·HCl** were incubated with IDO1 in the presence of SYPRO orange, a fluorescent staining agent, and heated to determine the thermal denaturation temperature (T_m) of the enzyme.²³⁶ As the temperature is increased the protein begins to denature, exposing hydrophobic surfaces that the SYPRO dye can bind to. Once bound, the SYPRO emits a fluorescent signal which can be used to infer the level of denaturation. The result is a bell shape curve that represents the thermal denaturation profile of the protein in question and allows for the determination of the protein T_m .

The binding of small molecules to an enzyme has been demonstrated to have an impact on the thermal stability of the protein.²³⁷ Shifts in the T_m value, versus the control, therefore implies a binding even between the protein and the inhibitor.

Control experiments demonstrated that the IDO1/SYPRO dye ratio was critical for reliable data (Figure 41). High IDO1/SYPRO ratios (1/500) resulted in an overall decrease in the control T_m value to ~30 °C. As the IDO1/SYPRO ratio was decreased, the thermal stability of the enzyme increased to a consistent value of ~37 °C. The instability of IDO1 at high SYPRO ratios is indicative of a destabilising interaction between IDO1 and SYPRO, likely induced by SYPRO binding to IDO1. Interestingly, when no SYPRO dye was used, a fluorescence signal was detected when IDO1 alone was subjected to the T_m assay conditions. It has been previously demonstrated that denaturation of heme-based proteins leads to the release of a readily fluorescent porphyrin species.²³⁸ Compound effects were therefore assessed in both the presence and absence of SYPRO.

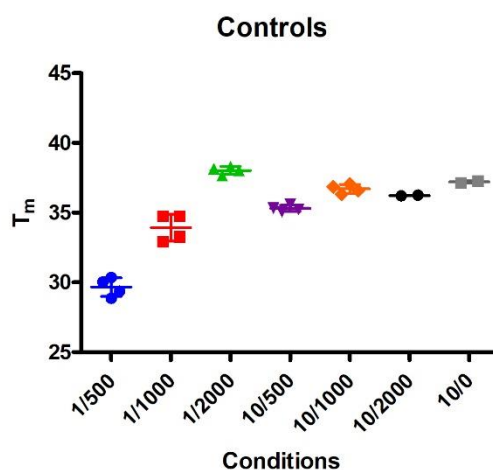


Figure 41 - Thermal shift assay control experiments: IDO/SYPRO dye ratio

Heating IDO1 and SYPRO dye (1/2000) in the presence of **6** (100 μ M) led to a significant increase in the T_m of IDO1, indicating a significant stabilisation afforded by the binding of **6** to IDO1 (Figure 42). Incubation of IDO1 with tryptophan analogue **100-HCl** failed to see an increase in the T_m versus the control suggesting no binding interaction has occurred. Similarly, no significant binding event was observed with **4**, which alongside the destabilising effects of SYPRO on the protein led to the hypothesis that SYPRO orange may be directly or indirectly affecting the interaction with these molecules.

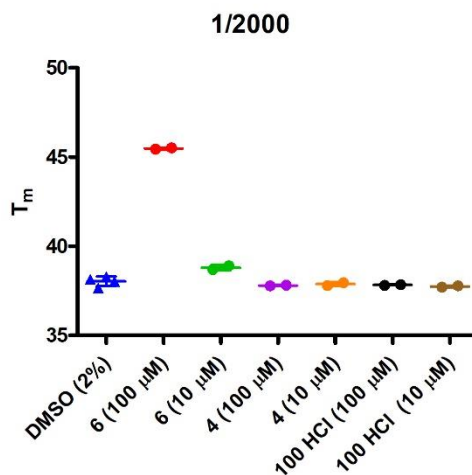


Figure 42 – T_m shift of IDO1 when incubated with **6**, **4** and **100-HCl** in the presence of SYPRO dye

We therefore decided to investigate the thermal shift using the heme detection endpoint. In this instance, the T_m for the IDO1-**6** complex remained unchanged with respect to the control (Figure 43). Increases in the T_m value begin to be observed when IDO1 is incubated with tryptophan analogue **100-HCl** at 100 μ M and even more so when **100-HCl** concentration is 500 μ M. The increase in T_m is indicative of a binding event between IDO1 and **100-HCl**.

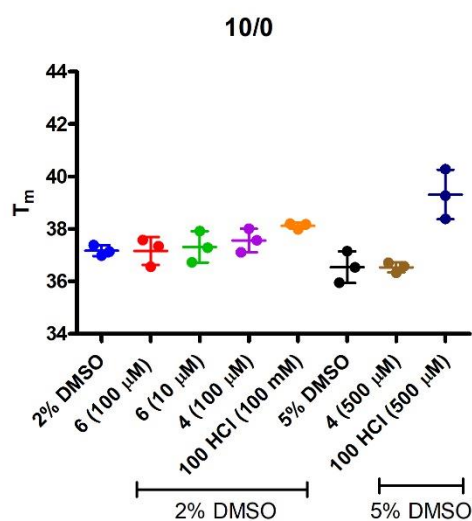


Figure 43 - T_m shifts of IDO1 when incubated with **6**, **4** and **100-HCl** in the absence of SYPRO dye

When the SYPRO dye is utilised as the protein staining agent, fluorescence gain is a result of a global change in the protein structure which allows for fluorescence detection. In the example where no SYPRO is used, the fluorescence gain is a result of a change in the heme-environment. This can therefore be interpreted as tryptophan **100-HCl** affording greater stability to the heme unit *via* a binding event.

Studies of **6**'s, and related analogues, competitive binding to the IDO1 active site implicate significant binding interactions between **6** and the IDO1 active site binding pockets.²³⁹ Through high affinity binding to the active site pocket, the thermal stability afforded to the IDO1-**6** complex, and as a result the increase in T_m , can be rationalised. In the case of **4** and **100-HCl**, the stabilisation afforded to the active site binding pockets will be minimal and as such, little increase in T_m was observed.

Without the SYPRO dye, and relying on changes in the heme-environment, alternative factors could dominate the observed T_m . For instance, liberation of the heme unit to form the fluorescence active porphyrin unit could be an early event upon exposing the enzyme to heat. If stabilised, the release of porphyrin would occur at a higher temperature leading to a shifted T_m . The shift in observed T_m value for the IDO-**100-HCl** (500 mM) experiment strongly implies a direct interaction between IDO1 and **100-HCl**. However, the relative effects of **6** and **100-HCl** compound requires further investigation.

Summary: Differential Scanning Fluorimetry/Thermal Shift Assay:

The most applicable conditions for determining the T_m value of IDO1-Binding substrate complexes were found to be at low ratios of IDO1 to SYPRO dye. High ratios lead to the suspected binding to the protein and resultant destabilisation.

In the presence of the SYPRO dye, a significant shift of T_m was observed when IDO1 was incubated with 100 μM **6** while no change in T_m was observed when IDO1 was pre-incubated with **4** or **100·HCl**.

Changes in fluorescence could also be observed in the absence of the SYPRO stain, this was thought to be a result of the liberation of a fluorescently active porphyrin from the IDO1 active site. Experiments to determine T_m subsequently gave contradictory results compared to the observed result in the experiments where SYPRO dye was used. It was rationalised that the two assays were surveying two distinct denaturing events that could lead to observed differences in the measured T_m value, however this was not experimentally verified. Further investigation would be required to confirm this hypothesis.

1.8 – Conclusions and Future Work

A novel route to 1,2- Δ -tryptophan **61·HCl** was developed that relied on the *in situ* generation of a reactive diazo intermediate in the presence of an amino acrylate (Scheme 52).^{145, 154} The route avoided the use of harsh reagents employed in the prior synthesis of **61** and proceeded in excellent overall yield.¹⁴³

Targeted 1,2- Δ -tryptophan **61·HCl**, 1,2- Δ -tryptamine **99** and homologated 1,2- Δ -tryptamine **182** were unstable under aerobic conditions which resulted in the production of a highly coloured impurity or complete degradation of the compound. Both factors prevented the biological evaluation of compounds **61·HCl**, **99**, and **182**.

The instability of the 1,2-cyclopropane cores was hypothesised to be a result of the polarisation of the cyclopropane ring by electron-withdrawing and donating groups. 1,1'- Δ -Tryptophan **100·HCl** and tryptamine **101·HCl** were thus designed and successfully synthesised. Compounds **100·HCl** and **101·HCl** were stable to aerobic conditions and were therefore viable candidates for evaluation. A small library of sulfenylindoles was also successfully synthesised.

Whole cell evaluation (Figure 21 & Figure 22) in IFN γ stimulated HeLa cells demonstrated that the assayed compounds were poor inhibitors of IDO1 activity. Sulfenylindole **102** and cyclopropyl ester **181** displayed the most promising inhibition profile, however significant cellular toxicity was seen at >300 μ M which ultimately complicated the interpretation of these results. It was not possible to determine from the whole cell assay data whether the lack of IDO1 inhibition was a result of limited interaction with IDO1 or the failure of the compounds to cross the cell membrane.

To establish whether the synthesised inhibitors demonstrated any interaction with IDO1, a biochemical assay was developed to assay compounds **61·HCl**, **100·HCl**, **101·HCl**, and **102**. These assays identified 1,1'- Δ -tryptophan **100·HCl** as a potential inhibitor of IDO1. Further investigation of **100·HCl** led to the observation of time-dependent inhibition and the inability to overturn its inhibitory activity with excess substrate – two characteristics that are suggestive of irreversible inhibition.

A novel assay was developed for the detection of *N*-formyl-*L*-kynurenine *via* fluorescence spectroscopy. The K_m was successfully determined for Trp with respect to IDO F164A and this finding was used to inform appropriate substrate concentrations for use in a Dixon plot analysis to determine the K_i values for **6** and **100·HCl**. Dixon plot analysis of **6** and **100·HCl** failed to give reliable data, due to faults in the assay design, and as such it was not possible to determine the K_i value for **6** and **100·HCl**.

Thermal shift analysis of IDO1, in the presence of the fluorescent dye SYPRO orange, demonstrated that at high IDO1:SYPRO ratios IDO1 displayed high thermal instability – a suspected result of SYPRO orange binding destabilising the protein. In the absence of a dye, IDO1 demonstrated a clear change in fluorescence signal upon heating. This was hypothesised to be due to the release of a highly fluorescent porphyrin ring as the enzyme denatures. In the SYPRO-free experiment, IDO1 incubation with **100·HCl** demonstrated a significant shift in the T_m value, which was suggestive of an IDO1-**100·HCl** interaction. Further investigation would be required to confirm the presence of an interaction between IDO1 and **100·HCl**.

Moving forward, further X-ray and mass spectrometry-based experiments could help decipher any interactions between tryptophan analogue **100·HCl** and IDO1. To assist with the mass spectrometry-based experiments, propargyl ester **235** could be synthesised to allow for the ligation of a photoaffinity probe to enhance the detection of any potential inhibitor-protein adducts (Figure 44).²⁴⁰

If inhibition is demonstrated by these methods, further evaluation of tryptophan analogue **100·HCl** in a whole cell model should be carried out; principally to identify if crossing the cell membrane is the limiting factor in the observation of IDO1 inhibitory activity. Further to this, a pro-drug approach to administering tryptophan analogue **100·HCl** should be considered.

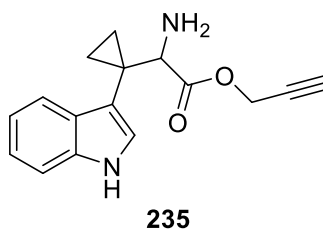


Figure 44 – Propargyl ester **235**

Chapter 2:

Design, Synthesis and Evaluation of PROTAC-degraders of JAK2

2.1 – Therapeutic Intervention of the JAK/STAT Pathway

In mammalian systems there are multiple pathways to transduce extracellular stimuli into an intracellular transcriptional response. An example of such a pathway is the Janus Kinase/Signal Transducers and Activators of Transcription (JAK/STAT) pathway, which mediates cellular events that are vital to a wide variety of processes including adipogenesis, hematopoiesis and immune development.²⁴¹

Propagation of external signals through the JAK/STAT pathway begins with a cytokine-induced multimerisation of JAK-associated cytokine receptors. Being in close proximity allows the JAK proteins to trans-phosphorylate which then begins the process of phosphorylation of a number of other targets, including STAT proteins. Phosphorylated STAT allows for STAT dimerisation which is then followed by migration to the nucleus, binding to regulatory sequences and activation or deactivation of the transcription process. Constant activation or failed regulation of JAK signalling can have a profound effect on protein transcription and lead to auto-immune diseases, erythrocytosis and Leukaemia.²⁴¹

There are four members of the JAK family of proteins: JAK1, JAK2, JAK3 and TYK2. With different family members associated with various transmembrane cytokine receptors which, upon activation by extracellular cytokines, phosphorylate one or more of seven STAT proteins, resulting in a wide range of transcriptional responses.

2.1.1 – Interferon γ Induction of the JAK/STAT Pathway

Interferon- γ (IFN γ) is one of a number of pro-inflammatory cytokines secreted by T-cells, natural killer (NK) and other immune cells in response to pathogenic invasion.^{242, 243} Under regular cellular function, IFN γ serves roles in both the innate and adaptive immune system, for example by promoting increased antigen presentation on macrophages and recruitment of T-helper cells to stimulate a full T-cell response.^{242, 244} In addition to its well-studied role as a pro-inflammatory cytokine, recent studies have pointed toward a contradictory role of IFN γ and have uncovered the pro-tumour functionality of the cytokine.

The balance between the anti and pro-tumour capacity of IFN γ depends largely on the signalling intensity, tumour specificity and microenvironment it exists within.²⁴² The pro-tumour role of IFN γ is at least partly mediated by its role in stimulating the expression of two well-studied immunosuppressive proteins: Indoleamine-2,3-dioxygenase 1 (IDO1) and Programmed Death-Ligand 1 (PD-L1).²⁴⁵⁻²⁴⁸ Expression of IDO1 leads to an increase in the concentration of metabolites that are cytotoxic to naïve T-cells, development of T-regulatory cells and suppress cytotoxic T-lymphocytes (CTLs).²⁴⁹ Expression of PD-L1 serves to directly

interact with PD-1 presenting T-cells, thus suppressing T-cell activity.²⁴⁷ Initially, T-cells have an anti-tumour effect but as they become activated and recruit other immune cells, *via* the secretion of IFN γ , the tumour responds through the upregulation of IDO1 and PD-L1.

Successful studies to understand the mechanism of tumour immune resistance through protein knock-down or direct protein inhibition have highlighted therapeutic intervention opportunities for JAK proteins.^{15, 250, 251} The cytokine receptor responsible for binding IFN γ requires either JAK1 or 2 for signal propagation. JAK1 and 2 play a key role in the immune escape and, as a result, inhibition of these proteins has proven efficacious in treating myelofibrosis.^{251, 252} Signalling of IL-2 and IL-15 through JAK3 has been demonstrated to be important in the development of T-cells with inhibition of JAK3 showing significant slowing of T-cell proliferation.²⁵³⁻²⁵⁵ Inhibition of the JAK family of proteins must therefore be selective for JAK1/2 to avoid undesirable side-effects when treating cancers. Selective JAK3 inhibition however has shown efficacious in treating autoimmune diseases such as rheumatoid arthritis.^{256, 257}

2.1.2 – Selective Inhibitors of JAK1 and 2

Many JAK1 and/or 2 selective inhibitors have been developed and evaluated in against a variety of cancers – Table 8 summarises the cell-free IC₅₀ data for the JAK family kinases.

Table 8 – Common JAK inhibitors and their cell-free IC₅₀ (nM) values against the JAK family of kinases

	JAK1	JAK2	JAK3	TKY2
Itacitinib ²⁵⁸ INCB039110	2	63	>2000	795
Ruxolitinib ²⁵⁹ INCB018424	3.3	2.8	>430	ND
Pacritinib ²⁶⁰ SB1518	1280	23	520	50
Gandotinib ²⁶¹ LY2784544	19.8	3	48	ND
Momelotinib ²⁶² CYT-387/GS-0387	11	18	155	ND
Fedratinib ²⁶³ TG101348/SAR302503	~90	3	~900	~300
BMS-911543 ²⁶⁴	360	1.1	75	66

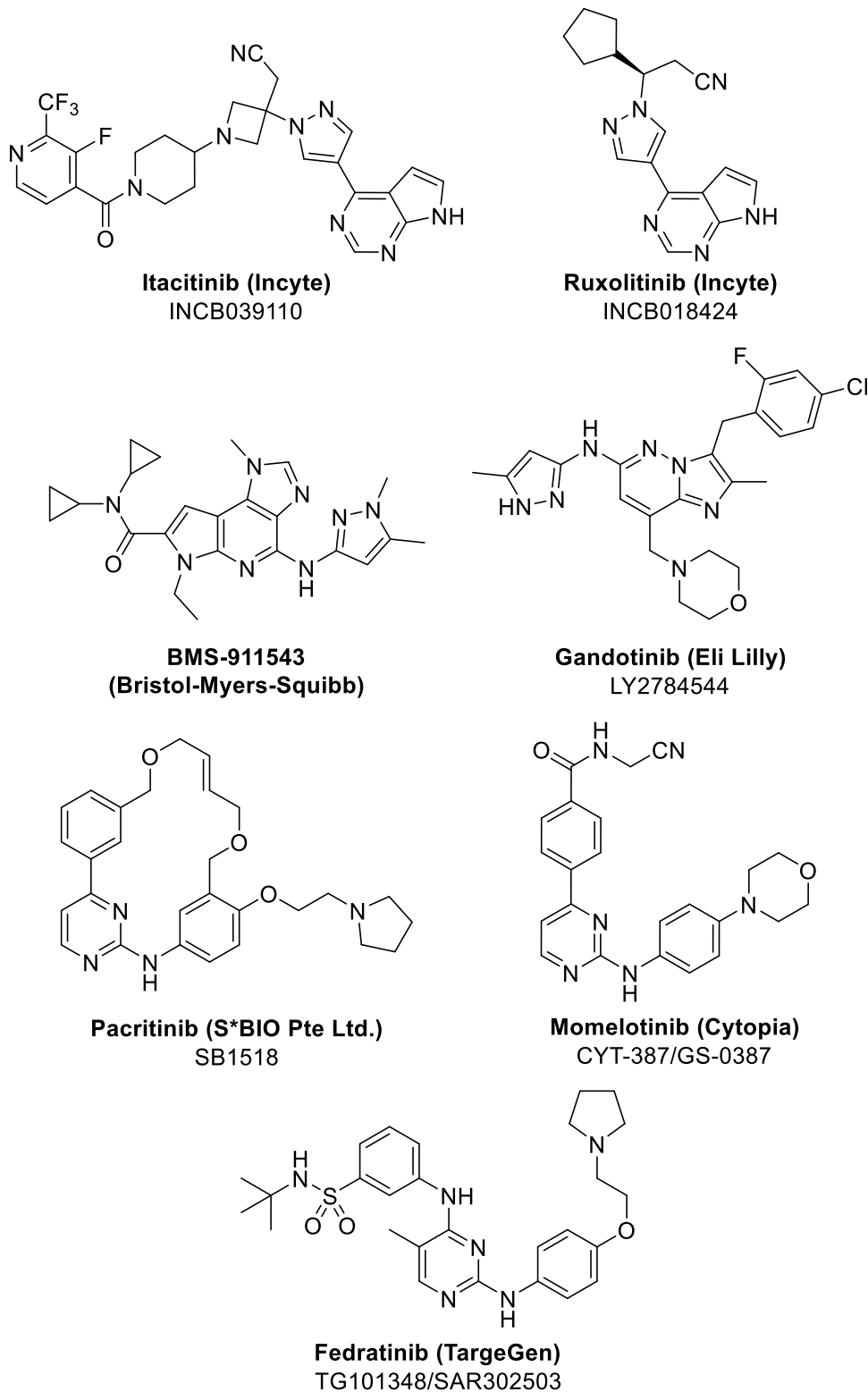


Figure 45 – Clinically evaluated JAK inhibitors for treatment of various cancers

Of the JAK1 and 2 selective inhibitors currently under clinical evaluation or patent protection, two core scaffolds are most commonly present: amino pyrimidines and fused diazine-based heterocycles, namely pyrrolo[2,3-d]pyrimidines and imidazo[1,2-b]pyridazines (Figure 45).

Docking studies performed by Caflisch and Hantschel suggested that ruxolitinib and fedratinib both utilise L932 residue binding in the hinge region of JAK2.²⁶⁵ Their study corroborated with *in vitro* observations of resistance-causing point mutations that places a bulky side-chain in a position that prevents this binding event.²⁶⁶

Inctye developed a number of pyrrolo[2,3-d]pyrimidine based scaffolds, most notably Ruxolitinib.²⁶⁷ Ruxolitinib achieved a >130-fold selectivity for JAK1/2 over JAK3 and currently is marketed as a treatment for high-risk myelofibrosis (MF) and polycythemia vera (PCV) serving as the best available therapy.^{259, 268} However, patients exposed to ruxolitinib often experience anaemia as a result of its myelosuppressive activity – an effect linked to ruxolitinib's antagonistic action on JAK2.²⁶⁹ Structurally related itacitinib gave lower binding affinities for JAK2 and JAK3 displaying a 31- and >1000-fold, respectively, binding preference for JAK1 with an IC₅₀ of 2 nM.²⁵⁸ Selective inhibition of JAK1 is thought to improve symptoms of myelosuppression related to JAK2 inhibition.²⁷⁰ Itacitinib is currently in phase III evaluation for Graft-Vurses-Host Disease (GVHD) and phase II myeloproliferative Neoplasms (MPN).^{271, 272}

Amongst those with myeloproliferative cancers, the JAK2 V617F mutation is commonplace and is associated with a very poor prognosis.^{273, 274} Imidazo[1,2-b]pyridazine-containing gandotinib demonstrated greater antiproliferative activity in mutation-driven cells; in whole cell models gandotinib demonstrated an IC₅₀ of 68 nM in mutation driven cells, compared to 1.36 µM in non-mutation-driven cells.²⁶¹ Gandotinib was most recently evaluated in phase II trials in patients with MPNs, PCV, MF or essential thrombocythemia (ET), including those who have failed to respond to, or have shown disease progression whilst being treating with ruxolitinib.²⁷⁵

BMS reported a series of JAK2-selective inhibitors with BMS-911543 currently under clinical evaluation for treatment of myelofibrosis.^{264, 276} Pre-clinical studies of BMS-911543 demonstrated a promising ADMET profile in animal models.²⁶⁴ The inhibitor is >300 fold more selective for JAK2 over JAK1, but only ~70 fold more selective for JAK2 over JAK3, suggesting treatment with the inhibitor could incur inhibition of T-cell proliferation and reduced effectiveness.

Amino pyrimidine-containing JAK inhibitors pacritinib and momelotinib have been evaluated against ruxolitinib in patients with myelofibrosis who have experienced lack of efficacy or toxic haematological effects with ruxolitinib. Pacritinib has demonstrated high selectivity for JAK2 over JAK1 and 3 (>50 and >20-fold, respectively) but only 2-fold over TYK2 in cell-free studies. Lack of TYK2 function has been demonstrated in mice models to lead to an impaired ability to detect tumours.²⁷⁷ However, patients with a low red blood cell count saw improvements in their disease states after treatment with Pacritinib when compared to ruxolitinib.^{278, 279} Pacritinib

satisfied the two co-primary end points of spleen volume reduction (SVR) and total symptom score (TSS) in the phase III study.^{279, 280} Momelotinib, which was also trialled against ruxolitinib, failed to satisfy its end point of SVR however the trial demonstrated that momelotinib improved anaemia symptoms in patients.^{281, 282}

Another important amino pyrimidine-containing JAK inhibitor is fedratinib. In cell-free studies fedratinib displayed high selectivity for JAK2 with an IC₅₀ of 3 nM, with IC₅₀ values 30- and 300-fold lower than that reported for JAK1 and JAK3 respectively. The JAK2 selective inhibitor showed a 100-fold higher IC₅₀ for TKY2 and also inhibited FLT3 and RET with IC₅₀ values of 15 and 48 nM, respectively.²⁶³ Mutations in FLT3 and RET are common in myeloid leukaemia and are often associated with a poor prognosis, inhibition of FLT3 and/or RET has shown efficacy but often lead to severe side effects or rapid resistance.^{283, 284} Phase II clinical evaluation of fedratinib in myelofibrosis patients exceeded its primary end point of SVR by 20%, with over half of the cohort achieving 55% SVR.^{275, 285} However, suspected cases of Wernicke's encephalopathy in a small number of patients in other fedratinib trials led to the early termination of the study.^{285, 286} Cases of Wernicke's encephalopathy, caused by thiamine deficiency, were attributed to fedratinib's adverse effects of vomiting and diarrhoea exacerbating symptoms malnutrition in patients. These findings ultimately pointed toward improving patient management rather than a specific toxicity of the drug.²⁸⁷ Separate studies conducted in rat models later concluded Fedratinib does not inhibit thiamine uptake.^{287, 288}

In late 2018, Celgene began phase III evaluation of fedratinib in patients with myelofibrosis with the FDA announcing in early 2019 that fedratinib earned priority review status for myelofibrosis treatment.^{289, 290} In August 2019, under the trade name of INREBIC[®], fedratinib was granted FDA approval – the first new treatment for myelofibrosis approved in nearly a decade.^{291, 292}

2.1.3 – Studying the Role of JAK2 *in vivo*

It is well established that IFN γ signals through JAK2 to induce PD-L1 expression which is implicated in aiding tumour immune escape.^{243, 293-295} While IDO1 has similarly been implicated in aiding tumour immune escape, the link between IDO1 expression and IFN γ JAK2 signalling is less well established.²⁹⁶

Unpublished work conducted by Celentyx Ltd has demonstrated in IFN γ stimulated SKOV3 cells, an ovarian cancer cell line, that the expression of PD-L1 and IDO1 can be suppressed though treatment with JAK inhibitor ruxolitinib (Figure 46).

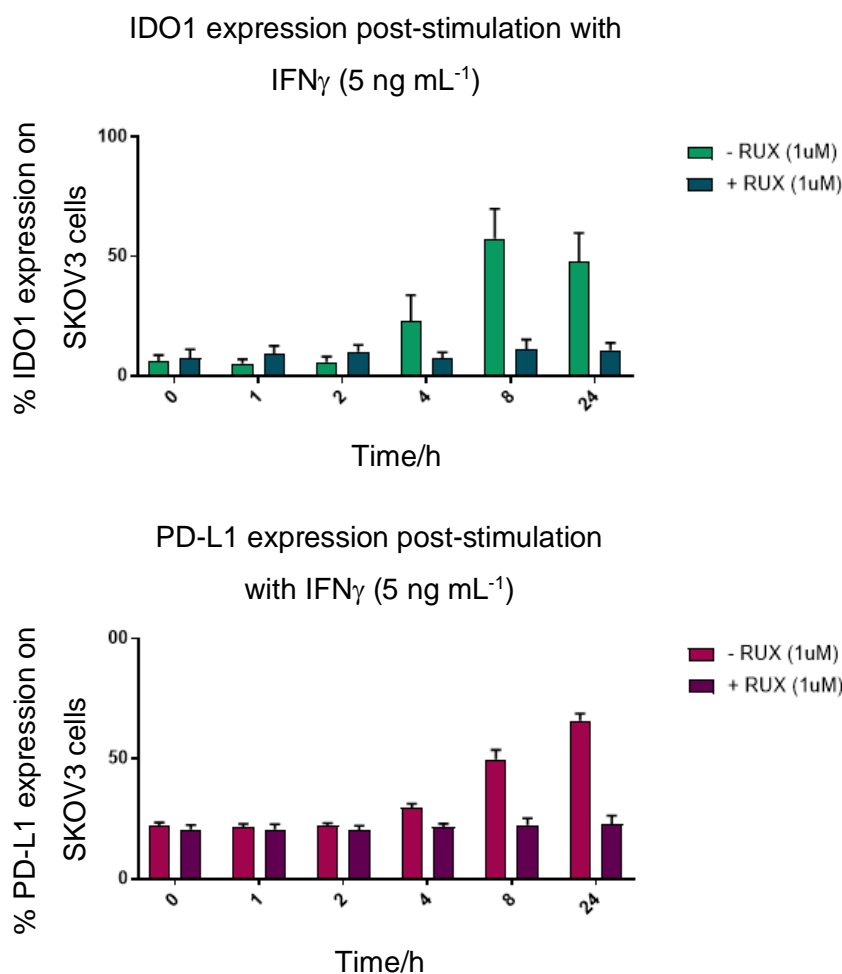


Figure 46 – % IDO1 and PD-L1 expression data with and without ruxolitinib

Both ruxolitinib and the structurally distinct and potentially more JAK2 selective inhibitor BMS-911543 (BMS) have a negligible effect on CD8+ cell viability in isolation or as a CD8+/SKOV3 co-culture at concentrations of up to 1000 nM (Figure 47a & b, e & f). Stimulation of isolated CD8+ cells with CD3/CD28 beads leads to a significant increase in proliferating CD8+ cells, accompanied by a smaller increase in live T-cell count at this time point. Co-treatment with either ruxolitinib or BMS reduces the percentage of proliferating cells in a dose dependent manner, indicating that T-cell activation is suppressed by these compounds (Figure 47c, g). As would be expected, given the lack of toxicity of these drugs, the proliferation changes are reflected in an overall reduction in live T-cells at higher concentrations.

Co-culture of CD8+ cells with SKOV3s results in a significant reduction in proliferating CD8+ cells following stimulation, consistent with the SKOV3 cells inhibiting T-cell activation (Figure 47d, h). In addition there is some evidence of both T-cell death and increased proliferation in unstimulated cells, however these effects are comparatively small and inconsistent between experiments. In contrast to the effects on T-cells alone, when the stimulated co-cultures are

treated with ruxolitinib or BMS a dose-dependent increase in the overall percentage of proliferating cells is observed (Figure 47d, h). However, this increase is only marginal, with a percentage increase of roughly 1.5% for both JAK inhibitors (compared to % proliferation at 0 nM [inhibitor] and when dosed at 1000 nM).

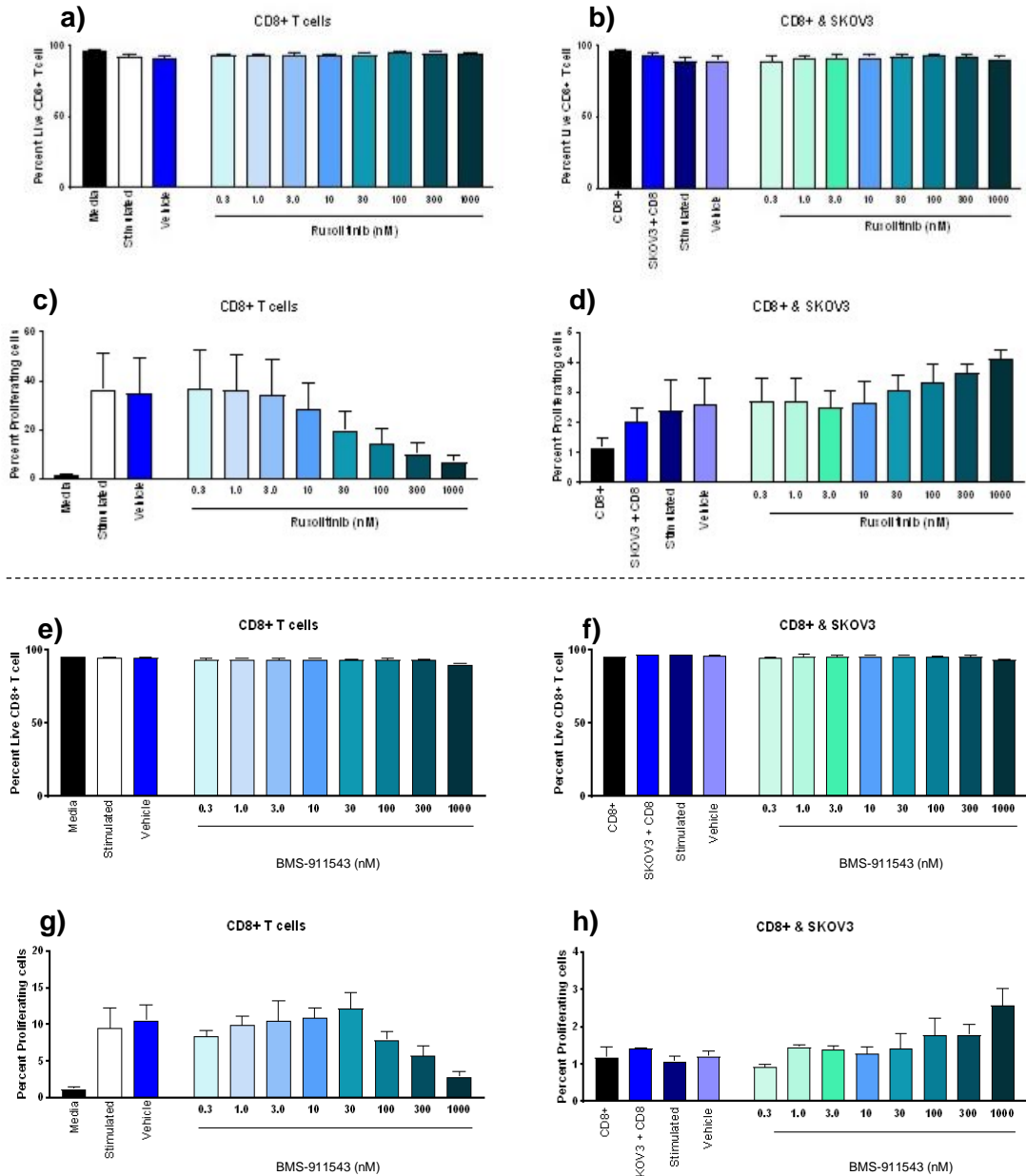


Figure 47 – Ruxolitinib (a-d) and BMS (e-h) data

This change can be explained by a dual effect of the JAK inhibitor where direct suppression of T-cell activation overlays a reduction in the SKOV3 cells ability to inhibit CD8+ cell proliferation, potentially mediated by reduced expression of PD-L1 and IDO1 as observed in earlier experiments (Figure 46).

A comparative study was conducted with selective-IDO1 inhibitor epacadostat **6** (INCB). In stimulated CD8+ T-cells or CD8+/SKOV3 co-cultures, **6** had no effect on cell viability, nor did the inhibitor have any significant impact on CD8+ cell count in both cultures (Figure 48a & b). The percentage of proliferating cells in stimulated CD8+ cells predictably remained unchanged when treated with increasing concentrations of **6** (Figure 48c). However when a stimulated CD8+/SKOV3 co-culture was treated with increasing concentrations of **6**, the number of proliferating CD8+ cells increased rapidly with an inhibitor dosing of 300 nM seeing a >35% increase in percentage proliferating CD8+ cells (Figure 48d). This demonstrates the importance of IDO1 in the ability of SKOV3 cells to suppress the proliferation of CD8+ cells; this also supports the idea that the JAK inhibitors ruxolitinib and BMS are having a significant impact on T-cell proliferation.

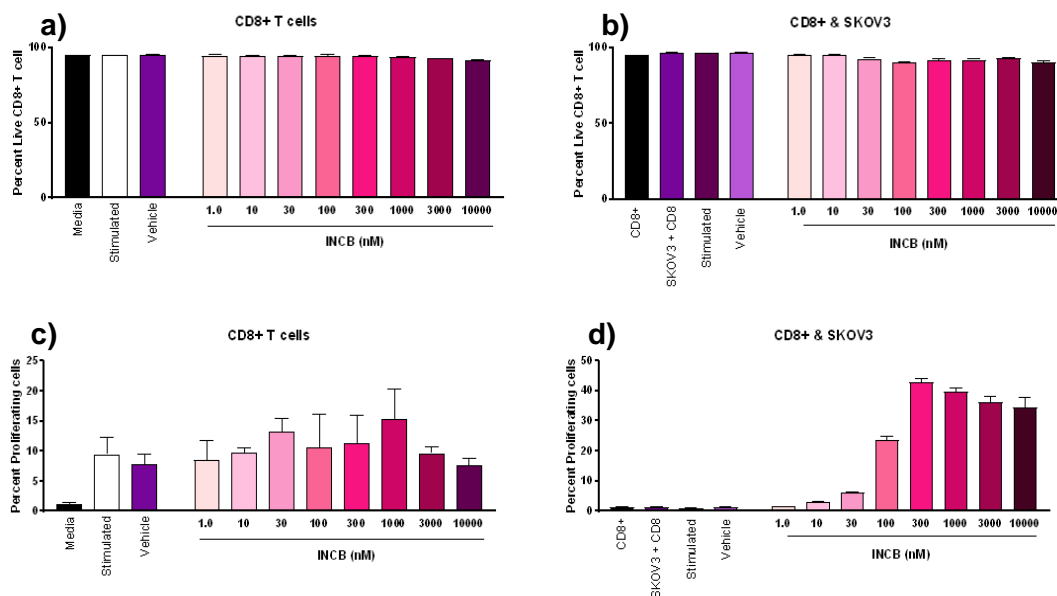


Figure 48 – INCB 6 data

In a final study, a CD8+/SKOV3 co-culture was treated with 30 nM epacadostat and increasing concentrations of BMS. At 0.3 nM BMS, the percentage of proliferating cells was reported at 5%, rising to ~10% with 1000 nM BMS. Comparatively, the epacadostat/BMS combination therapy improved the percentage of proliferating T-cells over that of BMS treatment alone (Figure 49d). The increase in percentage proliferation can be attributed to the further inhibition of PD-L1/IDO afforded by JAK2 inhibition, further reducing the ability of SKOV3 cells to suppress the immune system.

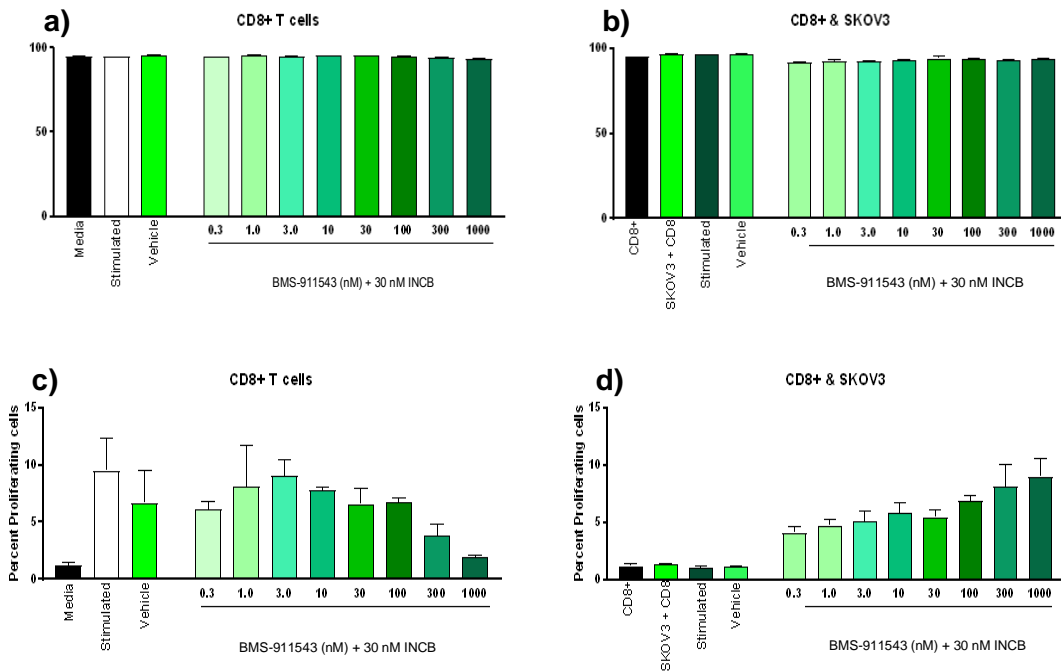


Figure 49 – BMS + INCB data

These experiments illustrate that studying the effects of JAK2 inhibition in the immune response to cancer cells is complicated by an impaired ability of T-cells to respond to the tumour after treatment with JAK inhibitors. The impaired function of the T-cells is likely to arise from a lack of fully selective JAK1 or 2 inhibition; inhibition of T-cell JAK3 has been demonstrated to lead to a significant slowing in cell proliferation.²⁵³⁻²⁵⁵

2.2 – Protein Degradation as a Therapeutic Tool

Outside of surgical intervention, one of the main avenues in cancer treatment is the use of targeted cancer drugs.²⁹⁷

Monoclonal antibodies are a common class of anticancer drugs that act as highly selective and potent inhibitors of oncogenic proteins that are either non-cell associated or presented on the cell surface. In the clinic anti-cancer mAbs are generally used in one of two ways: by triggering the immune system or by directly acting on cancer cells; for example, rituximab binds CD20 on B-cells and causes cell apoptosis while pembrolizumab binds PD-1 on T-cells to prevent deactivation from PD-L1 presented by tumour cells.^{298, 299} Currently the technology is limited by inconsistent translation from pre-clinical models to human trials and the susceptibility of these highly specific and expensive medicines to complete failure due to minor changes in antigen structure.³⁰⁰

Unlike mAb approaches, gene-silencing therapies such as siRNA rely on cellular entry for effect. Through the use of siRNAs it is possible to selectively degrade the mRNA coding for the target protein, preventing the expression of oncogenic proteins and inhibit both functional and any scaffolding roles of the protein.^{301, 302} Development of effective drugs has been limited by the challenges faced in effective intracellular delivery of the non-permeable siRNA oligonucleotides to poorly perfused tissues, such as many tumours; however progress has been made *via* the use of lipids, polymers and gold nanoparticles.^{303, 304}

By far the largest area of targeted drug therapies is that of small molecule inhibitors and they continue to be a mainstay of medicinal chemistry research. Typically small molecule inhibitors function through binding intracellular targets with high affinity and impeding their function. Various inhibitory modes exist including competitive, non-competitive, and allosteric. Small molecule inhibitors have provided excellent therapeutic benefit for patients, particularly in cancer treatments, however they suffer limitations that prevent their use against all prospective oncogene-derived targets.³⁰⁵ Firstly, to inhibit a protein, binding must alter or cease the protein's function. A number of proteins do not have easily 'druggable' sites, such as active sites, and instead are often featureless, hydrophobic surfaces which are difficult to bind and complicate drug development.³⁰⁶ Secondly, high dosing regimens often required in small molecule inhibitors limits usage by increasing the possibility of off-target effects.³⁰⁷ Finally, sustained usage of small molecule inhibitors increases the likelihood of somatic mutations of proteins and eventual drug resistance.³⁰⁸

2.2.1 – Proteolysis Targeting Chimeras

The use of protein degradation induced by Proteolysis Targeting Chimeras (PROTACs) has become an increasingly well studied strategy to overcome the limitations of current therapeutic approaches.³⁰⁹⁻³¹³ This technology harnesses the ability of E3-ligases to ubiquitinate proteins, marking them for destruction *via* the proteasome.³¹⁴ PROTACs are heterobifunctional molecules containing a warhead for protein-of-interest (POI) binding tethered to an E3-ligase recruiting ligand *via* a linker unit (Figure 50).³¹⁴

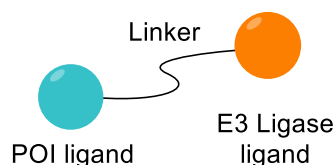
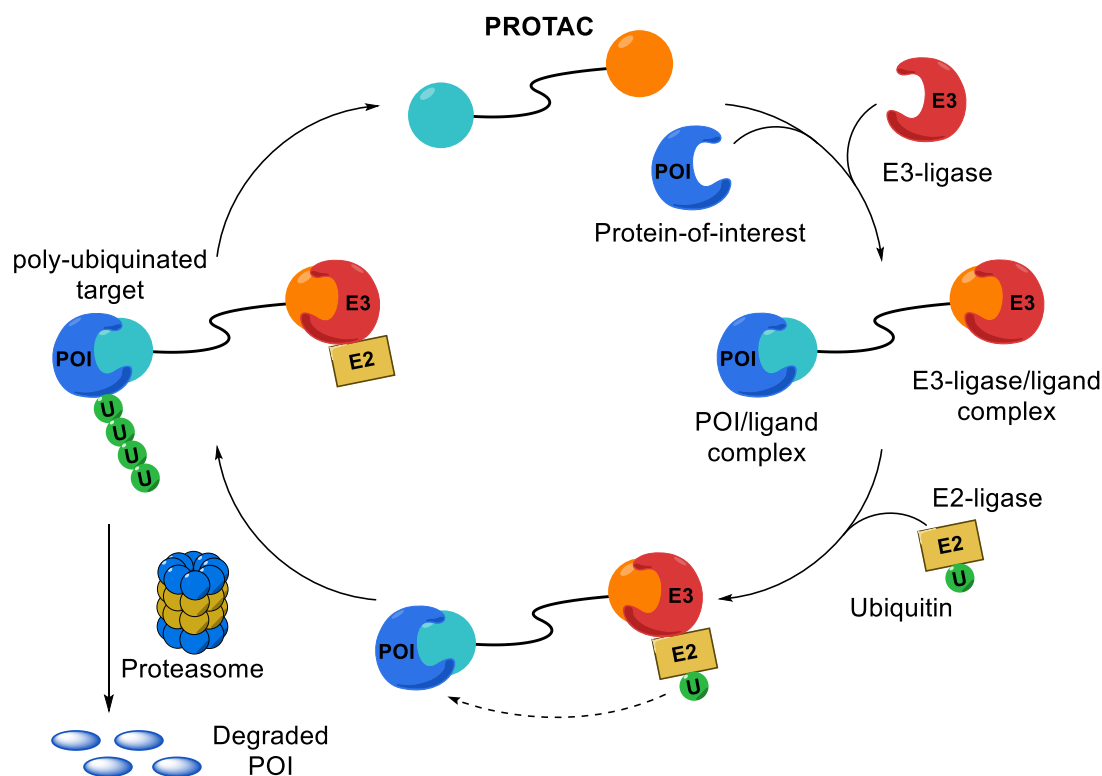


Figure 50 – Anatomy of a PROTAC

PROTACs function through the binding of the POI and an E3-ligase to form a ternary complex, the purpose of this is to bring the POI and E3-ligase in close proximity and to facilitate poly-ubiquitination. Formation of the ternary complex is followed by the recruitment of an E2-ligase which serves as a ubiquitin-conjugating enzyme, poly-ubiquitinating a lysine residue on the protein surface. Poly-ubiquitinated lysine residues of the POI are then recognised by the proteasome, the cell's protein degradation machinery, and the POI is degraded (Scheme 97). Radiolabelling studies later showed PROTACs to be catalytic in their activity, causing the degradation of multiple substrate proteins.³¹⁵ There are many competing events that must be satisfied to favour progression from a ternary complex to a degraded protein. Firstly, the PROTAC must bind the POI and the E3-ligase concomitantly to form the ternary complex. Secondly, the proteins must bind in a conformation to allow for ubiquitination of a suitably positioned lysine on the POI to allow ubiquitination.³¹⁶ Further to this, the rate of polyubiquitination must also be greater than the rate of deubiquitination performed by deubiquitinases (DUBs).³¹⁷ Finally, the ubiquitination pattern on the substrate protein must allow for recognition by the proteasome – many ubiquitin chain lengths and topologies are possible however linear K48-linked ubiquitin are thought to be favoured.³¹⁸



Scheme 97 – Catalytic cycle of PROTAC-mediated protein degradation

2.2.2 – Development of PROTAC Technology

Examples of induced protein degradation by the ubiquitin-dependent proteasomal system can be traced back to the early 1990s, however in these examples ligation to other proteins was utilised to initiate degradation.³¹⁹⁻³²¹ It wasn't until 2001 that Crews reported the first protein degrader with a small molecule warhead that the term PROTAC was coined.³¹⁴ Ovalicin, a known inhibitor of aminopeptidase Met-AP2, was linked to I κ B α phosphopeptide, a known binder of E3 ligase SCF ^{β -TRCP}, and used to ubiquitinate Met-AP2. Crews' PROTAC, designated Protac-1, initiated rapid proteasomally-dependent degradation of Met-AP2 (Figure 51).³¹⁴

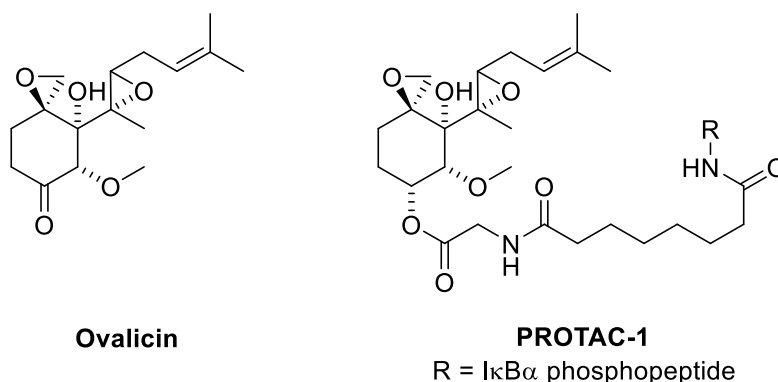


Figure 51 – Ovalicin and Crews' ovalicin-derived PROTAC, Protac-1

Protac-1's utility as a therapeutic was however limited due to its inability to cross cell membranes – with later peptidic-PROTACs, targeting the estrogen receptors (ER) and androgen receptors (AR), being introduced *via* microinjection to show efficacy in cells.³²²

A large step forward in PROTAC technology was achieved in 2008 with nutlin, an MDM2 binder, serving as the E3-ligase recruiting moiety creating the first 'small molecule' PROTAC (Figure 52).³²³ The SARM-nutlin PROTAC was also the first PROTAC able to cross the cell membrane without need for microinjection. When AR-expressing HeLa cells were treated with 10 μ M of the SARM-nutlin PROTAC, partial proteasomal degradation of the AR was observed.³²³

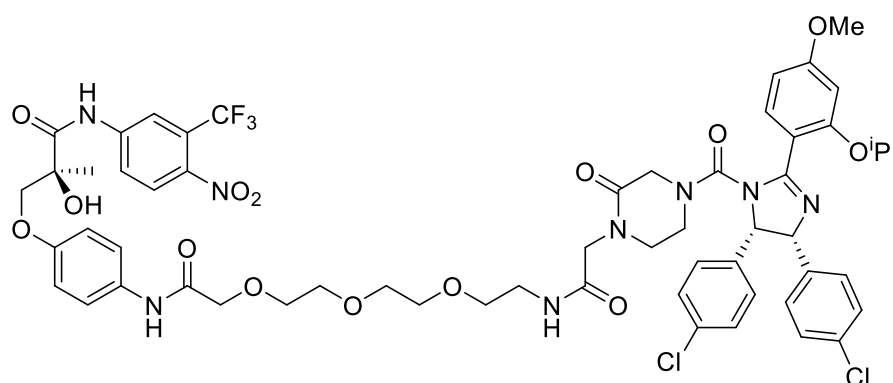


Figure 52 – Crews' cell-permeable SARM-nutlin PROTAC

Building on the success of the MDM2 ligand, a collaborative effort between Crews, Ciulli and GSK lead to the discovery of a series of small molecule recruiters of the E3-ligase von Hippel–Lindau (VHL). Through X-ray and biophysical analysis, the groups were able to identify non-natural peptide ligands to mimic the natural substrate of the VHL ligase (Figure 53).^{324, 325} When tethered to a receptor-interacting protein kinase 2 (RIPK2) ligand, Crews discovered cellular potencies of around 1 nM with the VHL-ligand.³¹⁵ Ciulli later utilised the VHL-ligand to target bromodomain and extraterminal domain (BET) family member BRD4, achieving a DC_{50} value of 149 nM.³²⁶

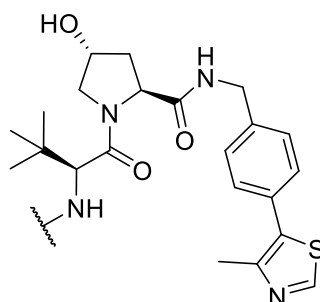


Figure 53 – von Hippel-Lindau ligand

Recruitment of the cellular inhibitor of apoptosis protein 1 (cIAP1), an E3 ligase commonly overexpressed in cancers, has also been utilised in recent protein degraders.^{327, 328} cIAP

recruiting degraders are known as specific and non-genetic inhibitor of apoptosis-dependent protein erasers (SNIPERs) however, like PROTACs, they rely on the same process of poly-ubiquitination and proteasomal degradation. Ligands used to target the cIAP ligase are non-natural peptidic substrate mimics (Figure 54). The first cIAP recruiting protein degrader, described by Itoh, was a bestatin-based ligand which was used to degrade cellular retinoic acid-binding proteins (CRABP-I and II).³²⁷ Later examples utilised derivatives of MV1, a potent inhibitor of cIAP, to induce estrogen receptor- α degradation.³²⁹⁻³³² Many proline-based IAP recruiting ligands are now known and used under the umbrella term of ‘IAP-ligands’ (Figure 54).

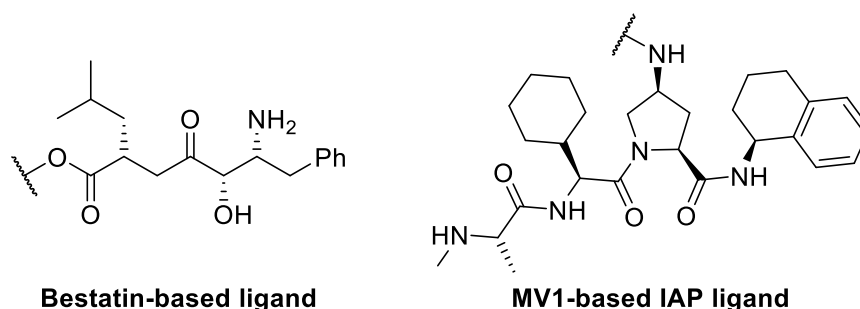


Figure 54 – Bestatin-based and MV1-based IAP E3 ligase ligands

Advances in the understanding of thalidomide’s binding to the cereblon (CRBN) E3-ligase lead to the incorporation of thalidomide, and the structurally similar lenalidomide and pomalidomide, into PROTAC scaffolds (Figure 55).^{326, 333, 334} The groups of Bradner and Crews independently reported the use of cereblon ligands for the degradation of BRD4, both achieving significant protein degradation at low doses.^{334, 335}

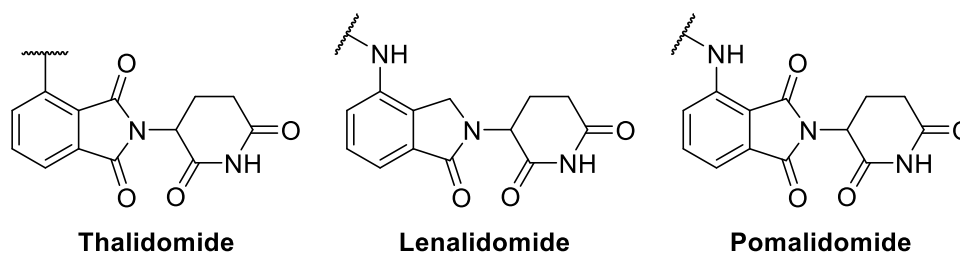


Figure 55 – Cereblon ligands

While there is much still to be understood about the function and translational potential of PROTAC molecules, the discovery of these more ‘drug-like’ PROTACs attracted great interest in the drug discovery community. As the field has progressed, a variety of proteins have been targeted and degraded using PROTACs, many of which are summarised in the numerous reviews of the field.^{309-313, 336, 337}

2.2.3 – PROTACs Verses Small Molecule Inhibitors *in vivo*

Possible benefits of PROTACs over small molecule inhibitors include higher cellular potencies owing to their catalytic nature, higher observed selectivity's than the constituent POI binder and their differences in pharmacodynamics. PROTACs also offer the opportunity to access previously inaccessible pharmacology.

Cellular Potency

Small molecule inhibitors rely on high target occupancy for effect, often translating to high and frequent dosing regimens. Higher dosing quantities increases the chances of off-target effects and the likelihood of somatic mutations – the lead driving force for inhibitor resistance. Many small molecule inhibitors display impressive cell-free EC_{50} values, yet cellular EC_{50} values suffer and are often higher than the molecules K_d value. For PROTACs, low levels of target occupancy has been demonstrated to be sufficient for protein degradation, particularly if the rate of ubiquitination and subsequent proteasomal degradation is high. Combined with the catalytic nature of PROTACs, cellular EC_{50} values well below the intrinsic K_d for the target binder can often be observed.³¹⁵

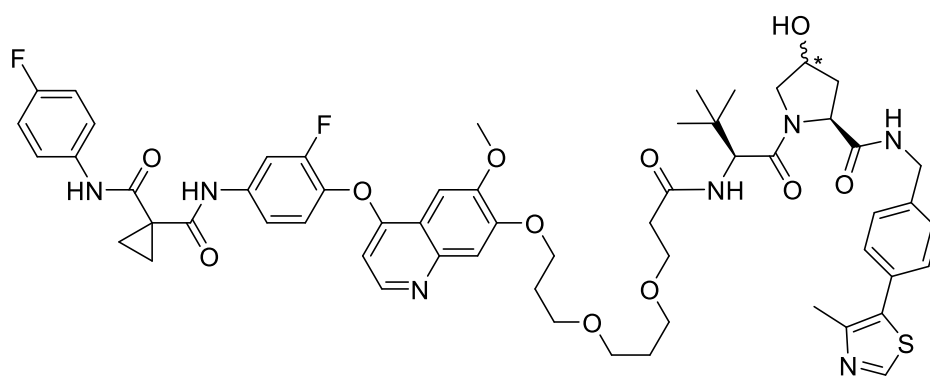
Selectivity Profiles

Small molecule selectivity is principally driven by the ratio between target K_d and the off-target(s) K_d values with the level of selectivity inferred by the gap in this ratio. In drug development, focus on driving more selective interactions *in vivo* is a high priority. Dosing of small molecule inhibitors becomes a challenge to balance the desired effect with undesired off-target, and potentially toxic, side effects.

Simple binding affinity is not the only factor that effects PROTAC selectivity. The discovery that conjugation of JQ1, a non-selective BET-family inhibitor, to a VHL-recruiting ligand gave selective degradation of BRD4 over BRD2 and 3 suggested other factors contributed (Figure 56).³²⁶ Ciulli rationalised this observation as either more effective ubiquitination of BRD4 over 2 and 3 or cooperative protein-protein stabilisation between the VHL ligase and BRD4.³²⁶

respect to p38 α was 210 nM while its K_d was 11 μ M.³³⁹ Crews' also identified that high affinity binding of the same PROTAC to AXL (K_d = 26 nM) did not lead to degradation at concentrations of up to 10 μ M.³³⁹ By using glutathione S-transferase (GST) tagged VHL proteins, Crews' was able to identify ternary complexes that formed in the presence of a PROTAC. Gratuitously, a strong correlation was found for proteins that co-operatively interacted with the GST-tagged VHL and those that were degraded in prior experiments. Control experiments using a functionally inactive epimer of the foretinib-PROTAC saw no ternary complex formation. Proteins which displayed high binding affinity to the PROTAC, such as AXL, also showed no detectable ternary complex formation suggesting either steric clashing or binding-induced conformation change of the PROTAC preventing ligase recruitment. Molecular modelling of the ternary complex formed between p38 α :PROTAC:VHL-ligase highlighted a protein-protein interaction surface of 800 \AA^2 . The model also identified Arg69 of VHL and Ala40 of p38 α as key residues that allow for the stabilisation of the linker region. Crews experimentally validated this model by performing single point mutation studies, mutating p38 α Ala40 to either Lys or Val. As predicted the Lys-mutant destroyed favourable interactions and prevented formation of the ternary complex while the Val-mutant had minimal effect versus the wild-type.³³⁹

In the same study Crews' also identified that although the foretinib-VHL PROTAC bound over 50 kinases, less than 10 were degraded. Changing the ligase recruiter to the alternative CRBN ligands also saw a similar effect – highlighting the broader importance of co-operative protein interactions in successful protein degradation across different PROTAC scaffolds.



Foretinib-VHL PROTAC

*Figure 58 – Crews' foretinib-PROTAC, * = R-, functionally active; * = S-, functionally inactive*

Promiscuous kinase binders conjugated to ligase recruiters have also been used in a chemoproteomic approach to probe kinase susceptibility to degradation.³⁴⁰ Over 30 kinases were susceptible to degradation over two cell lines and selective degraders of FLT3 and BTK were developed from this screen. Gray's work highlighted the applicability of PROTACs not

only as potential therapeutic agents, but also as agents that can play an important role in phenotypic assays, target identification and the study of protein function.^{337, 341}

The work of Crews' and Ciulli recognised the importance of co-operative protein-protein interactions and the roles that the linker and the surface residues play in the formation of the ternary complex. PROTAC design was initially approached with a plug-and-play attitude. As the field progresses, better understanding of the influencing factors on productive protein degradation have been made leading to enhanced selectivities of degraders synthesised. The additional binding events identified by Crews and Ciulli gives medicinal chemists further scope to tune selectivity profiles and potentiate novel pharmacology previously inaccessible with small molecule inhibitors.

Differences in Pharmacodynamics

Small molecule inhibitors operate *via* highly efficient reversible binding to their target protein. The principal limitation of this mode of inhibition is that only one small molecule inhibitor can inhibit one target protein. PROTACs, due to their catalytic nature, demonstrate the ability to initiate the degradation of multiple target proteins. Once the cellular protein level is diminished the PROTAC only has to degrade the protein as it is resynthesised which, for many proteins, is a relatively slow process.³⁴² This has the potential to result in extended pharmacodynamics, resulting in lower dosing frequencies, further reducing the chance of negative off-target effects. However, a greater understanding of the rate of protein degradation and regeneration within the target cells needs to be understood for clinicians to fully utilise *in vivo* protein degradation.

2.2.4 – PROTACs in the Clinic

The development of PROTACs currently in the clinic was driven by the founding of Arvinas in 2013 by Craig Crews. Since then several small biotech have been founded whose sole focus are PROTACs or degrader technology development, while many large pharmaceutical companies also have major projects involving PROTAC technology.³⁴³ Arvinas were the first to enter a PROTAC-based drug, ARV-110, into phase I clinical evaluation in early 2019. ARV-110 is a degrader of the androgen receptor (AR) and is being evaluated in patients with metastatic castration-resistant prostate cancer (mCRPC) who have failed to respond to enzalutamide or abiraterone.³⁴⁴

Criticisms of PROTACs as clinically useful therapeutics included questions surrounding cell permeability, SAR development and metabolic stability.³¹⁰ Thus far, PROTACS have displayed a remarkable ability to cross cell membranes despite their high molecular weights and SAR has been successfully developed for many PROTACs, including those described here by

Crews, Ciulli and Gray. However, exploration of their efficacy and pharmacokinetics in humans has yet to be fully assessed. Trials in mice, bama pigs and rhesus monkeys demonstrated global protein degradation of FKBP12, a Ca²⁺-ion channel regulating protein, within 2-3 days. Withdrawal of treatment after 15 days saw the recovery of protein concentration to near basal levels in most tissues after 5–7 days.³⁴⁵ Sun highlights the potential utility of PROTACs over technologies such as siRNA and CRISPR-Cas9 however no investigation into the PROTAC pharmacokinetics were reported. ARV-110 is therefore serving as a first-in-class test to determine how PROTACs perform in humans and in the clinic – with many pharmaceutical on-lookers following the results closely.³⁴³

The full structure of ARV-110 is yet to be published, however a recent patent filed by Arvinas disclosed the structures of a series of AR-degrading PROTACs (Figure 59).³⁴⁶ A closer look at the disclosed structures shows an overall shortening of the linker and, in many cases, an increase in rigidity over those used in published *in vivo* studies. Shorter, rigid and more lipophilic linkers seen in the development of the AR-degrading PROTACs suggests an intentional move toward more ‘drug-like’ chemical space. Detailed SAR data for ARV-110 is currently not available and limited pre-clinical data has been released for ARV-110.³⁴⁷

As of November 2019, Arvinas has reported positive results from dose escalation studies (35–140 mg) of ARV-110. The AR-degrading PROTAC was well tolerated in patients with no dose-limiting toxicity or adverse patient reactions observed. The ADMET studies indicate that the tumours have been exposed to levels of ARV-110 associated with tumour growth inhibition in pre-clinical models. Increases in dose were also complimented by increases in tumour exposure concentrations to ARV-110. Moving forward, Arvinas have stated that the dose escalation will be further increased and further evaluation of drug safety and pharmacokinetic properties.³⁴⁸

Further PROTACs targeting other proteins are set to soon enter clinical evaluation. Arvinas’ ARV-471, an ER-degrader for treatment of breast cancer, is set to enter clinical evaluation in Q3 2019.³⁴⁹ Kymera’s IRAK4-degrading PROTAC, KYM-001, is also set to enter phase I clinical evaluation in the first half of 2020.³⁵⁰

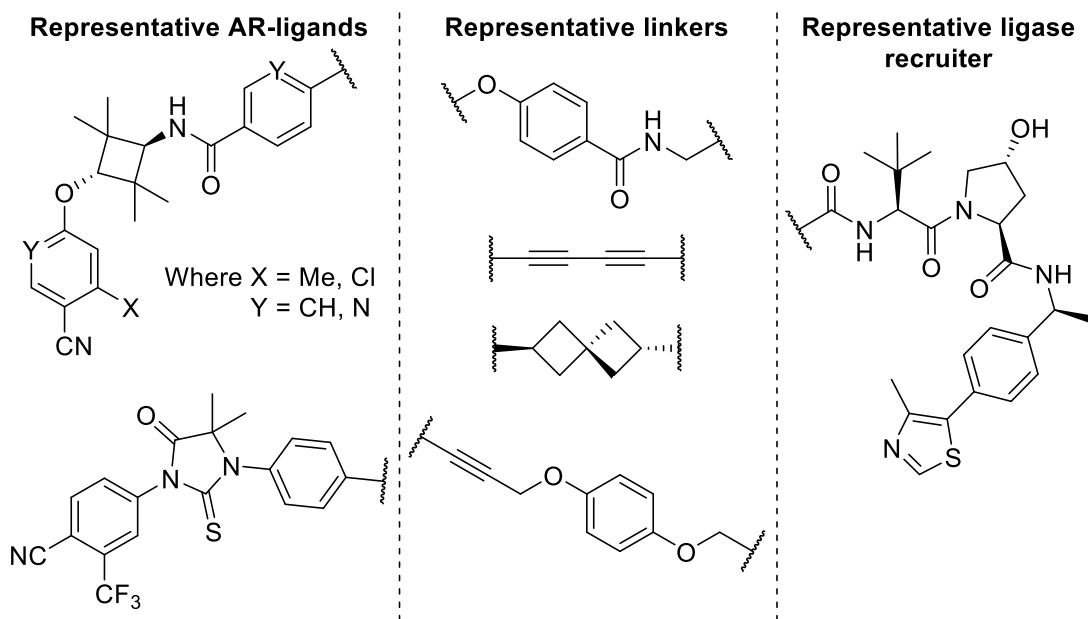


Figure 59 – Representative AR-ligands, linkers and ligase recruiter disclosed in the Arvinas patent

2.3 – Aims and Objectives

Studying the role of JAK2 in tumour immune escape using JAK inhibitors ruxolitinib and BMS-991543 has been complicated by its lack of selectivity for JAK2 over other JAK family proteins. Celentyx data demonstrates that non-selective JAK inhibition has an anti-proliferative effect on T-cells, with this activity preventing understanding of the immune response to JAK2-inhibited tumour cells.

In order to disconnect the effects on tumour and immune cells, JAK2 deficient tumour lines could be accessed through gene therapy and gene expression suppressor technology, however these methodologies often come at high cost and require specialist attention. Treatment of tumour cells with a JAK2-selective PROTAC could provide sufficient *in vivo* knockdown of JAK2 to allow investigation of the effect of T-cells on JAK2-deficient tumour lines. A JAK2 deficient tumour line could be achieved by allowing selective JAK2 degradation in the tumour cells or by inducing JAK2 degradation ahead of introduction of the T-cells into the system. If successful this approach would provide a cheaper, time-efficient and potentially more translatable method for studying JAK2's role in tumour immune escape.

JAK2 PROTAC Design

While there are a large number of well-characterised JAK inhibitors, not all are amenable to conversion to PROTACs due to their target binding topology. Fedratinib was identified as a suitable ligand to incorporate into a PROTAC as analysis of co-crystal structures of the structurally related JAK2 ligand TG101209 **236** suggests a suitable region for introduction of the ligase binder-linker complex (Figure 60).³⁵¹ In addition, this class of 2,4-diphenylaminopyrimidine warhead has been successfully incorporated into PROTAC scaffolds by other groups targeting FAK and ALK.^{352, 353}

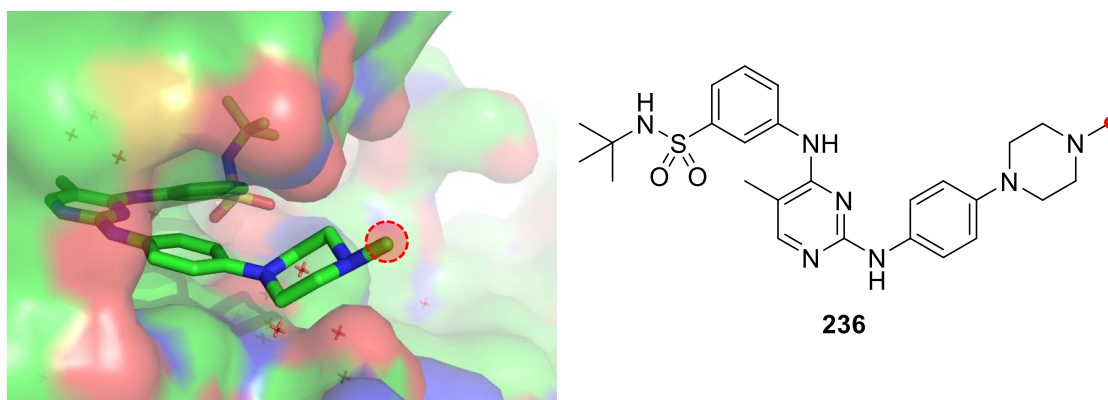


Figure 60 – Co-crystal structure of TG101209 bound to JAK2 with the red dot identifying the portion of the ligase binder that is orientated away from the protein (PDB N° 4JI9)

Fedratinib **237** is therefore hypothesised to participate in key protein-ligand interactions through the aryl sulfonamide and amino pyrimidine units; the phenoxyethyl pyrrolidine group, however, extends out into solvent and plays a limited role in protein binding (Figure 61). Substituting the pyrrolidine ring for a piperazine ring is envisaged to have minimal effect on binding while providing a handle for linker conjugation *via* formation of an amide bond. As such, modified JAK2 ligand **238** is proposed to act as a suitable PROTAC warhead.

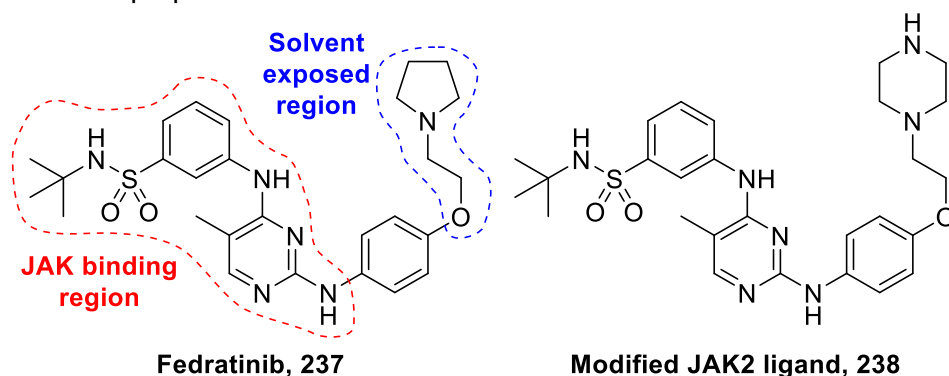


Figure 61 – Protein binding analysis of fedratinib and the proposed novel JAK2 ligand

PROTAC-mediated protein degradation is generally reliant on the ‘correct’ combination of protein and ligase ligands.³⁵⁴ Currently there are four E3 ligases that are publicly validated as valuable ligases for PROTAC recruitment and subsequent protein degradation: MDM2, CRBN, VHL and IAP.³¹¹ To increase the chance of JAK2 degradation, 4 ligase recruiting ligands have been selected to recruit either the CRBN, VHL or IAP classes of E3-ligase (Figure 62).

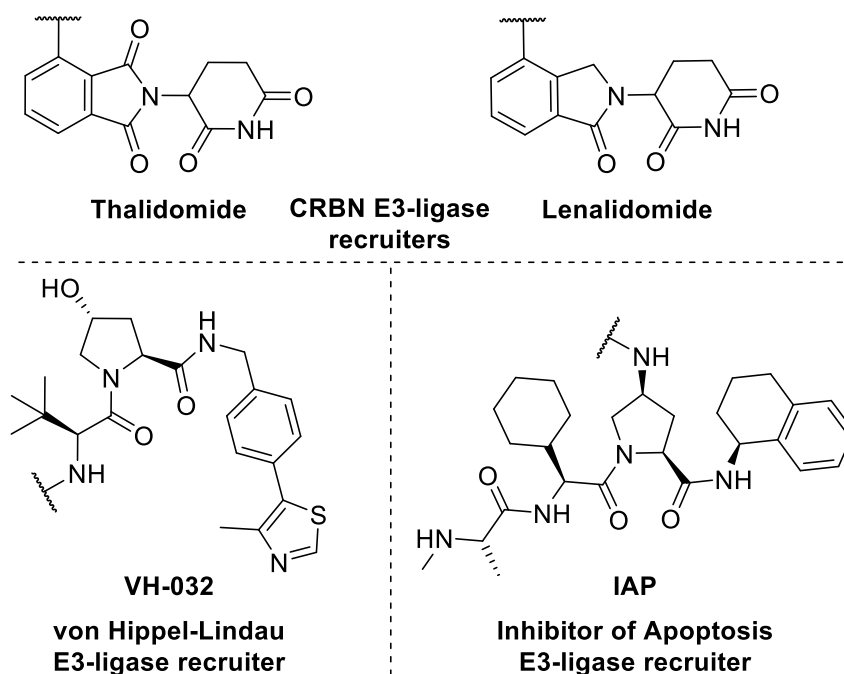


Figure 62 – Selected E3-ligase recruiters

Joining of the JAK2 ligand and the ligase ligand will be achieved with a variety of 5 or 6 carbon linkers (Figure 63). The linkers have been designed to contain alkynes and alkanes, allowing modulation of the linkers' rigidity – a characteristic that has been demonstrated to be important in PROTAC SAR.³⁵⁵

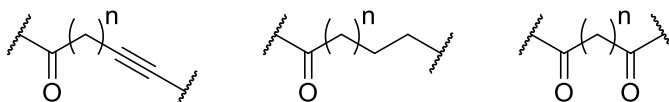


Figure 63 – Linker design, $n = 2$ or 3

The initial study therefore aims to synthesise a small library of eight PROTACs based on the fedratinib-like warhead; results from this preliminary study will inform future SAR efforts. Thalidomide-based PROTACs **239–241** (Figure 64), lenalidomide-based PROTACs **242–244** (Figure 65), VH-032 and IAP-based PROTACs **245** and **246** (Figure 66) will be synthesised and evaluated by Celentyx Ltd in HeLa cells for JAK2 degradation.

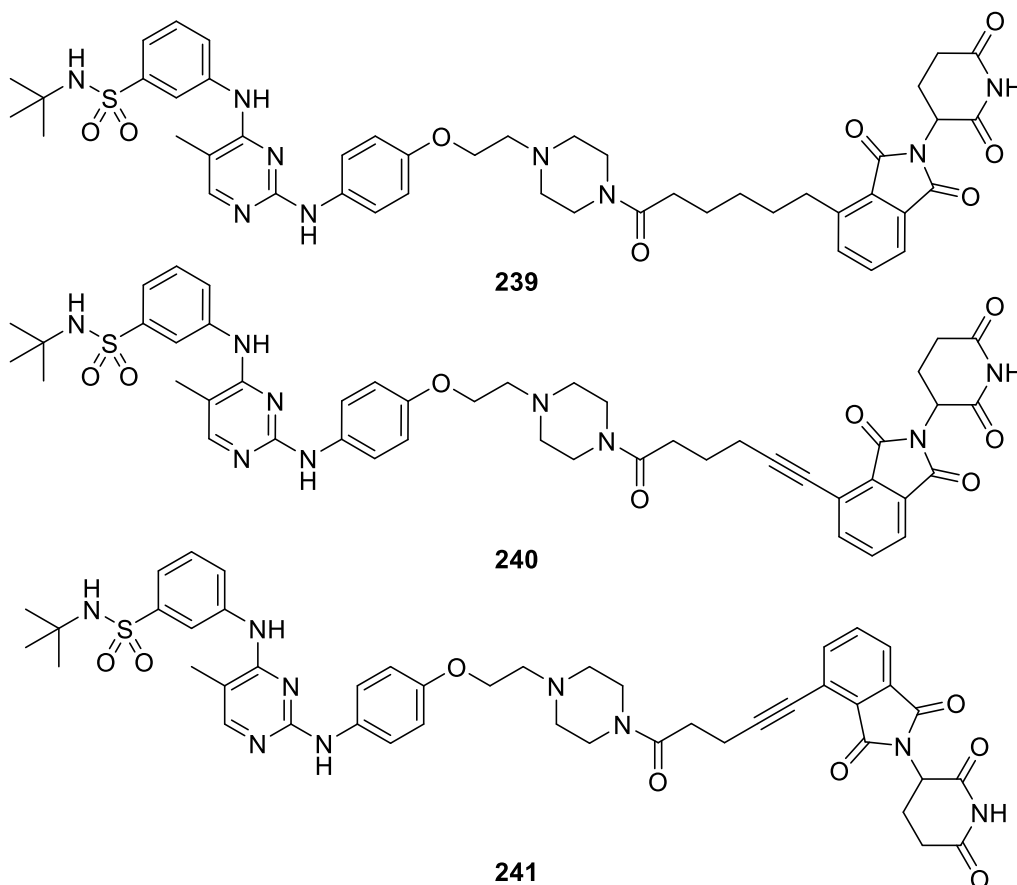


Figure 64 – Targeted thalidomide-based PROTACs **239–241**

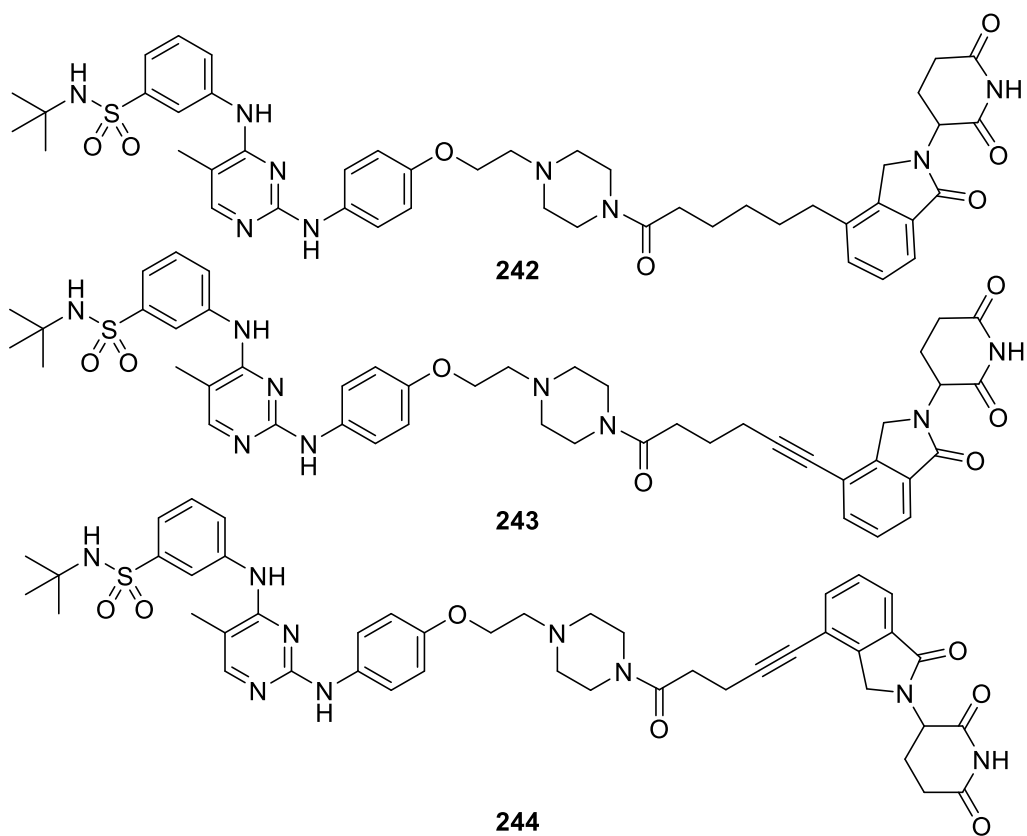


Figure 65 – Targeted lenalidomide-based PROTACs 242–244

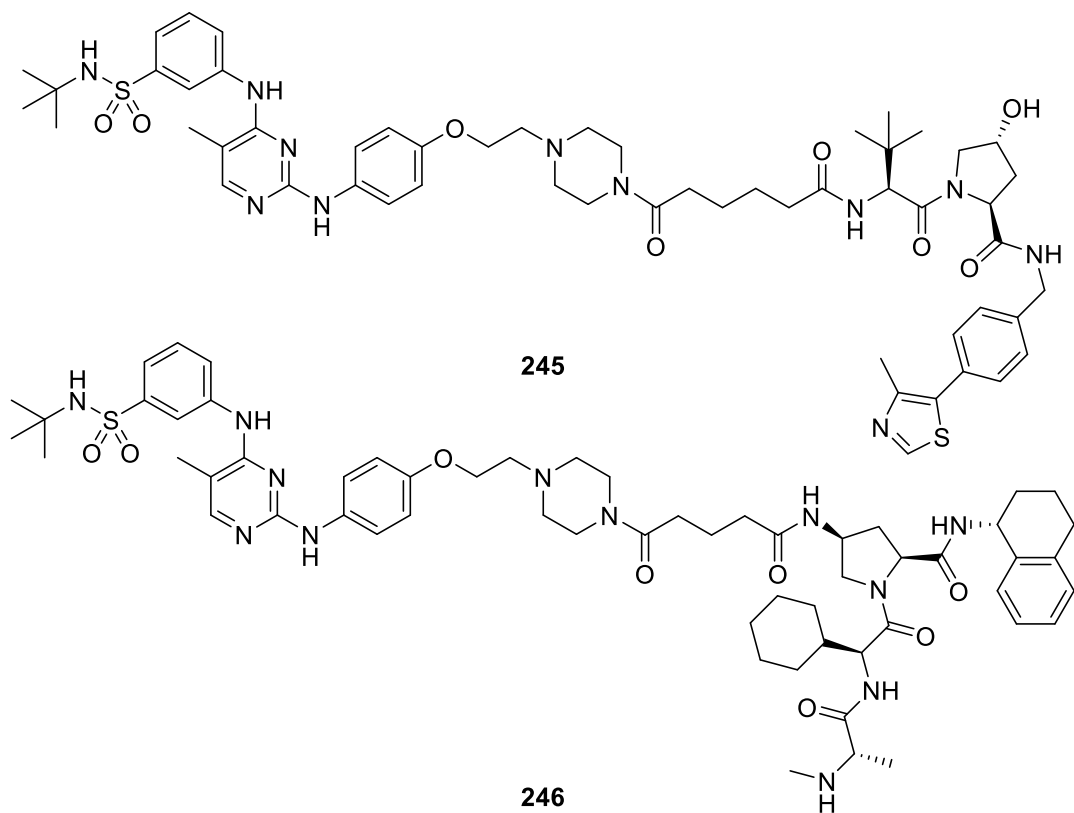


Figure 66 – Targeted VH-032 and IAP-based PROTACs 245 and 246

2.4 – Synthesis of a Series of JAK2-Targeting PROTACs

PROTACs are typically large in size and often structurally complex, however their synthesis can be approached in a modular manner. A simple retrosynthetic analysis can be performed to identify the constituent components (Figure 67).

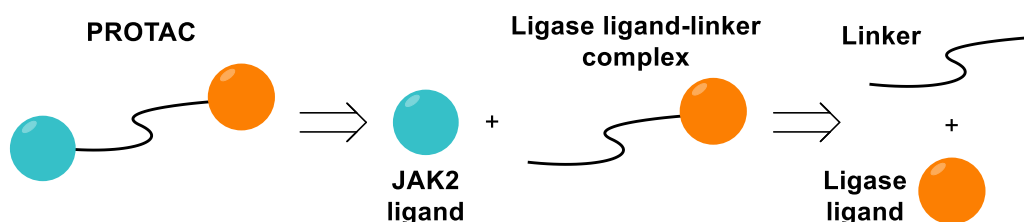
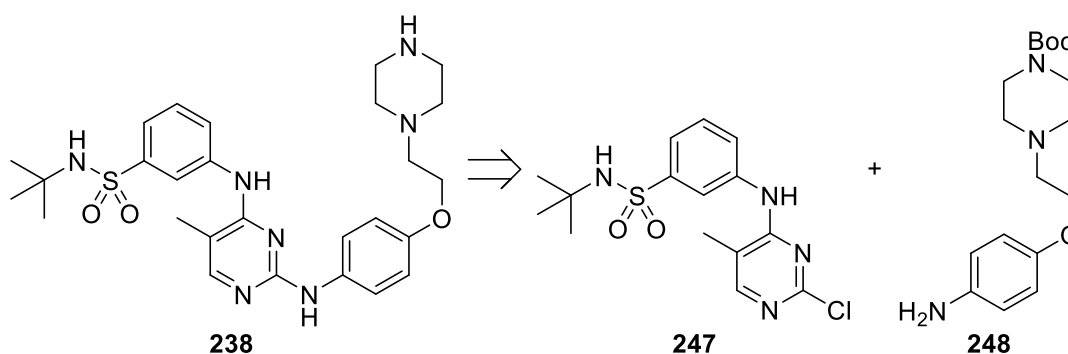


Figure 67 – Retrosynthetic analysis of the PROTAC synthesis

Formation of the ligase ligand-linker complex would be achieved *via* palladium-catalysed cross-coupling, amide coupling, or ring-opening of cyclic anhydrides – depending on the ligase ligand in use. The ligase ligand-linker complexes will be terminated with a masked acid which, upon deprotection, would be coupled with the JAK2 ligand to give the desired PROTAC. Due to the modular nature of the synthesis, the JAK2 ligand and the ligase ligands can be synthesised on scale and libraries of PROTACs can be generated rapidly.

2.4.1 – JAK2 Ligand Synthesis

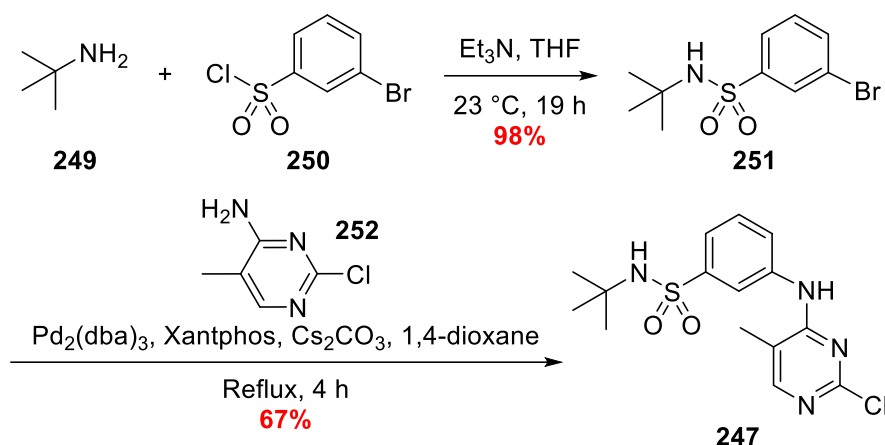
The synthesis of fedratinib **237** is well characterised within the patent literature providing a good starting point to synthesise JAK2 ligand **238**.³⁵⁶ By splitting fedratinib mimic **238**, two easily accessible halves remained: diaryl chloropyrimidine **247** and *p*-alkoxyaniline **248**. The reported synthesis of fedratinib, and a number of other structural analogues, utilised a variety of methods to join the two halves, all of which proceeded in poor yield.³⁵⁶ A screen would therefore be performed to access the most applicable method for the modified JAK2 ligand **238**.



Scheme 98 – Retrosynthetic analysis of **238**

Synthesis of Diaryl Chloropyrimidine **247**

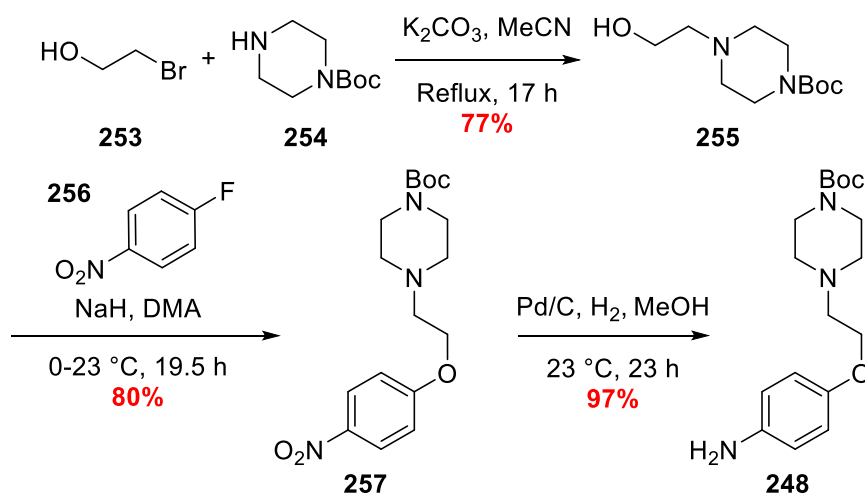
The synthesis of diaryl chloropyrimidine **247** began with the sulfonylation of *tert*-butylamine **249** with commercially available 3-bromobenzenesulfonyl chloride **250** to give sulfonamide **251** in excellent yield. The use of excess *tert*-butylamine **249** promoted complete conversion to sulfonamide **251**. A subsequent Buchwald-Hartwig cross-coupling of aryl bromide **251** and aminopyrimidine **252** afforded diaryl **247** in good yield (Scheme 99).



Scheme 99 – Synthesis of diaryl aminopyrimidine **247**

Synthesis of *p*-Alkoxyaniline **248**

To access *p*-alkoxyaniline **248**, an alkylation of piperazine **254** with 2-bromoethanol **253** was performed to give alcohol **255** which was then subjected to an $\text{S}_{\text{N}}\text{Ar}$ reaction with *p*-fluoronitrobenzene **256** to yield the *p*-nitrophenol derivative **257**. A Pd/C-mediated reduction of nitrophenol **257** gave clean conversion to the alkoxyaniline **248** in excellent yield. The ability to purify nitro **257** *via* recrystallisation and use of a heterogeneous reduction catalyst increased the scalability of the synthesis.



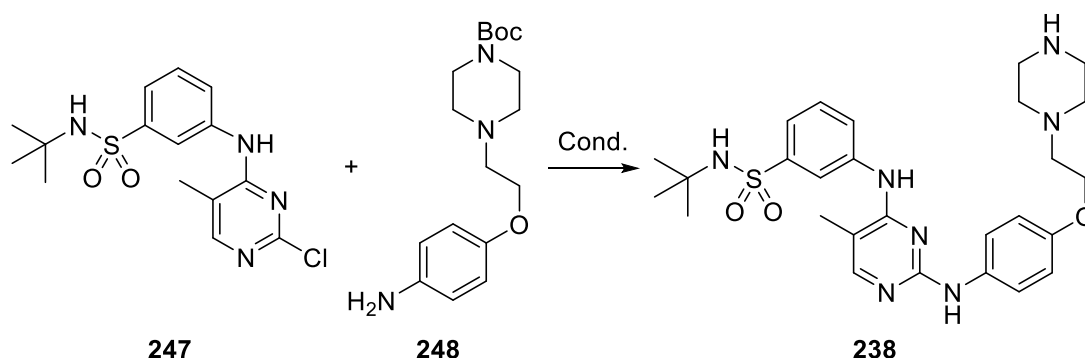
Scheme 100 – Synthesis of *p*-alkoxyaniline **248**

Synthesis of JAK2 Ligand **238**

With the two constituent halves in hand, methodology had to be developed to enable efficient access to ligand **238** (Scheme 101, Table 9). Initial attempts at the literature Buchwald-Hartwig cross-coupling failed with no product mass peak detected *via* LC-MS (Table 9, Entry 1).³⁵⁶ Targegen's patent reports the yield of the equivalent reaction as 11%, suggesting the poor suitability of cross-couplings on this scaffold. Later attempts utilising a reported palladium-catalysed addition-elimination reaction also failed to see any conversion to the desired ligand (Table 9, Entry 2).³⁵⁷

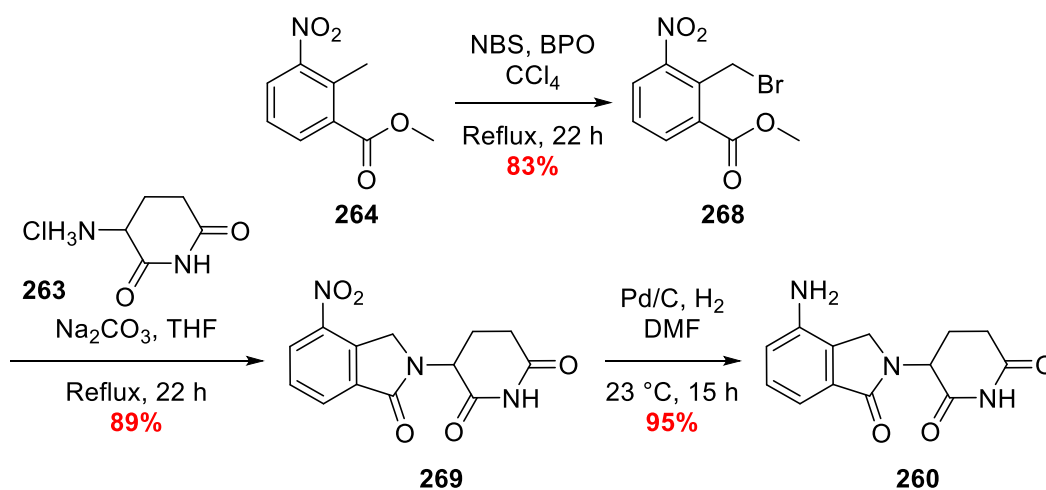
The first sign of success was achieved when heating a solution of chloropyrimidine **247** and amine **248** in AcOH; after 70 h trace amounts of the product mass could be detected by LC-MS, yet the dominant mass peak was the Boc-protected product (Table 9, Entry 3). When considering the reaction conditions, concomitant Boc-deprotection would not be surprising. However, due to the scale of the recovered material, it was not possible to determine whether the loss of the Boc group was occurring during the reaction or during the LC-MS experiment. This result spurred further investigation of Brønsted acid-catalysed addition-eliminations.

Several reports cite microwave irradiation as an efficient method to promote Brønsted acid-catalysed addition-elimination reactions of anilines to chloropyrimidines.³⁵⁸⁻³⁶⁰ An ethanolic solution chloropyrimidine **241** and amine **242** was therefore subjected to microwave irradiation, in the presence of sub-stoichiometric quantities of a hydrogen chloride solution, for 20 min at 150 °C. The reaction gave ligand **238** in moderate yield and unsurprisingly proceeded with concomitant Boc-deprotection. It was later found that increasing the reaction time to 30 min and completing the reaction on >1 mmol scale gave reproducible 60% yields (Table 9, Entry 4).



Scheme 101 – Synthesis of JAK2 ligand **238**

The synthesis of lenalidomide **260** began with the radical bromination of methyl 2-methyl-3-nitrobenzoate **264**, affording benzyl bromide **268** in a good yield. Synthesis of the core of the ligase binder was completed with the one-pot S_N2/amidation reaction of benzyl bromide **268** with amine hydrochloride **263**. Reduction of the nitro group initially proved problematic due to solubility issues of the starting material with the reaction proceeding in poor yield (Table 10, Entry 1). Use of a MeOH/CH₂Cl₂ solvent system lead to a minor increase in yield due to increased solubility of nitrobenzene **269** (Table 10, Entry 2). An alternative reduction catalyst, PtO₂, was also trialled in the reduction of nitrobenzene **269**; however the PtO₂ catalyst performed poorly in a MeOH/1,4-dioxane solvent system (Table 10, Entry 3). Reluctantly, due to the potential for difficult removal post-reaction, nitro **269** was solubilised in DMF. Despite the complete solubilisation of nitro **269**, use of PtO₂ again lead to poor recovery of lenalidomide **260** (Table 10, Entry 4). In a final attempt to reduce nitrobenzene **269**, Pd/C in DMF was employed and gave clean conversion to lenalidomide **260** in excellent yield (Table 10, Entry 5).



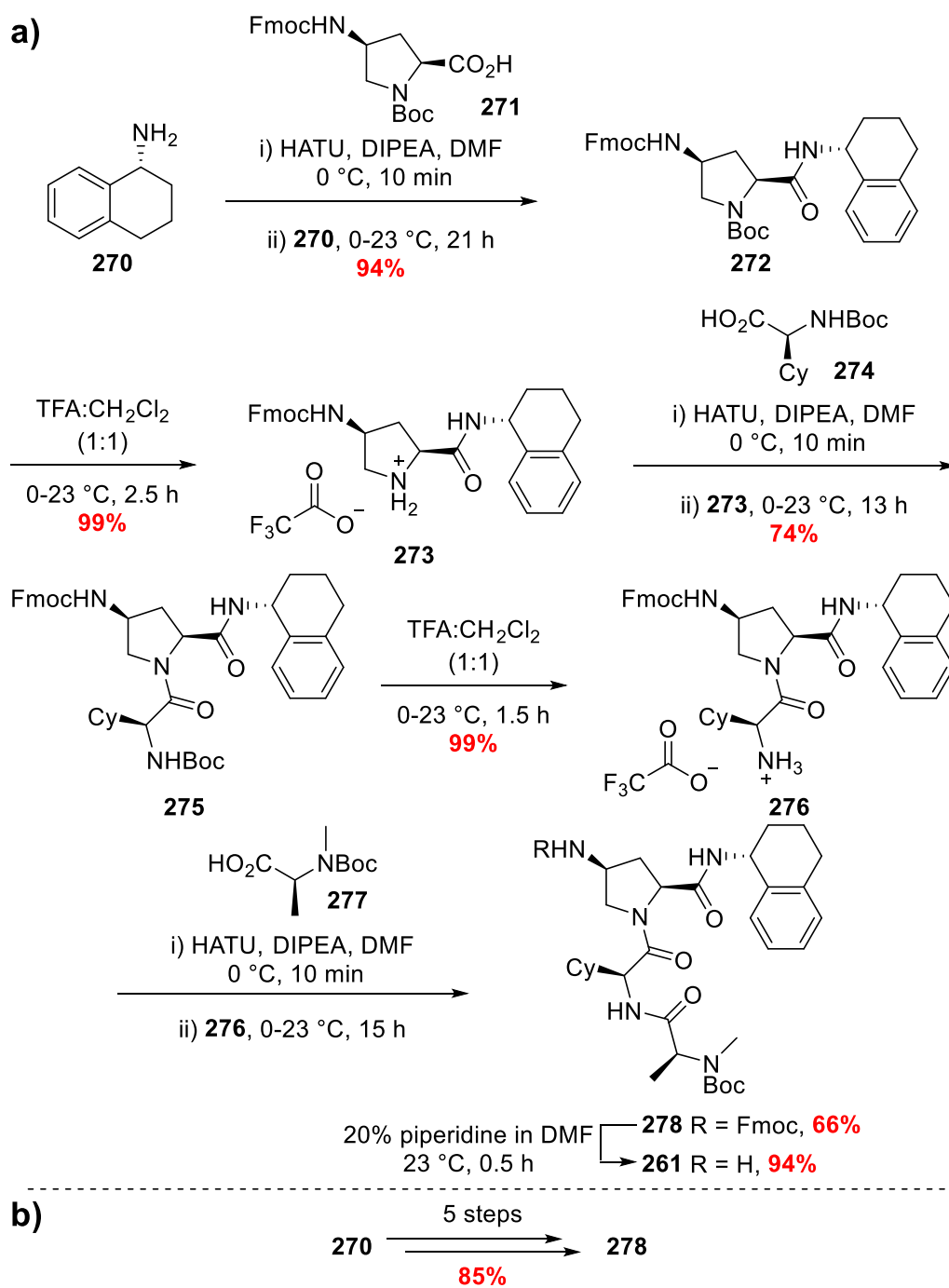
Scheme 105– Synthesis of Lenalidomide **260**

Table 10 – Optimisation of nitro-reduction conditions

Entry	Conditions	Result
1	Pd/C (10% wt.), H ₂ , MeOH, 23 °C, 15 h	260 , 21%
2	Pd/C (10% wt.), H ₂ , MeOH/CH ₂ Cl ₂ (3:1), 23 °C, 6 h	260 , 44%
3	PtO ₂ , H ₂ , MeOH/1,4-Dioxane (3:1), 23 °C, 14 h	269
4	PtO ₂ , H ₂ , DMF, 23 °C, 16 h	Trace 260
5	Pd/C (10% wt.), H ₂ , DMF, 23 °C, 15 h	260 , 95%

IAP Ligase Recruiter Synthesis

The synthesis of **278** involved sequential HATU-mediated amide couplings and TFA Boc-deprotections. Purification of each intermediate gave a yield of 45% over 5 steps (Scheme 106a). The synthesis of **278** was improved by completing the 5 steps without purification of the intermediates – by this method, an 85% yield was achieved over 5 steps on >11 mmol scale (Scheme 106b). A piperidine-mediated Fmoc-deprotection gave IAP ligand **261** in excellent yield.

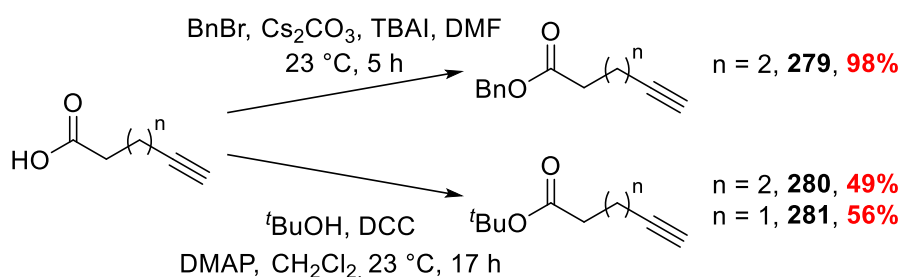


Scheme 106 – Synthesis of IAP ligand **261**

2.4.3 – Linker Synthesis

The identified linkers (Figure 63, *vide supra*) would be joined to JAK2 ligand **238** *via* an amide coupling; thus it is a prerequisite that the linkers must be terminated with a carboxylic acid functionality. For the IAP ligand the linker would also be bound *via* an amide bond – this would be achieved *via* ring opening of a cyclic anhydride or a direct amide coupling reaction.

However, for the thalidomide and lenalidomide CRBN ligands **258** and **259**, the linkers would be attached *via* a Sonogashira cross-coupling reaction. As such, alkyne-terminated aliphatic acids would be required; judicious choice of acid protecting group would allow for facile modulation of the linker topology during the later deprotection step. Benzyl and *tert*-butyl **279**–**281** esters were therefore synthesised from the corresponding alkyne-terminated aliphatic acids (Scheme 107).



Scheme 107 – Synthesis of benzyl and *tert*-butyl esters **273**–**275**

2.4.4 – Ligase Binder-Linker Synthesis

For the first series of PROTACs, eight structures were identified requiring the synthesis of three equivalent thalidomide and lenalidomide-linker complexes and one IAP-linker complex. VHL-linker complex **282** would be purchased from Tocris. For the thalidomide and lenalidomide complexes, 5-carbon alkyne, 6-carbon alkyne and 6-carbon alkane-based linkers were selected. For the IAP linker complex, a 5-carbon alkane-based linker was selected. The linker-length and rigidity was decided based on reported observations of shorter, more rigid linkers improving PROTAC performance.³⁵⁵

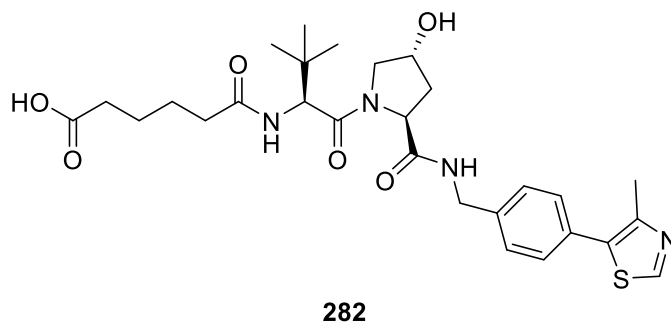
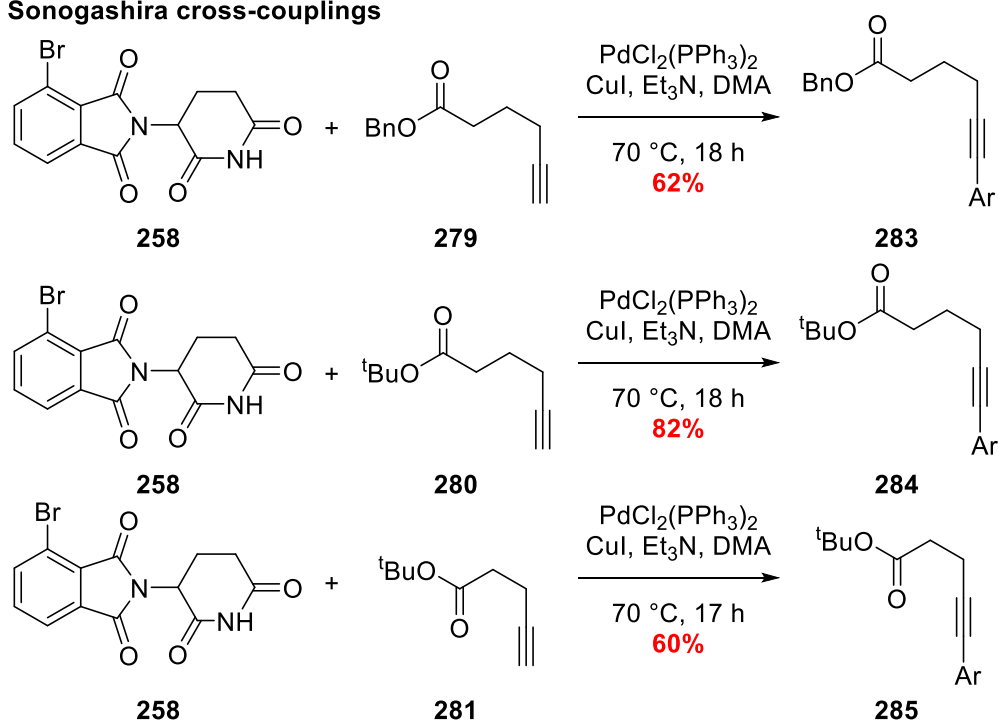


Figure 68 – VHL-linker complex **282** purchased from Tocris

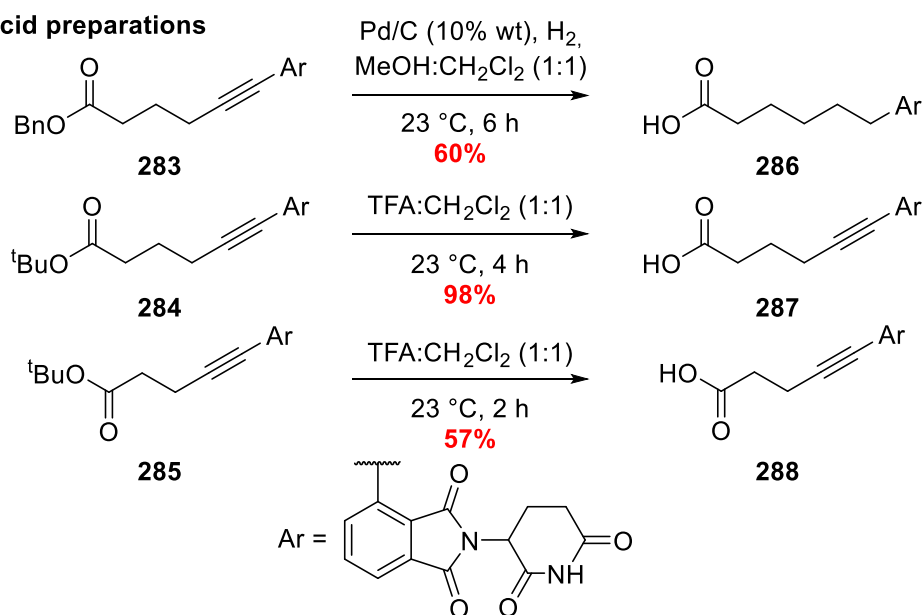
Synthesis of Thalidomide-Linker Complexes

The synthesis began with the Sonogashira cross-coupling of alkynes **279–281** with bromothalidomide **258**, which proceeded in moderate to good yields. Subsequent de-esterifications afforded the desired thalidomide-linker complexes **286–288**. For benzyl ester **283**, the reaction conditions also lead to the concomitant reduction of the alkyne to afford the desired alkane-based linker complex **286**. Due to sample impurities acids **286** and **288** were purified by flash column chromatography, leading to reduced isolated yields (Scheme 108).

Sonogashira cross-couplings



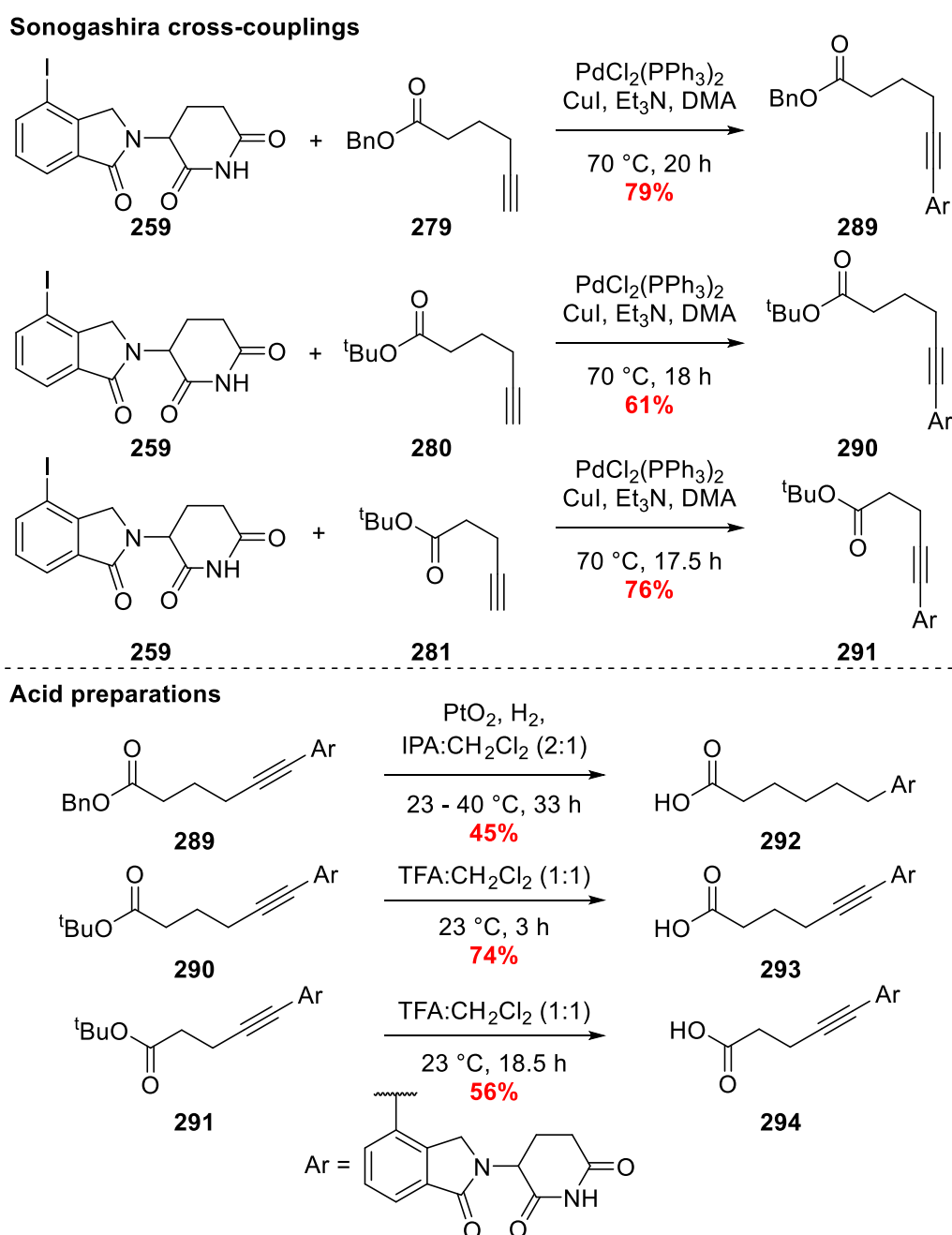
Acid preparations



Scheme 108 – Synthesis of thalidomide-linker complexes **286–288**

Synthesis of the Lenalidomide-Linker Complexes

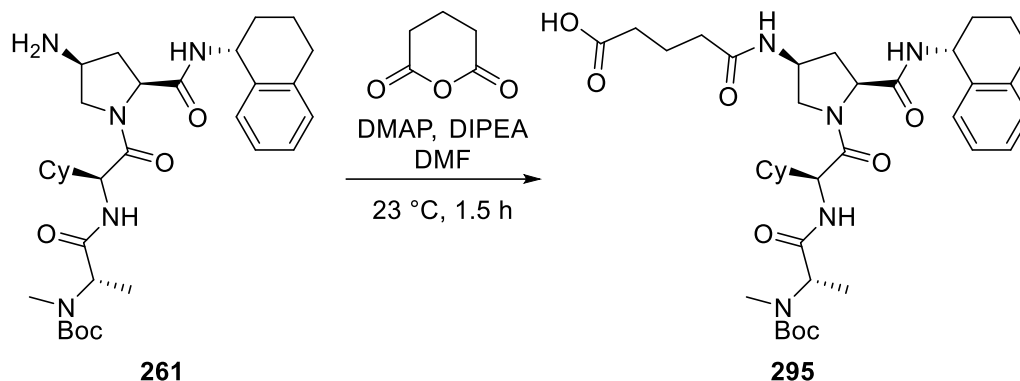
Aryl iodide **259** was subjected to three separate Sonogashira cross-couplings with alkynes **279–281** to give the corresponding ligase binder-linker complexes **289–291** in good yield. Treatment of *tert*-butylesters **290** and **291** with TFA gave the respective lenalidomide-linker complexes **293** and **294**. Concomitant hydrogenolysis and alkyne reduction of benzyl ester **289** failed using Pd/C. PtO₂ at 40 °C gave conversion to acid **292**, unfortunately significant losses during purification lead to poor recovery and hence low isolated yield (Scheme 109).



Scheme 109 – Synthesis of lenalidomide-linker complexes **292–294**

Synthesis of the IAP-Linker Complex **295**

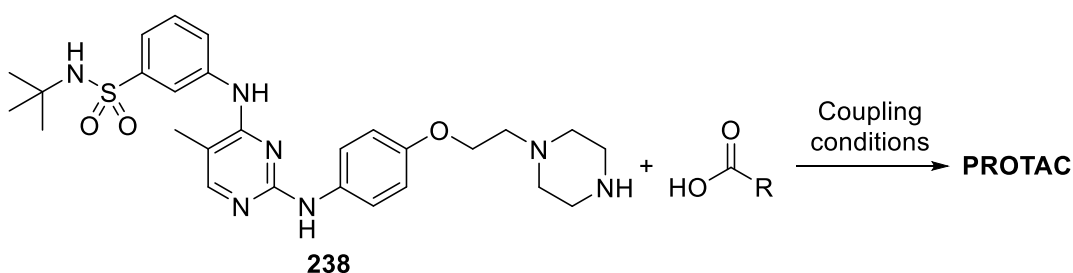
A DMAP-catalysed ring opening of glutaric anhydride followed by subsequent reaction with amine **261** gave access to the desired IAP-linker complex **295** (Scheme 110). Due to the anticipated difficulties in standard phase purification, IAP-linker complex **295** was not isolated and characterised, but its formation was evidenced *via* LC-MS.



Scheme 110 – Synthesis of IAP-linker complex **295**

2.4.5 – JAK2 Ligand and Ligase Binder-Linker Complex Coupling

With the JAK2 ligand and the eight ligase binder-linker complexes in hand, the final amide couplings remained to give the targeted PROTACs (Scheme 111). Due to the small quantities of the ligase binder-linker complexes, a coupling agent screen would not be carried out for the synthesis of a single PROTAC – it would be instead be carried out on a reaction-to-reaction basis (Figure 69).



Scheme 111 – Generic coupling overview to synthesise the targeted PROTACs

In the synthesis of PROTAC **239**, the coupling agent used was the cyclic phosphonic anhydride, T3P. In the presence of NMM, in a CH_2Cl_2 solution, the conversion was low and the isolated yield was very poor (Table 11, Entry 1). The following coupling to yield PROTAC **240** was carried out in a solution of DMA, in the presence of EDCI-HCl and HOBT (Table 11, Entry 2). Use of a highly polar solvent overcame the solubility issues and the use of a more reactive coupling agent partnership lead to an increased yield. However, this higher yield was only achieved through increasing the temperature to 50 °C and an extended reaction time of 45 h. After initial success with a benzotriazole-based coupling agent, the widely used coupling agent

HATU was utilised in the synthesis of PROTAC **241**. In the case of PROTAC **241** this had the effect of affording a higher yield over a significantly shorter time period without the need to heat the reaction mixture (Table 11, Entry 3). PROTACs **242–245** and **296** were subsequently synthesised using HATU-based couplings, generally proceeding in low yield but in sufficient quantities for evaluation purposes.

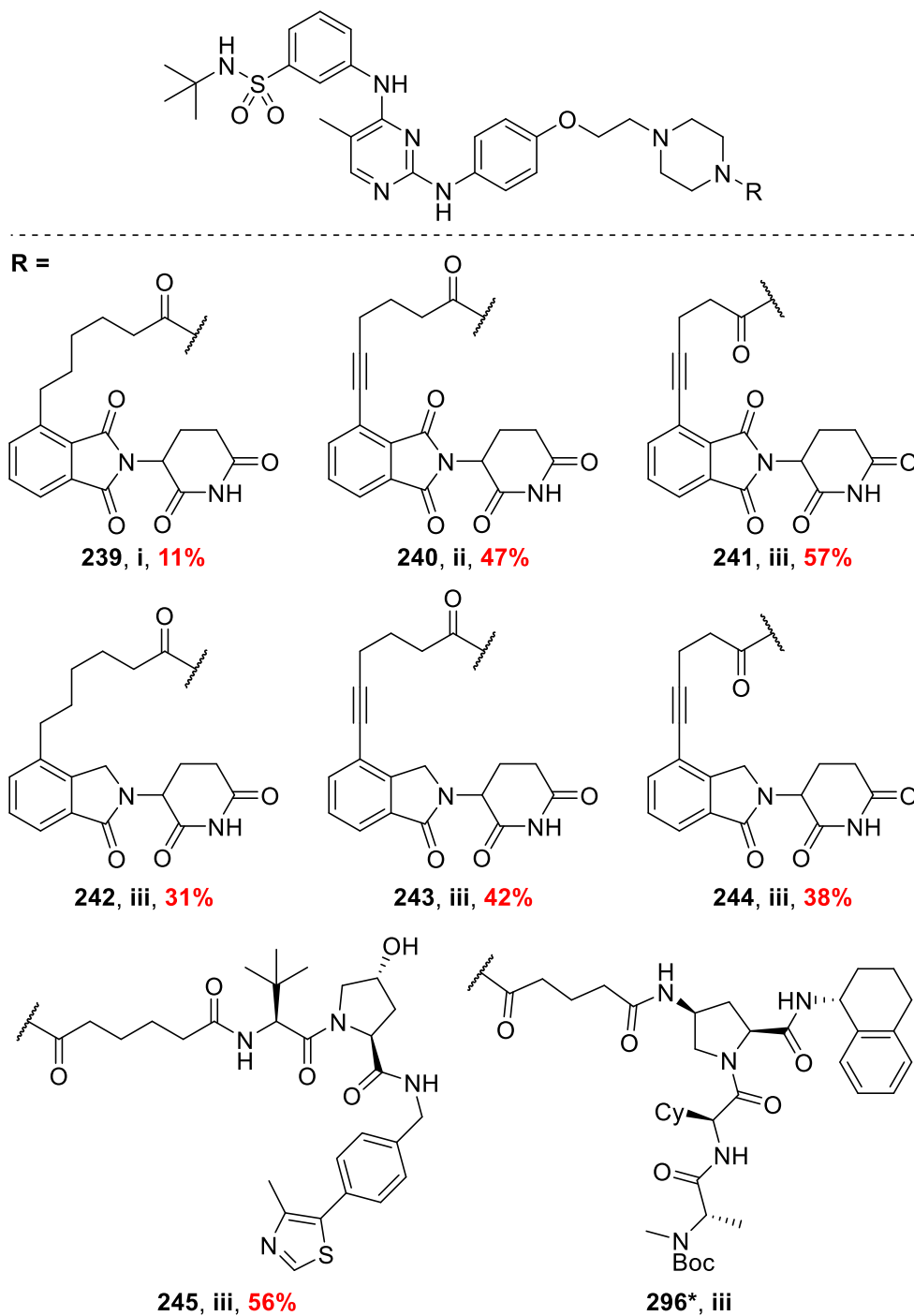
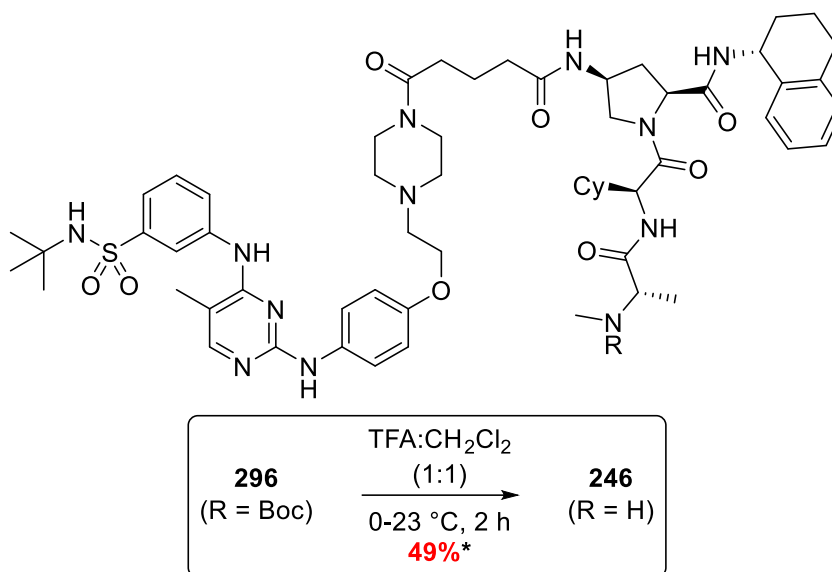


Figure 69 – PROTACs synthesised, *Not isolated and purified

Table 11 – Conditions used for amide couplings

Conditions	Reagents
i	T3P, NMM, CH ₂ Cl ₂ , 23 °C, 24 h
ii	EDCI·HCl, HOBT, Et ₃ N, DMA, 23–50 °C, 45 h
iii	HATU, DIPEA, DMA, 23 °C, 3–23 h

For *N*-Boc PROTAC **296** a final Boc-deprotection was required to access the active PROTAC. Treatment of **296** with TFA followed by elution through an SCX column afforded the free amine **246** in good yield (Scheme 112).



Scheme 112 – Boc-deprotection of PROTAC **246**, *yield over 2 steps

2.5 – Biological Evaluation of the Synthesised PROTACs

Prior to studying the effect of subjecting a JAK2-deficient tumour line to simulated CD8+ cells, the PROTACs were validated with respect to their ability to degrade JAK2. The mechanism of PROTACs involves multiple stages and to date there are no reliable methods for assessing their activity in cell-free experiments. As a result, the synthesised PROTACs were assessed for their ability to degrade JAK2 in HeLa cells: a cervical cancer cell line which expresses JAK2 and demonstrates IFN γ -dependant IDO expression.

Initially four PROTACs were selected: **239**, **244**, **245** and **246**. PROTACs **245** and **246** were selected based on the differences in E3-ligase recruitment whereas PROTACs **239** and **244** were selected based on differing ligands used to recruit the CRBN E3-ligase – this approach was taken to maximise the chance of observing JAK2 degradation. HeLa cells were then exposed to 10, 1 or 0.1 μ M PROTAC individually for a period of 24 hours before the protein level was assessed by western-blot analysis by Celentyx Ltd.

The western-blot data shows 2 proteins detected by the JAK2 antibody, of which the major band appears at below the expected M_w region for full length JAK2 (~130 kDa). To date the nature of these bands is not fully understood, however the results for PROTACs **245** and **246** were unfortunately not indicative of degradation of either 'JAK2' protein under these conditions. (Figure 70).

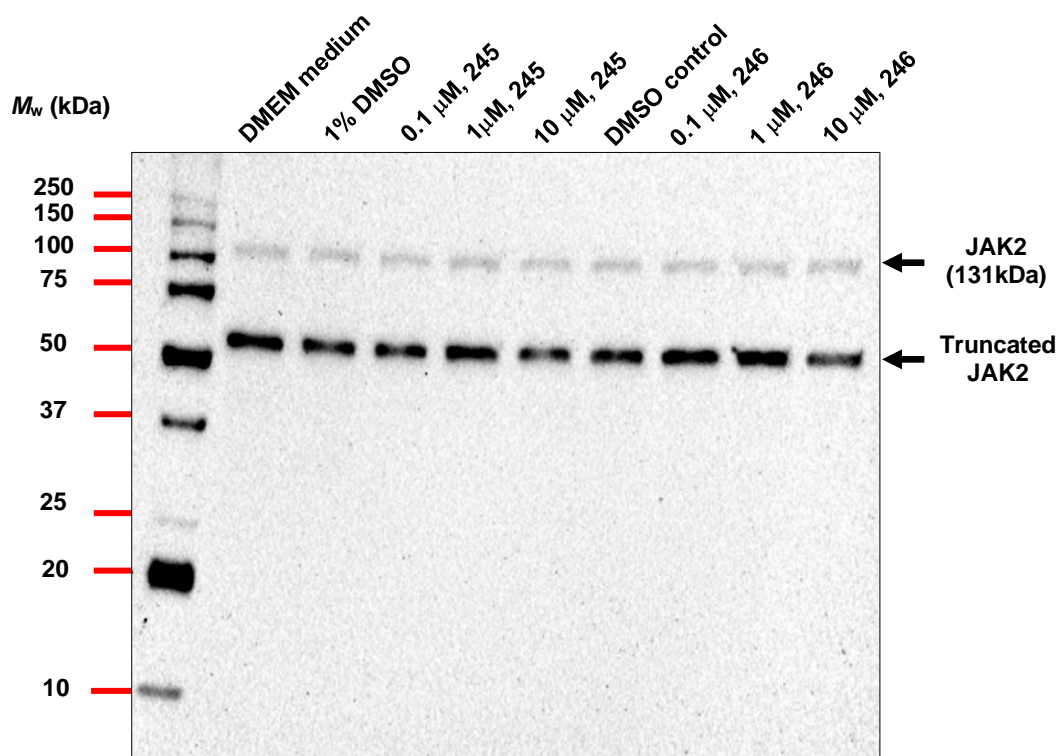


Figure 70 – Western blot analysis for the PROTACs **245** and **246**

Disappointingly, a similar result was observed in the western blot analysis of PROTACs **239** and **244**. No JAK2 degradation in HeLa cells was observed in the presence of PROTACs **239** and **244** (Figure 71).

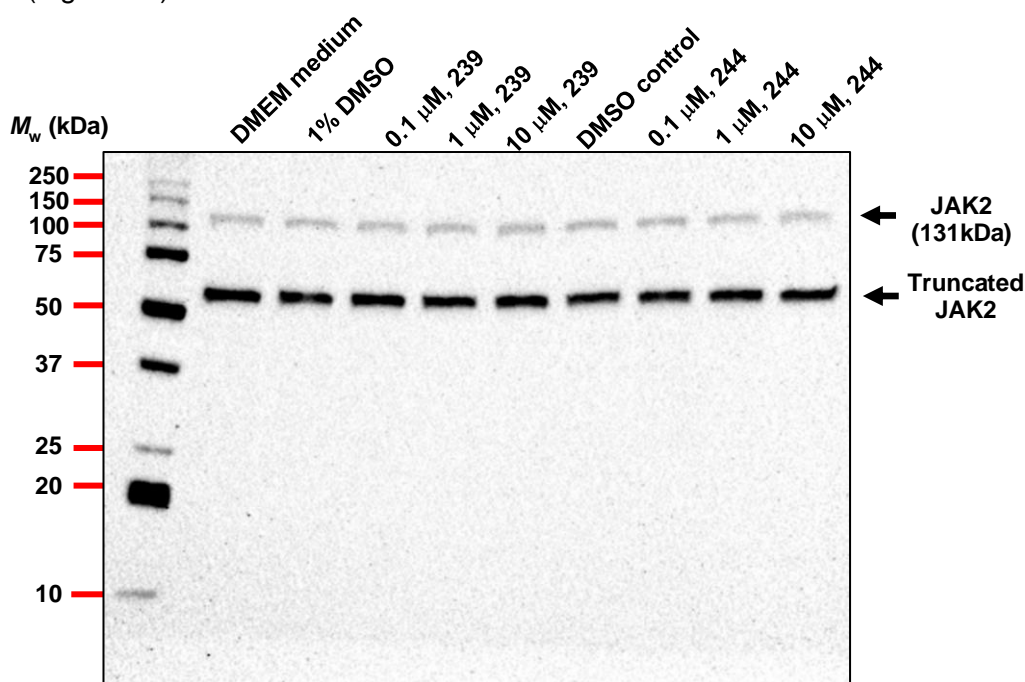


Figure 71 – Western blot analysis for PROTACs **239** and **244**

In the preliminary western blot analysis, no loading control was run. If effect had been seen, loading controls would have been completed to allow the quantification of JAK2 concentration.

The rationale behind the lack of observed degradation of the assayed PROTACs is more nuanced than just a lack of target binding. Fedratinib is a well characterised, FDA-approved inhibitor of JAK2 and when considering the changes made to the fedratinib-based modified warhead (Figure 61) it is difficult to rationalise a complete drop-off in JAK2 binding ability. Based on the current understanding of PROTAC SAR, it is possible that a number of factors were not optimised for successful degradation of JAK2 in these experiments, the mostly likely of which is the failure to form a productive ternary complex.

The work of Crews and Ciulli has demonstrated that co-operative protein-protein interaction is key to affect protein degradation *via* the use of PROTACs. Crews demonstrated an inverse relationship between the PROTAC intrinsic K_d for a target protein and its subsequent DC_{50} , demonstrating that high target occupancy was not a prerequisite for protein degradation.³³⁴ Ciulli also completed detailed studies on the interactions at the protein-protein surface in the ternary complex and demonstrated the linker unit can have a profound impact on target degradation.³²⁶ By considering these analyses, PROTACs **239**, **244**, **245** and **246** could have prevented the formation of a co-operatively bound ternary complex through their linker topology.

Other groups working on structurally related 2,4-diphenylaminopyrimidine PROTAC TL13-12 have noticed that the PROTAC is a ligand of the ABCB1 (ATP Binding Cassette Subfamily B member 1) efflux transporter protein.³⁵² ABCB1 is a class of protein that has been demonstrated to remove hydrophobic and amphipathic compounds *via* active transport.³⁶⁴ In high expressing ABCB1 cell lines, TL13-12 had a low anti-proliferative effect. Co-treatment of cells with TL13-12 with ABCB1 inhibitor tariquidar demonstrated a significant increase in the anti-proliferative activity.^{352, 365} HeLa cells are known to express ABCB1 proteins.³⁶⁶ It was therefore hypothesised that, due to the efflux of structurally related PROTAC TL13-12, efflux of PROTACs **239**, **244**, **245** and **246** was a plausible explanation of the lack of observed JAK2 degradation.

2.6 – Conclusions and Future Work

Based on the JAK2 inhibitor fedratinib, a modified warhead that would enable conjugation to a ligase binder-linker complex, *via* an amide linkage, was designed and successfully synthesised. During the synthesis of modified warhead **238**, a reproducible acid-catalysed S_NAr/elimination was developed to link chloropyrimidine **247** and *p*-alkoxyaniline **248** (Scheme 101).

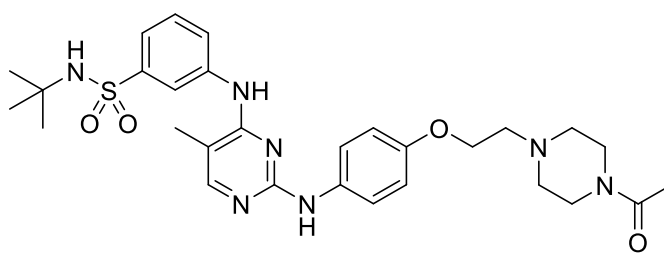
Two syntheses were developed to access lenalidomide-like cores **259** and **260** which would allow the joining of the linker unit *via* an amide linkage or a Sonogashira cross-coupling (Scheme 104 & Scheme 105). A series of successful Sonogashira cross-couplings was then performed to access three lenalidomide- and three thalidomide-based ligase-binder-linker complexes (Scheme 108 & Scheme 109). A large-scale synthesis of IAP ligand **278** was also developed and achieved in an 85% yield over 5 steps (Scheme 106).

The warhead and ligase binder-linker units were then subjected to a dynamic screen of amide coupling conditions; HATU was found to be the most efficacious coupling agent (Figure 69).

Eight PROTACs were synthesised and four (**239**, **244**, **245** and **246**) were subjected to biological evaluation to assess their ability to degrade JAK2 in a whole cell model. Disappointingly, no significant JAK2 degradation in HeLa cells was observed and no definitive rationale was established (Figure 70 & Figure 71). It was hypothesised that the lack of degradation could have been in part due no productive ternary complex formation. Based on literature precedent, it was hypothesised that the 2,4-diphenylaminopyrimidine core is a ligand of the ABCB1 efflux protein. PROTACs **239**, **244**, **245** and **246** could have been recognised and actively transported out of the cell prior to having effect.

Looking forward, several measures could be taken to enable better understanding of the modified warhead and the SAR of this class of JAK2 PROTAC.

Firstly, *N*-acetylated analogue **297** of modified fedratinib ligand **238** could be synthesised and its ability to inhibit JAK2 function evaluated in a whole cell model (Figure 72). Acetylated warhead **297** would serve to validate whether the modifications made to fedratinib **237** (Figure 61) are tolerated with respect to JAK2 binding and provide validation for the choice of warhead and the modifications made.



297

Figure 72 – N-Acetylated warhead 297

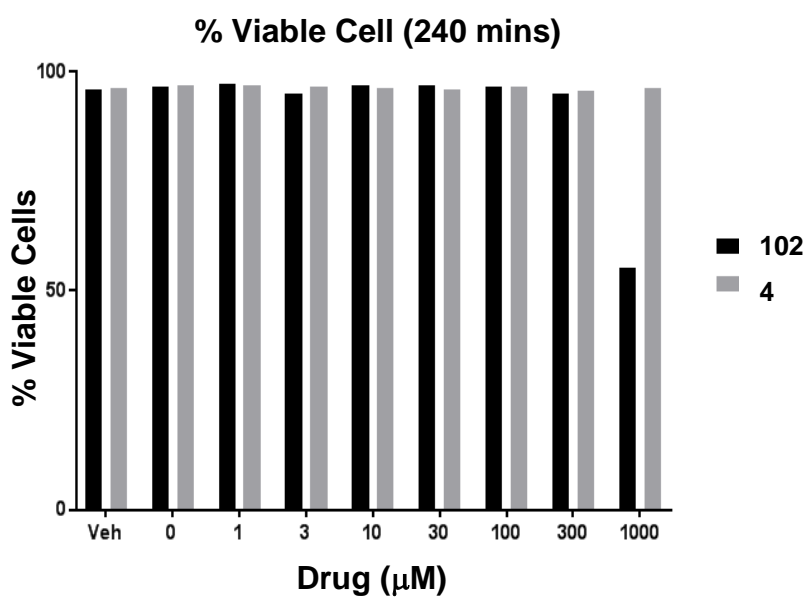
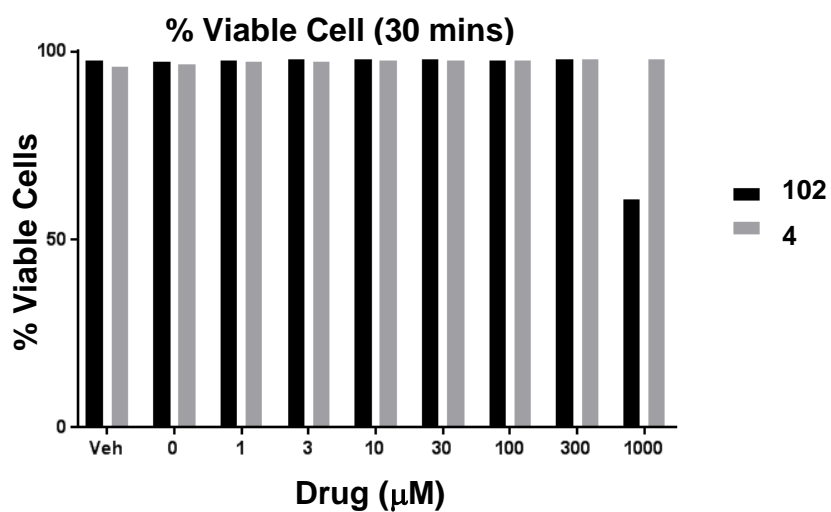
Building on this work, the SAR for a JAK2 PROTAC could be developed by carbon linker units of different length. Prior work has demonstrated that the linker length, and topology, can have a profound impact on the degradation capacity of a PROTAC.^{326, 355} To this effect, incrementally increasing the linker length to ten-carbons would help survey the relationship, if any, between linker length and target degrading ability of the PROTACs. To maximise the chance of degradation, the suite of previously discussed ligase binders should be employed in future study.

In order to fully evaluate the current and any future PROTACs, the molecules should be tested in a wider range of cell lines and under conditions where the JAK2 detection gives clearer results. By evaluating PROTACs in range of cell lines, it is possible to examine cellular environments that demonstrate differing levels of E3-ligase or ABCB1 efflux protein expression. To evaluate the impact of permeability and efflux in HeLa cells, the PROTACs should also be co-administered with ABCB1 inhibitors.

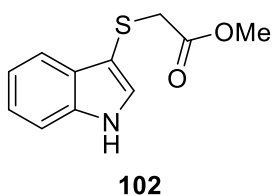
Chapter 3:

Appendix

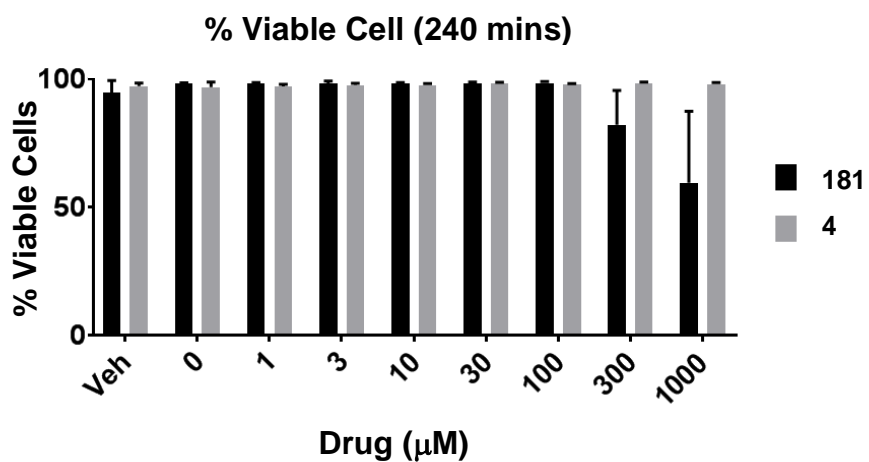
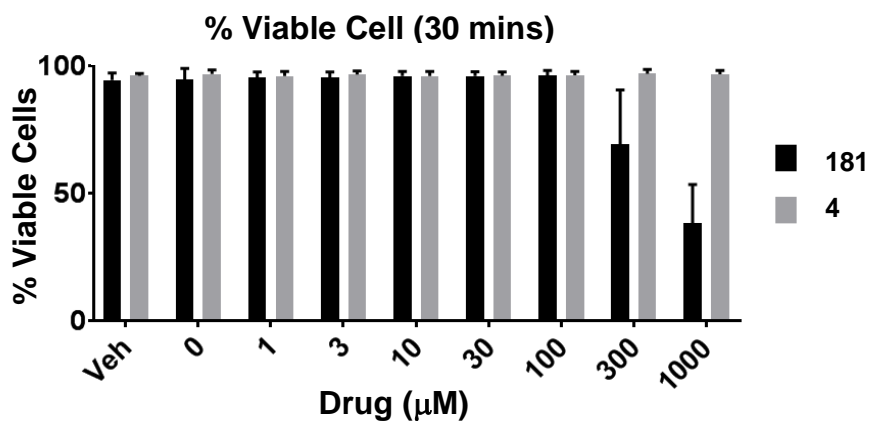
Appendix 1 – % Viable Cell Data for Sulfenylindole **102**



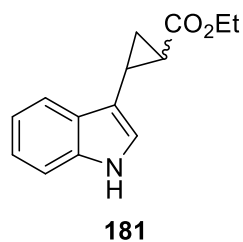
Time dependent cell-viability data for sulfenylindole **102**. Below 300 mM **102** demonstrated no significant cellular toxicity. No time dependent toxicity effects were observed.



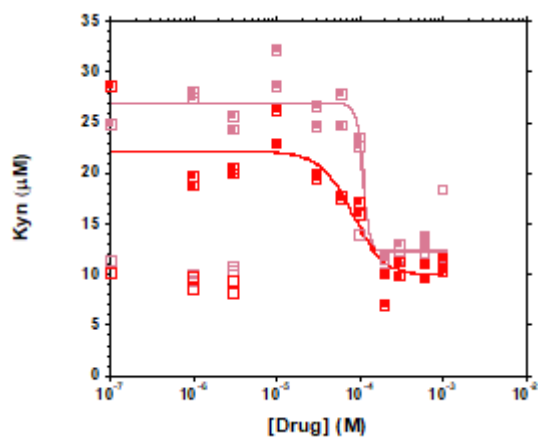
Appendix 2 – % Viable Cell Data for Cyclopropyl Ester **181**



Time dependent cell-viability data for cyclopropyl ester **181**. Below 100 mM **181** demonstrated no significant cellular toxicity. No time dependent toxicity effects were observed.



Appendix 3 – Dose Response Data for Sulfenylindole **102**



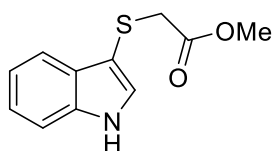
30 mins

y = m4-(m1*((m0^m3)/((m0^m3)...		
	Value	Error
m1	14.586	1.0056
m2	109uM	0.00013009
m3	11.843	152.32
m4	26.799	0.59698
Chisq	61.585	NA
R	0.97044	NA

240 mins

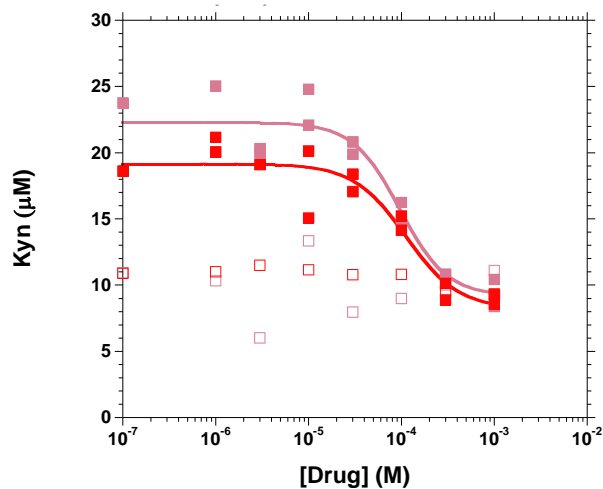
y = m4-(m1*((m0^m3)/((m0^m3)...		
	Value	Error
m1	12.254	1.8061
m2	83.1uM	2.0981e-05
m3	2.2802	1.2352
m4	22.071	1.0219
Chisq	123.45	NA
R	0.90695	NA

Dose response data for sulfenylindole **102**, IC₅₀ value is represented by the m2 value. No significant change in IC₅₀ was observed between to two dose-response time points.



102

Appendix 4 – Dose Response Data for Cyclopropyl Ester **181**



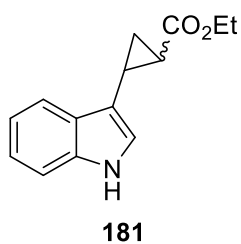
30 mins

y = m4-(m1*((m0^m3)/((m0^m3)...		
	Value	Error
m1	13.104	1.7847
m2	96uM	2.5982e-05
m3	1.7174	0.75139
m4	22.288	0.73575
Chisq	35.137	NA
R	0.95893	NA

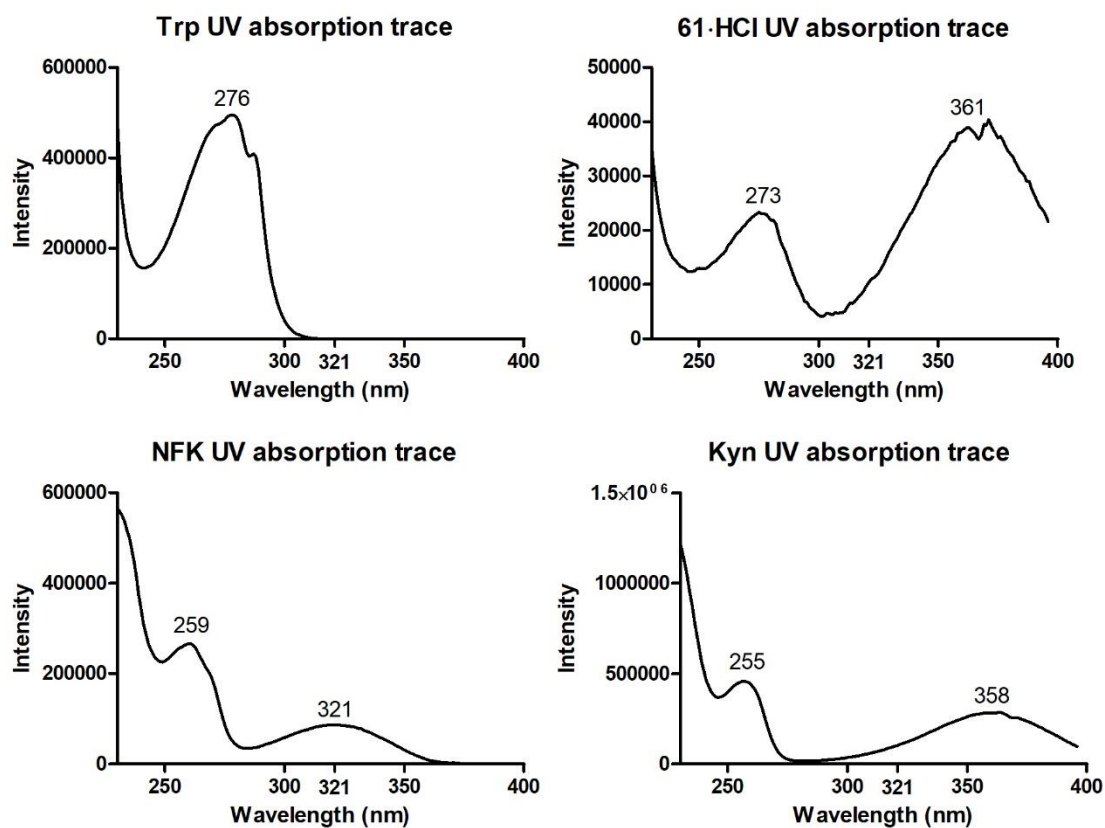
240 mins

y = m4-(m1*((m0^m3)/((m0^m3)...		
	Value	Error
m1	10.951	1.79
m2	112uM	3.6918e-05
m3	1.5357	0.6957
m4	19.152	0.6382
Chisq	25.584	NA
R	0.95351	NA

Dose response data for cyclopropyl ester **181**, IC₅₀ value is represented by the m2 value. No significant change in IC₅₀ was observed between to two dose-response time points.



Appendix 5 – UV absorption data for Trp, **61·HCl**, NFK and Kyn

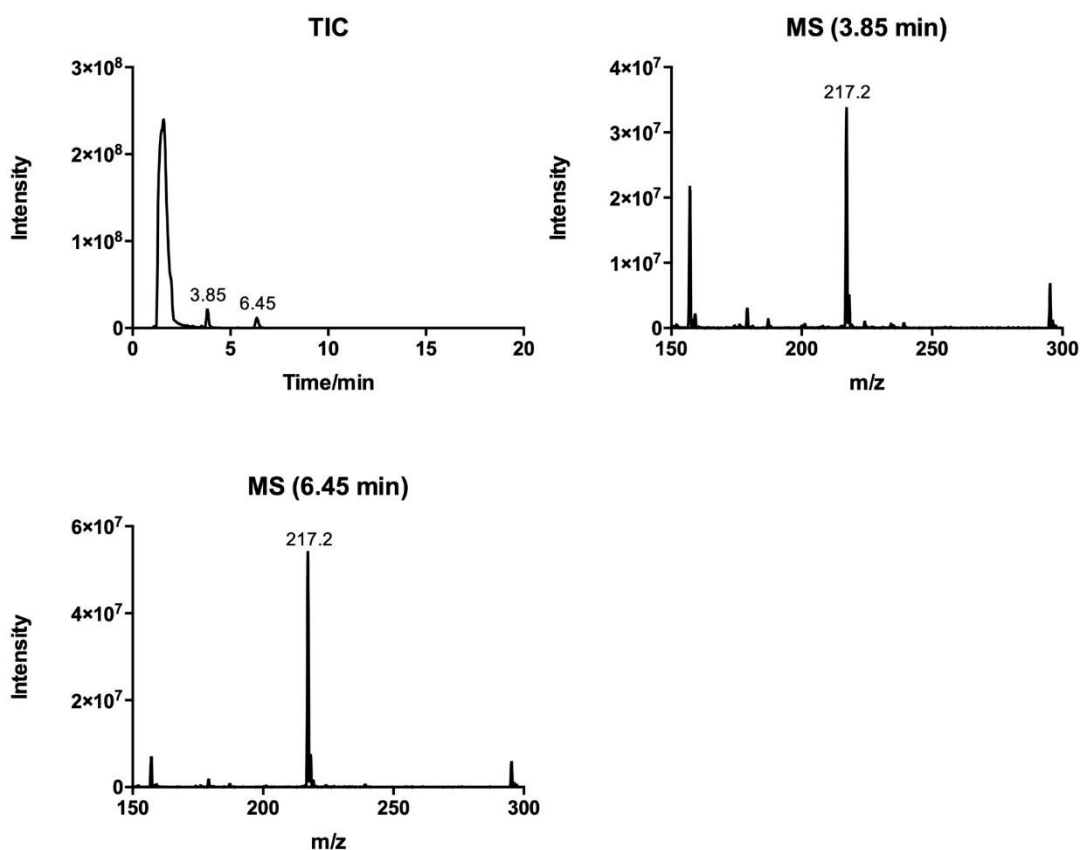


The UV trace data was extracted from LC-MS experiments. Trp demonstrates no absorption at 321 nm while **61·HCl** demonstrates a significant absorption at 321 nm – contributing to the background absorption. NFK and Kyn UV traces are presented for comparison.

Appendix 6 – Steady-State Assay, compound and assay media LC-MS data for **61·HCl**, **100·HCl**, **101·HCl** and **102**

Appendix 6.1 – Data for 1,2- Δ -Tryptophan **61·HCl**

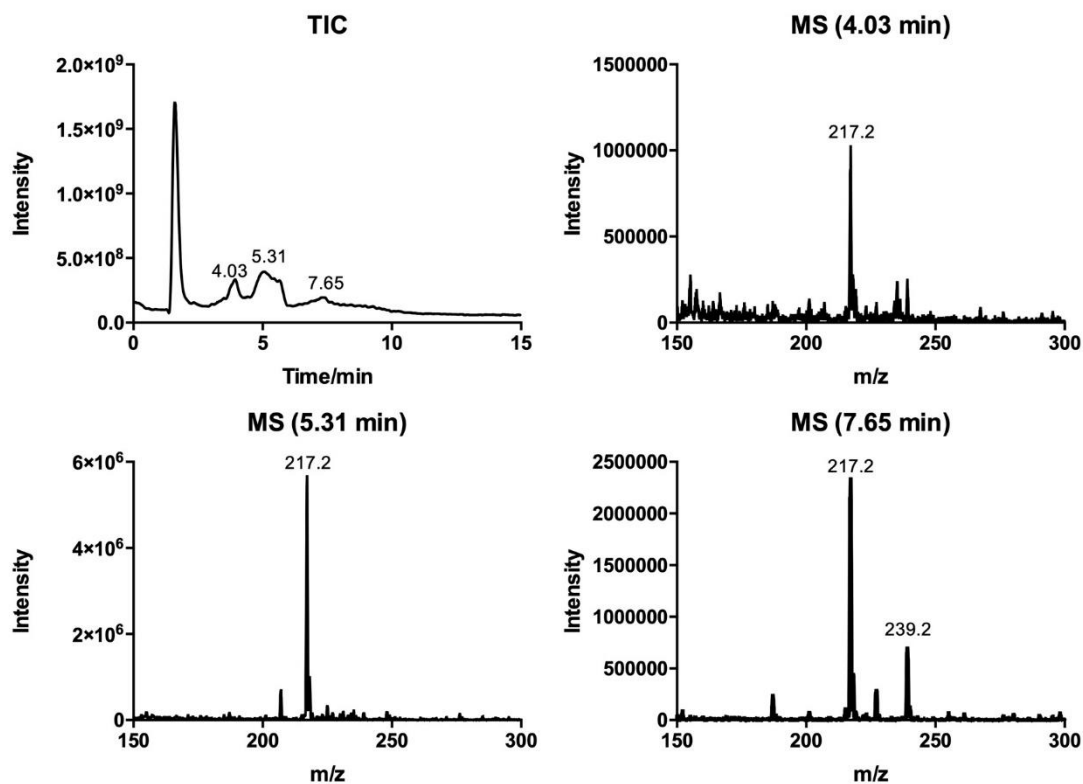
Steady-State Assay LC-MS Data



LC: 100% water, 30 min. M_w (1,2- Δ -Tryptophan **61·HCl**) = 216.1 g mol⁻¹.

Two LC-fractions were observed to contain the mass ion for 1,2- Δ -Tryptophan **61·HCl**. This observation could be a result of diastereomer separation, however this was not verified.

Compound LC-MS data

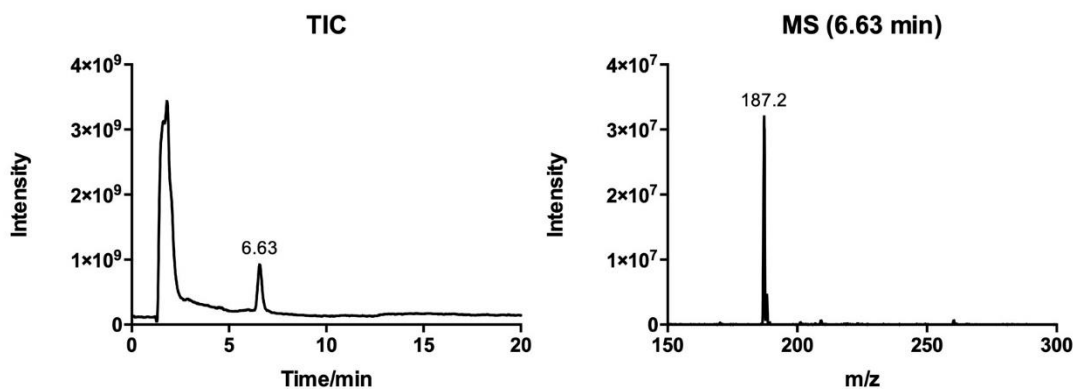


LC: 100% Water, 30 min. M_w (1,2- Δ -Tryptophan **61**·HCl) = 216.1 g mol⁻¹.

The broad elution profile of 1,2- Δ -Tryptophan **61**·HCl could be a result of protonation of the α -amine during the trichloroacetic acid assay quench procedure. No additional mass ions were identified that would align with the predicted mass outcomes.

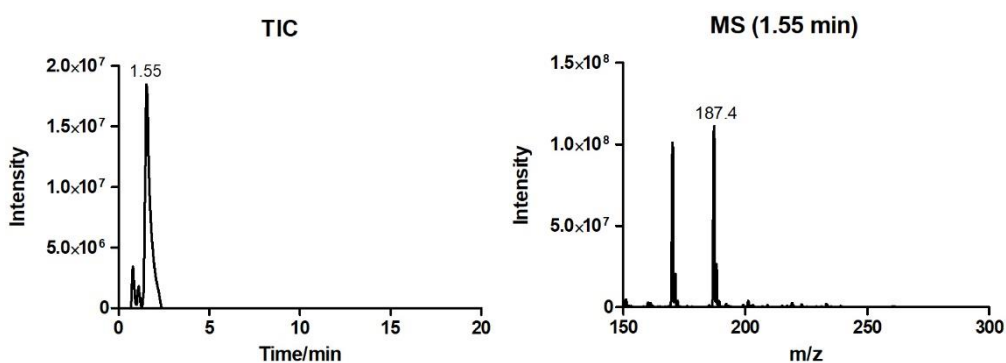
Appendix 6.2 – Steady-State Assay LC-MS Data for 1,1'- Δ -Tryptamine **101·HCl**

Steady-State Assay LC-MS Data



LC: 90–10% water in MeOH, 60 min, M_w (1,1'- Δ -Tryptamine **101·HCl**) = 186.4 g mol⁻¹.

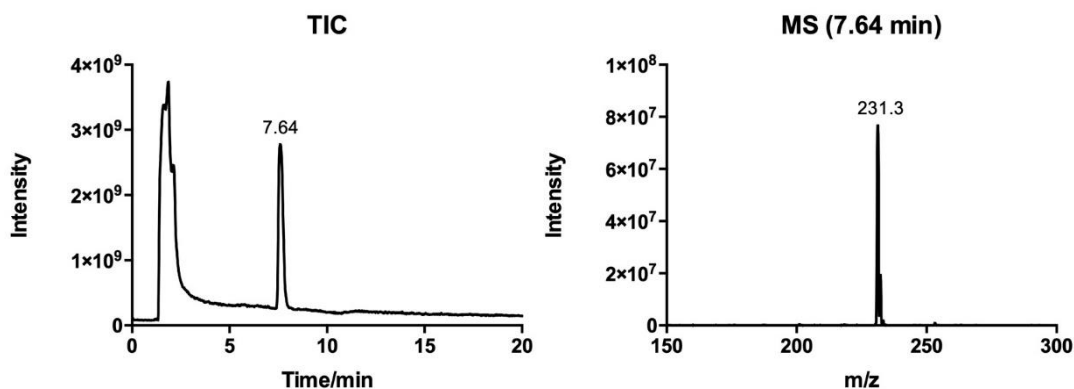
Compound LC-MS Data



LC: 90–10% water in MeOH, 60 min, M_w (1,1'- Δ -Tryptamine **101·HCl**) = 186.4 g mol⁻¹. No additional mass peaks were observed that correlated to the predicted mass outcomes for IDO1 mediated dioxygenation of tryptamine **101·HCl**.

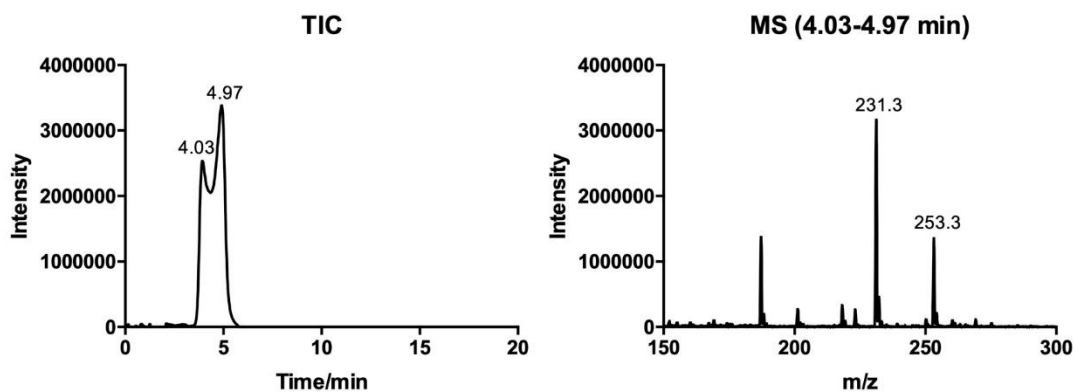
Appendix 6.3 – Steady-State Assay LC-MS Data for 1,1'- Δ -Tryptophan **100**·HCl

Steady-State Assay LC-MS Data



LC: 90–10% water in MeOH, 60 min, M_w (1,1'- Δ -Tryptophan **100**·HCl) = 230.3 g mol⁻¹.

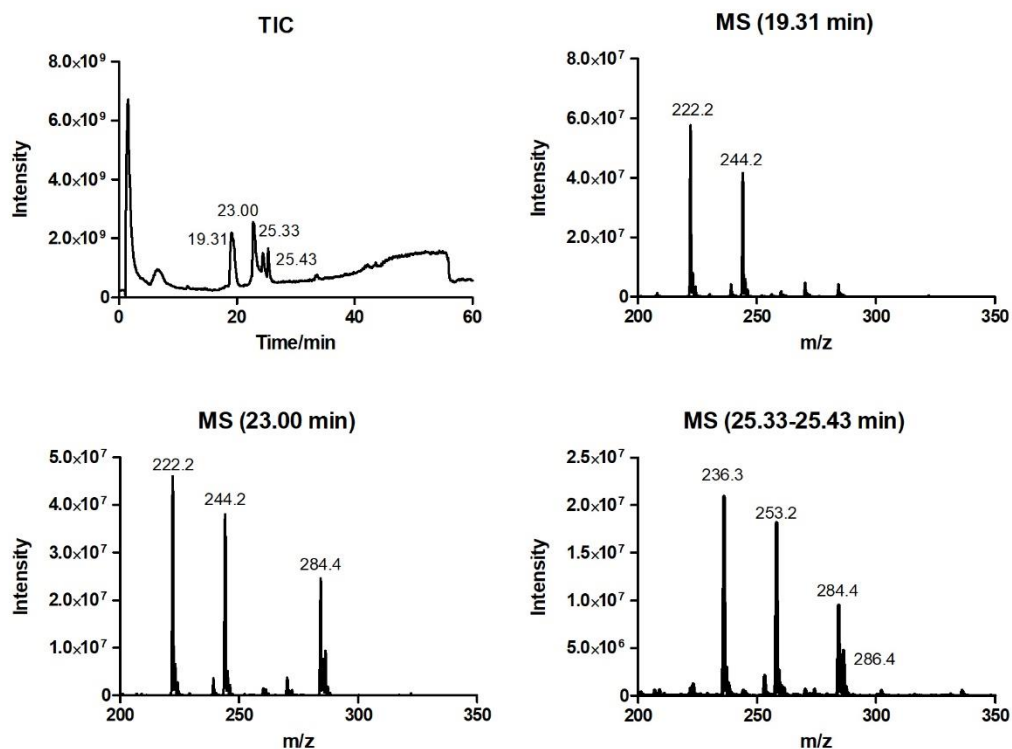
Compound LC-MS Data



LC: 90–88% water in MeOH, 30 min. M_w (1,1'- Δ -Tryptophan **100**·HCl) = 230.3 g mol⁻¹. No additional mass peaks were observed that correlated to the predicted mass outcomes for IDO1 mediated dioxygenation of tryptophan **100**·HCl.

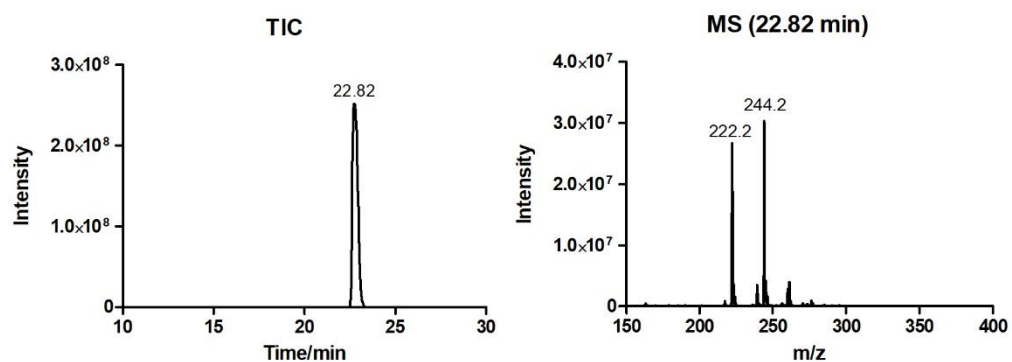
Appendix 6.4 – Steady-State Assay LC-MS Data for Sulfenylindole **102**

Steady-State Assay LC-MS Data



LC method: 90–10% water in MeOH, 60 min, M_w (Sulfenylindole **102**) = 221.2 g mol⁻¹.

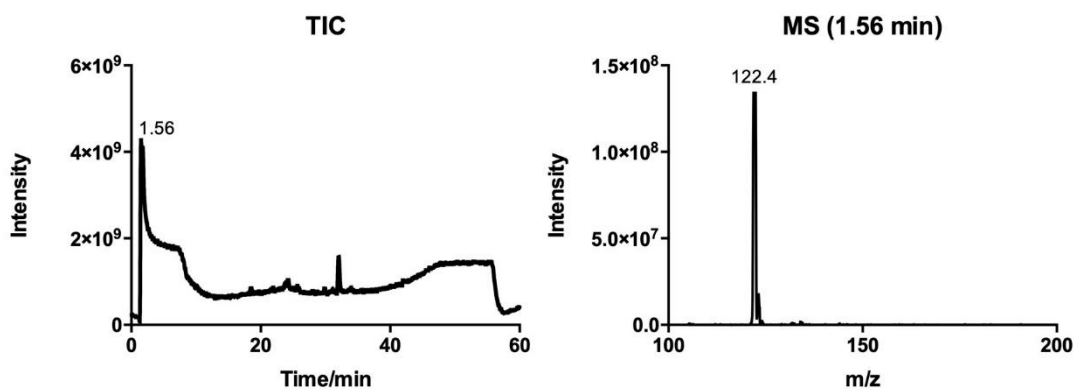
Compound LC-MS data



LC method: 90–10% water in MeOH, 60 min M_w (Sulfenylindole **102**) = 221.2 g mol⁻¹.

Two elution peaks are present which contain the molecular ion for sulfenylindole **102**. Methylene blue is responsible for mass peaks at 284.4 g mol⁻¹. The 236.3 and 253.2 g mol⁻¹ mass peaks did not

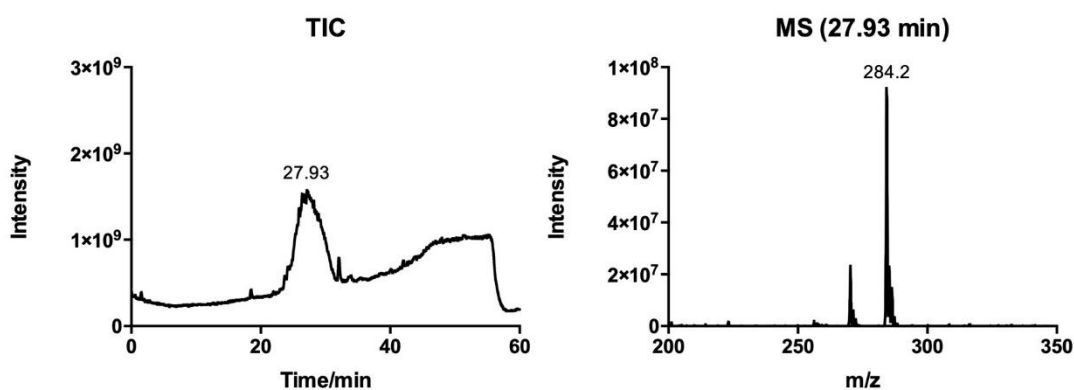
Appendix 6.5 – Steady-State Assay Control LC-MS Data for Tris solution



LC method: 90–10% water in MeOH, 60 min

M_w (Tris/tris(hydroxymethyl)aminomethane) = 121.4 g mol^{-1}

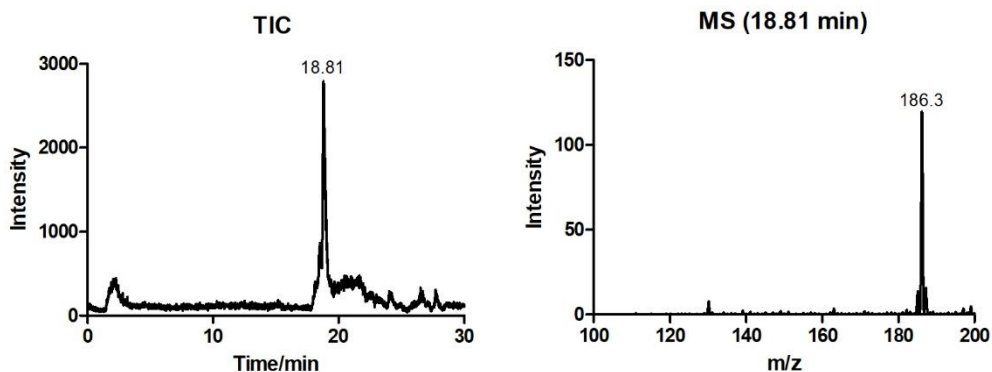
Appendix 6.6 – Steady-State Assay Control LC-MS Data for Methylene Blue



LC method: 90–10% water, 60 min

M_w (Methylene blue) = 319.9 g mol^{-1} (methylene blue is a chloride salt, thus the observable mass is 284.5 g mol^{-1})

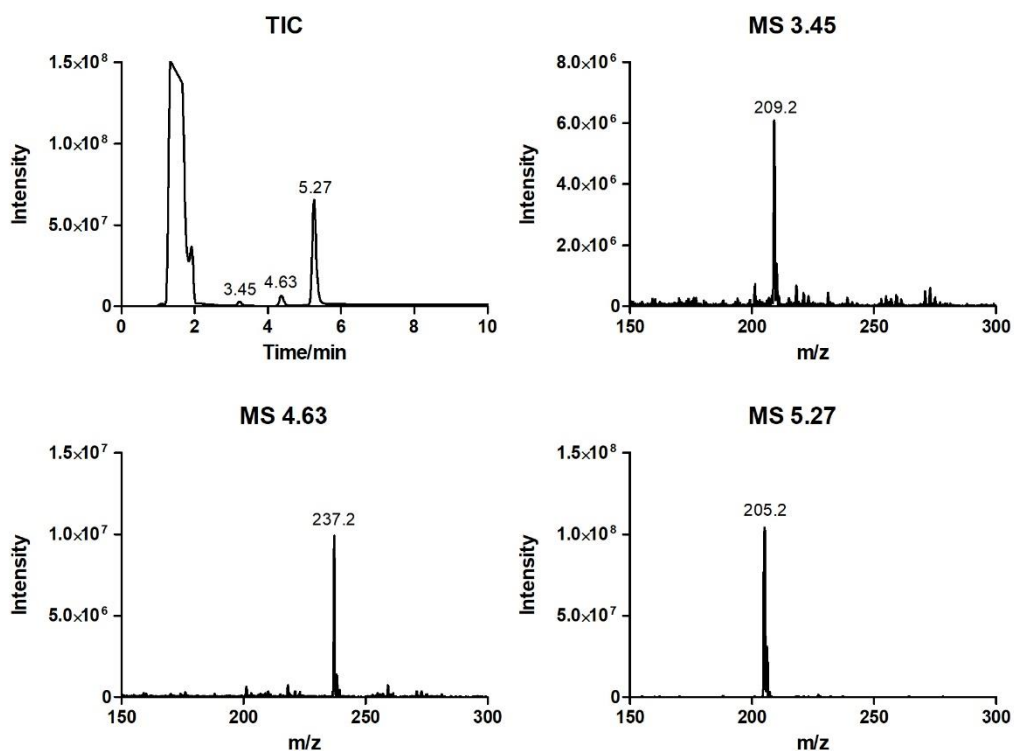
Appendix 6.7 – Steady-State Assay Control LC-MS Data for trichloroacetic acid



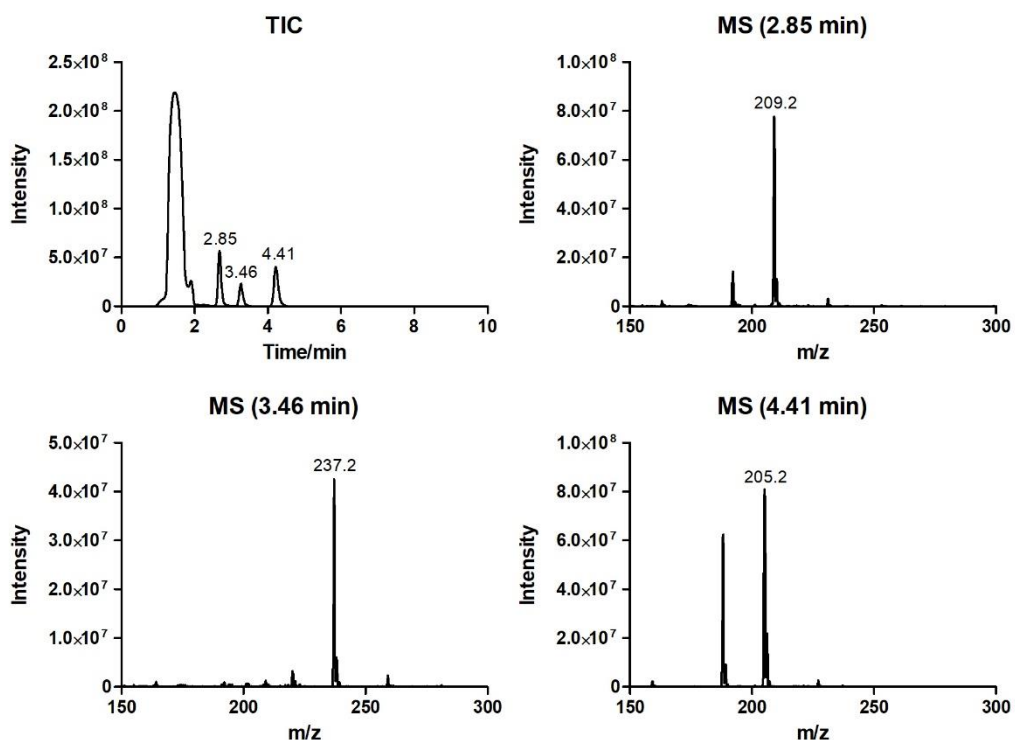
LC method: 100% water, 30 min, M_w (TCA/trichloroacetic acid) = 163.3 g mol⁻¹

Appendix 7 – LC-MS data for the 15 min and 30 min pre-incubation experiments

Appendix 7.1 – 30 min Pre-Incubation Period (30 min 90-92% MeCN:H₂O LC gradient)

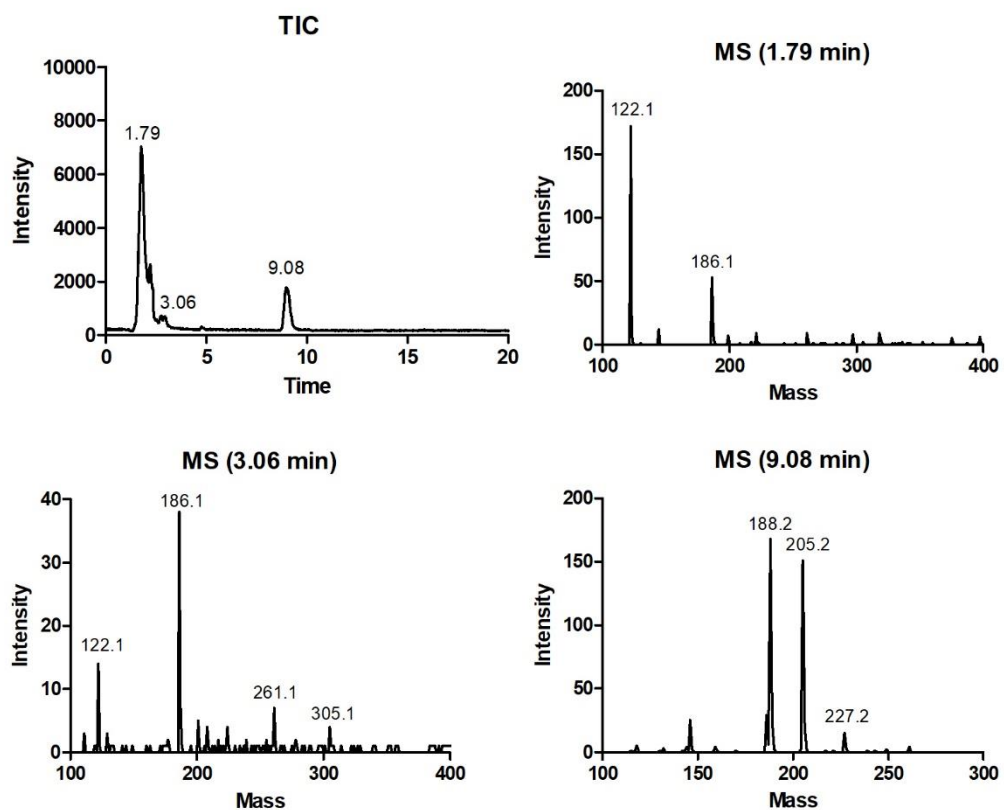


Appendix 7.2 – 15 min Pre-Incubation Period (60 min 90-80% MeCN:H₂O LC gradient)



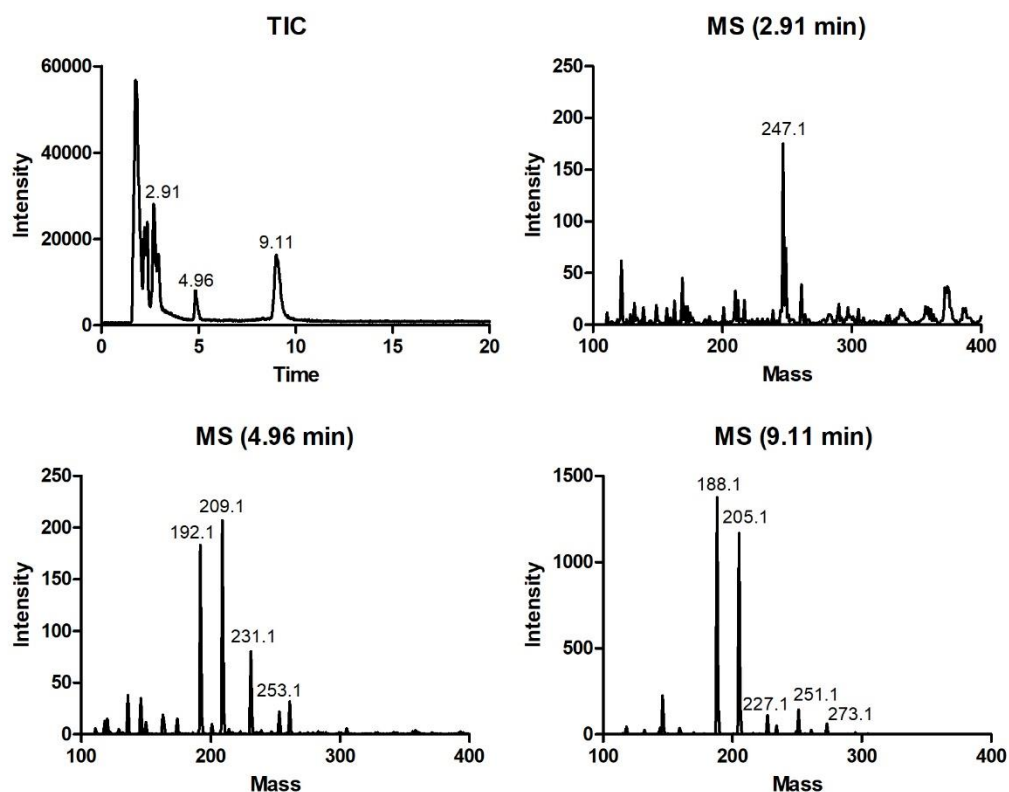
A 30 min pre-incubation period lead to a significant reduction in IDO1 activity, as evidenced by the reduction absorbance at 321 nm and in the detected NFK ($R_t = 4.63$ min, $M_w = 236.2$ g mol⁻¹) and Kyn ($R_t = 5.27$ min, $M_w = 208.2$ g mol⁻¹). A 15 min pre-incubation period gave a superior result with an increased detection of NFK *via* absorption at 321 nm and the increase in detected NFK ($R_t = 3.46$ min, $M_w = 236.2$ g mol⁻¹) and Kyn ($R_t = 4.41$ min, $M_w = 208.2$ g mol⁻¹).

Appendix 8 – LC-MS data for the INCB, **6**, control experiment



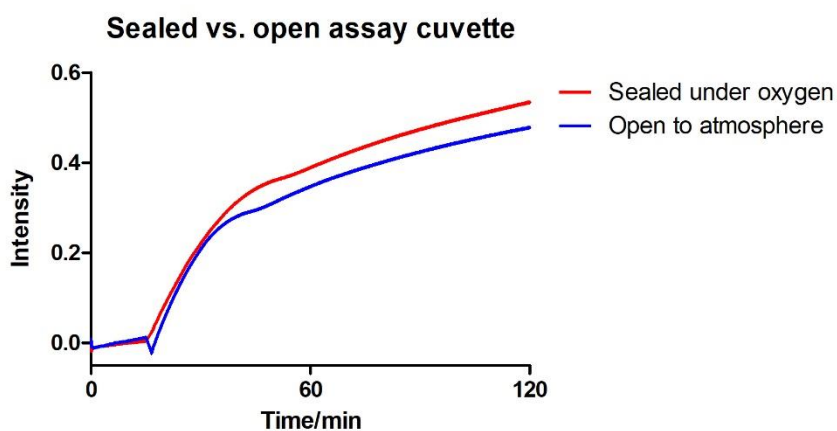
Excess **6** completely inhibited IDO1 activity and no NFK or Kyn was evidenced by LC-MS analysis.

Appendix 9 – LC-MS data for the 1-MT, 4, control experiment



Use of **4** as a positive control lead to the reduced activity of IDO1 though substrate competition. As **4** acts as a weak substrate of IDO1, metabolic products 1-MeNFK ($R_t = 9.11$ min, $M_w = 250.1$ g mol⁻¹) was observed alongside Trp metabolic products Kyn ($R_t = 4.96$ min, $M_w = 250.1$ g mol⁻¹).

Appendix 10 – Trp turnover in oxygen sealed and open to atmosphere assay mixtures ($n = 1$)



Chapter 4:
Experimental Methods

Biological Evaluation Methods

General Experimental

All reagents and solutions were purchased from Sigma-Aldrich or ThermoFisher at 99.5% purity or higher. Molecular biology grade water was used to make up all stock solutions, stock solutions of sodium ascorbate and catalase were stored for a maximum period of 6 weeks before a fresh solution was prepared.

The assays (with the exception of the thermal shift assay) were performed using the same component solutions, at the same concentrations but with differing volumes – volumes will be stated in the assay descriptions. Stock solution refers to a mixture of tris·HCl, pH 8 buffer (50 mM), sodium ascorbate (20 mM) and methylene blue (10 μ M) – fresh stock solution was prepared for each experiment. Catalase (10 μ g mL⁻¹) was prepared from a suspension of catalase solution (24 mg mL⁻¹) with an assayed activity of 11895 units mL⁻¹. Samples of recombinant IDO1 F164A were kindly provided by Prof. Emma L. Raven (University of Bristol, School of Chemistry) for use in the cell-free assays (5 μ M). Trichloroacetic acid (TCA, 30% in water) was used to quench the assays prior to LC-MS analysis.

'UV-Vis' refers to UV-visible spectra recorded using a Varian Cary50 UV-Visible spectrophotometer measuring continuous (10 readings s⁻¹) absorbance at 321 nm.²³⁰ 'Fluorimeter' refers to a Jasco FP-8500 fluorescence spectrometer. 'Plate reader' refers to a BMG Labtech CLARIOstar plate reader fitted with a monochromator. In all cases, fluorescence events were stimulated by an excitation wavelength of 325 nm and fluorescence emission was recorded at 434 nm, as per the literature value for *N*-formyl-*L*-kynurenine.²³² LC-MS analysis was performed using either a Waters e2695 separation module coupled with a Waters SQD MS-detector (raw data was processed and extracted using MassLynx V4.1 SCN855), or a ThermoFisher LCQ-fleet LC-MS (raw data was processed and extracted using Xcaliber). All data was processed with Prism 5 or 6. All graphs were generated from the data analysis performed in Prism.

Whole Cell Evaluation Methods

Whole Cell Assay (Performed by Celentyx Ltd.)

SKOV-3 cell culture media: DMEM with glutamine, 10% FBS, 1% P/S. Kyn staining solution: *p*-dimethylaminobenzaldehyde (~0.07 M), ethanol (96%) and glacial acetic acid (4%). Whole cell assays were carried out at 37 °C. Two assays were run, one in the absence of Trp and one in the presences of Trp (100 µM). Each compound data point: n = 2 or 3.

The SKOV-3 cells were transferred in the cell culture media to a 96-well plate and stimulated with IFN γ . After a period of 24 h, the cells were washed with fresh media to remove excess IFN γ . The cells were the treated with inhibitor (variable concentration) or vehicle and the resulting solution was allowed to rest for 2 h. Water or Trp (100 µM) was then added to the assay mixture and allowed to rest for a further 2 h. The assay mixtures were then transferred to a separate 96-well plate containing TCA_(aq) (30%, 10 µL) to quench the mixtures. The quenched mixtures were transferred to Eppendorf vials and centrifuged to remove the remaining cell debris. The media of each quenched assay solution was then heated to 65 °C to hydrolyse any remaining NFK to Kyn. To visualise the Kyn, assay media (140 µL) was treated with Ehrlich's reagent and absorbance readings were recorded at 490 nm and compared against a standard curve to determine Kyn concentration.

Cell Viability Assays (Performed by Celentyx Ltd.)

Cell viability was determined *via* staining with Zombie dye following a literature protocol.³⁶⁷

Western Blot Analysis

SKOV-3 cell culture media: DMEM with glutamine, 10% FBS, 1% P/S.

SKOV-3 cells were plated into six-well plates and were incubated at 37 °C for 24 h. After 24 h, the cultures were treated with PROTAC (variable concentration) and incubated at 37 °C. After a further 24 h, the cells were lysed by addition of 1 mL cold RIPA solution and the cells were scraped and vortexed. The resulting lysated were cooled on ice for 30 min before being subjected to centrifugation (16,000g, 15 min). The collected supernatants were subjected to a BCA protein assay to determine the protein levels in each sample.³⁶⁸ The western blot was performed using a BIO-RAD Precast gel using standard protocols and the samples were blotted using a BIO-RAD transblot turbo system. The following antibodies were used to visualise JAK2: Rabbit polyclonal anti-JAK2 (1:2000) as the primary antibody and anti-rabbit

HRP conjugated (1:3000). JAK2 bands on the blot were detected using a ChemiDoc imaging system.

Biochemical Evaluation Methods

Steady State Assay

Total assay volume = 1 mL, performed in a sealed quartz cuvette of 1.2 mL maximum volume. Oxygenated stock solution (O₂ gas passed through the stock solution for 10 min) was transferred to the UV cuvette. Catalase and IDO1 was added to the oxygenated stock solution and the cuvette was sealed under an atmosphere O₂. After 5 min, Trp/1-MT/inhibitor (1 mM) was added, the cuvette was re-sealed under an atmosphere of O₂, the cuvette was transferred to the UV-vis spectrometer and absorbance readings were initiated to detect *N*-formyl-*L*-kynurenine (Abs = 321 nm). After 2 h, the absorbance readings were ceased, and the assay mixture was transferred to an Eppendorf vial containing TCA (100 μL). The assay mixture was subjected to centrifugation (13,000 rpm, 5 min), transferred to a HPLC vial and submitted for LC-MS analysis.

UV-vis-based Inhibition Assay

Total assay volume = 1 mL, performed in a sealed quartz cuvette of 1.2 mL maximum volume. Oxygenated stock solution (O₂ gas passed through the stock solution for 10 min) was transferred to the UV cuvette. Catalase and IDO1 was added to the oxygenated stock solution and the cuvette was sealed under an atmosphere O₂. After 5 min, inhibitor (Varied concentrations) was added, the cuvette was re-sealed under an atmosphere of O₂, the cuvette was transferred to the UV-vis spectrometer and absorbance readings were initiated (Abs = 321 nm). After 15 min, the UV recording was paused, Trp (1 mM) was added and then UV recording was resumed. After a further 1.75 h, the absorbance readings were ceased, and the assay mixture was transferred to an Eppendorf vial containing TCA (100 μL). The assay mixture was subjected to centrifugation (13,000 rpm, 5 min), transferred to a HPLC vial and submitted for LC-MS analysis.

Fluorescence-Based Inhibition Assay

Total assay volume = 1 mL, performed in a sealed 90° quartz cuvette of 1.2 mL maximum volume. Oxygenated stock solution (O₂ gas passed through the stock solution for 10 min) was transferred to the UV cuvette. Catalase and IDO1 was added to the oxygenated stock solution and the cuvette was sealed under an atmosphere O₂. After 5 min, inhibitor (Varied concentrations) was added, the cuvette was re-sealed under an atmosphere of O₂, the cuvette

was transferred to the fluorimeter and fluorescence readings were taken every 2 min to detect *N*-formyl-*L*-kynurenine. After 15 min, Trp (1 mM) was added and fluorescence readings were recorded for a further 35 min. The assay mixture was transferred to an Eppendorf vial containing TCA (100 μ L), subjected to centrifugation (13,000 rpm, 5 min) and then submitted for LC-MS analysis.

Throughout the assay aliquots (50 μ L) of the assay mixture were taken at the 10, 20, 25, 30, 40 and 50 min time points and quenched by addition to separate wells of a 96-well plate containing DMSO (50 μ L). The plate was then read *via* a plate reader under.

IDO1 F164A-Tryptophan 384-Well Plate Control Experiment

Total assay volume = 50 μ L, performed in Greiner black wall and base 384-well plates, focal height 6.2 mm, gain = 1000. Oxygenated stock solution (O_2 gas passed through the stock solution for 10 min) was transferred to the 384-well plate. IDO1 and catalase were added and the assay mixtures were allowed to equilibrate. After 15 min, Trp (1 mM) was added, the fluorescence readings were initiated and recorded once a minute for 45 min.

IDO1 F164A-Tryptophan K_m Determination Assay

Total assay volume = 50 μ L, performed in Greiner black wall and base 384-well plates, focal height 6.2 mm, gain = 1250, each assay included three repeats of each Trp concentration. Oxygenated stock solution (O_2 gas passed through the stock solution for 10 min) was transferred to the 384-well plate. IDO1 and catalase were added and the wells were allowed to equilibrate. After 5 min, Trp (12 concentrations, 3 mM–50 nM) was added, fluorescence readings were initiated and recorded for 1 h. The triplicate time course data was plotted in an intensity vs. time plot with errors. V_0 was calculated by taking the first 5 min of data (during the linear phase), performing a linear regression of each triplicate data set with the gradient of the linear regression representing the V_0 value. The gradient of the linear regression was plotted against Trp concentration and then fitted to the Michaelis-Menten equation to estimate the K_m .

IDO1-F164A-6/100-HCl K_i Determination Assay

Total assay volume = 50 μ L, performed in Greiner black wall and base 384-well plates, focal height 6.2 mm, gain = 1250. A 384-well plate was loaded with 3 rows of **6** or **100-HCl** (11 concentrations and 1 blank, **6** 10 μ M–170 pM, **100-HCl** 1 mM–17 nM). Oxygenated stock solution (O_2 gas passed through the stock solution for 10 min) was transferred to the 384-well plate. IDO1 and catalase were added and the wells were allowed to equilibrate. After 15 min, Trp (3, 30, or 300 μ M) was added, fluorescence readings were initiated and recorded for 20

min. The triplicate time course data, for each concentration of Trp used, was plotted in an intensity vs. time plot with errors. V_0 was calculated by taking the first 5 min of data (during the linear phase), performing a linear regression of each triplicate data set with the gradient of the linear regression representing the V_0 value. To account for error when plotting the inverse V_0 value, $V_0 \pm$ the error was calculated to give three values: V_0 , $V_0 +$ error & $V_0 -$ error. This analysis was performed for each of the Trp concentration assays (3, 30 and 300 μM). The reciprocal of the three values was then taken and plotted as standard error mean values in a $1/V_0$ vs **6/100-HCl** plot. A linear regression was performed for each of the Trp concentration data sets and the regression line was extrapolated back to find the point at which all three lines intersect. The corresponding X value at which the three lines intersect is equivalent to $-K_i$.

Differential Scanning Fluorimetry/Thermal Shift Assay

Thermal melting experiments were carried out at the University of Manchester by Roseanna Hare using a Stratagene Mx3005p Real Time PCR machine (Agilent Technologies). All experiments were conducted at 200 μL volume in 96-well PCR plates, using 20 mM HEPES, pH 7.5, 140 mM NaCl, containing either 2% or 5% DMSO. IDO1 protein was used at a final concentration of 1 or 10 μM as required. Compounds were diluted into buffer from a 10 mM DMSO stock solution and added at a final concentration of 10 μM , 100 μM or 500 μM . Where required SYPRO Orange (Molecular Probes) was added as a fluorescence probe at a final dilution of 1:500, 1:1000 or 1:2000 (v/v). Excitation and emission filters for the SYPRO-Orange dye were set to 465 nm and 590 nm, respectively. The temperature was raised with a step of 1 $^\circ\text{C}$ per minute from 25 $^\circ\text{C}$ to 96 $^\circ\text{C}$, and fluorescence readings were taken at each interval. Experiments were performed in triplicate and the observed temperature shifts, ΔT_m^{obs} , were recorded as the difference between the transition midpoints of sample and reference wells containing protein without ligand in the same conditions and determined by non-linear least squares fit of the initial fluorescence event, reported in $^\circ\text{C}$.

Chemical Synthesis Methods

General Experimental

Heated reactions were performed on Heidolph Hei-Tec stirrer hotplates using fitted heating-mantels with the temperature being controlled *via* an external probe. Reactions that required cooling were performed with one of the following: ice/water (0 °C), ice/sodium chloride (-20 °C) or dry ice/acetone (-78 °C) bath. The term 'warmed passively to X °C' refers to the act of leaving a cooled reaction mixture in a non-maintained cooling bath to warm to the stated temperature. Microwave reactions were conducted using a CEM Discover SP microwave, with PC interface, in 35 mL volume vials containing a magnetic stirrer bead. The microwave vials were fitted with CEM Activent™ caps.

Unless stated otherwise, all solvents and reagents were used without further purification, from one of the following outlets: Alfa Aesar, Acros Organics, Fisher, Fluorochem, Sigma Aldrich, TCI, Merck or VWR chemicals. Petroleum ether refers to 'Petroleum ether 60:40'. Anhydrous solvents were either collected from a solvent purification system using alumina columns or dried from the bottle *via* activated (300 °C, >6 h, <1 mbar) 3 or 4 Å molecular sieves. Any reference to 'water' use refers to purified water collected from a PURELAB option-S 7 reverse osmosis water purifier.

Thin-layer chromatography (TLC) was performed using Merck silica gel F254, aluminium-backed TLC plates. Flash column chromatography was carried out using Sigma-Aldrich silica gel (Technical grade, 60 Å pore size, 230 – 400 mesh, 40–63 µm particle size) with the column diameter and collected fraction size determined using Still's reference guide.³⁶⁹ Automated flash column chromatography was performed using a Teledyne Combi-Flash™ 300+.

Melting points were determined *via* a Stuart SMP10 melting point apparatus with a digital temperature reading (1 °C graduations). Melting points are quoted as ranges where applicable; the term 'Dec.' refers to samples that have decomposed upon heating. Infrared Spectra (IR) were recorded using either a Varian 660 FT-IR spectrometer (with UATR attachment for solid samples) or a Perkin Elmer Spectrum 100 FT-IR spectrometer at 23 °C. For ¹H-NMR spectra recorded at 400 MHz either a Bruker AVIII400, AV NEO 400 or NEO400 NMR spectrometer was used; for ¹H-NMR spectra recorded at 500 MHz a Bruker AV NEO 500 was used. ¹³C-NMR spectra were recorded at 101 MHz using a Bruker AVIII400, AV NEO 400 or NEO400 NMR spectrometer and are proton decoupled, unless otherwise stated. All ¹H-NMR and ¹³C-NMR spectra were recorded at 25 °C, unless stated otherwise, and the data processed using MestReNova 12.0.2. Chemical shifts (δ) are reported in ppm relative to the standard solvent shift of the deuterated solvent used with coupling constants (J) expressed in units of Hertz

(Hz). Proton assignments are presented in condensed formula form with the assigned proton being highlighted in italics (i.e. CH₃*CH*₂CH₃) and will proceed from left to right on the structure of the compound being assigned. COSY, HSQC, HMBC and pendant techniques were used to unambiguously assign both ¹H-NMR and ¹³C-NMR spectra, JMOD, DEPT45 and/or 135 experiments were used to identify quaternary carbons. The following abbreviations were used to assign resonance multiplicity: s = singlet, d = doublet, t = triplet, q = quartet, dd = double doublet, td = triple doublet, dt = double triplets, tt = triple triplets, ddd = double double doublets, tdd = triple double doublets, dddd = double double double doublets, quin. = quintet, *app.* = apparent. 'Stack' is used to describe a resonance structure in which two or more non-equivalent nuclei are coincident. 'Multiplet', m, is used to describe a resonance that arises from a single, or multiple equivalent, nuclei where the coupling patterns cannot be identified and assigned. Low and high resolution mass spectra were recorded *via* electrospray (ES), electron impact (EI), affinity-purification (AP) or matrix-assisted laser desorption ionisation (MALDI) using a Waters Xevo G2-XS or Synapt G2S TOF Mass Spectrometer in positive or negative mode (technique and charge detection method stated in each MS report). LC-MS analysis was performed using either a Waters e2695 separation module coupled with a Waters SQD MS-detector (raw data was processed and extracted using MassLynx V4.1 SCN855), or a ThermoFisher LCQ-fleet LC-MS (raw data was processed and extracted using Xcaliber).

General Synthetic Procedures

Any deviations from the following general procedures will be denoted by an asterisk (*).

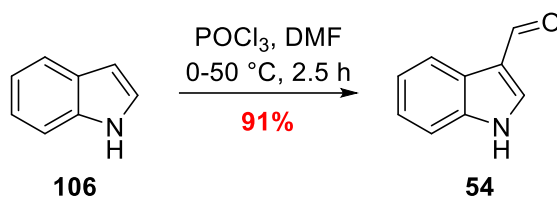
General procedure A: Cyclopropanation of the tosyl hydrazone derivatives

A flame-dried 100 mL Schlenk flask was charged with anhydrous toluene, hydrazone (1 eq.), caesium carbonate (1 eq.) and benzyltriethylammonium chloride (0.1 eq) and stirred vigorously at 23 °C under an atmosphere of argon for 1.5 h. Alkene (0.75 eq) was then added, a dried reflux condenser fitted and the temperature increased to 90 °C for 20 h. The reaction mixture was transferred to a single-neck round-bottom flask and the toluene removed under reduced pressure. The resulting residue was re-suspended in ethyl acetate and the solids were removed *via* suction filtration. The mother liquor was collected and diluted with water. Upon separation of the phases, the aqueous was back-extracted with ethyl acetate (2 × 20 mL) and the combined organics washed with water (2 × 20 mL) and brine (1 × 30 mL). The organics were combined, dried over MgSO₄, filtered and concentrated under reduced pressure to afford the crude material.

General Procedure B: Sonogashira cross-coupling

A flame-dried flask was charged with aryl halide (1 eq.), alkyne (1.5 eq.), PdCl₂(PPh₃)₂ (10 mol%) and CuI (20 mol%), and solubilised in a 4:1 mixture of anhydrous DMA and freshly distilled Et₃N. The resulting solutions were heated to 70 °C and the reactions were monitored *via* TLC. Upon completion, the reactions were taken off the heat, allowed to cool and the solids were collected *via* suction filtration. The mother liquor was further diluted with ethyl acetate and then partitioned with water. The phases were separated: the aqueous was extracted with ethyl acetate (15 mL) and the combined organics were washed with water (5 × 10 mL) and brine (20 mL). The organics were dried over MgSO₄, filtered to remove the solids and then concentrated under reduced pressure. The crude material was subjected to purification *via* flash column chromatography and/or recrystallisation to yield the desired aryl alkynes.

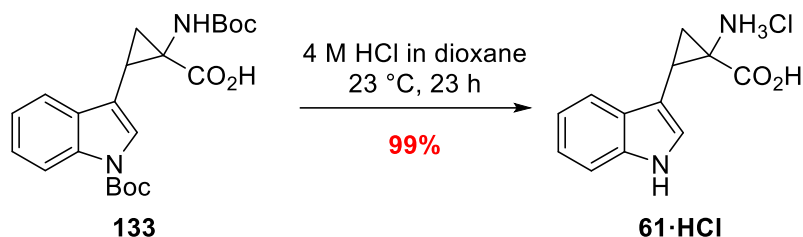
54) Indole-3-carbaldehyde



Distilled phosphorus(V) oxychloride (1.91 mL, 20.4 mmol) was added to anhydrous *N,N*-dimethylformamide (4 mL) at 0 °C in a flame-dried round-bottom flask and stirred under an atmosphere of argon for 30 min. To this solution, indole **106** (2.00 g, 17.0 mmol) in anhydrous dimethylformamide (16 mL) was added. The resultant solution was heated to 50 °C and stirred for a further 2 h, after which the reaction was judged complete *via* TLC ($R_f = 0.3$, 1:1 ethyl acetate:*n*-hexane). The reaction mixture was allowed to cool to 23 °C, ice (~10 g) was added, and stirred vigorously. The resultant solution was brought to pH 11, *via* dropwise addition of aqueous sodium hydroxide (1 M), forming a colourless precipitate. The suspension was brought to reflux for 15 min and then allowed to cool to 23 °C before the solid was collected *via* suction filtration. The solid was dried under reduced pressure to afford aldehyde **54**, with no need for further purification, as a white crystalline solid (2.24 g, 91%); $\nu_{\text{max}}/\text{cm}^{-1}$ (neat) 3166 (conj. NH), 2979 (CH), 2931 (CH), 2892 (CH), 2820.5 (CH), 1629.9 (conj. CO); δ_H (400 MHz; CD_3OD) 7.23 (1H, td, $J = 7.2, 1.2$, CHCHCC or CHCHCNH), 7.27 (1H, td, $J = 7.2, 1.2$, CHCHCC or CHCHCNH), 7.45–7.49 (1H, m, CHCHCC or CHCHCNH), 8.08 (1H, s, CCHNH), 8.14–8.17 (1H, m, CHCHCC or CHCHCNH), 9.88 (1H, s, CHO); δ_C (101 MHz; CD_3OD) 113.1 (CH), 120.1, (CH), 122.4 (CH), 123.6 (CH), 125.0 (CH), 125.7 (C), 138.9 (C), 139.6 (CH), 187.3 (CH); LRMS m/z (ES+) 146.1 ($[\text{M} + \text{H}]^+$, 100%), 118.1 (18).

*A known compound prepared according to a literature procedure.*³⁷⁰ *The recorded data are in agreement with that reported in the literature.*³⁷¹

61·HCl) 1-Amino-2-(1H-indol-3-yl)cyclopropane-1-carboxylic acid hydrochloride

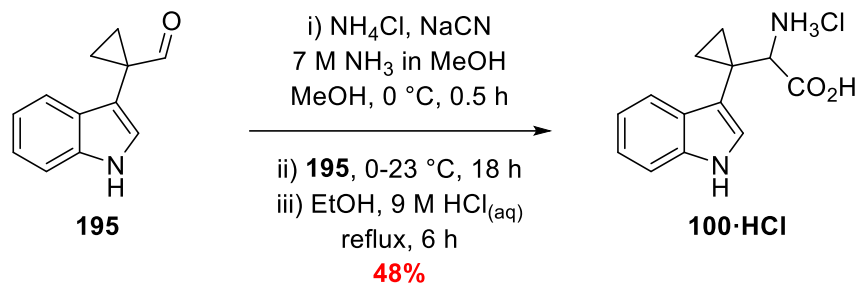


Acid **133** (80 mg, 0.19 mmol) was dissolved in a solution of hydrogen chloride in 1,4-dioxane (4 M, 2 mL) and stirred at 23 °C under an atmosphere of argon for 23 h. The resultant suspension was diluted with diethyl ether (5 mL) and the solid collected *via* suction filtration, the solid was washed further with diethyl ether (2 × 10 mL), transferred to a flask and dried under high-vacuum to afford a diastereomeric mixture (87:13, *E/Z*) of the indole **61·HCl** as a red solid (48 mg, 99%); **mp** = 260–261 °C; $\nu_{\max}/\text{cm}^{-1}$ (neat) 3372 (NH), 2863 br (OH), 1703 (CO); δ_{H} (400 MHz; CD_3OD) Resonances assignable to the major *E*-diastereomer: 1.97 (1 H, dd, $J = 10.2, 6.4$, CHCHH'C), 2.19 (1 H, dd, $J = 8.4, 6.4$, CHCHH'C), 2.93–2.98 (1 H, m, CCHCHH', overlap with minor diastereomer), 7.22–7.27 (1 H, m, CHCHCC or CHCHCNH), 7.31 (1 H, *app.* dd, $J = 7.3, 1.3$, CHCHCC or CHCHCNH), 7.56 (1 H, *app.* d, $J = 1.3$, CCHNH), 7.71–7.75 (1 H, *app.* d, $J = 7.0$, CHCHCC or CHCHCNH), 8.13 (1 H, *app.* d, $J = 8.1$, CHCHCC or CHCHCNH). Resonances assignable to the minor *Z*-diastereomer: 1.91 (1 H, dd, $J = 10.2, 6.2$, CHCHH'C), 2.96–3.05 (1 H, m, CHCHH'C), 7.03 (1 H, *app.* t, $J = 7.3$, CHCHCC or CHCHCNH), 7.07–7.12 (1 H, m, CHCHCC or CHCHCNH), 7.13 (1 H, s, CCHNH), 7.34 (1 H, d, $J = 6.9$, CHCHCC or CHCHCNH), 7.69 (1 H, d, $J = 7.8$, CHCHCC or CHCHCNH), CHCHH'C resonance missing, assumed to be overlapping with the resonance at 2.19 ppm of the major diastereomer; δ_{C} (101 MHz; CD_3OD) Resonances assignable to the major *E*-diastereomer: 17.6 (CH_2), 23.2 (CH), 40.5 (C), 116.2 (CH), 119.8 (CH), 123.9 (CH), 125.7 (CH), 126.6 (CH), 131.7 (C), 136.8 (C), 153.1 (C), 169.5 (C). Resonances assignable to the minor *Z*-diastereomer: 17.7 (CH_2), 24.4 (CH), 40.9 (C), 108.9 (CH), 112.4 (CH), 119.1 (CH), 120.1 (CH), 122.6 (CH), 125.5 (CH), 129.1 (C), 137.9 (C), 169.9 (C), missing C(8) of the indole

ring; LRMS m/z (ASAP+) 200.1 ($[M - NH_2]^+$, 100%); HRMS m/z (ASAP+) calcd. for $C_{12}H_{10}NO_2$ 200.0712, found 200.0720.

A known compound prepared according to a standard procedure.¹⁴³

100·HCl) 2-(1-(1H-Indol-3-yl)cyclopropyl)-2-aminoacetic acid hydrochloride

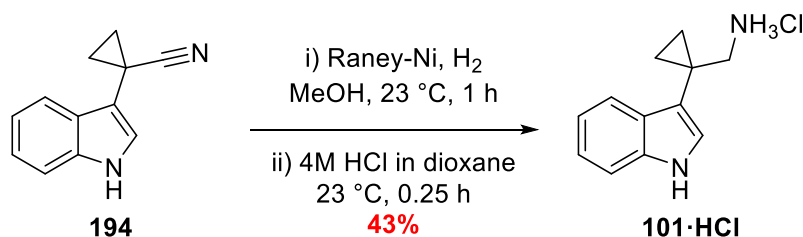


A solution of NH_3 in methanol (7 M, 47 μ L) was added to a suspension of NH_4Cl (29 mg, 0.54 mmol) and $NaCN$ (26 mg 0.54 mmol) in methanol (1 mL) and stirred vigorously at 0 °C. After 30 min, a solution of **195** (100 mg, 0.54 mmol) in methanol (1 mL) was added dropwise over 2 min and then the solution was allowed to warm to 23 °C. After 72 h, the aldehyde was no longer visible *via* TLC so the reaction mixture was diluted with water (5 mL), $NaHCO_{3(aq)}$ (sat. soln., 10 drops) was added and then the organics were extracted with ethyl acetate (2 \times 10 mL). The organic was extracted with $HCl_{(aq)}$ (1 M, 3 \times 10 mL) and the acidic aqueous layers combined, taken to \sim pH 12 *via* the addition of $NaOH_{(aq)}$ (1 M, 35 mL) and the remaining organic residues extracted with ethyl acetate (3 \times 10 mL). The organics were combined, dried over $MgSO_4$, the solids filtered off and concentrated to afford the intermediate cyanoamine. The intermediate was immediately re-solubilised in EtOH (0.5 mL) and $HCl_{(aq)}$ (9 M, 4 mL) was added and heated to reflux. After 24 h, the solution was allowed to cool to 23 °C, concentrated to dryness and dried under high vacuum to afford tryptophan analogue **100·HCl** as an off-white solid (69 mg, 48%); **mp** = 137–139 °C; ν_{max}/cm^{-1} (neat) 3243 br (COOH), 1614 br (CO); δ_H (400 MHz; $CDCl_3$) 0.89 (1 H, ddd, $J = 9.2, 6.2, 4.2$, $CH^1H^2CH^3H^4$), 1.02 (1 H, ddd, $J = 9.2, 6.0, 4.5$, $CH^1H^2CH^3H^4$), 1.16 (1 H, ddd, $J = 9.7, 6.0, 4.2$, $CH^1H^2CH^3H^4$), 1.35 (1 H, ddd, $J = 9.5, 6.2, 4.5$, $CH^1H^2CH^3H^4$), 3.47 (1 H, s, $CHNH_3ClCO_2H$), 7.03 (1 H, ddd, $J = 7.9, 7.0, 1.0$,

CHCHCC or CHCHCNH), 7.09 (1 H, ddd, $J = 8.1, 7.0, 1.2$, CHCHCC or CHCHCNH), 7.24 (1 H, s, CCHNH), 7.33 (1 H, dt, $J = 8.1, 1.0$, CHCHCC or CHCHCNH), 7.85 (1 H, dt, $J = 7.9, 1.2$, CHCHCC or CHCHCNH); δ_c (101 MHz; CDCl₃) 12.1 (CH₂), 13.5 (CH₂), 19.5 (C), 63.7 (C), 112.4 (CH), 114.8 (C), 120.2 (Stack, 2 × CH), 122.7 (CH), 126.9 (CH), 128.7 (C), 138.1 (C); LRMS m/z (ES+) 253.1 ([M + Na]⁺, 20%); 231.1 ([M + H]⁺, 14); HRMS m/z (ES+) calcd for C₁₃H₁₄N₂O₂Na 253.0953, found 253.0952.

A known compound prepared according to a modified literature procedure.³⁷² The recorded data are in agreement with that reported in the literature with the exception of the missing COOH resonance in the ¹³C-NMR spectra.³⁷²

101·HCl (1-(1H-Indol-3-yl)cyclopropyl)methanamine hydrochloride

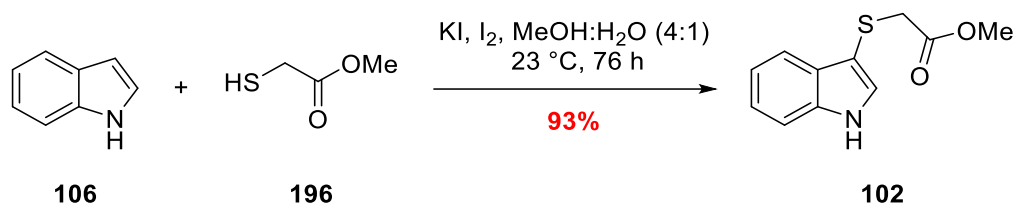


A spatula tip of Raney-Ni (suspended in H₂O) was added to a solution of nitrile **194** (50 mg, 0.27 mmol) in methanol (4 mL) and stirred vigorously at 23 °C. Hydrogen gas was then bubbled through the reaction mixture for 10 min, upon which the hydrogen source was removed from the solution and suspended above the solution to maintain a hydrogen atmosphere. After 1 h, the reaction was determined complete *via* TLC and the reaction mixture was passed through a celite bung, eluted with methanol (3 × 5 mL) and the collected liquor was concentrated under reduced pressure. The crude was re-solubilised in 1,4-dioxane (1.5 mL) and cooled to 0 °C. A solution of HCl in 1,4-dioxane (4 M, 5 drops) was then added and the resulting mixture was allowed to sit. After 0.25 h, a white precipitate had formed. The mixture was diluted with Et₂O and the solid was collected *via* suction filtration. Further drying of the solid under high vacuum afforded ammonium salt **101·HCl** as a fine white solid (26 mg, 43%); mp = 110–112 °C; $\nu_{\max}/\text{cm}^{-1}$ (neat) 3256 (NH), 3003 (CH), 2957 (CH), 2908 (CH); δ_H (500 MHz; CD₃OD) 0.97 (2 H, AA'BB', Cyclopropane CH₂), 1.01 (2 H, AA'BB', Cyclopropane CH₂), 3.16 (2 H, s,

CH₂NH₃Cl), 7.06 (1 H, ddd, *J* = 8.0, 7.0, 1.1, CHCHCC or CHCHCNH), 7.13 (1 H, ddd, *J* = 8.3, 7.0, 1.2, CHCHCC or CHCHCNH), 7.24 (1 H, s, CCHNH), 7.38 (1 H, dt, *J* = 8.3, 1.2, CHCHCC or CHCHCNH), 7.68 (1 H, dt, *J* = 8.0, 1.1, CHCHCC or CHCHCNH); δ_c (101 MHz; CD₃OD) 12.3 (2 × CH₂), 17.1 (C), 48.6 (CH₂), 112.8 (CH), 114.7 (C), 119.4 (CH), 120.3 (CH), 123.0 (CH), 126.1 (CH), 126.7 (C), 128.2 (C); LRMS *m/z* (ES+) 187.1 ([M + H]⁺, 48%), 170.1 ([M – NH₂]⁺, 95); HRMS *m/z* (ES+) calcd for C₁₂H₁₅N₂ 187.1235, found 187.1232.

A known compound prepared according to a modified literature procedure.³⁷³ The recorded data are in agreement with that reported in the literature.³⁷³

102) Methyl 2-((1H-indol-3-yl)thio)acetate

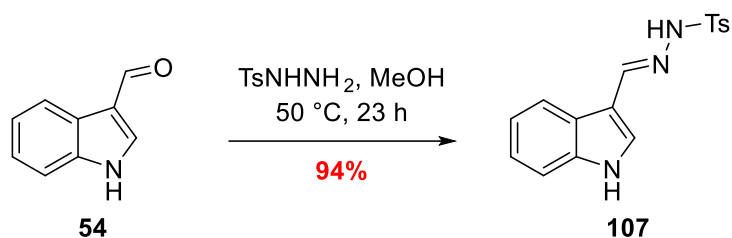


A solution of I₂ (3.60 g, 14.2 mmol) and KI (2.35 g, 14.2 mmol) in MeOH:H₂O (4:1, 14 mL) was added dropwise over 10 h to a solution of indole **106** (2.00 g, 17.0 mmol) and thioglycolic acid **196** (1.27 mL, 14.2 mmol) in MeOH:H₂O (4:1, 30 mL) at 23 °C. The reaction mixture was stirred for 76 h before being quenched by the addition of NaHCO_{3(aq)} (Sat. Soln., 40 mL) and then diluted further with ethyl acetate (35 mL). The resultant phases were separated, and the organic phase was washed sequentially with Na₂S₂O_{3(aq)} (Sat. Soln., 20 mL), NaOH_(aq) (1 M, 20 mL), water (20 mL) and brine (30 mL). The organic was then dried over MgSO₄, filtered and concentrated under reduced pressure. The resulting crude material was subjected to flash column chromatography (*R_f* = 0.3, 6:4 *n*-hexane:ethyl acetate) to give sulfenylindole **102** as a colourless oil* (2.91 g, 93%); ν_{\max} /cm⁻¹ (neat) 3364 (NH), 2950 (CH), 1720 (CO); δ_H (400 MHz; CDCl₃) 3.46 (2 H, s, SCH₂CO₂CH₃), 3.67 (3 H, s, CO₂CH₃), 7.22–7.30 (2 H, Stack, CHCHCC and CHCHCNBoc), 7.38–7.42 (2 H, Stack, CHCHCC or CHCHCNBoc, and CCHNH), 7.76–7.81 (1 H, m, CHCHCC or CHCHCNBoc), 8.45 (1 H, s, NH); δ_c (101 MHz; CDCl₃) 38.8 (CH₂), 52.4 (CH₃), 104.5 (C), 111.8 (CH), 119.2 (CH), 120.8

(CH), 123.0 (CH), 129.1 (C), 130.5 (CH), 136.3 (C), 171.1 (C); **LRMS m/z (ES+)** 244.0 ([M + Na]⁺, 94%), 222.0 ([M + H]⁺, 100); **HRMS m/z (ES+)** calcd for C₁₁H₁₂NO₂S 222.0589, found 222.0596.

*A novel compound prepared according to a literature procedure.²²³ No spectral data is available within the literature. *Oil browns on standing with no detectable change in its ¹H-NMR.*

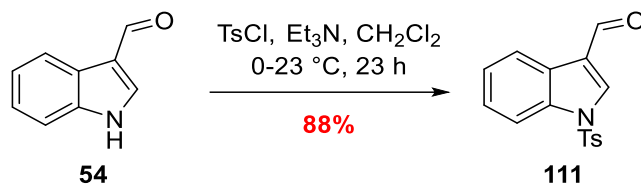
107) *E-N*-((Indol-3-yl)methylene)-4-methylbenzenesulfonylhydrazide



p-Toluenesulfonyl hydrazide (2.02 g, 10.9 mmol) was added to a solution of aldehyde **54** (1.50 g, 10.9 mmol) and stirred at 50 °C for 23 h. The reaction mixture was allowed to cool to 23 °C before the solution was concentrated under reduced pressure. The crude solid was suspended in dichloromethane (20 mL) and collected by suction filtration. The solid was washed sequentially with dichloromethane (3 × 10 mL), collected and dried under high vacuum to give hydrazide **107** as the *E*-olefin, with no need for further purification, as a fine yellow powder (3.05 g, 94%); $\nu_{\max}/\text{cm}^{-1}$ (neat) 3371 (NH), 3150 (NH), 3066 (CH), 1396 (SO), 1163 (SO); δ_{H} (400 MHz; (CD₃)₂SO) 2.33 (3 H, s, Ts-CH₃), 7.12 (1 H, td, *J* = 7.4, 1.2, CHCHCC or CHCHCNH), 7.17 (1 H, td, *J* = 7.6, 1.5, CHCHCC or CHCHCNH), 7.37–7.41 (3 H, Stack, Ts-CH and CHCHCC or CHCHCNH), 7.71 (1 H, d, *J* = 2.8, CCHNH), 7.79–7.83 (2 H, AA'BB', Ts-CH), 7.97 (1 H, dd, *J* = 7.5, 1.3, CHCHCC or CHCHCNH), 8.08 (1 H, s, CCHNHTs), 11.50 (1 H, d, *J* = 2.8, CHNHC); δ_{C} (101 MHz; (CD₃)₂SO) 20.9 (CH₃) 111.1 (C), 111.8 (CH), 120.4 (CH), 121.5 (CH), 122.5 (CH), 124.0 (C), 127.3 (CH), 129.4 (CH), 130.3 (CH), 136.3 (C), 136.9 (C), 143.1 (C), 145.0 (CH); **LRMS m/z (ES+)** 336.1 ([M + Na]⁺, 100%), 314.1 ([M + H]⁺, 53).

A known compound prepared according to a literature procedure.³⁷⁴ The recorded data are in agreement with that reported in the literature.³⁷⁴

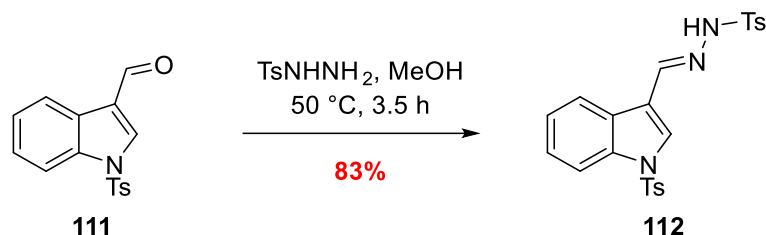
111) 1-Tosyl-indole-3-carbaldehyde



Indole **54** (1.00 g, 6.90 mmol) and triethylamine (2.64 mL, 13.8 mmol) were solubilised in dichloromethane (20 mL) and stirred at 0 °C for 5 min. *p*-Toluenesulfonyl chloride (1.44 g, 7.60 mmol) was added and the reaction mixture was allowed to warm to 23 °C. After 23 h, the reaction was determined complete *via* TLC ($R_f = 0.3$, 3:1 petroleum ether:diethyl ether). The reaction was quenched by addition of water (10 mL) and the resulting mixture was extracted with dichloromethane (2 × 10 mL). The combined organic layers were then washed with water (10 mL), HCl_(aq) (1 M, 10 mL) and brine (15 mL), dried over MgSO₄ and the solids filtered off. Concentration under reduced pressure afforded *N*-Tosyl indole **111**, with no need for further purification, as a colourless solid (1.81 g, 88%); $\nu_{\text{max}}/\text{cm}^{-1}$ (neat) 3136 (CH), 3063 (CH), 2850 (CH), 1662 (conj. CO), 1339 (SO), 1127 (SO); δ_{H} (400 MHz; CDCl₃) 2.37 (3 H, s, CH₃), 7.30 (2 H, AA'BB', *Ar-H*), 7.36 (1 H, td, CHCHCC or CHCHCNTs), 7.41 (1 H, td, CHCHCC or CHCHCNTs), 7.85 (2 H, AA'BB', *Ar-H*), 7.93–7.96 (1 H, m, CHCHCC or CHCHCNTs), 8.23 (1 H, s, CCHNTs), 8.24–8.27 (1 H, m, CHCHCC or CHCHCNTs), 10.09 (1 H, s, CHO); δ_{C} (101 MHz; CDCl₃) 21.7 (CH₃), 113.3 (CH), 122.4 (CH), 122.6 (CH), 125.0 (CH), 126.3 (C), 127.2 (CH), 130.3 (CH), 134.4 (C), 135.2 (C), 136.2 (C), 146.1 (C), 185.3 (CHO); LRMS *m/z* (ES+) 300.1 ([M + H]⁺, 65%).

*A known compound prepared according to a literature procedure.*³⁷⁵ *The recorded data are in agreement with that reported in the literature.*³⁷⁵

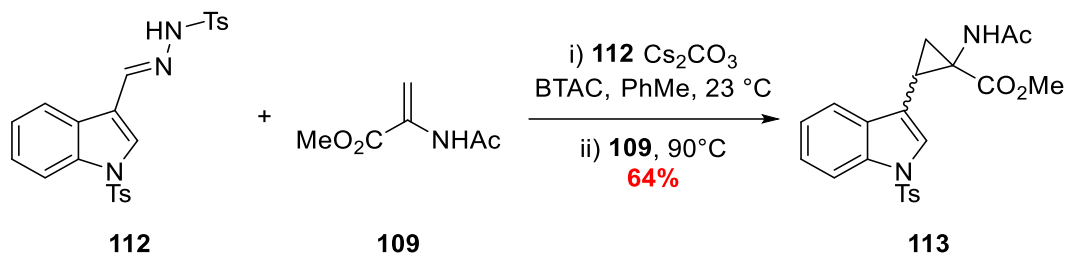
112) E-4-Methyl-N'-((1-tosyl-indol-3-yl)methylene)methylbenzenesulfonohydrazide



Aldehyde **111** (5.00 g, 17.0 mmol) was suspended in methanol (100 mL) and stirred at 50 °C for 5 minutes. *p*-toluenesulfonyl hydrazide (3.11 g, 17.0 mmol) was added and stirred for a further 3.5 h at 50 °C until the reaction was determined complete *via* TLC ($R_f = 0.7$, 7:3 ethyl acetate:*n*-hexane). The reaction mixture was allowed to cool to 23 °C, the precipitate was collected, *via* suction filtration, and washed portion-wise with cold methanol (3 × 30 mL). Drying under high vacuum afforded hydrazide **112**, with no need for further purification, as a fine white powder (6.49 g, 83%); **mp** = 206–208 °C; $\nu_{\text{max}}/\text{cm}^{-1}$ (neat) 3167 (NH), 1396 (SO), 1343 (SO), 1163 (SO), 1128 (SO); δ_H (400 MHz; CDCl_3) 1.62 (1 H, s, NH), 2.34 (3 H, s, CH_3), 2.38 (3 H, s, CH_3), 7.19–7.41 (6 H, Stack, *Ar-H*), 7.70 (1 H, s, CCHNTs), 7.75 (2 H, m, *Ar-H*), 7.88 (1 H, s, CCHNNH), 7.90 (2 H, m, *Ar-H*), 7.94 (1 H, m, CHN), 8.14 (1 H, m, *Ar-H*); δ_C (101 MHz; CDCl_3) 21.6 (2 × CH_3), 113.3 (CH), 117.3 (C), 123.2 (CH), 124.3 (CH), 125.8 (CH), 126.9 (CH), 127.2 (C), 128.0 (CH), 128.9 (CH), 129.7 (CH), 130.1 (CH), 134.7 (C), 135.2 (C), 135.4 (C), 142.2 (CH), 144.4 (C), 145.6 (C); **LRMS m/z (ES+)** 490.1 ($[\text{M} + \text{Na}]^+$, 100%), 468.1 ($[\text{M}]^+$, 40); **HRMS m/z (ES+)** calcd for $\text{C}_{23}\text{H}_{21}\text{N}_3\text{O}_4\text{S}_2\text{Na}$ 490.0871, found 490.0877.

*A novel compound prepared according to a modified literature procedure.*¹⁴⁵

113) Methyl-1-acetamido-2-(1-tosyl-indol-3-yl)cyclopropane-1-carboxylate



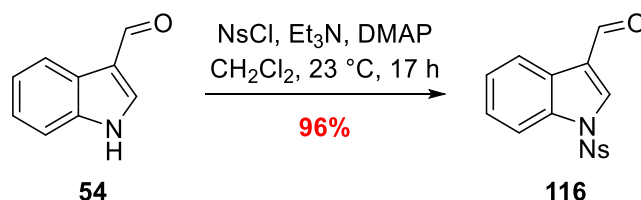
General method **A** was utilised to synthesise **113**: **112** (1.50 g, 3.20 mmol), caesium carbonate (1.05 g, 3.20 mmol), benzyltriethylammonium chloride (73 mg, 0.32 mmol), acrylate **109** (230 mg, 1.60 mmol*), anhydrous toluene (40 mL). Analysis of the crude by ¹H-NMR revealed a 89:11 d.r., (*E/Z*). Purification *via* flash column chromatography (1:1 ethyl acetate:petroleum ether to 100% ethyl acetate) afforded the separated diastereomers of the cyclopropane **113** as a white solids (*E*-**113** 381 mg, 58%; *Z*-**113** 57 mg, 6%); mp = 171–172 °C; $\nu_{\max}/\text{cm}^{-1}$ (neat) 3275 (NH), 3062 (CH), 2946 (CH), 1736 (CO), 1647 (CO), 1548 (SO), 1169 (SO); δ_{H} (400 MHz; CDCl₃) Resonances assignable to the major *E*-diastereomer: 1.69 (1 H, dd, $J = 9.7$, 5.4, CHCHH'C), 2.06 (3 H, s, COCH₃), 2.16 (1 H, dd, $J = 8.3$, 5.4, CHCHH'C), 2.32 (3 H, s, Ts-CH₃), 2.71 (1 H, ddd, $J = 9.7$, 8.2, 1.4, CCHCH₂), 3.17 (3 H, s, COOCH₃), 6.26 (1 H, s, NHAc), 7.18–7.21 (2 H, AA'BB', *Ar-H*), 7.23 (1 H, td, $J = 7.5$, 1.3, CHCHCC or CHCHCNTs), 7.28 (1 H, td, $J = 7.5$, 1.3, CHCHCC or CHCHCNTs), 7.40 (1 H, d, $J = 1.4$, CCHNTs), 7.72–7.75 (2 H, AA'BB', *Ar-H*), 7.86 (1 H, dt, $J = 7.5$, 0.9, CHCHCC or CHCHCNTs), 7.92 (1 H, dt, $J = 7.5$, 0.9, CHCHCC or CHCHCNTs). Resonances assignable to the minor *Z*-diastereomer: 1.65 (1 H, dd, $J = 7.9$, 5.7, CHCH₂C), 1.75 (3 H, s, COCH₃), 2.29–2.33 (1 H, m, CHCH₂C), 2.34 (3 H, s, Ts-CH₃), 2.85 (1 H, ddd, $J = 9.4$, 7.9, 1.1, CCHCH₂), 3.77 (3 H, s, COOCH₃), 5.31 (1 H, s, NHAc), 7.21–7.25 (2 H, AA'BB', *Ar-H*), 7.26–7.31 (1 H (appears at 2H in spectrum due to proximity to ref. peak, m, CHCHCC or CHCHCNTs), 7.38 (1 H, ddd, $J = 8.4$, 7.2, 1.3, CHCHCC or CHCHCNTs), 7.52 (1 H, dt, $J = 7.8$, 1.2, CHCHCC or CHCHCNTs), 7.73–7.77 (2 H, AA'BB', *Ar-H*), 8.02 (1 H, dt, $J = 8.4$, 0.9, CHCHCC or CHCHCNTs); δ_{C} (101 MHz; CDCl₃) Resonances assignable to the major *E*-diastereomer:

21.2 (CH₂), 21.7 (CH₃), 23.5 (CH₃), 25.8 (CH₃), 40.1 (C), 52.1 (CH₃), 113.6 (CH), 117.9 (C), 120.3 (CH), 123.5 (CH), 124.9 (CH), 125.6 (CH), 127.0 (CH), 129.9 (CH), 131.2 (C), 135.1 (C), 135.5 (C), 144.9 (C), 169.6 (C), 171.1 (C). **Resonances assignable to the minor Z-diastereomer:** 21.7 (CH₃), 21.9 (CH₂), 23.1 (CH₃), 23.5 (CH₃), 38.6 (C), 53.0 (CH₃), 114.1 (CH), 117.3 (C), 119.3 (CH), 123.8 (CH), 124.3 (CH), 125.5 (CH), 126.9 (CH), 130.1 (CH), 130.8 (C), 135.3 (CH), 145.4 (C), 171.3 (C), 172.1 (C); **LRMS *m/z* (ES⁺)** 449.1 ([M + Na]⁺, 100%); **HRMS *m/z* (ES⁺)** calcd for C₂₂H₂₂N₂O₅SNa 449.1147, found 449.1148.

*General procedure deviation: 0.5 eq. of methyl-2-acetamidoacrylate used.

A novel compound prepared according to a modified literature procedure.¹⁴⁵

116) 1-((4-Nitrophenyl)sulfonyl)-indole-3-carbaldehyde

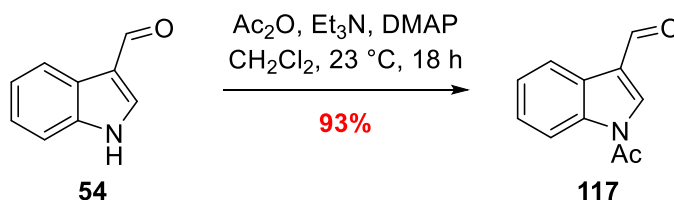


Triethylamine (2.15 mL, 15.5 mmol) and 4-dimethylaminopyridine (101 mg, 0.830 mmol) was added to a solution of indole **54** (1.50 g, 10.3 mmol) in dichloromethane (20 mL) and stirred at 23 °C for 10 min. To this, a solution of *p*-nitrobenzenesulfonyl chloride (2.52 g, 11.4 mmol) in dichloromethane (20 mL) was added dropwise over 5 min. The resulting solution was stirred for 17 h after which the reaction mixture was diluted with HCl_(aq) (1 M, 20 mL) and stirred vigorously for a further 10 min. The layers were separated and the organic was washed with water (2 × 20 mL) and brine (1 × 20 mL), dried over MgSO₄, filtered and concentrated to afford *N*-Nosyl indole **116**, with no need for further purification, as a pale yellow powdered solid (3.29 g, 96%); $\nu_{\text{max}}/\text{cm}^{-1}$ (neat) 3111 (CH), 3061 (CH), 1683 (CO), 1528 (SO), 1179 (SO); δ_{H} (400 MHz; CDCl₃) 7.41 (1 H, td, $J = 7.6, 1.2$, CHCHC₂N₂ or CHCHCC), 7.46 (1 H, td, $J = 8.2, 1.4$, CHCHC₂N₂ or CHCHCC), 7.95 (1 H, dt, $J = 8.6, 1.0$, CHCHCC), 8.16 (2 H, AA'BB', *Ar-H*), 8.21 (1 H, s, CCHN₂), 8.27 (1 H, dt, $J = 8.4, 1.0$, CHCHC₂N₂), 8.35 (2 H, AA'BB', *Ar-H*), 10.12 (1 H, s, CHO); δ_{C} (101 MHz; CDCl₃) 113.2 (CH), 123.2 (CH), 123.6 (C),

125.1 (CH), 125.9 (CH), 126.6 (C), 127.1 (CH), 128.6 (CH), 135.3 (C), 135.6 (CH), 142.8 (C), 151.3 (C), 185.2 (CHO); **LRMS m/z (AP+)** 331.0 ($[M + H]^+$, 100%).

A known compound prepared according to a literature procedure.¹⁶³ The recorded data are in agreement with that reported in the literature.¹⁶³

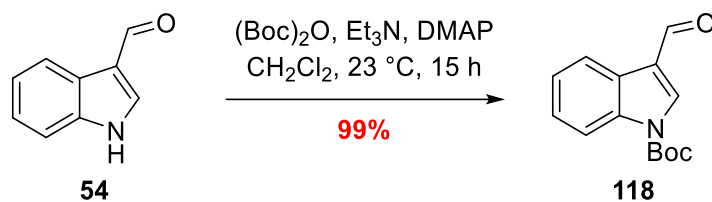
117) 1-Acetyl-indole-3-carbaldehyde



Triethylamine (1.72 mL, 12.4 mmol) and 4-dimethylaminopyridine (126 mg, 1.03 mmol) was added to a solution of indole **54** (1.50 g, 10.3 mmol) in dichloromethane (20 mL) and stirred at room temperature for 10 min. To this, a solution of acetic anhydride (1.17 mL, 12.4 mmol) in dichloromethane (20 mL) was added dropwise over 10 min. Progress was monitored *via* TLC and the reaction was determined complete after 18 h ($R_f = 0.3$, 1:1, ethyl acetate:*n*-hexane). The acidic reaction mixture was brought to neutral pH by the addition of $\text{NaHCO}_{3(\text{aq})}$ (sat. soln., ~20 mL). Upon neutralisation, the reaction mixture was diluted with ethyl acetate (20 mL) and stirred for a further 10 min. The resulting phases were separated and the organic phase washed with water (2×20 mL) and brine (30 mL), dried over MgSO_4 , filtered and concentrated under reduced pressure to afford *N*-Acyl indole **117**, with no need for further purification, as a pale yellow solid (1.80 g, 93 %); $\nu_{\text{max}}/\text{cm}^{-1}$ (neat) 3122 (CH), 3075 (CH), 2927 (CH), 1731 (CO), 1670 (CO); δ_H (400 MHz; CDCl_3) 2.74 (3 H, s, Ac- CH_3), 7.43 (2 H, Stack, CHCHC and CHCHCNAC), 8.07 (1 H, s, CCHNAC), 8.27 (1 H, dt, $J = 7.9, 1.2$, CHCHC or CHCHCNAC), 8.40 (1 H, dt, $J = 7.9, 1.2$, CHCHC or CHCHCNAC), 10.13 (1 H, s, CHO); δ_C (101 MHz; CDCl_3) 24.1 (CH_3), 116.5 (CH), 122.1 (CH), 122.9 (C), 125.6 (CH), 126.2 (C), 127.0 (CH), 135.2 (CH), 136.5 (C), 168.6 (CO), 185.7 (CO); **LRMS m/z (AP-MALDI+)** 188.1 ($[M + H]^+$, 10%).

A known compound prepared according to a literature procedure.¹⁶⁴ The recorded data are in agreement with that reported in the literature.¹⁶⁴

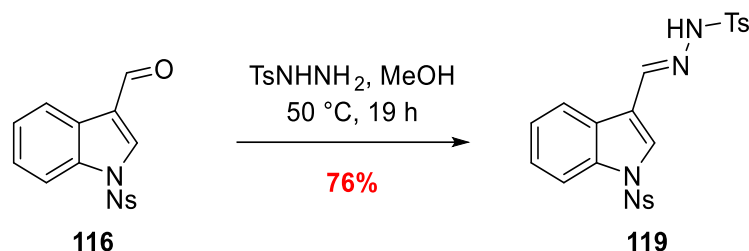
118) 3-Formyl-indole-1-*tert*-butyl carboxylate



Di-*tert*-butyl dicarbonate (3.38 g, 15.5 mmol) was dissolved in dichloromethane (35 mL) and stirred. To this solution, indole **54** (1.50 g, 10.3 mmol), triethylamine (2.16 mL, 15.5 mmol) and DMAP (126 mg, 1.03 mmol) was added and stirred at 23 °C for 15 h until determined complete *via* TLC ($R_f = 0.7$, 100% ethyl acetate). The reaction mixture was diluted with water (20 mL) and stirred for a further 5 minutes. The layers were separated and the organic washed with water (2 × 30 mL) and brine (1 × 40 mL), dried over MgSO_4 , filtered and concentrated under reduced pressure to *N*-Boc indole **118** as a pale yellow solid in sufficient purity (2.52 g, 99%); $\nu_{\text{max}}/\text{cm}^{-1}$ (neat) 1741.8 (CO), 1677.5 (CO); δ_{H} (400 MHz; CDCl_3) 1.71 (9 H, s, $\text{C}(\text{CH}_3)_3$), 7.34–7.44 (2 H, Stack, *CHCHC* and *CHCHCNBoc*), 8.15 (1 H, m, *CHCHC* or *CHCHCNBoc*), 8.23 (1 H, s, *CCHNBoc*), 8.26–8.30 (1 H, m, *CHCHC* or *CHCHCNBoc*), 10.09 (1 H, s, *CHO*); δ_{C} (101 MHz; CDCl_3) 28.1 (CH_3), 45.9 (C), 85.7 (C), 115.2 (CH), 121.6 (C), 122.1 (CH), 124.6 (CH), 126.1 (CH), 136.0 (C), 136.5 (CH), 148.8 (C), 185.8 (CO); LRMS m/z (AP+) 246.2 ($[\text{M} + 1]^+$, 2%), 190.1 ($[\text{M} - \text{tBu} + \text{H}]^+$, 100), 146.1 ($[\text{M} - \text{Boc}]^+$, 21).

*A known compound prepared according to a literature procedure.*¹⁶⁵ *The recorded data are in agreement with that reported in the literature.*¹⁶⁵

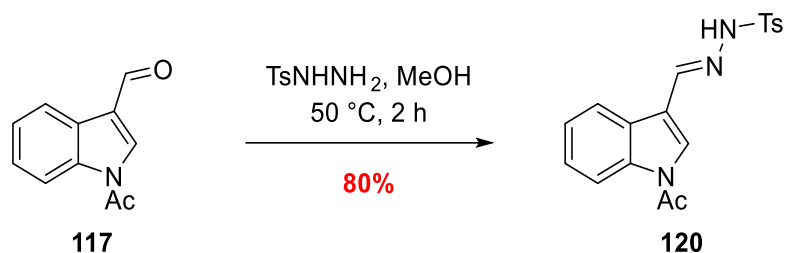
119) *E*-1-((4-Nitrophenyl)sulfonyl)-3-((2-(*p*-tolyl)hydrazono)methyl)-indole



p-Toluenesulfonyl hydrazide (846 mg, 4.54 mmol) was added to a solution of aldehyde **54** (1.50 g, 4.54 mmol) in methanol (40 mL) and stirred at 50 °C for 19 h. The reaction was determined complete *via* TLC and allowed to cool to 23 °C. The resulting precipitate was collected *via* suction filtration and washed portion-wise with cold methanol (3 × 20 mL). Further drying of the solid under high vacuum gave hydrazide **119** as the *E*-olefin, with no need for further purification, as a fine yellow powder (1.68 g, 76%); **mp** = 224–226 °C; $\nu_{\max}/\text{cm}^{-1}$ (neat) 3169 (conj. NH), 3109 (CH), 1617 (CN), 1532 (NO), 1333 (SO), 1164 (NO), 1127 (SO); δ_{H} (400 MHz; $(\text{CD}_3)_2\text{CO}$) 2.34 (3 H, s, Ts-CH₃), 7.37 (2 H, AA'BB', Ts-CH), 7.41 (1 H, td, $J = 7.8, 1.2$, CHCHCNNs or CHCHCC), 7.46 (1 H, td, $J = 7.8, 1.2$, CHCHCNNs or CHCHCC), 7.86 (2 H, AA'BB', Ts-CH), 8.02 (1 H, dt, $J = 7.8, 1.2$, CHCNNs or CHCHCC), 8.10 (1 H, d, $J = 0.9$, CCHNNH), 8.19 (1 H, d, $J = 0.9$, NNSCHC), 8.25 (1 H, dt, $J = 7.8, 1.2$, CHCNNs or CHCHCC), 8.29 (2 H, AA'BB', *Ar-H*), 8.38 (2 H, AA'BB', *Ar-H*); δ_{C} (101 MHz; $(\text{CD}_3)_2\text{CO}$) 21.5 (CH₃), 114.3 (CH), 120.1 (C), 124.5 (CH), 125.8 (CH), 126.0 (CH), 127.2 (CH), 128.4 (C), 128.8 (CH), 129.6 (CH), 130.3 (CH) 130.6 (CH), 136.3 (C), 137.5 (C), 142.5 (CH), 143.4 (C), 144.9 (C), 152.3 (C); **LRMS m/z (ES+)** 521.1 ($[\text{M} + \text{Na}]^+$, 100%), 499.1 ($[\text{M} + \text{H}]^+$, 48); **HRMS m/z (ES+)** calcd for C₂₂H₁₈N₄O₆S₂Na 521.0656, found 521.0564.

*A novel compound prepared according to a modified literature procedure.*¹⁴⁵

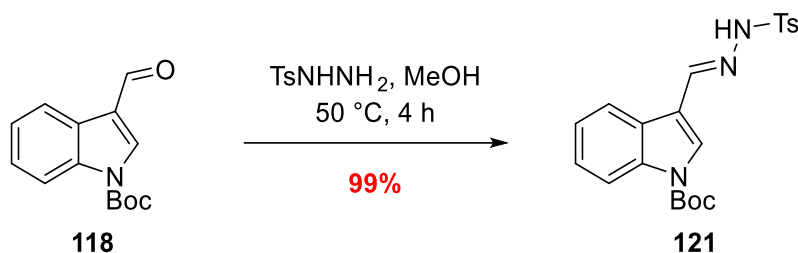
120) *E-N*-((1-Acetyl-indol-3-yl)methylene)-4-methylbenzenesulfonylhydrazide



p-Toluenesulfonyl hydrazide (1.49 g, 8.01 mmol) was added to a solution of aldehyde **54** (1.50 g, 8.01 mmol) in methanol (40 mL) and stirred at 50 °C for 2 h, at which point a white precipitate had formed. The reaction mixture was taken off heat and allowed to cool to 23 °C. Once cool, the solid was collect *via* suction filtration. The solid was washed portion-wise with cold methanol (3 × 30 mL) to afford hydrazide **120** as the *E*-olefin, with no need for further purification, as a white powdered solid (2.27 g, 80%); **mp** = 208–210 °C; $\nu_{\text{max}}/\text{cm}^{-1}$ (neat) 3182 (conj. NH), 3136 (CH), 1704 (CO), 1556 (SO), 1163 (SO); δ_{H} (400 MHz; $(\text{CD}_3)_2\text{CO}$) 2.36 (3 H, s, Ts-CH₃), 2.67 (3 H, s, NCOCH₃), 7.36–7.43 (4 H, m, Ts-CH and CHCHCNAc and CHCHCC), 7.89 (2 H, AA'BB', Ts-CH), 8.07 (1 H, s, CCHN), 8.18 (1 H, s, CCHNAc), 8.25–8.29 (1 H, m, CHCHCNAc or CCHCC), 8.37–8.42 (1 H, m, CHCHCNAc or CCHCC); δ_{C} (101 MHz; $(\text{CD}_3)_2\text{CO}$) 21.4 (CH₃), 23.9 (CH₃), 117.0 (CH), 118.0 (C), 123.4 (CH), 125.0 (CH), 126.6 (CH), 127.8 (C), 128.7 (CH), 130.4 (CH), 130.8 (CH), 137.3 (C), 137.5 (C), 143.4 (CH), 144.7 (C), 169.8 (CO); **LRMS *m/z* (ES⁺)** 378.1 ([M + Na]⁺, 100%), 356.1 ([M + H]⁺, 70); **HRMS *m/z* (ES⁺)** calcd for C₁₈H₁₇N₃O₃SNa 378.0888, found 378.0885.

*A known compound prepared according to a modified literature procedure.*¹⁴⁵ *The recorded data are in agreement with that reported in the literature.*³⁷⁶

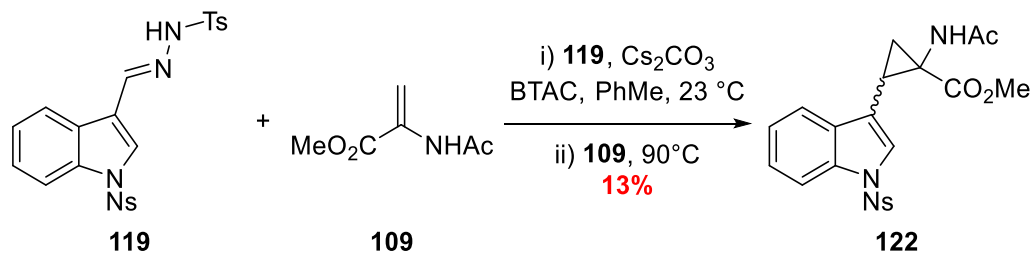
121) *E*-*tert*-Butyl-3-((2-tosylhydrazono)methyl)-indole-1-carboxylate



p-Toluenesulfonyl hydrazide (1.50 g, 6.10 mmol) was added to a solution of aldehyde **118** (1.14 g, 6.10 mmol) in methanol (30 mL) and stirred at 50 °C for 4 h until determined complete *via* TLC ($R_f = 0.3$, 1:1 ethyl acetate: *n*-hexanes). The reaction was taken off heat and allowed to cool to 23 °C before the methanol was removed under reduced pressure to afford hydrazide **121** as the *E*-olefin, with no need for further purification, as a crystalline yellow solid (2.51 g, 99%); **mp** = 86–88 °C; $\nu_{\max}/\text{cm}^{-1}$ (neat) 3194 (NH), 2979 (CH), 1736 (CO), 1551 (SO), 1151 (SO); δ_H (400 MHz; CDCl_3) 1.66 (9 H, s, $\text{C}(\text{CH}_3)_3$), 2.38 (3 H, s, Ts- CH_3), 7.30 (2 H, AA'BB', Ts-CH), 7.33 (1 H, td, $J = 7.8, 1.2$, CHCHCC or CHCHCNBoc), 7.38 (1 H, td, $J = 7.8, 1.2$, CHCHCC or CHCHCNBoc), 7.73 (1 H, s, CCHN), 7.83 (1 H, s, NH), 7.91 (2 H, AA'BB', *Ar-H*), 7.95 (1 H, s, CCHNBoc), 8.11 (1 H, d, $J = 7.8$, CHCHCC or CHCHCNBoc), 8.19 (1 H, dt, $J = 7.8, 1.5$, CHCHCC or CHCHCNBoc); δ_C (101 MHz; CDCl_3) 21.7 (CH_3), 28.3 (CH_3), 84.9 (C), 115.2 (CH), 116.0 (C), 122.9 (CH), 123.9 (CH), 125.7 (CH), 126.9 (C), 128.2 (CH), 129.3 (CH), 129.8 (CH), 135.4 (C), 136.0 (C), 143.6 (CH), 144.4 (C), 149.2 (C), quaternary carbamate CO not observed; **LRMS m/z (ES+)** 436.1 ($\{M + \text{Na}\}^+$, 100%), 414.2 ($\{M + \text{H}\}^+$, 33); **HRMS m/z (ES+)** calcd for $\text{C}_{21}\text{H}_{23}\text{N}_3\text{O}_4\text{SNa}$ 436.1307, found 436.1306.

*A novel compound prepared according to a modified literature procedure.*¹⁴⁵

122) Methyl 1-acetamido-2-(1-((4-nitrophenyl)sulfonyl)-1*H*-indol-3-yl)cyclopropane-1-carboxylate



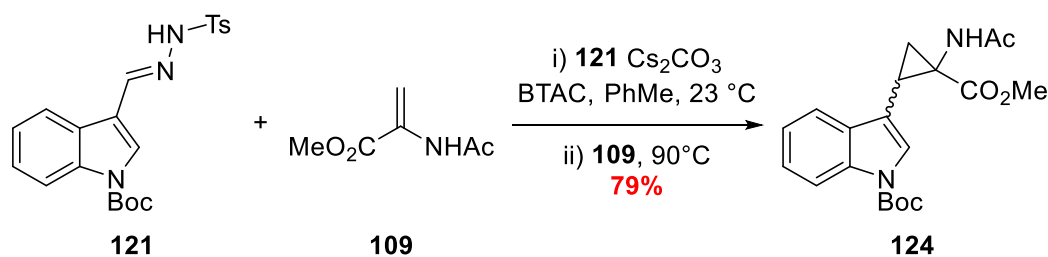
General method A was utilised to synthesise **122**: **119** (1.50 g, 3.01 mmol), caesium carbonate (980 mg, 3.01 mmol), benzyltriethylammonium chloride (91 mg, 0.40 mmol), acrylate **109** (288 mg, 2.01 mmol), anhydrous toluene (30 mL). Analysis of the crude by ¹H-NMR revealed a 95:5 d.r.. (*E/Z*). Purification *via* flash column chromatography (*R_f* = 0.3, 9.5:0.5, *n*-hexane:ethyl acetate) afforded a diastereomeric mixture (95:5, *E/Z*) of cyclopropane **122** as a pale yellow solid (115 mg, 13%); **mp** = 157–158 °C; $\nu_{\max}/\text{cm}^{-1}$ 3279 (NH), 2923 (CH), 2853 (CH), 1731 (CO), 1672 (CO), 1654 (CO), 1532 (SO), 1173 (SO); δ_{H} (**400 MHz**; (CD₃)₂CO) 1.62 (1 H, dd, *J* = 9.4, 5.2, CHCHH'C), 1.92 (3 H, s, NHCOCH₃), 2.22 (1 H, dd, *J* = 8.2, 5.2, CHCHH'C), 2.75 (1 H, ddd, *J* = 9.4, 8.2, 1.4, CCHCHH'), 3.16 (3 H, s, CO₂CH₃), 7.27 (1 H, ddd, *J* = 8.3, 7.3, 1.0, CHCHCC or CHCHCNNs), 7.35 (1 H, ddd, *J* = 8.4, 7.3, 1.3, CHCHCC or CHCHCNNs), 7.57 (1 H, d, *J* = 1.4, CCHNNs), 7.95 (1 H, dt, *J* = 8.3, 1.0, CHCHCC or CHCHCNNs), 8.02 (1H, dt, *J* = 7.3, 1.0, CHCHCC or CHCHCNNs), 8.06 (1 H, s, CCHNNs), 8.18–8.22 (2 H, AA'BB', *Ar-H*), 8.34–8.39 (2 H, m, AA'BB', *Ar-H*); δ_{C} (**101 MHz**; (CD₃)₂CO) 21.5 (CH₂), 22.9 (CH₃), 25.7 (CH₃), 40.7 (C), 52.0 (CH), 114.2 (CH), 121.1 (C), 121.8 (CH), 124.7 (CH), 125.5 (CH), 126.0 (CH), 126.4 (CH), 129.3 (CH), 132.6 (C), 135.9 (C), 143.6 (C), 170.3 (CO), 170.9 (CO); **LRMS *m/z* (ES⁺)** 480.1 ([M + Na]⁺, 100%), 458.1 ([M + H]⁺, 18); **HRMS *m/z* (ES⁺)** calcd for C₂₁H₁₉N₃O₇Na 480.0841, found 480.0846.

*A novel compound prepared according to a modified literature procedure.*¹⁴⁵

21.3 (CH₂), 23.4 (CH₃), 24.1 (CH₃, Overlap with minor), 26.0 (CH₃), 40.0 (C), 52.5 (CH), 116.7 (CH), 117.6 (C), 118.6 (CH), 123.9 (CH), 124.2 (CH), 125.4 (CH), 130.4 (C), 135.8 (C), 168.6 (CO), 171.2 (CO), 171.7 (CO). **Resonances assignable to the minor Z-diastereomer:** 21.7 (CH₂), 23.3 (CH), 23.4 (CH₃), 24.1 (CH₃, Overlap with major), 38.6 (C), 53.0 (CH), 117.0 (CH), 117.2 (C), 119.4 (CH), 123.8 (CH), 124.5 (CH), 126.1 (CH), 130.8 (C), 136.1 (C), 168.5 (CO), 169.7 (CO), 172.2 (CO); **LRMS *m/z* (ES+)** 337.1 ([M + Na]⁺, 100%); **HRMS *m/z* (ES+)** calcd for C₁₇H₁₈N₂O₄Na 337.1267, found 337.1264.

A novel compound prepared according to a modified literature procedure.¹⁴⁵

124) *tert*-Butyl 3-(2-acetamido-2-(methoxycarbonyl)cyclopropyl)-indole-1-carboxylate

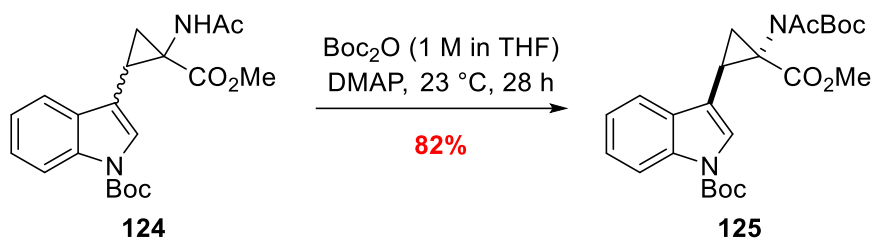


General method A was utilised to synthesise **124**: **121** (1.40 g, 3.24 mmol), caesium carbonate (1.06 g, 3.24 mmol), benzyltriethylammonium chloride (74 mg, 0.32 mmol), acrylate **109** (348 mg, 2.43 mmol), anhydrous toluene (43 mL). Analysis of the crude by ¹H-NMR revealed a 92:8 d.r. (*E/Z*). Purification *via* flash column chromatography (*R*_f (minor) = 0.3, *R*_f (major) = 0.2, 4:1 *n*-hexane:ethyl acetate) afforded a diastereomerically enriched mixture (93:7, *E/Z*) of cyclopropane **124** as a white solid (716 mg, 79%); **mp** = 161–163 °C; **v**_{max}/cm⁻¹ 3278 (NH), 3066 (CH), 2991 (CH), 1730 (CO), 1655 (CO), 1652 (CO); **δ**_H (400 MHz; CDCl₃) **Resonances assignable to the major E-diastereomer:** 1.66 (9 H, s, C(CH₃)₃), 1.67–1.71 (1 H, m, CHCHH'C), 2.08 (3 H, s, NHCOCH₃), 2.20 (1 H, dd, *J* = 8.2, 5.3, CHCHH'C), 2.70 (1 H, ddd, *J* = 9.6, 8.2, 1.4, CCHHH'), 3.35 (3 H, s, COOCH₃), 6.34 (1 H, s, NH), 7.23 (1 H, td, *J* = 7.5, 1.3, CHCHCC or CHCHCNBoc), 7.29 (1 H, td, *J* = 7.3, 1.3, CHCHCC or CHCHCNBoc), 7.42 (1 H, s, CCHNBoc), 7.84 (1 H, dt, *J* = 7.5, 1.3, CHCHCC or CHCHCNBoc), 8.08 (1 H, d, *J* = 7.3, CHCHCC or CHCHCNBoc). **Resonances assignable to the minor Z-diastereomer:**

1.83 (3 H, s, NHCOCH_3), 1.73 (1 H, m, $\text{CHCHH}'\text{C}$), 2.32 (1 H, m, CHCHHC), 2.86 (1 H, m, CCHCHH'), 3.79 (3 H, s, COOCH_3), 6.84 (1H, s, NH), 7.32 (1 H, s, CCHNBoc), 7.37 (1 H, ddd, $J = 8.4, 7.3, 1.3, \text{CHCHCC}$ or CHCHCNBoc), 7.50–7.55 (1 H, m, CHCHCC or CHCHCNBoc).
 Missing resonances: $\text{C}(\text{CH}_3)_3$, CHCHCC and CHCHCNBoc ; δ_{c} (101 MHz; CDCl_3) 21.3 (CH_2), 23.4 (CH_3), 26.0 (CH_3), 28.4 (CH_3), 39.9 (CH), 52.4 (C), 83.8 (C), 115.3 (CH), 115.9 (C), 119.6 (CH), 122.8 (CH), 124.5 (CH), 125.2 (CH), 130.8 (C), 135.4 (C), 149.7 (CO), 169.9 (CO), 171.2 (CO). **Resonances assignable to the minor diastereomer:** No detectable resonances;
LRMS m/z (ES+) 395.2 ($[\text{M} + \text{Na}]^+$, 100%), 373.2 ($[\text{M} + \text{H}]^+$, 7); **HRMS m/z (ES+)** calcd for $\text{C}_{20}\text{H}_{24}\text{N}_2\text{O}_5\text{Na}$ 395.1538, found 395.1585.

A novel compound prepared according to a modified literature procedure.¹⁴⁵

125) *tert*-Butyl 3-(2-(*N*-(*tert*-butoxycarbonyl)acetamido)-2-(methoxycarbonyl)cyclopropyl)-1*H*-indole-1-carboxylate

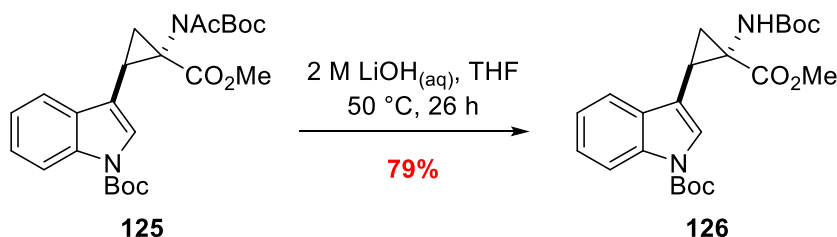


Amide **124** (305 mg, 0.82 mmol) and DMAP (100 mg, 0.82 mmol) were added to a flame-dried flask and purged with argon. After 5 min, di-*tert*-butyl dicarbonate (1 M in tetrahydrofuran, 4.10 mL, 4.10 mmol) was added and stirred at 23 °C for 27 h until determined complete *via* TLC ($R_f = 0.3, 8.5:1.5$ *n*-hexane:ethyl acetate). The reaction mixture was diluted with water (10 mL), stirred for a further 5 min and then extracted with ethyl acetate (10 mL). After separation of the phases, the aqueous layer was back-extracted with ethyl acetate (2×10 mL) and combined with the organic layer. The combined organic layers were then washed sequentially with water (2×10 mL) and brine (20 mL), dried over MgSO_4 , filtered to remove the solids and concentrated under reduced pressure. The resulting crude was subjected to flash column chromatography ($R_f = 0.3, 8.5:1.5$ *n*-hexane:ethyl acetate) to yield only the *E*-diastereomer of *N*-Boc amide **125** as a white solid (248 mg, 64%); **mp** = 133–134 °C; $\nu_{\text{max}}/\text{cm}^{-1}$ 2979 (CH),

1730 (br, CO); δ_H (400 MHz; $CDCl_3$) 1.52 (10 H, Stack, $C(CH_3)_3$ and $CHCHH'C$), 1.66 (9 H, s, $C(CH_3)_3$), 2.29 (1 H, dd, $J = 8.9, 5.7$, $CHCHH'C$), 2.46–2.60 (3 H, m, $NHCOCH_3$), 2.83–2.91 (1 H, m, $CCHCHH'C$), 3.45 (3 H, s, CO_2CH_3), 7.22–7.33 (2 H, Stack, $CHCHCC$ and $CHCHCNBoc$), 7.48 (1 H, m, $CHCHCC$ or $CHCHCNBoc$), 8.10 (1 H, *app. d*, $J = 7.3$, $CHCHCC$ or $CHCHCNBoc$); δ_C (101 MHz; $CDCl_3$) 23.7 (CH_2), 26.9 (CH), 28.1 ($C(CH_3)_3$), 28.3 ($C(CH_3)_3$), 29.6 (CH_3), 44.0 (CH_2), 52.3 (CH_3), 83.6 (C), 115.0 (CH), 115.7 (C), 120.6 (CH), 122.8 (CH), 124.3 (CH), 125.7 (CH), 130.9 (C), 135.5 (C), 149.8 (CO), 153.4 (CO), 169.2 (CO), 172.9 (CO); LRMS m/z (ES+) 495.2 ($[M + Na]^+$, 100%); HRMS m/z (ES+) calcd for $C_{25}H_{32}N_2O_7Na$ 495.2107, found 495.2108.

A novel compound prepared according to a literature procedure.¹⁴³ No quaternary ^tBu-carbon resonance was observed in the ¹³C resonance.

126) tert-Butyl 3-(2-((tert-butoxycarbonyl)amino)-2-(methoxycarbonyl)cyclopropyl)-1H-indole-1-carboxylate

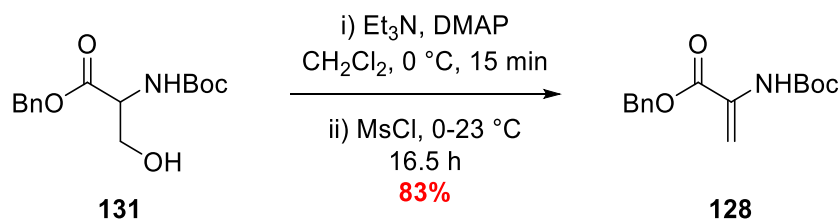


N-Boc amide **125** (208 mg, 0.44 mmol) was solubilised in tetrahydrofuran (0.44 mL) and $LiOH_{(aq)}$ (2 M, 0.44 mL) and the solution heated to 50 °C. After 26 h the reaction was allowed to cool to room temperature before the reaction mixture was diluted with $HCl_{(aq)}$ (1 M, 5 mL). The diluted mixture was stirred for a further 5 min and then extracted with ethyl acetate (10 mL). Upon separation of the phases, the aqueous was back extracted with ethyl acetate (2 × 10 mL) and combined with the organic phase. The combined organics was then washed with water (2 × 10 mL) and brine (10 mL). Drying over $MgSO_4$ and concentration under reduced pressure afforded the crude material as an orange oil. The crude was subjected to flash column chromatography ($R_f = 0.5$; 8:2 *n*-hexanes:ethyl acetate) to afford carbamate **E-126** as a white solid (149 mg, 79%); mp = 177–179 °C; ν_{max}/cm^{-1} 3359 (NH), 2978 (CH), 2931 (CH), 1725

(CO), 1721 (CO); δ_H (400 MHz; $CDCl_3$) 1.49 (9 H, s, $(CH_3)_3$), 1.66 (9 H, s, $(CH_3)_3$), 1.72 (1 H, m, $CHCH_2C$), 2.17 (1 H, dd, $J = 8.6, 5.2$, $CHCH_2C$), 2.66 (1 H, *app. t*, $J = 8.6$, $CCHCH_2$), 3.38 (3 H, s, OCH_3), 5.40 (1 H, s, NH), 7.23 (1 H, td, $J = 7.5, 1.3$, $CHCHCC$ or $CHCHCNBoc$), 7.29 (1 H, td, $J = 7.5, 1.3$, $CHCHCC$ or $CHCHCNBoc$), 7.41 (1 H, s, $CCHNBoc$), 7.70 (1 H, s, $CHCHCC$ or $CHCHCNBoc$), 8.09 (1 H, d, $J = 7.5$, $CHCHCC$ or $CHCHCNBoc$); δ_C (101 MHz; $CDCl_3$) 26.0 (CH), 28.3 ($C(CH_3)_3$), 28.5 ($C(CH_3)_3$), 52.2 (CH_3), 80.5 ($2 \times C$), 83.7 (C), 115.3 (CH), 119.2 (CH), 122.7 (CH), 124.5 (CH), 125.0 (CH), 130.8 (C), 135.4 (C), 149.7 (C), 155.9 ($2 \times CO$), 170.5 (CO); LRMS m/z (ES+) 453.2 ($[M + Na]^+$, 100%); HRMS m/z (ES+) calcd for $C_{23}H_{30}N_2O_6Na$ 453.2002, found 453.2001.

A novel compound prepared according to a standard procedure.

128) Benzyl 2-((*tert*-butoxycarbonyl)amino)acrylate

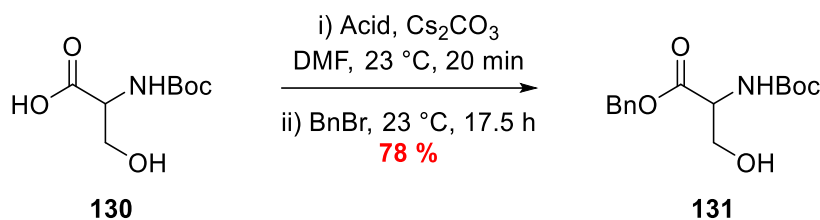


A solution of alcohol **131** (8.52 g, 28.9 mmol), triethylamine (10.1 mL, 72.1 mmol) and 4-dimethylaminopyridine (3.52 mg, 28.9 mmol) in anhydrous dichloromethane (150 mL) was cool to 0 °C and stirred under an atmosphere of argon for 15 min. Methanesulfonyl chloride (3.70 mL, 37.5 mmol) was then added dropwise over the course of 5 min, the resultant mixture was allowed to warm to 23 °C over-night. After 16.5 h, the reaction mixture was diluted with $HCl_{(aq)}$ (1 M, 10 mL). The organic and aqueous layers were separated and the organic was washed with $HCl_{(aq)}$ (1M, 10 mL), water (2×10 mL) and brine (20 mL). This organic solution was dried with $MgSO_4$ and concentrated under reduced pressure to give a light brown oil. The crude was subjected to flash column chromatography ($R_f = 0.3$, 9:1 *n*-hexane:ethyl acetate) to afford amino acrylate **128** as a white solid (6.64 g, 83%); ν_{max}/cm^{-1} (neat) 3397 (NH), 2980 (CH), 1705 (CO), 1630 (CC); δ_H (400 MHz; $CDCl_3$) 1.48 (9 H, s, $C(CH_3)_3$), 5.26 (2 H, s,

PhCH₂CO₂), 5.79 (1 H, d, *J* = 1.5, CCH_aH_b or CCH_aH_b), 6.18 (1 H, *app. s*, CCH_aH_b or CCH_aH_b), 7.03 (1 H, s, NH), 7.32–7.40 (5 H, m, *Ar-H*); δ_c (101 MHz; CDCl₃) 28.4 (CH₃), 67.8 (CH₂), 80.9 (C), 105.6 (CH₂), 128.3 (CH), 128.7 (CH), 128.8 (CH), 131.5 (C), 135.3 (C), 152.7 (CO), 164.0 (CO); LRMS *m/z* (ES+) 300.1 ([M + Na]⁺, 100%).

A known compound prepared according to a literature procedure.³⁷⁷ The recorded data are in agreement with that reported in the literature.³⁷⁷

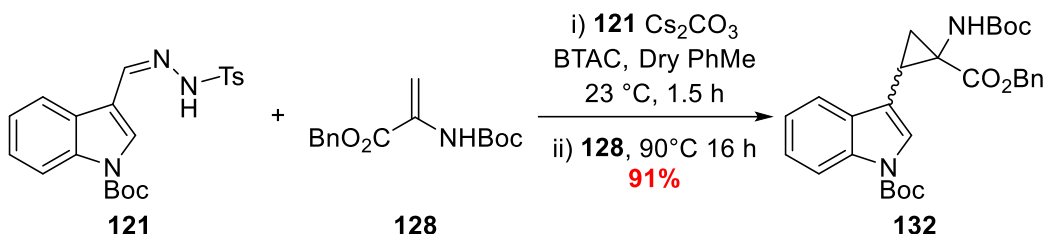
131) Benzyl (tert-butoxycarbonyl)serinate



N-Boc Serine **130** (2.00 g, 9.27 mmol) was dissolved in a suspension of caesium carbonate (3.81 g, 11.7 mmol) in *N,N*-dimethylformamide (40 mL) and stirred vigorously at 23 °C for 20 min. Benzyl bromide (1.39 mL, 11.7 mmol) was then added dropwise over 3 min and the reaction allowed to stir. After 17.5 h, the reaction mixture was diluted with water (20 mL) and extracted with ethyl acetate (30 mL). The organic and aqueous layers were separated and the organic was washed with water (2 × 15 mL) and brine (20 mL), dried over MgSO₄, filtered and concentrated under reduced pressure. The crude mixture was subjected to flash column chromatography (*R_f* = 0.2, 2:1 *n*-hexanes:ethyl acetate) to yield benzyl ester **131** compound as a colourless oil (2.23 g, 78%); $\nu_{\text{max}}/\text{cm}^{-1}$ (neat) 3391 (OH), 2976 (CH), 1688 (CO); δ_H (400 MHz; CDCl₃) 1.44 (9 H, s, C(CH₃)₃), 2.18 (1 H, t, *J* = 6.2, CHCH₂), 3.92 (1 H, dd, *J* = 6.2, 3.7, CHCH₂), 3.99 (1 H, dd, *J* = 6.2, 3.7, CHCH₂), 4.43 (1 H, s, OH), 5.20 (1 H, d, *J* = 12.4, PhCHH'CO₂), 5.22 (1 H, d, *J* = 12.4, PhCHH'CO₂), 5.44 (1 H, s, NH), 7.31–7.40 (5 H, m, *Ar-H*); δ_c (101 MHz; CDCl₃) 28.4 (CH₃), 56.0 (CH), 63.7 (CH₂), 67.5 (CH₂), 128.3 (CH), 128.6 (CH), 128.8 (CH), 135.3 (C), 155.9 (CO) 170.8 (CO); LRMS *m/z* (ES+) 318.1 ([M + Na]⁺ 100%).

A known compound prepared according to a literature procedure.³⁷⁸ The recorded data are in agreement with that reported in the literature with the exception of the missing quaternary carbon of the ^tBu-group in the ¹³C-NMR spectrum.³⁷⁹

132) tert-Butyl 3-(2-((benzyloxy)carbonyl)-2-((tert-butoxycarbonyl)amino)cyclopropyl)-1*H*-indole-1-carboxylate

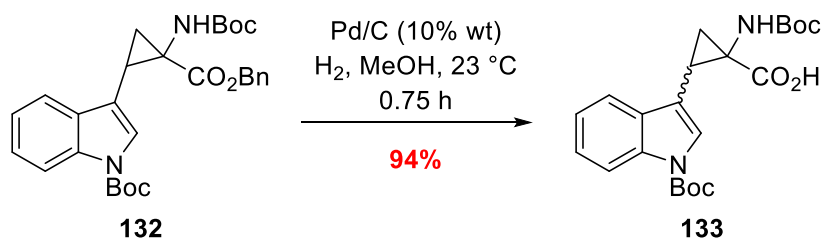


An oven-dried two-neck flask, fitted with an oven-dried condenser, was charged with **121** (2.02 g, 4.88 mmol), caesium carbonate (1.59 g, 4.88 mmol), benzyltriethylammonium chloride (111 mg, 0.49 mmol) and anhydrous toluene (40 mL). The resulting suspension was stirred vigorously under an atmosphere of argon for 1.5 h to yield a bright white suspension. A solution of **128** (1.02 g, 3.67 mmol) in anhydrous toluene (40 mL) was then added and the overall solution was heated at 90 °C for 16 h until complete loss of the acrylate was seen *via* TLC. The reaction mixture was allowed to cool and the remaining solids were removed *via* suction filtration, the collected solids were washed with ethyl acetate (2 × 20 mL). The combined organics were diluted with water (20 mL), separated and the resultant organic phase was washed further with water (2 × 20 mL) and brine (30 mL). Drying over MgSO₄ and concentration under reduced pressure afforded the crude mixture. Analysis of the crude by ¹H-NMR revealed an 92:8 d.r.. (*E/Z*). The crude was subjected to flash column chromatography (*R*_f = 0.2, 8.5:1.5 *n*-hexane:ethyl acetate) to yield diastereomeric mixture (86:14, *E/Z*) of cyclopropane **132** as a pale yellow solid (1.69 g, 91%); **mp** = 126–128 °C; **v**_{max}/**cm**⁻¹ (neat) 3254 (NH), 2976 (CH), 1731 (CO), 1726 (CO), 1678 (CO); **δ**_H (**400 MHz; CDCl**₃) **Resonances assignable to the major *E*-diastereomer**: 1.46 (9 H, s), 1.65 (9 H, s), 2.16–2.22 (1 H, m), 2.69 (1 H, app. t, *J* = 8.8, CCHCHH'), 4.74 (2 H, m, CO₂CH₂Ph), 5.43 (1 H, s, NH), 6.88 (2 H, m, Ph-CH), 7.12–7.23 (4 H, m, 3 × Ph-CH & CHCHCC or CHCHCNBoc), 7.30 (1 H, ddd, *J* = 8.4, 7.2, 1.4,

CHCHCC or CHCHCNBoc), 7.34–7.37 (1 H, m, CCHNBoc), 7.73 (1 H, s, CHCHCC or CHCHCNBoc), 8.08 (1 H, d, $J = 8.1$, CHCHCC or CHCHCNBoc). **Resonances assignable to the minor *Z*-diastereomer:** 2.27 (1 H, m), 2.88 (1 H, app. t, $J = 8.7$, CCHCHH'). Used for purposes of identifying the diastereomer ratio; δ_C (101 MHz; CDCl₃) **Resonances assignable to the major *E*-diastereomer:** 21.4 (CH₂), 26.2 (CH), 28.4 (CH₃), 28.5 (CH₃), 67.1 (CH₂), 83.7 (C), 115.4 (CH), 119.4 (CH), 122.8 (CH), 124.5 (CH), 125.0 (C), 125.2 (CH), 128.0 (CH), 128.1 (CH), 128.3 (CH), 130.8 (C), 135.4 (C), 144.9 (C), 149.6 (C), 155.9 (C), 170.1 (C). Both quaternary C(CH₃)₃ carbons not observed. **Resonances assignable to the minor *Z*-diastereomer:** No resonances assignable; **LRMS m/z (ES+)** 529.2 ([M + Na]⁺, 100%); **HRMS m/z (ES+)** calcd for C₂₉H₃₄N₂O₆Na 529.2315, found 529.2317.

A novel compound prepared according to a modified literature procedure.¹⁴⁵

133) 2-(1-(*tert*-Butoxycarbonyl)-1*H*-indol-3-yl)-1-((*tert*-butoxycarbonyl)amino)cyclopropane-1-carboxylic acid



10% Pd/C (100 mg) was suspended in a solution of **132** (200 mg, 0.39 mmol) in methanol (8 mL) and stirred in a round-bottom flask fitted with a septa. Hydrogen was then bubbled through the solution for 10 min *via* balloon and then for the remainder of the reaction the balloon needle was left above the surface of the solution. After 45 min, the reaction was determined complete *via* TLC. The reaction mixture was passed through a celite bung and was eluted with methanol (2 × 5 mL). The resulting liquor was collected and concentrated under reduced pressure to give a diastereomeric mixture of acid **133** (91:9, *E/Z*) as a white solid (154 mg, 94%); **mp** = 153–154 °C; $\nu_{\max}/\text{cm}^{-1}$ (neat) 2978 (CH), 1726 (CO), 1702 (CO), Br. COOH absorbance seen but with no definable centre; δ_H (400 MHz; CD₃OD) **Resonances assignable to the major *E*-diastereomer:** 1.49 (9 H, s C(CH₃)₃), 1.56–1.60 (1 H, m,

CHCHH'C), 1.66 (9 H, s, C(CH₃)₃), 2.10 (1 H, dd, *J* = 8.2, 5.1, CHCHH'C), 2.67 (1 H, td, *J* = 8.8, 8.1, 1.5, CCHCHH'), 7.21 (1 H, td, *J* = 7.4, 1.3, CHCHCC or CHCHCNBoc), 7.24–7.29 (1 H, m, CHCHCC or CHCHCNBoc), 7.39–7.41 (1 H, m, CCHNBoc), 7.89 (1 H, d, *J* = 7.6, CHCHCC or CHCHCNBoc), 8.05 (1 H, d, *J* = 8.1, CHCHCC or CHCHCNBoc). **Resonances assignable to the minor Z-diastereomer:** 2.80 (1 H, m, CCHCHH'). Used for purposes of identifying the diastereomer ratio; **δ_c (101 MHz; CDCl₃) Resonances assignable to the major E-diastereomer:** 21.7 (CH₂), 26.3 (CH), 28.4 (CH₃), 28.8 (CH₃), 41.2 (C), 80.5 (C), 84.8 (C), 115.8 (CH), 117.8 (C), 120.9 (CH), 123.6 (CH), 125.3 (CH), 125.8 (CH), 132.3 (C), 136.7 (C), 151.0 (C), 158.6 (C), 173.9 (C). **Resonances assignable to the minor Z-diastereomer:** No resonances assignable; **LRMS *m/z* (ES+)** 439.2 ([M + Na]⁺, 100%); **HRMS *m/z* (ES+)** calcd for C₂₂H₂₈N₂O₆Na 439.1845, found 439.1851.

A novel compound prepared according to a standard procedure.

151) *E*-3-(2-Nitrovinyl)-1H-indole

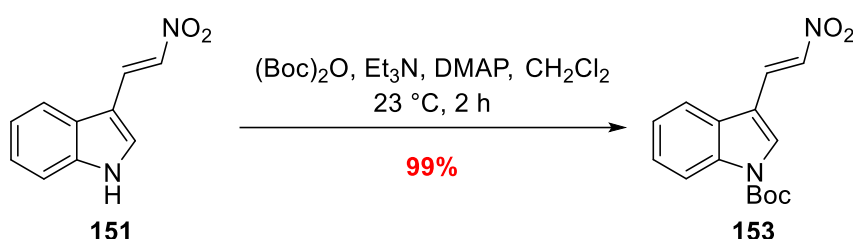


Aldehyde **54** (1.00g, 6.89 mmol) and ammonium acetate (531 mg, 6.89 mmol, recrystallised from hot MeOH before use) was solubilised in nitromethane (3.7 mL) and heated to reflux for 3 h. Once the reaction was determined complete *via* TLC (*R_f* = 0.6, 1:1 ethyl acetate:*n*-hexane), the reaction mixture allowed to cool to room 23 °C before being quenched by addition of water (10 mL) and extracted with CH₂Cl₂ (10 mL). The two phases were separated, and the organic was washed sequentially with water (2 × 10 mL) and brine (20 mL). The combined organics were dried over MgSO₄, filtered to remove the solids and then concentrated to give the crude material. The resulting solid was recrystallised from hot CH₂Cl₂ to give *E*-nitroalkene **151** as a brown crystalline solid (449 mg, 35%); **ν_{max}/cm⁻¹** (neat) 3404 (NH), 3108 (vinyl-CH), 3032 (CH), 1614 (Conj. C=C), 1577 (NO), 1305 (NO); **δ_H (400 MHz; CDCl₃)** 7.31–7.39 (2 H, Stack,

CHCHCC and CHCHCNH), 7.46–7.51 (1 H, m, CHCHCC or CHCHCNH), 7.68 (1 H, d, $J = 3.0$ CCHNH), 7.77–7.84 (2 H, Stack, CHCHNO₂ and CHCHCC or CHCHCNH), 8.30 (1 H, d, $J = 13.5$, CHCHNO₂), 8.74 (1 H, s, NH); δ_c (101 MHz; CDCl₃) 109.9 (C), 112.4 (CH), 120.7 (CH), 122.8 (CH), 124.5 (CH), 124.8 (C), 132.4 (CH), 133.2 (CH), 133.6 (CH), 137.4 (C); LRMS m/z (ES⁻) 187.0 ([M – H]⁻, 100%).

A known compound prepared according to a literature procedure.¹⁷⁷ The recorded data are in agreement with that reported in the literature.¹⁷⁷

153) *tert*-Butyl *E*-3-(2-nitrovinyl)-indole-1-carboxylate

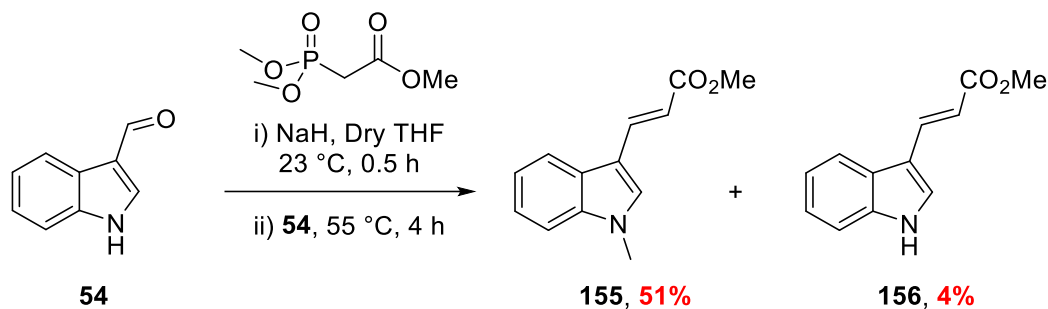


Nitroalkene **151** (100 mg, 0.53 mmol), 4-dimethylaminopyridine (7 mg, 0.05 mmol) and triethylamine (0.11 mL, 0.80 mmol) were solubilised in dichloromethane (10 mL) and stirred at 23 °C. After 10 min, di-*tert*-butyl dicarbonate (174 mg, 0.80 mmol) was added and stirred vigorously at 25 °C for a further 2 h until the reaction was determined complete *via* TLC ($R_f = 0.9$, *n*-hexane:ethyl acetate). The reaction mixture was quenched by addition of HCl_(aq) (1 M, 5 mL). The resulting phases were separated and the organic layer washed with HCl_(aq) (1 M, 10 mL), water (2 × 10 mL) and brine (15 mL) before being dried over MgSO₄ and filtered. Concentration of the dried organic phase yield *N*-Boc indole **153** as an orange oil with no need for further purification (153 mg, 99%); $\nu_{\max}/\text{cm}^{-1}$ 3129 (CH), 2978 (CH), 2931 (CH), 1736 (CO), 1545 (NO), 1338 (NO); δ_H (400 MHz; CDCl₃) 1.70 (9 H, s, (CH₃)₃), 7.39 (1 H, td, $J = 7.6, 1.2$, CHCHCC or CHCHCNBoc), 7.44 (1 H, td, $J = 7.6, 1.2$, CHCHCC or CHCHCNBoc), 7.72 (1 H, dt, $J = 7.6, 1.2$, CHCHCC or CHCHCNBoc), 7.79 (1 H, d, $J = 13.7$, CCHCHNO₂), 8.03 (1 H, d, $J = 0.6$, CCHNBoc), 8.18 (1 H, dd, $J = 13.7, 0.6$, CCHCHNO₂), 8.21–8.26 (1 H, dt, $J = 7.6, 1.2$, CHCHCC or CHCHCNBoc); δ_c (101 MHz; CDCl₃) 28.2 (CH₃), 85.7 (C), 112.6 (C), 116.1 (CH),

120.3 (CH), 124.4 (CH), 126.1 (CH), 127.0 (C), 131.7 (CH), 132.3 (CH), 136.0 (CH), 136.5 (C), 148.8 (C); **LRMS m/z (ES⁺)** 289.3 ([M + H]⁺, 8%), 189.3 ([M – Boc]⁺, 10).

A known compound prepared according to a literature procedure.³⁸⁰ The recorded data are in agreement with that reported in the literature.³⁸⁰

155) Methyl *E*-3-(1-methyl-1H-indol-3-yl)acrylate

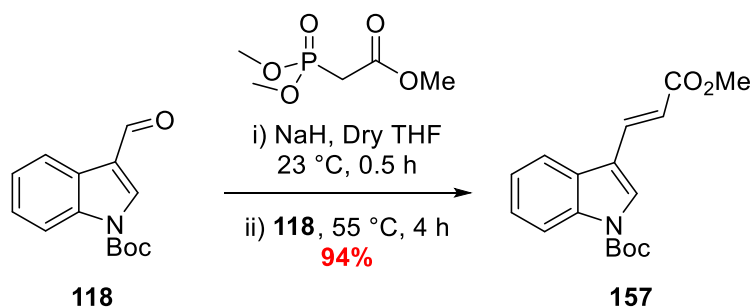


Freshly triturated (from hexanes, 2 × 5 mL) and dried sodium hydride (103 mg, 4.28 mmol) was suspended in a solution of trimethyl phosphonoacetate (0.70 mL, 4.28 mmol) in anhydrous tetrahydrofuran (30 mL) and stirred under an atmosphere of argon at 23 °C. After 0.5 h, aldehyde **54** (300 mg, 2.07 mmol) was added and the temperature increased to 55 °C for 4 h. Upon complete consumption of starting material, as determined *via* TLC (R_f = 0.3, 3:1 *n*-hexane:ethyl acetate), the reaction mixture was diluted with water (25 mL) and the organic extracted with ethyl acetate (25 mL). The resultant phases were separated and the organic layer washed with water (2 × 10 mL) and brine (20 mL). Drying over MgSO₄, filtration and concentration under reduced pressure afforded the crude material. The crude material was subjected to flash column chromatography (R_f = 0.3, 3:1 *n*-hexane:ethyl acetate) to give two fractions: fraction 1, **155**, as a white solid (228 mg, 51%) and fraction 2, **156**, as a white solid (18 mg, 4%); **Characterisation data for 155 (fraction 1):** $\nu_{\max}/\text{cm}^{-1}$ (neat) 3109 (vinyl-CH), 3050 (CH), 2939 (CH), 1700 (conj. CO), 1616 (conj. C=C); δ_H (400 MHz; CDCl₃) 3.81 (3 H, s, NCH₃ or CO₂CH₃), 3.81 (3 H, s, NCH₃ or CO₂CH₃), 6.42 (1 H, d, J = 15.9, CHCHCO₂CH₃), 7.23–7.38 (4 H, Stack, CHCHCC and CHCHCNCH₃ and CCHNH and CHCHCC or CHCHCNCH₃) 7.86–7.94 (2 H, Stack, CHCHCC or CHCHCNCH₃ and CHCHCO₂CH₃); δ_C (101 MHz; CDCl₃) 33.3 (CH₃), 51.5 (CH₃), 110.1 (CH), 112.2 (CH), 112.3 (C), 120.7 (CH),

121.4 (CH), 123.1 (CH), 126.2 (C), 133.2 (CH), 138.2 (C), 138.3 (CH), 168.9 (CO); **LRMS m/z (ES+)** 238.1 ([M + Na]⁺, 100%), 216.1 ([M + H]⁺, 25). **Characterisation data for 156 (fraction 2):** $\nu_{\max}/\text{cm}^{-1}$ (neat) 3368 (NH), 3100 (vinyl-CH), 2950 (CH), 1704 (conj. CO), 1621 (conj. C=C); δ_H (**300 MHz; CDCl₃**) 3.82 (3 H, s, CO₂CH₃), 6.47 (1 H, d, $J = 16.0$, CHCHCO₂CH₃), 7.22–7.32 (3 H, Stack,), 7.40–7.45 (1 H, m), 7.50 (1 H, d, $J = 2.8$, CCHNH), 7.89–7.98 (2 H, Stack, CHCHCC or CHCHCNCH₃ and CHCHCO₂CH₃), 8.51 (1 H, s, NH); **LRMS m/z (EI+)** 201.1 ([M]⁺, 95%), 170.1 ([M – OMe]⁺, 95%).

Both **155** and **156** are known compounds prepared via a novel procedure.³⁸¹ The recorded data are in agreement with that reported in the literature.³⁸¹ No carbon data was recorded for fraction 2.

157) tert-Butyl E-3-(3-methoxy-3-oxoprop-1-en-1-yl)-1H-indole-1-carboxylate

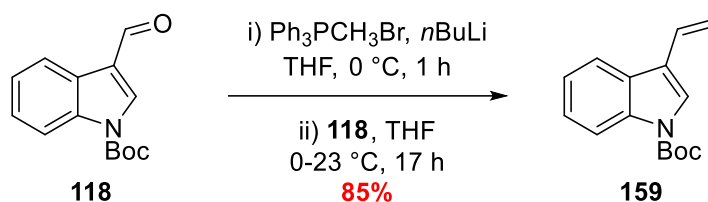


Freshly triturated (from hexanes, 2 × 5 mL) and dried sodium hydride (32 mg, 1.35 mmol) was suspended in a solution of trimethyl phosphonoacetate (0.22 mL, 1.35 mmol) in anhydrous tetrahydrofuran (25 mL) and stirred under an atmosphere of argon at 23 °C. After 0.5 h, aldehyde **118** (300 mg, 1.22 mmol) was added and the temperature increased to 55 °C for 4 h. Upon complete consumption of starting material, the reaction mixture was diluted with water (25 mL) and the organic extracted with ethyl acetate (25 mL). The resultant phases were separated and the organic layer washed with water (2 × 10 mL) and brine (20 mL). Drying over MgSO₄, filtration and concentration under reduced pressure afford *E*-olefin **157**, with no need for further purification, as a pale yellow solid (345 mg, 94%); $\nu_{\max}/\text{cm}^{-1}$ 2953 (CH), 1738 (CO), 1712 (CO); δ_H (**400 MHz; CDCl₃**) 1.69 (9 H, s, (CH₃)₃), 3.83 (3 H, s, OCH₃), 6.54 (1 H, dd, $J = 16.1, 0.6$, CHCHCOOMe), 7.33 (1 H, td, $J = 7.4, 1.4$, CHCHCC or CHCHCNBoc), 7.39

(1 H, ddd, $J = 7.4, 1.4$, CHCHCC or CHCHCNBoc), 7.81–7.87 (3 H, Stack, CHCHCOOMe and [CHCHCC or CHCHCNBoc] and CCHNBoc*), 8.20 (1 H, d, $J = 7.4$, CHCHCC or CHCHCNBoc); δ_c (101 MHz; CDCl₃) 28.3 ((CH₃)₃), 51.8 (OCH₃), 84.8 (C), 115.7 (CH), 116.9 (C), 117.2 (CH), 120.4 (CH), 123.7 (CH), 125.4 (CH), 128.1 (C), 128.8 (CH), 136.4 (C), 136.8 (CH), 149.3 (C), 168.0 (C); LRMS m/z (ES+) 302.38 ([M + H]⁺, 44%), 202.3 ([M – Boc]⁺, 33).

A known compound prepared via a novel sequence – the protocol used was developed from protocols to synthesise similar compounds.^{382, 383} The recorded data are in agreement with that reported in the literature.³⁸²

159) *tert*-Butyl 3-vinyl-1*H*-indole-1-carboxylate



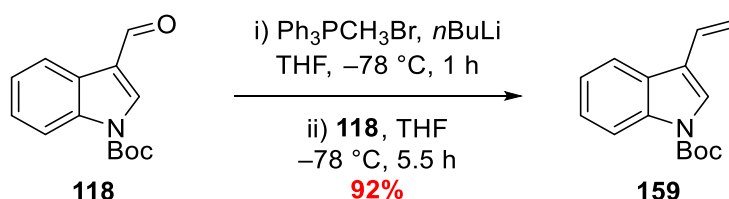
Initial *n*BuLi method

Methyl triphenylphosphonium bromide (874 mg, 2.45 mmol) was suspended in anhydrous tetrahydrofuran (10 mL), cooled to 0 °C and stirred for 10 min in a flame-dried two-neck round-bottom flask under an atmosphere of argon. To this, a solution of *n*BuLi in hexanes (~2.1 M, 0.87 mL, 1.83 mmol) was added dropwise over 10 min to give a bright yellow solution. The yellow solution was stirred for a further 10 min at 0 °C, upon which the flask was removed from the ice-bath and allowed to warm to 23 °C. In a separate flame-dried two-neck round-bottom flask, a solution of aldehyde **118** (300 mg, 1.22 mmol) in anhydrous tetrahydrofuran (15 mL) was prepared and cooled to 0 °C under an atmosphere of argon. After 5 min, the freshly-prepared ylide solution was transferred, *via* dried glass syringe, to the aldehyde/anhydrous tetrahydrofuran solution. The resultant reaction mixture was removed from the ice-bath and allowed to warm to 23 °C passively. After 17 h, the reaction was quenched with NH₄Cl_(aq) (Sat. soln., 20 mL) and the organics extracted with ethyl acetate (10 mL). The resultant layers were separated and the organic layers washed with water (2 × 10 mL) and brine (20 mL), dried over MgSO₄, filtered and concentrated under reduced pressure to afford a yellow oil. The oil was

subjected to flash column chromatography ($R_f = 0.3$, 9:1 *n*-hexane:ethyl acetate) to afford alkene **159** as a pale yellow oil (254 mg, 85%); $\nu_{\max}/\text{cm}^{-1}$ (neat) 2978 (CH), 1730 (CO), 1637 (CC); δ_H (400 MHz; CDCl_3) 1.70 (9 H, s, $(\text{CH}_3)_3$), 5.35 (1 H, dd, $J = 11.3, 1.2$, CCHCH₂, *cis*), 5.84 (1 H, dd, $J = 17.8, 1.2$, CCHCH₂, *trans*), 6.83 (1 H, ddd, $J = 17.8, 11.3, 0.8$, CCHCH₂), 7.28 – 7.33 (1 H, m, CHCHNBoc or CHCHCC), 7.37 (1 H, ddd, $J = 8.4, 7.2, 1.4$, CHCHNBoc or CHCHCC), 7.65 (1 H, s, CCHNBoc), 7.79–7.85 (1 H, m, CHCHCNBoc or CHCHCC), 8.20 (1 H, d, $J = 8.4$, CHCHCNBoc or CHCHCC); δ_C (101 MHz; CDCl_3) 28.3 (CH_3), 83.9 (C), 114.5 (CH), 115.5 (CH), 119.4 (C), 120.1 (CH), 123.0 (CH), 124.1 (CH), 124.7 (CH), 128.3 (CH), 128.9 (CH_2), 136.1 (C), 149.7 (C); LRMS m/z (ES+) 244.1 ($[\text{M} + 1]^+$, 12%), 243.1 ($[\text{M}]^+$, 51%), 187.0 ($[\text{M} - \text{tBu} + \text{H}]^+$, 86), 143.1 ($[\text{M} - \text{Boc}]^+$, 100).

A known compound prepared according to a literature procedure.³⁸⁴ The recorded data are in agreement with that reported in the literature.³⁸⁴

159) *tert*-Butyl 3-vinyl-1*H*-indole-1-carboxylate



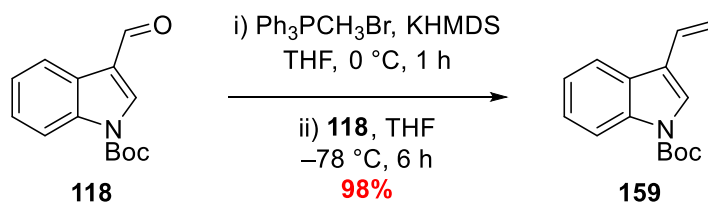
Optimised *n*BuLi method

Methyl triphenylphosphonium bromide (1.31 mg, 3.67 mmol) was suspended in anhydrous tetrahydrofuran (9 mL), cooled to 0 °C and stirred for 10 min in a flame-dried two-neck round-bottom flask under an atmosphere of argon. To this, a solution of *n*BuLi (2 M in hexanes, 1.68 mL, 3.36 mmol) was added dropwise over 5 min to give a bright yellow solution. The ylide was allowed to mature at 0 °C, after 1 h the solution was cooled to $-78\text{ }^\circ\text{C}$. A solution of aldehyde **118** (750 mg, 3.06 mmol) in anhydrous tetrahydrofuran (9 mL) was then added dropwise over 1 h to the cooled ylide solution. The resultant reaction mixture was maintained at $-78\text{ }^\circ\text{C}$ for 5.5 h. Once determined complete *via* TLC ($R_f = 0.7$, 3:1 *n*-hexane:ethyl acetate) the reaction was quenched with $\text{NH}_4\text{Cl}_{(\text{aq})}$ (Sat. soln., 20 mL) and then extracted with ethyl acetate (10 mL). The resultant layers were separated and the organic layers washed with water (2 × 10 mL)

and brine (20 mL), dried over MgSO₄, filtered and concentrated under reduced pressure to afford a yellow oil. The oil was subjected to flash column chromatography (*R*_f = 0.3, 9:1 hexanes:ethyl acetate) to afford olefin **159** as a pale yellow oil (687 mg, 92%); $\nu_{\max}/\text{cm}^{-1}$ (neat) 2978 (CH), 1730 (CO), 1637 (CC); δ_{H} (400 MHz; CDCl₃) 1.70 (9 H, s, (CH₃)₃), 5.35 (1 H, dd, *J* = 11.3, 1.2, CCHCH₂, *cis*), 5.84 (1 H, dd, *J* = 17.8, 1.2, CCHCH₂, *trans*), 6.83 (1 H, ddd, *J* = 17.8, 11.3, 0.8, CCHCH₂), 7.28–7.33 (1 H, m, CHCHNBoc or CHCHCC), 7.37 (1 H, ddd, *J* = 8.4, 7.2, 1.4, CHCHNBoc or CHCHCC), 7.65 (1 H, s, CCHNBoc), 7.79–7.85 (1 H, m, CHCHCNBoc or CHCHCC), 8.20 (1 H, d, *J* = 8.4, CHCHCNBoc or CHCHCC); δ_{C} (101 MHz; CDCl₃) 28.3 (CH₃), 83.9 (C), 114.5 (CH), 115.5 (CH), 119.4 (C), 120.1 (CH), 123.0 (CH), 124.1 (CH), 124.7 (CH), 128.3 (CH), 128.9 (CH₂), 136.1 (C), 149.7 (C); LRMS *m/z* (ES⁺) 244.1 ([M + 1]⁺, 12%), 243.1 ([M]⁺, 51%), 187.0 ([M - tBu + H]⁺, 86), 143.1 ([M - Boc]⁺, 100).

A known compound prepared according to a literature procedure.³⁸⁴ The recorded data are in agreement with that reported in the literature.³⁸⁴

159) *tert*-Butyl 3-vinyl-1*H*-indole-1-carboxylate



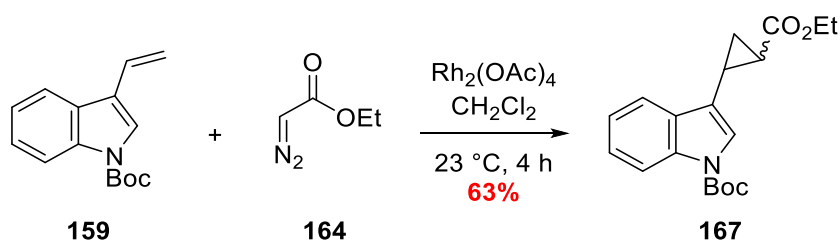
KHMDS method

Methyl triphenylphosphonium bromide (1.31 g, 3.66 mmol) was suspended in anhydrous tetrahydrofuran (10 mL), cooled to 0 °C and stirred for 10 min in a flame-dried two-neck round-bottom flask under an atmosphere of argon. To this, a solution of KHMDS (0.7 M in PhMe, 4.8 mL, 3.36 mmol) was added dropwise over 5 min to give a bright orange solution. The ylide solution was allowed to mature for 1 h at 0 °C, upon which the flask was cooled to -78 °C. A solution of **118** (750 mg, 3.06 mmol) in anhydrous tetrahydrofuran (8 mL) was then added dropwise over 1 h to the cooled ylide solution. The resultant reaction mixture was maintained

at $-78\text{ }^{\circ}\text{C}$ for 6 h. Once determined complete *via* TLC ($R_f = 0.7$, 3:1 *n*-hexane:ethyl acetate) the reaction was quenched with $\text{NH}_4\text{Cl}_{(\text{aq})}$ (Sat. soln., 20 mL) and then extracted with ethyl acetate (10 mL). The resultant layers were separated and the organic layers washed with water ($2 \times 10\text{ mL}$) and brine (20 mL), dried over MgSO_4 , filtered and concentrated under reduced pressure to afford a yellow oil. The oil was subjected to flash column chromatography ($R_f = 0.3$, 9:1 *n*-hexane:ethyl acetate) to afford olefin **159** as a pale yellow oil (729 mg, 98%); $\nu_{\text{max}}/\text{cm}^{-1}$ (neat) 2978 (CH), 1730 (CO), 1637 (CC); δ_{H} (400 MHz; CDCl_3) 1.70 (9 H, s, $(\text{CH}_3)_3$), 5.35 (1 H, dd, $J = 11.3, 1.2$, CCHCH₂, *cis*), 5.84 (1 H, dd, $J = 17.8, 1.2$, CCHCH₂, *trans*), 6.83 (1 H, ddd, $J = 17.8, 11.3, 0.8$, CCHCH₂), 7.28–7.33 (1 H, m, CHCHNBoc or CHCHCC), 7.37 (1 H, ddd, $J = 8.4, 7.2, 1.4$, CHCHNBoc or CHCHCC), 7.65 (1 H, s, CCHNBoc), 7.79–7.85 (1 H, m, CHCHCNBoc or CHCHCC), 8.20 (1 H, d, $J = 8.4$, CHCHCNBoc or CHCHCC); δ_{C} (101 MHz; CDCl_3) 28.3 (CH₃), 83.9 (C), 114.5 (CH), 115.5 (CH), 119.4 (C), 120.1 (CH), 123.0 (CH), 124.1 (CH), 124.7 (CH), 128.3 (CH), 128.9 (CH₂), 136.1 (C), 149.7 (C); LRMS *m/z* (ES+) 244.1 ($[\text{M} + 1]^+$, 12%), 243.1 ($[\text{M}]^+$, 51%), 187.0 ($[\text{M} - \text{tBu} + \text{H}]^+$, 86), 143.1 ($[\text{M} - \text{Boc}]^+$, 100).

A known compound prepared according to a literature procedure.³⁸⁴ The recorded data are in agreement with that reported in the literature.³⁸⁴

167) *tert*-Butyl 3-(2-(ethoxycarbonyl)cyclopropyl)-indole-1-carboxylate

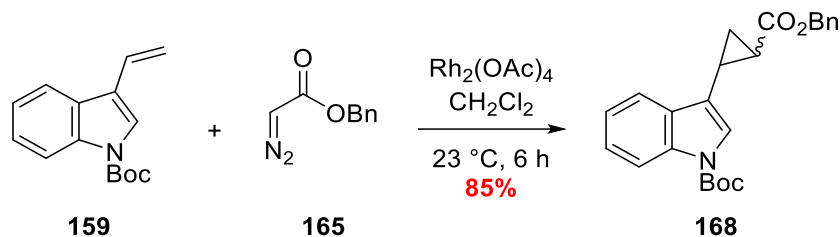


A solution of **159** (517 mg, 2.12 mmol) in anhydrous dichloromethane (9 mL) was added to an oven-dried flask containing rhodium acetate (19 mg, 0.04 mmol) under an atmosphere of argon and stirred at $23\text{ }^{\circ}\text{C}$. To this, a solution of ethyl diazoacetate **164** (0.34 mL, 3.19 mmol) in anhydrous dichloromethane (0.66 mL) was added over 1 h. After a further 5 hours, the reaction mixture was passed through a pad of celite and eluted with dichloromethane. The resultant

organic solution was concentrated under reduced pressure to give a yellow oil. The crude material was subjected to flash column chromatography ($R_f = 0.2$, 9:1 *n*-hexane:ethyl acetate) to give a 3:1 (*E*:*Z*) diastereomeric mixture, of cyclopropylester **167** as a colourless oil (438 mg, 63%); $\nu_{\max}/\text{cm}^{-1}$ 2979 (CH), 2934 (CH), 1722 (Br., 2 \times CO); δ_H (400 MHz; CDCl_3) **Resonances assignable to the major *E*-diastereomer:** 1.29–1.33 (4 H, Stack, CH_2CH_3 , $\text{CHCHH}'\text{CH}$ or $\text{CHCHH}'\text{CH}$), 1.56–1.63 (1 H, m, $\text{CHCHH}'\text{CH}$ or $\text{CHCHH}'\text{CH}$), 1.66 (9 H, s, $\text{C}(\text{CH}_3)_3$), 1.90 (1 H, ddd, $J = 8.3, 5.1, 4.2$, CHCO_2Et), 2.54 (1 H, dddd, $J = 9.1, 6.5, 4.2, 1.2$, CCHCHH'), 4.21 (2 H, q, $J = 7.2$, CH_2CH_3), 7.24–7.28 (1 H, m, CHCHNBoc or CHCHCC), 7.30 (1 H, d, $J = 1.2$, CCHNBoc), 7.33 (1 H, ddd, $J = 8.3, 7.2, 1.4$, CHCHNBoc or CHCHCC), 7.61 (1 H, dd, $J = 7.7, 1.4$, CHCHCNBoc or CHCHCC), 8.11 (1 H, d, $J = 8.3$, CHCHCNBoc or CHCHCC); **Resonances assignable to the major *Z*-diastereomer:** 0.94 (3 H, t, $J = 7.1$, CH_2CH_3), 1.36–1.44 (1 H, m), 1.66 (10 H, Stack, $\text{C}(\text{CH}_3)_3$ and $\text{CHCHH}'\text{CH}$ or $\text{CHCHH}'\text{CH}$), 2.16 (1 H, ddd, $J = 8.9, 7.8, 5.6$, CHCO_2Et), 2.43 (1 H, *app.* tdd, $J = 8.9, 8.7, 7.2, 1.5$, CCHCHH'), 3.76–3.83 (1 H, m, $\text{CO}_2\text{CHH}'\text{CH}_3$), 3.83–3.90 (1H, m $\text{CO}_2\text{CHH}'\text{CH}_3$), 7.21 (1 H, *app.* td, $J = 7.6, 7.3, 1.3$, CHCHNBoc or CHCHCC), 7.26–7.31 (1 H, m, CHCHNBoc or CHCHCC), 7.41 (1 H, s, CCHNBoc), 7.60 (1 H, dd, $J = 7.6, 1.3$, CHCHCNBoc or CHCHCC), 8.09 (1 H, *app.* s, CHCHCNBoc or CHCHCC); δ_C (101 MHz; CDCl_3) **Resonances assignable to the major *E*-diastereomer:** 14.5 (CH), 15.5 (CH_2), 17.3 (CH), 21.9 (CH_3), 28.4 ($\text{C}(\text{CH}_3)_3$), 60.9 (CH_2), 83.8 (C), 115.4 (CH), 119.2 (CH), 120.5 (C), 122.1 (CH), 122.7 (CH), 124.8 (CH), 130.6 (C), 135.6 (C), 149.8 (CO), 173.7 (CO); **Resonances assignable to the major *Z*-diastereomer:** 11.2 (CH_2), 14.1 (CH), 16.0 (CH), 20.3 (CH_3), 28.3 ($\text{C}(\text{CH}_3)_3$), 60.4 (CH_2), 83.5 (C), 115.4 (CH), 116.9 (C), 119.0 (CH), 122.5 (CH), 124.4 (CH), 124.8 (CH), 131.2 (C), 135.5 (C), 149.8 (CO), 171.1 (CO); **LRMS m/z (TOF ES $^+$)** 352.2 ($[\text{M} + \text{Na}]^+$, 50%); **HRMS m/z (TOF ES $^+$)** calcd for $\text{C}_{19}\text{H}_{23}\text{NO}_4\text{Na}$ 352.1525, found 352.1530.

*A known compound prepared according to a modified literature procedure.*¹⁷⁵ The recorded data are in agreement with that reported in the literature.^{175, 385}

168) *tert*-Butyl 3-(2-((benzyloxy)carbonyl)cyclopropyl)-indole-1-carboxylate

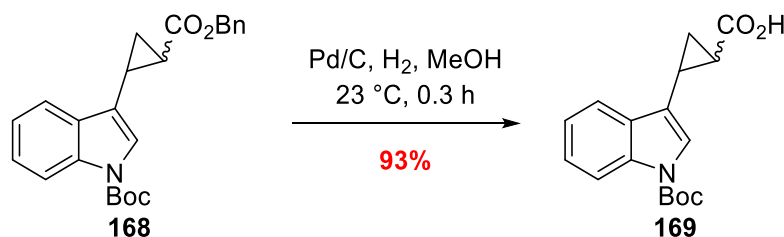


A solution of vinyl **159** (459 mg, 1.89 mmol) in anhydrous dichloromethane (9 mL) was added to a flame-dried flask containing dirhodium tetraacetate (17 mg, 0.04 mmol) under an atmosphere of argon and stirred at 23 °C. To this, a solution of benzyl diazoacetate **165** (0.47 mL, 2.83 mmol) in anhydrous dichloromethane (0.53 mL) was added over 1 h. After 5 hours, the reaction mixture was passed through a plug of celite and eluted with dichloromethane. The resultant organic solution was concentrated under reduced pressure to give a yellow oil. The crude material was subjected to flash column chromatography ($R_f = 0.3$, 8.5:1.5 *n*-hexane:ethyl acetate) to give a 3:1 (*E:Z*) diastereomeric mixture of benzyl ester **168** as a colourless oil (627 mg, 85%); $\nu_{\max}/\text{cm}^{-1}$ (neat) 2977 (CH), 1723 (CO), 1668 (CO); δ_H (400 MHz; CDCl_3) Resonances assignable to the major diastereomer: 1.34 (1 H, ddd, $J = 8.3$, 6.6, 4.3, CHCHH'CH or CHCHH'CH), 1.62–1.65 (1 H, m, CHCHH'CH or CHCHH'CH), 1.67 (13 H, s, $\text{C}(\text{CH}_3)_3$, appears at 13 H due to overlap with major isomer CHCHH'CH or CHCHH'CH, and minor isomer CHCHH'CH or CHCHH'CH), 1.98 (1 H, ddd, $J = 8.2$, 5.0, 4.2, CHH'CHCO₂Bn), 2.58 (1 H, dddd, $J = 9.0$, 6.5, 4.2, 1.1, CCHCHH'), 5.21 (2 H, s, CO₂CH₂Ph), 7.21 (1 H, td, $J = 6.6$, 1.3, CHCHCC or CHCHCNBoc), 7.23–7.28 (1 H, m, CHCHCC or CHCHCNBoc, appears as 2 H due to overlap with ref. peak), 7.34 (1 H, t, $J = 1.2$, CCHNBoc), 7.35–7.42 (5 H, m, *Ar-H*, appears as 6.5 H due to overlap with minor isomer *Ar-H* resonances), 7.59 (1 H, dt, $J = 7.7$, 1.0, CHCHCC or CHCHCNBoc), 8.12 (1 H, app. d, $J = 8.0$, CHCHCC or CHCHCNBoc). Resonances assignable to the minor diastereomer: 1.43 (1 H, td, $J = 8.1$, 4.8, CHCHH'CH or CHCHH'CH), 1.68–1.71 (1 H, m, CHCHH'CH or CHCHH'CH), 2.24 (1 H, ddd, $J = 8.9$, 7.8, 5.6, CHH'CHCO₂Bn), 2.48 (1 H, tdd, $J = 8.7$, 7.2, 1.4, CCHCHH'), 4.76 (1 H, d, $J = 12.3$), 4.82 (1 H, d, $J = 12.3$), unable to unambiguously assign aromatic resonances due

to overlapping resonances; δ_c (101 MHz; CDCl₃) Resonances assignable to the major diastereomer: 15.7 (CH₂), 21.9 (CH), 28.3 (CH₃), 66.7 (CH₂), 83.8 (C), 115.4 (CH), 119.1 (CH), 122.8 (CH), 124.8 (CH), 130.6 (C), 133.9 (C), 136.1 (CH), 149.7 (C), 164.8 (C), 173.6 (C), unable to unambiguously assign 1 quaternary and 4 tertiary carbons. Resonances assignable to the minor diastereomer: 11.4 (CH₂), 16.4 (CH), 20.4 (CH), 28.4 (CH₃), 66.4 (CH₂), 73.5 (C), 116.7 (CH), 118.9 (CH), 122.6 (CH), 124.5 (CH), 131.2 (C), 135.3 (C), 135.9 (C), 171.0 (C), unable to unambiguously assign 2 quaternary and 4 tertiary carbons; LRMS m/z (ES+) 414.2 ([M + Na]⁺, 100%); HRMS m/z (ES+) calcd for C₂₄H₂₅NO₄Na 414.1680, found 414.1681.

A novel compound prepared according to a modified literature procedure.³⁸⁵

169) 2-(1-(*tert*-Butoxycarbonyl)-indol-3-yl)cyclopropane-1-carboxylic acid

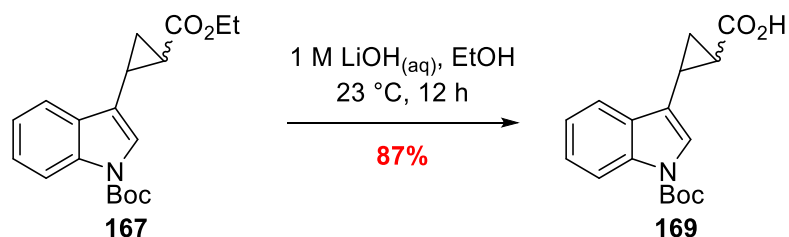


10% Pd/C (130 mg) was suspended in a solution of **168** (261 mg, 0.67 mmol) in methanol (6 mL) and stirred in a sealed flask. Hydrogen gas was then bubbled through the solution for 10 min and then the needle for the hydrogen feed was left in the flask above the solution. The mixture was stirred for 20 min before the reaction was determined complete *via* TLC. The catalyst was filtered off and the liquor collected was concentrated under reduced pressure to afford a diastereomeric mixture (79:21) of cyclopropyl acid **169** as a pale orange solid (187 mg, 93%); mp = 207–209 °C; ν_{max}/cm^{-1} 2978 (CH), 2934 (COOH), 1726 (CO, acid), 1688 (CO, carbamate); δ_H (400 MHz; CD₃OD) Resonances assignable to the major diastereomer: 1.38 (1 H, ddd, J = 8.3, 6.5, 4.2, CHCH H' CH or CHCH H' CH), 1.51–1.55 (1 H, m, CHCH H' CH or CHCH H' CH, appears as 2 H due to overlap with minor diastereomer resonances), 1.66 (9 H, s, C(CH₃)₃), 1.82 (1 H, ddd, J = 8.2, 5.0, 4.2, CH H' CHCO₂Bn), 2.45–2.51 (1 H, m,

CCHCHH'), 7.22–7.27 (1 H, m, CHCHCC or CHCHCNBoc), 7.31 (1 H, ddd, $J = 8.5, 7.2, 1.4$, CHCHCC or CHCHCNBoc), 7.35 (1 H, d, $J = 1.2$, CCHNBoc), 7.60 (1 H, ddd, $J = 7.7, 1.4, 0.7$, CHCHCC or CHCHCNBoc), 8.08 (1 H, d, $J = 8.3$, CHCHCC or CHCHCNBoc). **Resonances assignable to the minor diastereomer:** 1.40–1.45 (1 H, m CHCHH'CH or CHCHH'CH), 1.51–1.55 (1 H, m, CHCHH'CH or CHCHH'CH, Overlap with major diastereomer resonances), 1.67 (9 H, s, C(CH₃)₃), 2.17 (1 H, ddd, $J = 9.0, 7.7, 5.6$, CHH'CHCO₂Bn), 2.50–2.55 (1 H, m, CCHCHH'), 7.15–7.21 (1 H, m, CHCHCC or CHCHCNBoc), 7.64 (1 H, ddd, $J = 7.6, 1.4, 0.7$, CHCHCC or CHCHCNBoc), 8.04 (1 H, m, CHCHCC or CHCHCNBoc, overlap with major diastereomer resonance). Unable to unambiguously assign one of the CHCHCC or CHCHCNBoc protons, or the CCHNBoc proton, due to overlapping resonances; δ_c (101 MHz; CD₃OD) **Resonances assignable to the major diastereomer:** 15.6 (CH₂), 18.1 (CH), 22.7 (CH), 28.4 (CH₃), 84.9 (C), 116.2 (CH), 119.9 (CH), 121.7 (C), 122.9 (CH), 123.8 (CH), 125.7 (CH), 129.1 (C), 131.8 (C), 150.9 (C), 177.2 (C). **Resonances assignable to the minor diastereomer:** 11.8 (CH₂), 16.9 (CH), 21.2 (CH), 28.7 (CH₃), 29.8 (C), 116.0 (CH), 120.0 (CH), 123.5 (CH), 125.3 (CH), 134.0 (C), 136.9 (C), 151.0 (C), 177.1 (C). Unable to assign 1 quaternary and 1 tertiary carbon; **LRMS m/z (ES+)** 324.1 ([M + Na]⁺, 20%); **HRMS m/z (ES+)** calcd for C₁₇H₁₉NO₄Na 324.1212, found 324.1214.

A novel compound prepared according to a standard procedures.

169) 2-(1-(*tert*-Butoxycarbonyl)-indol-3-yl)cyclopropane-1-carboxylic acid

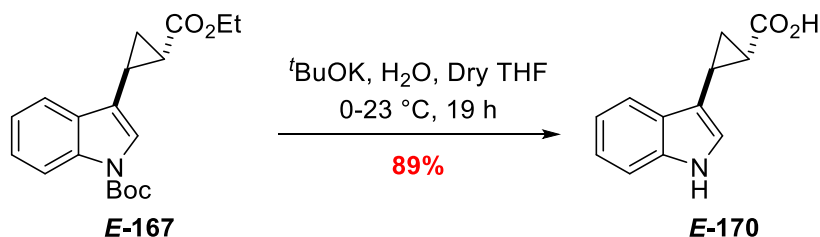


A solution of LiOH_(aq) (1 M, 0.61 mL, 0.61 mmol) was added to a solution of ester **167** (101 mg, 0.31 mmol) in EtOH (3 mL) and stirred at 23 °C. After 12 h, the reaction was determined complete *via* TLC ($R_f = 0.2$, 4:1 ethyl acetate:*n*-hexane). The reaction mixture was transferred to a separating funnel and then extracted with ethyl acetate (2 × 10 mL) to remove any neutral

organics remaining. The aqueous was acidified by addition of $\text{HCl}_{(\text{aq})}$ (1 M, 5 mL) and then extracted with ethyl acetate (3×10 mL). The combined organics were then washed with brine (30 mL), dried over MgSO_4 , filtered to remove the solids and then concentrated under reduced pressure to give acid **169** as an off-white solid (72 mg, 87%); **mp** = 210–212 °C; $\nu_{\text{max}}/\text{cm}^{-1}$ (neat) 2978 (CH), 2934 (COOH), 1726 (CO, acid), 1688 (CO, carbamate); δ_{H} (400 MHz; CD_3OD) **Resonances assignable to the major diastereomer**: 1.38 (1 H, ddd, $J = 8.3, 6.5, 4.2$, $\text{CHCHH}'\text{CH}$ or $\text{CHCHH}'\text{CH}$), 1.51–1.55 (1 H, m, $\text{CHCHH}'\text{CH}$ or $\text{CHCHH}'\text{CH}$, appears as 2 H due to overlap with minor diastereomer resonances), 1.66 (9 H, s, $\text{C}(\text{CH}_3)_3$), 1.82 (1 H, ddd, $J = 8.2, 5.0, 4.2$, $\text{CHH}'\text{CHCO}_2\text{Bn}$), 2.45–2.51 (1 H, m, CCHCHH'), 7.22–7.27 (1 H, m, CHCHCC or CHCHCNBoc), 7.31 (1 H, ddd, $J = 8.5, 7.2, 1.4$, CHCHCC or CHCHCNBoc), 7.35 (1 H, d, $J = 1.2$, CCHNBoc), 7.60 (1 H, ddd, $J = 7.7, 1.4, 0.7$, CHCHCC or CHCHCNBoc), 8.08 (1 H, d, $J = 8.3$, CHCHCC or CHCHCNBoc). **Resonances assignable to the minor diastereomer**: 1.40–1.45 (1 H, m $\text{CHCHH}'\text{CH}$ or $\text{CHCHH}'\text{CH}$), 1.51–1.55 (1 H, m, $\text{CHCHH}'\text{CH}$ or $\text{CHCHH}'\text{CH}$, Overlap with major diastereomer resonances), 1.67 (9 H, s, $\text{C}(\text{CH}_3)_3$), 2.17 (1 H, ddd, $J = 9.0, 7.7, 5.6$, $\text{CHH}'\text{CHCO}_2\text{Bn}$), 2.50–2.55 (1 H, m, CCHCHH'), 7.15–7.21 (1 H, m, CHCHCC or CHCHCNBoc), 7.64 (1 H, ddd, $J = 7.6, 1.4, 0.7$, CHCHCC or CHCHCNBoc), 8.04 (1 H, m, CHCHCC or CHCHCNBoc , overlap with major diastereomer resonance). Unable to unambiguously assign one of the CHCHCC or CHCHCNBoc protons, or the CCHNBoc proton, due to overlapping resonances; δ_{C} (101 MHz; CD_3OD) **Resonances assignable to the major diastereomer**: 15.6 (CH_2), 18.1 (CH), 22.7 (CH), 28.4 (CH_3), 84.9 (C), 116.2 (CH), 119.9 (CH), 121.7 (C), 122.9 (CH), 123.8 (CH), 125.7 (CH), 129.1 (C), 131.8 (C), 150.9 (C), 177.2 (C). **Resonances assignable to the minor diastereomer**: 11.8 (CH_2), 16.9 (CH), 21.2 (CH), 28.7 (CH_3), 29.8 (C), 116.0 (CH), 120.0 (CH), 123.5 (CH), 125.3 (CH), 134.0 (C), 136.9 (C), 151.0 (C), 177.1 (C). Unable to assign 1 quaternary and 1 tertiary carbon; **LRMS m/z (ES⁺)** 324.1 ($[\text{M} + \text{Na}]^+$, 20%); **HRMS m/z (ES⁺)** calcd for $\text{C}_{17}\text{H}_{19}\text{NO}_4\text{Na}$ 324.1212, found 324.1214.

A novel compound prepared according to a standard procedure.

E-170) 2-(Indol-3-yl)cyclopropane-1-carboxylic acid

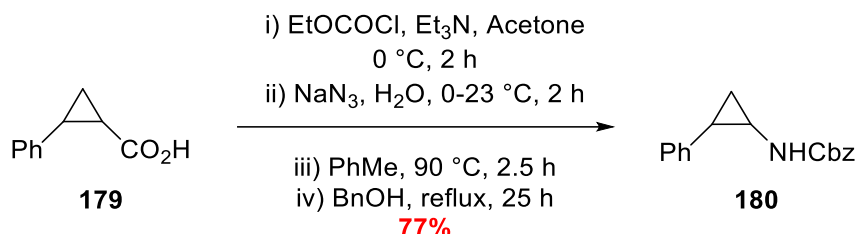


A flame-dried flask was charged with a suspension of $t\text{BuOK}$ (1.23 g, 11.0 mmol) in anhydrous tetrahydrofuran (10 mL) and sealed under an atmosphere of argon. The resulting solution was cooled to 0 °C and water (50 μL) was added. After 10 min, a solution of ester **E-167** (421 mg, 1.28 mmol) in anhydrous tetrahydrofuran (10 mL) was added dropwise over 5 min to the cooled solution causing the mixture to change colour from a white precipitate to a dark brown solution. The reaction mixture was then allowed to passively warm to 23 °C. After 19 h, the reaction was determined complete *via* TLC ($R_f = 0.1$, 100% ethyl acetate) and was subsequently quenched by the addition of water (20 mL). The basic quenched solution was then extracted with ethyl acetate (2×10 mL) to remove any remaining organic material. After acidification of the collected aqueous portion with $\text{HCl}_{(\text{aq})}$ (1 M, 15 mL), the aqueous was extracted with ethyl acetate (5×10 mL). The combined organics were washed with water (2×10 mL) and brine (20 mL) and dried over MgSO_4 . The solids were removed by suction filtration and the mother liquor was concentrated under reduced pressure to give acid **E-170** as a pale brown solid (230 mg, 89%) with no need for further purification; **mp** = 234–235 °C; $\nu_{\text{max}}/\text{cm}^{-1}$ (neat) 3391 (NH), 2924 (COOH), 1673 (CO); δ_{H} (400 MHz; CDCl_3) 1.35 (1 H, ddd, $J = 8.2, 6.6, 4.0$, CCHCHH'CHCO₂H), 1.51 (1 H, ddd, $J = 9.1, 5.0, 4.0$, CCHCHH'CHCO₂H), 1.76 (1 H, ddd, $J = 8.2, 5.0, 4.1$, CCHCHH'CHCO₂H), 2.54 (1 H, dddd, $J = 9.1, 6.6, 4.1, 1.0$, CCHCHH'CHCO₂H), 6.98 (1 H, d, $J = 1.0$, CCHNH), 7.01 (1 H, ddd, $J = 7.9, 7.0, 1.2$, CHCHCC or CHCHCNH), 7.09 (1 H, ddd, $J = 8.1, 7.0, 1.2$, CHCHCC or CHCHCNH), 7.29–7.34 (1 H, m, $J = 8.1, 1.2$, CHCHCC or CHCHCNH), 7.56 (1 H, dd, $J = 7.9, 1.2$, CHCHCC or CHCHCNH); δ_{C} (101 MHz; CDCl_3) 16.0 (CH₂), 19.4 (CH), 23.1 (CH), 112.3 (CH), 115.5 (C), 119.2 (CH), 119.9 (CH), 122.4 (CH), 122.6 (CH), 128.8 (C), 138.1 (C), 178.1 (CO); **LRMS m/z (ES⁺)** 224.1

([M + Na]⁺, 100%), 201.1 ([M + H]⁺, 90); **HRMS *m/z* (ES⁺)** calcd for C₁₂H₁₁NO₂Na 224.0687, found 224.0693.

*A novel compound prepared according to a literature procedure.*²⁰⁰

180) Benzyl (2-phenylcyclopropyl)carbamate

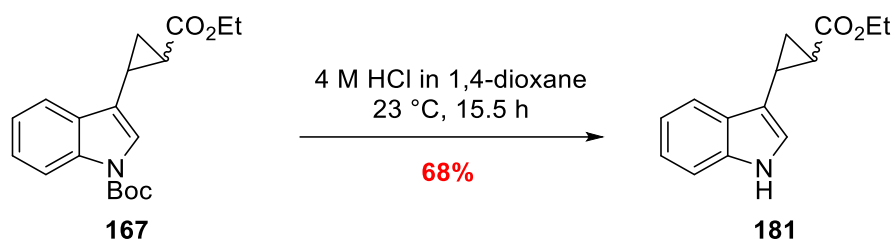


Acid **179** (200 mg, 1.23 mmol) was solubilised in a solution of anhydrous acetone (mL) and triethylamine (0.22 mL, 1.60 mmol) and cooled to 0 °C under an atmosphere of argon. Ethyl chloroformate (0.18 mL, 1.85 mmol) was then added dropwise over 1 min and the resulting solution was stirred until all the starting material had been consumed by TLC. A solution of sodium azide (289 mg, 4.44 mmol) in water (3 mL) was then added to the acyl carbonate and stirred vigorously for 2 h until no acyl carbonate was visible by TLC (acyl carbonate R_f = 0.3, acyl azide R_f = 0.4, 4:1 *n*-hexane:ethyl acetate). The resulting mixture was poured into water (10 mL) and was extracted with toluene (2 × 10 mL), the combined organic washes were then washed with water (2 × 10 mL) and brine (20 mL), dried over MgSO₄ and concentrated to ~5 mL and then heated to 90 °C. After 2.5 h, the solution was reduced to a fifth of its volume and BnOH (0.64 mL, 6.16 mmol) was then added and heated to reflux. After 25 h, the reaction was determined complete *via* TLC (R_f = 0.3, 4:1 *n*-hexane:ethyl acetate) and was concentrated under reduced pressure to remove the volatiles. The crude was loaded directly on to silica and purified *via* flash column chromatography (R_f = 0.3, 4:1 *n*-hexane:ethyl acetate) to yield carbamate **180** as a white crystalline solid (255 mg, 77%); $\nu_{\max}/\text{cm}^{-1}$ (neat) 3252 (NH), 3130 (CH), 3059 (CH), 2942 (CH), 1701 (CO); δ_H (400 MHz; CDCl₃) 1.06 (1 H, m, CHCHH'CH or CHCHH'CH), 1.33 (1 H, m, CHCHH'CH or CHCHH'CH), 2.29 (1 H, m, PhCH), 2.99 (1 H, m, CHNHCbz), 4.40 (1 H, s, NH), 4.96 (1 H, d, J = 12.2, CO₂CHH'), 5.07 (1 H, d, J = 12.2,

CO₂CHH'), 7.10–7.42 (10 H, Stack, *Ar-H*); δ_c (101 MHz; CDCl₃) 12.1 (CH₂), 21.9 (CH), 29.2 (CH), 66.6 (CH₂), 119.1 (C) 126.6 (CH), 128.1 (CH), 128.4 (CH), 128.5 (CH), 128.8 (CH), 142.0 (C), 153.5 (CO); LRMS *m/z* (ES+) 290.4 ([M + Na + H]⁺, 100%).

A known compound prepared according to a modified literature procedure.^{208, 386} The recorded data are in agreement with that reported in the literature.³⁸⁶ Starting material 179 was prepared via a literature protocol.³⁸⁵

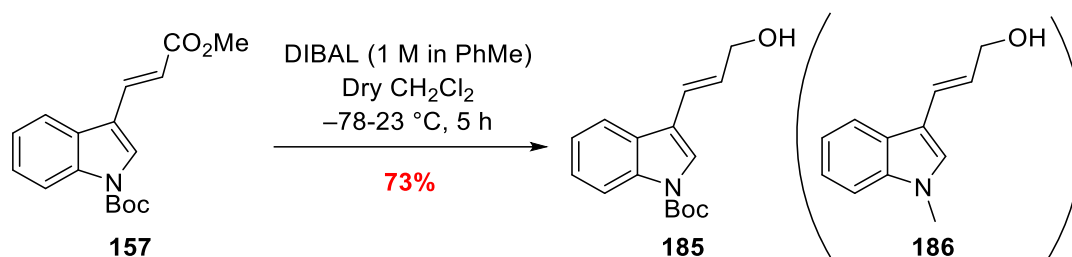
181) Ethyl 2-(indol-3-yl)cyclopropane-1-carboxylate



N-Boc indole **167** was solubilised in a solution of HCl in 1,4-dioxane (4 M, 5 mL) and stirred at 23 °C. After 15 h, the reaction was determined complete *via* TLC (*R_f* = 0.2, ethyl acetate: *n*-hexane) and was concentrated under reduced pressure. The crude material was loaded on to silica and purified by elution through a 3 cm silica plug (2 × 30 mL 1:1 ethyl acetate:*n*-hexane then 10% MeOH in ethyl acetate 30 mL). The methanolic fraction was concentrated under reduced pressure to yield ester **181** as a light brown oil (54 mg, 68%); $\nu_{\max}/\text{cm}^{-1}$ (neat) 3405 (NH), 2981 (CH), 1703 (CO); δ_H (400 MHz; CDCl₃) 1.26–1.35 (4 H, Stack, CH₂CH₃ and CHCHH'CH or CHCHH'CH), 1.58 (1 H, ddd, *J* = 9.1, 5.0, 4.1, CHCHH'CH or CHCHH'CH), 1.90 (1 H, ddd, *J* = 8.3, 5.0, 4.1, CCHCHH'CHCO₂H), 2.62 (1 H, dddd, *J* = 9.1, 6.5, 4.1, 1.0, CCHCHH'CHCO₂H), 4.21 (2 H, q, *J* = 7.1, CH₂CH₃), 6.95 (1 H, dd, *J* = 2.5, 1.0, CCHNH), 7.14 (1 H, ddd, *J* = 7.9, 7.0, 1.1, CHCHCC or CHCHCNH), 7.21 (1 H, ddd, *J* = 8.2, 7.0, 1.4, CHCHCC or CHCHCNH), 7.35 (1 H, dd, *J* = 8.2, 1.1, CHCHCC or CHCHCNH), 7.68 (1 H, dd, *J* = 7.9, 1.4, CHCHCC or CHCHCNH), 7.98 (1 H, s, NH); δ_c (101 MHz; CDCl₃) 14.5 (CH), 15.7 (CH₂), 18.2 (CH), 22.2 (CH₃), 60.7 (CH₂), 111.3 (CH), 116.0 (C), 119.1 (CH), 119.8 (CH), 121.1 (CH), 122.5 (CH), 127.6 (C), 136.4 (C), 174.3 (CO); LRMS *m/z* (ES+) 230.1 ([M + H]⁺, 53%), 184.1 ([M – OEt]⁺, 100); HRMS *m/z* (ES+) calcd for C₁₄H₁₆NO₂ 230.1181, found 230.1187.

A novel compound prepared according to a standard procedure.

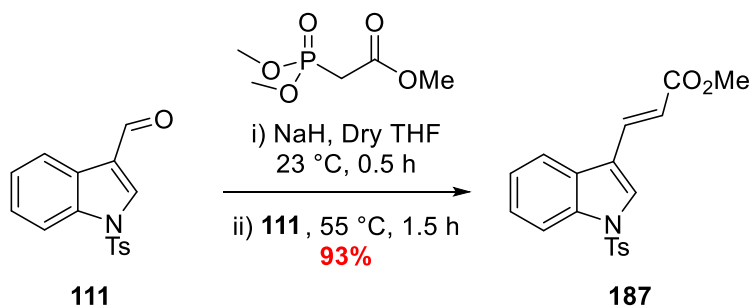
185) tert-Butyl E-3-(3-hydroxyprop-1-en-1-yl)-indole-1-carboxylate



Ester **157** (500 mg, 1.66 mmol) was solubilised in anhydrous CH₂Cl₂ (15 mL) and cooled to -78 °C under an atmosphere of argon. DIBAL (1 M in PhMe, 3.98 mmol, 4.0 mL) was then added to the cooled solution dropwise over 5 min resulting in a colour change of the reaction mixture from clear orange to a clear yellow solution. The reaction mixture was stirred for 3.5 h at -78 °C and then allowed to warm to 23 °C. After a further 1.5 h, the reaction was determined complete *via* TLC ($R_f = 0.5$, 1:1 ethyl acetate:*n*-hexane) and quenched *via* the slow addition of water (5 mL). The resulting solution was further diluted with a solution of sodium potassium tartrate (Sat. Soln, 20 mL) and stirred vigorously. After 1 h, the solution was extracted with ethyl acetate (10 mL) and the resulting phases were separated. The organic phase was washed with water (2 × 10 mL) and brine (20 mL), dried over MgSO₄, filtered and concentrated under reduced pressure. The crude oil was subjected to flash column chromatography ($R_f = 0.5$, 1:1 ethyl acetate:*n*-hexane) to yield *E*-allylic alcohol **185** as a white solid (333 mg, 73%); $\nu_{\max}/\text{cm}^{-1}$ (neat) 3377 (OH), 2978 (CH), 2929 (CH), 1730 (CO); δ_H (400 MHz; CDCl₃) 1.68 (9 H, s, C(CH₃)₃), 4.33–4.42 (2 H, d, $J = 5.8$, CHCH₂OH), 6.46 (1 H, dt, $J = 16.0, 5.8$), 6.72 (1 H, d, $J = 16.0$), 7.25–7.36 (2 H, Stack, CHCHCC and CHCHCNBoc), 7.62 (1 H, s, CCHNBoc), 7.78 (1 H, d, $J = 8.1$, CHCHCC or CHCHCNBoc), 8.17 (1 H, d, $J = 8.1$, CHCHCC or CHCHCNBoc); δ_C (101 MHz; CDCl₃) 28.3 (C(CH₃)₃), 64.4 (CH₂), 84.1 (C), 115.5 (CH), 118.3 (C), 120.0 (CH), 122.8 (CH), 123.1 (CH), 124.1 (CH), 124.8 (CH), 128.9 (CH), 136.0 (C), 149.7 (C); LRMS m/z (ES⁻) 239.1 ([M - ^tBu + Na]⁻, 100%), 223.1 ([M - ^tBu]⁻, 30).

A known compound prepared via a novel procedure.³⁸¹ The recorded data are in agreement with that reported in the literature with the exception of a the missing carbamate carbonyl resonance from the ¹³C-NMR spectrum.³⁸¹ **186** was evidenced via LC-MS (ES+) 188.3.

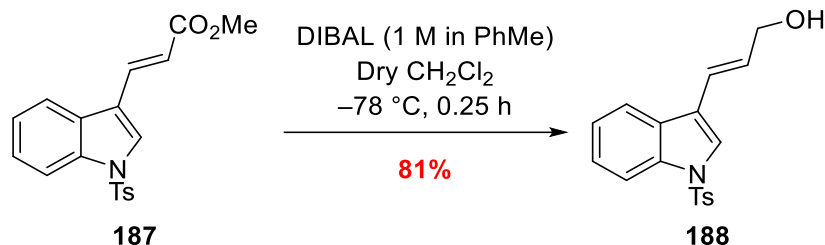
187) Methyl *E*-3-(1-tosylindol-3-yl)acrylate



Freshly triturated (from *n*-hexane, 2 × 5 mL) and dried sodium hydride (295 mg, 5.51 mmol) was suspended in a solution of trimethyl phosphonoacetate (0.22 mL, 1.35 mmol) in anhydrous tetrahydrofuran (25 mL) and stirred under an atmosphere of argon at 23 °C. After 0.5 h, aldehyde **111** (1.50 g, 5.01 mmol) was added and the temperature increased to 55 °C for 1.5 h. Upon complete consumption of starting material, the reaction mixture was diluted with water (25 mL) and the organic extracted with ethyl acetate (25 mL). The resultant phases were separated and the organic layer washed with water (2 × 10 mL) and brine (20 mL), dried over MgSO₄, filtered and concentrated under reduced pressure to give pure ester **187** as a pale orange solid (1.65 g, 93%); $\nu_{\max}/\text{cm}^{-1}$ (neat) 3118 (vinyl-CH), 3063 (CH), 2956 (CH), 1706 (CO), 1635 (Conj. C=C), 1318 (SO), 1159 (SO); δ_{H} (400 MHz; CDCl₃) 2.35 (3 H, s, Ts-CH₃), 3.82 (3 H, s, CO₂C), 6.52 (1 H, d, *J* = 16.1, CCHCHCO₂CH₃), 7.24 (2 H, Stack, Ts *Ar*-H), 7.32 (1 H, ddd, *J* = 8.4, 7.2, 1.1, CHCHCC or CHCHCNTs), 7.38 (1 H, ddd, *J* = 8.4, 7.2, 1.1, CHCHCC or CHCHCNTs), 7.75–7.87 (5 H, Stack, Ts *Ar*-H and CCHCHCO₂CH₃ and CHCHCC or CHCHCNTs), 8.00 (1 H, dt, *J* = 8.2, 1.1, CHCHCC or CHCHCNTs); δ_{C} (101 MHz; CDCl₃) 21.8 (CH₃), 51.9 (CH₃), 114.0 (CH), 118.0 (CH), 118.2 (C), 120.8 (CH), 124.2 (CH), 125.7 (CH), 127.1 (CH), 128.2 (C), 128.6 (CH), 130.3 (CH), 134.9 (C), 135.7 (C), 136.0 (CH), 145.7 (C), 167.7 (CO); LRMS *m/z* (ES+) 356.1 ([M + H]⁺, 45%), 324.1 ([M – OMe + H]⁺, 100).

A known compound prepared according to a modified literature procedure.^{212, 383} The recorded data are in agreement with that reported in the literature.²¹²

188) *E*-3-(1-Tosylindol-3-yl)prop-2-en-1-ol

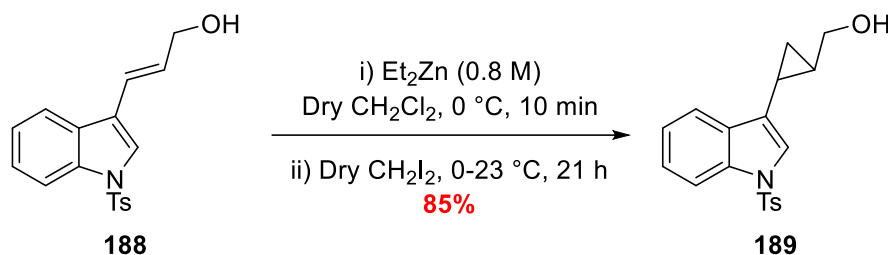


A flame-dried flask containing ester **187** (1.30 g, 3.66 mmol) was charged with anhydrous CH₂CH₂ and the resulting solution was cooled to -78 °C under an atmosphere of argon. A solution of DIBAL (8.4 mL, 8.41 mmol, 1 M in PhMe) was added dropwise over a period of 5 min. After 15 min, the reaction was determined complete *via* TLC ($R_f = 0.1$, 3:1 *n*-hexane:ethyl acetate) and, whilst still at -78 °C, was quenched by addition of MeOH (6 mL). The resulting solution was stirred vigorously, removed from the dry ice/acetone bath and allowed to warm to 23 °C. The quenched solution was diluted further with a solution of Rochelle's salt (Sat. Soln, 25 mL) and stirred. After a period of 1 h, the solution was extracted with CH₂Cl₂ (20 mL) and the two resulting phases were separated. The aqueous phase was washed with CH₂Cl₂ (20 mL) and the combined organics were washed with water (4 × 20 mL) and brine (30 mL). The organics were then dried over MgSO₄, filtered to remove the solids and then concentrated under reduced pressure. The crude material was subjected to flash column chromatography ($R_f = 0.3$, 1:1 *n*-hexane:ethyl acetate) to yield alcohol **188** as a white solid (971 mg, 81%); $\nu_{\max}/\text{cm}^{-1}$ (neat) 3584 (OH), 3125 (vinyl-CH), 3057 (CH), 2868 (CH), 1593 (C=C), 1363 (SO), 1170 (SO); δ_H (400 MHz; CDCl₃) 2.33 (3 H, s, Ts-CH₃), 4.35 (2 H, dd, $J = 5.7, 1.6$, CHCH₂OH), 6.44 (1 H, dt, $J = 16.0, 5.7$, CCHCHCH₂), 6.69 (1 H, d, $J = 16.0$, CCHCHCH₂), 7.19–7.23 (2 H, AA'BB', Ts *Ar-H*), 7.27 (1 H, ddd, $J = 8.4, 7.4, 1.3$, CHCHCC or CHCHCNTs), 7.33 (1 H, ddd, $J = 8.4, 7.4, 1.1$, CHCHCC or CHCHCNTs), 7.59 (1 H, s, CCHNTs), 7.72 (1 H, dt, $J = 7.4, 1.1, 1.1$), 7.76 (1 H, AA'BB', Ts *Ar-H*), 7.99 (1 H, dt, $J = 8.4, 1.1$, CHCHCC or CHCHCNTs); δ_C (101 MHz; CDCl₃) 21.7 (CH₃), 64.1 (CH₂), 113.9 (CH), 120.1 (C), 120.5 (CH), 121.9 (CH),

123.7 (CH), 124.2 (CH), 125.1 (CH), 127.0 (CH), 129.1 (C), 129.9 (CH), 130.1 (CH), 135.2 (C), 135.6 (C), 145.2 (C); **LRMS m/z (ES+)** 310 ($[M - OH + H]^+$, 100%).

A known compound prepared according to a literature procedure.³⁸⁷ The recorded data are in agreement with that reported in the literature.³⁸⁷

189) (2-(1-Tosylindol-3-yl)cyclopropyl)methanol

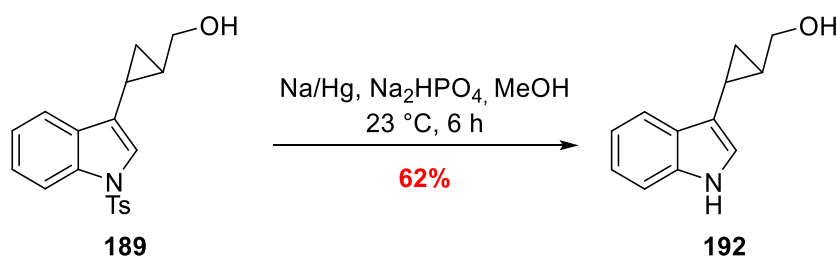


A flame-dried flask containing alkene **188** (900 mg, 2.75 mmol) was charged with anhydrous CH_2Cl_2 (20 mL) and the resulting solution was cooled to 0 °C under an atmosphere of argon. Once at 0 °C, Et_2Zn (15.5 mL, 12.4 mmol, 0.8 M in hexanes) was added *via* a flame-dried glass syringe and metal needle over a period of 5 min. After a 15 min maturation period, a solution of anhydrous CH_2I_2 (1.0 mL, 12.4 mmol) in anhydrous CH_2Cl_2 (2 mL) was added dropwise over a period of 5 min. The reaction mixture was allowed to passively warm to 23 °C and after a period of 21 h the reaction was determined complete *via* TLC ($R_f = 0.3$, 1:1 *n*-hexane:ethyl acetate, the product has the same R_f as the starting material but completion was determined by a lack of staining when exposed to iodine-dip). The reaction mixture was cooled to 0 °C and a solution of $\text{Na}_2\text{SO}_4(\text{aq})$ (Sat. Soln., ~5 mL) was added dropwise until the effervescence ceased, at this point the reaction mixture was exposed to air and diluted further with additional $\text{Na}_2\text{SO}_4(\text{aq})$ (Sat. Soln., 40 mL). After 15 minutes of vigorous stirring, the solution was acidified with $\text{HCl}(\text{aq})$ (4 M, 20 mL), extracted with CH_2Cl_2 (20 mL) and then the two phases were separated. The aqueous layer was washed with CH_2Cl_2 (2×20 mL) and the combined organics were washed with water (2×30 mL), dried over MgSO_4 , filtered to remove the solids and concentrated under reduced pressure. The crude material was then subjected to flash column chromatography ($R_f = 0.3$, 1:1 *n*-hexane:ethyl acetate) to yield cyclopropane **189** as a white solid (795 mg, 85%) $\nu_{\text{max}}/\text{cm}^{-1}$ (neat) 3373 (OH), 2920 (CH), 1365 (SO), 1171 (SO); δ_H (400

MHz; CDCl₃) 0.90 (1 H, dt, $J = 8.5, 5.1$, CHCHH'CH), 0.96 (1 H, dt, $J = 8.5, 5.1$, CHCHH'CH), 1.33–1.43 (1 H, m, CHCHH'CH), 1.48 (1 H, app. t, $J = 4.0$, OH), 1.79 (1 H, dddd, $J = 8.6, 5.5, 4.5, 1.2$, CCHCHH'CH), 2.33 (3 H, s, Ts-CH₃), 3.62 (1 H, ddd, $J = 10.8, 6.5, 4.0$, CHCHH'OH), 3.71 (1 H, ddd, $J = 10.8, 6.5, 4.0$, CHCHH'OH), 7.20 (3 H, Stack, Ts Ar-H and CCHNTs), 7.23 (1 H, m, CHCHCC or CHCHCNTs), 7.31 (1 H, ddd, $J = 8.4, 7.2, 1.0$, CHCHCC or CHCHCNTs), 7.62 (1 H, dt, $J = 7.8, 1.0$, CHCHCC or CHCHCNTs), 7.71–7.75 (2 H, AA'BB', Ts Ar-H), 7.96 (1 H, dt, $J = 8.3, 1.0$, CHCHCC or CHCHCNTs); δ_c (**101 MHz; CDCl₃**) 11.3 (CH₂), 11.9 (CH), 21.7 (CH₃), 23.1 (CH), 66.6 (CH₂), 113.9 (CH), 119.7 (CH), 121.9 (CH), 123.2 (CH), 124.5 (C), 124.9 (CH), 126.9 (CH), 127.5 (C), 130.0 (CH), 131.4 (C), 135.4 (C), 144.9 (C); **LRMS m/z (ES⁺)** 342.1 ([M + H]⁺, 25%), 324 ([M - OH - H]⁺, 100).

A known compound prepared according to a literature procedure.³⁸⁸ The recorded data are in agreement with that reported in the literature.³⁸⁸

192) (2-(Indol-3-yl)cyclopropyl)methanol

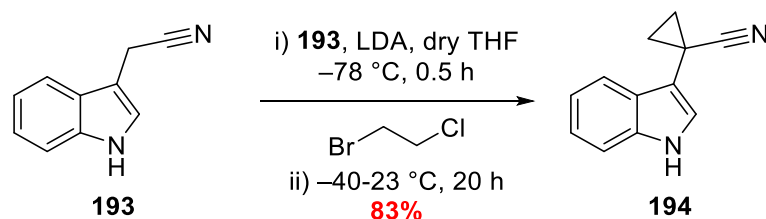


A flame-dried flask containing *N*-tosyl indole **189** (50 mg, 0.15 mmol), Na₂HPO₄ (83 mg, 0.59 mmol) and freshly ground sodium amalgam (101 mg, 20% Na) was charged with anhydrous MeOH (1.5 mL) and the resulting solution was stirred vigorously at 23 °C. After 6 h, the reaction was determined complete *via* TLC ($R_f = 0.4$, 3:1 ethyl acetate:*n*-hexane, product and starting material have very similar masses but the two could be discriminated *via* vanillin staining) and was quenched by addition of water (10 mL). The quenched solution was extracted with ethyl acetate (10 mL) and the resultant phases were separated. The organic phase was then washed with water (2 × 10 mL), brine (20 mL), dried over MgSO₄, filtered to remove the solids and concentrated under reduced pressure. The crude material was later subjected to flash column chromatography ($R_f = 0.4$, 6:4 ethyl acetate:*n*-hexane) to yield indole **192** as a

colourless oil (17 mg, 62%); $\nu_{\max}/\text{cm}^{-1}$ (neat) 3407 (NH), 3304 (OH), 3057 (CH), 3004 (CH), 2923 (CH); δ_H (400 MHz; CDCl_3) 0.87 (1 H, ddd, $J = 8.7, 5.3, 4.5$, CHCHH'CH), 0.96 (1 H, ddd, $J = 8.3, 5.3, 4.5$, CHCHH'CH), 1.38–1.47 (1 H, m, CHCHH'CH), 1.63 (1 H, s, OH), 1.90 (1 H, dddd, $J = 8.7, 5.3, 4.5, 1.0$, CCHCHH'CH), 3.68 (1 H, d, $J = 0.9$, CHCHH'OH), 3.70 (1 H, d, $J = 0.9$, CHCHH'OH), 6.90 (1 H, dd, $J = 2.5, 1.0$, CCHNH), 7.14 (1 H, ddd, $J = 7.9, 7.0, 1.3$, CHCHCC or CHCHCNH), 7.20 (1 H, ddd, $J = 8.2, 7.0, 1.2$, CHCHCC or CHCHCNH), 7.34 (1 H, dt, $J = 8.2, 1.2$, CHCHCC or CHCHCNH), 7.73 (1 H, dt, $J = 7.9, 1.3$, CHCHCC or CHCHCNH), 7.93 (1 H, d, $J = 2.5$, NH); δ_C (101 MHz; CDCl_3) 11.4 (CH_2), 12.4 (CH), 22.9 z, 67.2 (CH_2), 111.3 (CH), 117.7 (C), 119.1 (CH), 119.5 (CH), 120.7 (CH), 122.3 (CH), 127.9 (C), 136.4 (C); LRMS m/z (EI+) 187.2 ($[\text{M}]^+$, 10%); HRMS m/z (EI+) calcd for $\text{C}_{12}\text{H}_{13}\text{NO}$ 187.0997, found 187.0998.

A novel compound prepared according to a literature procedure.²¹²

194) 1-(Indol-3-yl)cyclopropane-1-carbonitrile

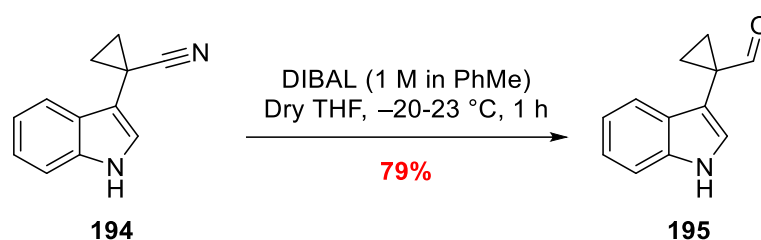


A solution of *n*-BuLi in hexanes (2.25 M, 22.8 mL, 51.2 mmol) was added to a flame-dried, two-neck round-bottom flask that had been charged with anhydrous tetrahydrofuran (5 mL) and cooled to -40 °C under an atmosphere of argon. Freshly distilled (*i*-Pr)₂NH (7.20 mL, 51.2 mmol) was then added to the cooled *n*-BuLi/tetrahydrofuran solution dropwise over 5 min while maintaining the temperature at -40 °C. After 0.5 h, the resulting LDA solution was transferred *via* cannula (by positive pressure of argon) to a solution of nitrile **193** (2.00 g, 12.8 mmol) in anhydrous tetrahydrofuran (20 mL) which had been cooled to -78 °C. The resulting solution was allowed to mature for 0.5 h, in which time a yellow suspension had formed signifying the formation of the nitrile anion. 1-bromo-2-chloroethane (1.60 mL, 19.2 mmol) was then added in one portion and the solution immediately turned to a brown translucent solution. The

resulting brown solution was allowed to warm passively to 23 °C and after 20 h the reaction was determined complete *via* TLC. The reaction mixture was quenched by slow addition of water (20 mL) and then diluted further with ethyl acetate (20 mL). The two layers were separated and the organic was washed with HCl_(aq) (2 M, 2 × 20 mL), water (20 mL) and brine (40 mL). After drying over MgSO₄, the solids were filtered off and the organic was concentrated to give the crude as a brown oil. The crude was subjected to flash column chromatography (R_f = 0.5, 1:1 *n*-hexane:ethyl acetate) and the product-containing fractions were combined, concentrated and recrystallised from hot *n*-hexane and ethyl acetate to afford 1,1'-cyclopropane **194** as pale-yellow needle-like crystals (1.94 g, 83%); **mp** = 168–170°C; $\nu_{\text{max}}/\text{cm}^{-1}$ (neat) 3392 (NH), 3126 (CH), 2093 (CH), 3057 (CH), 2227 (CN); δ_H (400 MHz; CDCl₃) 1.34–1.39 (2 H, AA'BB', Cyclopropane CH₂), 1.64–1.69 (2 H, AA'BB', Cyclopropane CH₂), 7.11 (1 H, d, J = 2.6, CCHNH), 7.21 (1 H, td, J = 8.1, 7.2, 1.4, CHCHCC or CHCHCNH), 7.26 (1 H, td, J = 7.7, 7.2, 1.4, CHCHCC or CHCHCNH), 7.38 (1 H, dd, J = 8.1, 1.4, CHCHCC or CHCHCNH), 7.83 (1 H, dd, J = 7.7, 1.4, CHCHCC or CHCHCNH), 8.13 (1 H, s, NH); δ_C (101 MHz; CDCl₃) 5.9 (C), 15.5 (2 × CH₂), 111.7 (CH), 112.0 (C), 119.0 (CH), 120.5 (CH), 123.1 (CH), 123.3 (CH), 126.5 (C), 136.3 (C), one quaternary-C (CN) resonance was not observed; **LRMS m/z (ES+)** 183.1 ([M + H]⁺, 100%), 156.1 ([M – CN]⁺, 95); **HRMS m/z (ES+)** calcd for C₁₂H₁₁N₂183.0922, found 183.0921.

A reported compound prepared according to a modified literature procedure.²²⁰ No reference data is available to compare the recorded spectra to.

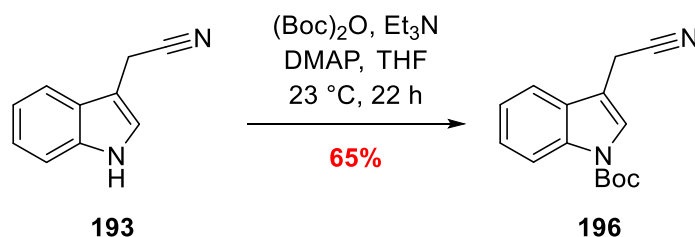
195) 1-(Indol-3-yl)cyclopropane-1-carbaldehyde



A solution of DIBAL (4.30 mL, 4.28 mmol, 1.0 M) in toluene was added dropwise over 20 min to a stirred solution of nitrile **194** (600 mg, 3.29 mmol) in anhydrous tetrahydrofuran (10 mL) which had been cooled to $-20\text{ }^{\circ}\text{C}$ under argon. After a further 40 min, the reaction was determined complete *via* TLC. Upon completion, the remaining DIBAL was quenched *via* dropwise addition of MeOH (2.5 mL) over 5 min. The reaction mixture was then diluted further with a solution of Rochelle's salt (Sat. soln, 20 mL) and allowed to stir. After 1 h, the mixture was extracted with ethyl acetate (15 mL). The two-phases were separated and the aqueous was back-extracted with ethyl acetate ($2 \times 10\text{ mL}$) and the combined organics were washed with water ($2 \times 10\text{ mL}$) and brine (20 mL), dried over MgSO_4 , filtered and concentrated to afford the crude as a yellow oil. The crude oil was subjected to flash column chromatography ($R_f = 0.4$, 6:4 *n*-hexane:ethyl acetate) to afford aldehyde **195** as a colourless oil (481 mg, 79%); $\nu_{\text{max}}/\text{cm}^{-1}$ (neat) 3376 s (NH), 3092 (CH), 3055 (CH), 3009 (CH), 2829 (CH – aldehyde), 2721 (CH – aldehyde), 1699 (CO); δ_{H} (400 MHz; CDCl_3) 1.38–1.42 (2 H, AA'BB', CH_2), 1.63–1.67 (2 H, AA'BB', CH'_2), 7.12 (1 H, d, $J = 2.5$, CCHNH), 7.15 (1 H, ddd, $J = 8.2, 7.2, 1.3$, CHCHCC or CHCHCNH), 7.24 (1 H, ddd, $J = 8.2, 7.2, 1.3$, CHCHCC or CHCHCNH), 7.39 (1 H, dt, $J = 8.1, 0.9$, CHCHCC or CHCHCNH), 7.59 (1 H, dt, $J = 8.1, 0.9$, CHCHCC or CHCHCNH), 8.13 (1 H, s, NH), 9.45 (1 H, s, CHO); δ_{C} (101 MHz; CDCl_3) 16.5 ($2 \times \text{CH}_2$), 29.0 (C), 111.6 (CH), 113.7 (C), 119.2 (CH), 120.1 (CH), 122.7 (CH), 124.3 (CH), 128.0 (C), 136.4 (C), 202.3 (CHO); LRMS m/z (ES+) 208.1 ($[\text{M} + \text{Na}]^+$, 100%); 186.1 ($[\text{M} + \text{H}]^+$, 5); HRMS m/z (TOF ES+) calcd for $\text{C}_{12}\text{H}_{11}\text{NONa}$ 208.0739, found 208.0738.

A literature compound prepared according to a modified literature procedure.²²⁰ The recorded data are in agreement with that reported in the literature.³⁸⁹

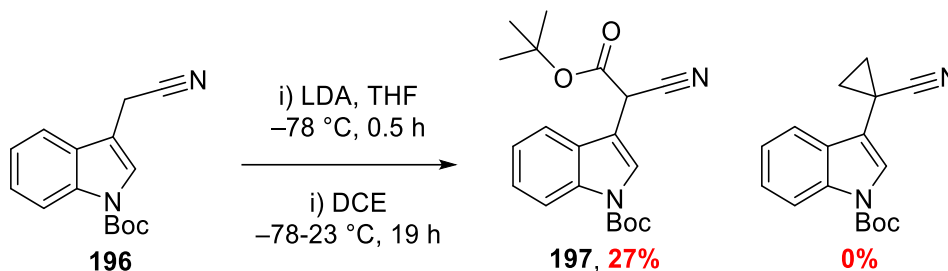
196) *tert*-Butyl 3-(cyanomethyl)-indole-1-carboxylate



Indole **193** (2.00 g, 12.8 mmol) was dissolved in a solution of Di-*tert*-butyl dicarbonate (3.63 g, 16.6 mmol), triethylamine (2.30 mL, 16.6 mmol) and DMAP (156 mg, 1.28 mmol) in tetrahydrofuran (25 mL). The resulting solution was stirred at 23 °C for 22 h until determined complete *via* TLC ($R_f = 0.7$, 1:1 *n*-hexane:ethyl acetate). The reaction mixture was quenched by the addition of with $\text{HCl}_{(\text{aq})}$ (1 M, 20 mL) and stirred for 5 minutes. The layers were separated and the organic washed with water (2 × 20 mL) and brine (1 × 30 mL), dried over MgSO_4 , filtered and concentrated under reduced pressure. The crude material was subjected to flash column chromatography ($R_f = 0.3$, 4:1 *n*-hexane:ethyl acetate) to give *N*-Boc indole **196** as a white powder (2.13 g, 65%); $\nu_{\text{max}}/\text{cm}^{-1}$ (neat) 3126 (CH), 3011 (CH), 2978 (CH), 2250 (CN), 1742 (CO); δ_H (400 MHz; CDCl_3) 1.68 (9 H, s, $\text{C}(\text{CH}_3)_3$), 3.77 (2 H, d, $J = 1.3$, CCH_2CN), 7.30 (1 H, ddd, $J = 8.2, 7.3, 1.1$, CHCHCC or CHCHCNBoc), 7.38 (1 H, ddd, $J = 8.5, 7.3, 1.3$, CHCHCC or CHCHCNBoc), 7.48–7.55 (1 H, m, CHCHCC or CHCHCNBoc), 7.64 (1 H, t, $J = 1.3$, CCHNBoc), 8.18 (1 H, d, $J = 8.3$, CHCHCC or CHCHCNH); δ_C (101 MHz; CDCl_3) 14.5 (CH_2), 28.3 ($\text{C}(\text{CH}_3)_3$), 86.0 (C), 109.6 (C), 115.7 (CH), 117.2 (C), 118.3 (CH), 123.1 (CH), 124.4 (CH), 125.3 (CH), 149.4 (C), 161.7 (CO); LRMS m/z (ES+) 257.3 ($[\text{M} + \text{H}]^+$, 100%).

*A known compound prepared according to a literature procedure. The recorded data are in agreement with that reported in the literature.*³⁹⁰

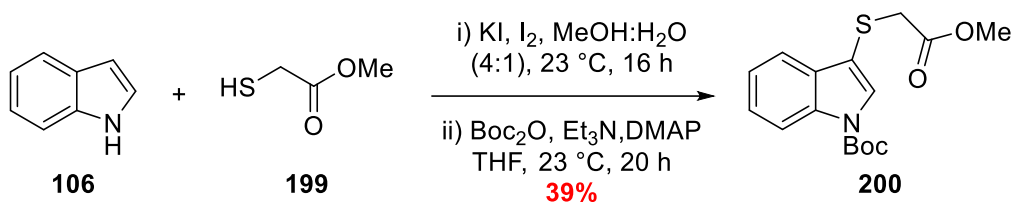
197) tert-Butyl 3-(2-(tert-butoxy)-1-cyano-2-oxoethyl)-indole-1-carboxylate



A solution of *n*BuLi (2.29 M, 1.56 mL, 3.90 mmol) was added to a cooled ($0\text{ }^{\circ}\text{C}$) solution of freshly distilled (*i*Pr)₂NH (0.55 mL, 3.90 mmol) in anhydrous tetrahydrofuran (5 mL) and allowed to mature for 0.5 h before being cooled to $-78\text{ }^{\circ}\text{C}$. A solution of nitrile **196** (400 mg, 1.56 mmol) in anhydrous tetrahydrofuran (5 mL) was added dropwise to the freshly prepared LDA solution over 5 min. The resulting solution was stirred for 0.5 h before a solution of 1,2-dichloroethane (0.18 mL, 2.34 mmol) in anhydrous tetrahydrofuran (5 mL) was added dropwise over a period of 2 h. Upon completion of the addition, the reaction was maintained at $-78\text{ }^{\circ}\text{C}$ before being allowed to passively warm to $23\text{ }^{\circ}\text{C}$. After 19 h, the reaction was quenched by the slow addition of NH₄Cl_(aq) (Sat. soln, 15 mL) over a 10 min period – the quenched solution was extracted with ethyl acetate (10 mL). The resulting layers were separated and the organics were washed with water ($2 \times 10\text{ mL}$) and brine (20 mL), dried over MgSO₄, filtered and concentrated under reduced pressure. The crude material was subjected to flash-column chromatography ($R_f = 0.1$, 9:1 *n*-hexane:ethyl acetate) to afford the Claisen-adduct **197** as the only identifiable product (148 mg, 27%); $\nu_{\text{max}}/\text{cm}^{-1}$ (neat) 3045 (CH), 2988 (CH), 2259 (CN), 1752 (CO), 1701 (CO); δ_H (400 MHz; CDCl₃) 1.38–1.51 (9 H, s, C(CH₃)₃), 1.57–1.81 (9 H, s, C(CH₃)₃), 4.83 (1 H, d, $J = 4.2$, CCH(CO₂^tBu)CN), 7.28–7.33 (1 H, m, CHCHCC or CHCHCNBoc), 7.34–7.42 (1 H, m, CHCHCC or CHCHCNBoc), 7.66 (1 H, d, $J = 8.1$, CHCHCC or CHCHCNBoc), 7.75 (1 H, d, $J = 4.6$, CCHNBoc), 8.19 (1 H, d, $J = 8.5$, CHCHCC or CHCHCNBoc); δ_C (101 MHz; CDCl₃) 27.9 (C(CH₃)₃), 28.3 (C(CH₃)₃), 36.9 (CH), 84.6 (C), 85.1 (C), 110.3 (C), 115.4 (CH), 115.7 (CH), 119.2(CH), 123.2 (CH), 125.3 (CH), 125.4 (C), 135.7 (C), 149.3 (C), 163.4 (CO), 185.0 (CO); LRMS *m/z* (ES⁺) 257.3 ([M + H]⁺, 100%).

A novel compound prepared according to a literature procedure.

200) *tert*-Butyl 3-((2-methoxy-2-oxoethyl)thio)-1H-indole-1-carboxylate

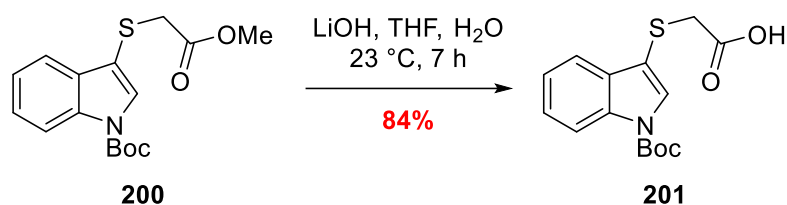


A solution of I₂ (1.80 g, 7.09 mmol) and KI (1.18 g, 7.09 mmol) in MeOH:H₂O (4:1, 10 mL) was added dropwise over 5 h to a solution of indole **106** (1.00 g, 8.51 mmol) and thioglycolic acid **199** (0.63 mL, 7.09 mmol) in MeOH:H₂O (4:1, 10 mL) at 23 °C. The reaction mixture was stirred for 16 h before being quenched *via* the addition of NaHCO_{3(aq)} (Sat. Soln., 25 mL) and then diluted further with ethyl acetate (20 mL). The resultant phases were separated, and the organic phase was washed sequentially with Na₂S₂O_{3(aq)} (Sat. Soln., 2 × 10 mL), water (10 mL) and brine (20 mL), dried over MgSO₄, filtered to remove the solids and the concentrated under reduced pressure. The crude material was then dried under high vacuum. After 3 hours, the crude material was re-solubilised in tetrahydrofuran (15 mL) and Boc₂O (1.71 g, 7.82 mmol), Et₃N (1.10 mL, 7.82 mmol) and DMAP (87 mg, 0.71 mmol) was added and stirred at 23 °C. After 20 h, the reaction was determined complete *via* TLC and the reaction mixture was quenched with HCl_(aq) (1 M, 20 mL) then further diluted with ethyl acetate (20 mL). The layers were separated and the organic was washed with HCl_(aq) (1M, 10 mL), water (2 × 10 mL) and brine (20 mL), dried over MgSO₄, filtered to remove the solids and concentrated under reduced pressure. The resulting crude was subjected to flash column chromatography (*R_f* = 0.3, 9:1 *n*-hexane:ethyl acetate) to afford *N*-Boc sulfenylindole **200** as a pale-brown oil (1.04 g, 39%); $\nu_{\max}/\text{cm}^{-1}$ (neat) 2978 (CH), 1732 (CO), 1643 (CO); δ_H (400 MHz; CDCl₃) 1.67 (9 H, s, C(CH₃)₃), 3.50 (2 H, s, SCH₂CO₂CH₃), 3.67 (3 H, s, CO₂CH₃), 7.31 (1 H, td, *J* = 7.5, 7.3, 1.2, CHCHCC or CHCHCNBoc), 7.36 (1 H, td, *J* = 8.3, 7.2, 1.5, CHCHCC or CHCHCNBoc), 7.67 (1 H, dt, *J* = 7.6, 1.5, CHCHCC or CHCHCNBoc), 7.77 (1 H, s, CCHNBoc), 8.15 (1 H, *app. d*, *J* = 8.1, CHCHCC or CHCHCNBoc); δ_C (101 MHz; CDCl₃) 28.3 ((CH₃)₃), 37.7 (CH₂), 52.5

(CH₃), 84.5 (C), 110.9 (C), 115.6 (CH), 119.5 (CH), 123.3 (CH), 125.2 (CH), 130.4 (CH), 130.9 (C), 135.6 (C), 149.2 (C), 170.4 (C); **LRMS *m/z* (ES+)** 322.3 ([M + H]⁺, 38%), 221.7 ([M - Boc]⁺, 100).

A novel compound prepared according to a modified literature procedure.²²³ No available spectral data is available within the literature.

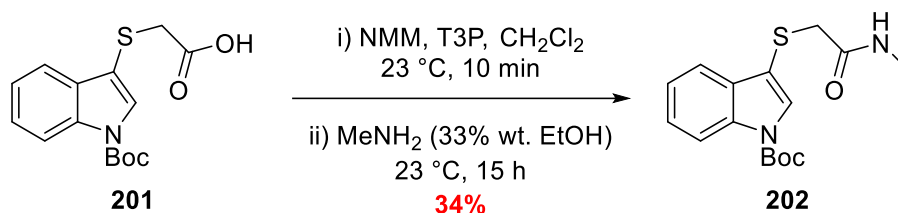
201) 2-((1-(*tert*-Butoxycarbonyl)-indol-3-yl)thio)acetic acid



Sulfenylindole **200** (550 mg, 1.71 mmol) was dissolved in tetrahydrofuran (20 mL) and stirred at 23 °C. To this, a solution of lithium hydroxide (123 mg, 5.13 mmol) in distilled water (5 mL) was added and stirred for 7 h. The reaction mixture was then partitioned between water (20 mL) and ethyl acetate (20 mL), the resultant phases were separated. The aqueous was acidified with HCl_(aq) (1 M, 10 mL) and extracted with ethyl acetate (20 mL). The resulting organic was then subjected to further water (2 × 10 mL) and brine (20 mL) washes. After washing the organic was dried over MgSO₄ and concentrated to afford acid **201** as a pale orange solid (444 mg, 84%); **mp** = 174–177 °C; $\nu_{\max}/\text{cm}^{-1}$ (neat) 2994 (CH), 1732 (CO), 1702 (CO), COOH observed but centre of absorbance is indistinguishable; δ_{H} (**400 MHz; CDCl₃**) 1.67 (9 H, s, C(CH₃)₃), 3.52 (2 H, s, SCH₂CO₂H), 7.30 (1 H, td, *J* = 7.7, 7.3, 1.3, CHCHCC or CHCHCNBoc), 7.36 (1 H, td, *J* = 8.3, 7.4, 1.3, CHCHCC or CHCHCNBoc), 7.69 (1 H, ddd, *J* = 7.7, 1.4, 0.7, CHCHCC or CHCHCNBoc), 7.80 (1 H, s, CCHNBoc), 8.15 (1 H, *app.* d, *J* = 8.3, CHCHCC or CHCHCNBoc); δ_{C} (**101 MHz; CDCl₃**) 28.3 ((CH₃)₃), 37.6 (CH₂), 84.6 (C), 110.5 (C), 115.6 (CH), 119.4 (CH), 123.4 (CH), 125.3 (CH), 130.6 (CH), 130.7 (C), 135.6 (C), 149.1 (CO), 175.8 (CO); **LRMS *m/z* (ES+)** 330.1 ([M + Na]⁺, 58%), 208.0 ([M - Boc + H]⁺, 100); **HRMS *m/z* (ES+)** calcd for C₁₅H₁₇NO₄SNa 330.0776, found 330.0777.

A novel compound prepared according to a modified literature procedure.³⁹¹

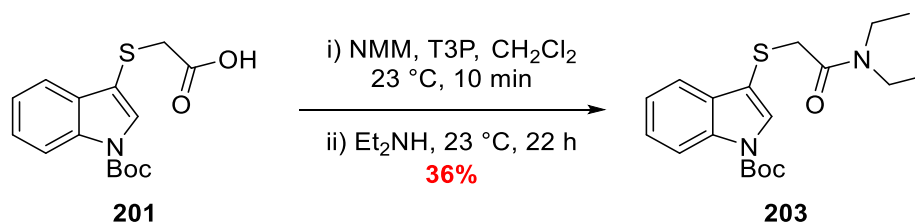
202) *tert*-Butyl 3-((2-(methylamino)-2-oxoethyl)thio)-indole-1-carboxylate



NMM (43 μ L, 0.39 mmol) was added to a solution of acid **201** (100 mg, 0.33 mmol) in dichloromethane (1 mL) and then immediately after T3P (50% wt in CH₂Cl₂, 124 mg of T3P/248 mg of T3P soln., 0.39 mmol) was added and stirred at 23 °C. After 10 min, methylamine solution (33% in EtOH, 48 μ L, 0.39 mmol) was added and stirred for a further 15 h after which point the reaction was determined complete *via* TLC (R_f = 0.4, 3:1 ethyl acetate:*n*-hexane). The reaction was quenched *via* the addition of HCl_(aq) (1 M, 5 mL) and the quenched solution was then poured into a separating funnel containing ethyl acetate (5 mL). The layers were separated and the organic phase was washed sequentially with NaOH_(aq) (1 M, 2 \times 10 mL), water (10 mL) and brine (20 mL). After drying over MgSO₄, the solids were filtered off and the solution was concentrated under reduced pressure. The crude mixture was subjected to flash column chromatography (R_f = 0.2, 9:1 ethyl acetate:*n*-hexane) to yield methylamide **202** as a colourless oil (35 mg, 34%); $\nu_{\max}/\text{cm}^{-1}$ (neat) 3246 (NH), 2995 (CH), 1723 (CO); δ_H (400 MHz; CDCl₃) 1.67 (9 H, s, C(CH₃)₃), 2.80 (3 H, d, J = 4.9, NHCH₃), 3.48 (2 H, s, SCH₂CO), 6.64 (1 H, s, NH), 7.30 (1 H, td, J = 7.5, 7.4, 1.1, CHCHCC or CHCHCNBoc), 7.36 (1 H, *app.* td, J = 8.3, 7.2, CHCHCC or CHCHCNBoc), 7.62 (1 H, dt, J = 7.6, 1.1, CHCHCC or CHCHCNBoc), 7.67 (1 H, s, CCHNBoc), 8.13 (1 H, d, J = 8.3, CHCHCC or CHCHCNBoc); δ_C (101 MHz; CDCl₃) 26.7 (CH₃), 28.3 ((CH₃)₃), 39.2 (CH₂), 84.6 (C), 111.1 (C), 115.6 (CH), 119.2 (CH), 123.3 (CH), 125.4 (CH), 128.7 (CH), 130.4 (C), 135.6 (C), 149.1 (CO), 168.9 (CO); LRMS m/z (ES⁺) 343.1 ([M + Na]⁺, 70%), 221.1 ([M - Boc + H]⁺, 100); HRMS m/z (ES⁺) calcd for C₁₆H₂₀N₂O₃SNa 343.1092, found 343.1098.

*A novel compound prepared according to a modified literature procedure.*³⁹²

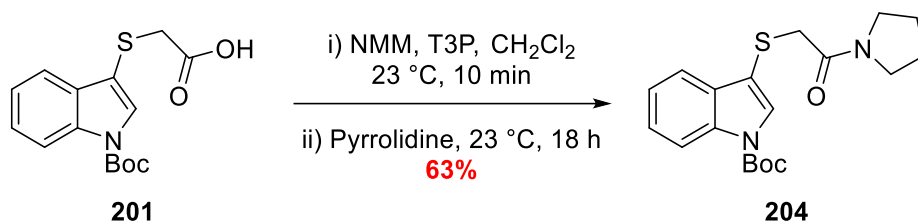
203) *tert*-Butyl 3-((2-(diethylamino)-2-oxoethyl)thio)-indole-1-carboxylate



NMM (43 μ L, 0.39 mmol) was added to a solution of acid **201** (100 mg, 0.330 mmol) in dichloromethane (1 mL) and then immediately after T3P (50% wt in CH₂Cl₂, 124 mg of T3P/248 mg of T3P soln., 0.390 mmol) was added and stirred at 23 °C. After 10 min, diethylamine (29 μ L, 0.39 mmol) was added and stirred for a further 22 h after which point the reaction was determined complete *via* TLC (R_f = 0.4, 1:1 ethyl acetate:*n*-hexane). The reaction was quenched *via* the addition of HCl_(aq) (1 M, 5 mL) and the quenched solution was then poured into a separating funnel containing ethyl acetate (5 mL). The layers were separated, and the organic phase was washed sequentially with NaOH_(aq) (1 M, 10 mL), water (10 mL) and brine (20 mL). After drying over MgSO₄, the solids were filtered off and the solution was concentrated under reduced pressure. The crude mixture was subjected to flash column chromatography (R_f = 0.4, 1:1 ethyl acetate:*n*-hexane) to yield diethylamide **203** as a colourless oil (42 mg, 36%); $\nu_{\max}/\text{cm}^{-1}$ (neat) 3062 (CH), 2955 (CH), 2871 (CH), 1713 br (2 \times CO); δ_H (400 MHz; CDCl₃) 1.09 (3 H, t, J = 7.2, CH₃CH₂N(R)CH₂CH₃ or CH₃CH₂N(R)CH₂CH₃), 1.12 (3 H, t, J = 7.2, CH₃CH₂N(R)CH₂CH₃ or CH₃CH₂N(R)CH₂CH₃), 1.66 (9 H, s, C(CH₃)₃), 3.23 (2 H, q, J = 7.1, CH₂N(R)CH₂ or CH₂N(R)CH₂), 3.35 (2 H, q, J = 7.1, CH₂N(R)CH₂ or CH₂N(R)CH₂), 3.61 (2 H, s, SCH₂CON), 7.29 (1 H, td, J = 7.4, 7.3, 1.4, CHCHCC or CHCHCNBoc), 7.35 (1 H, td, J = 8.3, 7.3, 1.4, CHCHCC or CHCHCNBoc), 7.68–7.71 (1 H, m, CHCHCC or CHCHCNBoc), 7.74 (1 H, s, CCHNBoc), 8.14 (1 H, d, J = 8.3, CHCHCC or CHCHCNBoc); δ_C (101 MHz; CDCl₃) 13.0 (CH₃), 14.5 (CH₃), 28.3 ((CH₃)₃), 37.8 (CH₂), 40.5 (CH₂), 42.6 (CH₂), 84.3 (C), 111.1 (C), 115.5 (CH), 119.5 (CH), 123.2 (CH), 125.1 (CH), 130.1 (CH), 131.2 (C), 135.6 (C), 149.2 (CO), 167.8 (CO); LRMS m/z (ES⁺) 363.2 ([M + H]⁺, 44%), 263.2 ([M – Boc + H]⁺, 100); HRMS m/z (ES⁺) calcd for C₁₉H₂₇N₂O₃S 363.17425, found 363.1741.

A novel compound prepared according to a modified literature procedure.³⁹²

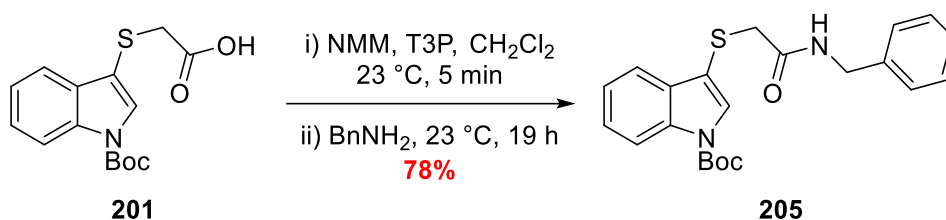
204) *tert*-Butyl 3-((2-oxo-2-(pyrrolidin-1-yl)ethyl)thio)-indole-1-carboxylate



NMM (50 μ L, 0.46 mmol) was added to a solution of acid **201** (117 mg, 0.380 mmol) in dichloromethane (1 mL) and then immediately after T3P (50% wt in CH₂Cl₂, 145 mg of T3P/290 mg of T3P soln., 0.460 mmol) was added and stirred at 23 °C. After 10 min, pyrrolidine (38 μ L, 0.46 mmol) was added and stirred for a further 18 h after which point the reaction was determined complete *via* TLC (R_f = 0.3, 3:1 ethyl acetate:*n*-hexane). The reaction was quenched *via* the addition of HCl_(aq) (1 M, 5 mL) and the quenched solution was then poured into a separating funnel containing ethyl acetate (5 mL). The layers were separated and the organic phase was washed sequentially with NaOH_(aq) (1 M, 10 mL), water (10 mL) and brine (20 mL). After drying over MgSO₄, the solids were filtered off and the solution was concentrated under reduced pressure and then dried under high vacuum to afford pyrrolo-amide **204**, without need for further purification, as a pale-yellow oil (86 mg, 63%); $\nu_{\max}/\text{cm}^{-1}$ (neat) 2974 (CH), 2874 (CH), 1732 (CO), 1637 (CO); δ_H (400 MHz; CDCl₃) 1.66 (9 H, s, C(CH₃)₃), 1.74–1.82 (4 H, Stack, CH₂CH₂N(R)CH₂CH₂ and CH₂CH₂N(R)CH₂CH₂), 3.30 (2 H, t, J = 6.4, CH₂N(R)CH₂ or CH₂N(R)CH₂), 3.42 (2 H, t, J = 6.4, CH₂N(R)CH₂ or CH₂N(R)CH₂), 3.53 (2 H, s, SCH₂CON), 7.29 (1 H, td, J = 7.4, 7.3, 1.4, CHCHCC or CHCHCNBoc), 7.34 (1 H, td, J = 8.3, 7.2, 1.4, CHCHCC or CHCHCNBoc), 7.67 (1 H, dd, J = 7.6, 1.5, CHCHCC or CHCHCNBoc), 7.76 (1 H, s, CCHNBoc), 8.13 (1 H, d, J = 8.3, CHCHCC or CHCHCNBoc); δ_C (101 MHz; CDCl₃) 24.4 (CH₂), 26.2 (CH₂), 28.3 ((CH₃)₃), 38.9 (CH₂), 46.2 (CH₂), 47.0 (CH₂), 84.4 (C), 111.2 (C), 115.5 (CH), 119.6 (CH), 123.2 (CH), 125.1 (CH), 130.2 (CH), 131.2 (C), 135.6 (C), 149.2 (CO), 167.3 (CO); LRMS m/z (ES+) 383.1 ([M + Na]⁺, 44%), 361.2 ([M + H]⁺, 74), 261.1 ([M - Boc + H]⁺, 100); HRMS m/z (ES+) calcd for C₁₉H₂₅N₂O₃S 361.1586, found 361.1590.

A novel compound prepared according to a modified literature procedure.³⁹²

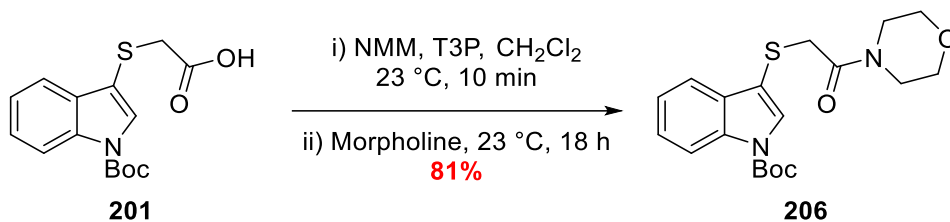
205) tert-Butyl 3-((2-(benzylamino)-2-oxoethyl)thio)-indole-1-carboxylate



NMM (43 μ L, 0.39 mmol) was added to a solution of acid **201** (100 mg, 0.330 mmol) in dichloromethane (1 mL) and then immediately after T3P (50% wt in CH₂Cl₂, 124 mg of T3P/248 mg of T3P soln., 0.390 mmol) was added and stirred at 23 °C. After 5 min, BnNH₂ (43 μ L, 0.39 mmol) was added and stirred for a further 19 h after which point the reaction was determined complete *via* TLC (R_f = 0.4, 1:1 ethyl acetate:*n*-hexane). The reaction was quenched *via* the addition of HCl_(aq) (1 M, 5 mL) and the quenched solution was extracted with ethyl acetate (5 mL). The layers were separated, and the organic phase was washed sequentially with NaOH_(aq) (1 M, 10 mL), water (10 mL) and brine (20 mL). After drying over MgSO₄, the solids were filtered and the solution was concentrated under reduced pressure and dried under high vacuum to afford benzylamide **205**, with no need for further purification, as a colourless oil (101 mg, 78%); $\nu_{\max}/\text{cm}^{-1}$ (neat) 3285 (NH), 3063 (CH), 2979 (CH), 2930 (CH), 1734 (CO), 1649 (CO); δ_H (400 MHz; CDCl₃) 1.58 (9 H, s, C(CH₃)₃), 3.46 (2 H, s, SCH₂CONH), 4.31 (2 H, d, J = 5.7, CONHCH₂Ph), 6.81 (1 H, d, J = 5.7, NH), 7.02–7.06 (2 H, m, *Ar-H*), 7.16–7.21 (4 H, Stack, *Ar-H* and CHCHCC or CHCHCNBoc), 7.28 (1 H, td, J = 8.3, 7.3, 1.3, CHCHCC or CHCHCNBoc), 7.52 (1 H, dt, J = 7.7, 1.1, CHCHCC or CHCHCNBoc), 7.56 (1 H, s, CCHNBoc), 8.06 (1 H, d, J = 8.3, CHCHCC or CHCHCNBoc); δ_C (101 MHz; CDCl₃) 28.3 ((CH₃)₃), 39.1 (CH₂), 44.0 (CH₂), 84.6 (C), 110.8 (C), 115.6 (CH), 119.2 (CH), 123.4 (CH), 125.4 (CH), 127.7 (CH), 127.8 (CH), 128.8 (CH), 128.9 (CH), 130.4 (C), 135.6 (C), 137.6 (C), 149.0 (CO), 168.3 (CO); LRMS m/z (ES⁺) 419.1 ([M + Na]⁺, 100%), 297.1 ([M – Boc + H]⁺, 34); HRMS m/z (ES⁺) calcd for C₂₂H₂₄N₂O₃SNa 419.1405, found 419.1408.

A novel compound prepared according to a modified literature procedure.³⁹²

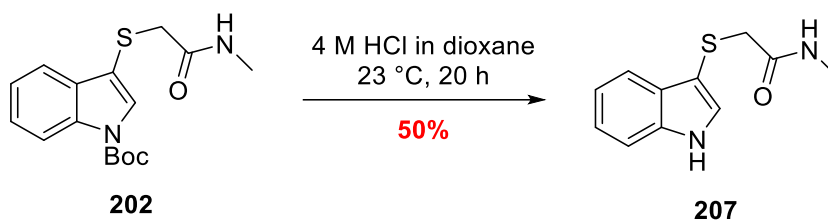
206) *tert*-Butyl 3-((2-morpholino-2-oxoethyl)thio)-indole-1-carboxylate



NMM (43 μ L, 0.39 mmol) was added to a solution of acid **201** (100 mg, 0.330 mmol) in dichloromethane (1 mL) and then immediately after T3P (50% wt in CH₂Cl₂, 124 mg of T3P/248 mg of T3P soln., 0.390 mmol) was added and stirred at 23 °C. After 10 min, morpholine (34 μ L, 0.39 mmol) was added and stirred for a further 18 h after which point the reaction was determined complete *via* TLC (R_f = 0.3, 3:1 ethyl acetate:*n*-hexane). The reaction was quenched *via* the addition of HCl_(aq) (1 M, 5 mL) and the quenched solution was then poured into a separating funnel containing ethyl acetate (5 mL). The layers were separated, and the organic phase was washed sequentially with NaOH_(aq) (1 M, 10 mL), water (10 mL) and brine (20 mL). After drying over MgSO₄, the solids were filtered off and the solution was concentrated under reduced pressure and then dried under high vacuum to afford morpholine amide **206**, without need for further purification, as a colourless oil (97 mg, 81%); $\nu_{\max}/\text{cm}^{-1}$ (neat) 2977 (CH), 2925 (CH), 2855 (CH), 1733 (CO), 1640 (CO); δ_H (400 MHz; CDCl₃) 1.67 (9 H, s, C(CH₃)₃), 3.37 (2 H, dd, J = 5.8, 3.9, CH₂NCH'₂ or CH₂NCH'₂), 3.53 (2 H, dd, J = 5.8, 3.9, CH₂NCH'₂ or CH₂NCH'₂), 3.55–3.59 (1 H, m, CH₂OCH'₂ or CH₂OCH'₂), 3.59–3.64 (4 H, Stack, SCH₂CON and CH₂OCH'₂ or CH₂OCH'₂), 7.31 (1 H, td, J = 7.4, 7.3, 1.4, CHCHCC or CHCHCNBoc), 7.36 (1 H, td, J = 8.3, 7.3, 1.4, CHCHCC or CHCHCNBoc), 7.65–7.70 (1 H, m, CHCHCC or CHCHCNBoc), 7.77 (1 H, s, CCHNBoc), 8.14 (1 H, d, J = 8.3, CHCHCC or CHCHCNBoc); δ_C (101 MHz; CDCl₃) 28.3 ((CH₃)₃), 37.0 (CH₂), 42.3 (1 \times N(CH₂)₂), 46.9 (1 \times N(CH₂)₂), 66.6 (1 \times O(CH₂)₂), 66.9 (1 \times O(CH₂)₂), 84.6 (C), 110.6 (C), 115.7 (CH), 119.4 (CH), 123.4 (CH), 125.3 (CH), 130.3 (CH), 131.1 (C), 135.6 (C), 149.1 (CO), 167.6 (CO); LRMS m/z (ES⁺) 399.1 ([M + Na]⁺, 100%), 377.1 ([M + H]⁺, 10), 299.1 ([M – Boc + Na]⁺, 90), 277.1 ([M – Boc + H]⁺, 68); HRMS m/z (ES⁺) calcd for C₁₉H₂₄N₂O₄SNa 399.1354, found 399.1369.

A novel compound prepared according to a modified literature procedure.³⁹²

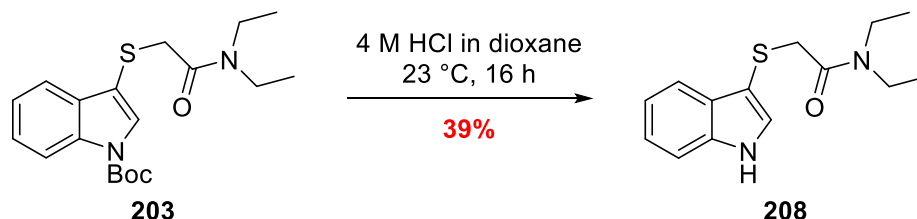
207) 2-((1H-Indol-3-yl)thio)-N-methylacetamide



N-Boc indole **202** (32 mg, 0.10 mmol) was solubilised in a solution of HCl in 1,4-dioxane (4 M, 2 mL) and stirred at 23 °C. After 20 h, the reaction mixture was concentrated under reduced pressure and the crude material was recrystallised from hot *n*-hexane and ethyl acetate to give indole **207** as a white solid (11 mg, 50%); mp = 243–244 °C; $\nu_{\max}/\text{cm}^{-1}$ (neat) 3338 (NH), 3277 (NH), 2931 (CH), 1632 (CO); δ_{H} (400 MHz; CDCl_3) 2.78 (3 H, d, $J = 4.9$, CONHCH_3), 3.42 (2 H, s, $\text{SCH}_2\text{CONHCH}_3$), 6.60 (1 H, s, CONHCH_3), 7.21 (2 H, Stack, CHCHCC and CHCHCNH), 7.28 (1 H, d, $J = 2.5$, CCHNH), 7.37 (1 H, d, $J = 7.3$, CHCHCC or CHCHCNH), 7.70 (1 H, d, $J = 8.4$, CHCHCC or CHCHCNH), 8.75 (1 H, s, CHNHC); δ_{C} (101 MHz; CDCl_3) 26.7 (CH_3), 40.8 (CH_2), 104.5 (C), 112.0 (CH), 118.9 (CH), 120.9 (CH), 123.1 (CH), 128.6 (CH), 129.2 (C), 136.4 (C), 170.0 (CO); LRMS m/z (ES+) 243.1 ($[\text{M} + \text{Na}]^+$, 100%); HRMS m/z (ES+) calcd for $\text{C}_{11}\text{H}_{12}\text{N}_2\text{OSNa}$ 243.0568, found 243.0569.

A novel compound prepared according to a modified literature procedure.³⁹³

208) 2-((1H-Indol-3-yl)thio)-*N,N*-diethylacetamide

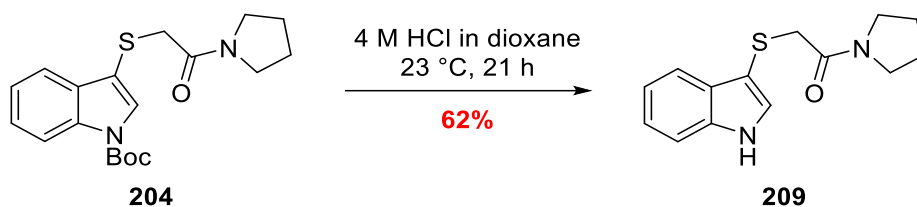


N-Boc indole **203** (42 mg, 0.12 mmol) was solubilised in a solution of HCl in 1,4-dioxane (4 M, 1 mL) and stirred at 23 °C. After 16 h, the reaction was determined complete *via* TLC and was quenched *via* the addition of $\text{NaHCO}_3(\text{aq})$ (Sat. Soln., 5 mL) and the diluted further by the addition of ethyl acetate (5 mL). The two phases were separated, and the organic phase was

washed with water (2 × 10 mL) and brine (20 mL), dried over MgSO₄, filtered to remove the solids and concentrated under reduced pressure. The crude material was then subjected to flash column chromatography (*R_f* = 0.3, 9:1 ethyl acetate:*n*-hexane) to yield amide **208** as a white solid (12 mg, 39%); **mp** = 163–164 °C; $\nu_{\max}/\text{cm}^{-1}$ (neat) 3231 (NH), 2974 (CH), 2931 (CH), 1616 (CO); δ_{H} (400 MHz; CDCl₃) 1.07 (4 H, t, *J* = 7.1, CH₃CH₂N(R)CH₂CH₃ or CH₃CH₂N(R)CH₂CH₃), 1.13 (3 H, t, *J* = 7.1, CH₃CH₂N(R)CH₂CH₃ or CH₃CH₂N(R)CH₂CH₃), 3.26 (2 H, q, *J* = 7.1, CH₂N(R)CH₂ or CH₂N(R)CH₂), 3.35 (2 H, q, *J* = 7.1, CH₂N(R)CH₂ or CH₂N(R)CH₂), 3.54 (2 H, s, SCH₂CON), 7.15–7.22 (2 H, Stack, CHCHCC and CHCHCNH), 7.30 (1 H, d, *J* = 2.7, CCHNH), 7.31–7.34 (1 H, m, CHCHCC or CHCHCNH), 7.72–7.77 (1 H, m, CHCHCC or CHCHCNH), 8.91 (1 H, s, NH); δ_{C} (101 MHz; CDCl₃) 13.0 (CH₃), 14.5 (CH₃), 38.7 (CH₂), 40.5 (CH₂), 42.6 (CH₂), 104.1 (C), 111.9 (CH), 119.1 (CH), 120.6 (CH), 122.7 (CH), 129.3 (C), 130.6 (CH), 136.4 (C), 168.9 (CO); **LRMS *m/z* (ES⁺)** 285.1 ([M + Na]⁺, 32%), 263.1 ([M + H]⁺, 100); **HRMS *m/z* (ES⁺)** calcd for C₁₄H₁₉N₂OS 263.1218, found 263.1217.

A novel compound prepared according to a modified literature procedure.³⁹³

209) 2-((1H-Indol-3-yl)thio)-1-(pyrrolidin-1-yl)ethan-1-one

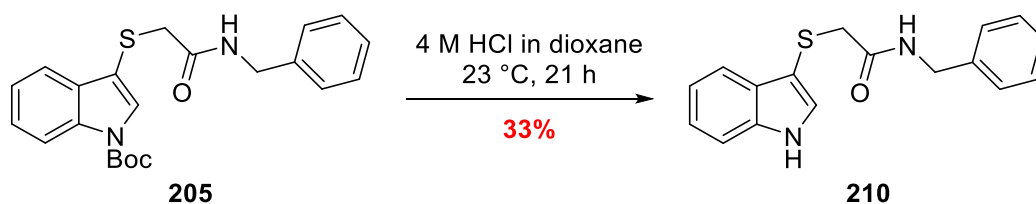


N-Boc indole **204** (78 mg, 0.22 mmol) was solubilised in a solution of HCl in 1,4-dioxane (4 M, 2 mL) and stirred at 23 °C. After 21 h, the reaction mixture was concentrated under reduced pressure and the crude material was subjected to flash column chromatography (*R_f* = 0.2, 4:1 ethyl acetate:*n*-hexane to ethyl acetate) to yield indole **209** as a pale-yellow solid (46 mg, 62%); **mp** = 145–147 °C; $\nu_{\max}/\text{cm}^{-1}$ (neat) 3147 (NH), 2973 (CH), 1620 (CO); δ_{H} (300 MHz; CDCl₃) 1.71–1.79 (4 H, Stack, CH₂CH₂N(R)CH₂CH₂ and CH₂CH₂N(R)CH₂CH₂), 3.30 (2 H, t, *J* = 6.6, CH₂N(R)CH₂ or CH₂N(R)CH₂), 3.39 (2 H, t, *J* = 6.6), 3.45 (2 H, s, SCH₂CON), 7.12–7.20 (2 H, Stack, CHCHCC and CHCHCNH), 7.24 (1 H, d, *J* = 2.6, CCHNH), 7.28–7.34 (1 H, m,

CHCHCC or CHCHCNH), 7.67–7.74 (1 H, m, CHCHCC or CHCHCNH), 9.51 (1 H, s, NH); δ_c (101 MHz; CDCl₃) 24.4 (CH₂), 26.1 (CH₂), 39.8 (CH₂), 46.3 (CH₂), 47.0 (CH₂), 103.3 (C), 112.0 (CH), 118.9 (CH), 120.4 (CH), 122.5 (CH), 129.5 (C), 131.1 (CH), 136.4 (C), 168.5 (CO); LRMS m/z (ES+) 283.1 ([M + Na]⁺, 100%); HRMS m/z (ES+) calcd for C₁₄H₁₆N₂OSNa 283.0881, found 283.882.

A novel compound prepared according to a modified literature procedure.³⁹³

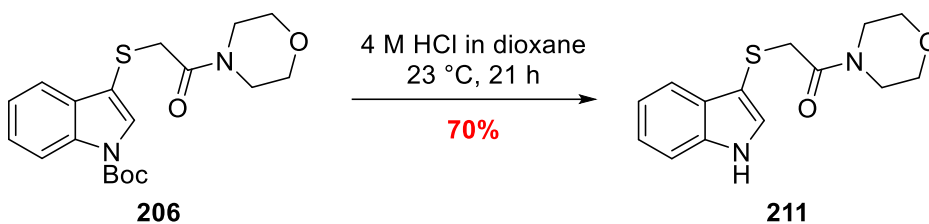
210) 2-((1H-Indol-3-yl)thio)-N-benzylacetamide



N-Boc indole **205** (84 mg, 0.21 mmol) was solubilised in a solution of HCl in 1,4-dioxane (4 M, 2 mL) and stirred at 23 °C. After 21 h, the reaction mixture was concentrated under reduced pressure and the crude material was recrystallised from hot MeOH to give indole **210** as a white solid (21 mg, 33%); mp = 280–281 °C; $\nu_{\max}/\text{cm}^{-1}$ (neat) 3419 (NH), 3256 (NH), 3064 (CH), 2920 (CH), 1643 (CO); δ_H (400 MHz; (CD₃)₂CO) 3.41 (2 H, s, SCH₂CON), 4.35 (2 H, d, J = 5.9, CONHCH₂Ph), 7.11 (1 H, td, J = 8.0, 7.1, 1.3, CHCHCC or CHCHCNH), 7.14–7.29 (6 H, Stack, *Ar-H* and CHCHCC or CHCHCNH), 7.44 (1 H, s, CCHNH), 7.44–7.47 (1 H, m, CHCHCC or CHCHCNH), 7.62 (1 H, s, CONHCH₂), 7.70 (1 H, dd, J = 8.0, 1.3, CHCHCC or CHCHCNH), 10.52 (1 H, s, NH); δ_c (101 MHz; (CD₃)₂CO) 41.1 (CH₂), 43.8 (CH₂), 104.7 (C), 112.8 (CH), 119.6 (CH), 120.8 (CH), 123.0 (CH), 125.8 (C), 127.7 (CH), 128.4 (CH), 129.1 (CH), 130.0 (C), 131.5 (CH), 140.3 (C), 169.4 (CO); LRMS m/z (ES+) 319.2 ([M + Na]⁺, 100%), 297.2 ([M + H]⁺, 44); HRMS m/z (ES+) calcd for C₁₇H₁₇N₂OS 297.1586, found 297.1587

A novel compound prepared according to a modified literature procedure.³⁹³

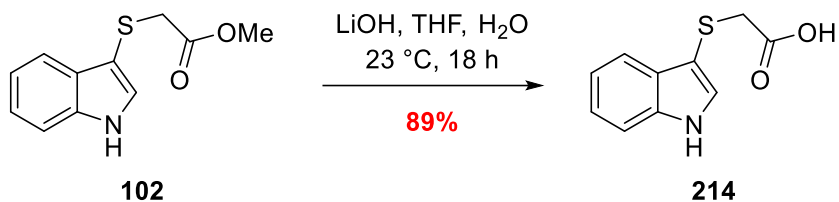
211) 2-((1H-indol-3-yl)thio)-1-morpholinoethan-1-one



N-Boc indole **206** (84 mg, 0.21 mmol) was solubilised in a solution of HCl in 1,4-dioxane (4 M, 2 mL) and stirred at 23 °C. After 21 h, the reaction mixture was concentrated under reduced pressure and the crude material was subjected to flash column chromatography ($R_f = 0.1$, 4:1 ethyl acetate:*n*-hexane to ethyl acetate) to yield indole **211** as a pale-yellow solid (46 mg, 70%); **mp** = 211–212 °C; $\nu_{\max}/\text{cm}^{-1}$ (neat) 3223 (NH), 2959 (CH), 2918 (CH), 2854 (CH), 1621 (CO); δ_H (400 MHz; CDCl_3) 3.31 (2 H, dd, $J = 5.7, 3.9$, $\text{CH}_2\text{NCH}'_2$ or $\text{CH}_2\text{NCH}'_2$), 3.41 (2 H, dd, $J = 5.7, 3.9$, $\text{CH}_2\text{NCH}'_2$ or $\text{CH}_2\text{NCH}'_2$), 3.53 (2 H, s, SCH_2CON), 3.57 (4 H, Stack, $\text{CH}_2\text{OCH}'_2$ and $\text{CH}_2\text{OCH}'_2$), 7.16–7.23 (2 H, Stack, CHCHCC and CHCHCNH), 7.28 (1 H, d, $J = 2.6$, CCHNH), 7.31–7.34 (1 H, m, CHCHCC or CHCHCNH), 7.70–7.75 (1 H, m, CHCHCC or CHCHCNH), 9.09 (1 H, s, NH); δ_C (101 MHz; CDCl_3) 37.8 (CH_2), 42.3 (CH_2), 46.9 (CH_2), 66.5 (CH_2), 66.8 (CH_2), 103.4 (C), 112.0 (CH), 118.9 (CH), 120.7 (CH), 122.9 (CH), 129.3 (C), 130.7 (CH), 136.4 (C), 168.6 (CO; **LRMS** m/z (**ES+**) 299.1 ($[\text{M} + \text{Na}]^+$, 100%), 277.1 ($[\text{M} + \text{H}]^+$, 12); **HRMS** m/z (**ES+**) calcd for $\text{C}_{14}\text{H}_{16}\text{N}_2\text{O}_2\text{SNa}$ 299.0830, found 299.0827.

*A novel compound prepared according to a modified literature procedure.*³⁹³

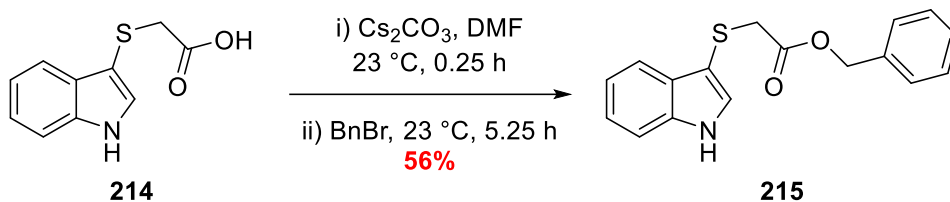
214) 2-((1H-Indol-3-yl)thio)acetic acid



Lithium hydroxide (182 mg, 7.59 mmol) in water (3 mL) was added to a solution of ester **102** (560 mg, 2.53 mmol) in tetrahydrofuran (15 mL) and stirred at 23 °C. After 18 h, the reaction mixture was diluted with water (10 mL) and ethyl acetate (10 mL). The two phases were separated, and the aqueous phase was extracted with ethyl acetate (10 mL). After, the pH of the aqueous phase was adjusted to ~pH 1 *via* the addition of HCl_(aq) (1 M, 15 mL) and then extracted with ethyl acetate (3 × 15 mL). The combined organics were then washed with water (10 mL) and brine (20 mL), dried over MgSO₄ and the solids filtered off. The dried organic phase was then concentrated under reduced pressure and dried further under high vacuum to afford acid **214**, with no need for further purification, as a pale-green solid (468 mg, 89%); **mp** = 108–110 °C; $\nu_{\max}/\text{cm}^{-1}$ (neat) 3361 (NH), 3000 br (COOH), 2921 (CH), 1698 (CO); δ_{H} (400 MHz; CDCl₃) 3.44 (2 H, s, SCH₂CO₂H), 7.19–7.28 (2 H, Stack, CHCHCC and CHCHCNH), 7.37–7.40 (1 H, m, CHCHCC or CHCHCNH), 7.41 (1 H, d, *J* = 2.7, CCHNH), 7.77 (1 H, dd, *J* = 7.3, 1.7, CHCHCC or CHCHCNH), 8.32 (1 H, s, NH); δ_{C} (101 MHz; CDCl₃) 38.6 (CH₂), 104.3 (C), 111.8 (CH), 119.2 (CH), 121.0 (CH), 123.1 (CH), 128.9 (CH), 130.6 (C), 136.3 (C), 175.5 (CO); **LRMS *m/z* (ES⁻)** 206.0 ([M - H]⁺, 100%); **HRMS *m/z* (ES⁻)** calcd for C₁₀H₈NO₂S 306.0276, found 206.0278.

*A novel compound prepared according to a modified literature procedure.*³⁹¹ COOH was not observed in the ¹H-NMR.

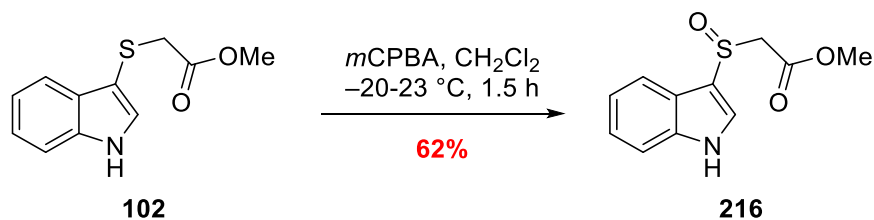
215) Benzyl 2-((1H-indol-3-yl)thio)acetate



Caesium carbonate (189 mg, 0.58 mmol) was added to a solution of acid **214** (100 mg, 0.48 mmol) in DMF (5 mL) and stirred vigorously at 23 °C. After 0.25 h, benzyl bromide (69 μL , 0.58 mmol) was added dropwise over 2 min and the resulting solution was stirred for a further 5 h upon which the reaction was determined complete *via* TLC. The reaction was quenched *via* the addition of $\text{NaHCO}_3(\text{aq})$ (Sat. Soln., 10 mL) and the quenched solution was diluted further with ethyl acetate (10 mL). The two phases were separated and the organic phase was washed with water (2 \times 10 mL) and brine (20 mL), dried over MgSO_4 , filtered to remove the solids and concentrated under reduced pressure. The crude material was then subjected to flash column chromatography ($R_f = 0.2$, 4:1 ethyl acetate:*n*-hexane) to afford benzyl ester **215** as a white solid (80 mg, 56%); **mp** = 173–175 °C; $\nu_{\text{max}}/\text{cm}^{-1}$ (neat) 3373 (NH), 3034 (CH), 1717 (CO); δ_{H} (400 MHz; CDCl_3) 3.47 (2 H, s, SCH_2CO_2), 5.07 (2 H, s, $\text{CO}_2\text{CH}_2\text{Ph}$), 7.19–7.27 (5 H, Stack, 3 \times Ph-*H* and CHCHCC and CHCHCNH), 7.31–7.37 (4 H, Stack, 2 \times Ph-*H* and CCHNH and CHCHCC or CHCHCNH), 7.76 (1 H, m, CHCHCC or CHCHCNH), 8.36 (1 H, s, *NH*); δ_{C} (101 MHz; CDCl_3) 38.8 (CH_2), 67.0 (CH_2), 104.2 (C), 111.7 (CH), 119.2 (CH), 120.8 (CH), 122.9 (CH), 128.4 (2 CH, Stack), 128.6 (CH), 129.0 (C), 130.7 (CH), 135.7 (C), 136.3 (C), 170.6 (CO); **LRMS m/z (ES+)** 320.0 ($[\text{M} + \text{Na}]^+$, 100%), 298.0 ($[\text{M} + \text{H}]^+$, 81); **HRMS m/z (ES+)** calcd for $\text{C}_{17}\text{H}_{16}\text{NO}_2\text{S}$ 298.0902, found 298.0903.

*A novel compound prepared according to a literature procedure.*³⁷⁸

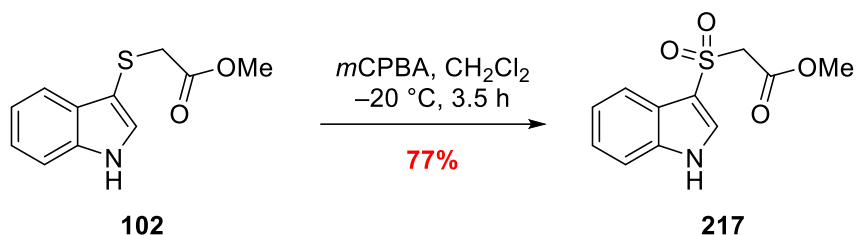
216) Methyl 2-((1H-Indol-3-yl)sulfinyl)acetate



Sulfenylindole **102** (105 mg, 0.47 mmol) was dissolved in dichloromethane (1 mL) and cooled to $-20\text{ }^{\circ}\text{C}$. To this solution, *m*CPBA (57 mg, 0.33 mmol) dissolved in dichloromethane (1 mL) was added dropwise over 5 min and the reaction mixture was allowed to warm to $23\text{ }^{\circ}\text{C}$. After 1.5 h the reaction was determined complete *via* TLC and the reaction mixture was quenched *via* the addition of $\text{NaHCO}_{3(\text{aq})}$ (Sat. Soln., 5 mL) and stirred for a further 5 min. The quenched reaction mixture was diluted further with ethyl acetate (10 mL), the phases separated and the organic washed with $\text{NaHCO}_{3(\text{aq})}$ (Sat. Soln., $2 \times 10\text{ mL}$), water (10 mL) and brine (20 mL). After drying over MgSO_4 and filtration of the solids, the organic was concentrated under reduced pressure. The resultant crude was subjected to flash column chromatography ($R_f = 0.2$, 4:1 ethyl acetate:*n*-hexane \rightarrow ethyl acetate) to afford sulfinylindole **216** as a white solid (70 mg, 62%); **mp** = $147\text{--}148\text{ }^{\circ}\text{C}$; $\nu_{\text{max}}/\text{cm}^{-1}$ (neat) 3105 (NH), 2951 (CH), 1736 (CO), 1272 (SO); δ_{H} (400 MHz; $(\text{CD}_3)_2\text{SO}$) 3.61 (3 H, s, CO_2CH_3), 4.18 (1 H, d, $J = 13.7$, $\text{SOCHH}'\text{CO}_2\text{CH}_3$), 4.42 (1 H, d, $J = 13.7$, $\text{SOCHH}'\text{CO}_2\text{Me}$), 7.17 (1 H, td, $J = 8.2, 7.1, 1.2$, CHCHCC or CHCHCNH), 7.25 (1 H, td, $J = 8.2, 7.1, 1.2$, CHCHCC or CHCHCNH), 7.52 (1 H, dt, $J = 8.0, 1.1$, CHCHCC or CHCHCNH), 7.87 (1 H, dt, $J = 8.0, 1.1$, CHCHCC or CHCHCNH), 7.99 (1 H, s, CCHNH), 11.94 (1 H, s, NH); δ_{C} (101 MHz; $(\text{CD}_3)_2\text{SO}$) 52.2 (CH_3), 58.2 (CH_2), 112.7 (CH), 114.4 (C), 119.0 (CH), 120.8 (CH), 122.8 (CH), 123.7 (C), 128.5 (CH), 136.8 (C), 166.1 (C); **LRMS** m/z (**ES+**) 260.0 ($[\text{M} + \text{Na}]^+$, 100%); **HRMS** m/z (**ES+**) calcd for $\text{C}_{11}\text{H}_{11}\text{NO}_3\text{SNa}$ 260.0357, found 260.0358.

*A novel prepared according to a modified literature procedure.*³⁹⁴

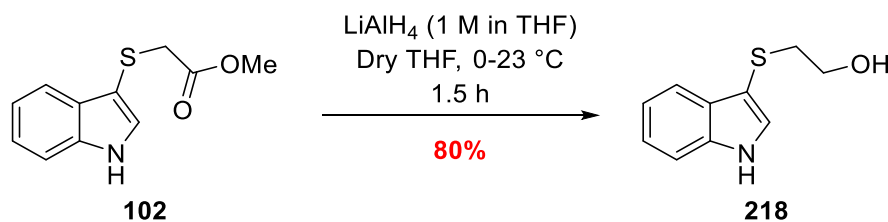
217) *tert*-Butyl 3-((2-methoxy-2-oxoethyl)sulfonyl)-1H-indole-1-carboxylate



Sulfenylindole **102** (100 mg, 0.45 mmol) was dissolved in dichloromethane (1 mL) and cooled to $-20\text{ }^\circ\text{C}$. A solution of *m*-CPBA (172 mg, 0.99 mmol) in dichloromethane (1 mL) was then added dropwise over 5 min and the reaction mixture was allowed to warm to at $23\text{ }^\circ\text{C}$. After 3.5 h, the reaction was determined complete *via* TLC and was quenched with $\text{NaHCO}_3(\text{aq})$ (Sat. Soln., 5 mL) and extracted with ethyl acetate (10 mL). The two phases were then separated and the organic was washed sequentially with NaHCO_3 (Sat. soln., $2 \times 10\text{ mL}$), water (10 mL) and then brine (20 mL). The crude material was then subjected to flash column chromatography ($R_f = 0.2$, 6:4 ethyl acetate:*n*-hexane) to yield sulfenylindole **217** as a pale blue oil (88 mg, 77%); $\nu_{\text{max}}/\text{cm}^{-1}$ (neat) 3332 (NH), 1733 (CO), 1298 (SO), 1119 (SO); δ_{H} (400 MHz; CDCl_3) 3.64 (3 H, s, CO_2CH_3), 4.22 (2 H, s, $\text{SOCH}_2\text{CO}_2\text{CH}_3$), 7.26–7.33 (2 H, Stack, *CHCHCC* and *CHCHCNH*), 7.46–7.50 (1 H, m, *CHCHCC* or *CHCHCNH*), 7.82 (1 H, d, $J = 3.2$, *CCHNH*), 7.86–7.92 (1 H, m, *CHCHCC* or *CHCHCNH*), 9.64 (1 H, s, *NH*); δ_{C} (101 MHz; CDCl_3) 53.1 (CH_3), 61.5 (CH_2), 112.7 (CH), 113.5 (C), 119.2 (CH), 123.0 (CH), 123.8, 124.4 (CH), 132.1 (CH), 136.3 (C), 163.7 (CO); **LRMS m/z (ES⁺)** 276.0 ($[\text{M} + \text{Na}]^+$, 100%); **HRMS m/z (ES⁺)** calcd for $\text{C}_{11}\text{H}_{11}\text{NO}_4\text{SNa}$ 276.0306, found 276.0309.

*A novel prepared according to a modified literature procedure.*³⁹⁴

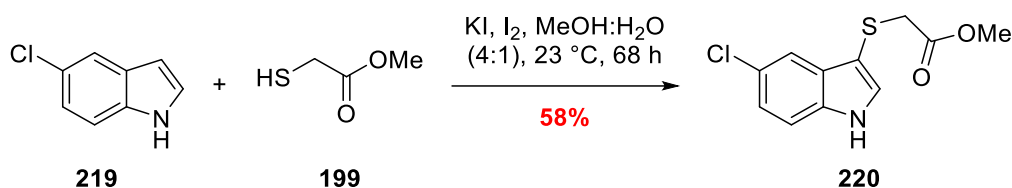
218) 2-((1H-Indol-3-yl)thio)ethan-1-ol



A solution of **102** (100 mg, 0.45 mmol) in anhydrous tetrahydrofuran (3 mL) was cooled to 0 °C under an atmosphere of argon and then LiAlH₄ (1 M in tetrahydrofuran, 0.68 mL, 0.68 mmol) was added. After 0.5 h, the reaction mixture was removed from the ice bath and allowed to warm to 23 °C to stir for 1 h before the reaction was determined complete *via* TLC. The reaction mixture was quenched by slow addition of Rochelle's salt (Sat. soln, 1 mL) and then diluted further with water (5 mL) and ethyl acetate (10 mL). The two phases were separated, and the organic phase was washed with water (2 × 10 mL) and brine (20 mL), dried over MgSO₄, filtered to remove the solids and concentrated under reduced pressure. The crude material was then subjected to flash column chromatography (*R_f* = 0.3, 6:4 ethyl acetate:*n*-hexane) to alcohol **218** as a colourless oil (70 mg, 80 %); $\nu_{\max}/\text{cm}^{-1}$ (neat) 3398 (NH), 3293 br (OH), 30.57 (CH), 2922 (CH), 2874 (CH), δ_{H} (400 MHz; CDCl₃) 2.29 (1 H, s, OH), 2.77 (2 H, t, *J* = 5.8, SCH₂CH₂OH), 3.53 (2 H, t, *J* = 5.8, SCH₂CH₂OH), 7.10–7.19 (2 H, Stack, CHCHCC and CHCHCNH), 7.23 (1 H, d, *J* = 2.6, CCHNH), 7.26–7.31 (1 H, m, CHCHCC or CHCHCNH), 7.68 (1 H, dd, *J* = 7.2, 1.9, CHCHCC or CHCHCNH), 8.35 (1 H, s, NH); δ_{C} (101 MHz; CDCl₃) 39.2 (CH₂), 60.3 (CH₂), 103.9 (C), 111.8 (CH), 119.2 (CH), 120.8 (CH), 123.0 (CH), 129.3 (C), 130.1 (CH), 136.4 (C); LRMS *m/z* (ES+) 194.1 ([M + H]⁺, 100%); HRMS *m/z* (ES+) calcd for C₁₀H₁₂NOS 194.0640, found 194.0641.

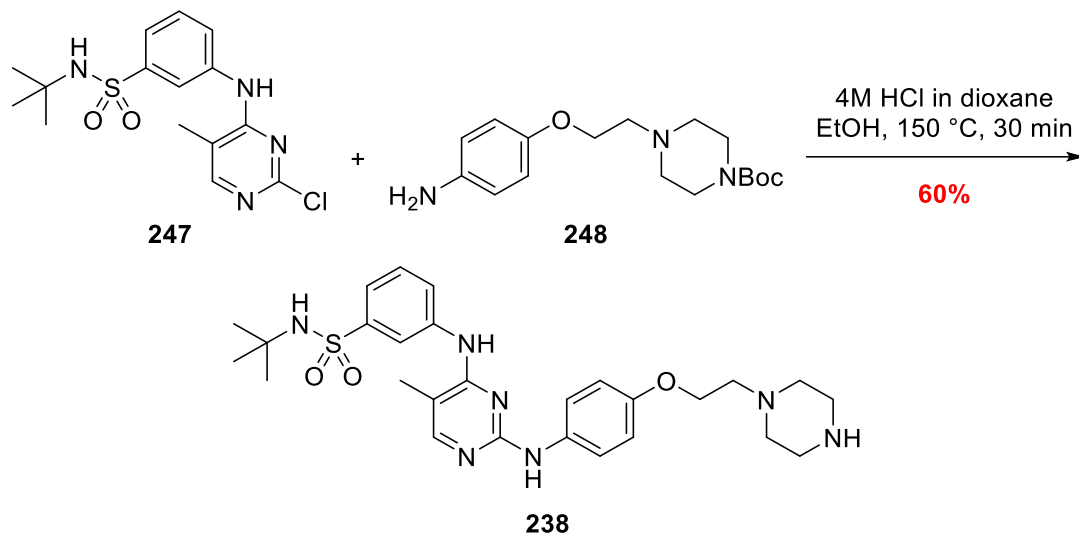
*A novel preparation of a known compound.*³⁹⁵ *The recorded data are in agreement with that reported in the literature.*³⁹⁵ *The protocol followed is based on a literature procedure.*³⁹⁶

220) Methyl 2-((5-chloro-1H-indol-3-yl)thio)acetate



A solution of I₂ (279 mg, 1.10 mmol) and KI (183 mg, 1.10 mmol) in MeOH:H₂O (4:1, 2.5 mL) was added dropwise over 10 h to a solution of 5-chloroindole **220** (200 mg, 1.32 mmol) and thioglycolic acid **199** (0.10 mL, 1.10 mmol) in MeOH:H₂O (4:1, 2.5 mL) at 23 °C. The reaction mixture was stirred for 68 h before being quenched by the addition of NaHCO_{3(aq)} (Sat. Soln., 5 mL) and then diluted further with ethyl acetate (5 mL). The resultant phases were separated and the organic phase was washed sequentially with Na₂S₂O_{3(aq)} (Sat. Soln., 10 mL), NaOH_(aq) (1 M, 20 mL), water (10 mL) and brine (20 mL). The organic was then dried over MgSO₄, filtered and concentrated under reduced pressure. The resulting crude material was subjected to flash column chromatography (*R_f* = 0.3, 6:4 *n*-hexane:ethyl acetate) to give 5-chlorosulfenylindole **220** as a colourless solid (197 mg, 58%); **mp** = 87–89 °C; $\nu_{\max}/\text{cm}^{-1}$ (neat) 3311 (NH), 3089 (CH), 2957 (CH), 1723 (CO); δ_{H} (400 MHz; CDCl₃) 3.40 (2 H, s, SCH₂CO₂CH), 3.67 (3 H, s, CO₂CH₃), 7.13 (1 H, dd, *J* = 8.6, 2.1, ClCCHCH), 7.19 (1 H, d, *J* = 8.6, CHCHC), 7.30 (1 H, d, *J* = 2.7, CCHNH), 7.69 (1 H, d, *J* = 2.1, ClCCHC), 8.80 (1 H, s, NH); δ_{C} (101 MHz; CDCl₃) 38.7 (CH₂), 52.5 (CH₃), 103.6 (C), 112.9 (CH), 118.5 (CH), 123.2 (CH), 126.6 (C), 130.2 (C), 131.9 (CH), 134.6 (CCl), 171.3 (CO); **LRMS *m/z* (ES⁺)** 278.0 ([M + Na]⁺, 100%), 256.0 ([M + H]⁺, 50); **HRMS *m/z* (ES⁺)** calcd for C₁₁H₁₀NO₂S³⁵ClNa 278.0018, found 278.0023.

*A novel compound prepared according to a literature procedure.*²²³

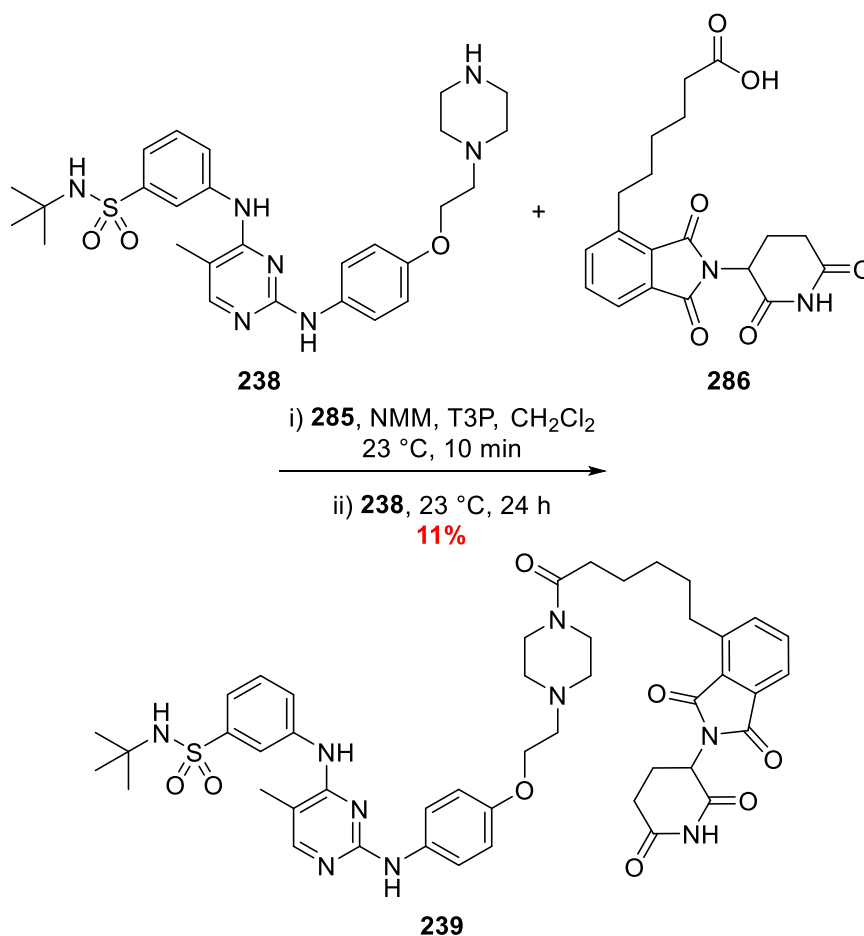
238) *N*-(*tert*-Butyl)-3-((5-methyl-2-((4-(2-(piperazin-1-yl)ethoxy)phenyl)amino)pyrimidin-4-yl)amino)benzenesulfonamide

A solution of HCl in 1,4-dioxane (4 M, 10 drops from a syringe) was added to a suspension of chloropyrimidine **247** (622 mg, 1.75 mmol) and aniline **248** (592 mg, 1.84 mmol) in EtOH (5 mL) in a microwave tube immediately before placing it in the microwave. The reaction mixture was ramped to 150 °C (100W), whilst stirring, and held at this temperature for 30 min. The reaction mixture was allowed to cool and then was poured into a separating funnel containing NaHCO_{3(aq)} (Sat. Soln., 10 mL) and the organics were extracted with ethyl acetate (10 mL). The two phases were separated and the organic was washed with water (2 × 10 mL) and brine (20 mL), dried over MgSO₄, filtered to remove the solids and concentrated under reduced pressure. The crude material was subjected to reverse-phase column chromatography (Combi-Flash 300+, 30g C-18 column, MeCN:NH₄OH/H₂O gradient) to yield **238** as an off-white solid (567 mg, 60%); **mp** = 241–242 °C; $\nu_{\max}/\text{cm}^{-1}$ (neat) 3334 (NH), 2942 (CH), 2827 (CH), 1305 (SO), 1137 (SO); δ_H (400 MHz; CDCl₃) 1.19 (9 H, s, C(CH₃)₃), 2.15 (3 H, d, $J = 0.9$, CH₃), 2.63 (4 H, m, CH₂N(CH₂)₂ or (CH₂)₂NH), 2.80 (2 H, t, $J = 5.5$, NCH₂CH₂OAr), 2.93 (4 H, t, $J = 5.0$, CH₂N(CH₂)₂ or (CH₂)₂NH), 4.11 (2 H, t, $J = 5.5$, NCH₂CH₂OAr), 6.84 (2 H, AA'BB', *Ar-H*), 7.38 (2 H, AA'BB', *Ar-H*), 7.44 (1 H, t, $J = 7.9$, CHCHCH), 7.58 (1 H, ddd, $J = 7.8, 1.9, 1.0$, SO₂CCHCH, or CHCHCNH), 7.80 (1 H, d, $J = 0.9$, CH₃CCHN), 7.93–7.97

(1 H, m, SO₂CCHCH, or CHCHCNH), 8.16 (1 H, *app.* t, $J = 1.9$, CCHCNH); δ_c (101 MHz; CDCl₃) 13.5 (CH₃), 30.4 ((CH₃)₃), 45.8 (CH₂), 54.7 (CH₂), 54.9 (C), 58.8 (CH₂), 66.7 (CH₂), 115.8 (CH), 121.2 (CH), 122.2 (CH), 123.2 (CH), 127.0 (CH), 128.8 (CH), 130.0 (C), 135.0 (C), 141.8 (C), 145.7 (C), 155.6 (CH), 156.4 (C), 160.2 (C), 161.2 (C); LRMS m/z (ES+) 540.3 ([M + H]⁺, 26%); HRMS m/z (ES+) calcd for C₂₇H₃₈N₇O₃S 540.2757, found 540.2756.

*A novel compound prepared according to a modified literature procedure.*³⁹⁷

239) *N*-(*tert*-Butyl)-3-((2-((4-(2-(4-(6-(2-(2,6-dioxopiperidin-3-yl)-1,3-dioxoisindolin-4-yl)hexyl)piperazin-1-yl)ethoxy)phenyl)amino)-5-methylpyrimidin-4-yl)amino)benzenesulfonamide

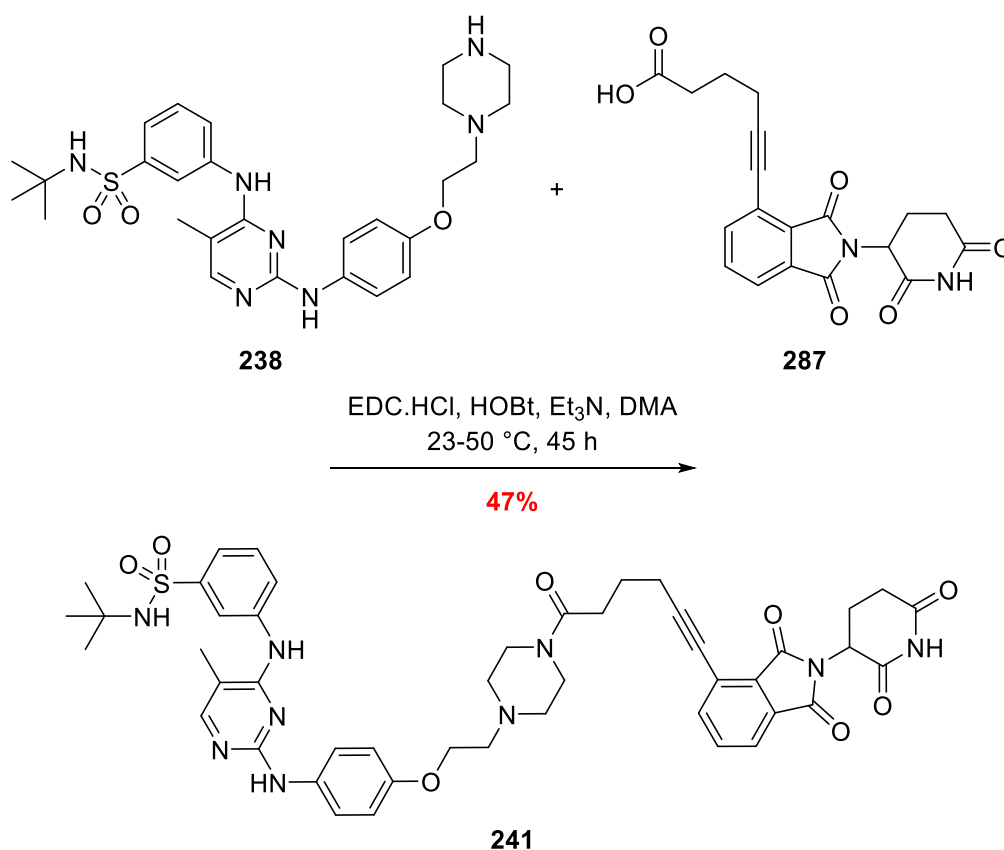


T3P (50% wt in CH₂Cl₂, 124 mg of T3P/248 mg of T3P soln., 0.390 mmol) was added to a solution of acid **286** (53 mg, 0.14 mmol) and NMM (16 μL, 0.14 mmol) in dichloromethane (0.8 mL) and stirred at 23 °C. After 10 min, amine **238** (51 mg, 0.09 mmol) was added and stirred for a further 24 h after which point the reaction was determined complete *via* TLC (R_f = 0.2, 10% MeOH in ethyl acetate). The reaction mixture was concentrated, re-solubilised and loaded onto an SCX column. The SCX column was eluted sequentially with MeOH (3 × 3 mL) and then the desired material was collected from the column though elution with a methanolic solution of NH₃ (7 M, 2 × 3 mL). The collected crude was subjected to column chromatography (R_f = 0.2, 10% MeOH in ethyl acetate) to yield PROTAC **239** as a white solid (9 mg, 11%); **mp** = 129–131 °C; $\nu_{\max}/\text{cm}^{-1}$ (neat) 3306 (NH), 2925 (CH), 1708 br (CO), 1321 (SO), 1145 (SO);

δ_H (400 MHz; $CDCl_3$) 1.18 (9 H, s, $C(CH_3)_3$), 1.25 (1 H, s), 1.39–1.49 (3 H, Stack), 1.53–1.83 (8 H, Stack), 2.12 (3 H, d, $J = 0.9$, CH_3CCHN), 2.29–2.36 (2 H, Stack), 2.51–2.64 (4 H, m, $CH_2N(CH_2)_2$ or $(CH_2)_2NH$), 2.78–2.91 (4 H, m, $CH_2N(CH_2)_2$ or $(CH_2)_2NH$), 2.98–3.13 (2 H, m, $NCO(CH_2)_3CH_2(CH_2)_1C$), 3.48 (2 H, t, $J = 5.3$, $ArOCH_2CH_2N$), 3.56–3.65 (1 H, m), 3.66–3.74 (1 H, m), 4.13 (2 H, t, $J = 5.4$, $ArOCH_2CH_2N$), 4.67 (1 H, s, NH), 4.93–5.01 (1 H, m, $NCHCO$), 6.50 (1 H, s, NH), 6.85–6.89 (2 H, AA'BB', $Ar-H$), 7.37–7.43 (3 H, Stack, contains AA'BB' $Ar-H$), 7.52 (1 H, dd, $J = 7.7, 1.1$, CH_2CCH or $CHCHCCO$), 7.56 (1 H, ddd, $J = 7.9, 1.8, 1.0$, $O_2SCCHCHCHNH$), 7.63 (1 H, *app.* t, $J = 7.5$, $CH_2CCHCHCHCCO$), 7.72 (1 H, dd, $J = 7.4, 1.1$, CH_2CCH or $CHCHCCO$), 7.81 (1 H, ddd, $J = 8.2, 2.3, 1.0$, $O_2SCCHCH$), 7.92 (1 H, d, $J = 0.9$, CH_3CCHN), 8.15 (1 H, t, $J = 2.0$, $SO_2CCHCNH$), 9.66 (1 H, s, NH); **δ_C (101 MHz; $CDCl_3$)** 13.4 (CH_3), 22.9 (CH_2), 25.1 (CH_2), 29.2 (CH_2), 29.8 (CH_2), 30.3 ($C(CH_3)_3$), 30.7 (CH_2), 31.4 (CH_2), 31.6 (CH_2), 33.0 (CH_2), 41.6 (CH_2), 45.7 (CH_2), 49.2 (CH), 53.4 (CH_2), 53.7 (CH_2), 54.7 (CH_2), 57.2 (CH_2), 60.6 (C), 66.2 (CH_2), 105.1 (C), 115.2 (CH), 118.5 (CH), 121.3 (CH), 121.7 (H), 122.0 (CH), 122.3 (CH), 124.4 (CH), 128.2 (C), 129.4 (CH), 132.4 (C), 133.3 (C), 134.2 (CH), 136.2 (CH), 139.8 (C), 143.6 (C), 144.2 (C), 154.3 (C), 158.8 (C), 159.0 (C), 167.5 (CO), 168.0 (CO), 169.0 (CO), 171.7 (CO), 171.8 (CO); **LRMS m/z (ES+)** 895.4 ($[M + H]^+$, 45%), 894.4 ($[M]^+$, 100); **HRMS m/z (ES+)** calcd for $C_{46}H_{56}N_9O_8S$ 894.3973, found 894.3976.

*A novel compound prepared according to a literature procedure.*³⁹⁸

240) *N*-(*tert*-butyl)-3-((2-((4-(2-(4-(6-(2-(2,6-dioxopiperidin-3-yl)-1,3-dioxoisindolin-4-yl)hex-5-ynoyl)piperazin-1-yl)ethoxy)phenyl)amino)-5-methylpyrimidin-4-yl)amino)benzenesulfonamide

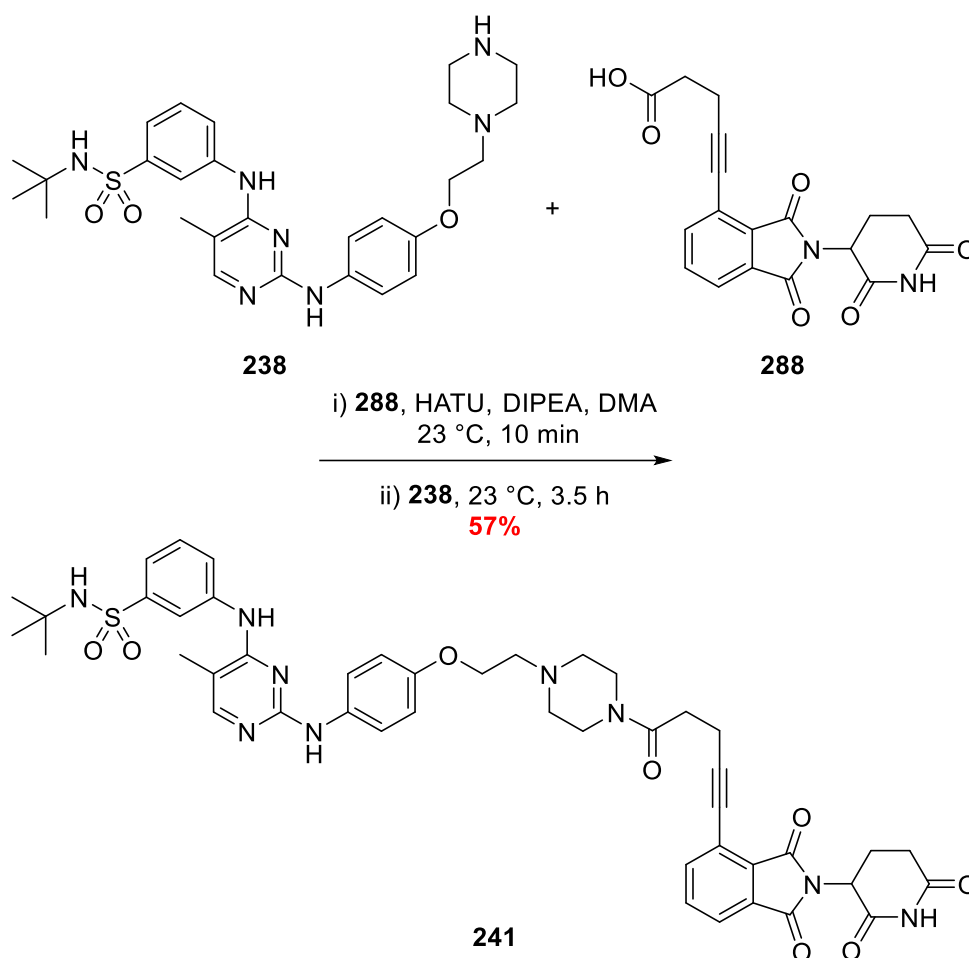


Et₃N (20 μ L, 0.16 mmol) was added to a solution of amine **238** (40 mg, 0.07 mmol), acid **287** (27 mg, 0.07 mmol), EDCI·HCl (16 mg, 0.08 mmol), HOBT (11 mg, 0.08 mmol) in anhydrous DMA (1 mL) and stirred at 23 °C. After 18 h, poor reaction progress was observed by TLC so the reaction temperature was increased to 50 °C. After a further 27 h, the reaction was determined complete *via* TLC (R_f = 0.2, 10% MeOH in ethyl acetate) the reaction mixture was diluted with ethyl acetate (10 mL) and then quenched by the addition of water (10 mL). The resulting phases were separated and the organic was washed sequentially with water (4 \times 10 mL) and brine (20 mL), dried over MgSO₄, filtered to remove the solids and concentrated under reduced pressure. The resulting crude material was subjected to flash column chromatography (R_f = 0.2, 10% MeOH in ethyl acetate) to yield PROTAC **240** as a white solid (31 mg, 47%); **mp** = 153–155 °C; $\nu_{\max}/\text{cm}^{-1}$ (neat) 3314 (NH), 2932 (CH), 2228 (C \equiv C), 1769 (CO), 1710 br (CO), 1321 (SO), 1144 (SO); δ_H (400 MHz; (CD₃)₂SO) 1.12 (9 H, s, C(CH₃)₃), 1.80 (2 H,

app. p, $J = 7.1$, $\text{COCH}_2\text{CH}_2\text{CH}_2$), 2.03–2.09 (1 H, m), 2.10–2.14 (3 H, m, CH_3), 2.23 (2 H, m), 2.45 (3 H, Stack), 2.59 (3 H, Stack), 2.65–2.71 (1 H, m), 3.48 (1 H, m), 3.55–3.62 (4 H, m, $\text{N}(\text{CH}_2)_2$ or $(\text{CH}_2)_2\text{NCO}$), 4.01 (2 H, *app.* t, $J = 5.7$, OCH_2CH_2), 4.10–4.18 (4 H, m, $\text{N}(\text{CH}_2)_2$ or $(\text{CH}_2)_2\text{NCO}$), 5.14 (1 H, dd, $J = 12.8$, 5.4, NCHCHH'), 6.78–6.82 (2 H, AA'BB', *Ar-H*), 7.46–7.50 (2 H, Stack), 7.50–7.55 (2 H, AA'BB', *Ar-H*), 7.57 (1 H, s, *Ar-H*), 7.81–7.84 (1 H, m, *Ar-H*), 7.86 (1 H, m, *Ar-H*), 7.90 (1 H, d, $J = 0.9$, CH_3CCH), 8.09–8.15 (2 H, Stack, *Ar-H*), 8.54 (1 H, s, *NH*), 8.79 (1 H, s, *NH*), 11.17 (1 H, s, *NH*); δ_{C} (101 MHz; $(\text{CD}_3)_2\text{SO}$) 12.81 (CH_3), 29.0 (CH_2), 29.8 ($\text{C}(\text{CH}_3)_3$), 30.8 (CH_2), 31.3 (CH_2), 44.8 (C), 46.5 (CH), 49.0 (CH_2), 53.2 (CH_2), 56.6 (CH_2), 62.8 (CH_2), 68.4 (CH_2), 69.7 (CH_2), 76.6 (C), 98.4 (C), 105.6 (C), 114.3 (CH), 118.9 (CH) 119.9 (C), 120.0 (CH), 120.2 (CH), 122.7 (CH), 124.8 (CH), 128.9 (CH), 130.3 (C), 132.0 (C), 134.3 (C), 134.7 (CH), 138.2 (CH), 140.5 (C), 144.4 (C), 158.3 (C), 159.0 (C), 166.3 (CO), 169.8 (CO), 170.1 (CO), 172.8 (CO), 175.3 (CO); LRMS m/z (ES+) 891.4 ($[\text{M} + \text{H}]^+$, 50%), 890.4 ($[\text{M}]^+$, 100); HRMS m/z (ES+) calcd for $\text{C}_{46}\text{H}_{52}\text{N}_9\text{O}_8\text{S}$ 890.3660, found 890.3671.

A novel compound prepared according to a literature procedure.³⁹⁹ One aromatic CH and quaternary C were not observed in the ^{13}C -NMR spectrum.

241) *N*-(*tert*-Butyl)-3-((2-((4-(2-(4-(5-(2-(2,6-dioxopiperidin-3-yl)-1,3-dioxoisindolin-4-yl)pent-4-ynoyl)piperazin-1-yl)ethoxy)phenyl)amino)-5-methylpyrimidin-4-yl)amino)benzenesulfonamide

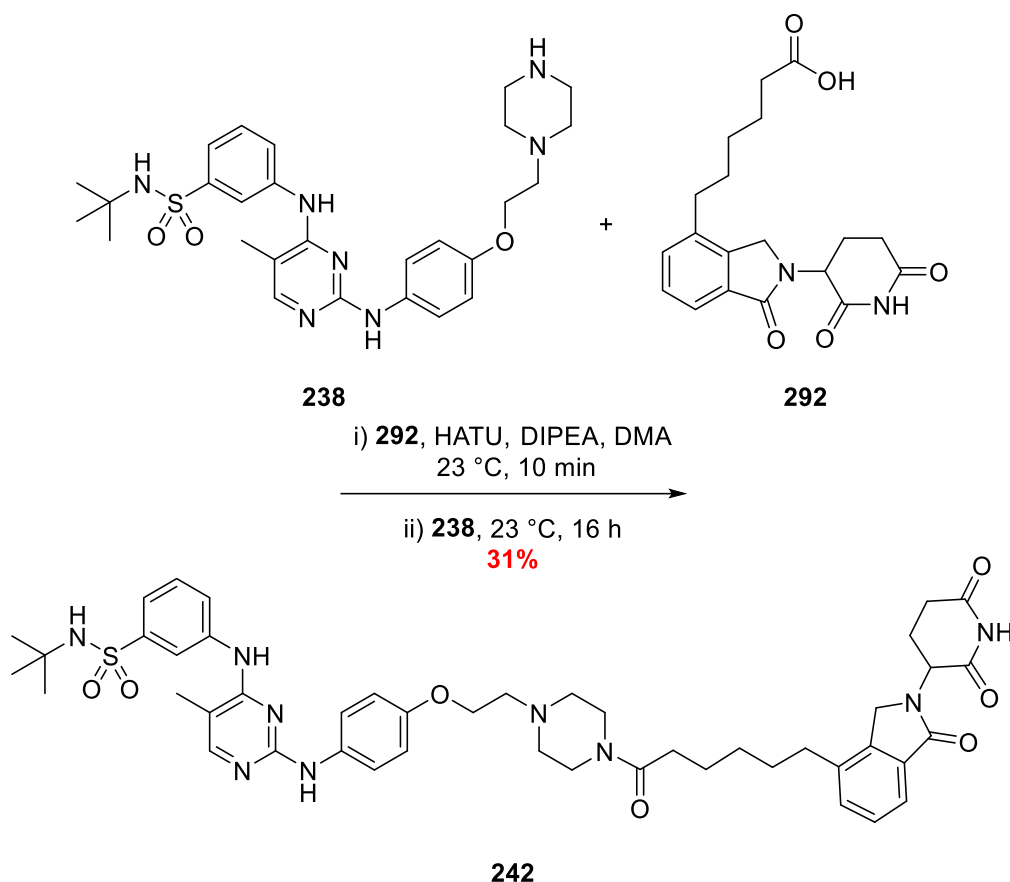


HATU (31 mg, 0.08 mmol) was added to a solution of acid **288** (26 mg, 0.07 mmol) and DIPEA (26 μ L, 0.15 mmol) in anhydrous DMA (0.5 mL) and the resulting solution was stirred at 23 °C. After 10 min, a solution of amine **238** (40 mg, 0.07 mmol) in anhydrous DMA (0.5 mL) was added and the stirring was continued. After 3.5 h, the reaction was determined complete *via* TLC ($R_f = 0.2$, 10% MeOH in CH_2Cl_2) and the reaction mixture was quenched by addition of water (5 mL) and extracted with ethyl acetate (10 mL). The two phases were then separated and the organic washed with water (3 \times 10 mL) and brine (20 mL), dried over MgSO_4 , filtered to remove the solids and concentrated under reduced pressure. The crude material was subjected to flash column chromatography ($R_f = 0.2$, 10% MeOH in CH_2Cl_2) to yield PROTAC **241** as a white solid (37 mg, 57%); **mp** = 178–179 °C; $\nu_{\text{max}}/\text{cm}^{-1}$ (neat) 3310 (NH), 2928 (CH),

2236 (C≡C), 1773 (CO), 1710 br (CO), 1321 (SO), 1144 (SO); δ_H (400 MHz; (CD₃)₂SO) 1.12 (9 H, s, C(CH₃)₃), 2.01–2.08 (1 H, m), 2.12 (3 H, s, CH₃C), 2.45 (6 H, s, Stack), 2.58 (2 H, Stack), 2.70 (6 H, Stack), 2.82–2.95 (1 H, m), 3.48 (4 H, *app.* s, N(CH₂)₂ or (CH₂)₂NCO), 4.02 (2 H, t, *J* = 5.7, 5.7, OCH₂CH₂N), 5.14 (1 H, dd, *J* = 12.9, 5.4, NCHCHH'), 6.77–6.83 (2 H, AA'BB', *Ar-H*), 7.47–7.50 (2 H, m, *Ar-H*), 7.53 (2 H, AA'BB', *Ar-H*), 7.58 (1 H, s, *Ar-H*), 7.79–7.83 (1 H, m, *Ar-H*), 7.84–7.88 (1 H, m, *Ar-H*), 7.90 (1 H, s, *Ar-H*), 8.08–8.17 (2 H, Stack, *Ar-H*), 8.55 (1 H, s, NH), 8.80 (1 H, s, NH), 11.15 (1 H, s); δ_C (101 MHz; (CD₃)₂SO) 13.5 (CH₃), 15.3 (CH₂), 21.9 (CH₂), 29.8 (C(CH₃)₃), 30.9 (CH₂), 31.1 (CH₂), 49.0 (CH), 52.8 (C), 53.2 (CH₂), 56.6 (CH₂), 65.5 (CH₂), 76.0 (C), 98.4 (C), 105.6 (C), 114.3 (CH), 118.9 (CH), 120.0 (CH), 120.2 (CH), 122.7 (CH), 124.8 (C), 128.9 (CH), 130.2 (C), 132.0 (C), 134.3 (C), 134.7 (CH), 138.2 (CH), 140.5 (C), 144.4 (C), 152.8 (CH), 156.0 (CH), 158.2 (C), 159.0 (C), 165.7 (CO), 166.3 (CO), 168.6 (CO), 169.8 (CO), 172.8 (CO); LRMS *m/z* (ES+) 877.4 ([M + H]⁺, 40%), 890.4 ([M]⁺, 100); HRMS *m/z* (ES+) calcd for C₄₅H₅₀N₉O₈S 876.3503, found 876.3508.

A novel compound prepared according to a literature procedure.⁴⁰⁰ The ¹³C-NMR data is missing a CH₂ resonance signal.

242) *N*-(*tert*-Butyl)-3-((2-((4-(2-(4-(6-(2-(2,6-dioxopiperidin-3-yl)-1-oxoisindolin-4-yl)hexanoyl)piperazin-1-yl)ethoxy)phenyl)amino)-5-methylpyrimidin-4-yl)amino)benzenesulfonamide

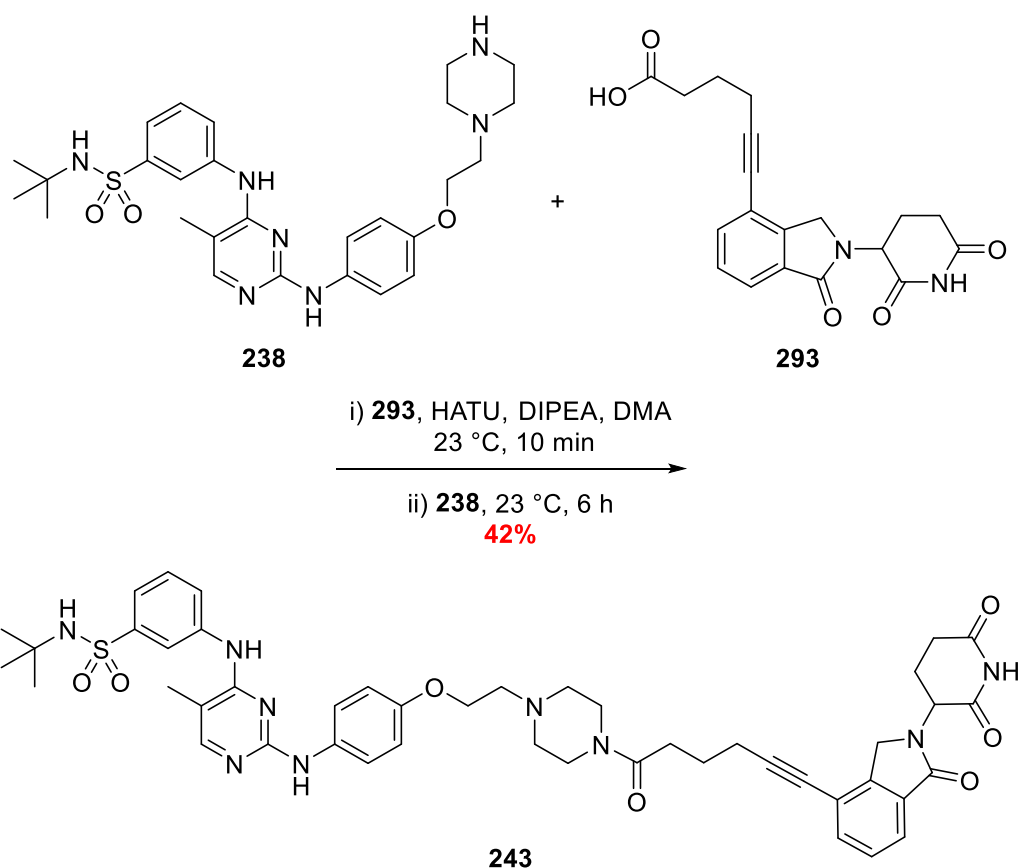


HATU (43 mg, 0.11 mmol) was added to a solution of acid **292** (31 mg, 0.09 mmol) and DIPEA (30 μ L, 0.17 mmol) in anhydrous DMA (0.5 mL) and the resulting solution was stirred at 23 °C. After 10 min, a solution of amine **238** (47 mg, 0.09 mmol) in anhydrous DMA (1 mL) was added and the stirring was continued. After 16 h, the reaction was determined complete *via* TLC (R_f = 0.2, 10% MeOH in CH_2Cl_2) and the reaction mixture was quenched by addition of water (5 mL) and extracted with ethyl acetate (10 mL). The two phases were then separated and the organic washed with water (2 \times 10 mL) and brine (20 mL), dried over MgSO_4 , filtered to remove the solids and concentrated under reduced pressure. The crude material was subjected to flash column chromatography (R_f = 0.2, 10% MeOH in CH_2Cl_2) to yield PROTAC **242** as a white solid (24 mg, 31%); **mp** = 151–152 °C; $\nu_{\text{max}}/\text{cm}^{-1}$ (neat) 3310 (NH), 2934 (CH), 1685 br (CO), 1320 (SO), 1144 (SO); δ_H (400 MHz; $(\text{CD}_3)_2\text{SO}$) 1.12 (9 H, s, $\text{C}(\text{CH}_3)_3$), 1.29–1.38 (2 H,

m), 1.53 (2 H, *app.* p, $J = 7.5$), 1.61 (2 H, *app.* p, $J = 7.9$), 1.96–2.05 (1 H, m), 2.12 (3 H, d, $J = 0.9$, CH_3CCHN), 2.29 (2 H, *app.* t, $J = 7.4$), 2.37–2.47 (7 H, Stack), 2.63 (2 H, *app.* t, $J = 7.7$), 2.68 (2 H, m), 2.86–2.98 (1 H, m), 3.43 (4 H, s, $\text{N}(\text{CH}_2)_2$ or $(\text{CH}_2)_2\text{NCO}$), 4.03 (2 H, d, $J = 5.6$, OCH_2CH_2), 4.30 (1 H, d, $J = 17.2$, $\text{CCHH}'\text{N}$), 4.46 (1 H, d, $J = 17.2$, $\text{CCHH}'\text{N}$), 5.13 (1 H, dd, $J = 13.3$, 5.1, NCHCHH'), 6.77–6.83 (2 H, AA'BB', *Ar-H*), 7.43–7.46 (2 H, m, *Ar-H*), 7.47–7.50 (1 H, m, *Ar-H*), 7.51–7.54 (2 H, m, AA'BB', *Ar-H*), 7.54–7.56 (1 H, m, *Ar-H*) 7.57 (1 H, s, *Ar-H*), 7.90 (1 H, d, $J = 0.9$, CH_3CCHN), 8.13 (2 H, Stack, *Ar-H*), 8.55 (1 H, s, *NH*), 8.80 (1 H, s, *NH*), 11.00 (1 H, s, *NH*); δ_{C} (**101 MHz; $(\text{CD}_3)_2\text{SO}$**) 13.5 (CH_3), 22.5 (CH_2), 24.6 (CH_2), 28.7 (CH_2), 29.1 (CH_2), 29.8 ($\text{C}(\text{CH}_3)_3$), 31.2 (CH_2), 32.1 (CH_2), 44.8 (C) 46.2 (CH_2), 51.5 (CH), 53.2 (CH_2), 56.5 (CH_2), 65.4 (CH_2) 105.6 (C), 108.8 (C) 114.3 (CH), 119.0 (CH), 120.0 (Stack, 2 \times CH), 120.2 (CH), 120.6 (CH), 124.8 (C), 128.3 (CH), 128.9 (CH), 131.5 (CH), 134.3 (C), 137.5 (C), 140.5 (C), 144.4 (CH), 152.8 (C), 156.0 (C), 158.2 (C), 159.0 (C), 168.4 (CO), 170.5 (CO), 171.1 (CO), 172.9 (CO); **LRMS m/z (ES $^+$)** 881.4 ($[\text{M} + \text{H}]^+$, 40%), 880.4 ($[\text{M}]^+$, 100); **HRMS m/z (ES $^+$)** calcd for $\text{C}_{46}\text{H}_{58}\text{N}_9\text{O}_7\text{S}$ 880.4180, found 880.4179.

*A novel compound prepared according to a literature procedure.*⁴⁰⁰

243) *N*-(*tert*-Butyl)-3-((2-((4-(2-(4-(5-(2-(2,6-dioxopiperidin-3-yl)-1-oxoisindolin-4-yl)pent-4-ynoyl)piperazin-1-yl)ethoxy)phenyl)amino)-5-methylpyrimidin-4-yl)amino)benzenesulfonamide

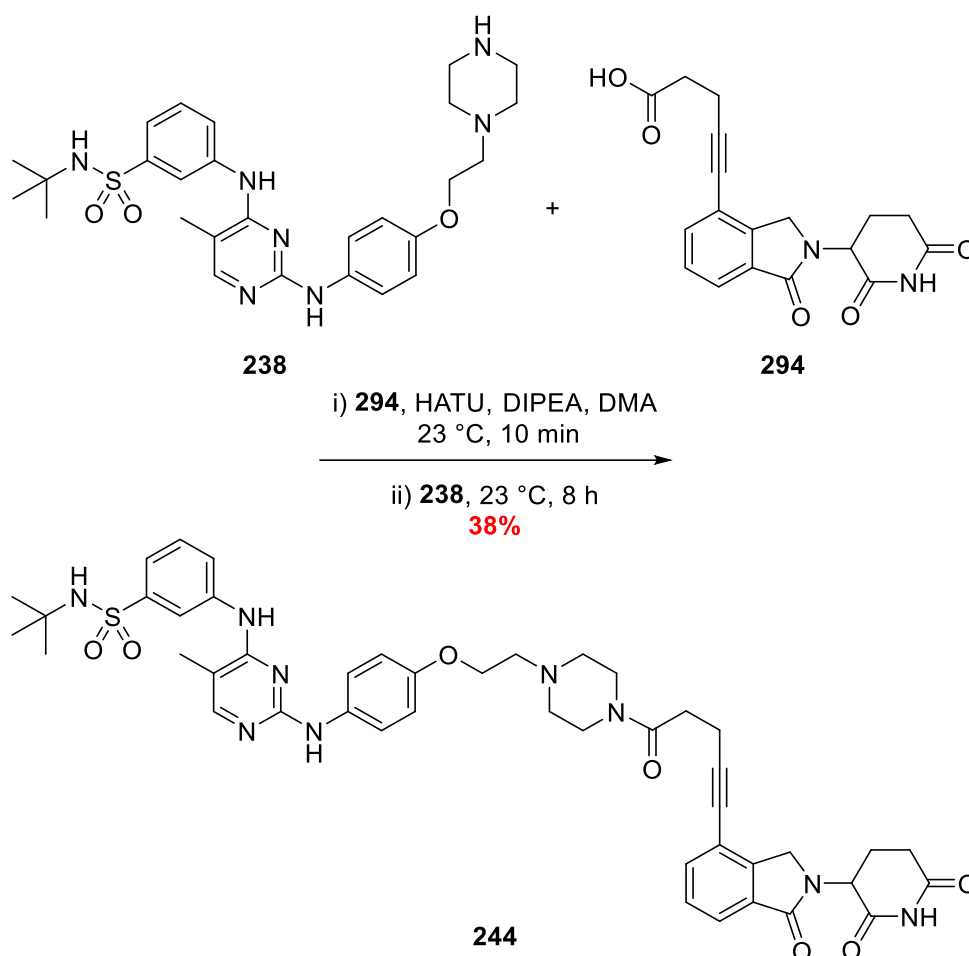


HATU (34 mg, 0.09 mmol) was added to a solution of acid **293** (26 mg, 0.07 mmol) and DIPEA (26 μ L, 0.15 mmol) in anhydrous DMA (0.5 mL) and the resulting solution was stirred at 23 °C. After 10 min, a solution of amine **238** (40 mg, 0.07 mmol) in anhydrous DMA (1 mL) was added and the stirring was continued. After 6 h, the reaction was determined complete *via* TLC (R_f = 0.2, 10% MeOH in CH_2Cl_2) and the reaction mixture was quenched by addition of water (5 mL) and extracted with ethyl acetate (10 mL). The two phases were then separated and the organic washed with water (2 \times 10 mL) and brine (20 mL), dried over MgSO_4 , filtered to remove the solids and concentrated under reduced pressure. The crude material was subjected to flash column chromatography (R_f = 0.2, 10% MeOH in CH_2Cl_2) to yield PROTAC **243** as a white solid (27 mg, 42%); **mp** = 175–177 °C; $\nu_{\text{max}}/\text{cm}^{-1}$ (neat) 3307 (NH), 2917 (CH), 2228 w ($\text{C}\equiv\text{C}$), 1691 br (CO), 1319 (SO), 1144 (SO); δ_H (400 MHz; CDCl_3) 1.17 (9 H, s), 1.96 (3 H,

Stack), 2.08 (3 H, d, $J = 0.9$, CH_3CCHN), 2.18–2.21 (1 H, m), 2.33–2.45 (1 H, m), 2.46–2.65 (7 H, Stack), 2.74–2.94 (4 H, Stack), 3.48 (2 H, q, $J = 5.0$, $\text{ArOCH}_2\text{CH}_2\text{N}$), 3.55–3.71 (1 H, m), 4.09 (2 H, t, $J = 5.0$, $\text{ArOCH}_2\text{CH}_2\text{N}$), 4.35 (1 H, d, $J = 16.8$, $\text{CCHH}'\text{N}$), 4.46 (1 H, d, $J = 16.8$, $\text{CCHH}'\text{N}$), 5.06 (1 H, s, NH), 5.26 (1 H, dd, $J = 13.3, 5.2$, NCHCHH'), 6.62 (1 H, s, NH), 6.80–6.86 (2 H, AA'BB', Ar-H), 7.34 (1 H, t, $J = 8.0$), 7.37–7.45 (3 H, Stack, contains AA'BB' Ar-H), 7.50–7.58 (3 H, Stack), 7.79 (2 H, Stack), 7.90 (1 H, d, $J = 0.9$, CH_3CCHN), 8.14 (1 H, t, $J = 1.9$, $\text{O}_2\text{SCCHCNH}$), 10.4 (1 H, s, NH); δ_{C} (101 MHz; CDCl_3) 13.4 (CH_3), 19.2 (CH), 23.6 (CH), 24.2 (CH), 30.3 ($\text{C}(\text{CH}_3)_3$), 31.7 (CH_2), 31.9 (CH_2), 41.7 (CH_2), 45.6 (CH_2), 47.1 (CH_2), 51.9 (CH), 53.2 (CH_2), 53.5 (CH_2), 54.6 (C), 57.2 (CH_2), 66.1 (CH_2), 95.4 (C), 105.1 (C), 115.1 (CH), 118.5 (CH), 121.1 (C), 121.8 (CH), 123.4 (CH), 124.5 (CH), 128.5 (CH), 129.3 (CH), 131.8 (CH), 133.5 (C), 134.7 (C), 139.8 (C), 143.7 (C), 144.3 (C), 154.1 (C), 155.9 (CH), 158.8 (C), 159.0 (C), 169.2 (CO), 170.5 (CO), 170.8 (CO), 172.3 (CO); **LRMS m/z (ES+)** 898.3 ([M + Na]⁺, 100%); **HRMS m/z (ES+)** calcd for $\text{C}_{46}\text{H}_{53}\text{N}_9\text{O}_7\text{S}$ 898.3686, found 898.3688.

*A novel compound prepared according to a literature procedure.*⁴⁰⁰

244) *N*-(*tert*-Butyl)-3-((2-((4-(2-(4-(5-(2-(2,6-dioxopiperidin-3-yl)-1-oxoisindolin-4-yl)pent-4-ynoyl)piperazin-1-yl)ethoxy)phenyl)amino)-5-methylpyrimidin-4-yl)amino)benzenesulfonamide

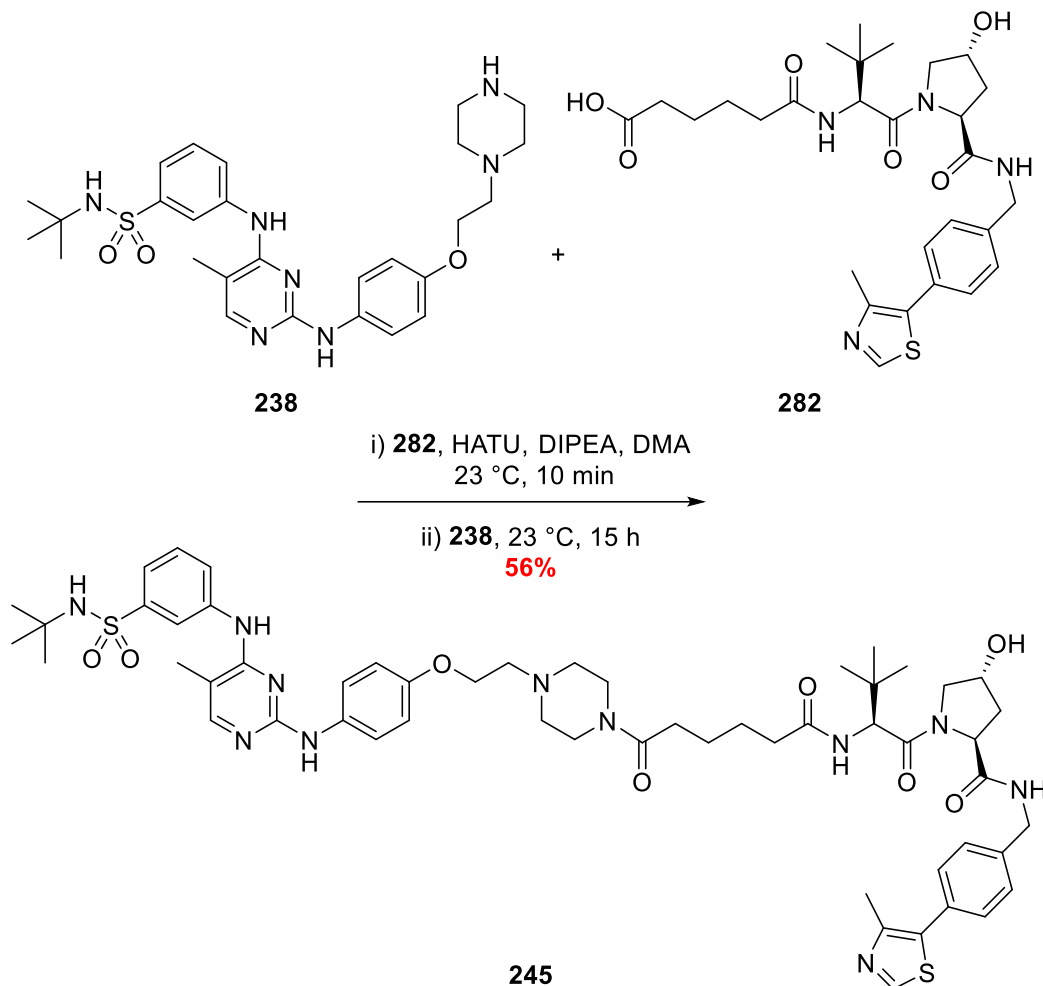


HATU (31 mg, 0.08 mmol) was added to a solution of acid **294** (25 mg, 0.07 mmol) and DIPEA (26 μ L, 0.15 mmol) in anhydrous DMA (0.5 mL) and the resulting solution was stirred at 23 °C. After 10 min, a solution of amine **238** (40 mg, 0.07 mmol) in anhydrous DMA (1 mL) was added and the stirring was continued. After 8 h, the reaction was determined complete *via* TLC (R_f = 0.2, 10% MeOH in CH_2Cl_2) and the reaction mixture was quenched by addition of water (5 mL) and extracted with ethyl acetate (10 mL). The two phases were then separated and the organic washed with water (3 \times 10 mL) and brine (20 mL), dried over MgSO_4 , filtered to remove the solids and concentrated under reduced pressure. The crude material was subjected to flash column chromatography (R_f = 0.2, 10% MeOH in CH_2Cl_2) to yield PROTAC **244** as a white solid (24 mg, 38%); **mp** = 155–158 °C; $\nu_{\text{max}}/\text{cm}^{-1}$ (neat) 3303 (NH), 2923 (CH), 2231 ($\text{C}\equiv\text{C}$),

1686 br (CO), 1320 (SO), 1144 (SO); δ_H (400 MHz; $CDCl_3$) 1.17 (9 H, s, $C(CH_3)_3$), 2.03–2.13 (3 H, m), 2.17–2.23 (1 H, m), 2.32–2.44 (1 H, m), 2.50–2.71 (6 H, Stack), 2.73–2.97 (6 H, Stack), 3.44–3.57 (2 H, m), 3.64–3.69 (2 H, m), 4.09 (2 H, t, $J = 5.4, 5.4$), 4.35 (1 H, d, $J = 16.9$, CCHH'N), 4.48 (1 H, d, $J = 16.9$, CCHH'N), 4.93 (1 H, s, NH), 5.27 (1 H, dd, $J = 13.3, 5.1$, NCHCHH'), 6.57 (1 H, s, NH), 6.80–6.87 (2 H, AA'BB', Ar-H), 7.35 (1 H, t, $J = 8.0$, Ar-H), 7.38–7.46 (3 H, Stack), 7.51–7.58 (2 H, Stack, Ar-H), 7.75–7.83 (2 H, Stack, Ar-H), 7.92 (1 H, d, $J = 0.9$, CH_3CCHN), 8.16 (1 H, t, $J = 2.0$, $O_2SCCHCNH$), 10.04 (1 H, s, NH); δ_C (101 MHz; $CDCl_3$) 13.4 (CH_3), 15.8 (CH_2), 29.8 (C), 30.3 ($C(CH_3)_3$), 31.7 (CH_2), 32.4 (CH_2), 41.9 (CH_2), 45.6 (C), 47.1 (CH_2), 51.9 (CH), 53.3 (CH_2), 53.5 (CH_2), 54.7 (CH_2), 57.2 (CH_2), 66.1 (C), 95.2 (C), 105.1 (C), 115.2 (CH), 118.5 (CH), 119.4 (C), 121.2 (CH), 121.9 (CH), 123.5 (CH), 124.5 (CH), 128.5 (CH), 129.4 (CH), 131.7 (C), 133.4 (C), 134.7 (CH), 139.8 (C), 149.6 (C), 154.2 (C), 156.0 (CH), 159.0 (C), 169.2 (CO), 169.4 (CO), 170.4 (CO), 172.2 (CO); LRMS m/z (ES+) 873.2 ($[M + H]^+$, 50%), 862.2 ($[M]^+$, 100); HRMS m/z (ES+) calcd for $C_{45}H_{52}N_9O_7S$ 862.3710, found 862.3713.

A novel compound prepared according to a literature procedure.⁴⁰⁰ The 1H -NMR spectrum is missing 2 proton resonances.

245) (2S,4R)-1-((S)-2-(6-(4-(2-(4-((3-(*N*-(*tert*-Butyl)sulfamoyl)phenyl)amino)-5-methylpyrimidin-2-yl)amino)phenoxy)ethyl)piperazin-1-yl)-6-oxohexanamido)-3,3-dimethylbutanoyl)-4-hydroxy-*N*-(4-(4-methylthiazol-5-yl)benzyl)pyrrolidine-2-carboxamide

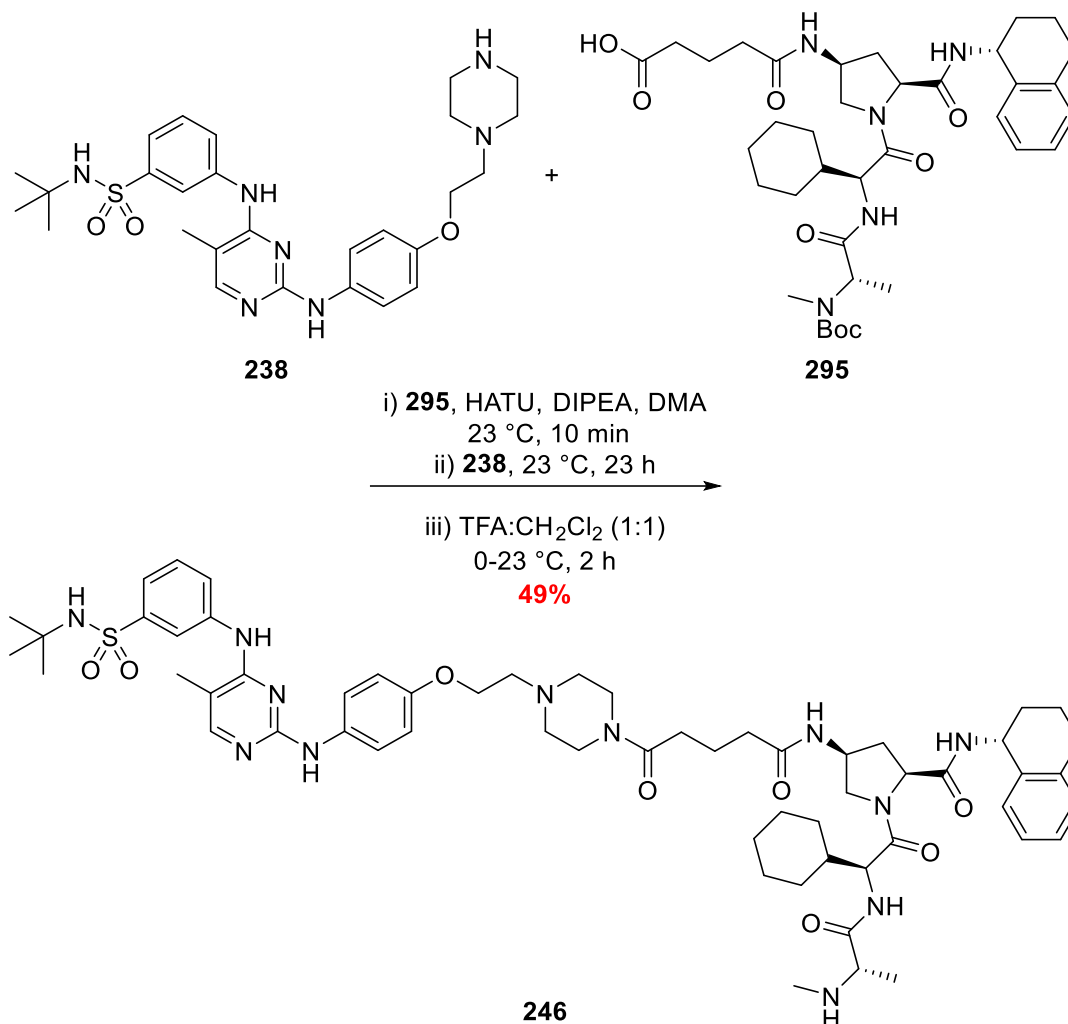


HATU (18 mg, 0.05 mmol) was added to a solution of **282** (25 mg, 0.04 mmol) and DIPEA (34 μ L, 0.20 mmol) in anhydrous DMA (0.25 mL) and the resulting solution was stirred at 23 °C. After 10 min, a solution of amine **238** (24 mg, 0.04 mmol) in anhydrous DMA (0.25 mL) was added and the stirring was continued. After 15 h, the reaction was determined complete *via* TLC (R_f = 0.3, 15% MeOH in CH_2Cl_2) and the reaction mixture was quenched by addition of water (5 mL) and extracted with ethyl acetate (10 mL). The two phases were then separated and the organic washed with water (5 \times 10 mL) and brine (20 mL), dried over MgSO_4 , filtered to remove the solids and concentrated under reduced pressure. The crude material was subjected to flash column chromatography (R_f = 0.3, 15% MeOH in CH_2Cl_2) to yield PROTAC

245 as a white solid (27 mg, 56%); **mp** = 239–240 °C; $\nu_{\max}/\text{cm}^{-1}$ (neat) 3281 br (NH), 29.35 (CH), 1672 br (CO); δ_{H} (**400 MHz; CDCl₃**) 0.93 (9 H, s, C(CH₃)₃), 1.10 (9 H, s, C(CH₃)₃), 1.48 (5 H, Stack), 1.90 (1 H, ddd, *J* 12.9, 8.4, 4.6), 1.98–2.07 (1 H, m), 2.12 (4 H, Stack), 2.23–2.34 (4 H, m), 2.44 (3 H, s, CH₃CCS), 3.45 (4 H, *app.* s), 3.60–3.72 (2 H, m), 4.07 (2 H, *app.* s), 4.21 (1 H, dd, *J* = 15.9, 5.5), 4.35 (1 H, s), 4.40–4.47 (1 H, m), 4.54 (1 H, *app.* d, *J* = 9.4), 5.14 (1 H, *app.* d, *J* = 3.6, CHOH), 6.82 (2 H, AA'BB', *Ar-H*), 7.38 (2 H, AA'BB', *Ar-H*), 7.42 (2 H, AA'BB', *Ar-H*), 7.47–7.51 (2 H, Stack, *Ar-H*), 7.53 (1 H, AA'BB', *Ar-H*), 7.58 (1 H, s, *Ar-H*), 7.88 (1 H, d, *J* = 9.6, *Ar-H*), 7.90 (1 H, s, CH₃CCH), 8.05–8.20 (2 H, Stack), 8.58 (2 H, Stack, *Ar-H*), 8.84 (1 H, s, NH), 8.98 (1 H, s, NH); δ_{C} (**101 MHz; CDCl₃**) 13.5 (CH₃), 16.0 (CH₃), 24.4 (CH₂), 25.2 (CH₂), 26.4 (C(CH₃)₃), 29.8 (C(CH₃)₃), 31.9 (CH₂), 34.7 (CH₂), 35.3 (CH₂), 38.0 (CH₂), 41.6 (CH₂), 43.2 (CH), 53.2 (CH₂), 56.3 (CH₂), 58.7 (CH), 64.9 (CH₂), 68.9 (CH), 81.4 (C), 99.2 (C), 105.7 (C), 107.9 (C), 114.4 (CH), 119.0 (CH), 120.3 (CH), 124.9 (CH), 127.4 (CH), 128.7 (CH), 128.8 (C),_z 128.9 (CH), 129.6 (C), 131.2 (C), 139.5 (C), 140.5 (C), 144.4 (C), 147.7 (CH), 151.5 (CH), 157.1 (CH), 158.1 (C), 159.0 (C), 169.7 (CO), 170.2 (CO), 170.5 (CO), 172.0 (CO); **LRMS *m/z* (ES⁺)** 1102.5 ([M + Na - H]⁺, 70%), 1080.5 ([M]⁺, 75); **HRMS *m/z* (ES⁺)** calcd for C₅₅H₇₃N₁₁O₈S₂Na 1102.4983, found 1102.5026.

*A novel compound prepared according to a literature procedure.*⁴⁰⁰ *One aromatic quaternary carbon resonance was not observed in the ¹³C-NMR.*

246) tert-Butyl ((S)-1-(((S)-2-((2S,4S)-4-(5-(4-(2-(4-((4-((3-(N-(tert-butyl)sulfamoyl)phenyl)amino)-5-methylpyrimidin-2-yl)amino)phenoxy)ethyl)piperazin-1-yl)-5-oxopentanamido)-2-(((R)-1,2,3,4-tetrahydronaphthalen-1-yl)carbamoyl)pyrrolidin-1-yl)-1-cyclohexyl-2-oxoethyl)amino)-1-oxopropan-2-yl)(methyl)carbamate

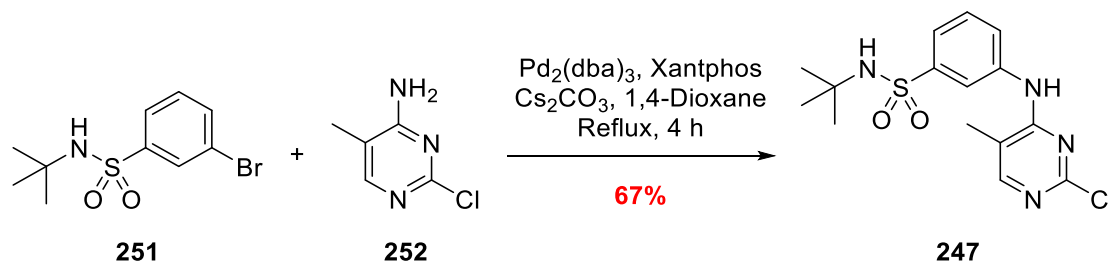


HATU (17 mg, 0.05 mmol) was added to a solution of acid **289** (29 mg, 0.04 mmol) and DIPEA (32 μ L, 0.18 mmol) in anhydrous DMA (0.50 mL) and the resulting solution was stirred at 23 °C. After 10 min, a solution of amine **232** (22 mg, 0.04 mmol) in anhydrous DMA (0.50 mL) was added and the stirring was continued. After 23 h, the reaction was determined complete *via* TLC ($R_f = 0.2$, 10% MeOH in CH₂Cl₂) and the reaction mixture was quenched by addition of water (5 mL) and extracted with ethyl acetate (10 mL). The two phases were then separated and the organic washed with water (4 \times 10 mL) and brine (20 mL), dried over MgSO₄, filtered to remove the solids and concentrated under reduced pressure. The crude material was

immediately re-solubilised in CH₂Cl₂ (1 mL) and treated with trifluoroacetic acid (1 mL) – the resulting solution was then stirred at 23 °C. After 2h, the reaction mixture was concentrated under reduced pressure, re-solubilised in MeOH (1 mL) and then loaded onto an SCX column. The column was eluted with MeOH (3 × 3 mL) and the desired material was removed from the column *via* elution with methanolic NH₃ (7 M, 2 × 3 mL). After concentration, PROTAC **246** was isolated with no need for further purification as a white solid (22 mg, 49%); **mp** = 130–131 °C; $\nu_{\max}/\text{cm}^{-1}$ (neat) 3292 (NH), 2929 (CH), 1648 br (CO), 1321 (SO), 1146 (SO); δ_{H} (400 MHz; CDCl₃) 1.01–1.11 (3 H, Stack), 1.20 (9 H, s, C(CH₃)₃), 1.21–1.29 (4 H, m), 1.38 (3 H, s), 1.47–1.72 (4 H, Stack), 1.75–1.89 (3 H, Stack), 1.91–2.03 (4 H, Stack), 2.07–2.16 (5 H, Stack), 2.26–2.36 (6 H, Stack), 2.40 (2 H, m), 2.53 (2 H, *app.* t, *J* = 5.2), 2.56–2.60 (2 H, *app.* t, *J* = 5.2), 2.71–2.86 (4 H, Stack), 3.00 (1 H, *app.* q, *J* = 6.9), 3.46–3.55 (2 H, m), 3.57–3.68 (4 H, Stack), 4.02–4.13 (3 H, Stack) 4.34 (2 H, *app.* p, *J* = 6.8), 4.50–4.63 (1 H, m), 4.66–4.75 (1 H, m), 4.95 (1 H, s, NH), 5.05–5.15 (1 H, m, CONHCHCHH'), 6.59 (1 H, s, NH), 6.81–6.89 (2 H, AA'BB', *Ar-H*), 7.02–7.18 (4 H, Stack), 7.30–7.43 (3 H, Stack), 7.50–7.62 (2 H, Stack), 7.66–7.75 (1 H, m), 7.78–7.86 (1 H, m), 7.84–7.91 (1 H, m), 7.97–8.04 (1 H, Stack), 8.09–8.17 (1 H, Stack); δ_{C} (101 MHz; CDCl₃) 13.3 (CH₃), 19.5 (CH₃), 20.0 (CH₂), 21.2 (CH₂), 25.8 (CH₂), 26.0 (CH₂), 28.6 (CH₂), 29.1 (CH₂), 29.9 (CH₂), 30.2 (C(CH₃)₃), 30.5 (CH), 31.3 (CH₂), 32.6 (CH₂), 35.1 (CH), 35.7 (CH₂), 40.5 (CH₃), 41.5 (CH), 45.5, 48.0 (CH), 49.3 (CH), 53.3 (CH₂), 53.7 (CH₂), 54.7 (CH), 55.8 (CH₂), 57.2 (CH₂), 60.2 (CH₂), 66.1 (C), 105.1 (C), 115.0 (CH), 118.4 (CH), 121.0 (CH), 121.9 (CH), 124.2 (C), 126.1 (CH), 127.3 (CH), 128.3 (CH), 129.2 (CH), 129.3 (CH), 133.2(C), 136.0 (C), 137.3 (C), 144.1 (C), 154.3 (C), 156.3 (CH), 158.9 (C), 170.8 (CO), 171.1 (CO), 172.4 (CO), 173.2 (CO), 175.0 (CO); **LRMS *m/z* (ES+)** 1141.5 ([M + Na – H]⁺, 100%), 1119.5 ([M]⁺, 60); **HRMS *m/z* (ES+)** calcd for C₅₉H₈₂N₁₂O₈SNa 1141.5991, found 1141.6040.

*A novel compound prepared according to a literature procedure.*⁴⁰⁰

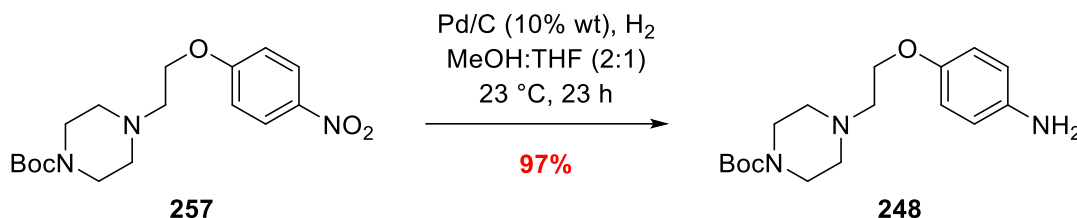
247) *N*-(*tert*-Butyl)-3-((2-chloro-5-methylpyrimidin-4-yl)amino)benzenesulfonamide



A flame-dried, two-neck flask fitted with a condenser was charged with pyrimidine **252** (500 mg, 3.48 mmol), aryl bromide **251** (1.22 g, 4.18 mmol), Cs_2CO_3 (2.58 g, 7.31 mmol), $\text{Pd}_2(\text{dba})_3$ (191 mg, 0.21 mmol), Xantphos (242 mg, 0.42 mmol) and then purged with argon. Anhydrous DMA (10 mL) was then added to the flask and the resulting solution heat to reflux. After 4 h, the reaction was deemed complete *via* TLC ($R_f = 0.2$, 6:4 ethyl acetate:*n*-hexane, N.B. 'Pyrimidine' and the product share similar R_f values, however 'pyrimidine' stains yellow and fades to clear in ~10 min with ninhydrin while the product stains blue and remains) and was allowed to cool to 23 °C. The reaction mixture was filtered through a celite bung and eluted with ethyl acetate (3 × 10 mL). The liquor was then poured into a separating funnel and washed with water (2 × 10 mL) and brine (20 mL), dried over MgSO_4 , filtered to remove the solids and concentrated under reduced pressure. The crude solid was then washed sequentially with Et_2O (3 × 20 mL), collected and the dried under high vacuum to afford chloropyrimidine **247**, with no need for further purification, as a pale-yellow solid (828 mg, 67%); **mp** = 198–200 °C; $\nu_{\text{max}}/\text{cm}^{-1}$ (neat) 3355 (NH), 2973 (CH), 2867 (CH), 1305 (SO), 1148 (SO); δ_H (400 MHz; CDCl_3) 1.23 (9 H, s, $\text{C}(\text{CH}_3)_3$), 2.24 (3 H, d, $J = 1.0$, CH_3), 7.52 (1 H, t, $J = 8.0$, CHCHCH), 7.65 (1 H, ddd, $J = 8.0, 2.0, 1.4$, SO_2CCHCH , or CHCHCNH), 7.83 (1 H, ddd, $J = 8.0, 2.0, 1.4$, SO_2CCHCH , or CHCHCNH), 7.98–8.04 (1 H, d, $J = 1.0$, CH_3CCHN), 8.24 (1 H, *app.* t, $J = 1.4$, CCHCNH); δ_C (101 MHz; CDCl_3) 13.6 (CH_3), 30.5 ($(\text{CH}_3)_3$), 68.1 (C), 115.9 (C), 122.1 (CH), 123.4 (CH), 126.8 (CH), 130.3 (CH), 140.4 (C), 145.9 (C), 157.0 (CH). **LRMS m/z (ES+)** 355.1 ($[\text{M}^{35}\text{Cl} + \text{H}]^+$, 100%), 357.1 ($[\text{M}^{37}\text{Cl} + \text{H}]^+$, 33); **HRMS m/z (ES+)** calcd for $\text{C}_{15}\text{H}_{20}\text{N}_4\text{O}_2\text{S}^{35}\text{Cl}$ 355.0995, found 355.0996.

A known compound prepared according to a literature procedure.⁴⁰¹ The recorded data are in agreement with that reported in the literature with the exception of two missing quaternary-carbon resonances in the ¹³C-NMR spectrum.⁴⁰¹

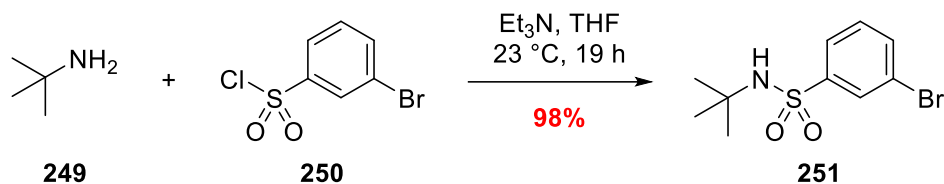
248) *tert*-Butyl 4-(2-(4-aminophenoxy)ethyl)piperazine-1-carboxylate



Palladium on carbon (10% wt., 348 mg) was added to a solution of nitrophenol **257** (1.92 g, 5.46 mmol) in MeOH:tetrahydrofuran (2:1, 30 mL) and stirred under a sealed atmosphere at 23 °C. Hydrogen gas was then bubbled continuously through the solution, with a vent in the septum, for 10 min and then the vent was removed and the hydrogen source was suspended above the solution to maintain a hydrogen atmosphere. This process was repeated twice throughout the course of the reaction. After 23 h, the reaction was determined complete *via* TLC ($R_f = 0.2$, 4:1 ethyl acetate:*n*-hexane) and the reaction mixture was filtered through a celite bung and eluted with MeOH (3 × 20 mL). The resulting liquor was concentrated under reduced pressure to give *p*-alkoxyaniline **248** as a brown solid (1.70 g, 97%); mp = 111–112 °C; $\nu_{\text{max}}/\text{cm}^{-1}$ (neat) 3453 (NH), 3344 (NH), 2951 (CH), 2834 (CH), 1675 (CO); δ_H (400 MHz; CDCl_3) 1.45 (9 H, s, $\text{C}(\text{CH}_3)_3$), 2.85 (4 H, t, $J = 5.3$, $\text{BocN}(\text{CH}_2)_2$ or $(\text{CH}_2)_2\text{NCH}_2$), 3.07 (2 H, t, $J = 5.1$, $\text{NCH}_2\text{CH}_2\text{OAr}$), 3.65 (4 H, d, $J = 5.3$, $\text{BocN}(\text{CH}_2)_2$ or $(\text{CH}_2)_2\text{NCH}_2$), 4.23 (2 H, t, $J = 5.1$, $\text{NCH}_2\text{CH}_2\text{OAr}$), 6.60–6.66 (2 H, m, AA'BB', *Ar-H*), 6.70–6.76 (2 H, m, AA'BB', *Ar-H*); δ_C (101 MHz; CDCl_3) 28.5 ($(\text{CH}_3)_3$), 42.1 (CH_2), 53.1 (CH_2), 57.1 (CH_2), 65.1 (CH_2), 80.6 (C), 115.9 (CH), 116.5 (CH), 140.8 (C), 151.1 (C), 154.4 (CO); LRMS m/z (ES+) 322.4 ($[\text{M} + \text{H}]^+$, 85%), 222.3 ($[\text{M} - \text{Boc} + \text{H}]^+$, 100); HRMS m/z (ES+) calcd for $\text{C}_{17}\text{H}_{28}\text{N}_3\text{O}_3$ 322.2131, found 322.2130.

A known compound prepared according to a literature procedure.⁴⁰² The recorded data are in agreement with that reported in the literature.⁴⁰²

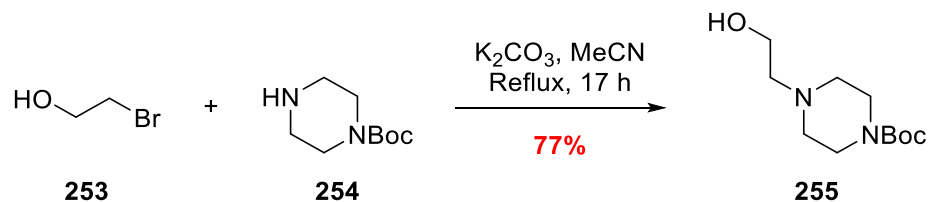
251) 3-Bromo-N-(tert-butyl)benzenesulfonamide



tert-Butylamine **249** (1.23 mL, 11.7 mmol) was added to a solution of 3-bromobenzenesulfonyl chloride **250** (1.13 mL, 7.83 mmol) and Et₃N (1.64 mL, 11.7 mmol) in tetrahydrofuran (15 mL) and stirred at 23 °C. After 19 h, the reaction was quenched *via* the addition of HCl_(aq) (2 M, 20 mL) and the organic material was extracted with ethyl acetate (15 mL). The two phases were separated and the organic was washed with water (2 × 15 mL) and brine (30 mL), dried over MgSO₄, filtered to remove the solids and concentrated under reduced pressure. Further drying under high vacuum gave sulfonamide **251** with no need for further purification as a white solid (2.24 g, 98%); mp = 89–90 °C; $\nu_{\max}/\text{cm}^{-1}$ (neat) 3271 (NH), 3082 (CH), 2978 (CH), 1314 (SO), 1148 (SO); δ_{H} (400 MHz; CDCl₃) 1.22 (9 H, s, C(CH₃)₃), 5.29 (1 H, s, NH), 7.36 (1 H, t, $J = 7.9$, CHCHCH), 7.65 (1 H, ddd, $J = 7.9, 1.9, 1.0$, CHCHCBr), 7.84 (1 H, ddd, $J = 7.9, 1.9, 1.0$, O₂SCCHCH), 8.04 (1 H, t, $J = 1.9$, O₂SCCHCBr); δ_{C} (101 MHz; CDCl₃) 30.2 ((CH₃)₃), 55.1 (C), 122.8 (C), 125.5 (CH), 129.9 (CH), 130.6 (CH), 135.3 (CH), 145.4 (C); LRMS m/z (ES+) 316.0 ([M⁸¹Br + Na]⁺, 100%), 314.0 ([M⁷⁹Br + Na]⁺, 96); HRMS m/z (ES+) calcd for C₁₀H₁₄NO₂S⁷⁹BrNa 313.9826, found 313.9825

*A known compound prepared according to a literature procedure.*⁴⁰³ *The recorded data are in agreement with that reported in the literature.*⁴⁰³

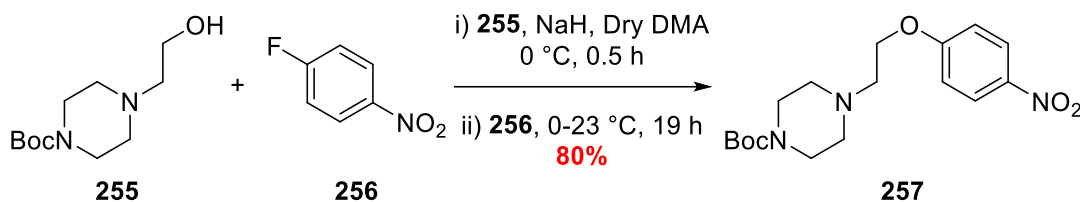
255) *tert*-Butyl 4-(2-hydroxyethyl)piperazine-1-carboxylate



A solution of 2-bromoethanol **253** (1.14 mL, 16.1 mmol), *N*-Boc piperazine **254** (2.00 g, 10.7 mmol) and K₂CO₃ (3.71 g, 26.8 mmol) in MeCN (20 mL) was prepared and heated to reflux. After 17 h, the reaction determined complete *via* TLC and was taken off the heat and allow to cool to 23 °C. Once cool, the reaction mixture was passed through a celite bung to remove the solids and eluted with MeCN (3 × 10 mL). The resulting liquor was concentrated under reduced pressure and the crude material subject to flash column chromatography (*R*_f = 0.2, 12% MeOH in ethyl acetate) to yield ethyl alcohol **255** as a colourless oil (1.89 g, 77%); ν_{\max} /cm⁻¹ (neat) 3418 br (OH), 2975 (CH), 2934 (CH), 2813 (CH), 1693 (CO); δ_H (400 MHz; CDCl₃) 1.45 (9 H, s, C(CH₃)₃), 2.45 (4 H, t, *J* = 5.1, BocN(CH₂)₂ or (CH₂)₂NCH₂), 2.55 (2 H, t, *J* = 5.4, NCH₂CH₂OH), 2.63 (1 H, s, OH), 3.43 (4 H, t, *J* = 5.1, BocN(CH₂)₂ or (CH₂)₂N), 3.62 (2 H, t, *J* = 5.4, NCH₂CH₂OH); δ_C (101 MHz; CDCl₃) 28.6 ((CH₃)₃), 43.6 (CH₂), 52.8 (CH₂), 57.8 (CH₂), 59.5 (CH₂), 79.9 (C), 154.8 (CO); LRMS *m/z* (EI+) 230.2 ([M]⁺, 12%); HRMS *m/z* (EI+) calcd for C₁₁H₂₂N₂O₃ 230.1630, found 230.1628.

*A known compound prepared according to a literature procedure.*⁴⁰⁴ *The recorded data are in agreement with that reported in the literature.*⁴⁰⁴

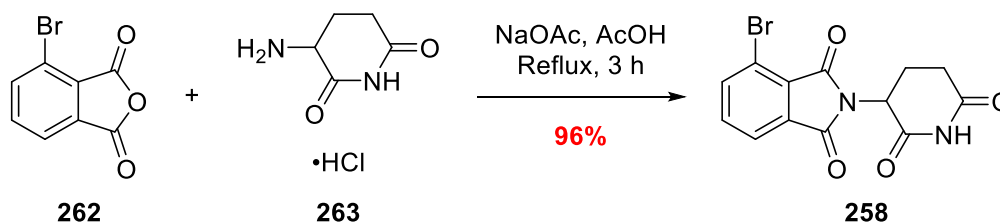
257) *tert*-Butyl 4-(2-(4-nitrophenoxy)ethyl)piperazine-1-carboxylate



A solution of **255** (1.79 g, 7.78 mmol) in anhydrous DMA (5 mL) was added dropwise over 2 min to freshly triturated (3 × 2 mL hexane then the solid was dried under high vacuum) NaH (260 mg, 11.7 mmol) that had been suspended in anhydrous DMA and cooled to 0 °C. The solution effervesced and formed a white precipitate. After 30 min, a solution of 1-fluoro-4-nitrobenzene **256** (1.32 g, 9.33 mmol) in anhydrous DMA (5 mL) was added dropwise over 5 min and the resulting mixture was allowed to warm to 23 °C. After 19 h, the reaction was determined complete *via* TLC ($R_f = 0.1$, ethyl acetate) and quenched *via* the addition of water (15 mL). The resulting solution was then poured into a separating funnel containing ethyl acetate (25 mL) and the two phases were separated. The organic phase was washed with water (3 × 20 mL) and brine (2 × 20 mL) before being dried over MgSO₄ and filtered to remove the solids. The liquor was concentrated to yield a yellow solid which was recrystallised (Hot *n*-hexane/ethyl acetate) to yield nitrophenol **257** as a pale-yellow solid (2.17 g, 80%); **mp** = 132–134 °C; $\nu_{\max}/\text{cm}^{-1}$ (neat) 3081 (CH), 2948 (CH), 2804 (CH), 1682 (CO); δ_H (400 MHz; CDCl₃) 1.46 (9 H, s, C(CH₃)₃), 2.52 (4 H, t, $J = 5.1$, BocN(CH₂)₂ or (CH₂)₂NCH₂), 2.85 (2 H, t, $J = 5.7$, NCH₂CH₂OAr), 3.45 (4 H, t, $J = 5.1$, BocN(CH₂)₂ or (CH₂)₂NCH₂), 4.19 (2 H, t, $J = 5.7$, NCH₂CH₂OAr), 6.91–7.01 (2 H, AA'BB', *Ar-H*), 8.15–8.24 (2 H, AA'BB', *Ar-H*); δ_C (101 MHz; CDCl₃) 28.6 ((CH₃)₃), 43.2 (CH₂), 53.6 (CH₂), 57.1 (CH₂), 66.9 (CH₂), 79.9 (C), 114.4 (C), 114.7 (CH), 126.1 (CH), 154.8 (C), 163.8 (CO); **LRMS m/z (ES⁺)** 352.5 ([M + H]⁺, 49%); **HRMS m/z (ES⁺)** calcd for C₁₇H₂₆N₃O₅ 352.1872, found 352.1870.

*A known compound prepared via a novel procedure.*⁴⁰⁵ The recorded ¹H-NMR spectral data is in agreement with that reported in the literature..⁴⁰⁵ The recorded ¹³C-NMR data shows a very weak signal for the CH₂ resonance at 43.1 ppm, the presence of the CH₂ resonance was confirmed by HSQC which displays a strong cross-peak.

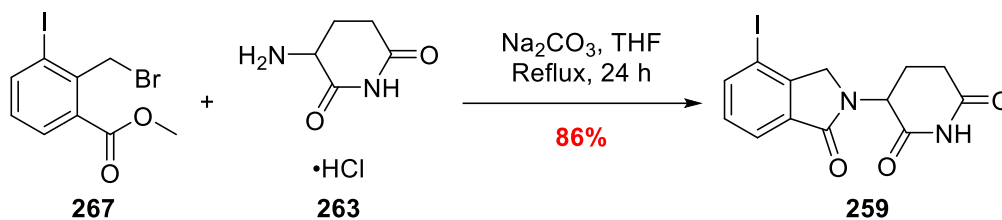
258) 4-Bromo-2-(2,6-dioxopiperidin-3-yl)isoindoline-1,3-dione



3-Bromophthalic anhydride **262** (1.00g 4.41 mmol), ammonium salt **263** (798 mg, 4.85 mmol) and NaOAc (452 mg, 5.51 mmol) were suspended in AcOH (10 mL) and heated to reflux. After 3 h, the reaction was determined complete *via* TLC ($R_f = 0.3$, 1:1 ethyl acetate:*n*-hexane), removed from the heat and allowed to cool to 23 °C. The resulting suspension was collected *via* suction filtration and the solid was washed sequentially with water (2 × 20 mL) and EtOH (20 mL). The solid was then transferred to a round-bottom flask and dried over-night under high vacuum to give bromothalidomide **258**, with no need for further purification, as a pale-purple powder (1.43 g, 96%); **mp** = 300 °C (dec.); $\nu_{\max}/\text{cm}^{-1}$ (neat) 3200 (NH), 3088 (CH), 29.23 (CH), 1786 (CO), 1712 (CO), 1693 (CO), 1679 (CO); δ_H (400 MHz; $(\text{CD}_3)_2\text{SO}$) 2.07 (1 H, dtd, $J = 13.0, 5.3, 2.2$, NCHCHH'CH₂), 2.45–2.54 (2 H, Stack), 2.55–2.65 (1 H, m), 2.89 (1 H, ddd, $J = 16.9, 13.8, 5.4$, NCHCHH'CH₂), 5.16 (1 H, dd, $J = 12.8, 5.4$), 7.78 (1 H, dd, $J = 8.1, 7.4$, CHCHC), 7.94 (1 H, dd, $J = 7.4, 0.9$, CHCBrC or CHCHC), 8.06 (1 H, dd, $J = 8.1, 0.9$, CHCBrC or CHCHC), 11.18 (1 H, s, NH); δ_C (101 MHz; $(\text{CD}_3)_2\text{SO}$) 21.8 (CH₂), 30.9 (CH₂), 49.2 (CH), 117.6 (C), 122.9 (CH), 128.7 (C), 133.7 (C), 136.3 (CH), 139.2 (CH), 165.2 (CO), 165.6 (CO), 169.8 (CO), 172.9 (CO); **LRMS m/z (ES+)** 361.0 ($[\text{M}^{81}\text{Br} + \text{Na}]^+$, 91%), 359.0 ($[\text{M}^{79}\text{Br} + \text{Na}]^+$, 100); **HRMS m/z (ES+)** calcd for C₁₃H₉N₂O₄⁷⁹BrNa 358.9643, found 358.9646.

A known compound prepared according to a literature procedure.⁴⁰⁶ The recorded data are in agreement with that reported in the literature.⁴⁰⁶

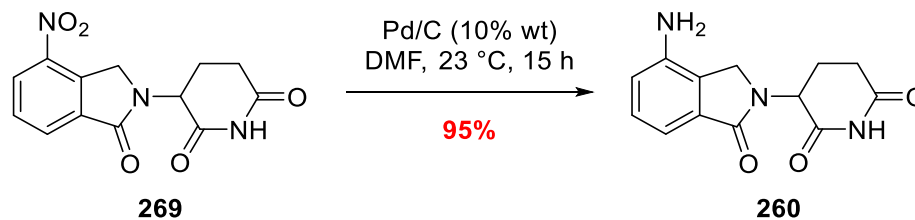
259) 3-(4-Iodo-1-oxoisindolin-2-yl)piperidine-2,6-dione



Benzyl bromide **267** (3.25 g, 9.17 mmol) was added to a stirred solution of ammonium salt **263** (1.51 g, 9.17 mmol) and Na_2CO_3 (2.91 g, 27.5 mmol) in anhydrous tetrahydrofuran (30 mL) and the resulting solution was heated to reflux. After 24 h, a purple suspension had formed and was determined complete *via* TLC ($R_f = 0.1$, 1:1 *n*-hexane:ethyl acetate). The reaction mixture was allowed to cool to 23 °C, diluted with water (20 mL) and stirred vigorously. The remaining solid was collected *via* suction filtration and was washed sequentially with water (2 × 20 mL) and EtOH (4 × 20 mL) until the blue colouration stopped eluting. The solid was collected and dried under high vacuum to give iodo-lenalidomide **259** as a pale blue solid (1.27 g, 76%); mp = 193–195 °C; $\nu_{\text{max}}/\text{cm}^{-1}$ (neat) 3175 (CH), 3086 (CH), 1705 (CO), 1664 (CO); δ_H (400 MHz; $(\text{CD}_3)_2\text{SO}$) 2.01 (1 H, dtd, $J = 12.6, 5.4, 5.3, 2.1$, CHCHH'CHH'CO or CHCHH'CHH'CO), 2.42–2.55 (1 H, Stack, CHCHH'CHH'CO or CHCHH'CHH'CO and DMSO residual resonance), 2.59 (1 H, ddd, $J = 17.2, 4.4, 2.2$, CHH'CHH'CO or CHH'CHH'CO), 2.91 (1 H, ddd, $J = 17.1, 13.6, 5.4$, CHH'CHH'CO or CHH'CHH'CO) 4.14 (1 H, d, $J = 17.5$, CCHH'N), 4.29 (1 H, d, $J = 17.5$, CCHH'N), 5.15 (1 H, dd, $J = 13.3, 5.1$, NCHCHH'), 7.35 (1 H, *app. t*, $J = 7.6$, CHCHCCO), 7.77 (1 H, dd, $J = 7.5, 0.9$, CHCHCCO or CHCIC), 8.04 (1 H, dd, $J = 7.8, 0.9$, CHCHCCO or CHCIC), 11.02 (1 H, s, NH); δ_C (101 MHz; $(\text{CD}_3)_2\text{SO}$) 22.7 (CH₂), 31.7 (CH₂), 51.6 (CH₂), 52.1 (CH), 92.2 (C), 123.4 (CH), 130.7 (CH), 133.8 (C), 141.0 (CH), 146.9 (C), 168.1 (CO), 171.4 (CO), 173.4 (CO); LRMS m/z (AP+) 371.0 ($[\text{M} + \text{H}]^+$, 100%); HRMS m/z (AP+) calcd for $\text{C}_{13}\text{H}_{12}\text{N}_2\text{O}_3^{127}\text{I}$ 370.9893, found 370.9892.

A known compound prepared according to a modified literature procedure.⁴⁰⁷ The mass spectra data is in agreement with that reported in the literature – no mp, IR, ¹H/¹³H-NMR or HRMS data has been reported.⁴⁰⁷

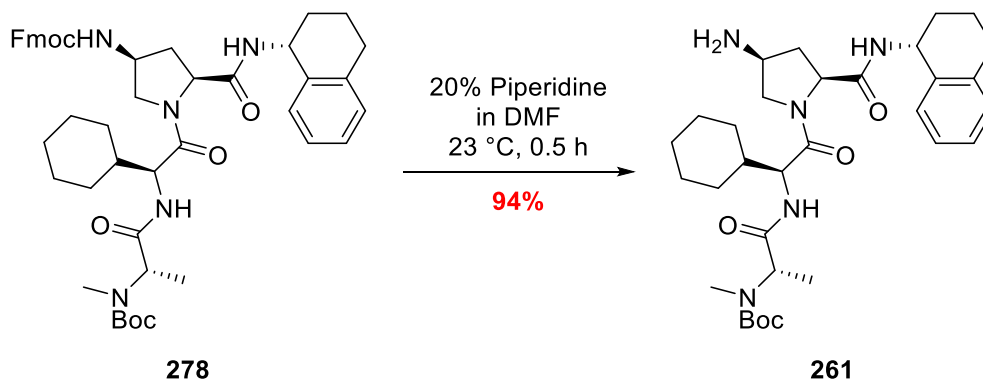
260) 3-(4-Amino-1-oxoisindolin-2-yl)piperidine-2,6-dione



Palladium on carbon (10% wt., 10 mg) was added to a solution of nitrobenzene **269** (100 mg, 0.35 mmol) in *N,N*-dimethylformamide (4 mL) and stirred under a sealed atmosphere at 23 °C. Hydrogen gas was then bubbled continuously through the solution, with a vent in the septum, for 10 min and then the vent was removed and the hydrogen source was suspended above the solution to maintain a hydrogen atmosphere. After 15 h, the reaction was determined complete *via* TLC ($R_f = 0.2$, 5% MeOH in ethyl acetate) and the reaction mixture was filtered through a celite bung and eluted with MeOH (3 × 10 mL). The resulting liquor was concentrated under reduced pressure to give lenalidomide **260** as a white solid (85 mg, 95%); **mp** = 290 °C (dec.); $\nu_{\text{max}}/\text{cm}^{-1}$ (neat) 3365 (NH), 3093 (CH), 2849 (CH), 1667 br (3 × CO); δ_H (**400 MHz; (CD₃)₂SO**) 2.02 (1 H, ddd, $J = 12.9, 5.2, 2.1$, CH₂CHH'CO), 2.30 (1 H, ddd, $J = 13.3, 13.3, 12.9$, CH₂CHH'CO), 2.61 (1 H, *app.* ddd, $J = 17.2, 13.5, 3.6$, CHCHHCH₂), 2.92 (1 H, *app.* ddd, $J = 17.2, 13.5, 5.4$, CHCHH'CH₂), 4.10 (1 H, d, $J = 17.0$, CCHH'N), 4.21 (1 H, d, $J = 17.0$, CCHH'N), 5.11 (1 H, dd, $J = 13.5, 5.1$, NCHCH₂), 6.81 (1 H, dd, $J = 7.9, 0.9$), 6.93 (1 H, dd, $J = 7.4, 0.9$), 7.19 (1 H, *app.* t, $J = 7.6$, CHCHCCO), 11.01 (1 H, s, NH); δ_C (**101 MHz; (CD₃)₂SO**) 22.8 (CH₂), 31.3 (CH₂), 45.5 (CH₂), 51.5 (CH₂), 110.6 (CH), 116.6 (CH), 125.8 (C), 128.9 (CH), 132.3 (C), 143.3 (C), 168.9 (CO), 171.3 (CO), 172.9 (CO); **LRMS m/z (ES⁺)** 282.1 ([M + Na]⁺, 100%), 260.1 ([M + H]⁺, 47); **HRMS m/z (ES⁺)** calcd for C₁₃H₁₃N₃O₃Na 282.0855, found 282.0854.

*A known compound prepared according to a literature procedure.*⁴⁰⁸ *The recorded data are in agreement with that reported in the literature.*⁴⁰⁸

261) *tert*-Butyl ((*S*)-1-(((*S*)-2-((2*S*,4*S*)-4-amino-2-(((*R*)-1,2,3,4-tetrahydronaphthalen-1-yl)carbamoyl)pyrrolidin-1-yl)-1-cyclohexyl-2-oxoethyl)amino)-1-oxopropan-2-yl)(methyl)carbamate

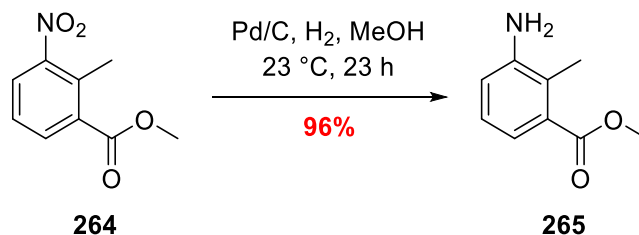


A solution of *N*-Fmoc amine **278** (667 mg, 0.84 mmol) in 20% piperidine in *N,N*-dimethylformamide (5 mL) was stirred at 23 °C for 0.5 h, after which time the reaction was determined complete *via* TLC. The reaction mixture was diluted with ethyl acetate (15 mL) and then quenched by addition of water (20 mL). The subsequent layers were separated and the organic was washed with water (5 × 10 mL) and brine (20 mL), dried over MgSO₄, filtered to remove the solids and concentrated under reduced pressure. The resulting crude mixture was purified by flash-column chromatography (*R*_f = 0.2 [in 10% MeOH in CH₂Cl₂], 10-50% MeOH in CH₂Cl₂) to yield amine **261** as a white solid (462 mg, 94%); **mp** = 118–120 °C; $\nu_{\max}/\text{cm}^{-1}$ (neat) 3312 br (NH), 2929 (CH), 2855 (CH), 1656 (CO), 1638 (CO); δ_{H} (400 MHz; CDCl₃) 0.83–1.19 (6 H, m), 1.26 (3 H, d, *J* = 7.1, CH₃NBocCHCH₃), 1.44 (9 H, s, C(CH₃)₃), 1.62 (6 H, Stack), 1.80 (3 H, Stack), 2.00 (1 H, tt, *J* = 11.5, 11.5, 5.8, 5.8), 2.17–2.30 (2 H, m), 2.75 (4 H, Stack, contains CH₃NBoc), 3.56 (1 H, *app.* d, *J* = 10.8), 3.69 (2 H, s, NH₂), 3.98 (1 H, dd, *J* = 11.0, 5.4), 4.42 (1 H, *app.* t, *J* = 7.8), 4.48–4.59 (1 H, m), 4.65 (1 H, s, NH), 5.09 (1 H, dd, *J* = 9.7, 4.9), 6.71 (1 H, s, NH), 7.04 (1 H, dd, *J* = 7.3, 1.9, CCHCH or CHCHC), 7.10 (2 H, *app.* td, *J* = 7.3, 7.0, 1.9, CHCHCHCH and CHCHCHCH), 7.22 (1 H, dd, *J* = 7.0, 1.7, CCHCH or CHCHC); δ_{C} (101 MHz; CDCl₃) 20.1 (CH₂), 25.8 (CH₂), 26.0 (CH₂), 26.1 (CH₂), 28.4 (C(CH₃)₃), 29.3 (CH₂), 29.7 (CH₂), 30.0 (CH₂), 40.8 (CH), 47.8 (CH), 55.2 (CH), 60.3 (CH), 80.7 (C), 126.2 (CH), 127.3 (CH), 128.7 (CH), 129.2 (CH), 136.5 (C), 137.4 (C), 156.3 (CO), 171.0 (CO),

171.5 (CO), 171.9 (CO); **LRMS m/z (ES+)** 606.4 ($[M + Na]^+$, 30%), 584.4 ($[M + H]^+$, 100);
HRMS m/z (ES+) calcd for $C_{32}H_{50}N_5O_5$ 584.3812, found 584.3811.

A known compound prepared according to a literature procedure.⁴⁰⁹ The recorded mass spectrometry data is in agreement with that reported in the literature; no mp, IR, HRMS, 1H - or ^{13}C -NMR has been reported.⁴⁰⁹

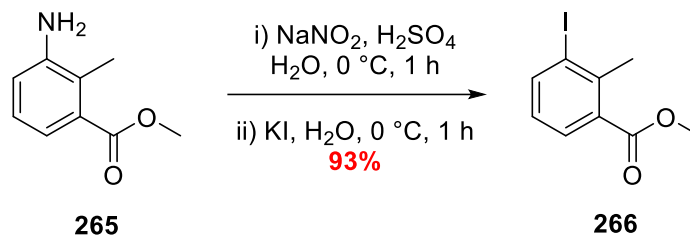
265) Methyl 3-amino-2-methylbenzoate



A solution of nitrobenzene **258** (1.89 g, 9.68 mmol) in MeOH (25 mL) containing 10% wt Pd/C (189 mg) was saturated with hydrogen gas, *via* a sparging frit, and stirred at 23 °C. After 23 h, the reaction was determined complete *via* TLC ($R_f = 0.2$, 3:1 *n*-hexane:ethyl acetate). The reaction mixture was passed through a celite bung to collect the solids and the filter cake was washed with MeOH (3 × 10 mL). The mother liquor was concentrated and then subjected to flash column chromatography ($R_f = 0.3$, 6:4 *n*-hexane:ethyl acetate) to yield aniline **259** as a white solid (1.59 g, 96%); ν_{max}/cm^{-1} (neat) 3472 (NH), 3380 (NH), 3014 (CH), 2950 (CH), 1707 (CO); δ_H (400 MHz; $CDCl_3$) 2.34 (3 H, s, CH_3), 3.73 (2 H, s, NH_2), 3.87 (3 H, s, CO_2CH_3), 6.80 (1 H, dd, $J = 7.9, 1.3$, $CHC(NO_2)C$ or $CHCCO_2CH_3$), 7.04 (1 H, t, $J = 7.8$, $CHCHCCO_2CH_3$), 7.21 (1 H, dd, $J = 7.8, 1.3$, $CHC(NO_2)C$ or $CHCCO_2CH_3$); δ_C (101 MHz; $CDCl_3$) 13.9 (CH_3), 52.0 (CH_3), 118.2 (CH), 120.4 (CH), 122.9 (C), 126.1 (CH), 131.7 (C), 145.6 (C), 169.2 (CO); **LRMS m/z (EI+)** 165.0 ($[M]^+$, 100%).

A known compound prepared according to a literature procedure.⁴¹⁰ The recorded data are in agreement with that reported in the literature.⁴¹⁰

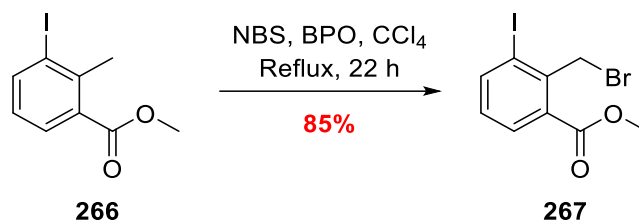
266) Methyl 3-iodo-2-methylbenzoate



Aniline **265** (2.87 g, 17.4 mmol) was suspended in water (17 mL) and cooled to 0 °C. H₂SO₄ (98%, 3.4 mL) in water (17 mL) was added followed by the dropwise addition of solution of NaNO₂ (1.26 g, 18.3 mmol) in water (17 mL) over a period of 2 min. After 1 h, a solution of KI (4.33 g, 26.1 mmol) in water (17 mL) was added dropwise over 5 min – addition of KI was followed by an immediate colour change from a pale yellow solution to a dark orange solution. After a further 1 h, the reaction mixture was diluted with ethyl acetate (40 mL) and stirred vigorously. The resultant phases were separated and the organic layer was washed sequentially with Na₂S₂O_{3(aq)} (Sat. soln., 2 × 20 mL), water (20 mL) and brine (30 mL). The organic was dried over MgSO₄, filtered to remove the solids and concentrated under reduced pressure to yield aryl iodide **266** as a white solid (4.47 g, 93%) with no need for further purification; $\nu_{\max}/\text{cm}^{-1}$ (neat) 2949 (CH), 1718 (CO); δ_{H} (400 MHz; CDCl₃) 2.66 (3 H, *app.* q, $J = 0.5$, CCH₃), 3.90 (3 H, s, CO₂CH₃), 6.92 (1 H, *app.* tq, $J = 7.8, 7.8, 0.5$, CHCHCO₂CH₃), 7.73 (1 H, ddd, $J = 7.8, 1.4, 0.5$, CHCl or CHCHCO₂CH₃), 7.97 (1 H, ddd, $J = 7.8, 1.4, 0.5$, CHCl or CHCHCO₂CH₃); δ_{C} (101 MHz; CDCl₃) 26.5 (CH₃), 52.3 (CH₃), 104.1 (C), 127.1 (CH), 130.0 (CH), 131.9 (C), 141.5 (C), 142.6 (CH), 167.9 (CO); LRMS m/z (ES⁺) 276.0 ([M]⁺, 100%).

A known compound prepared according to a literature procedure.³⁶³ The recorded data are in agreement with that reported in the literature.³⁶³

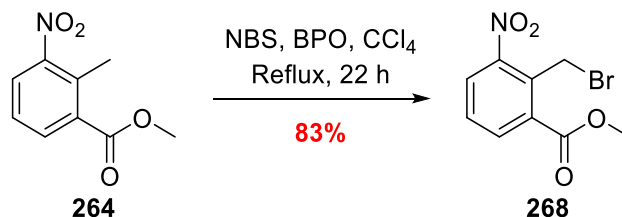
267) Methyl 2-(bromomethyl)-3-iodobenzoate



Aryl iodide **266** (2.03 g, 7.35 mmol) was solubilised in a solution of *N*-bromosuccinimide (1.57 g, 8.82 mmol) and benzoyl peroxide (70%, 509 mg, 1.47 mmol) in tetrachloromethane (20 mL) and heated to reflux. After 22h, the reaction was determined complete *via* TLC ($R_f = 0.3$, 9:1 petroleum ether:diethyl ether), took off the heat and allowed to cool. Upon cooling, a white solid precipitated which was removed *via* suction filtration. The mother liquor was concentrated under reduced pressure and the crude was subjected to column chromatography ($R_f = 0.3$, 9:1 petroleum ether:diethyl ether) and the product containing fractions were combined and concentrated to give an off-white solid. The solid was recrystallised from hot *n*-hexane to yield benzyl bromide **267** as white needle-like crystals (2.22 g, 85%); $\nu_{\max}/\text{cm}^{-1}$ (neat) 3069 (CH), 2949 (CH), 1719 (CO); δ_H (400 MHz; CDCl₃) 3.98 (3 H, s, CO₂CH₃), 5.15 (2 H, s, CH₂Br), 7.07 (1 H, *app. t*, $J = 7.9$, CHCHCCO₂CH₃), 7.92 (1 H, *dd*, $J = 7.8, 1.3$, CHCl or CHCHCCO₂CH₃), 8.07 (1 H, *dd*, $J = 7.9, 1.3$, CHCl or CHCHCCO₂CH₃); δ_C (101 MHz; CDCl₃) 36.2 (CH₂), 52.7 (CH₃), 103.6 (C), 129.5 (C), 129.7 (CH), 131.3 (CH), 140.6 (C), 144.0 (CH), 166.5 (CO); LRMS m/z (EI+) 356.0 ([M⁸¹Br]⁺, 5%), 354.0 ([M⁷⁹Br]⁺, 5), 275.0 ([M⁷⁹Br - ⁷⁹Br and M⁸¹Br - ⁸¹Br]⁺, 100).

A known compound prepared according to a modified literature procedure.⁴¹¹ The recorded data are in agreement with that reported in the literature.⁴¹¹

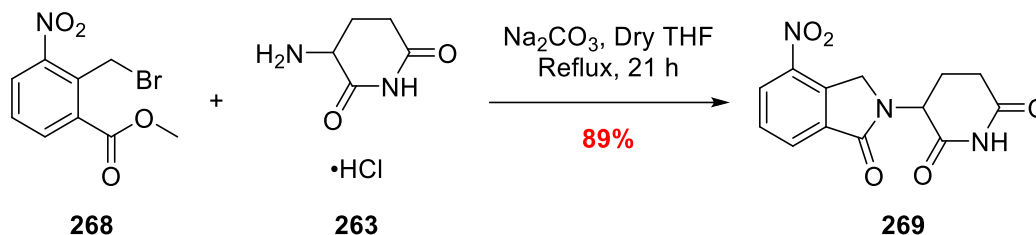
268) Methyl 2-(bromomethyl)-3-nitrobenzoate



Benzoyl peroxide (70%, 355 mg, 1.02 mmol) and *N*-bromosuccinimide (2.19 g, 12.3 mmol) were added to a solution of methyl 2-methyl-3-nitrobenzoate **264** (2.00 g, 10.2 mmol) in CCl₄ (20 mL) and heated to reflux. After 22 h, the reaction was deemed complete *via* TLC, taken off the heat and allowed to cool to 23 °C. On cooling, a white precipitate appeared which was filtered off *via* suction filtration and the solid was washed with CHCl₃ (2 × 10 mL). The liquor was transferred to a separating funnel and washed with water (3 × 20 mL), dried over MgSO₄, filtered to remove the solids and concentrated under reduced pressure. The resulting crude material was subjected to flash column chromatography (*R*_f = 0.3, 4:1 *n*-hexane:ethyl acetate) to yield benzyl bromide **268** as a yellow solid (2.32 g, 83%); **mp** = 69–70 °C; **v**_{max}/cm⁻¹ (neat) 3088 (CH), 2954 (CH), 1724 (CO), 1532 (NO), 1354 (NO); **δ**_H (400 MHz; CDCl₃) 3.99 (3 H, s, CO₂CH₃), 5.15 (2 H, s, CCH₂Br), 7.53 (1 H, *app. t.*, *J* = 8.0, CHCHCO₂), 7.95 (1 H, dd, *J* = 8.1, 1.5, CHCHCO₂ or CHCNO₂), 8.10 (1 H, dd, *J* = 7.8, 1.5, CHCHCO₂ or CHCNO₂); **δ**_C (101 MHz; CDCl₃) 22.9 (CH₃), 53.2 (CH₂), 128.0 (CH), 129.2 (CH), 132.5 (C), 132.8 (C), 134.9 (CH), 150.7 (C), 166.0 (CO); **LRMS m/z (AP+)** 276.0 ([M⁸¹Br + H]⁺, 5%), 274.0 ([M⁷⁹Br + H]⁺, 5), 194.0 (([M^{79/81}Br - ^{79/81}Br + H]⁺, 100); **HRMS m/z (AP+)** calcd for C₉H₉NO₄⁷⁹Br 273.9715, found 273.9708.

*A known compound prepared according to a literature procedure.*⁴¹² *The recorded data are in agreement with that reported in the literature.*⁴¹²

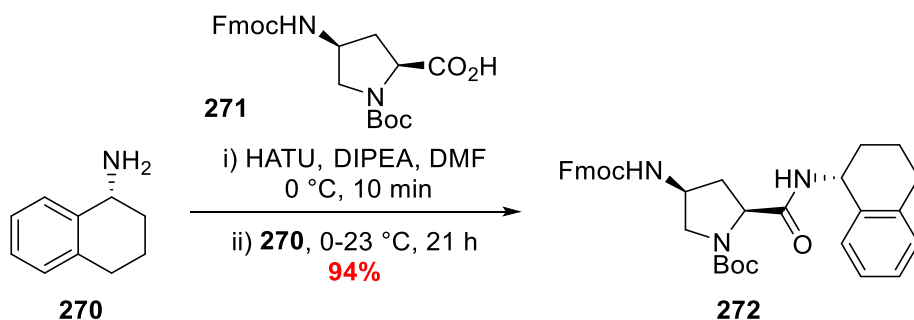
269) 3-(4-Nitro-1-oxoisindolin-2-yl)piperidine-2,6-dione



A flame-dried flask was charged with benzyl bromide **268** (2.19 g, 7.99 mmol), ammonium salt **263** (1.31 g, 7.99 mmol), Na_2CO_3 (2.54 g, 24.0 mmol) and anhydrous tetrahydrofuran (20 mL) and heated to reflux. After 21 h, the reaction was deemed complete *via* TLC ($R_f = 0.4$, 5% MeOH in ethyl acetate), taken off the heat and allowed to cool to 23 °C. Once cool, the reaction mixture was diluted with water (20 mL), stirred vigorously for 5 min and then the remaining precipitate was collection *via* suction filtration. The collected solid was washed with water (4 × 20 mL) and EtOH (2 × 20 mL), transferred to a round-bottom flask and dried azeotropically with toluene (5 mL). The solid was then dried under high vacuum over-night to afford nitrobenzene **269** as a blue powder (2.05 g, 89%); **mp** = 279 °C (dec.); $\nu_{\text{max}}/\text{cm}^{-1}$ (neat) 3097 (CH), 3046 (CH), 2912 (CH), 1707 (CO), 1663 (CO), 1634 (CO), 1539 (NO), 1344 (NO); δ_{H} (400 MHz; $(\text{CD}_3)_2\text{SO}$) 2.02 (1 H, *app.* ddd, $J = 16.7, 14.1, 5.4$, CHCHH'CH₂), 2.53–2.64 (2 H, m, CHH'CH₂CO), 2.92 (1 H, *app.* ddd, $J = 16.7, 14.1, 5.4$, CHCHH'CH₂), 4.80 (1 H, *app.* d, $J = 19.3$, CCHH'CH), 4.91 (1 H, *app.* d, $J = 19.3$, CCHH'CH), 5.18 (1 H, dd, $J = 13.1, 5.2$, NCHCH₂), 7.85 (1 H, dd, $J = 8.2, 7.5$ CHCHCH), 8.19 (1 H, dd, $J = 7.5, 1.0$, CHC(NO₂)C or CH CCO), 8.48 (1 H, dd, $J = 8.2, 1.0$, CHC(NO₂)C or CH CCO), 11.04 (1 H, s, NH). δ_{C} (101 MHz; $(\text{CD}_3)_2\text{SO}$) 22.2 (CH₂), 31.2 (CH₂), 48.5 (CH₂), 51.8 (CH), 127.1 (CH), 129.7 (CH), 130.2 (CH), 134.7 (C), 137.5 (C), 143.4 (C), 166.0 (CO), 170.7 (CO), 172.8 (CO); **LRMS** m/z (ES+) 290.1 ($[\text{M} + \text{H}]^+$, 100%); **HRMS** m/z (ES+) calcd for C₁₃H₁₂N₃O₅ 290.0777, found 290.0775.

A known compound prepared according to a literature procedure.⁴¹³ The recorded data are in agreement with that reported in the literature.⁴¹³

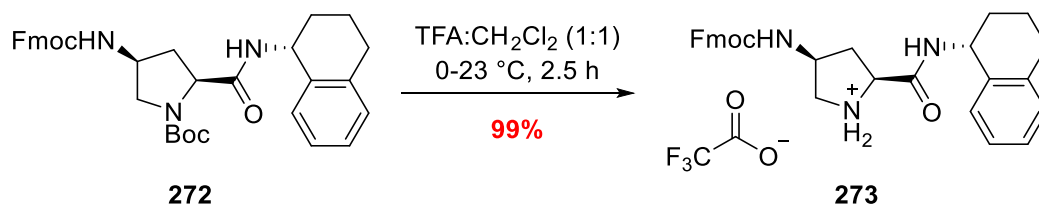
272) tert-Butyl (2S,4S)-4-(((9H-fluoren-9-yl)methoxy)carbonyl)amino)-2-(((R)-1,2,3,4-tetrahydronaphthalen-1-yl)carbamoyl)pyrrolidine-1-carboxylate



HATU (370 mg, 0.97 mmol) was added to a solution of acid **271** (400 mg, 0.88 mmol) and DIPEA (0.69 mL, 3.98 mmol) in DMF (4 mL) and the resulting solution was stirred at 0 °C. After 10 min, a solution of amine **270** (130 mg, 0.88 mmol) in DMF (0.5 mL) was added dropwise over 2 min. The resulting solution was allowed to stir while passively warming to 23 °C. After 21 h, the reaction was determined complete *via* TLC and the reaction mixture was quenched by addition of water (5 mL) and extracted with ethyl acetate (10 mL). The two phases were then separated and the organic washed with water (5 × 10 mL) and brine (20 mL), dried over MgSO₄, filtered to remove the solids and concentrated under reduced pressure. The crude material was then subjected to flash column chromatography (*R_f* = 0.2, 1:1 *n*-hexane:ethyl acetate) to yield amide **272** as a white solid (481 mg, 94%); *mp* = 191–192 °C; $\nu_{\max}/\text{cm}^{-1}$ (neat) 3320 (NH), 2938 (CH), 1684 br. (CO), 1655 br. (CO); δ_{H} (400 MHz; CDCl₃) 1.41 (9 H, s, C(CH₃)₃), 1.87 (3 H, Stack), 2.08–2.24 (2 H, m), 2.45–2.53 (1 H, m), 2.71–2.89 (2 H, m), 3.47–3.64 (2 H, m), 4.21–4.30 (2 H, m), 4.32–4.52 (3 H, Stack), 5.18 (1 H, s, CONHCH), 7.38 (8 H, Stack, Fmoc *Ar-H*), 7.61–7.66 (2 H, Stack, *Ar-H*), 7.69–7.79 (2 H, Stack, *Ar-H*); δ_{C} (101 MHz; CDCl₃) 20.4 (CH₂) 28.4 (C(CH₃)₃), 29.4 (CH₂), 30.3 (CH₂), 32.0 (CH₂), 47.4 (CH), 48.4 (CH), 50.9 (CH₂), 55.4 (CH), 59.8 (C), 67.2 (CH₂), 81.2 (C), 120.1 (CH), 125.4 (CH), 125.5 (CH), 126.3 (CH), 127.2 (CH), 127.8 (CH), 129.2 (CH), 137.5 (C), 141.4 (C), 144.1 (C), 156.3 (CO), 171.9 (CO). **LRMS *m/z* (ES⁺)** 604.1 ([M + Na]⁺, 100%), 582.4 ([M + H]⁺, 10); **HRMS *m/z* (ES⁺)** calcd for C₃₅H₃₉N₃O₅Na 604.2787, found 604.2786.

A known compound prepared according to a literature procedure.⁴⁰⁹ The recorded mass spectrometry data is in agreement with that reported in the literature; no mp, IR, HRMS, ¹H- or ¹³C-NMR has been reported.⁴⁰⁹ The recorded ¹³C-NMR spectra is missing a carbamate carbonyl signal.

273) (2S,4S)-4-(((9H-Fluoren-9-yl)methoxy)carbonyl)amino)-2-(((R)-1,2,3,4-tetrahydronaphthalen-1-yl)carbamoyl)pyrrolidin-1-ium trifluoroacetate

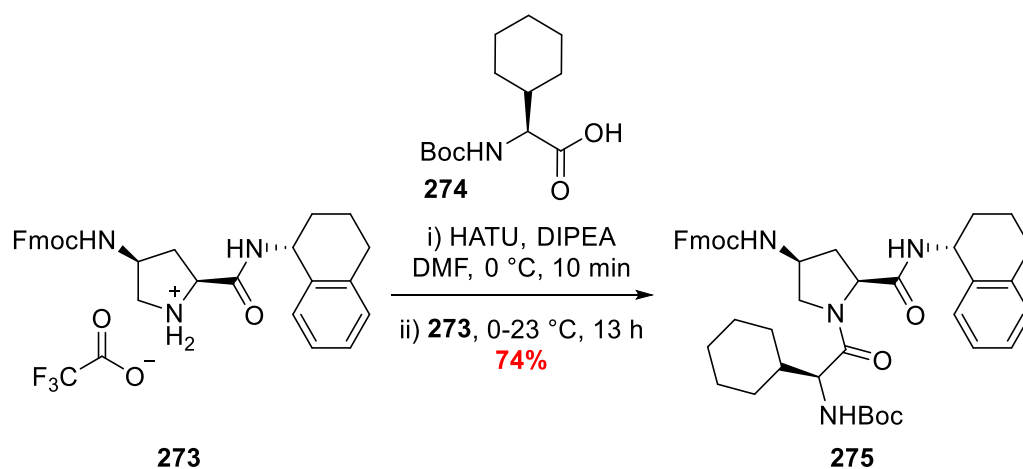


N-Boc proline **272** (393 mg, 0.68 mmol) was solubilised in dichloromethane (4 mL) the resulting solution was cooled to 0 °C. After 10 min, trifluoroacetic acid (4 mL) was added and the resulting mixture was allowed to stir and warm to 23 °C passively. After 2.5 h the reaction was determined complete *via* TLC (*R_f* = 0.1, 5% MeOH in CH₂Cl₂) and the mixture was concentrated under reduced pressure to afford the crude solid. The solid was then re-suspended in diethyl ether (10 mL) and sonicated for 5 min. Filtration of the suspension and sequential washing with diethyl ether (3 × 10 mL) afforded ammonium salt **273** as a fine white powder (398 mg, 99%) with no need for further purification; **mp** = 205–207 °C; $\nu_{\max}/\text{cm}^{-1}$ (neat) 3305 (NH), 2937 (CH), 1716 (CO), 1678 (CO), 1657 (CO); δ_{H} (400 MHz; CDCl₃) 1.64–1.94 (5 H, Stack), 2.58 (1 H, m), 2.65–2.85 (2 H, m), 3.11 (1 H, s), 3.43 (1 H, s), 4.20 (3 H, Stack), 4.38 (2 H, *app.* d, *J* = 6.5, CO₂CH₂C), 5.00 (1 H, m), 7.10–7.23 (4 H, m), 7.34 (2 H, *app.* t, *J* = 7.4, 2 × *Ar-H*), 7.42 (2 H, *app.* t, *J* = 7.5, 2 × *Ar-H*), 7.55 (1 H, *app.* d, *J* = 6.5), 7.68 (2 H, *app.* d, *J* = 7.5, 2 × *Ar-H*), 7.90 (2 H, Stack, 2 × *Ar-H*), 8.77 (1 H, s, NH), 8.85 (1 H, *app.* d, *J* = 8.3, CONHCH), 9.47 (1 H, s, NH); δ_{C} (101 MHz; CDCl₃) 19.4 (CH₂), 28.6 (CH₂), 29.4 (CH₂), 34.8 (CH₂), 46.7 (CH), 47.1 (CH), 48.9 (CH₂), 49.4 (CH), 57.9 (CH), 65.5 (CH₂), 120.2 (CH), 125.0 (CH), 125.9 (CH), 127.1 (CH), 127.2 (CH), 127.7 (CH), 128.5 (CH), 128.9 (CH), 136.1 (C), 137.2 (C), 140.8 (C), 143.7 (C), 155.6 (CO), 166.7 (CO); **LRMS** *m/z* (ES⁺) 504.2 ([M +

Na]⁺, 40%), 482.2 ([M + H]⁺, 100); **HRMS *m/z* (ES⁺)** calcd for C₃₀H₃₂N₃O₃ 482.2444, found 482.2445.

A known compound prepared according to a literature procedure.⁴⁰⁹ The recorded mass spectrometry data is in agreement with that reported in the literature; no mp, IR, HRMS, ¹H- or ¹³C-NMR has been reported.⁴⁰⁹ The recorded ¹³C-NMR data is missing either a carbamate or amide carbonyl resonance.

275) (9H-Fluoren-9-yl)methyl ((3S,5S)-1-((S)-2-((tert-butoxycarbonyl)amino)-2-cyclohexylacetyl)-5-(((R)-1,2,3,4-tetrahydronaphthalen-1-yl)carbamoyl)pyrrolidin-3-yl)carbamate

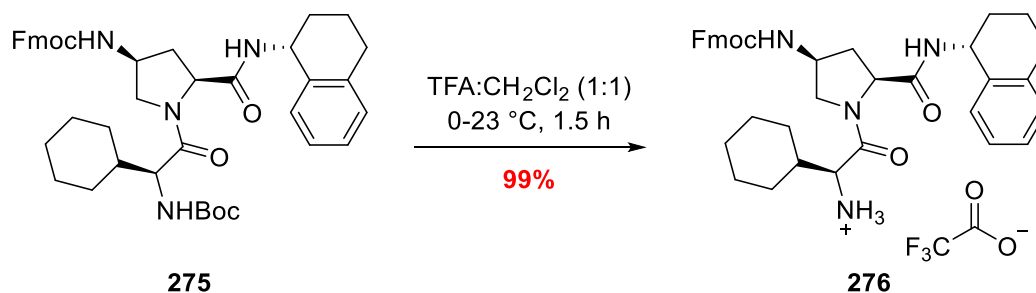


HATU (370 mg, 0.97 mmol) was added to a solution of acid **274** (188 mg, 0.66 mmol) and DIPEA (0.57 mL, 3.28 mmol) in DMF (2 mL) and the resulting solution was stirred at 0 °C. After 10 min, a solution of ammonium salt **273** (391 mg, 0.66 mmol) in DMF (3 mL) was added dropwise over 2 min. The resulting solution was allowed to stir while passively warming to 23 °C. After 13 h, the reaction was determined complete *via* TLC and the reaction mixture was quenched by addition of water (5 mL) and extracted with ethyl acetate (10 mL). The two phases were then separated and the organic washed with water (5 × 10 mL) and brine (20 mL), dried over MgSO₄, filtered to remove the solids and concentrated under reduced pressure. The crude material was then subjected to flash column chromatography (*R_f* = 0.3, 6:4 *n*-hexane:ethyl acetate) to yield *N*-Boc amine **275** as a white solid (348 mg, 74%); **mp** = 120–122 °C; $\nu_{\max}/\text{cm}^{-1}$ (neat) 3290 (NH), 2929 (CH), 2854 (CH), 1710 (CO), 1654 br (CO); δ_{H} (400 MHz; CDCl₃) 1.01–1.15 (5 H, Stack), 1.40 (9 H, s, (C(CH₃)₃)), 1.47–1.72 (4 H, Stack),

1.80–1.91 (3 H, Stack), 1.99–2.09 (1 H, m), 2.18–2.29 (1 H, m), 2.50 (1 H, *app. d*, $J = 13.8$), 2.69–2.89 (3 H, m), 3.71 (1 H, *app. d*, $J = 10.9$), 4.01 (1 H, dd, $J = 10.8, 5.2$), 4.14 (1 H, *app. t*, $J = 8.0$), 4.22–4.34 (2 H, m), 4.37–4.43 (1 H, m), 4.48 (1 H, *app. q*, $J = 6.3$), 4.77 (1 H, *app. d*, $J = 8.9$), 5.01 (1 H, d, $J = 9.1$), 5.18 (1 H, *app. q*, $J = 6.9$), 7.07 (2 H, *app. d*, $J = 7.6$), 7.10–7.21 (2 H, m, Fmoc *Ar-H*), 7.31 (2 H, ddd, $J = 7.4, 6.2, 1.3$, Fmoc *Ar-H*), 7.39 (2 H, tt, $J = 7.4, 1.3$, Fmoc *Ar-H*), 7.65 (2 H, *app. d*, $J = 7.8$), 7.69 (1 H, s, NH), 7.77 (2 H, *app. d*, $J = 7.5$); δ_c (**101 MHz; CDCl₃**) 19.9 (CH₂), 25.9 (CH₂), 26.0 (CH₂), 26.1 (CH₂), 28.2 (CH₂), 28.3, 29.2 (CH₂), 29.5 (CH₂), 29.9 (CH₂), 31.6 (CH₂), 40.8 (CH), 47.2 (CH), 47.9 (CH), 51.1 (CH), 55.7 (CH₂), 60.2 (CH), 67.2 (CH₂), 79.7 (C), 120.0 (CH), 125.3 (CH), 126.2 (CH), 127.1 (CH), 127.4 (CH), 127.7 (CH), 128.5 (CH), 129.2 (CH), 136.0 (C), 137.3 (C), 141.3 (C), 144.1 (C), 155.7 (CO), 156.1 (CO), 170.8 (CO), 173.7 (CO); **LRMS m/z (ES⁺)** 743.4 ([M + Na]⁺, 100%), 721.4 ([M + H]⁺, 20); **HRMS m/z (ES⁺)** calcd for C₄₃H₅₂N₄O₆Na 743.3785, found 743.3790.

A known compound prepared according to a literature procedure.⁴⁰⁹ The recorded mass spectrometry data is in agreement with that reported in the literature; no mp, IR, HRMS, ¹H- or ¹³C-NMR has been reported.⁴⁰⁹

276) (S)-2-((2S,4S)-4-(((9H-Fluoren-9-yl)methoxy)carbonyl)amino)-2-(((R)-1,2,3,4-tetrahydronaphthalen-1-yl)carbamoyl)pyrrolidin-1-yl)-1-cyclohexyl-2-oxoethan-1-aminium trifluoroacetate

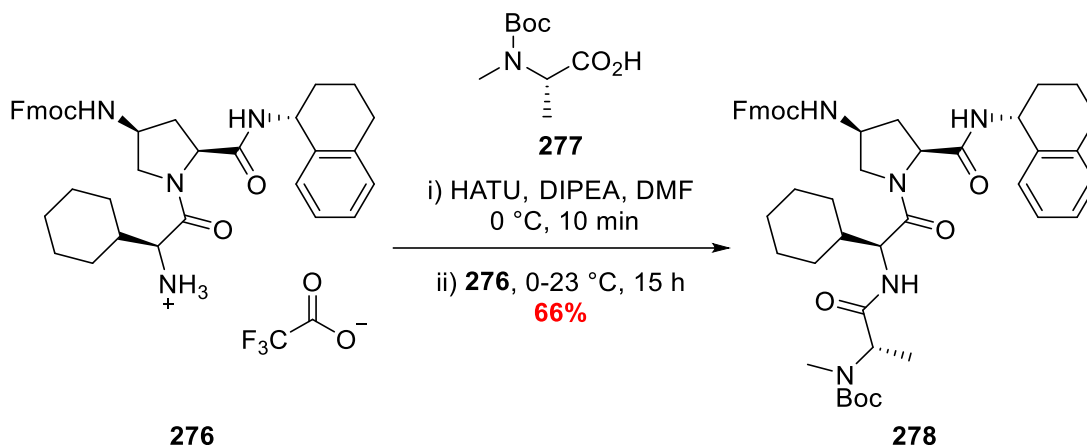


Carbamate **275** (328 mg, 0.45 mmol) was solubilised in dichloromethane (4 mL) and the resulting solution was cooled to 0 °C. After 10 min, trifluoroacetic acid (4 mL) was added and the resulting mixture was allowed to stir and warm to 23 °C passively. After 1.5 h the reaction was determined complete *via* TLC ($R_f = 0.1$, 10% MeOH in CH₂Cl₂) and the mixture was concentrated under reduced pressure to afford the crude solid. The solid was then re-

suspended in diethyl ether (10 mL) and sonicated for 5 min. Filtration of the suspension and sequential washing with diethyl ether (3 × 10 mL) afforded ammonium salt **276** as a fine white powder (332 mg, 99%) with no need for further purification; **mp** = 141–142 °C; $\nu_{\max}/\text{cm}^{-1}$ (neat) 3299 br (NH), 2930 (CH), 2857 (CH), 1699 br (CO), 1661 (CO); δ_{H} (**400 MHz; CDCl₃**) 0.96–1.21 (6 H, Stack), 1.54–1.91 (11 H, Stack), 2.00–2.17 (2 H, Stack, CONHCHCHH'), 2.29 (1 H, *app.* q, $J = 8.1$), 2.59–2.76 (2 H, m), 3.57 (1 H, *app.* d, $J = 10.8$), 3.76 (1 H, dd, $J = 10.8, 5.2$), 3.85 (1 H, *app.* d, $J = 5.7$), 4.01 (1 H, *app.* t, $J = 8.9$), 4.18 (1 H, *app.* t, $J = 7.4$), 4.28 (1 H, dd, $J = 10.1, 7.4$), 4.41 (1 H, *app.* d, $J = 6.8$), 4.50–4.58 (1 H, m), 5.16 (1 H, *app.* q, $J = 7.6$), 6.94–6.99 (1 H, m, Fmoc *Ar-H*), 7.05 (2 H, m, Fmoc *Ar-H*), 7.19–7.25 (1 H, m, Fmoc *Ar-H*), 7.27–7.36 (2 H, m, Fmoc *Ar-H*), 7.36–7.44 (2 H, m, Fmoc *Ar-H*), 7.58 (2 H, dd, $J = 7.6, 2.5$, *Ar-H*), 7.77 (2 H, dd, $J = 7.6, 1.1$, *Ar-H*), 7.93 (1 H, s, NH), 7.99 (3 H, s, NH₃); δ_{C} (**101 MHz; CDCl₃**) 20.7 (CH₂), 25.6 (CH₂), 25.9 (CH₂), 27.7 (CH₂), 28.4 (CH₂), 29.2 (CH₂), 30.0 (CH₂), 33.6 (CH₂), 39.8 (CH), 47.1 (CH), 48.4 (CH), 51.0 (CH), 55.4 (CH₂), 56.3 (CH), 60.3 (CH), 67.4 (CH₂), 116.3 (q, $J = 290.7$, F₃CCO₂H), 120.1 (CH), 125.3 (CH), 125.4 (CH), 126.0 (CH), 127.2 (CH), 127.9 (CH), 128.0 (CH), 129.3 (CH), 136.7 (C), 137.5 (C), 141.4 (C), 144.0 (C), 156.3 (CO), 161.6 (q, $J = 36.2, 36.2, 36.1$, F₃CCO₂H), 168.6 (CO), 171.5 (CO); **LRMS m/z (ES⁺)** 643.3 ([M + Na]⁺, 25%), 621.3 ([M + H]⁺, 100); **HRMS m/z (ES⁺)** calcd for C₃₈H₄₅N₄O₄ 621.3441, found 621.3440.

A known compound prepared according to a literature procedure.⁴⁰⁹ The recorded mass spectrometry data is in agreement with that reported in the literature; no mp, IR, HRMS, ¹H- or ¹³C-NMR has been reported.⁴⁰⁹

278) tert-Butyl ((S)-1-(((S)-2-((2S,4S)-4-(((9H-fluoren-9-yl)methoxy)carbonyl)amino)-2-(((R)-1,2,3,4-tetrahydronaphthalen-1-yl)carbamoyl)pyrrolidin-1-yl)-1-cyclohexyl-2-oxoethyl)amino)-1-oxopropan-2-yl)(methyl)carbamate

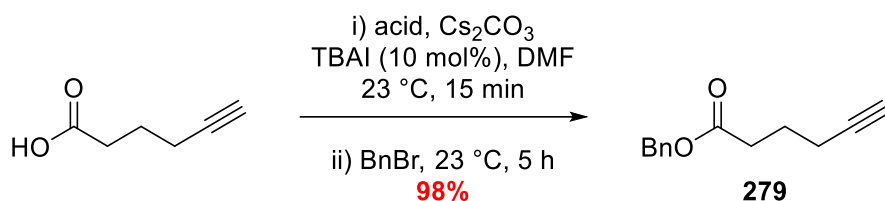


HATU (189 mg, 0.50 mmol) was added to a solution of acid **277** (101 mg, 0.50 mmol) and DIPEA (0.39 mL, 2.26 mmol) in DMF (2 mL) and the resulting solution was stirred at 0 °C. After 10 min, a solution of ammonium salt **276** (332 mg, 0.45 mmol) in DMF (2 mL) was added dropwise over 2 min. The resulting solution was allowed to stir while passively warming to 23 °C. After 15 h, the reaction was determined complete *via* TLC and the reaction mixture was quenched by addition of water (5 mL) and extracted with ethyl acetate (10 mL). The two phases were then separated and the organic washed with water (5 × 10 mL) and brine (20 mL), dried over MgSO₄, filtered to remove the solids and concentrated under reduced pressure. The crude material was then subjected to flash column chromatography (R_f = 0.3, 9:1 ethyl acetate:*n*-hexane) to yield *N*-Fmoc amine **278** as a white solid (241 mg, 66%); **mp** = 161–163 °C; $\nu_{\text{max}}/\text{cm}^{-1}$ (neat) 3299 (NH), 3063 (CH), 2930 (CH), 1699 (CO), 1661 (CO); δ_H (**400 MHz**; **CDCl**₃) 1.05 (3 H, Stack), 1.29 (3 H, *app.* d, J = 8.1, CH₃NBocCHCH₃), 1.46 (9 H, s, C(CH₃)₃), 1.50–1.72 (6 H, Stack), 1.87 (4 H, *app.* d, J = 6.2), 2.00–2.10 (1 H, m), 2.23 (1 H, ddd, J =14.6, 9.0, 6.6), 2.49 (1 H, *app.* d, J =13.8), 2.75 (5 H, Stack, Contains CH₃NBoc), 3.68–3.77 (1 H, m), 4.07 (1 H, m), 4.23–4.32 (2 H, Stack), 4.34–4.43 (1 H, m), 4.47 (1 H, *app.* q, J = 6.3), 4.64 (1 H, s, NH), 4.75 (1 H, *app.* d, J = 8.1, NBocCHCH₃), 5.15–5.23 (1 H, m, CONHCHCH₂), 6.64 (1 H, s, NH), 7.07 (2 H, d, J = 7.8, Fmoc *Ar-H*), 7.10–7.23 (2 H, m, Fmoc

Ar-H), 7.31 (2 H, ddd, $J = 7.6, 6.5, 1.2$, Fmoc *Ar-H*), 7.35–7.43 (2 H, m, Fmoc *Ar-H*), 7.54–7.71 (3 H, Stack, *Ar-H* and *NH*), 7.73–7.79 (2 H, m, *Ar-H*); δ_C (101 MHz; $CDCl_3$) 20.1 (CH_2), 25.9 (CH_2), 26.1 (CH_2), 28.5 ($C(CH_3)_3$), 28.6, 29.3 (CH_2), 29.5 (CH_2), 30.1 (CH_2), 31.7 (CH_2), 40.7 (CH), 47.3 (CH), 48.0 (CH), 51.2 (CH), 55.3 (CH), 56.0 (CH_2), 60.3 (CH), 67.3 (CH_2), 80.8 (C), 120.1 (CH), 125.4 (CH), 126.3 (CH), 127.2 (CH), 127.4 (CH), 127.8 (CH), 128.5 (CH), 129.3 (CH), 136.2 (C), 137.4 (C), 141.4 (C), 144.2 (C), 156.3 (CO), 170.9 (CO), 171.6 (CO), 173.0 (CO); LRMS m/z (ES+) 828.4 ($[M + Na]^+$, 100%), 805.4 ($[M + H]^+$, 5); HRMS m/z (ES+) calcd for $C_{47}H_{59}N_5O_7Na$ 828.4312, found 828.4309.

A known compound prepared according to a literature procedure.⁴⁰⁹ The recorded mass spectrometry data is in agreement with that reported in the literature; no mp, IR, HRMS, 1H - or ^{13}C -NMR has been reported.⁴⁰⁹ The recorded ^{13}C -NMR spectrum is missing a carbamate carbonyl resonance signal.

279) Benzyl hex-5-ynoate

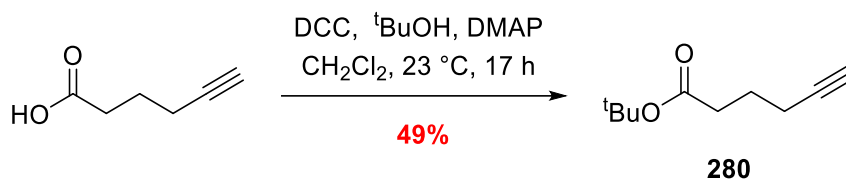


Hex-5-ynoic acid (0.98 mL, 8.92 mmol) was added dropwise over 5 min to a solution of Cs_2CO_3 (4.72 g, 13.4 mmol) and TBAI (329 mg, 0.89 mmol) in DMF (36 mL) and vigorously stirred at 23 °C. After 15 min, benzyl bromide (1.60 mL, 13.4 mmol) was added dropwise of 5 min and the resulting mixture was stirred for a further 5 hours before the reaction was determined complete *via* TLC. The reaction was quenched *via* the slow addition of $HCl_{(aq)}$ (2 M, 20 mL) and the organics were extracted with ethyl acetate (20 mL). The two phases were separated and the organics were washed with water (4 × 20 mL) and brine (30 mL), dried over $MgSO_4$, filtered to remove the solids and concentrated under reduced pressure. The crude material was then subjected to flash column chromatography ($R_f = 0.3$, 92:8 *n*-hexane:ethyl acetate) to yield benzyl ester **279** as a colourless oil (1.77 g, 98%); ν_{max}/cm^{-1} (neat) 3292 (alkyne-CH), 3034 (CH), 2942 (CH), 2117 w ($C\equiv C$), 1731 (CO); δ_H (400 MHz; $CDCl_3$) 1.88 (3 H, *app* qnt, J

= 7.1), 1.97 (1 H, t, $J = 2.6$), 2.27 (2 H, td, $J = 7.1, 2.7$, $\text{CH}_2\text{CH}_2\text{CCH}$), 2.51 (2 H, t, $J = 7.1$, $\text{O}_2\text{CCH}_2\text{CH}_2$), 5.13 (2 H, s, $\text{PhCH}_2\text{O}_2\text{C}$), 7.29–7.42 (5 H, Stack, Ar-H); δ_{C} (101 MHz; CDCl_3) 18.0 (CH_2), 23.7 (CH_2), 33.0 (CH_2), 66.4 (CH_2), 69.3 (C), 83.3 (C), 128.3 (CH), 128.4 (CH), 128.7 (CH), 136.1 (C), 173.0 (CO); LRMS m/z (EI+) 202.1 ($[\text{M}]^+$, 13%).

A known compound prepared according to a literature procedure.⁴¹⁴ The recorded data are in agreement with that reported in the literature.⁴¹⁴

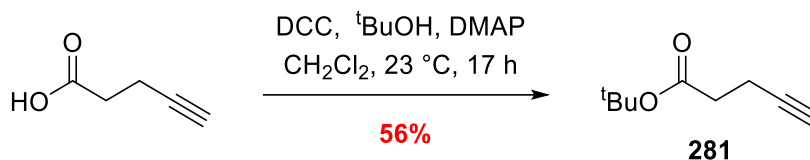
280) *tert*-Butyl hex-5-ynoate



Hex-5-ynoic acid (500 mg, 4.46 mmol) was solubilised in a solution of dicyclohexylcarbodiimide (1.01 g, 4.91 mmol), $t\text{BuOH}$ (661 mg, 8.92 mmol) and DMAP (54 mg, 0.45 mmol) in anhydrous CH_2Cl_2 (10 mL) and the resulting solution was stirred at 23 °C. After 17 h, the reaction was determined complete *via* TLC and was cooled to 0 °C to precipitate the remaining DCC and dicyclohexylurea. The solids were collected *via* suction filtration and the filter cake was washed with CH_2Cl_2 (2 \times 10 mL). The mother liquor was treated with a solution of $\text{HCl}_{(\text{aq})}$ (2 M, 10 mL) and the resultant phases were separated. The organic portion was washed with water (2 \times 10 mL) and brine (20 mL), dried over MgSO_4 , filtered to remove the solids and then concentrated under reduced pressure. The crude material was subjected to flash column chromatography ($R_f = 0.3$, 9:1 *n*-hexane:ethyl acetate) to yield *tert*-butyl ester **280** as a colourless oil (365 mg, 49%); $\nu_{\text{max}}/\text{cm}^{-1}$ (neat) 3302 (alkyne-CH), 2979 (CH), 2934 (CH), 2122 w ($\text{C}\equiv\text{C}$), 1726 (CO); δ_{H} (400 MHz; CDCl_3) 1.43 (9 H, s, $\text{C}(\text{CH}_3)_3$), 1.79 (1 H, *app. p*, $J = 7.1$, $\text{CH}_2\text{CH}_2\text{CH}_2$), 1.95 (1 H, t, $J = 2.6$, CCH), 2.23 (2 H, td, $J = 7.0, 2.7$, $\text{CH}_2\text{CH}_2\text{CCH}$), 2.34 (2 H, t, $J = 7.2$, $t\text{BuO}_2\text{CCH}_2\text{CH}_2$); δ_{C} (101 MHz; CDCl_3) 18.0 (CH_2), 23.9 (CH_2), 28.2 ($\text{C}(\text{CH}_3)_3$), 34.4 (CH_2), 69.0 (CH), 80.4 (C), 83.6 (C), 172.5 (CO); LRMS m/z (AP+) 169.2 ($[\text{M} + \text{H}]^+$, 10%).

A known compound prepared according to a modified literature procedure.^{415, 416} The recorded data are in agreement with that reported in the literature.⁴¹⁵

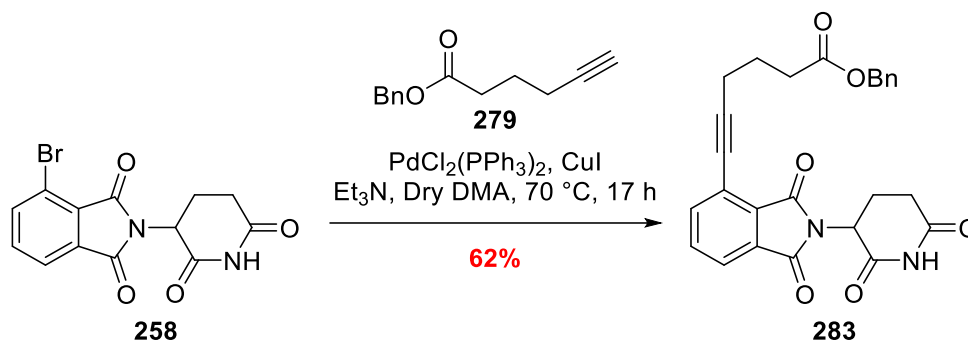
281) *tert*-Butyl pent-4-ynoate



Pent-4-ynoic acid (500 mg, 5.10 mmol) was solubilised in a solution of dicyclohexylcarbodiimide (1.16 g, 45.61 mmol), *t*BuOH (750 mg, 10.2 mmol) and DMAP (62 mg, 0.51 mmol) in anhydrous CH₂Cl₂ (10 mL) and the resulting solution was stirred at 23 °C. After 17 h, the reaction was determined complete *via* TLC ($R_f = 0.4$, 9:1 *n*-hexane:ethyl acetate) and was cooled to 0 °C to precipitate the remaining DCC and dicyclohexylurea. The solids were collected *via* suction filtration and the filter cake was washed with CH₂Cl₂ (2 × 10 mL). The mother liquor was treated with a solution of HCl_(aq) (2 M, 15 mL) and the resultant phases were separated. The organic portion was washed sequentially with HCl_(aq) (1 M, 10 mL), water (15 mL) and brine (30 mL), dried over MgSO₄, filtered to remove the solids and then concentrated under reduced pressure. The crude material was subjected to flash column chromatography ($R_f = 0.3$, 92:8 → 9:1 *n*-hexane:ethyl acetate) to yield *tert*-butyl ester **281** as a colourless oil (441 mg, 56%); $\nu_{\max}/\text{cm}^{-1}$ (neat) 3304 (alkyne-CH), 2980 (CH), 2931 (CH), 2120 (C≡C), 1728 (CO); δ_H (400 MHz; CDCl₃) 1.45 (9 H, s, (C(CH₃)₃), 1.93–1.97 (1 H, m, CH), 2.45 (4 H, Stack, 2 × CH₂); δ_C (101 MHz; CDCl₃) 14.6 (CH₂), 28.2 (C(CH₃)₃), 34.6 (CH₂), 68.9 (CH), 80.9 (C), 82.9 (C), 171.2 (CO); LRMS m/z (AP+) 155.2 ([M + H]⁺, 12%).

A known compound prepared according to a modified literature procedure.^{415, 416} The recorded data are in agreement with that reported in the literature.⁴¹⁵

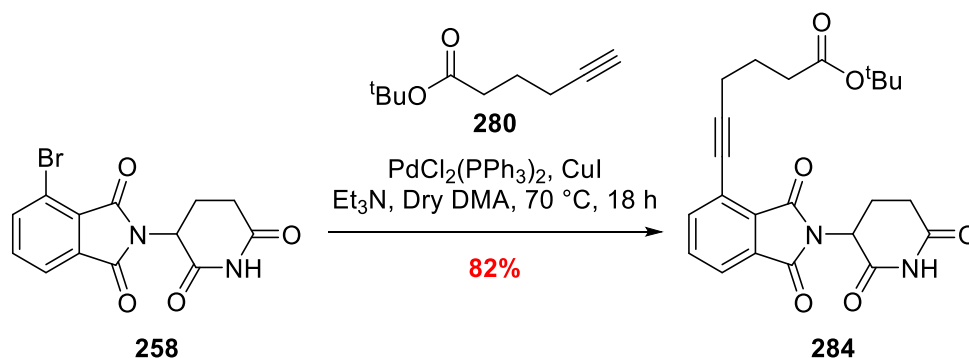
283) Benzyl 6-(2-(2,6-dioxopiperidin-3-yl)-1,3-dioxoisoindolin-4-yl)hex-5-ynoate



General method B was utilised to synthesise **283**: Aryl bromide **258** (300 mg, 0.89 mmol), alkyne **279** (360 mg, 1.78 mmol*), $\text{PdCl}_2(\text{PPh}_3)_2$ (62 mg, 0.09 mmol) and CuI (34 mg, 0.18 mmol), and solubilised in a mixture of anhydrous DMA and freshly distilled Et_3N (4:1, 5 mL). Heated at 70°C for 18 h ($R_f = 0.3$, 1:1 ethyl acetate:*n*-hexane). The reaction crude was diluted with diethyl ether (~10 mL) and cooled to -20°C . The resulting solid was collected and dried under high vacuum to yield aryl alkyne **283** as a white solid (251 mg, 62%); **mp** = 201–202 $^\circ\text{C}$; $\nu_{\text{max}}/\text{cm}^{-1}$ (neat) 3188 (NH), 3085 (CH), 2236 ($\text{C}\equiv\text{C}$), 1705 br. ($5 \times \text{CO}$); δ_{H} (400 MHz; CDCl_3) 2.02 (2 H, *app.* p, $J = 7.1$, $\text{CH}_2\text{CH}_2\text{CH}_2$), 2.07–2.17 (1 H, m, CHCHH' or CHCHH), 2.61 (2 H, t, $J = 7.0$, CCCH_2CH_2), 2.65 (2 H, *app.* t, $J = 7.5$, $\text{CH}_2\text{CH}_2\text{CO}_2^t\text{Bu}$), 2.69–2.95 (3 H, Stack, $\text{CHH}'\text{CHH}'\text{CO}$, $\text{CHH}'\text{CHH}'\text{CO}$ and CHCHH' or CHCHH), 4.96 (1 H, dd, $J = 12.4$, 5.3, NCHCHH'), 5.14 (2 H, s, $\text{CO}_2\text{CH}_2\text{Ph}$), 7.29–7.38 (5 H, Stack, *Ar-H*), 7.63–7.71 (2 H, Stack, CHCHC and $\text{CHCC}\equiv\text{C}$ or CHCHCCO), 7.78 (1 H, dd, $J = 6.9$, 1.5, $\text{CHCC}\equiv\text{C}$ or CHCHCCO), 7.98 (1 H, s, *NH*); δ_{C} (101 MHz; CDCl_3) 19.3 (CH_2), 22.7 (CH_2), 23.6 (CH_2), 31.5 (CH_2), 33.1 (CH_2), 49.4 (CH), 66.4 (C), 98.2 (C), 121.6 (C), 122.8 (CH), 128.3 ($2 \times \text{CH}$), 128.7 ($2 \times \text{CH}$), 130.8 (C), 132.3 (C), 134.0 (CH), 136.1 (C), 138.6 (CH), 166.1 (CO), 166.6 (CO), 167.9 (CO), 170.8 (CO), 173.1 (CO); **LRMS m/z (ES+)** 481.1 ($[\text{M} + \text{Na}]^+$, 100%); **HRMS m/z (ES+)** calcd for $\text{C}_{26}\text{H}_{22}\text{N}_2\text{O}_6\text{Na}$ 481.1376, found 481.1378.

A novel compound prepared according to a literature procedure.⁴⁰⁶ *2 eq. used.

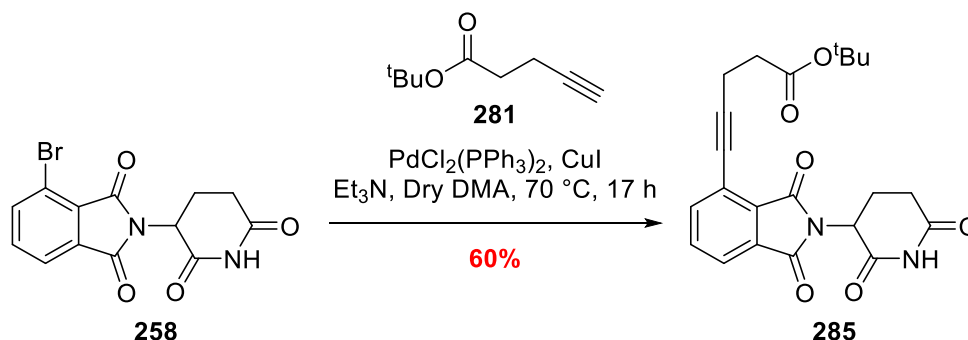
284) tert-Butyl 6-(2-(2,6-dioxopiperidin-3-yl)-1,3-dioxoisindolin-4-yl)hex-5-ynoate



General method B was utilised to synthesise **284**: Aryl bromide **258** (399 mg, 1.18 mmol), alkyne **280** (172 mg, 1.78 mmol), $\text{PdCl}_2(\text{PPh}_3)_2$ (83 mg, 0.12 mmol) and CuI (45 mg, 0.24 mmol), and solubilised in a mixture of anhydrous DMA and freshly distilled Et_3N (4:1, 5 mL). Heated at 70°C for 18 h ($R_f = 0.3$, 1:1 ethyl acetate:*n*-hexane). Purified by flash column chromatography ($R_f = 0.3$, 6:4 *n*-hexane:ethyl acetate) to yield aryl alkyne **284** as a white solid (413 mg, 82%); **mp** = $170\text{--}172^\circ\text{C}$; $\nu_{\text{max}}/\text{cm}^{-1}$ (neat) 3227 (NH), 2976 (CH), 2331 ($\text{C}\equiv\text{C}$), 1708 br. ($5 \times \text{CO}$); δ_{H} (400 MHz; CDCl_3) 1.44 (9 H, s, $\text{C}(\text{CH}_3)_3$), 1.94 (2 H, *app.* p, $J = 7.2$, $\text{CH}_2\text{CH}_2\text{CH}_2$), 2.09–2.17 (1 H, m, CHCHH' or CHCHH), 2.46 (2 H, *app.* t, $J = 7.4$, CCCH_2CH_2), 2.58 (2 H, t, $J = 7.0$, $\text{CH}_2\text{CH}_2\text{CO}_2^t\text{Bu}$), 2.69–2.93 (3 H, Stack, $\text{CHH}'\text{CHH}'\text{CO}$, $\text{CHH}'\text{CHH}'\text{CO}$ and CHCHH' or CHCHH), 4.98 (1 H, dd, $J = 12.4$, 5.3, NCHCHH'), 7.67 (2 H, Stack, CHCHC and $\text{CHCC}\equiv\text{C}$ or CHCHCCO), 7.77 (1 H, dd, $J = 7.1$, 1.4, $\text{CHCC}\equiv\text{C}$ or CHCHCCO), 8.29 (1 H, s, NH); δ_{C} (101 MHz; CDCl_3) 19.3 (CH_2), 22.7 (CH_2), 23.9 (CH_2), 28.2 ($\text{C}(\text{CH}_3)_3$), 31.5 (CH_2), 34.4 (CH_2), 49.3 (CH), 76.6 (C), 80.5 (C), 98.6 (C), 121.7 (C), 122.8 (CH), 130.7 (C), 132.3 (C), 134.0 (CH), 138.7 (CH), 166.1 (CO), 166.6 (CO), 168.1 (CO), 171.1 (CO), 172.6 (CO); **LRMS** m/z (**ES+**) 447.2 ($[\text{M} + \text{Na}]^+$, 100%); **HRMS** m/z (**ES+**) calcd for $\text{C}_{23}\text{H}_{24}\text{N}_2\text{O}_6\text{Na}$ 447.1532, found 447.1534.

A novel compound prepared according to a literature procedure.⁴⁰⁶

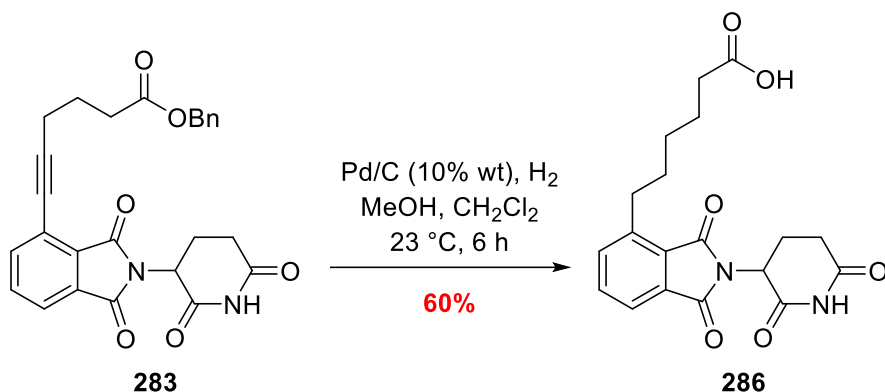
285) tert-Butyl 5-(2-(2,6-dioxopiperidin-3-yl)-1,3-dioxoisindolin-4-yl)pent-4-ynoate



General method B was utilised to synthesise **285**: Aryl bromide **258** (250 mg, 0.74 mmol), alkyne **281** (172 mg, 1.11 mmol), $\text{PdCl}_2(\text{PPh}_3)_2$ (52 mg, 0.07 mmol) and CuI (28 mg, 0.12 mmol), and solubilised in a mixture of anhydrous DMA and freshly distilled Et_3N (4:1, 5 mL). Heated at 70°C for 17 h ($R_f = 0.2$, 1:1 ethyl acetate:*n*-hexane). Purified by flash column chromatography ($R_f = 0.3$, 3:1 ethyl acetate:*n*-hexane) and the product containing fractions were precipitated from CH_2Cl_2 with *n*-hexane to yield aryl alkyne **278** as a white solid (182 mg, 60%); **mp** = $158\text{--}160^\circ\text{C}$; $\nu_{\text{max}}/\text{cm}^{-1}$ (neat) 3274 (NH), 2977 (CH), 2233 ($\text{C}\equiv\text{C}$), 1709 br. ($5 \times \text{CO}$); δ_{H} (400 MHz; CDCl_3) 1.45 (9 H, s, $\text{C}(\text{CH}_3)_3$), 2.07–2.18 (1 H, m, CHCHH' or CHCHH), 2.56–2.65 (2 H, m, $\text{C}\equiv\text{CCH}_2$), 2.67–2.98 (5 H, Stack, $\text{CH}_2\text{CO}_2^t\text{Bu}$, $\text{CHH}'\text{CHH}'\text{CO}$, $\text{CHH}'\text{CHH}\text{CO}$ and CHCHH' or CHCHH), 4.98 (1 H, dt, $J = 12.2, 2.9$, NCHCHH'), 7.61–7.70 (2 H, Stack, CHCHCCO and $\text{CHCC}\equiv\text{C}$ or CHCHCCO), 7.76 (1 H, dd, $J = 6.7, 1.8$, $\text{CHCC}\equiv\text{C}$ or CHCHCCO), 8.42 (1 H, s, NH); δ_{C} (101 MHz; CDCl_3) 15.9 (CH_2), 22.7 (CH_2), 28.2 ($\text{C}(\text{CH}_3)_3$), 31.5 (CH_2), 34.4 (CH_2), 49.4 (CH), 76.3 (C), 81.0 (C), 97.7 (C), 121.5 (C), 122.8 (CH), 130.8 (C), 132.3 (C), 134.0 (CH), 138.6 (CH), 166.0 (CO), 166.6 (CO), 168.1 (CO), 171.1 (CO), 171.2 (CO); **LRMS m/z (ES+)** 433.1 ($[\text{M} + \text{Na}]^+$, 100%); **HRMS m/z (ES+)** calcd for $\text{C}_{22}\text{H}_{22}\text{N}_2\text{O}_6\text{Na}$ 433.1376, found 433.1377.

*A novel compound prepared according to a literature procedure.*⁴⁰⁶

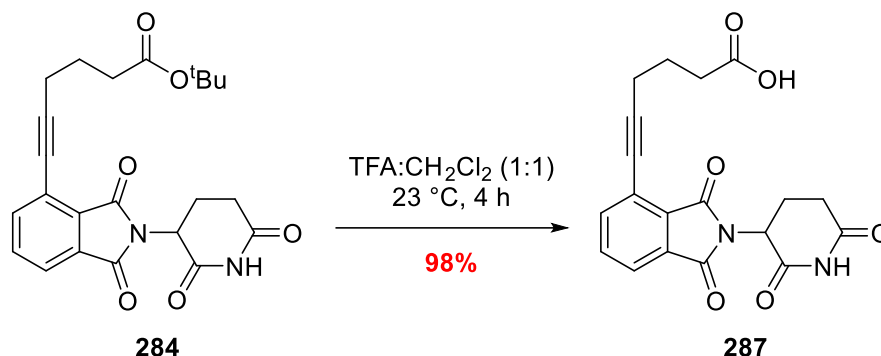
286) 6-(2-(2,6-Dioxopiperidin-3-yl)-1,3-dioxisoindolin-4-yl)hexanoic acid



A solution of benzyl ester **283** (280 mg, 0.61 mmol) and 10 wt% Pd/C (56 mg) in a mixture of MeOH and CH₂Cl₂ (1:1, 12 mL) was saturated with hydrogen gas and stirred at 23 °C. After 6 h, the reaction was determined complete *via* TLC ($R_f = 0.1$, 6:4 ethyl acetate:*n*-hexane) and then passed through a celite bung to remove the solids. The mother liquor was concentrated under reduced pressure and subjected to flash column chromatography ($R_f = 0.3$, 6:4 ethyl acetate:*n*-hexane + 1% AcOH) to yield acid **286** as a white solid (136 mg, 60%); **mp** = 139–141 °C; $\nu_{\max}/\text{cm}^{-1}$ (neat) 3277 (NH), 2928 (CH), 1767 (CO), 1699 br (4 × CO) – no distinct COOH stretch observed; δ_H (400 MHz; CDCl₃) 1.37–1.49 (3 H, Stack, CCH₂(CH₂)₄CO₂H and CHCHH' or CHCHH'), 1.64–1.72 (4 H, Stack, C(CH₂)₂CH₂CH₂(CH₂)₁CO₂H and C(CH₂)₂CH₂CH₂(CH₂)₁CO₂H), 2.35 (2 H, *app. t*, $J = 7.4$, C(CH₂)₄CH₂CO₂H), 2.69–2.95 (3 H, Stack, CHH'CHH'CO, CHH'CHH'CO and CHCHH' or CHCHH'), 3.05–3.12 (2 H, m, C(CH₂)₁CH₂(CH₂)₃CO₂H), 4.98 (1 H, dd, $J = 12.3, 5.3$, NCHCHH'), 7.52 (1 H, dd, $J = 7.8, 1.1$, CHCCH₂ or CHCHCCO), 7.63 (1 H, *app. t*, $J = 7.5$, CHCHCCO), 7.72 (1 H, dd, $J = 7.4, 1.1$, CHCCH₂ or CHCHCCO), 8.44 (1 H, s, NH); δ_C (101 MHz; CDCl₃) 22.8 (CH₂), 24.5 (CH₂), 28.8 (CH₂), 29.8 (CH₂), 30.5 (CH₂), 31.2 (CH₂), 31.5 (CH₂), 33.8 (CH₂), 49.2 (CH₂), 51.0 (CH), 121.8 (CH), 128.2 (C), 132.4 (C), 134.3 (CH), 136.1 (CH), 143.5 (C), 167.4 (CO), 168.0 (CO), 168.5 (CO), 171.3 (CO), 178.2 (CO); **LRMS m/z (ES+)** 395.1 ([M + Na]⁺, 100%); **HRMS m/z (ES+)** calcd for C₁₉H₂₀N₂O₆Na 395.12.19, found 395.1222.

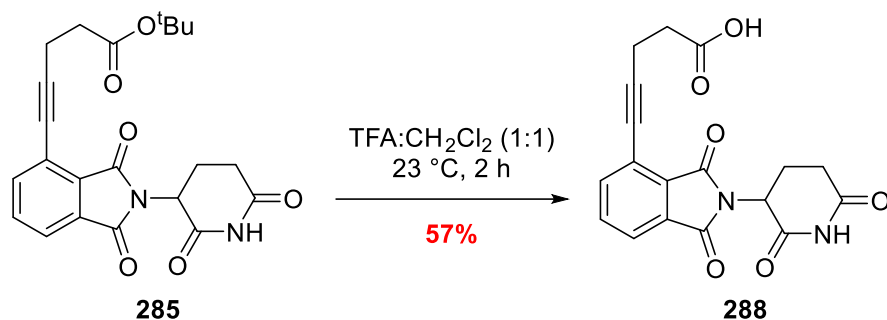
A novel compound prepared according to a standard procedure. COOH proton was not observed in the ¹H-NMR.

287) 6-(2-(2,6-Dioxopiperidin-3-yl)-1,3-dioxoisindolin-4-yl)hex-5-ynoic acid



Trifluoroacetic acid (1 mL) was added to a solution of *tert*-butyl ester **284** (100 mg, 0.24 mmol) in CH₂Cl₂ (1 mL) and stirred at 23 °C. After 4 h, the reaction was determined complete *via* TLC (*R_f* = 0.1, 3:1 ethyl acetate:*n*-hexane) and concentrated under reduced pressure to afford acid **287** as an off-white solid (86 mg, 98%) with no need for further purification; **mp** = 155–156 °C; $\nu_{\max}/\text{cm}^{-1}$ (neat) 3216 (NH), 3100* br (COOH), 3086 (CH), 2896 (CH), 2236 (C≡C), 1769 (CO), 1746 (CO), 1708 br (2 × CO), 1677 (CO); δ_{H} (400 MHz; (CD₃)₂SO) 1.81 (2 H, *app.* p, *J* = 7.2, CH₂CH₂CH₂), 2.02–2.10 (1 H, m, CHH'CHH'CO or CHH'CHHCO), 2.47 (2 H, *app.* t, *J* = 7.4, C≡CCH₂), 2.53–2.64 (4 H, Stack, CH₂CH₂CO₂^tBu, CHCHH' or CHCHH' and CHH'CHH'CO or CHH'CHHCO), 2.89 (1 H, ddd, *J* = 16.7, 13.7, 5.2, CHCHH' or CHCHH'), 5.10–5.19 (1 H, dd, *J* = 12.9, 5.2, NCHCHH'), 7.81–7.89 (3 H, Stack, CHCC≡C, CHCHCCO and CHCHCCO), 11.14 (1 H, s, NH), 12.13 (1 H, s, CO₂H); δ_{C} (101 MHz; (CD₃)₂SO) 18.4 (CH₂), 21.9 (CH₂), 23.4 (CH₂), 30.9 (CH₂), 32.4 (CH₂), 49.0 (CH), 76.5 (C), 98.0 (C), 119.9 (C), 122.7 (CH), 130.2 (C), 132.0 (C), 134.7 (CH), 138.3 (CH), 165.8 (CO), 166.3(CO), 169.9 (CO), 172.8 (CO), 174.1 (CO); **LRMS *m/z* (ES⁺)** 391.1 ([M + Na]⁺, 100%); **HRMS *m/z* (ES⁺)** calcd for C₁₉H₁₆N₂O₆Na 391.0906, found 391.0905.

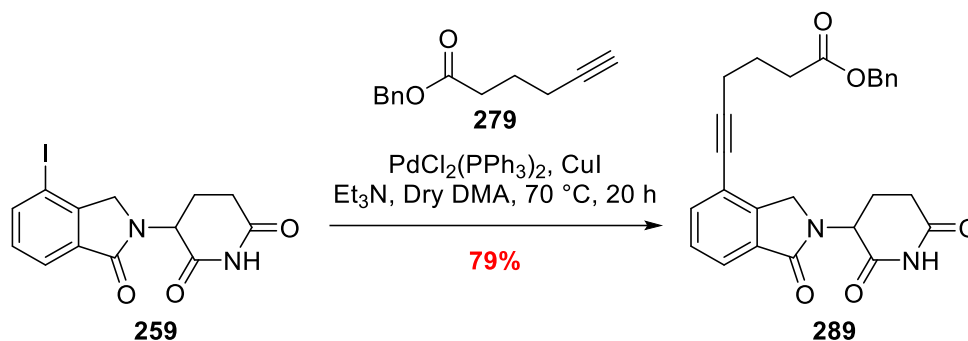
*A novel compound prepared according to a standard procedure. *arbitrary centre of broad trough caused by the COOH functionality.*

288) 5-(2-(2,6-Dioxopiperidin-3-yl)-1,3-dioxisoindolin-4-yl)pent-4-ynoic acid

Trifluoroacetic acid (3 mL) was added to a solution of *tert*-butyl ester **285** (182 mg, 0.44 mmol) in CH₂Cl₂ (3 mL) and stirred at 23 °C. After 2 h, the reaction was determined complete *via* TLC ($R_f = 0.1$, 3:1 ethyl acetate:*n*-hexane) and concentrated under reduced pressure. The crude material was then subjected to flash column chromatography ($R_f = 0.3$, 5% → 10% MeOH in CH₂Cl₂) to afford acid **288** as a white solid (89 mg, 57%); **mp** = 167–169 °C; $\nu_{\max}/\text{cm}^{-1}$ (neat) 3204 (NH), 3100* br (COOH), 3093 (CH), 2904 (CH), 2233 (C≡C), 1706 br (5 × CO); δ_H (400 MHz; (CD₃)₂SO) 2.00–2.11 (1 H, m, CHH'CHH'CO or CHH'CHH'CO), 2.52–2.66 (4 H, Stack, C≡CCH₂, CHCHH' or CHCHH' and CHH'CHH'CO or CHH'CHH'CO), 2.73 (2 H, *app. t*, $J = 7.2$, CH₂CH₂CO₂*t*Bu), 2.89 (1 H, m, CHCHH' or CHCHH'), 5.14 (1 H, dd, $J = 12.8, 5.4$, NCHCHH'), 7.76–7.90 (3 H, Stack, CHCC≡C, CHCHCCO and CHCHCCO), 11.13 (1 H, s, NH), 12.35 (1 H, s, CO₂H); δ_C (101 MHz; (CD₃)₂SO) 15.0 (CH₂), 21.9 (CH₂), 30.9 (CH₂), 32.6 (CH₂), 49.0 (CH), 76.1 (C), 97.6 (C), 119.7 (C), 122.8 (CH), 130.2 (C), 132.0 (C), 134.7 (CH), 138.2 (CH), 165.7 (CO), 166.3 (CO), 169.8 (CO), 172.7 (CO), 172.8 (CO); **LRMS m/z (AP+)** 335.1 ([M + H]⁺, 100%); **HRMS m/z (AP+)** calcd for C₁₈H₁₅N₂O₆Na 355.0930, found 355.0936.

*A novel compound prepared according to a standard procedure. *arbitrary centre of broad trough caused by the COOH functionality.*

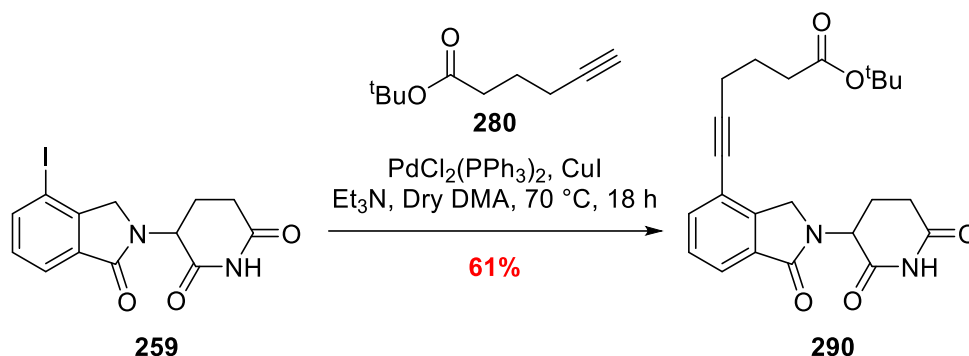
289) Benzyl 6-(2-(2,6-dioxopiperidin-3-yl)-1-oxoisindolin-4-yl)hex-5-ynoate



General method B was utilised to synthesise **289**: Aryl iodide **259** (150 mg, 0.41 mmol), alkyne **279** (123 mg, 0.61 mmol), $\text{PdCl}_2(\text{PPh}_3)_2$ (28 mg, 0.04 mmol) and CuI (15 mg, 0.08 mmol), and solubilised in a mixture of anhydrous DMA and freshly distilled Et_3N (4:1, 2.5 mL). Heated at 70°C for 20 h ($R_f = 0.2$, 4:1 ethyl acetate:*n*-hexane). Purified by flash column chromatography ($R_f = 0.2$, 4:1 ethyl acetate:*n*-hexane) to yield aryl alkyne **289** as a white solid (143 mg, 79%); $\text{mp} = 179\text{--}180^\circ\text{C}$; $\nu_{\text{max}}/\text{cm}^{-1}$ (neat) 3175 (NH), 3084 (CH), 2914 (CH), 2229 ($\text{C}\equiv\text{C}$), 1728 (CO), 1704 br ($2 \times \text{CO}$), 1664 (CO); δ_{H} (400 MHz; CDCl_3) 1.97 (2 H, *app.* p, $J = 7.2$, $\text{CH}_2\text{CH}_2\text{CH}_2$), 2.19 (1 H, m, $\text{CHH}'\text{CHH}'\text{CO}$ or $\text{CHH}'\text{CHH}'\text{CO}$), 2.37 (1 H, m, $\text{CHH}'\text{CHH}'\text{CO}$ or $\text{CHH}'\text{CHH}'\text{CO}$), 2.53 (2 H, t, $J = 7.0$, $\text{C}\equiv\text{CCH}_2$), 2.55 (2 H, *app.* t, $J = 7.4$, $\text{CH}_2\text{CH}_2\text{CO}_2^t\text{Bu}$), 2.77–2.94 (2 H, Stack, CHCHH' and CHCHH'), 4.33 (1 H, *app.* d, $J = 16.7$, $\text{CCHH}'\text{N}$), 4.48 (1 H, *app.* d, $J = 16.7$, $\text{CCHH}'\text{N}$), 5.13 (2 H, *app.* s, $\text{CO}_2\text{CH}_2\text{Ph}$), 5.22 (1 H, dd, $J = 13.3, 5.1$, NCHCHH'), 7.29 – 7.39 (5 H, Stack, *Ar-H*), 7.43 (1 H, *app.* t, $J = 7.6$, CHCHC), 7.56 (1 H, dd, $J = 7.6, 1.1$, $\text{CHCC}\equiv\text{C}$ or CHCHCCO), 7.80 (1 H, dd, $J = 7.6, 1.1$, $\text{CHCC}\equiv\text{C}$ or CHCHCCO), 8.04 (1 H, s, NH); δ_{C} (101 MHz; CDCl_3) 19.0 (CH_2), 23.4 (CH_2), 23.8 (CH_2), 31.6 (CH_2), 33.1 (CH_2), 47.0 (CH_2), 51.8 (CH), 66.4 (C), 77.2 (C), 94.6 (C), 119.3 (CH), 123.4 (CH), 128.2 (CH), 128.3 (CH), 128.4 (C), 128.6 (CH), 131.5 (C), 134.7 (CH), 143.5 (C), 169.0 (CO), 169.4 (CO), 171.0 (CO), 172.8 (CO); LRMS m/z (ES+) 467.2 ($[\text{M} + \text{Na}]^+$, 100%); HRMS m/z (ES+) calcd for $\text{C}_{26}\text{H}_{24}\text{N}_2\text{O}_5\text{Na}$ 467.1583, found 467.1584.

A novel compound prepared according to a literature procedure.⁴⁰⁶

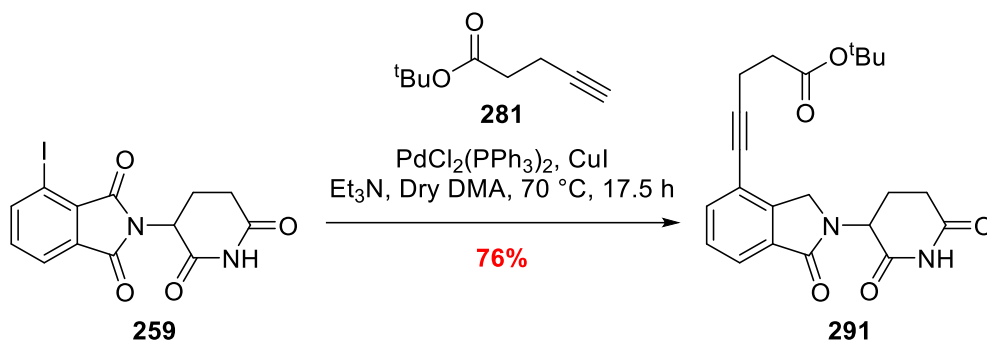
290) tert-Butyl 6-(2-(2,6-dioxopiperidin-3-yl)-1-oxoisindolin-4-yl)hex-5-ynoate



General method B was utilised to synthesise **290**: Aryl iodide **259** (200 mg, 0.54 mmol), alkyne **280** (136 mg, 0.81 mmol), $\text{PdCl}_2(\text{PPh}_3)_2$ (38 mg, 0.05 mmol) and CuI (21 mg, 0.11 mmol), and solubilised in a mixture of anhydrous DMA and freshly distilled Et_3N (4:1, 5 mL). Heated at $70\text{ }^\circ\text{C}$ for 18 h ($R_f = 0.2$, 4:1 ethyl acetate:*n*-hexane). Purified by flash column chromatography ($R_f = 0.2$, 4:1 ethyl acetate:*n*-hexane) to yield aryl alkyne **290** as a white solid (135 mg, 61%); **mp** = $202\text{--}203\text{ }^\circ\text{C}$; $\nu_{\text{max}}/\text{cm}^{-1}$ (neat) 3175 (NH), 3083 (CH), 2979 (CH), 2937 (CH), 2236 ($\text{C}\equiv\text{C}$), 1727 (CO), 1703 br ($2 \times \text{CO}$), 1664 (CO); δ_{H} (400 MHz; CDCl_3) 1.45 (9 H, s, $\text{C}(\text{CH}_3)_3$), 1.90 (2 H, *app.* p, $J = 7.3$, $\text{CH}_2\text{CH}_2\text{CH}_2$), 2.23 (1 H, m, $\text{CHH}'\text{CHH}'\text{CO}$ or $\text{CHH}'\text{CHH}'\text{CO}$), 2.40 (3 H, Stack, $\text{C}\equiv\text{CCH}_2$ and $\text{CHH}'\text{CHH}'\text{CO}$ or $\text{CHH}'\text{CHH}'\text{CO}$), 2.50 (2 H, *app.* t, $J = 7.1$, $\text{CH}_2\text{CH}_2\text{CO}_2^t\text{Bu}$), 2.78–2.97 (2 H, Stack, CHCHH' and CHCHH'), 4.35 (1 H, *app.* d, $J = 16.7$, $\text{CCHH}'\text{N}$), 4.49 (1 H, *app.* d, $J = 16.7$, $\text{CCHH}'\text{N}$), 5.24 (1 H, dd, $J = 13.4$, 5.1, NCHCHH'), 7.44 (1 H, *app.* t, $J = 7.6$, CHCHC), 7.57 (1 H, dd, $J = 7.6$, 1.1, $\text{CHCC}\equiv\text{C}$ or CHCHCCO), 7.80 (1 H, dd, $J = 7.6$, 1.1, $\text{CHCC}\equiv\text{C}$ or CHCHCCO), 8.03 (1 H, s, NH); δ_{C} (101 MHz; CDCl_3) 19.1 (CH_2), 23.6 (CH_2), 24.2 (CH_2), 28.3 ($\text{C}(\text{CH}_3)_3$), 31.7 (CH_2), 34.6 (CH_2), 47.1 (CH_2), 52.0 (CH), 77.4 (C), 80.7 (C), 95.1 (C), 119.5 (C), 123.5 (CH), 128.5 (CH), 131.7 (C), 134.8 (CH), 143.7 (C), 169.2 (CO), 169.5 (CO), 171.1 (CO), 172.5 (CO); **LRMS m/z (ES+)** 433.2 ($[\text{M} + \text{Na}]^+$, 100%); **HRMS m/z (ES+)** calcd for $\text{C}_{23}\text{H}_{26}\text{N}_2\text{O}_5\text{Na}$ 433.1739, found 433.1742.

A novel compound prepared according to a literature procedure.⁴⁰⁶

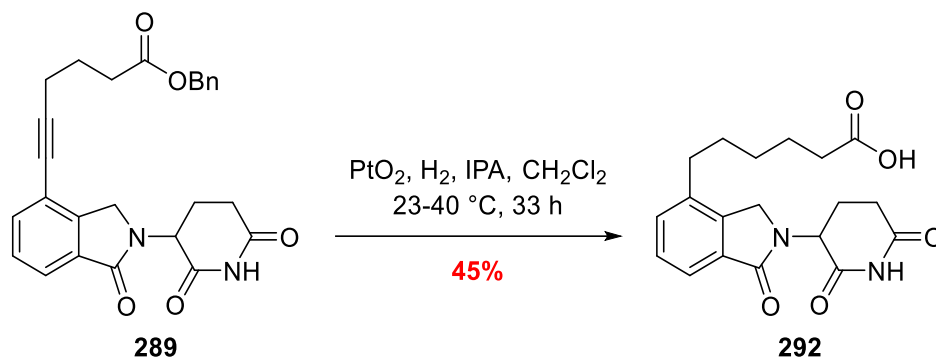
291) tert-Butyl 5-(2-(2,6-dioxopiperidin-3-yl)-1-oxoisindolin-4-yl)pent-4-ynoate



General method B was utilised to synthesise **291**: Aryl iodide **259** (200 mg, 0.54 mmol), alkyne **281** (125 mg, 0.81 mmol), $\text{PdCl}_2(\text{PPh}_3)_2$ (38 mg, 0.05 mmol) and CuI (21 mg, 0.11 mmol), and solubilised in a mixture of anhydrous DMA and freshly distilled Et_3N (4:1, 5 mL). Heated at $70\text{ }^\circ\text{C}$ for 17.5 h ($R_f = 0.2$, 4:1 ethyl acetate:*n*-hexane). Purified by flash column chromatography ($R_f = 0.2$, 4:1 ethyl acetate:*n*-hexane) to yield aryl alkyne **291** as a white solid (162 mg, 76%); **mp** = $219\text{--}221\text{ }^\circ\text{C}$; $\nu_{\text{max}}/\text{cm}^{-1}$ (neat) 3178 (NH), 3083 (CH), 2980 (CH), 2930 (CH), 2237 ($\text{C}\equiv\text{C}$), 1726 (CO), 1705 br ($2 \times \text{CH}$), 1663 (CH); δ_{H} (400 MHz; CDCl_3) 1.46 (9 H, s, $\text{C}(\text{CH}_3)_3$), 2.21 (1 H, m, $\text{CHH}'\text{CHH}'\text{CO}$ or $\text{CHH}'\text{CHH}'\text{CO}$), 2.38 (1 H, m, $\text{CHH}'\text{CHH}'\text{CO}$ or $\text{CHH}'\text{CHH}'\text{CO}$), 2.54 (2 H, *app. t*, $J = 7.2$, $\text{C}\equiv\text{CCH}_2$), 2.71 (2 H, *app. t*, $J = 7.2$, $\text{CH}_2\text{CH}_2\text{CO}_2^t\text{Bu}$), 2.78 – 2.96 (2 H, Stack, CHCHH' or CHCHH'), 4.33 (1 H, *app. d*, $J = 16.8$, $\text{CCHH}'\text{N}$), 4.46 (1 H, *app. d*, $J = 16.8$, $\text{CCHH}'\text{N}$), 5.24 (1 H, dd, $J = 13.3$, 5.2, NCHCHH'), 7.42 (1 H, *app. t*, $J = 7.6$, CHCHC), 7.54 (1 H, dd, $J = 7.7$, 1.1, $\text{CHCC}\equiv\text{C}$ or CHCHCCO), 7.80 (1 H, dd, $J = 7.6$, 1.1, $\text{CHCC}\equiv\text{C}$ or CHCHCCO), 8.26 (1 H, s, NH); δ_{C} (101 MHz; CDCl_3) 15.7 (CH_2), 23.6 (CH_2), 28.2 ($\text{C}(\text{CH}_3)_3$), 31.7 (CH_2), 34.8 (CH_2), 47.0 (CH_2), 51.9 (CH), 76.9 (C), 81.1 (C), 94.3 (C), 119.3 (C), 123.6 (CH), 128.5 (CH), 131.7 (C), 134.7 (CH), 143.8 (C), 169.1 (CO), 169.6 (CO), 171.1 (CO), 171.3 (CO); **LRMS m/z (ES⁺)** 419.2 ($[\text{M} + \text{Na}]^+$, 100%); **HRMS m/z (ES⁺)** calcd for $\text{C}_{22}\text{H}_{24}\text{N}_2\text{O}_5\text{Na}$ 419.1583, found 419.1586.

*A novel compound prepared according to a literature procedure.*⁴⁰⁶

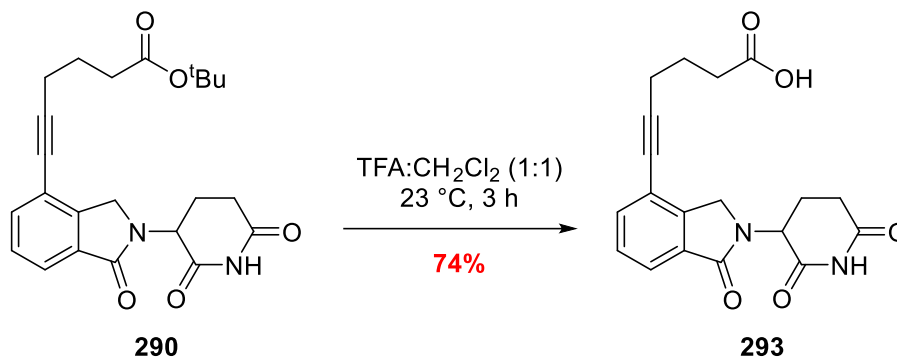
292) 6-(2-(2,6-Dioxopiperidin-3-yl)-1-oxoisindolin-4-yl)hexanoic acid



A solution of benzyl ester **289** (117 mg, 0.26 mmol) and PtO₂ (3 mg, 0.01 mmol) in a mixture of *i*PrOH and CH₂Cl₂ (1:1, 6 mL) was saturated with hydrogen gas and stirred at 23 °C. After 25 h only partial conversion was observed so the reaction temperature was elevated to 40 °C. After a further 8 h, the reaction was determined complete *via* TLC (*R_f* = 0.1, 100% ethyl acetate) and then passed through a celite bung to remove the solid catalyst. The mother liquor was concentrated under reduced pressure and subjected to flash column chromatography (*R_f* = 0.2, 10% MeOH in CH₂Cl₂) to yield acid **292** as a white solid (42 mg, 45%); **mp** = 188–190 °C; $\nu_{\max}/\text{cm}^{-1}$ (neat) 3183 (NH), 3050* br (COOH) 3062 (CH), 2931 (CH), 1690 (2 ×CO), 1665 (2 ×CO); δ_{H} (400 MHz; CD₃OD) 1.37–1.48 (2 H, m, CCH₂(CH₂)₄CO₂H), 1.61–1.74 (4 H, Stack, C(CH₂)₂CH₂CH₂(CH₂)₁CO₂H and C(CH₂)₂CH₂CH₂(CH₂)₁CO₂H), 2.19 (1 H, m, CHH'CHH'CO or CHH'CHH'CO), 2.29 (2 H, *app. t*, *J* = 7.7, C(CH₂)₁CH₂(CH₂)₃CO₂H), 2.47–2.60 (1 H, m, CHH'CHH'CO or CHH'CHH'CO), 2.69–2.75 (2 H, *app. t*, *J* = 7.7, C(CH₂)₄CH₂CO₂H), 2.79 (1 H, m, CHCHH' or CHCHH'), 2.91 (1 H, m, CHCHH' or CHCHH'), 4.45 (1 H, *app. d*, *J* = 17.0, CCHH'N), 4.52 (1 H, *app. d*, *J* = 17.0, CCHH'N), 5.17 (1 H, dd, *J* = 13.3, 5.2, NCHCHH'), 7.45–7.48 (2 H, Stack, CHCCH₂ and CHCHCCO), 7.64 (1 H, m, CHCHCCO); δ_{C} (101 MHz; CD₃OD) 24.1 (CH₂), 25.9 (CH₂), 30.0 (CH₂), 30.7 (CH₂), 32.4 (CH₂), 32.7 (CH₂), 34.9 (CH₂), 48.2 (CH₂), 53.7 (C), 122.1 (CH), 129.6 (CH), 132.6 (C), 133.3 (C), 139.1 (CH), 142.0 (C), 171.9 (CO), 172.3 (CO), 174.7 (CO), 177.7 (CO); **LRMS *m/z* (ES⁺)** 381.1 ([M + Na]⁺, 100%); **HRMS *m/z* (ES⁺)** calcd for C₁₉H₂₂N₂O₅Na 381.1426, 381.1425.

A novel compound prepared according to a standard procedure. *arbitrary centre of broad trough caused by the COOH functionality.

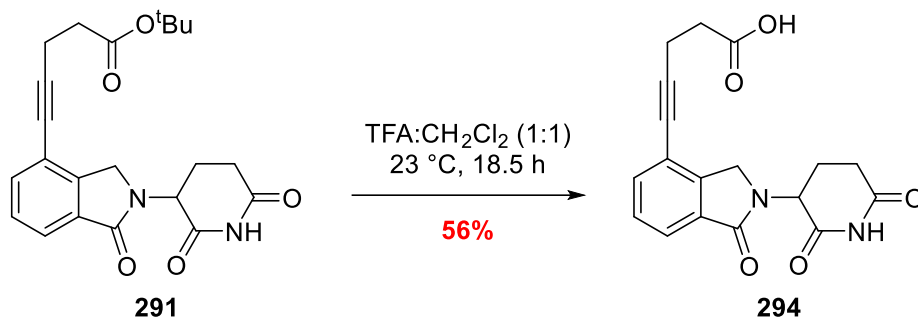
293) 6-(2-(2,6-Dioxopiperidin-3-yl)-1-oxoisoindolin-4-yl)hex-5-ynoic acid



Trifluoroacetic acid (2 mL) was added to a solution of *tert*-butyl ester **290** (135 mg, 0.33 mmol) in CH₂Cl₂ (2 mL) and stirred at 23 °C. After 3 h, the reaction was determined complete *via* TLC (*R_f* = 0.2, 4:1 ethyl acetate:*n*-hexane) and concentrated under reduced pressure to give the an impure solid. The crude solid was recrystallised from hot hexane, ethyl acetate a few drops of MeOH to give acid **293** as an off-white solid (86 mg, 74%); **mp** = 199–200 °C; $\nu_{\max}/\text{cm}^{-1}$ (neat) 3181 (NH), 3082 (CH), 2914 (CH), 2231 (C≡C), 1704 br (2 ×CO), 1665 (2 ×CO) – no distinct COOH stretch observed; δ_{H} (400 MHz; (CD₃)₂SO) 1.80 (2 H, *app.* p, *J* = 7.9, CH₂C), 2.00 (1 H, m, CHH'CHH'CO or CHH'CHH'CO), 2.36 (2 H, *app.* t, *J* = 7.3, C≡CCH₂), 2.39–2.48 (1 H, m, CHH'CHH'CO or CHH'CHH'CO), 2.50–2.54 (2 H, Stack, CH₂CO₂H and residual DMSO resonance), 2.59 (1 H, m, CHCHH' or CHCHH'), 2.84–3.00 (1 H, m, CHCHH' or CHCHH'), 4.31 (1 H, *app.* d, *J* = 17.8, CCHH'N), 4.46 (1 H, *app.* d, *J* = 17.8, CCHH'N), 5.14 (1 H, dd, *J* = 13.3, 5.0, NCHCHH'), 7.52 (1 H, *app.* t, *J* = 7.5, CHCHCCO), 7.64 (1 H, *app.* d, *J* = 7.5, CHC≡C or CHCHCCO), 7.71 (1 H, *app.* d, *J* = 7.5, CHCC≡C or CHCHCCO), 11.00 (1 H, s, NH), 12.24 (1 H, s, CO₂H); δ_{C} (101 MHz; (CD₃)₂SO) 18.3 (CH₂), 22.4 (CH₂), 23.8 (CH₂), 31.2 (CH₂), 33.0 (CH₂), 47.0 (CH₂), 51.6 (CH), 76.7 (C), 95.7 (C), 118.7 (C), 122.7 (CH), 128.6 (CH), 132.0 (C), 134.1 (C), 143.8 (CH), 167.7 (CO), 171.0 (CO), 172.9 (2 × CO); **LRMS *m/z* (ES⁺)** 355.1 ([M + H]⁺, 100%); **HRMS *m/z* (ES⁺)** calcd for C₁₉H₁₉N₂O₅ 355.1294, found 355.1295.

A novel compound prepared according to a standard procedure. Signals within the residual DMSO resonance were identified using HSQC and HMBC data.

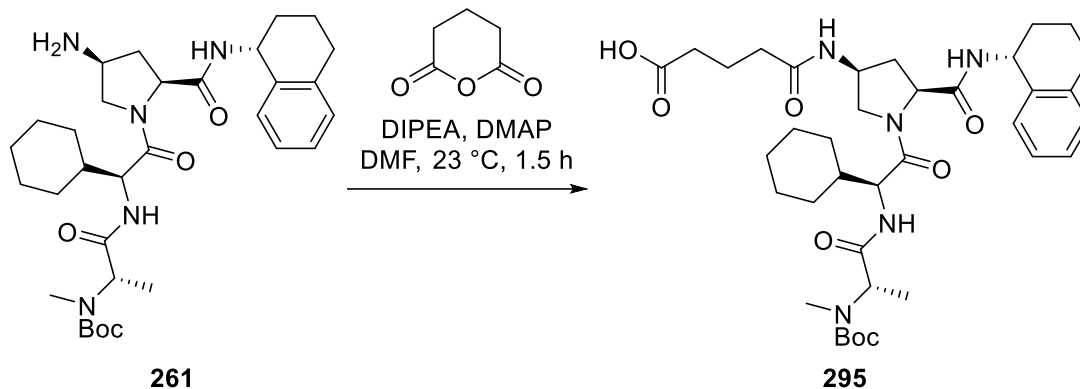
294) 5-(2-(2,6-Dioxopiperidin-3-yl)-1-oxoisoindolin-4-yl)pent-4-ynoic acid



Trifluoroacetic acid (4 mL) was added to a solution of *tert*-butyl ester **291** (160 mg, 0.40 mmol) in CH₂Cl₂ (4 mL) and stirred at 23 °C. After 18.5 h, the reaction was determined complete *via* TLC ($R_f = 0.1$, 4:1 ethyl acetate:*n*-hexane) and concentrated under reduced pressure to give the an impure solid. The crude solid was recrystallised from hot hexane, ethyl acetate a few drops of MeOH to give acid **294** as a fine white powder (77 mg, 56%); **mp** = 191–193 °C; $\nu_{\max}/\text{cm}^{-1}$ (neat) 3170 (NH), 3084 (CH), 2916 (CH), 2234 (C≡C), 1701 br (2 ×CO), 1664 (2 ×CO) – no distinct COOH stretch observed; δ_H (**400 MHz; (CD₃)₂SO**) 1.93–2.11 (1 H, m, CHH'CHH'CO or CHH'CHH'CO), 2.37–2.49 (1 H, m, CHH'CHH'CO or CHH'CHH'CO), 2.53–2.56 (3 H, Stack, C≡CCH₂ and CHCHH' or CHCHH'), 2.68 (2 H, *app.* t, $J = 7.0$, CH₂CO₂H), 2.93 (1 H, ddd, $J = 18.0, 13.3, 5.4$, CHCHH' or CHCHH'), 4.27 (1 H, *app.* d, $J = 17.8$, CCHH'N), 4.42 (1 H, *app.* d, $J = 17.8$, CCHH'N), 5.15 (1 H, dd, $J = 13.3, 5.1$, NCHCHH'), 7.52 (1 H, *app.* t, $J = 7.6$, CHCHCCO), 7.62 (1 H, *app.* d, $J = 7.5$, CHC≡C or CHCHCCO), 7.71 (1 H, *app.* d, $J = 7.5$ CHC≡C or CHCHCCO), 11.02 (1 H, s, NH), 12.39 (1 H, s, CO₂H); δ_C (**101 MHz; (CD₃)₂SO**) 15.0 (CH₂), 22.4 (CH₂), 31.2 (CH₂), 33.1 (CH₂), 46.9 (CH₂), 51.6 (CH), 76.4 (C), 95.3 (C), 118.6 (C), 122.8 (CH), 128.6 (CH), 132.0 (C), 133.9 (CH), 144.0 (C), 167.7 (CO), 171.0 (CO), 172.9 (CO), 173.0 (CO); **LRMS m/z (ES⁻)** 339.3 ([M - H]⁻, 100%); **HRMS m/z (ES⁻)** calcd for C₁₈H₁₅N₂O₅ 339.0981, found 339.0984.

A novel compound prepared according to a standard procedure.

295) 5-(((3S,5S)-1-((S)-2-((S)-2-((tert-Butoxycarbonyl)(methyl)amino)propanamido)-2-cyclohexylacetyl)-5-(((R)-1,2,3,4-tetrahydronaphthalen-1-yl)carbamoyl)pyrrolidin-3-yl)amino)-5-oxopentanoic acid



Amine **261** (50 mg, 0.09 mmol) was added to a solution of glutaric anhydride (12 mg, 0.10 mmol), DIPEA (18 μ L, 0.10 mmol) and DMAP (1 mg, 0.009 mmol) in DMF (1 mL) and stirred at 23 °C. After 1.5 h, the reaction was determined complete *via* TLC (R_f = 0.2, 15% MeOH in CH_2Cl_2). Acid **295** (34 mg) was isolated and used in the next step with no further purification. **LRMS m/z (ES+)** 720.6 ($[(M + \text{Na})^+]$, 100%), 398.7 ($[(M + \text{H})^+]$, 50).

*A novel compound prepared according to a literature procedure.*⁴¹⁷

Chapter 5:
References

References

1. S. Yamamoto and O. Hayaishi, *J. Biol. Chem.*, 1967, **242**, 5260-5266.
2. F. Hirata, O. Hayaishi, T. Tokuyama and S. Senoh, 1974, **249**, 1311-1313.
3. O. Hayaishi, *Acta Vitaminol. Enzym.*, 1975, **29**, 17-20.
4. R. Metz, J. B. DuHadaway, U. Kamasani, L. Laury-Kleintop, A. J. Muller and G. C. Prendergast, *Cancer Res*, 2007, **67**, 7082-7087.
5. H. J. Yuasa, M. Takubo, A. Takahashi, T. Hasegawa, H. Noma and T. Suzuki, *J Mol Evol*, 2007, **65**, 705-714.
6. H. J. Ball, A. Sanchez-Perez, S. Weiser, C. J. Austin, F. Astelbauer, J. Miu, J. A. McQuillan, R. Stocker, L. S. Jermiin and N. H. Hunt, *Gene*, 2007, **396**, 203-213.
7. N. D. Papadopoulou, M. Mewies, K. J. McLean, H. E. Seward, D. A. Svistunenko, A. W. Munro and E. L. Raven, *Biochemistry*, 2005, **44**, 14318-14328.
8. E. S. Booth, J. Basran, M. Lee, S. Handa and E. L. Raven, *J. Biol. Chem.*, 2015, **290**, 30924-30930.
9. N. Chauhan, J. Basran, I. Efimov, D. A. Svistunenko, H. E. Seward, P. C. E. Moody and E. L. Raven, *Biochemistry*, 2008, **47**, 4761-4769.
10. H. Sugimoto, S. I. Oda, T. Otsuki, T. Hino, T. Yoshida and Y. Shiro, *Proc. Natl. Acad. Sci. U. S. A.*, 2006, **103**, 2611-2616.
11. F. Forouhar, A. Lewis-Ballester, S. Lew, Karkashon, S., J. Seetharaman, C. Lu, M. Hussain, S.-R. Yeh, L. Tong and N. S. G. C. (NESG), Crystal structure of human indoleamine 2,3-dioxygenase (IDO1) in complex with L-Trp and cyanide, Northeast Structural Genomics Target HR6160, <http://www.rcsb.org/structure/6E35>.
12. A. B. Dounay, J. B. Tuttle and P. R. Verhoest, *J. Med. Chem.*, 2015, **58**, 8762-8782.
13. L. Vecsei, L. Szalardy, F. Fulop and J. Toldi, *Nat. Rev. Drug Discov.*, 2013, **12**, 64-82.
14. N. J. King and S. R. Thomas, *Int. J. Biochem. Cell. Biol.*, 2007, **39**, 2167-2172.
15. C. Uyttenhove, L. Pilotte, I. Theate, V. Stroobant, D. Colau, N. Parmentier, T. Boon and B. J. Van den Eynde, *Nat. med.*, 2003, **9**, 1269-1274.
16. R. Yoshida, Y. Urade, M. Tokuda and O. Hayaishi, *Proc. Natl. Acad. Sci. U. S. A.*, 1979, **76**, 4084-4086.
17. R. Yoshida and O. Hayaishi, *Proc. Natl. Acad. Sci. U. S. A.*, 1978, **75**, 3998-4000.
18. S. V. Schmidt and J. L. Schultze, *Front Immunol*, 2014, **5**, 384-384.
19. A. M. Mackler, E. M. Barber, O. Takikawa and J. W. Pollard, *J. Immunol.*, 2003, **170**, 823-830.
20. A. Curti, S. Trabanelli, V. Salvestrini, M. Baccarani and R. M. Lemoli, *Blood*, 2009, **113**, 2394-2401.

21. D. H. Munn, E. Shafizadeh, J. T. Attwood, I. Bondarev, A. Pashine and A. L. Mellor, *J. Exp. Med.*, 1999, **189**, 1363-1372.
22. G. K. Lee, H. J. Park, M. Macleod, P. Chandler, D. H. Munn and A. L. Mellor, *Immunology*, 2002, **107**, 452-460.
23. G. Frumento, R. Rotondo, M. Tonetti, G. Damonte, U. Benatti and G. B. Ferrara, *The Journal of experimental medicine*, 2002, **196**, 459-468.
24. M. Platten, W. Wick and B. J. Van den Eynde, *Cancer Res*, 2012, **72**, 5435-5440.
25. L. Hornyák, N. Dobos, G. Koncz, Z. Karányi, D. Páll, Z. Szabó, G. Halmos and L. Székvölgyi, *Front Immunol*, 2018, **9**, 151-151.
26. Y. Mandi and L. Vecsei, *J. Neural. Transm.*, 2012, **119**, 197-209.
27. Sarah J. Thackray, Christopher G. Mowat and Stephen K. Chapman, *Biochem. Soc. Trans.*, 2008, **36**, 1120.
28. R. Makino, E. Obayashi, H. Hori, T. Iizuka, K. Mashima, Y. Shiro and Y. Ishimura, *Biochemistry*, 2015, **54**, 3604-3616.
29. H. H. J. Soliman, E.; Neuger, T; Dees, E. C.; Harvey, R. D.; Han, H.; Ismail-Khan, R.; Minton, S.; Vahanian, N. N.; Link, C.; Sullivan, D. M.; Antonia, S., *Oncotarget*, 2014, **5**, 8136-8146.
30. W. P. Malachowski, M. Winters, J. B. DuHadaway, A. Lewis-Ballester, S. Badir, J. Wai, M. Rahman, E. Sheikh, J. M. LaLonde, S.-R. Yeh, G. C. Prendergast and A. J. Muller, *Eur. J. Med. Chem.*, 2016, **108**, 564-576.
31. Y.-H. Peng, S.-H. Ueng, C.-T. Tseng, M.-S. Hung, J.-S. Song, J.-S. Wu, F.-Y. Liao, Y.-S. Fan, M.-H. Wu, W.-C. Hsiao, C.-C. Hsueh, S.-Y. Lin, C.-Y. Cheng, C.-H. Tu, L.-C. Lee, M.-F. Cheng, K.-S. Shia, C. Shih and S.-Y. Wu, *J. Med. Chem.*, 2016, **59**, 282-293.
32. Y. Watanabe, M. Fujiwara and O. Hayaishi, *Biochem. Biophys. Res. Commun.*, 1978, **85**, 273-279.
33. N. Eguchi, Y. Watanabe, K. Kawanishi, Y. Hashimoto and O. Hayaishi, *Arch. Biochem. Biophys.*, 1984, **232**, 602-609.
34. S. G. Cady and M. Sono, *Arch. Biochem. Biophys.*, 1991, **291**, 326-333.
35. A. J. Muller, J. B. DuHadaway, P. S. Donover, E. Sutanto-Ward and G. C. Prendergast, *Nat. med.*, 2005, **11**, 312-319.
36. P. Gaspari, T. Banerjee, W. P. Malachowski, A. J. Muller, G. C. Prendergast, J. DuHadaway, S. Bennett and A. M. Donovan, *J. Med. Chem.*, 2006, **49**, 684-692.
37. S. Kumar, D. Jaller, B. Patel, J. M. LaLonde, J. B. DuHadaway, W. P. Malachowski, G. C. Prendergast and A. J. Muller, *J. Med. Chem.*, 2008, **51**, 4968-4977.
38. D. E. Williams, A. Steinø, N. J. de Voogd, A. G. Mauk and R. J. Andersen, *J. Nat. Prod.*, 2012, **75**, 1451-1458.
39. U. F. Röhrig, S. R. Majjigapu, P. Vogel, V. Zoete and O. Michielin, *J. Med. Chem.*, 2015, **58**, 9421-9437.

40. J. A. Balog, A. Huang, B. Chen, L. Chen, S. P. Seitz, A. C. Hart and J. A. Markwalder, *United States Pat.*, WO2014150677, 2014.
41. J. A. Balog, A. Huang, B. Chen, L. Chen and W. Shan, *United States Pat.*, WO2014150646, 2014.
42. J. A. Markwalder, J. A. Balog, A. Huang and S. P. Seitz, *United States Pat.*, WO2015006520, 2015.
43. J. A. Balog, E. C. Cherney, J. A. Markwalder, S. P. Seitz, W. Shan, D. K. Williams, S. J. Nara, S. Roy, S. Thangavel, R. K. Sistla, S. Cheruku, S. Thangathirupathy, Y. Kanyaboina, N. Pulicharla and H. Audris, WO2016161279, 2016.
44. Bristol-Myers Squibb: In the pipeline, <https://www.bms.com/research/pipeline/Pages/default.aspx>, (accessed 19/01/2017).
45. C. Jochems, M. Fantini, R. I. Fernando, A. R. Kwilas, R. N. Donahue, L. M. Lepone, I. Grenga, Y. S. Kim, M. W. Brechbiel, J. L. Gulley, R. A. Madan, C. R. Heery, J. W. Hodge, R. Newton, J. Schlom and K. Y. Tsang, *Oncotarget*, 2016, **7**, 37762-37772.
46. Incyte and Merck to Advance Clinical Development Program Investigating the Combination of Epacadostat with KEYTRUDA® (pembrolizumab), <http://www.mercknewsroom.com/news-release/oncology-newsroom/incyte-and-merck-advance-clinical-development-program-investigating-c>, (accessed 19/01/2017).
47. A. Philippidis, Incyte, Merck & Co. Halt Phase III Trial After Epacadostat/Keytruda Combination Fails in Melanoma, <https://www.genengnews.com/gen-news-highlights/incyte-merck-co-halt-phase-iii-trial-after-epacadostatkeytruda-combination-fails-in-melanoma/81255672>, (accessed 17/05/2018, 2018).
48. P. Taylor, BMS pulls IDO inhibitor trials as Incyte-prompted rout gathers pace, http://www.pmlive.com/pharma_news/bms_pulls_ido_inhibitor_trials_as_incyte-prompted_rout_gathers_pace_1234063, (accessed 17/05/2018, 2018).
49. J. M. T. Berg, J. L.; Stryer, L., *Biochemistry*, W.H.Freeman & Co Ltd, 5th edition edn., 2002.
50. J. Basran, I. Efimov, N. Chauhan, S. J. Thackray, J. L. Krupa, G. Eaton, G. A. Griffith, C. G. Mowat, S. Handa and E. L. Raven, *J. Am. Chem. Soc.*, 2011, **133**, 16251-16257.
51. M. Sono, M. P. Roach, E. D. Coulter and J. H. Dawson, *Chem. Rev.*, 1996, **96**, 2841-2888.
52. J. M. Leeds, P. J. Brown, G. M. McGeehan, F. K. Brown and J. S. Wiseman, *J. Biol. Chem.*, 1993, **268**, 17781-17786.
53. L. W. Chung, X. Li, H. Sugimoto, Y. Shiro and K. Morokuma, *J. Am. Chem. Soc.*, 2008, **130**, 12299-12309.
54. N. Chauhan, S. J. Thackray, S. A. Rafice, G. Eaton, M. Lee, I. Efimov, J. Basran, P. R. Jenkins, C. G. Mowat, S. K. Chapman and E. L. Raven, *J. Am. Chem. Soc.*, 2009, **131**, 4186-4187.

55. L. Capece, A. Lewis-Ballester, D. Batabyal, N. Di Russo, S. R. Yeh, D. A. Estrin and M. A. Marti, *J. Biol. Inorg. Chem.*, 2010, **15**, 811-823.
56. L. Capece, A. Lewis-Ballester, S.-R. Yeh, D. A. Estrin and M. A. Marti, *J. Phys. Chem. B*, 2012, **116**, 1401-1413.
57. C. Itagaki and Y. Nakayama, *Hoppe-Seylers Z. Physiol. Chem.*, 1941, **270**, 83-88.
58. W. E. Knox and A. H. Mehler, *J. Biol. Chem.*, 1950, **187**, 419-430.
59. O. Hayaishi and R. Y. Stanier, *J. Bacteriol.*, 1951, **62**, 691-709.
60. O. Hayaishi, S. Rothberg, A. H. Mehler and Y. Saito, *J. Biol. Chem.*, 1957, **229**, 889-896.
61. G. A. Hamilton, *Adv. Enzymol. Relat. Areas Mol. Biol.*, 1969, **32**, 55-&.
62. M. N. Dufour, A. L. Crumbliss, G. Johnston and A. Gaudemer, *J. Mol. Catal.*, 1980, **7**, 277-287.
63. M. Nakagawa, H. Watanabe, S. Kodato, H. Okajima, T. Hino, J. L. Flippen and B. Witkop, *Proc Natl Acad Sci U S A*, 1977, **74**, 4730-4733.
64. A. C. Terentis, S. R. Thomas, O. Takikawa, T. K. Littlejohn, R. J. W. Truscott, R. S. Armstrong, S. R. Yeh and R. Stocker, *J. Biol. Chem.*, 2002, **277**, 15788-15794.
65. B. Witkop and J. B. Patrick, *J. Am. Chem. Soc.*, 1951, **73**, 2196-2200.
66. B. Irena, E. Brooks and V. J. C., *J. Biolumin. Chemilumin.*, 1989, **4**, 99-111.
67. M. Czaun, G. Speier, J. Kaizer, N. El Bakkali-Taheri and E. Farkas, *Tetrahedron*, 2013, **69**, 6666-6672.
68. W. G. Young, A. C. McKinnis, I. D. Webb and J. D. Roberts, *J. Am. Chem. Soc.*, 1946, **68**, 293-296.
69. M. Matsumoto, *J. Photochem. Photobiol. C*, 2004, **5**, 27-53.
70. J. A. Joule and K. Mills, *Heterocyclic Chemistry*, Wiley-Blackwell, 2010.
71. Y. Zhang, S. A. Kang, T. Mukherjee, S. Bale, B. R. Crane, T. P. Begley and S. E. Ealick, *Biochemistry*, 2007, **46**, 145-155.
72. S. J. Thackray, C. Bruckmann, J. L. R. Anderson, L. P. Campbell, R. Xiao, L. Zhao, C. G. Mowat, F. Forouhar, L. Tong and S. K. Chapman, *Biochemistry*, 2008, **47**, 10677-10684.
73. G. Yagil, *Tetrahedron*, 1967, **23**, 2855-2861.
74. C. Lu, Y. Lin and S.-R. Yeh, *J. Am. Chem. Soc.*, 2009, **131**, 12866-12867.
75. I. Saito, T. Matsuura, M. Nakagawa and T. Hino, *Acc. Chem. Res.*, 1977, **10**, 346-352.
76. L. W. Chung, X. Li, H. Sugimoto, Y. Shiro and K. Morokuma, *J. Am. Chem. Soc.*, 2010, **132**, 11993-12005.
77. R. E. White, *Pharmacol. Ther.*, 1991, **49**, 21-42.
78. A. Lewis-Ballester, D. Batabyal, T. Egawa, C. Y. Lu, Y. Lin, M. A. Marti, L. Capece, D. A. Estrin and S. R. Yeh, *Proc. Natl. Acad. Sci. U. S. A.*, 2009, **106**, 17371-17376.

79. S. Yanagisawa, K. Yotsuya, Y. Hashiwaki, M. Horitani, H. Sugimoto, Y. Shiro, E. H. Appelman and T. Ogura, *Chem. Lett.*, 2010, **39**, 36-37.
80. I. Efimov, J. Basran, S. J. Thackray, S. Handa, C. G. Mowat and E. L. Raven, *Biochemistry*, 2011, **50**, 2717-2724.
81. E. S. Millett, I. Efimov, J. Basran, S. Handa, C. G. Mowat and E. L. Raven, *Curr. Opin. Chem. Biol.*, 2012, **16**, 60-66.
82. B. Meunier, S. P. de Visser and S. Shaik, *Chem. Rev.*, 2004, **104**, 3947-3980.
83. E. L. Raven, *JBIC, J. Biol. Inorg. Chem.*, 2017, **22**, 175-183.
84. H.-Y. Lee, D. K. Moon and J. S. Bahn, *Tetrahedron Lett.*, 2005, **46**, 1455-1458.
85. A. J. McCarroll and J. C. Walton, *Angew. Chem., Int. Ed.*, 2001, **40**, 2225-2248.
86. H. Miyabe and Y. Takemoto, *Chemistry (Weinheim an der Bergstrasse, Germany)*, 2007, **13**, 7280-7286.
87. G. Bar and A. F. Parsons, *Chem. Soc. Rev.*, 2003, **32**, 251-263.
88. R. Ilhyong and S. Noboru, *Angew. Chem., Int. Ed.*, 1996, **35**, 1050-1066.
89. G. J. Rowlands, *Tetrahedron*, 2009, **65**, 8603-8655.
90. G. J. Rowlands, *Tetrahedron*, 2010, **66**, 1593-1636.
91. H. Ishibashi, T. Sato and M. Ikeda, *Synthesis-Stuttgart*, 2002, 695-713.
92. D. M. Hodgson and L. H. Winning, *Org. Biomol. Chem.*, 2007, **5**, 3071-3082.
93. D. P. Curran, *Synlett*, 1991, **2**, 63-72.
94. D. Griller and K. U. Ingold, *Acc. Chem. Res.*, 1980, **13**, 317-323.
95. M. Newcomb, *Tetrahedron*, 1993, **49**, 1151-1176.
96. B. Roschek, K. A. Tallman, C. L. Rector, J. G. Gillmore, D. A. Pratt, C. Punta and N. A. Porter, *J. Org. Chem.*, 2006, **71**, 3527-3532.
97. in *Encyclopedia of Radicals in Chemistry, Biology and Materials*, 2012, DOI: doi:10.1002/9781119953678.rad007.
98. W. Zhao, R. P. Wurz, J. C. Peters and G. C. Fu, *J. Am. Chem. Soc.*, 2017, **139**, 12153-12156.
99. C. Walling, J. H. Cooley, A. A. Ponaras and E. J. Racah, *J. Am. Chem. Soc.*, 1966, **88**, 5361-5363.
100. C. Chatgililoglu, K. U. Ingold and J. C. Scaiano, *J. Am. Chem. Soc.*, 1981, **103**, 7739-7742.
101. S. U. Park, S. K. Chung and M. Newcomb, *J. Am. Chem. Soc.*, 1986, **108**, 240-244.
102. M. Newcomb, C. C. Johnson, M. B. Manek and T. R. Varick, *J. Am. Chem. Soc.*, 1992, **114**, 10915-10921.
103. H. G. Viehe, Z. Janousek, R. Merenyi and L. Stella, *Acc. Chem. Res.*, 1985, **18**, 148-154.

104. O. Ito, Y. Arito and M. Matsuda, *J. Chem. Soc, Perkin Trans. 2*, 1988, DOI: 10.1039/P29880000869, 869-873.
105. D. M. Hodgson, C. R. Maxwell and I. R. Matthews, *Synlett*, 1998, **12**, 1349-1350.
106. D. M. Z. Schmidt and D. G. McCafferty, *Biochemistry*, 2007, **46**, 4408-4416.
107. S. J. Cho, N. H. Jensen, T. Kurome, S. Kadari, M. L. Manzano, J. E. Malberg, B. Caldarone, B. L. Roth and A. P. Kozikowski, *J. Med. Chem.*, 2009, **52**, 1885-1902.
108. M. Bergmann, *Nature*, 1933, **131**, 662-664.
109. I. Wagner and H. Musso, *Angew. Chem., Int. Ed.*, 1983, **22**, 816-828.
110. A. Feldstein and K. K. Wong, *Anal. Biochem.*, 1965, **11**, 467-472.
111. T. Huang, G. Jander and M. de Vos, *Phytochemistry*, 2011, **72**, 1531-1537.
112. D. H. B. F.;, *Eur. J. Biochem.*, 1984, **138**, 9-37.
113. A. Neuberger, *Adv. Protein Chem.*, 1948, **4**, 297-383.
114. H. Sund and K. Weber, *Angew. Chem.-Int. Edit.*, 1966, **5**, 231-&.
115. G. V. Kryukov, S. Castellano, S. V. Novoselov, A. V. Lobanov, O. Zehtab, R. Guigó and V. N. Gladyshev, *Science*, 2003, **300**, 1439-1443.
116. A. G. Gornall, *Can. Med. Assoc. J.*, 1942, **47**, 421-423.
117. L. C. Gardner and T. M. Cox, *J. Biol. Chem.*, 1988, **263**, 6676-6682.
118. M. Watanabe, K. Maemura, K. Kanbara, T. Tamayama and H. Hayasaki, in *International Review of Cytology*, ed. W. J. Kwang, Academic Press, 2002, vol. Volume 213, pp. 1-47.
119. W. Derave, M. S. Özdemir, R. C. Harris, A. Pottier, H. Reyngoudt, K. Koppo, J. A. Wise and E. Achten, *J. Appl. Physiol.*, 2007, **103**, 1736-1743.
120. E. Calvaresi and J. Bryan, *J. Gerontol. B Psychol. Sci. Soc. Sci.*, 2001, **56**, P327-P339.
121. A. Wegkamp, W. van Oorschot, W. M. de Vos and E. J. Smid, *Appl. Environ. Microbiol.*, 2007, **73**, 2673-2681.
122. D. Majumdar and S. Guha, *J. Mol. Struct. Theochem*, 1988, **180**, 125-140.
123. P. Krogsgaardlarsen and G. A. R. Johnston, *J. Neurochem.*, 1978, **30**, 1377-1382.
124. P. R. Andrews and G. A. R. Johnston, *J. Theor. Biol.*, 1979, **79**, 263-273.
125. M. L. Vahatalo and A. I. Virtanen, *Acta Chem. Scand.*, 1957, **11**, 741-743.
126. L. F. Burroughs, *Nature*, 1957, **179**, 360-361.
127. H. Kakeya, H. P. Zhang, K. Kobinata, R. Onose, C. Onozawa, T. Kudo and H. Osada, *J. Antibiot.*, 1997, **50**, 370-372.
128. H. P. Zhang, H. Kakeya and H. Osada, *Tetrahedron Lett.*, 1997, **38**, 1789-1792.
129. M. Hara, S. Soga, M. Itoh, K. Shono, J. Eishima and T. Mizukami, *J. Antibiot.*, 2000, **53**, 720-723.

130. S. Khani-Oskouee, K. Ramalingam, D. Kalvin and R. W. Woodard, *Bioorg. Chem.*, 1987, **15**, 92-99.
131. J. N. Barlow, Z. Zhang, P. John, J. E. Baldwin and C. J. Schofield, *Biochemistry*, 1997, **36**, 3563-3569.
132. J. S. Thrower, R. Blalock, 3rd and J. P. Klinman, *Biochemistry*, 2001, **40**, 9717-9724.
133. R. K. Hill, S. R. Prakash, R. Wiesendanger, W. Angst, B. Martinoni, D. Arigoni, H. W. Liu and C. T. Walsh, *J. Am. Chem. Soc.*, 1984, **106**, 795-796.
134. T. Ogawa, H. Yoshitomi, H. Kodama, M. Waki, C. H. Stammer and Y. Shimohigashi, *FEBS Lett.*, 1989, **250**, 227-230.
135. I. MacInnes, D. C. Nonhebel, S. T. Orszulik, C. J. Suckling and R. Wrigglesworth, *J. Chem. Soc., Perkin Trans. 1*, 1983, **3**, 2771-2776.
136. C. J. Suckling, *Angew. Chem., Int. Ed.*, 1988, **27**, 537-552.
137. F. Brackmann and A. de Meijere, *Chem. Rev.*, 2007, **107**, 4493-4537.
138. C. K. Ingold, S. Sako and J. F. Thorpe, *J. Chem. Soc., Trans.*, 1922, **121**, 1177-1198.
139. F. Micheel, O. Eickenscheidt and I. Zeidler, *Chem. Ber.*, 1965, **98**, 3520-3522.
140. M. Suzuki, E. E. Gooch and C. H. Stammer, *Tetrahedron Lett.*, 1983, **24**, 3839-3840.
141. J. Vaughan and L. Phillips, *J. Chem. Soc.*, 1947, 1561-1565.
142. R. S. Hosmane and J. F. Liebman, *Struct. Chem.*, 2002, **13**, 501-503.
143. D. Donati, A. Garzon-Aburbbeh, B. Natalini, C. Marchioro and R. Pellicciari, *Tetrahedron*, 1996, **52**, 9901-9908.
144. A. B. Charette and B. Cote, *J. Am. Chem. Soc.*, 1995, **117**, 12721-12732.
145. L. A. Adams, V. K. Aggarwal, R. V. Bonnert, B. Bressel, R. J. Cox, J. Shepherd, J. de Vicente, M. Walter, W. G. Whittingham and C. L. Winn, *J. Org. Chem.*, 2003, **68**, 9433-9440.
146. T. N. Wheeler and J. A. Ray, *Synth. Commun.*, 1988, **18**, 141-149.
147. S. Ahmad, R. S. Phillips and C. H. Stammer, *J. Med. Chem.*, 1992, **35**, 1410-1417.
148. M. Kordes, H. Winsel and A. d. Meijere, *Eur. J. Org. Chem.*, 2000, **2000**, 3235-3245.
149. H. M. L. Davies, P. R. Bruzinski, D. H. Lake, N. Kong and M. J. Fall, *J. Am. Chem. Soc.*, 1996, **118**, 6897-6907.
150. M. C. Pirrung and J. Zhang, *Tetrahedron Lett.*, 1992, **33**, 5987-5990.
151. V. K. Aggarwal, E. Alonso, G. Hynd, K. M. Lydon, M. J. Palmer, M. Porcelloni and J. R. Studley, *Angew. Chem., Int. Ed.*, 2001, **40**, 1430-1433.
152. V. K. Aggarwal, E. Alonso, I. Bae, G. Hynd, K. M. Lydon, M. J. Palmer, M. Patel, M. Porcelloni, J. Richardson, R. A. Stenson, J. R. Studley, J.-L. Vasse and C. L. Winn, *J. Am. Chem. Soc.*, 2003, **125**, 10926-10940.

153. J. R. Wolf, C. G. Hamaker, J.-P. Djukic, T. Kodadek and L. K. Woo, *J. Am. Chem. Soc.*, 1995, **117**, 9194-9199.
154. C. Zhu, J. Li, P. Chen, W. Wu, Y. Ren and H. Jiang, *Org. Lett.*, 2016, **18**, 1470-1473.
155. J. V. Hunt and R. T. Dean, *Biochem. Biophys. Res. Commun.*, 1989, **162**, 1076-1084.
156. J. R. Fulton, V. K. Aggarwal and J. de Vicente, *Eur. J. Org. Chem.*, 2005, **2005**, 1479-1492.
157. I. Chataigner, C. Panel, H. Gérard and S. R. Piettre, *Chem. Comm.*, 2007, DOI: 10.1039/B705034H, 3288-3290.
158. M. Kazem-Rostami, N. G. Akhmedov and S. Faramarzi, *J. Mol. Struct.*, 2019, **1178**, 538-543.
159. K. Goswami, S. Paul, S. T. Bugde and S. Sinha, *Tetrahedron*, 2012, **68**, 280-286.
160. X. Wang and J. A. Porco, *J. Org. Chem.*, 2001, **66**, 8215-8221.
161. S. C. Bergmeier and P. P. Seth, *J. Org. Chem.*, 1999, **64**, 3237-3243.
162. C. M. Haskins and D. W. Knight, *Tetrahedron Lett.*, 2004, **45**, 599-601.
163. B. Pettersson, V. Hasimbegovic and J. Bergman, *J. Org. Chem.*, 2011, **76**, 1554-1561.
164. C. Bosset, P. Angibaud, I. Stanfield, L. Meerpoel, D. Berthelot, A. Guérinot and J. Cossy, *J. Org. Chem.*, 2015, **80**, 12509-12525.
165. J. E. Camp, D. Craig, K. Funai and A. J. P. White, *Org. Biomol. Chem.*, 2011, **9**, 7904-7912.
166. R. P. Sellers, L. D. Alexander, V. A. Johnson, C.-C. Lin, J. Savage, R. Corral, J. Moss, T. S. Slugocki, E. K. Singh, M. R. Davis, S. Ravula, J. E. Spicer, J. L. Oelrich, A. Thornquist, C.-M. Pan and S. R. McAlpine, *Bioorg. Med. Chem.*, 2010, **18**, 6822-6856.
167. A. I. Gerasyuto, M. A. Arnold, J. Wang, G. Chen, X. Zhang, S. Smith, M. G. Woll, J. Baird, N. Zhang, N. G. Almstead, J. Narasimhan, S. Peddi, M. Dumble, J. Sheedy, M. Weetall, A. A. Branstrom, J. V. N. Prasad and G. M. Karp, *J. Med. Chem.*, 2018, **61**, 4456-4475.
168. D. Sperandio, A. R. Gangloff, J. Litvak, R. Goldsmith, J. M. Hataye, V. R. Wang, E. J. Shelton, K. Elrod, J. W. Janc, J. M. Clark, K. Rice, S. Weinheimer, K.-S. Yeung, N. A. Meanwell, D. Hernandez, A. J. Staab, B. L. Venables and J. R. Spencer, *Bioorg. Med. Chem. Lett.*, 2002, **12**, 3129-3133.
169. L. Kisfaludy, F. Korenczki, T. Mohácsi, M. Sajgó and S. Femandjian, *Int. J. Pept. Protein Res.*, 1986, **27**, 440-442.
170. T. Ohta, S. Suzuki, M. Todo and T. Kurechi, *Chem. Pharm. Bull.*, 1981, **29**, 1767-1771.
171. W. E. Savige and A. Fontana, *Int. J. Pept. Protein Res.*, 1980, **15**, 285-297.
172. A. J. Downs and C. J. Adams, in *Comprehensive Inorganic Chemistry*, eds. J. C. Bailar, H. J. EmelÉUs, R. Nyholm and A. F. Trotman-Dickenson, Pergamon, Oxford, 1973, DOI: <https://doi.org/10.1016/B978-1-4832-8313-5.50020-6>, p. 1329.

173. A. Blackburn, D. M. Bowles, T. T. Curran and H. Kim, *Synth. Commun.*, 2012, **42**, 1855-1863.
174. W. S. Wadsworth Jr., *Synthetic Applications of Phosphoryl-Stabilized Anions*, John Wiley and Sons, 2005.
175. M. Davi and H. Lebel, *Chem. Comm.*, 2008, DOI: 10.1039/B810708D, 4974-4976.
176. M. P. Doyle, K.-L. Loh, K. M. DeVries and M. S. Chinn, *Tetrahedron Lett.*, 1987, **28**, 833-836.
177. M. S. C. Pedras and D. P. O. Okinyo, *Org. Biomol. Chem.*, 2008, **6**, 51-54.
178. Y. G. Gololobov, A. N. Nesmeyanov, V. P. Iysenko and I. E. Boldeskul, *Tetrahedron*, 1987, **43**, 2609-2651.
179. J. C. Lorenz, J. Long, Z. Yang, S. Xue, Y. Xie and Y. Shi, *J. Org. Chem.*, 2004, **69**, 327-334.
180. J. A. Ciaccio and C. E. Aman, *Synth. Commun.*, 2006, **36**, 1333-1341.
181. G. Zhu, X. Wang, F. Wang, Y. Mao and H. Wang, *J. Heterocycl. Chem.*, 2017, **54**, 2898-2901.
182. K. C. Nicolaou, K. Namoto, A. Ritzén, T. Ulven, M. Shoji, J. Li, G. D'Amico, D. Liotta, C. T. French, M. Wartmann, K.-H. Altmann and P. Giannakakou, *J. Am. Chem. Soc.*, 2001, **123**, 9313-9323.
183. D. M. Gooden, D. M. Z. Schmidt, J. A. Pollock, A. M. Kabadi and D. G. McCafferty, *Bioorg. Med. Chem. Lett.*, 2008, **18**, 3047-3051.
184. R. Ueda, T. Suzuki, K. Mino, H. Tsumoto, H. Nakagawa, M. Hasegawa, R. Sasaki, T. Mizukami and N. Miyata, *J. Am. Chem. Soc.*, 2009, **131**, 17536-17537.
185. M. Skvorcova, L. Grigorjeva and A. Jirgensons, *Org. Lett.*, 2015, **17**, 2902-2904.
186. A. F. G. Goldberg, N. R. O'Connor, R. A. Craig and B. M. Stoltz, *Org. Lett.*, 2012, **14**, 5314-5317.
187. R. K. Varshnaya and P. Banerjee, *J. Org. Chem.*, 2019, **84**, 1614-1623.
188. M. R. Fructos, T. R. Belderrain, M. C. Nicasio, S. P. Nolan, H. Kaur, M. M. Díaz-Requejo and P. J. Pérez, *J. Am. Chem. Soc.*, 2004, **126**, 10846-10847.
189. M. Bordeaux, V. Tyagi and R. Fasan, *Angew. Chem., Int. Ed.*, 2015, **54**, 1744-1748.
190. L. Pfeuffer and U. Pindur, *Helv. Chim. Acta*, 1988, **71**, 467-471.
191. R. Bergamasco, Q. Porter and C. Yap, *Aust. J. Chem.*, 1977, **30**, 1531-1544.
192. J. Cowell, M. Abualnaja, S. Morton, R. Linder, F. Buckingham, P. G. Waddell, M. R. Probert and M. J. Hall, *RSC Adv.*, 2015, **5**, 16125-16152.
193. L. R. Marcin, D. J. Denhart and R. J. Mattson, *Org. Lett.*, 2005, **7**, 2651-2654.
194. P. N. Naik, A. Khan and R. S. Kusurkar, *Tetrahedron*, 2013, **69**, 10733-10738.
195. J. N. Hernández, M. A. Ramírez and V. S. Martín, *J. Org. Chem.*, 2003, **68**, 743-746.

196. M. P. A. Lyle and P. D. Wilson, *Org. Lett.*, 2004, **6**, 855-857.
197. K. M. Peese, C. W. Allard, T. Connolly, B. L. Johnson, C. Li, M. Patel, M. E. Sorensen, M. A. Walker, N. A. Meanwell, B. McAuliffe, B. Minassian, M. Krystal, D. D. Parker, H. A. Lewis, K. Kish, P. Zhang, R. T. Nolte, J. Simmermacher, S. Jenkins, C. Cianci and B. N. Naidu, *J. Med. Chem.*, 2019, **62**, 1348-1361.
198. M. P. Doyle, R. L. Dorow, W. E. Buhro, J. H. Griffin, W. H. Tambllyn and M. L. Trudell, *Organometallics*, 1984, **3**, 44-52.
199. P. G. Gassman, P. K. G. Hodgson and R. J. Balchunis, *J. Am. Chem. Soc.*, 1976, **98**, 1275-1276.
200. P. G. Gassman and W. N. Schenk, *J. Org. Chem.*, 1977, **42**, 918-920.
201. P. Micuch and D. Seebach, *Helv. Chim. Acta*, 2002, **85**, 1567-1577.
202. W. Hu, F. Zhang, Z. Xu, Q. Liu, Y. Cui and Y. Jia, *Org. Lett.*, 2010, **12**, 956-959.
203. P. S. Baran, C. A. Guerrero, N. B. Ambhaikar and B. D. Hafensteiner, *Angew. Chem., Int. Ed.*, 2005, **44**, 606-609.
204. Z. Xu, Q. Li, L. Zhang and Y. Jia, *J. Org. Chem.*, 2009, **74**, 6859-6862.
205. T.-J. Lu and C.-K. Lin, *J. Org. Chem.*, 2011, **76**, 1621-1633.
206. A. K. Ghosh, A. Sarkar and M. Brindisi, *Org. Biomol. Chem.*, 2018, **16**, 2006-2027.
207. T. Shioiri, K. Ninomiya and S. Yamada, *J. Am. Chem. Soc.*, 1972, **94**, 6203-6205.
208. P. J. Jessup, C. B. Petty, J. Roos and L. E. Overman, *Org. Synth.*, 1979, **58**, 1-9.
209. E. Pretsch, P. Buhlmann and M. Badertscher, *Structure Determination of Organic Compounds: Tables of Spectral Data*, Springer, Berlin, Heidelberg, Berlin, 4th Edition edn., 2009.
210. M. E. Duggan and J. S. Imagire, *Synthesis-Stuttgart*, 1989, 131-132.
211. S. Vangveravong and D. E. Nichols, *J. Org. Chem.*, 1995, **60**, 3409-3413.
212. S. Vangveravong, A. Kanthasamy, V. L. Lucaites, D. L. Nelson and D. E. Nichols, *J. Med. Chem.*, 1998, **41**, 4995-5001.
213. T. T. Raj and M. R. Eftink, *Synth. Commun.*, 1998, **28**, 3787-3794.
214. M. A. Cavitt, L. H. Phun and S. France, *Chem. Soc. Rev.*, 2014, **43**, 804-818.
215. À. Cristòfol, E. C. Escudero-Adán and A. W. Kleij, *J. Org. Chem.*, 2018, **83**, 9978-9990.
216. P. Igel, E. Schneider, D. Schnell, S. Elz, R. Seifert and A. Buschauer, *J. Med. Chem.*, 2009, **52**, 2623-2627.
217. C. Oberhauser, V. Harms, K. Seidel, B. Schröder, K. Ekramzadeh, S. Beutel, S. Winkler, L. Lauterbach, J. S. Dickschat and A. Kirschning, *Angew. Chem., Int. Ed.*, 2018, **57**, 11802-11806.
218. Q. Li, T. Xia, L. Yao, H. Deng and X. Liao, *Chem. Sci.*, 2015, **6**, 3599-3605.

219. C. Aubry, P. R. Jenkins, S. Mahale, B. Chaudhuri, J.-D. Maréchal and M. J. Sutcliffe, *Chem. Comm.*, 2004, 1696-1697.
220. D. C. Horwell, M. J. McKiernan and S. Osborne, *Tetrahedron Lett.*, 1998, **39**, 8729-8732.
221. I. Peretto, S. Radaelli, C. Parini, M. Zandi, L. F. Raveglia, G. Dondio, L. Fontanella, P. Misiano, C. Bigogno, A. Rizzi, B. Riccardi, M. Biscaioli, S. Marchetti, P. Puccini, S. Catinella, I. Rondelli, V. Cenacchi, P. T. Bolzoni, P. Caruso, G. Villetti, F. Facchinetti, E. Del Giudice, N. Moretto and B. P. Imbimbo, *J. Med. Chem.*, 2005, **48**, 5705-5720.
222. C. Li, J. Ai, D. Zhang, X. Peng, X. Chen, Z. Gao, Y. Su, W. Zhu, Y. Ji, X. Chen, M. Geng and H. Liu, *ACS Med. Chem. Lett.*, 2015, **6**, 507-512.
223. P. R. Reid, T. M. Bridges, D. J. Sheffler, H. P. Cho, L. M. Lewis, E. Days, J. S. Daniels, C. K. Jones, C. M. Niswender, C. D. Weaver, P. J. Conn, C. W. Lindsley and M. R. Wood, *Bioorg. Med. Chem. Lett.*, 2011, **21**, 2697-2701.
224. B. Kakáč and Z. J. Vejdělek, *Handbuch der photometrischen Analyse organischer Verbindungen*, Verlag Chemie, 1974.
225. K.-A. Kovar and M. Laudszun, *Chemistry and Reaction Mechanisms of Rapid Tests for Drugs of Abuse and Precursors Chemicals*, Report SCITEC/6, United Nations Office on Drugs and Crime, Vienna, 1989.
226. J. B. Baell and J. W. M. Nissink, *ACS Chem. Biol.*, 2018, **13**, 36-44.
227. Sara A. Rafice, N. Chauhan, I. Efimov, J. Basran and Emma L. Raven, *Biochem. Soc. Trans.*, 2009, **37**, 408-412.
228. I. Efimov, J. Basran, X. Sun, N. Chauhan, S. K. Chapman, C. G. Mowat and E. L. Raven, *J. Am. Chem. Soc.*, 2012, **134**, 3034-3041.
229. N. Chauhan, J. Basran, S. A. Rafice, I. Efimov, E. S. Millett, C. G. Mowat, P. C. E. Moody, S. Handa and E. L. Raven, *FEBS J.*, 2012, **279**, 4501-4509.
230. J. Basran, S. A. Rafice, N. Chauhan, I. Efimov, M. R. Cheesman, L. Ghamsari and E. L. Raven, *Biochemistry*, 2008, **47**, 4752-4760.
231. N. Chauhan, PhD Thesis, University of Leicester, 2009.
232. Y. Fukunaga, Y. Katsuragi, T. Izumi and F. Sakiyama, *J. Biochem.*, 1982, **92**, 129-141.
233. M. Dixon, *Biochem J*, 1953, **55**, 170-171.
234. P. J. Butterworth, *Biochim. Biophys. Acta*, 1972, **289**, 251-253.
235. A. Lewis-Ballester, K. N. Pham, D. Batabyal, S. Karkashon, J. B. Bonanno, T. L. Poulos and S.-R. Yeh, *Nat Commun*, 2017, **8**, 1693.
236. T. H. Steinberg, L. J. Jones, R. P. Haugland and V. L. Singer, *Anal. Biochem.*, 1996, **239**, 223-237.
237. D. E. Koshland, *Proc. Natl. Acas. Sci. U.S.A*, 1958, **44**, 98-104.
238. S. Granick and R. D. Levere, *J. Cell. Biol.*, 1965, **26**, 167-176.

239. U. F. Röhrig, V. Zoete and O. Michielin, *Biochemistry*, 2017, **56**, 4323-4325.
240. E. Smith and I. Collins, *Future Med. Chem.*, 2015, **7**, 159-183.
241. J. S. Rawlings, K. M. Rosler and D. A. Harrison, *J. Cell Sci.*, 2004, **117**, 1281-1283.
242. M. R. Zaidi and G. Merlino, *Clin. Cancer Res.*, 2011, **17**, 6118-6124.
243. M. Mojic, K. Takeda and Y. Hayakawa, *Int. J. Mol.*, 2017, **19**, 89.
244. S. Lawrence, J. Reid and M. Whalen, *Environ. Toxicol.*, 2015, **30**, 559-571.
245. J. R. Brody, C. L. Costantino, A. C. Berger, T. Sato, M. P. Lisanti, C. J. Yeo, R. V. Emmons and A. K. Witkiewicz, *Cell Cycle*, 2009, **8**, 1930-1934.
246. J. B. Katz, A. J. Muller and G. C. Prendergast, *Immunol. Rev.*, 2008, **222**, 206-221.
247. M. Mandai, J. Hamanishi, K. Abiko, N. Matsumura, T. Baba and I. Konishi, *Clin. Cancer Res.*, 2016, **22**, 2329-2334.
248. K. Abiko, N. Matsumura, J. Hamanishi, N. Horikawa, R. Murakami, K. Yamaguchi, Y. Yoshioka, T. Baba, I. Konishi and M. Mandai, *Br. J. Cancer*, 2015, **112**, 1501.
249. G. C. Prendergast, *Oncogene*, 2008, **27**, 3889.
250. R. D. Dorand, J. Nthale, J. T. Myers, D. S. Barkauskas, S. Avril, S. M. Chirieleison, T. K. Pareek, D. W. Abbott, D. S. Stearns, J. J. Letterio, A. Y. Huang and A. Petrosiute, *Science*, 2016, **353**, 399-403.
251. D. M. Schwartz, Y. Kanno, A. Villarino, M. Ward, M. Gadina and J. J. O'Shea, *Nat. Rev. Drug Discovery*, 2017, **16**, 843.
252. A. Kontzias, A. Kotlyar, A. Laurence, P. Changelian and J. J. O'Shea, *Curr. Opin. Pharmacol.*, 2012, **12**, 464-470.
253. B. C. Betts, O. Abdel-Wahab, S. A. Curran, E. T. St Angelo, P. Koppikar, G. Heller, R. L. Levine and J. W. Young, *Blood*, 2011, **118**, 5330-5339.
254. M. A. Burchill, J. Yang, C. Vogtenhuber, B. R. Blazar and M. A. Farrar, *J. Immunol.*, 2007, **178**, 280-290.
255. T. Y. Wuest, J. Willette-Brown, S. K. Durum and A. A. Hurwitz, *J. Leukocyte Biol.*, 2008, **84**, 973-980.
256. Q. Qiu, Q. L. Feng, X. Y. Tan and M. X. Guo, *Expert Rev. Clin. Pharmacol.*, 2019, **12**, 547-554.
257. K. Yamaoka, *Expert Rev. Clin. Immunol.*, 2019, **15**, 577-588.
258. J. G. Kettle, A. Åstrand, M. Catley, N. P. Grimster, M. Nilsson, Q. Su and R. Woessner, *Expert Opin. Ther. Pat.*, 2017, **27**, 127-143.
259. A. Quintás-Cardama, K. Vaddi, P. Liu, T. Manshour, J. Li, P. A. Scherle, E. Caulder, X. Wen, Y. Li, P. Waeltz, M. Rupal, T. Burn, Y. Lo, J. Kelley, M. Covington, S. Shepard, J. D. Rodgers, P. Haley, H. Kantarjian, J. S. Fridman and S. Verstovsek, 2010, **115**, 3109-3117.

260. S. Hart, K. C. Goh, V. Novotny-Diermayr, C. Y. Hu, H. Hentze, Y. C. Tan, B. Madan, C. Amalini, Y. K. Loh, L. C. Ong, A. D. William, A. Lee, A. Poulsen, R. Jayaraman, K. H. Ong, K. Ethirajulu, B. W. Dymock and J. W. Wood, *Leukemia*, 2011, **25**, 1751.
261. L. Ma, J. R. Clayton, R. A. Walgren, B. Zhao, R. J. Evans, M. C. Smith, K. M. Heinz-Taheny, E. L. Kreklau, L. Bloem, C. Pitou, W. Shen, J. M. Strelow, C. Halstead, M. E. Rempala, S. Parthasarathy, J. R. Gillig, L. J. Heinz, H. Pei, Y. Wang, L. F. Stancato, M. S. Dowless, P. W. Iversen and T. P. Burkholder, *Blood Cancer J.*, 2013, **3**, e109.
262. A. Pardanani, T. Lasho, G. Smith, C. J. Burns, E. Fantino and A. Tefferi, *Leukemia*, 2009, **23**, 1441.
263. G. Wernig, M. G. Kharas, R. Okabe, S. A. Moore, D. S. Leeman, D. E. Cullen, M. Gozo, E. P. McDowell, R. L. Levine, J. Doukas, C. C. Mak, G. Noronha, M. Martin, Y. D. Ko, B. H. Lee, R. M. Soll, A. Tefferi, J. D. Hood and D. G. Gilliland, *Cancer Cell*, 2008, **13**, 311-320.
264. H. Wan, G. M. Schroeder, A. C. Hart, J. Inghrim, J. Grebinski, J. S. Tokarski, M. V. Lorenzi, D. You, T. McDevitt, B. Penhallow, R. Vuppugalla, Y. Zhang, X. Gu, R. Iyer, L. J. Lombardo, G. L. Trainor, S. Ruepp, J. Lippy, Y. Blat, J. S. Sack, J. A. Khan, K. Stefanski, B. Slecicka, A. Mathur, J.-H. Sun, M. K. Wong, D.-R. Wu, P. Li, A. Gupta, P. N. Arunachalam, B. Pragalathan, S. Narayanan, N. K.C, P. Kuppusamy and A. V. Purandare, *ACS Med. Chem. Lett.*, 2015, **6**, 850-855.
265. T. Zhou, S. Georgeon, R. Moser, D. J. Moore, A. Cafilisch and O. Hantschel, *Leukemia*, 2013, **28**, 404.
266. A. Deshpande, M. M. Reddy, G. O. M. Schade, A. Ray, T. K. Chowdary, J. D. Griffin and M. Sattler, *Leukemia*, 2012, **26**, 708-715.
267. J. D. Rodgers, S. Shepard, W. Zhu, L. Shao and J. Glenn, *United States Pat.*, WO2013173720, 2013.
268. A. Coltoff, D. Tremblay, M. Kremyanskaya, R. Hoffman and J. Mascarenhas, *Blood*, 2017, **130**, 2926-2926.
269. A. Ostojic, R. Vrhovac and S. Verstovsek, *Ther Clin Risk Manag*, 2012, **8**, 95-103.
270. J. Mascarenhas, *Leuk. Lymphoma*, 2015, **56**, 2493-2497.
271. clinicaltrials.gov, GRAVITAS-309: Itacitinib or Placebo in Combination With Corticosteroids as Initial Treatment for Chronic Graft-Versus-Host Disease, <https://clinicaltrials.gov/ct2/show/NCT03584516>, (accessed 06/08/2019).
272. clinicaltrials.gov, A Study of Itacitinib in Combination With Low-Dose Ruxolitinib or Itacitinib Alone Following Ruxolitinib in Subjects With Myelofibrosis, <https://clinicaltrials.gov/ct2/show/NCT03144687>, (accessed 06/08/2019).
273. P. J. Campbell, M. Griesshammer, K. Döhner, H. Döhner, R. Kusec, H. C. Hasselbalch, T. S. Larsen, N. Pallisgaard, S. Giraudier, M.-C. Le Bousse-Kerdilès, C. Desterke, B. Guerton, B. Dupriez, D. Bordessoule, P. Fenaux, J.-J. Kiladjian, J.-F. Viallard, J. Brière, C. N. Harrison, A. R. Green and J. T. Reilly, *Blood*, 2006, **107**, 2098-2100.

274. C. Nielsen, H. S. Birgens, B. G. Nordestgaard, L. Kjaer and S. E. Bojesen, *Haematologica*, 2011, **96**, 450-453.
275. clinicaltrials.gov, A Study of LY2784544 in Participants With Myeloproliferative Neoplasms, <https://clinicaltrials.gov/ct2/show/NCT01594723>, (accessed 06/08/2019).
276. Clinicaltrials.gov, Multiple Ascending Dose of BMS-911543, <https://clinicaltrials.gov/ct2/show/NCT01236352>, (accessed 27/10/2019).
277. N. R. Leitner, A. Witalisz-Siepracka, B. Strobl and M. Müller, *Cytokine*, 2017, **89**, 209-218.
278. J. Mascarenhas, R. Hoffman, M. Talpaz, A. T. Gerds, B. Stein, V. Gupta, A. Szoke, M. Drummond, A. Pristupa, T. Granston, R. Daly, S. Al-Fayoumi, J. A. Callahan, J. W. Singer, J. Gotlib, C. Jamieson, C. Harrison, R. Mesa and S. Verstovsek, *JAMA Oncology*, 2018, **4**, 652-659.
279. J. Mascarenhas, R. Hoffman, M. Talpaz, A. T. Gerds, B. Stein, V. Gupta, A. Szoke, M. Drummond, A. Pristupa, T. Granston, R. Daly, J. P. Dean, S. Al-Fayoumi, J. A. Callahan, J. W. Singer, J. Gotlib, C. Jamieson, C. Harrison, R. Mesa and S. Verstovsek, *Blood*, 2016, **128**, LBA-5-LBA-5.
280. clinicaltrials.gov, Oral Pacritinib Versus Best Available Therapy to Treat Myelofibrosis, <https://clinicaltrials.gov/ct2/show/NCT02055781>, (accessed 06/08/2019).
281. C. N. Harrison, A. M. Vannucchi, U. Platzbecker, F. Cervantes, V. Gupta, D. Lavie, F. Passamonti, E. F. Winton, H. Dong, J. Kawashima, J. D. Maltzman, J.-J. Kiladjan and S. Verstovsek, *Lancet Haematol.*, 2018, **5**, e73-e81.
282. Clinicaltrials.gov, Efficacy of Momelotinib Versus Best Available Therapy in Anemic or Thrombocytopenic Subjects With Primary Myelofibrosis (MF), Post-polycythemia Vera MF, or Post-essential Thrombocythemia MF (Simplify 2), (accessed 07/08/2019).
283. M. Wu, C. Li and X. Zhu, *J. Hematol. Oncol.*, 2018, **11**, 133.
284. L. Mendoza, *Oncol Rev*, 2018, **12**, 352-352.
285. C. N. Harrison, N. Schaap, A. M. Vannucchi, J.-J. Kiladjan, R. V. Tiu, P. Zachee, E. Jourdan, E. Winton, R. T. Silver, H. C. Schouten, F. Passamonti, S. Zweegman, M. Talpaz, J. Lager, Z. Shun and R. A. Mesa, *Lancet Haematol.*, 2017, **4**, e317-e324.
286. C. N. Harrison, R. A. Mesa, C. Jamieson, J. Hood, J. Bykowski, G. Zuccoli and J. Brewer, *Blood*, 2017, **130**, 2.
287. J. Hood and A. Hazell, *Blood*, 2017, **130**, 4993-4993.
288. A. S. Hazell, S. Afadlal, D. A. Cheresch and A. Azar, *Neurosci. Lett.*, 2017, **642**, 163-167.
289. clinicaltrials.gov, An Efficacy and Safety Trial of Fedratinib in Subjects With DIPSS, Intermediate or High-Risk Primary Myelofibrosis, Post-Polycythemia Vera Myelofibrosis, or Post-Essential Thrombocythemia Myelofibrosis and Previously Treated With Ruxolitinib (FREEDOM), <https://clinicaltrials.gov/ct2/show/NCT03755518>, (accessed 07/08/2019).

290. S. DiGrande, Fedratinib Earns Priority Review Status for Myelofibrosis From FDA, <https://www.ajmc.com/newsroom/fedratinib-earns-priority-review-status-for-myelofibrosis-from-fda>, (accessed 07/08/2019).
291. Celgene, U.S. FDA Approves INREBIC® (Fedratinib) as First New Treatment in Nearly a Decade for Patients With Myelofibrosis, <https://ir.celgene.com/press-releases/press-release-details/2019/US-FDA-Approves-INREBIC-Fedratinib-as-First-New-Treatment-in-Nearly-a-Decade-for-Patients-With-Myelofibrosis/default.aspx>, (accessed 30/08/2019).
292. U. S. F. a. D. Administration, FDA approves fedratinib for myelofibrosis, <https://www.fda.gov/drugs/resources-information-approved-drugs/fda-approves-fedratinib-myelofibrosis>, (accessed 30/08/2019).
293. F. Concha-Benavente and R. L. Ferris, *J. Immunother. Cancer*, 2014, **2**, P199.
294. R. Bellucci, A. Martin, D. Bommarito, K. Wang, S. H. Hansen, G. J. Freeman and J. Ritz, *Oncolmunology*, 2015, **4**, e1008824.
295. F. Castro, A. P. Cardoso, R. M. Gonçalves, K. Serre and M. J. Oliveira, 2018, **9**.
296. N. K. Bassal, B. P. Hughes and M. Costabile, *Prostaglandins, Leukotrienes Essent. Fatty Acids*, 2016, **110**, 48-54.
297. N. C. R. a. A. Service, Chemotherapy, Radiotherapy and Surgical Tumour Resections in England, http://www.ncin.org.uk/cancer_type_and_topic_specific_work/topic_specific_work/main_cancer_treatments, (accessed 07/08/2019).
298. R. M. Poole, *Drugs*, 2014, **74**, 1973-1981.
299. D. G. Maloney, A. J. GrilloLopez, C. A. White, D. Bodkin, R. J. Schilder, J. A. Neidhart, N. Janakiraman, K. A. Foon, T. M. Liles, B. K. Dallaire, K. Wey, I. Royston, T. Davis and R. Levy, *Blood*, 1997, **90**, 2188-2195.
300. F. Sewell, K. Chapman, J. Couch, M. Dempster, S. Heidel, L. Loberg, C. Maier, T. K. Maclachlan, M. Todd and J. W. van der Laan, *MAbs*, 2017, **9**, 742-755.
301. P. V. Scaria, R. M. Schifflers, A. Ansari, J. Xu, Q. Zhou, Q. Tang, G. Storm, G. Molema, P. Y. Lu and M. C. Woodle, *Proc. Amer. Assoc. Cancer Res.*, 2004, **64**, 542-542.
302. G. R. Devi, *Cancer Gene Ther.*, 2006, **13**, 819-829.
303. W. Guo, W. Chen, W. Yu, W. Huang and W. Deng, *Chin J Cancer*, 2013, **32**, 488-493.
304. G. Mahmoodi Chalbatani, H. Dana, E. Gharagouzloo, S. Grijalvo, R. Eritja, C. D. Logsdon, F. Memari, S. R. Miri, M. R. Rad and V. Marmari, *Int J Nanomedicine*, 2019, **14**, 3111-3128.
305. M. V. Gatzka, *Cancers (Basel)*, 2018, **10**, 155.
306. J. A. Wells and C. L. McClendon, *Nature*, 2007, **450**, 1001.
307. A. C. Lai and C. M. Crews, *Nat. Rev. Drug Discovery*, 2016, **16**, 101.

308. S. Dogan, R. Shen, D. C. Ang, M. L. Johnson, S. P. D'Angelo, P. K. Paik, E. B. Brzostowski, G. J. Riely, M. G. Kris, M. F. Zakowski and M. Ladanyi, *Clin Cancer Res*, 2012, **18**, 6169-6177.
309. S. An and L. Fu, *EBioMedicine*, 2018, **36**, 553-562.
310. I. Churcher, *J. Med. Chem.*, 2018, **61**, 444-452.
311. S. D. Edmondson, B. Yang and C. Fallan, *Bioorg. Med. Chem. Lett.*, 2019, **29**, 1555-1564.
312. J. Salami and C. M. Crews, *Science*, 2017, **355**, 1163-1167.
313. Y. Zou, D. Ma and Y. Wang, *Cell Biochem. Funct.*, 2019, **37**, 21-30.
314. K. M. Sakamoto, K. B. Kim, A. Kumagai, F. Mercurio, C. M. Crews and R. J. Deshaies, *Proc. Natl. Acad. Sci. U. S. A.*, 2001, **98**, 8554-8559.
315. D. P. Bondeson, A. Mares, I. E. D. Smith, E. Ko, S. Campos, A. H. Miah, K. E. Mulholland, N. Routly, D. L. Buckley, J. L. Gustafson, N. Zinn, P. Grandi, S. Shimamura, G. Bergamini, M. Faelth-Savitski, M. Bantscheff, C. Cox, D. A. Gordon, R. R. Willard, J. J. Flanagan, L. N. Casillas, B. J. Votta, W. den Besten, K. Famm, L. Kruidenier, P. S. Carter, J. D. Harling, I. Churcher and C. M. Crews, *Nat. Chem. Biol.*, 2015, **11**, 611.
316. M. D. Petroski, G. Kleiger and Raymond J. Deshaies, *Mol. Cell*, 2006, **24**, 523-534.
317. D. Komander, M. J. Clague and S. Urbé, *Nat. Rev. Mol. Cell Biol.*, 2009, **10**, 550.
318. Y. Kravtsova-Ivantsiv, T. Sommer and A. Ciechanover, *Angew. Chem., Int. Ed.*, 2013, **52**, 192-198.
319. M. Scheffner, K. Münger, J. M. Huibregtse and P. M. Howley, *EMBO J*, 1992, **11**, 2425-2431.
320. R. Dohmen, P. Wu and A. Varshavsky, *Science*, 1994, **263**, 1273-1276.
321. M. M. Gosink and R. D. Vierstra, *Proc. Natl. Acad. Sci. U. S. A.*, 1995, **92**, 9117-9121.
322. K. M. Sakamoto, K. B. Kim, R. Verma, A. Ransick, B. Stein, C. M. Crews and R. J. Deshaies, *Mol. Cell Proteomics*, 2003, **2**, 1350-1358.
323. A. R. Schneekloth, M. Pucheault, H. S. Tae and C. M. Crews, *Bioorg. Med. Chem. Lett.*, 2008, **18**, 5904-5908.
324. C. Galdeano, M. S. Gadd, P. Soares, S. Scaffidi, I. Van Molle, I. Birced, S. Hewitt, D. M. Dias and A. Ciulli, *J. Med. Chem.*, 2014, **57**, 8657-8663.
325. I. Van Molle, A. Thomann, Dennis L. Buckley, Ernest C. So, S. Lang, Craig M. Crews and A. Ciulli, *Chem. Biol.*, 2012, **19**, 1300-1312.
326. M. Zengerle, K.-H. Chan and A. Ciulli, *ACS Chem. Biol.*, 2015, **10**, 1770-1777.
327. Y. Itoh, M. Ishikawa, M. Naito and Y. Hashimoto, *J. Am. Chem. Soc.*, 2010, **132**, 5820-5826.
328. G. S. Salvesen and C. S. Duckett, *Nat. Rev. Mol. Cell Biol.*, 2002, **3**, 401-410.

329. E. Varfolomeev, J. W. Blankenship, S. M. Wayson, A. V. Fedorova, N. Kayagaki, P. Garg, K. Zobel, J. N. Dynek, L. O. Elliott, H. J. A. Wallweber, J. A. Flygare, W. J. Fairbrother, K. Deshayes, V. M. Dixit and D. Vucic, *Cell*, 2007, **131**, 669-681.
330. N. Ohoka, T. Misawa, M. Kurihara, Y. Demizu and M. Naito, *Bioorg. Med. Chem. Lett.*, 2017, **27**, 4985-4988.
331. N. Ohoka, Y. Morita, K. Nagai, K. Shimokawa, O. Ujikawa, I. Fujimori, M. Ito, Y. Hayase, K. Okuhira, N. Shibata, T. Hattori, T. Sameshima, O. Sano, R. Koyama, Y. Imaeda, H. Nara, N. Cho and M. Naito, *J. Biol. Chem.*, 2018, **293**, 6776-6790.
332. N. Ohoka, K. Okuhira, M. Ito, K. Nagai, N. Shibata, T. Hattori, O. Ujikawa, K. Shimokawa, O. Sano, R. Koyama, H. Fujita, M. Teratani, H. Matsumoto, Y. Imaeda, H. Nara, N. Cho and M. Naito, *J. Biol. Chem.*, 2017, **292**, 4556-4570.
333. E. S. Fischer, K. Böhm, J. R. Lydeard, H. Yang, M. B. Stadler, S. Cavadini, J. Nagel, F. Serluca, V. Acker, G. M. Lingaraju, R. B. Tichkule, M. Schebesta, W. C. Forrester, M. Schirle, U. Hassiepen, J. Ottl, M. Hild, R. E. J. Beckwith, J. W. Harper, J. L. Jenkins and N. H. Thomä, *Nature*, 2014, **512**, 49.
334. J. Lu, Y. Qian, M. Altieri, H. Dong, J. Wang, K. Raina, J. Hines, James D. Winkler, Andrew P. Crew, K. Coleman and Craig M. Crews, *Chem. Biol.*, 2015, **22**, 755-763.
335. G. E. Winter, D. L. Buckley, J. Paulk, J. M. Roberts, A. Souza, S. Dhe-Paganon and J. E. Bradner, *Science*, 2015, **348**, 1376-1381.
336. H. X. Pei, Y. R. Peng, Q. H. Zhao and Y. H. Chen, *RSC Adv.*, 2019, **9**, 16967-16976.
337. F. M. Ferguson and N. S. Gray, *Nat. Rev. Drug Discovery*, 2018, **17**, 353.
338. M. S. Gadd, A. Testa, X. Lucas, K.-H. Chan, W. Chen, D. J. Lamont, M. Zengerle and A. Ciulli, *Nat. Chem. Biol.*, 2017, **13**, 514.
339. D. P. Bondeson, B. E. Smith, G. M. Burslem, A. D. Buhimschi, J. Hines, S. Jaime-Figueroa, J. Wang, B. D. Hamman, A. Ishchenko and C. M. Crews, *Cell Chem. Biol.*, 2018, **25**, 78-87.e75.
340. H.-T. Huang, D. Dobrovolsky, J. Paulk, G. Yang, E. L. Weisberg, Z. M. Doctor, D. L. Buckley, J.-H. Cho, E. Ko, J. Jang, K. Shi, H. G. Choi, J. D. Griffin, Y. Li, S. P. Treon, E. S. Fischer, J. E. Bradner, L. Tan and N. S. Gray, *Cell Chem. Biol.*, 2018, **25**, 88-99.e86.
341. L. Tan and N. S. Gray, *Chin. J. Chem.*, 2018, **36**, 971-977.
342. B. Schwanhäusser, M. Gossen, G. Dittmar and M. Selbach, *Proteomics*, 2009, **9**, 205-209.
343. A. Mullard, *Nat. Rev. Drug Discovery*, 2019, **18**, 237-239.
344. clinicaltrials.gov, A Phase 1 Clinical Trial of ARV-110 in Patients With Metastatic Castration-resistant Prostate Cancer. (mCRPC), <https://clinicaltrials.gov/ct2/show/NCT03888612>, (accessed 27/08/2019).
345. X. Sun, J. Wang, X. Yao, W. Zheng, Y. Mao, T. Lan, L. Wang, Y. Sun, X. Zhang, Q. Zhao, J. Zhao, R.-P. Xiao, X. Zhang, G. Ji and Y. Rao, *Cell Discov.*, 2019, **5**, 10.

346. A. P. Crew, H. Dong, J. Wang, C. Ferraro, X. Chen and Y. Qian, *United States Pat.*, US20170327469A1, 2018.
347. T. Neklesa, L. B. Snyder, R. R. Willard, N. Vitale, K. Raina, J. Pizzano, D. Gordon, M. Bookbinder, J. Macaluso, H. Dong, Z. Liu, C. Ferraro, G. Wang, J. Wang, C. M. Crews, J. Houston, A. P. Crew and I. Taylor, Chicago, IL, 2018.
348. Arvinas.com, Press Releases: Arvinas Presents a Platform Update, Including Initial Data from the First Two Clinical Trials of PROTAC® Targeted Protein Degraders, <http://ir.arvinas.com/news-releases/news-release-details/arvinas-presents-platform-update-including-initial-data-first>, (accessed 13/11/2019).
349. Arvinas, Arvinas Pipeline, <http://arvinas.com/therapeutic-programs/pipeline/>, (accessed 29/08/2019).
350. Kymera, Kymera Pipeline, <https://www.kymeratx.com/pipeline/>, (accessed 29/08/2019).
351. M. Siu, R. Pastor, W. Liu, K. Barrett, M. Berry, W. S. Blair, C. Chang, J. Z. Chen, C. Eigenbrot, N. Ghilardi, P. Gibbons, H. He, C. A. Hurley, J. R. Kenny, S. Cyrus Khojasteh, H. Le, L. Lee, J. P. Lyssikatos, S. Magnuson, R. Pulk, V. Tsui, M. Ultsch, Y. Xiao, B.-y. Zhu and D. Sampath, *Bioorg. Med. Chem. Lett.*, 2013, **23**, 5014-5021.
352. C. E. Powell, Y. Gao, L. Tan, K. A. Donovan, R. P. Nowak, A. Loehr, M. Bahcall, E. S. Fischer, P. A. Jänne, R. E. George and N. S. Gray, *J. Med. Chem.*, 2018, **61**, 4249-4255.
353. P. M. Cromm, K. T. G. Samarasinghe, J. Hines and C. M. Crews, *J. Am. Chem. Soc.*, 2018, **140**, 17019-17026.
354. A. C. Lai, M. Toure, D. Hellerschmied, J. Salami, S. Jaime-Figueroa, E. Ko, J. Hines and C. M. Crews, *Angew. Chem., Int. Ed.*, 2016, **55**, 807-810.
355. C. Qin, Y. Hu, B. Zhou, E. Fernandez-Salas, C.-Y. Yang, L. Liu, D. McEachern, S. Przybranowski, M. Wang, J. Stuckey, J. Meagher, L. Bai, Z. Chen, M. Lin, J. Yang, D. N. Ziazadeh, F. Xu, J. Hu, W. Xiang, L. Huang, S. Li, B. Wen, D. Sun and S. Wang, *J. Med. Chem.*, 2018, **61**, 6685-6704.
356. J. C. Jianguo, J. Hood, D. Lohse, C. M. Ching, A. Mc Pheson, G. Noronha, V. Pathak, J. Renick, R. M. Soll and B. Zeng, *United States Pat.*, WO2007053452, 2007.
357. K. W. H. Chan, L. Fung, R. Sullivan, P. E. Erdman and F. Mercurio, *Uniter States Pat.*, WO2017201069, 2017.
358. H. Q. Zhang, Z. Xia, A. Vasudevan and S. W. Djuric, *Tetrahedron Lett.*, 2006, **47**, 4881-4884.
359. Y. Wang, W. Huang, M. Xin, P. Chen, L. Gui, X. Zhao, F. Tang, J. Wang and F. Liu, *Bioorg. Med. Chem.*, 2017, **25**, 75-83.
360. H. R. Lawrence, K. Mahajan, Y. Luo, D. Zhang, N. Tindall, M. Huseyin, H. Gevariya, S. Kazi, S. Ozcan, N. P. Mahajan and N. J. Lawrence, *J. Med. Chem.*, 2015, **58**, 2746-2763.
361. S. G. Stewart, D. Spagnolo, M. E. Polomska, M. Sin, M. Karimi and L. J. Abraham, *Bioorg. Med. Chem. Lett.*, 2007, **17**, 5819-5824.

362. W. B. Smith and O. C. Ho, *J. Org. Chem.*, 1990, **55**, 2543-2545.
363. C. Bressy, D. Alberico and M. Lautens, *J. Am. Chem. Soc.*, 2005, **127**, 13148-13149.
364. D. M. T. Yu, T. Huynh, A. M. Truong, M. Haber and M. D. Norris, in *Advances in Cancer Research*, eds. J. D. Schuetz and T. Ishikawa, Academic Press, 2015, vol. 125, pp. 139-170.
365. M. Roe, A. Folkes, P. Ashworth, J. Brumwell, L. Chima, S. Hunjan, I. Pretswell, W. Dangerfield, H. Ryder and P. Charlton, *Bioorg. Med. Chem. Lett.*, 1999, **9**, 595-600.
366. J. V. Chapman, V. Gouaze-Andersson and M. C. Cabot, *Int. J. Oncol.*, 2010, **37**, 1591-1597.
367. S. P. Perfetto, P. K. Chattopadhyay, L. Lamoreaux, R. Nguyen, D. Ambrozak, R. A. Koup and M. Roederer, *Curr Protoc Cytom*, 2010, **Chapter 9**, Unit-9.34.
368. F. He, *Bio-protocol*, 2011, **1**, e44.
369. W. C. Still, M. Kahn and A. Mitra, *J. Org. Chem.*, 1978, **43**, 2923-2925.
370. C. Zhang, D. Xu, J. Wang and C. Kang, *Russ. J. Gen. Chem.*, 2017, **87**, 3006-3016.
371. C. Zhao, Z. Ying, X. Tao, M. Jiang, X. Ying and G. Yang, *Nat. Prod. Res.*, 2018, **32**, 1548-1553.
372. B. W. P.;, M. de Kort, M. Enthoven, P. S. Hinchliffe, C. Paulie, C. M. Timmers, ; and S. Verkiak, *Netherlands Pat.*, WO2013041458, 2013.
373. K. Ohmoto, M. Kato, T. Mstsushita, S. Katsumata and M. Junichiro, *Japan Pat.*, EP1637521, 2006.
374. Z. Gao, M. Lv, Q. Li and H. Xu, *Bioorg. Med. Chem. Lett.*, 2015, **25**, 5092-5096.
375. A. P. Dieskau, M. S. Holzwarth and B. Plietker, *J. Am. Chem. Soc.*, 2012, **134**, 5048-5051.
376. L. Crespin, L. Biancalana, T. Morack, D. C. Blakemore and S. V. Ley, *Org. Lett.*, 2017, **19**, 1084-1087.
377. A.-S. Carlström and T. Frejd, *Synthesis*, 1989, 414 - 418.
378. J. J. Clemens, M. D. Davis, K. R. Lynch and T. L. Macdonald, *Bioorg. Med. Chem. Lett.*, 2003, **13**, 3401-3404.
379. B. L. Maheswara Rao, S. Nowshuddin, A. Jha, M. K. Divi and M. N. A. Rao, *Synth. Commun.*, 2017, **47**, 2127-2132.
380. W. Wrasidlo, E. M. Stocking, A. Hall and M. Maccoss, *Uniter States Pat.*, WO2018138085, 2018.
381. Y. Nakao, K. S. Kanyiva, S. Oda and T. Hiyama, *J. Am. Chem. Soc.*, 2006, **128**, 8146-8147.
382. A. García-Rubia, R. G. Arrayás and J. C. Carretero, *Angew. Chem., Int. Ed.*, 2009, **48**, 6511-6515.
383. M. Kurokawa, T. Watanabe and T. Ishikawa, *Helv. Chim. Acta*, 2007, **90**, 574-587.

384. J. Waser, B. Gaspar, H. Nambu and E. M. Carreira, *J. Am. Chem. Soc.*, 2006, **128**, 11693-11712.
385. C. L. Ladd, D. Sustac Roman and A. B. Charette, *Org. Lett.*, 2013, **15**, 1350-1353.
386. T. Ezawa, Y. Kawashima, T. Noguchi, S. Jung and N. Imai, *Tetrahedron: Asymmetry*, 2017, **28**, 1690-1699.
387. S. S. M. Spoehrle, T. H. West, J. E. Taylor, A. M. Z. Slawin and A. D. Smith, *J. Am. Chem. Soc.*, 2017, **139**, 11895-11902.
388. P. J. Gritsch, E. Stempel and T. Gaich, *Org. Lett.*, 2013, **15**, 5472-5475.
389. F. Turnu, A. Luridiana, A. Cocco, S. Porcu, A. Frongia, G. Sarais and F. Secci, *Org. Lett.*, 2019, **21**, 7329-7332.
390. C. Ferrer, A. Escribano-Cuesta and A. M. Echavarren, *Tetrahedron*, 2009, **65**, 9015-9020.
391. C. Wu, P. A. Miller and M. J. Miller, *Bioorg. Med. Chem. Lett.*, 2011, **21**, 2611-2615.
392. T. Leo and M. Michael, *Germany Pat.*, US2003162788 2003.
393. C. W. Zapf, J. R. Del Valle and M. Goodman, *Bioorg. Med. Chem. Lett.*, 2005, **15**, 4033-4036.
394. S. F. Wnuk and M. J. Robins, *J. Org. Chem.*, 1990, **55**, 4757-4760.
395. R. J. I. Tamargo, S. H. Kim and Y. R. Lee, *Adv. Synth. Catal.*, 2019, **361**, 4005-4015.
396. J. Zhou, R. He, K. M. Johnson, Y. Ye and A. P. Kozikowski, *J. Med. Chem.*, 2004, **47**, 5821-5824.
397. P.-C. Diao, W.-Y. Lin, X.-E. Jian, Y.-H. Li, W.-W. You and P.-L. Zhao, *Eur. J. Med. Chem.*, 2019, **179**, 196-207.
398. J. Schmitt, M. Bernd, B. Kutscher and H. Kessler, *Bioorg. Med. Chem. Lett.*, 1998, **8**, 385-388.
399. J. M. G. Nagano, K.-L. Hsu, L. R. Whitby, M. J. Niphakis, A. E. Speers, S. J. Brown, T. Spicer, V. Fernandez-Vega, J. Ferguson, P. Hodder, P. Srinivasan, T. D. Gonzalez, H. Rosen, B. J. Bahnson and B. F. Cravatt, *Bioorg. Med. Chem. Lett.*, 2013, **23**, 839-843.
400. M. Lamping, S. Enck and A. Geyer, *Eur. J. Org. Chem.*, 2015, **2015**, 7443-7448.
401. A. Pardanani, J. Hood, T. Lasho, R. L. Levine, M. B. Martin, G. Noronha, C. Finke, C. C. Mak, R. Mesa, H. Zhu, R. Soll, D. G. Gilliland and A. Tefferi, *Leukemia*, 2007, **21**, 1658.
402. R. A. Smith, S. K. Thompson and N. Laping, *United Kingdom Pat.*, WO2015038417, 2015.
403. C. Wallinder, M. Botros, U. Rosenström, M.-O. Guimond, H. Beaudry, F. Nyberg, N. Gallo-Payet, A. Hallberg and M. Alterman, *Bioorg. Med. Chem.*, 2008, **16**, 6841-6849.
404. D. A. Brown, M. Mishra, S. Zhang, S. Biswas, I. Parrington, T. Antonio, M. E. A. Reith and A. K. Dutta, *Bioorg. Med. Chem.*, 2009, **17**, 3923-3933.

405. V. T. H. Ngo, V.-H. Hoang, P.-T. Tran, N. Van Manh, J. Ann, E. Kim, M. Cui, S. Choi, J. Lee, H. Kim, H.-J. Ha, K. Choi, Y.-H. Kim and J. Lee, *Bioorg. Med. Chem.*, 2018, **26**, 3133-3144.
406. B. Zhou, J. Hu, F. Xu, Z. Chen, L. Bai, E. Fernandez-Salas, M. Lin, L. Liu, C.-Y. Yang, Y. Zhao, D. McEachern, S. Przybranowski, B. Wen, D. Sun and S. Wang, *J. Med. Chem.*, 2018, **61**, 462-481.
407. Y. Hu, C. Qin, F. Xu, J. Hu, W. Xiang and B. Zhou, *United States Pat.*, WO2018052949, 2018.
408. C. Chaulet, C. Croix, D. Alagille, S. Normand, A. Delwail, L. Favot, J.-C. Lecron and M.-C. Viaud-Massuard, *Bioorg. Med. Chem. Lett.*, 2011, **21**, 1019-1022.
409. S. G. Mischke, *United States Pat.*, WO2014090709, 2014.
410. N. Della Ca, G. Maestri, M. Malacria, E. Derat and M. Catellani, *Angew. Chem., Int. Ed.*, 2011, **50**, 12257-12261.
411. E. C. Taylor, L. D. Jennings, Z. Mao, B. Hu, J.-G. Jun and P. Zhou, *J. Org. Chem.*, 1997, **62**, 5392-5403.
412. P. G. Jagtap, G. J. Southan, E. Baloglu, S. Ram, J. G. Mabley, A. Marton, A. Salzman and C. Szabó, *Bioorg. Med. Chem. Lett.*, 2004, **14**, 81-85.
413. S. Hu, L. Yuan, H. Yan and Z. Li, *Bioorg. Med. Chem. Lett.*, 2017, **27**, 4075-4081.
414. D. C. M. Chan, H. Fu, R. A. Forsch, S. F. Queener and A. Rosowsky, *J. Med. Chem.*, 2005, **48**, 4420-4431.
415. G. Bartoli, M. Bosco, A. Carlone, R. Dalpozzo, E. Marcantoni, P. Melchiorre and L. Sambri, *Synthesis*, 2007, **2007**, 3489-3496.
416. B. Botta, I. D'Acquarica, G. Delle Monache, D. Subissati, G. Uccello-Barretta, M. Mastrini, S. Nazzi and M. Speranza, *J. Org. Chem.*, 2007, **72**, 9283-9290.
417. G. Lemercier, S. Gendreizig, M. Kindermann and K. Johnsson, *Angew. Chem., Int. Ed.*, 2007, **46**, 4281-4284.